Distribution Agreement

In presenting this thesis or dissertation as a partial fulfillment of the requirements for an advanced degree from Emory University, I hereby grant to Emory University and its agents the non-exclusive license to archive, make accessible, and display my thesis or dissertation in whole or in part in all forms of media, now or hereafter known, including display on the world wide web. I understand that I may select some access restrictions as part of the online submission of this thesis or dissertation. I retain all ownership rights to the copyright of the thesis or dissertation. I also retain the right to use in future works (such as articles or books) all or part of this thesis or dissertation.

Signature:

_____	_____
Jørn Hedløy Hansen	Date

SYNTHETIC AND QUANTUM-CHEMICAL EXPLORATION OF THE SELECTIVITY OF DONOR/ACCEPTOR-SUBSTITUTED METALLOCARBENOIDS

By

Jørn Hedløy Hansen

Doctor of Philosophy

Chemistry

_____

Dr. Huw M. L. Davies
Advisor

_____

Dr. Albert Padwa
Committee Member

_____

Dr. Fred Menger
Committee Member

Accepted:

_____

Lisa A. Tedesco, Ph.D.
Dean of the James T. Laney School of Graduate Studies

_____

Date

SYNTHETIC AND QUANTUM-CHEMICAL EXPLORATION OF THE SELECTIVITY OF DONOR/ACCEPTOR-SUBSTITUTED METALLOCARBENOIDS

By

Jørn Hedløy Hansen

Siv.ing./M.Sc., The Norwegian University of Science and Technology, 2005

Advisor: Huw M. L. Davies, Ph.D.

An abstract of

A dissertation submitted to the Faculty of the

James T. Laney School of Graduate Studies of Emory University

in partial fulfillment of the requirements for the degree of

Doctor of Philosophy

in Chemistry

2010

Abstract

SYNTHETIC AND QUANTUM-CHEMICAL EXPLORATION OF THE SELECTIVITY OF DONOR/ACCEPTOR-SUBSTITUTED METALLOCARBENOIDS

By Jørn Hedløy Hansen

Transient metallocarbenoids have become versatile intermediates for organic synthesis. Although a variety of applications have already been described, the broad spectrum of reactions displayed by these intermediates has led to an enormous growth in research efforts in later years. The donor/acceptor-substituted carbenoids, derived from aryl– and vinyldiazoacetates, are particularly stabilized and can effect highly stereo– and chemoselective transformations. In this work, factors controlling the selectivity of these species have been studied.

The rational syntheses of novel mixed-ligand dirhodium carboxylate catalysts of well-defined structure are described herein. The method can be used to generate several unique paddlewheel structures. A new class of chiral dirhodium tetracarboxylate catalysts has also been designed, that show considerable promise for asymmetric induction in carbenoid chemistry.

The selectivity of donor/acceptor-substituted rhodium carbenoids has been studied by Density Functional calculations. The calculations have demonstrated why these carbenoids are more selective than traditional carbenoid systems. A new model for the prediction of stereochemistry in intermolecular C–H insertions was also developed from these studies. The details of the mechanism of the combined C–H activation/Cope rearrangement have also been described, based on extensive studies of the potential energy surfaces.

The influence of metals, other than dirhodium complexes, on the selectivity and reactivity of donor/acceptor-substituted carbenoids has been studied. It was found that a new family of electron-deficient ruthenium(I) carbonyl carboxylates and silver salts greatly enhance vinylogous reactivity of their corresponding vinylcarbenoid intermediates. Heterobimetallic bismuth–rhodium carboxylate complexes were also shown to be effective catalysts for carbenoid transformations, although they were much less reactive than dirhodium catalysts. Comparative studies with analogous dirhodium complexes revealed that, axial coordination to the dirhodium catalysts during the catalytic cycle for carbenoid reactions, may greatly influence the reactivity.

A convenient and practical method for selective cross-dimerization of two diazo compounds has been developed. A variety of fumarates are available through this chemistry. The selectivity of the reaction was shown to rely on the preferred formation of donor/acceptor-substituted carbenoids during the catalytic cycle. Underlying control elements that determine the feasibility of cross-dimerization reactions were identified.

SYNTHETIC AND QUANTUM-CHEMICAL EXPLORATION OF THE SELECTIVITY OF DONOR/ACCEPTOR-SUBSTITUTED METALLOCARBENOIDS

By

Jørn Hedløy Hansen

Siv.ing. / M.Sc., The Norwegian University of Science and Technology, 2005

Advisor: Huw M. L. Davies, Ph.D.

A dissertation submitted to the Faculty of the

James T. Laney School of Graduate Studies of Emory University

in partial fulfillment of the requirements for the degree of

Doctor of Philosophy

in Chemistry

2010

Acknowledgements

The last five years has been a time of remarkable transformation for me – both at personal and professional levels. In this section, I would like to thank the people who have had a positive impact on my achievements during these years and, therefore, directly or indirectly, have contributed to this dissertation.

First of all, I would like to give sincere thanks to my advisor, Dr. Huw Davies, for accepting me into his research group, despite a rather lacking application that came three weeks after the deadline! I greatly admire his ability to achieve productivity and high-level research in his group, while maintaining a supportive atmosphere, where each individual is given a chance to develop and mature as a person and as a scientist. I strongly believe this is a rarity in high-level chemistry research groups, but indeed a strength! I would not have survived in the group without all the support.

I would also like to deeply thank Mrs. Angela Davies (Angie), for the tremendous amount of support I have received over the years – ranging from emergency grad-student psychotherapy, to stepping in as a reserve-mom in my wedding. You have had a great positive impact during my stay here in the U.S.!

During my time at UB, several of the faculty members significantly enhanced my professional development. For this, I would like to acknowledge Dr. Steven T. Diver, Dr. John P. Richard, Dr. Jerome B. Keister and Dr. David F. Watson. At Emory, I would like to thank my committee members Dr. Albert Padwa and Dr. Fred Menger for their support and advise during the last two years. Special thanks go to Dr. Padwa for his positive spirit, encouragement and his many enjoyable historical accounts of chemistry in the

group meetings. I would also like to thank Dr. Simon Blakey for his generous assistance with the printing of my dissertation!

The first months I spent in the U.S., I relied heavily on the assistance of several individuals. In this regard, I would like to thank Dr. Øystein Loe for his friendship and for greatly facilitating the transition to American culture. I appreciated all the hours spent showing me how things work, sharing his cultural experiences, and spending several weekends training me on the NMR. I would also like to thank Mr. Daniel Podolic, for providing a safe home for me during my first year, for supporting me as I was settling in, and helping me to get my first car! Dr. Janelle Thompson mentored me during my first months in the group. She taught me a great deal about the lab and how the chemistry department worked. I also appreciated how she always made sure that I was included in social events! Furthermore, I owe thanks to several people without whom I would not have been able to get to work during the first months. In particular, I thank Dr. Brian Peppers, Dr. Melissa Dunkle, Dr. Jessica France and Dr. Chris Pennington for their joint efforts in helping me out with this. In the lab, I have had the pleasure of receiving support and advice from several people. In particular, I would like to acknowledge Dr. Simon Hedley, Dr. Peter Scott, Dr. Mike Coleman, Dr. Xing Dai, Dr. Allison Dick and Dr. Daniel Morton for many helpful discussions and good advice! I also thank Dr. Philip Pelphrey, Dr. Jeremy Olson and Mr. Spandan Chennamadhavuni for putting up with me as their lab-mate (through good and bad times). Furthermore, I thank other past and present Davies group members that have contributed to my development.

On a more personal basis, I would like to thank Claudia Rivera-Vera, Dr. Mike Madden and Fred Briones for their friendship and coffee-breaks. Special thanks goes to

Dr. Etienne Nadeau for being a last-minute best-man in my wedding and for his unconditional friendship. My good friendship with Sven-Helge M. Larsen and Nina Ljones has also been very important to me, and I really appreciated their visit in Atlanta and their continued support.

Joining the chemistry department at Emory was a great experience. The supportive environment that exists here is quite unique. Firstly, I would like to give sincere thanks to Ms. Ann Dasher for always putting up with a bunch of questions and helping out when I needed guidance. Her contribution to the running of the department is highly undervalued. I would also like to thank Steve, Patti and Sarah in the stockroom, Dr Wang and Dr. Wu in the NMR center, Dr. Hardcastle (X-ray) as well as Dr. Stroebel in the mass spectrometry facility for greatly facilitating and supporting my research.

I have had the pleasure of having a superb selection of collaborators during the last five years that have greatly enhanced my studies. It has been quite educational to supervise several incoming graduate students, and I would like to acknowledge Mr. Brendan Parr, Mr. Clay Owens, Ms. Jennifer Bon and Mr. Changming Qin for their contribution to parts of this dissertation. Dr. Evgeny Dikarev and Dr. Marina Petrukhina at SUNY Albany are gratefully acknowledged for their generous contribution of diruthenium and bismuth–rhodium complexes. I would like to give sincere thanks to Dr. Jochen Autschbach at UB for sparking my interest in learning and applying computational chemistry to various research problems in the Davies group. Although much time and effort went into learning and understanding this tool, it has led to a great enhancement of my research program, as exemplified by the many applications detailed in this dissertation.

Although I have received much support by the people around me, the most important contribution has come from the family. I would like to thank Lill, Viktor, Tove, Daniel, Keiy, Alf and Nancy for their support, love and encouragement during many difficult times while I have been in the U.S. Even though we often talk about trivial things, the many phone/skype conversations over the last few years have been incredibly important to me. My wife, Stephanie Hansen, has unconditionally stood by me through all the difficult times over the last five years, accepted me despite my flaws and been my strongest supporter. I love you very much, and look forward to spending our lives together!

Last, but not least, I would like to thank my mom, without whom none of this would be possible, for the continued love and support throughout a too long education. Her contribution to this dissertation can not be overstated, and it started my first day in school when I was six years old, and lasted to this very day, about 23 years later. She has been there, unconditionally, all the way, and for that, this dissertation is dedicated to my loving mother.

Dedikeres til Mamma

Table of Contents

Chapter 1 Elements of Chiral Catalyst Design Based on the Rh(II)-Carboxylate Paddlewheel Scaffold 1

1.1 Introduction 1

1.2 Results and Discussion 24

1.2.1 Mixed Ligand Dirhodium Carboxylates 24

1.2.2 Design of a Novel Family of Chiral Dirhodium Tetracarboxylates 36

1.3 Conclusions 44

1.4 Experimental Section 45

1.4.1 General Considerations 45

1.5.2 Procedures and Characterization Data 46

References 59

Chapter 2 Density Functional Studies on the Selectivity of Donor/Acceptor-Substituted Rhodium Carbenoids 68

2.1 Introduction 68

2.2 Results And Discussion 81

2.2.1 Selectivity of Rhodium Carbenoids 81

2.2.2 Cyclopropenation Chemistry 103

2.2.3 The Combined C–H Activation/Cope Rearrangement 105

2.3 Conclusions 126

2.4 Experimental Section 128

2.4.1 General Considerations 128

2.4.2 Basis Sets and Pseudopotentials 129
2.4.3 Calculated Properties and Geometries 131
2.4.4 Single Point Energy Calculations 189
References 191

Chapter 3 Influence of Ru(I)- and Ag(I)-Catalysts on The Vinylogous *versus* Carbenoid Reactivity of Transient Metallovinylcarbenoids 197
3.1 Introduction 197
3.2 Results And Discussion 204
3.2.1 Electron-Deficient Ru(I) Carbonyl Carboxylates 204
3.2.2 Silver(I)-Catalyzed Reactions of Vinyldiazoacetates 210
3.3 Conclusions 230
3.4 Experimental Section 231
3.4.1 General Considerations 231
3.4.2 Procedures and Characterization Data 232
3.4.3 General Computational Considerations 256
3.4.4 Calculated Structures and Properties 257
3.4.5 Single Point Energy Calculations 268
References 269

Chapter 4 Bismuth–Rhodium Paddlewheel Carboxylates as Catalysts for Metallo-carbenoid Transformations 274
4.1 Introduction 274

4.2 Results And Discussion 279
4.2.1 Catalytic Activity: Cyclopropanation Chemistry 279
4.2.2 Reactivity 282
4.2.3 Electronic Effects 283
4.2.4 C–H Insertion Chemistry 286
4.2.5 Vinylogous Reactivity 288
4.2.6 Density functional studies 289
4.4 Conclusions 299
4.5 Experimental Section 300
4.5.1 General Considerations for Synthetic Studies 300
4.5.2 Procedures and Characterization Data 301
4.5.3 General Considerations for Computational Studies 308
4.5.4 Calculated Properties and Geometries 312
4.5.5 Single Point Energy Calculations 337
References 338

Chapter 5 On The Rhodium(II)-Catalyzed Dimerization of Diazo Compounds 346
5.1 Introduction 346
5.2 Results And Discussion 356
5.2.1 Synthetic Studies 356
5.2.3 Mechanistic Studies 363
5.3 Conclusions 376
5.4 Experimental Section 377

5.4.1 General Synthetic Considerations 377

5.4.2 Procedures And Characterization Data 378

5.5.3 General Considerations for Computational Studies 394

5.5.4 Calculated Properties and Geometries 395

References 411

Appendix A NMR Spectral Data for Representative Compounds 416

Appendix B X-Ray Crystallographic Data 422

List of Schemes

Scheme 1.1: Cyclopropanation reaction with 1.7. 8

Scheme 1.2: Generalized [4+3] Annulation. 9

Scheme 1.3: C–H Insertion reaction between 1.12 and adamantane. 10

Scheme 1.4: Combined C–H Activation/Cope rearrangement. 10

Scheme 1.5: Double intramolecular C–H insertion. 13

Scheme 1.6: Diastereoselective intermolecular C–H amination. 13

Scheme 1.7: Aziridination. 15

Scheme 1.8: Enantioselective carbonyl-ylide cycloaddition. 15

Scheme 1.9: Intramolecular cyclopropanation chemistry. 18

Scheme 1.10: Intramolecular C–H insertion. 18

Scheme 1.11: Oxonium ylide/[2,3]-sigmatropic rearrangement. 19

Scheme 1.12: Hetero Diels-Alder reaction. 19

Scheme 1.13: Synthesis of *trans*-1.49. 26

Scheme 1.14: Synthesis of mono-substituted complexes. 28

Scheme 1.15: Synthesis of *cis*-prolinate/acetate complexes. 29

Scheme 1.16: Synthesis of *trans*-series. 30

Scheme 1.17: Stepwise exchange mechanism. 30

Scheme 1.18: Catalyst evaluation in the cyclopropanation of styrene. 33

Scheme 1.19: Alkene cyclopropanation reactions. 35

Scheme 1.20: Synthesis of first dirhodium cyclopropane carboxylate catalyst. 37

Scheme 1.21: Evaluation of catalysts 1.61-1.63. 37

Scheme 1.22: Synthesis of catalyst 1.65. 40

Scheme 1.23: Test reaction 41

Scheme 1.24: Synthesis of bromo-complex 1.66. 42

Scheme 1.25: Catalyst evaluation 43

Scheme 2.1: Competition reactions with styrene using metallocarbenoids 69

Scheme 2.2: Potential energies of structures 72

Scheme 2.3: Cyclopropenation of alkynes 75

Scheme 2.4: C–H functionalization mechanism studied by Nakamura et. al 77

Scheme 2.5: The combined CH activation/Cope rearrangement reaction. 79

Scheme 2.6: Application of the CHCR reaction in medicinal synthesis. 79

Scheme 2.7: Reaction pathway for carbenoid formation 85

Scheme 2.8: C–H functionalization of cyclopentane. 91

Scheme 2.9: C–H insertions with 1,4-cyclohexadiene 93

Scheme 2.10: Computed *versus* experimental primary kinetic isotope effects. 98

Scheme 2.11: Predictions of stereochemical outcome 102

Scheme 2.12: Reaction model between styrylcarbenoid 2.24 and propene 105

Scheme 2.13: Model chemistries for the CHCR reaction. 106

Scheme 2.14: Mechanistic proposals for the CHCR reaction..... 108

Scheme 2.15: Vinylcarbenoid conformations..... 110

Scheme 2.16: IRC analyses 115

Scheme 2.17: IRC analyses. 116

Scheme 2.18: IRC analyses. 118

Scheme 2.19: Reaction between arylvinyldiazoacetate and 1,4-cyclohexadiene. 123

Scheme 2.20: Rationalization of stereochemical outcome. 124

Scheme 3.1: Vinylogous reactivity in metallovinylcarbenoids. 197

Scheme 3.2: Vinylogous reactivity in reaction with cyclopentadiene. 198

Scheme 3.3: Proposed reaction mechanism. 199

Scheme 3.4: Carbenoid versus vinylogous reactivity. 200

Scheme 3.5: Vinylogous reactivity in O–H insertion. 201

Scheme 3.6. Lewis acid catalyzed O–H insertions. 201

Scheme 3.7: Vinylogous alkylation of sterically hindered pyrroles and indoles. 202

Scheme 3.8: Catalytic activity of Ru(I)-complexes. 206

Scheme 3.9: Vinylogous reactivity in O–H insertions. 207

Scheme 3.10: Vinylogous reactivity in reaction with cyclopentadiene. 209

Scheme 3.11: Vinylogous reactivity in reaction with *N*-Boc pyrrole. 209

Scheme 3.12: O–H insertions with benzyl alcohol. 212

Scheme 3.13: O–H insertion with methanol..... 213

Scheme 3.14: X-H insertions with arylvinyldiazoacetates. 215

Scheme 3.15: O–H insertions with 3.23..... 216

Scheme 3.16: Vinylogous reactivity in C–C bond formation with *N*-Boc pyrrole..... 217

Scheme 3.17: Silver-catalyzed reaction of 3.9 with furan..... 218

Scheme 3.18: Mechanistic proposals for vinylogous O–H insertion..... 220

Scheme 3.19: Deuterium labelling studies. 221

Scheme 3.20: Model reaction for computational studies. 222

Scheme 3.21: Double bond shift..... 226

Scheme 3.22: Rationalization of stereoselectivity. 228

Scheme 3.23: Cyclopropanation of styrene with 3.42a.....229

Scheme 4.1: Cyclopropanation of styrene..... 280

Scheme 4.2: Reaction with furan. 281

Scheme 4.3: ReactIR study of cyclopropanation reaction. 283

Scheme 4.4: Competition studies..... 285

Scheme 4.5: C–H insertion of 1,4-cyclohexadiene..... 286

Scheme 4.6: Reaction with cyclohexene..... 288

Scheme 4.7: Reaction with cyclopentadiene. 289

Scheme 4.8: Mechanism for catalytic cyclopropanation by dirhodium complexes.....290

Scheme 5.1: Cu(II)-catalyzed homodimerization of 5.1. 347

Scheme 5.2: Mechanistic explanation for preferential formation of *Z*-stilbenes..... 347

Scheme 5.3: Homodimerization of aryldiazoalkanes by Rh(II). 348

Scheme 5.4: Selective homodimerization of ethyl diazoacetate..... 349

Scheme 5.5: Del Zottos cross-dimerization..... 350

Scheme 5.6: Homo- and heterocoupling 351

Scheme 5.7: Carbene cross-coupling with Fisher carbenes 5.15..... 352

Scheme 5.8: Barluengas formal [3+1]-coupling..... 352

Scheme 5.9: Dixneufs carbene cross-coupling..... 353

Scheme 5.10: Dimerization propensity..... 354

Scheme 5.11: Discovery of cross-dimerization. 355

Scheme 5.12: Test reaction for optimization of reaction conditions. 357

Scheme 5.13. Cross-coupling of aryldiazo compounds with 5.8..... 359

Scheme 5.14. Cross-coupling with vinyldiazoacetates. 360

Scheme 5.15: Cross-coupling of acceptor-diazo compounds with 5.25. 361

Scheme 5.16: Competition studies of cross-dimerization reaction..... 365

Scheme 5.17: Model chemistry for calculations of dimerization reaction..... 367

Scheme 5.18: Possible dimerization scenarios. 368

Scheme 5.19: Heterodimerization pathways via the donor/acceptor carbenoid..... 371

Scheme 5.20: Proposed catalytic cycle for productive cross-dimerization..... 375

List of Tables

Table 1.1: Effect of catalyst, solvent and temperature on asymmetric induction..... 34

Table 1.2: Evaluation of *cis*-1.55 conducted by Ms Jennifer Bon..... 35

Table 1.3: Initial evaluation of catalyst 1.65. 41

Table 1.4: Evaluation of 1.66 conducted by Mr. Changming Qin..... 43

Table 2.1: Contributions from gas-phase. 95

Table 2.2: Influence of substituent pattern. 110

Table 2.3: Basis set and pseudopotential specifications in the Gaussian input files. 129

Table 2.4: Single point energy calculations..... 189

Table 3.1: Vinylogous reactivity in reaction with cyclopentadiene. 199

Table 3.2: Influence of ester group and solvent 200

Table 3.3: Influence of catalyst on regioselectivity 201

Table 3.4: Lewis-acid catalyzed X–H insertion reported by Hu et. al. 202

Table 3.5: Cyclopropanation reactions 206

Table 3.6: O–H Insertions with Ru(I)-catalysts 208

Table 3.7. Reaction with cyclopentadiene 209

Table 3.8: Reaction with *N*-Boc pyrrole. 210

Table 3.9: Influence of loading and temperature on O–H insertion regioselectivity 212

Table 3.10: Complementary selectivity of various metals. 213

Table 3.11: X–H insertion scope. 215

Table 3.12: Catalyst influence on selectivity 217

Table 3.13: Single point energies and calculated E+ZPE 268

Table 4.1: Influence of carbenoid structure in cyclopropanation of styrene. 280

Table 4.2: Reaction between 4.6a and furan. 282

Table 4.3: C–H insertion. 287

Table 4.4: C–H insertion *versus* cyclopropanation. 288

Table 4.5: Vinylogous *vs* carbenoid reactivity. 289

Table 4.6: Product ratios obtained in competition studies. 304

Table 4.7: Basis set and pseudopotential definitions in the calculation input files. 309

Table 4.8: Calculated single-point energies. 337

Table 5.1: Influence of reaction conditions on cross-coupling selectivity 357

Table 5.2. Coupling of aryldiazoacetates with EDA 359

Table 5.3: Cross-coupling of various vinyldiazoacetates 360

Table 5.4: Influence of acceptor-substituted diazo compounds on cross-coupling. 362

Table 5.5: Influence of additive and molar ratio on conversion. 365

Table 5.6: Calculated gas-phase relative enthalpies and Gibbs free energies. 371

Table 5.7: Relative solution-phase enthalpies and Gibbs free energies. 373

List of Figures

Figure 1.1: Dirhodium paddlewheel catalyst structures. 3

Figure 1.2: Schematic representation 4

Figure 1.3: Arrangements of C_2-symmetric ligands. 5

Figure 1.4: Dirhodium tetraprolinates. 6

Figure 1.5: Second generation dirhodium prolinate complexes. 7

Figure 1.6: Representative phthaloyl- and naphthoyl-derived 12

Figure 1.7: Examples of unusual chiral dirhodium carboxylates. 14

Figure 1.8: Dirhodium(II) binaphthylphoshphonate complexes. 15

Figure 1.9: Dirhodium(II) carboxamidate complexes. 17

Figure 1.10: Bis-acetonitrile complex of *cis*-$Rh_2(TFA)_2(OAc)_2$. 21

Figure 1.11: Bis-acetonitrile complex of *trans*-$Rh_2(TFA)_2(OAc)_2$. 21

Figure 1.12: Symmetry considerations. 22

Figure 1.13: Time dependence 25

Figure 1.14**:** Observed intermediates 31

Figure 1.15: X-ray structure of bis-ethanol adduct of *trans*-1.55. 31

Figure 1.16: Enantioselectivity as a function of number of prolinate ligands. 34

Figure 1.17: Model system for styrene-derived dirhodium complex. 39

Figure 1.18: Model for triarylcyclopropane ligand system. 39

Figure 2.1: Hammett plots 69

Figure 2.2: Asymmetric synthetic technologies 70

Figure 2.3: D_2-symmetry of Rh_2(*S*-DOSP)$_4$ 73

Figure 2.4: Proposed approaches of terminal alkynes 75

Figure 2.5: First and second generation models 78

Figure 2.6: The structure of $Rh_2(OAc)_4 \bullet 2H_2O$. 83

Figure 2.7: Comparison of metal basis set influence 84

Figure 2.8: Calculated relative energies 87

Figure 2.9: Theoretical structures for the pathway with 2.3c. 88

Figure 2.10: Theoretical structures 89

Figure 2.11: Relative energies 92

Figure 2.12: Relative energies 94

Figure 2.13: Structural characteristics 96

Figure 2.14: Axial *versus* equatorial C–H insertion with cyclohexane 97

Figure 2.15: Approach modes of the C–H bond vector 100

Figure 2.16: Perspective of model for C–H insertion event. 101

Figure 2.17: Transition structure TS-X for the cyclopropenation of propene. 105

Figure 2.18: Important stereochemical considerations. 108

Figure 2.19: Most stable transition states found for the chemical models. 112

Figure 2.20: Concerted mechanism for the CHCR reaction. 113

Figure 2.21: Model potential energy surface bifurcation. 119

Figure 2.22: Forward IRCs. 121

Figure 2.23: Cope rearrangement transition states found from IRC geometries. 121

Figure 2.24: Aligned substrate with carbenoid for 1,3-cyclohexadiene reactions..... 125

Figure 3.1: Electrophilic diruthenium(I,I) carbonyl carboxylates. 204

Figure 3.2: Stuctural revision of the alkylated *N*-Boc pyrrole product 3.27. 219

Figure 3.3: Potential energy surface..... 224

Figure 3.4: LUMO frontier density plots 225

Figure 4.1: Various dirhodium catalysts. 275

Figure 4.2: RhBi carboxylate complexes 277

Figure 4.3: Disappearance of C=N=N stretch frequency 283

Figure 4.4: Hammet plot 285

Figure 4.5: Hammet plot 2..... 285

Figure 4.6: Potential energy surfaces. 292

Figure 4.7: Influence of axial coordination. 295

Figure 4.8: Potential energy surfaces. 297

Figure 4.9: Charge distribution on bimetallic core 298

Figure 5.1 Crystal structure determined for 5.39d. 363

Figure 5.2: Conversion rates..... 366

Figure 5.3: Lowest energy TS-I..... 369

Figure 5.4: Potential energy surface scan of homodimerization of 5.43..... 374

List of Charts

Chart 2.1: Complex marine natural products..... 79

Chart 3.1: Scope of vinylogous alkylation. 203

Chart 3.2: Other observed products. 218

Chart 3.3: Synthesis of novel diazo compounds..... 227

List of Abbreviations

$Rh_2(OAc)_4$	Dirhodium tetrakisacetate
BSP	Benzenesulfonylprolinate
DOSP	4-dodecyl phenylsulfonylprolinate
TBSP	4-(*tert*-butyl)phenylsulfonylprolinate
TISP	2,4,6-tri-isopropylphenylsulfonylprolinate
ee	Enantiomeric excess
EWG	Electron withdrawing group
de	Diastereomeric excess
BNP	Binaphthylphosphonate
Ns	4-nitrobenzenesulfonyl
TFA	Trifluoroacetate
DCM	Dichloromethane
TPCP	Triphenylcyclopropane
NMR	Nuclear Magnetic Resonance
TLC	Thin Layer Chromatography
TMS	Tetramethylsilane
FTIR	Fourier-transform Infrared
ρ	Hammett reaction constant
σ	Substituent parameter
EDG	Electron donating group
E	Energy
ZPE	Zero-point energy

LUMO	Lowest unoccupied molecular orbital
CHCR	The Combined C–H activation/Cope rearrangement
d.r.	Diastereomeric ratio
[Rh-LA2]	LANL2DZ basis set and pseudopotential for Rh
[Rh-RSC+4f]	Stuttgart RSC 1997 ECP for Rh, with a 4f-function.
d	distance
BO	Wiberg bond order
q	Mulliken charge
H	Enthalpy
G	Gibbs free energy
S	Entropy
$\mathbf{K_{rot}}$	Equilibrium constant for rotation
IRC	Intrinsic reaction coordinate
TST	Transition state theory
MEP	Minimum energy pathway
RSC	Relativistic small core
ECP	Effective core potential
Nu	Nucleophile
THF	Tetrahydrofuran
M	Metal
OHex	Hexanoate
OTf	Trifluoromethanesulfonate
OOct	Octanoate

HMBC	Heteronuclear multible bond correlation
nOe	Nuclear Overhauser effect
HSQC	Heteronuclear single quantum coherence
ε	Dielectric constant
[Ag-RSC+4f]	Stuttgart RSC 1997 ECP for Ag, with two 4f-functions
DBU	1,8-diazabicyclo[5.4.0]undec-7-ene
***p*-ABSA**	*para*-acetamidobenzenesulfonyl azide
HPLC	High-performance liquid chromatography
HRMS	High-resolution mass spectrometry
APCI	Atomspheric pressure chemical ionization
TFT	Trifluorotoluene
ESI	Electrospray ionization
TON	Turnover number
TOF	Turnover frequency
E_a	Arrhenius activation energy
R	Gas constant
T	Temperature
CAN	Cerium ammonium nitrate
OPiv	Pivaloate
PES	Potential energy surface
IEFPCM	Integral equation formalism polarizable continuum model
SCRF	Self-consistent reaction field

- Chapter 1 -

Elements of Chiral Catalyst Design Based on the Rh(II)-Carboxylate Paddlewheel Scaffold

---

1.1 Introduction

Dirhodium(II) complexes are exceptionally stable to heat, moisture and ambient atmosphere. They are also very active catalysts for a variety of transformations of diazo compounds.[1] The resulting rhodium carbenoids are capable of highly selective reactions, such as C–H insertions, cyclopropanation/propenation reactions and ylide formation.[1-13] They have also recently been shown to be effective in metallonitrenoid transformations[13-18] and Lewis acid-mediated cycloaddition chemistry.[19-23] Chiral catalysis within the dirhodium(II) regime has experienced immense growth since the discoveries in the early 1980's.[1] The potential of chiral rhodium(II)-complexes to catalyze asymmetric transformations has been convincingly demonstrated since – through ligand design and the development of a number of reaction types.[24,25] This section will highlight the advances in the field of chiral dirhodium(II)-catalysis and also emphasize that these complexes can possess high symmetry even though the ligands are of much lower symmetry.

Symmetry and Catalyst Design. Symmetry has played a major role in chiral metal catalysis since the first example of asymmetric transformations with a C_2-symmetrical chiral copper catalyst was reported by Pfaltz in the mid 1980s.[26] The high symmetry can

reduce the number of possible substrate approaches in a catalytic reaction occuring at the metal center, which can give more predictable and well-defined transition state structures. Elements that control asymmetric induction can then potentially be controlled. Traditionally, catalysts of high symmetry have been generated by using ligands of high symmetry, of which the most common class is the bidentate C_2-symmetric ligands. In metallocarbenoid chemistry, these complexes of copper (II)[27-31] and ruthenium[32-35] have been very effective catalysts. Complexes of higher symmetry have been described for metallocarbenoid chemistry that were based on porphyrin ligands of D_2- and D_4-symmetry.[36-39] Such complexes have, however, not been very practical to develop as the ligand synthesis often presents challenges.

Dirhodium(II) complexes are made up of a dimetallic core surrounded by four equatorial μ_2-ligands and two axial ligands, often referred to as a paddlewheel structure.[40-43] Each rhodium atom is considered to have octahedral geometry and the core is connected by a rhodium-rhodium single bond.[40-43] Dirhodium tetrakis(acetate), $Rh_2(OAc)_4$, (**1.1**, R = Me) is the parent complex of the dirhodium carboxylate class, and displays D_{4h} symmetry (Figure 1.1). Chiral dirhodium carboxylates can at best obtain D_4-symmetry. Another class of complexes is the dirhodium phosphonates (**1.2**) which have four phosphonate ligands surrounding the dimetallic core.[1-11] Complexes of carboxamides (**1.3**) have more complicated structural features, because the ligand spans the dirhodium core through an oxygen and a nitrogen. The *cis*-(2,2) configuration has been shown to be the preferred geometry, which implies that each rhodium is connected to two nitrogens and two oxygens in a *cis*-arrangement.[1-11] These complexes are inherently limited to C_2-symmetry because of the ligand binding propensity. For most dirhodium complexes, the

axially situated ligands are quite labile and these sites are therefore catalytically active. The paddlewheel structures are quite stable and generally considered to remain intact during reactions at the axial sites. Recently, models have emerged that propose catalytic reactions from en equatorial site following ligand dissociation, however, this is not yet generally accepted.[44,45]

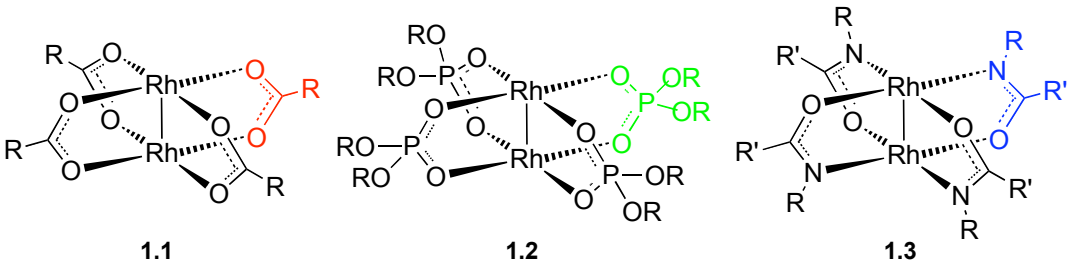

Figure 1.1: Dirhodium paddlewheel catalyst structures.

A simplified model must be introduced in order to describe how chiral ligands (R and R') influence the axial active sites of the dirhodium complexes.[46] In this model, the dirhodium complex is represented by a disk which corresponds to the O–Rh–O plane containing the active site in the center (Figure 1.2a). The two faces catalyst faces have arbitrarily been assigned as α (top) and β (bottom). Geometrical features must necessarily exist, such that the space above the O–Rh–O plane is restricted, leading to one favored substrate approach towards the axial ligand.[24] This means that "blocking groups" from equatorial ligands must be oriented towards the O–Rh–O plane.[24] Possible arrangements of chiral C_1-ligands can now be assessed. The blocking groups arising from the equatorial ligands, thereby creating the chiral influence, are pictured as rods (Figure 1.2b) (shaded rods represent groups influencing the α-face, unfilled rods the β-face).[46] If the blocking groups are oriented in the periphery of the catalyst (in the disk plane), asymmetric induction would presumably be unlikely to occur. Considering that the blocking groups

can orient themselves towards the α-face (up) or towards the β-face (down) of the catalyst, four permutations arise: (1) α, α, α, α (C_4-symmetry), (2) α, α, α, β (C_1-symmetry), (3) α, α, β, β (C_2-symmetry) and, (4) α, β, α, β (D_2-symmetry) (Figure 1.2b).[24,46] From these possible combinations, only the C_2-and D_2-symmetric complexes have two equivalent rhodium active sites.[46] Indeed, the major classes of effective chiral dirhodium catalysts are believed to possess C_2-and D_2-symmetry. The C_1-structure and C_4-symmetric complex contain inequivalent faces of the catalyst. Different levels of asymmetric induction on each face would be expected in such cases.[24]

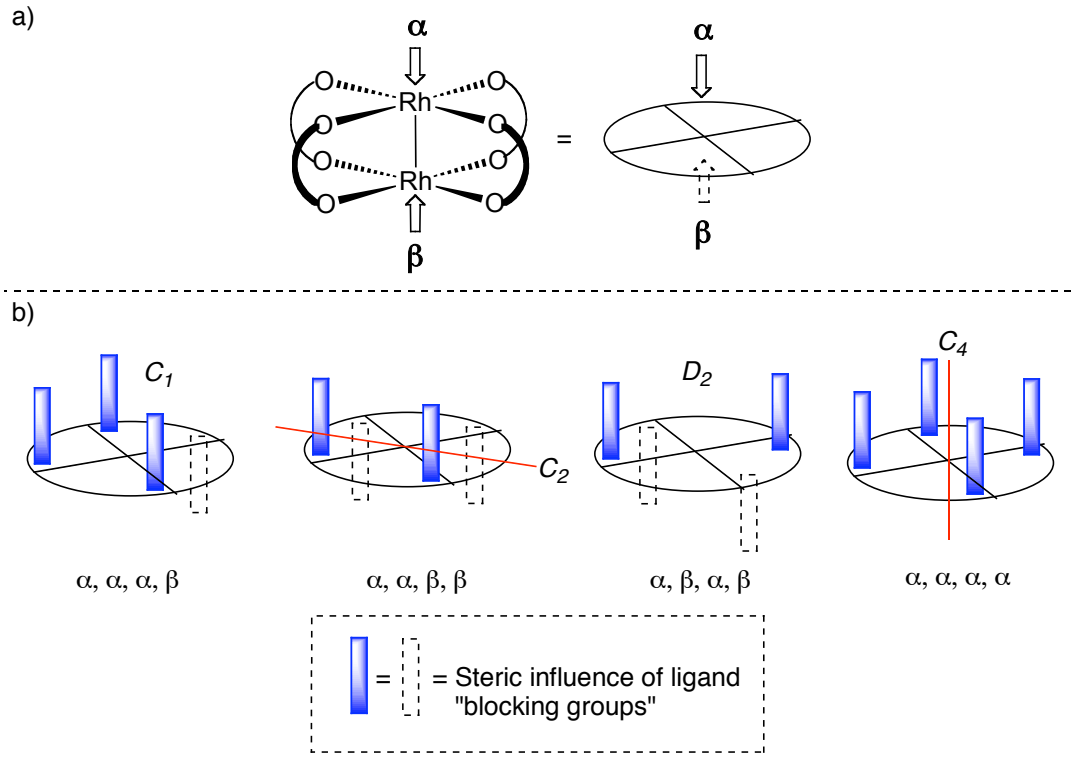

Figure 1.2: (a) Schematic representation of paddlewheel complexes. (b) Permutations of four coordinated ligands of C_1-symmetry.

Higher overall symmetry of dirhodium complexes is possible if the ligands possess C_2-symmetry. Both faces of the catalyst will be influenced by a C_2-symmetric ligand and

give overall D_2- or D_4-symmetry. D_4-symmetry will arise from four coordinated C_2-symmetric ligands.[24] D_2-symmetry is achieved with two *bridged* C_2-symmetric ligands, thereby affording a rigidified version of the α, β, α, β-form of complexes based on C_1-ligands (Figure 1.3).[24]

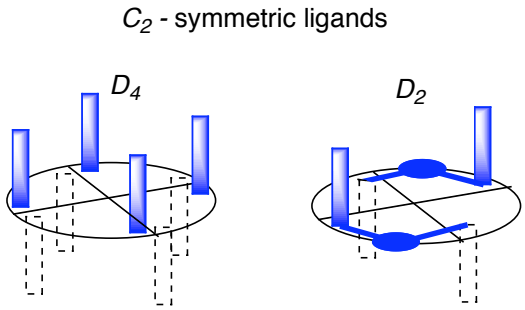

Figure 1.3: Arrangements of C_2-symmetric ligands.

The strengths involved in catalyst design based on the dirhodium paddlewheel motif, have been clearly articulated above. A modular approach can be employed in such systems to assemble a chiral complex. Four identical, low-symmetry chiral ligands can be coordinated to the highly symmetric bimetallic core, to afford an overall high-symmetry chiral catalyst.[24] It should be noted that, many factors are involved in determining the effectiveness of such chiral catalysts. For example, the preferred orientation of individual ligands, when coordinated to the dirhodium core, can be difficult to predict. An *a priori* assessment of whether a high-symmetry conformation will exist or not, in a complex consisting of four C_1-ligands, can not easily be given. Some controlling elements for such factors include solvent-effects, conformational flexibility and the electronic nature of the ligand.[24,46]

Survey of High-Symmetry Dirhodium Catalysts. The dirhodium(II) tetracarboxylates are very attractive catalysts in metallocarbenoid chemistry because of their high kinetic activity for decomposition of various diazo compounds.[1] The use of optically active carboxylic acids as ligands in dirhodium catalysis, was first evaluated by Brunner et. al. in cyclopropanation reactions between ethyl diazoacetate and styrene.[47] The poor results of this study (≤12% ee) led to the conclusion that dirhodium tetracarboxylates were ineffective catalysts in terms of achieving asymmetric induction.[48,49] As McKervey and Hashimoto demonstrated in the early 1990s that, moderate levels of asymmetric induction could be acheived in intramolecular C–H insertion chemistry, this idea was changing.[5,6,10] Up to 82% ee could be achieved with dirhodium prolinates in intramolecular C–H insertions.[50-52] Rh_2(*S*-BSP)$_4$ (**1.4a**) (Figure 1.4), the original prolinate complex developed by McKervey, was further developed by Davies to more soluble catalysts, such as Rh_2(*S*-TBSP)$_4$ (**1.4b**) and Rh_2(*S*-DOSP)$_4$ (**1.4d**). These were later on discovered to be exceptionally effective catalysts for reactions of donor/acceptor-substituted carbenoids.[46]

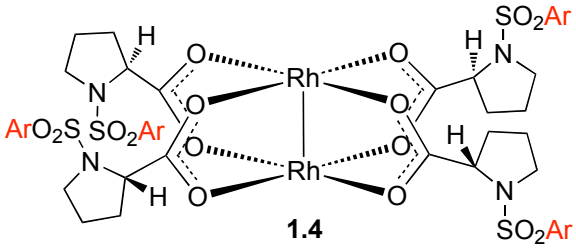

Ar =	C_6H_5	Rh_2(*S*-BSP)$_4$	**a**
	4-*t*-BuC_6H_4	Rh_2(*S*-TBSP)$_4$	**b**
	2,4,6-tri-*i*-PrC_6H_2	Rh_2(*S*-TISP)$_4$	**c**
	4-($C_{12}H_{25}$)C_6H_4	Rh_2(*S*-DOSP)$_4$	**d**

Figure 1.4: Dirhodium tetraprolinates.

The arylsulfonyl groups presumably exist in an up (α) or down (β) arrangement,[24] and the D_2-symmetric α,β,α,β-arrangement is believed to be the predominant structure in solution (non-polar solvents).[46] The D_2-symmetry of the structure has been proposed to

give rise to the high levels of asymmetric induction that can be achieved with such catalysts.[24] This form of the catalyst provides the most reasonable explanation of the observed enantioselectivities in many reactions, and also provides a predictive model for the sense of asymmetric induction in the products.[46,24,4] Furthermore, this picture is consistent with observed solvent effects.[24] High enantioselectivities are usually obtained in hydrocarbon solvents. Even with slightly polar solvents, such as dichloromethane, the enantioselectivity is significantly attenuated.[24] Jessop and co-workers studied complex **1.4b** in cyclopropanation reactions in supercritical media, and confirmed that enantioselectivity decreases with increasing dielectric constant.[53]

A second generation prolinate complexes were disgned based on the D_2-symmetry hypothesis, in which the arylsulfonyl groups were locked in the α, β, α, β-arrangement.[54] This was accomplished by using a C_2-symmetric dicarboxylate ligand containing two linked arylsulfonylproline moieties. This gave complexes **1.5** and **1.6** (Figure 1.5), both of which are locked in a D_2-symmetric arrangement due to the restricted conformation of the ligands.[24,46,54]

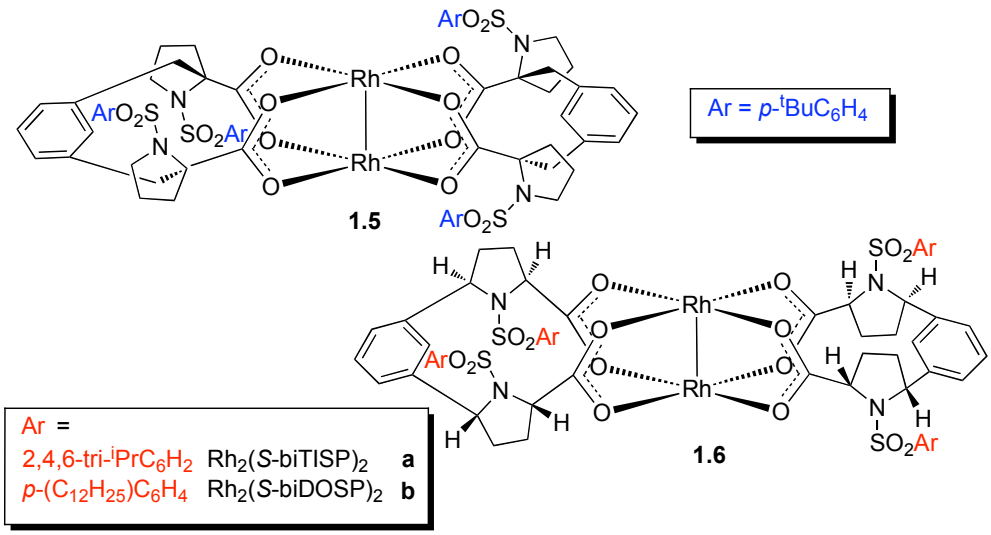

Figure 1.5: Second generation dirhodium prolinate complexes.

Cyclopropanation reactions can be effectively catalyzed by dirhodium(II)-catalysts *via* transient carbenoid intermediates.[1] The choice of chiral catalyst must be decided based on the structure of the diazo compounds and the reaction type. For cyclopropanation reactions with aryl– or vinyldiazoacetates in the intermolecular mode, dirhodium(II) prolinates are superior catalysts in terms of selectivity.[1] For example, in the cyclopropanation reaction between styrene and vinyldiazoacetate **1.7** (Scheme 1.1), the product **1.8** is obtained in 98% ee when using Rh_2(*S*-biTISP)$_2$ (**1.6a**).[19,46,55,56] Enantioselective cyclopropanantion reactions with Rh_2(*S*-DOSP)$_4$ have also been reported using aryl–,[57] heteroaryl–[57] and alkynyldiazoacetates.[58]

Scheme 1.1: Cyclopropanation reaction with **1.7**.

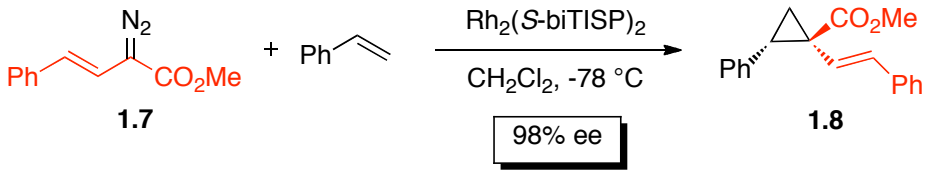

By using Rh_2(*S*-DOSP)$_4$ as catalyst in combination with vinyldiazoacetates (**1.9**) in the presence of 1,3-dienes **1.10**, a highly enantioselective formal [4+3]-cycloaddition occurs to yield cycloheptadienes **1.11** *via* a tandem cyclopropanantion/Cope rearrangement (Scheme 1.2). The relative stereochemistry of three stereogenic centers is fully controlled in this reaction.[10] The cycloheptadienes are formed in 73-98% ee. The intramolecular version of this transformation has been utilized in the enantioselective synthesis of *epi*-tremulane.[46]

Scheme 1.2: Generalized [4+3] Annulation.

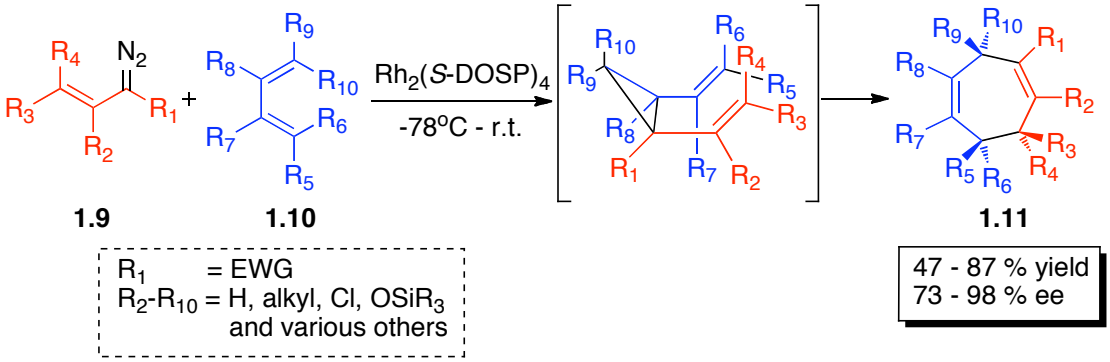

Dirhodium(II)-complexes of donor/acceptor-substituted carbenes can mediate highly enantioselective intermolecular C–H insertions. This has become a powerful technique for stereoselective functionalization of C–H bonds.[4] Dirhodium prolinates are the optimal catalysts for these transformations. The insertion can occur even into unactivated C–H bonds, and can afford very high regio-, diastereo- and enantioselectivity.[4] The reaction between aryldiazo compound **1.12** and adamantane generates a single C–H insertion product **1.13** in 90% ee (Scheme 1.3). Enantioselective C–H insertions α to heteroatoms, such as in THF and *N*-Boc pyrrole, have also been described.[59] Extensive applications of this transformation have been reported in synthesis, for example to prepare several pharmaceutical agents and natural products such as Ritalin, Imperanene,[60] Indatraline,[61] Cetiedil[62] and Venlafaxine.[62,63] The products of certain C–H insertions resemble those obtained through classical organic reactions, and are therefore surrogates for transformations such as the Aldol reaction,[64,65] the Claisen condensation[66] and the Mannich reaction.[67]

Scheme 1.3: C–H Insertion reaction between **1.12** and adamantane.

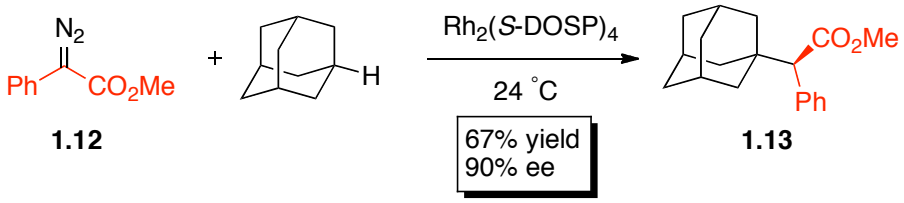

Another C–H functionalization reaction catalyzed by Rh_2(*S*-DOSP) is the combined C–H activation/Cope rearrangement.[68-70] This reaction has found numerous applications in the syntheses of pharmaceutical targets[63] and natural products. For example, a most impressive example is it utility as a key step in the total syntheses of colombiasin A and elisapterosin B (Scheme 1.4).[63] The reaction between vinyldiazoacetate **1.14** and dihydronaphthalene **1.15** results in an enantiodivergent reaction, in which one enantiomer of **1.15** undergoes the combined C–H activation/Cope rearrangement to give **1.16** in >95% ee.

Scheme 1.4: Combined C–H Activation/Cope rearrangement.

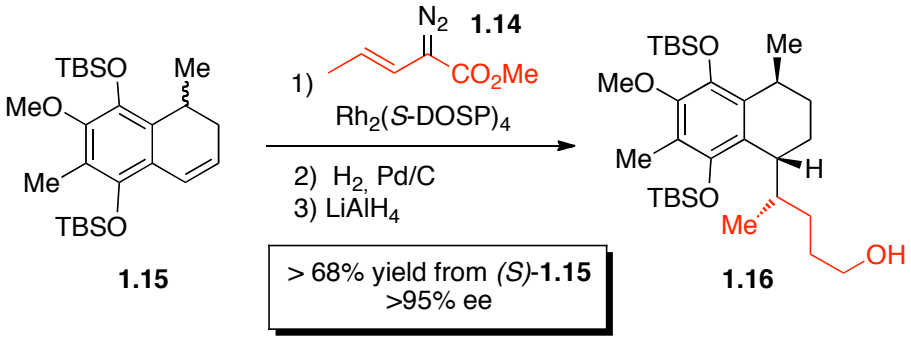

A series of phthaloyl protected amino acid derivatives were developed as ligands for Rh(II)-complexes by Hashimoto, Ikegami and co-workers (Figure 1.6).[1] Specific reactions can have certain optimal ligands, but the *tert*-leucine derived complex Rh_2(*S*-PTTL)$_4$ (**17d**) generally affords the highest asymmetric induction in a variety of

reactions.[1] Based on x-ray crystallographic data for Rh_2(*S*-PTPA)$_4$ (**17a**), which shows the phthaloyl groups oriented in a α,α,β,β-manner, it was proposed that these complexes, in their catalytically active conformation, would be C_2-symmetrical.[71] It has been assumed that this is the catalytically active conformation also in solution.[71] Recently, however, several reports have been claiming that the solution structure of related complexes is actually α,α,α,α (all up), based on x-ray data, and a range of new proposed mechanistic ideas have emerged from this.[72-74] Many derivatives of this class of complexes have been prepared by: extending the length of the phthaloyl moiety (**1.18a-e**), introducing halogens (**1.20a-b**) and by variation of the R-groups (**1.17a-f**, **1.19**) (Figure 1.6).[75-78] The same scaffold was used by Müller but with chages in the phthaloyl-portion to give complexes **1.21a-c.**[73,79] Davies et. al. have reported the adamantyl glycine derived complexes Rh_2(*S*-PTAD)$_4$ (**1.17f**) and Rh_2(*S*-TCPTAD)$_4$ (**1.20b**).[80,81] The phthaloyl protected dirhodium complexes are generally similar to the dirhodium prolinates in terms of activity.[1]

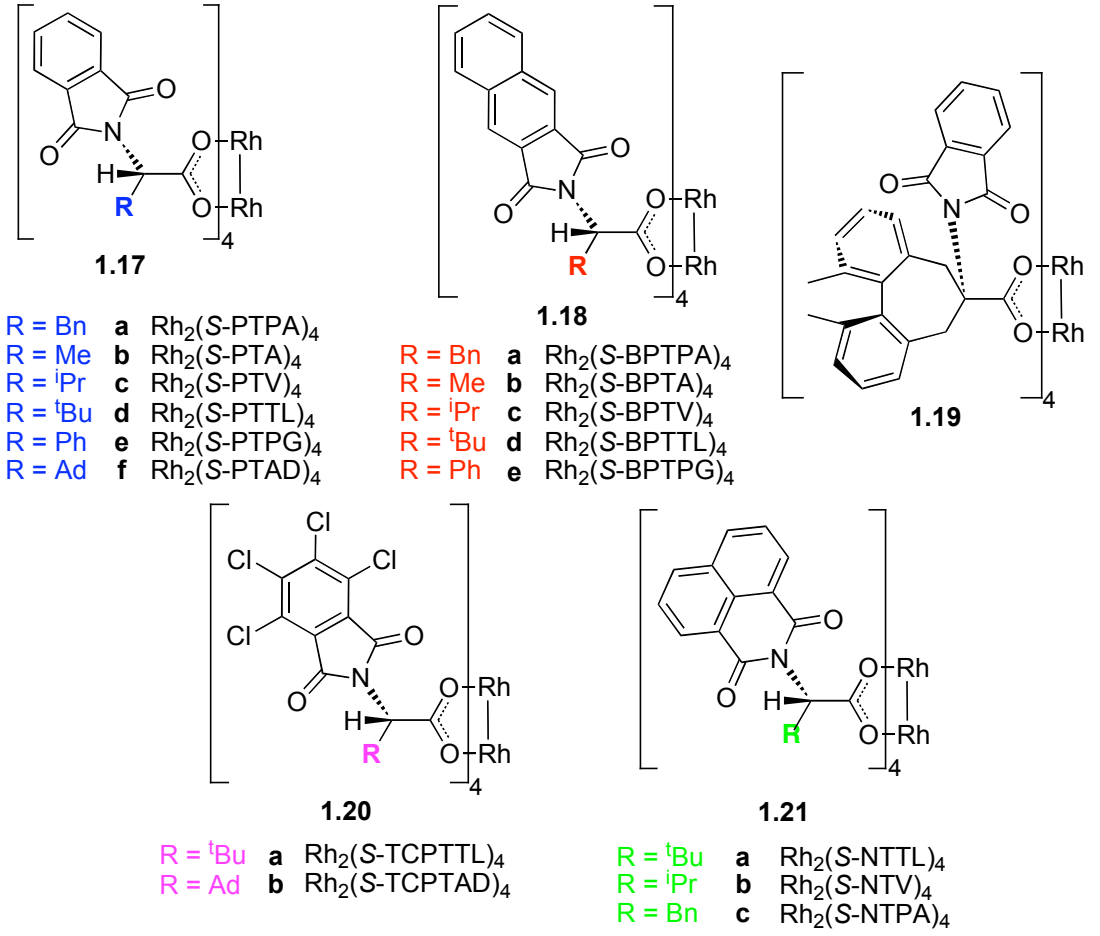

Figure 1.6: Representative phthaloyl- and naphthoyl-derived dirhodium(II) complexes.

Excellent enantiocontrol in intramolecular C–H insertions can be achieved with some of the phthaloyl-derived dirhodium complexes, particularly in syntheses of five-membered carbocycles[82] and β-lactams.[83] An example is the spirocyclization of **1.22** to ultimately afford **1.24** in 78% yield and 80% ee by double C–H insertion followed by decarboxylation (Scheme 1.5). The transformation was catalyzed by Rh_2(*S*-PTTL)$_4$ (**17d**).[84]

Scheme 1.5: Double intramolecular C–H insertion.

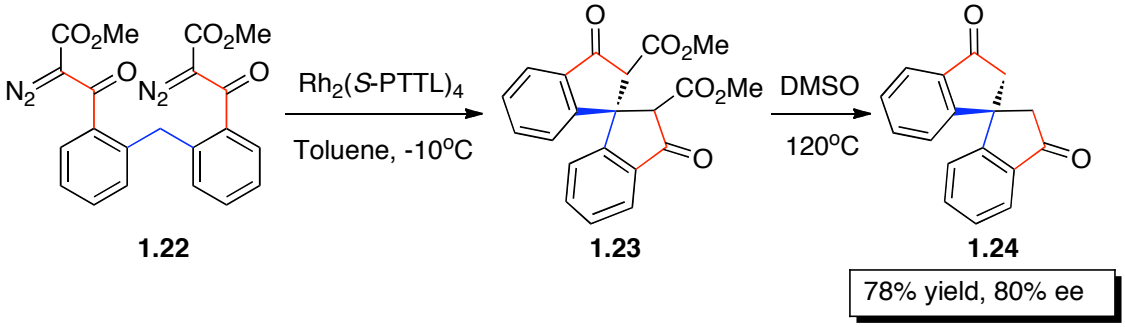

C–N bond formation through functionalization of C–H bonds has been a recent area of considerable attention since the transformation can catalyzed by dirhodium carboxylate-stabilized nitrenoids.[85] Excellent diastereocontrol was reported by Müller, Dodd, Dauban and co-workers in an intermolecular C–H amination of indene (>99% de) in 88% yield with Rh_2(*S*-NTTL)$_4$ (**21a**) to form **1.25**, using a chiral nitrene source (Scheme 1.6).[86]

Scheme 1.6: Diastereoselective intermolecular C–H amination.

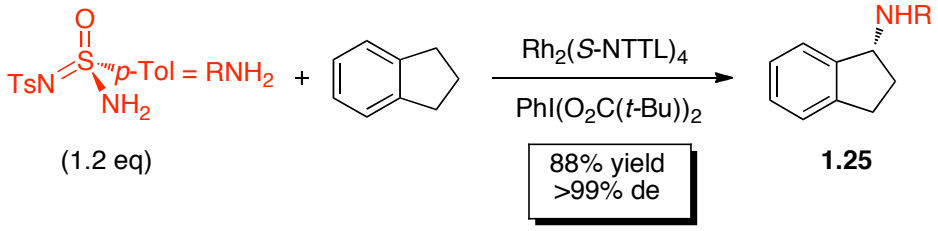

Many variants of chiral dirhodium(II) carboxylate complexes have been reported, some of which are shown in Figure 1.7 (**1.26-1.28a-d**).[87-89] To date, these complexes have not been developed as effective chiral catalysts, despite have some interesting features. Because of the C_2-symmetry of the ligands, complex **1.27** is D_4-symmetric. Although no structural data is available for complexes **1.28a-d**, these complexes could potentially form highly symmetrical conformations.[24] The atropisomeric, biaryl complex **1.26** was prepared by Hashimoto and co-workers.[28] The x-ray crystallographic data for

this complex demonstrated that the ligands are arranged in an α,α,β,β-conformation, thereby affording overall C_2-symmetry. However, poor enantiocontrol (50-52% ee) was obtained in an intramolecular C–H insertion.[28]

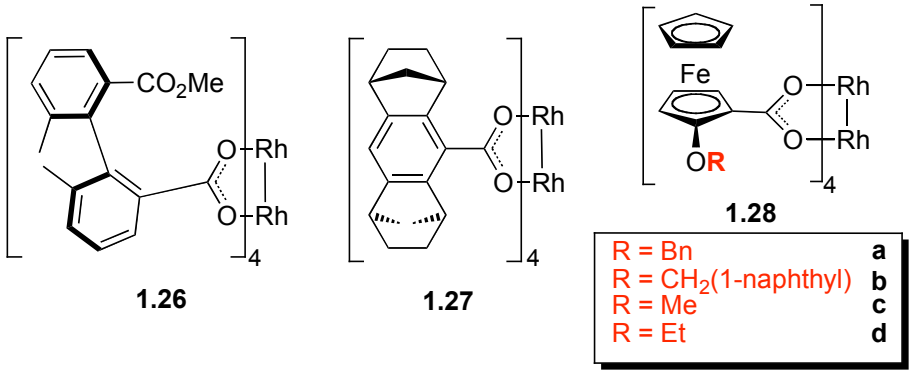

Figure 1.7: Examples of unusual chiral dirhodium carboxylates.

Rigid catalysts of high-symmetry can be obtained in the dirhodium(II) binaphthylphosphonate family of complexes, developed by McKervey and Pirrung independently.[90] The parent compound, Rh_2(*R*-BNP)$_4$, (**1.29a**) contains four binaphthylphosphonate ligands coordinated to the dirhodium core (Figure 1.8). Because of the C_2-symmetry of ligands, the overall complex is D_4-symmetrc. McKervey reported a mixed-ligand system Rh_2(*R*-BNP)$_2$(HCO$_3$)$_2$ (**1.30**),[91] which contains two equivalent C_2-symmetric ligands arranged in a *cis*-manner, giving overall a C_2-symmetric complex. The phosphonate catalysts are typically electron-deficient because of the relatively low basicity of the phosphonate anion.[1] A somewhat different reactivity profile is often displayed, compared to the amino acid derived complexes. Tetrakisphosphonate complexes are very promising chiral catalysts, resulting in the generation of several analogous structures (**1.29a-d**).[92] The most important is the dodecyl-substituted catalyst Rh_2(*R*-DDBNP)$_4$ (**1.29d**), because of its improved solubility.

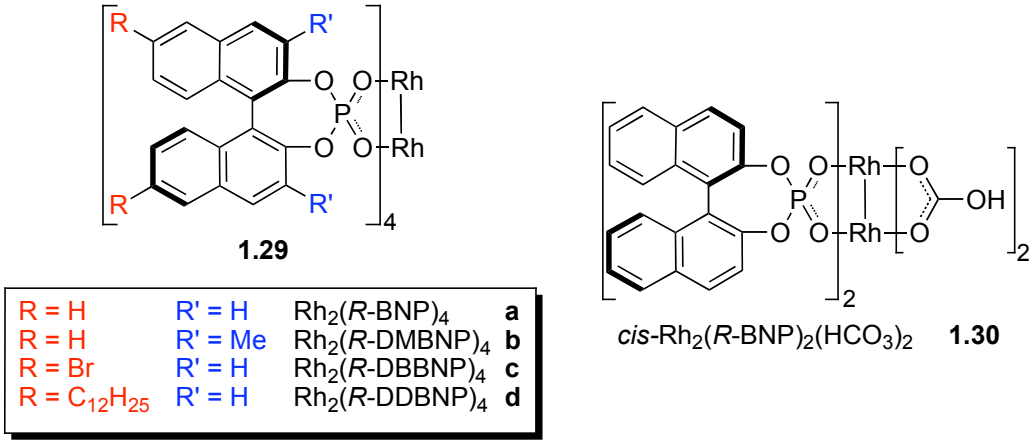

Figure 1.8: Dirhodium(II) binaphthylphoshphonate complexes.

Carbenoid ylide reactions and nitrenoid insertions have been the arenas for the most impressive applications of the binaphthylphosphonate catalysts.[92] Rh_2(*R*-BNP)$_4$ (**29a**) was used by Müller et. al. in an asymmetric aziridination reaction with styrenes. 73% ee was obtained with *cis*-β-methylstyrene **1.31** (Scheme 1.7).[93] Rh_2(*R*-DDBNP)$_4$ (**34d**) was employed in a carbonyl ylide-mediated intramolecular cycloaddition of **1.33** by Hodgson et. al., who reported the formation of **1.34** in 81% yield and 88% ee (Scheme 1.8).[92]

Scheme 1.7: Aziridination.

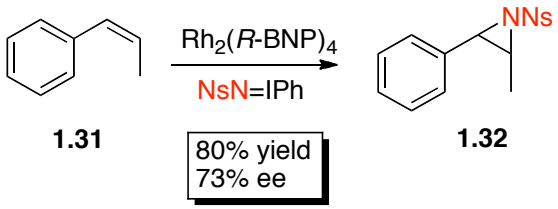

Scheme 1.8: Enantioselective carbonyl-ylide cycloaddition.

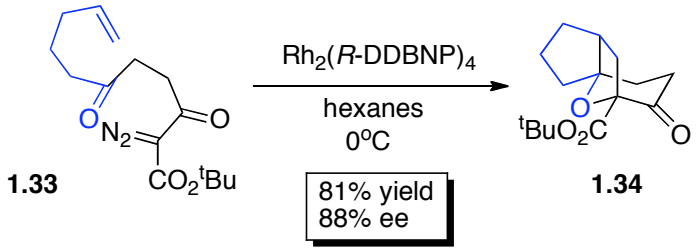

Chiral dirhodium tetracarboxamidate complexes are inherently C_2-symmetrical[1] due to the preferred *cis* (2,2)-configuration.[94,95] These catalysts are important, particularly in reactions of reactive carbenoids derived from diazoacetates and diazoacetamides.[1] The high basicity of the carboxamide ligands renders these complexes relatively electron-rich.[1] They are also very rigid, with virtually no ligand exchange occurring at ambient temperature.[94] The selectivity displayed in carbenoid reactions mediated by these complexes is relatively high because of their electron-rich nature, but it also diminishes the catalytic activity compared to dirhodium carboxylates.[1]

Doyle and co-workers initially developed chiral rhodium carboxamidates using ligands derived from optically pure α-carboxamides.[96,97] A plethora of ligands and ligand substituents have been described since (Figure 1.9). The most ligands are derived from 2-oxopyrrolidines,[98,99] 2-oxazolidinones,[100,101] *N*-acylimidazolidin-2-ones[102,103] and 2-acetidinones.[104] The structure of the carboxamidate ligands have considerable influence on the reactivity and selectivity of the corresponding catalyst complexes. The strained acetidinones, for example, lead to complexes with elongated Rh–Rh bonds and hence increases their reactivity.[105]

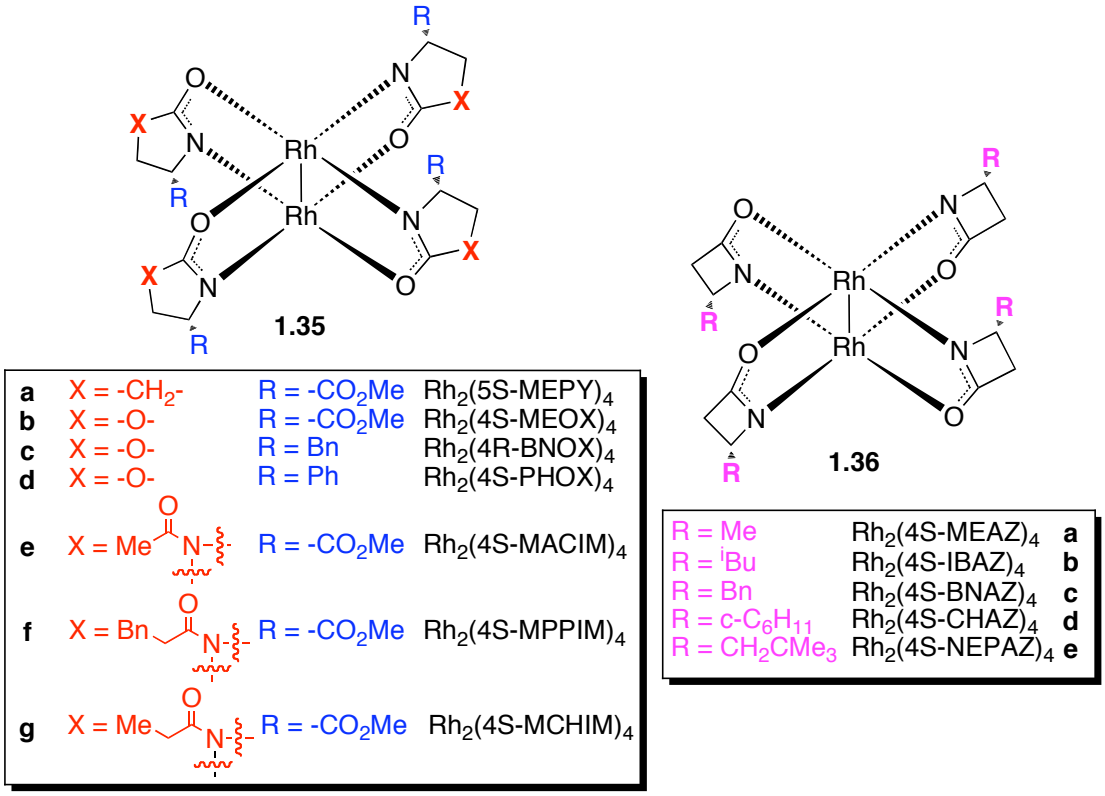

Figure 1.9: Dirhodium(II) carboxamidate complexes.

For intramolecular allylic cyclopropanantion reactions, dirhodium(II) carboxamidates are the catalysts of choice.[1,7] Intramolecular cyclopropanantion reactions of alkene tethered diazoacetates give high yields and moderate to excellent enantiocontrol with a variety of alkene substituents.[25] Complementary selectivity is often observed, for example, where Rh_2(5*S*-MEPY)$_4$ (**1.35a**) does not provide high stereocontrol, a better performance can be obtained with Rh_2(4*S*-MPPIM)$_4$ (**1.35f**).[5] The corresponding diazoamides are also amenable to the reaction and γ-lactams formation often occurs in high yields and with excellent enantioselectivity. The intramolecular cyclopropanation reaction of **1.37** to form lactam **1.38**, can be achieved with a variety of R_1 and R_2-groups with up to 95% ee (Scheme 1.9).[7] Intermolecular cyclopropanantions occur effectively, but with only moderate enantiocontrol, with these catalyst systems.[106]

Scheme 1.9: Intramolecular cyclopropanation chemistry.

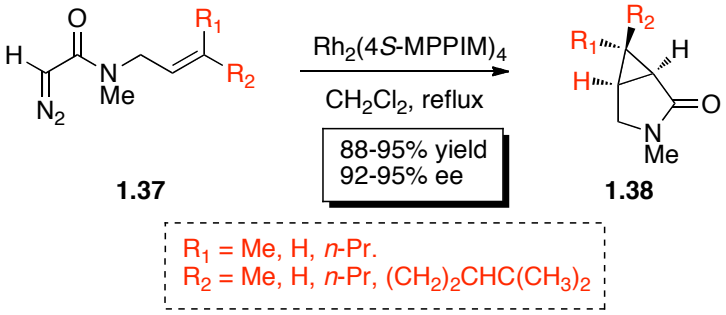

Asymmetric intramolecular C–H insertions to generate lactones or lactams are readily catalyzed by carboxamidate catalysts.[4] The formation of **1.41** is an example from a total synthesis, in which intermediate **1.40** was generated in 86% yield and 96% de from precursor **1.39** catalyzed by **1.35e** (Scheme 1.10).[4] Selectivity, yield and enantioselectivity are all routinely high (>90% ee) for many systems.[107] This has been utilized in synthesis on several occations, including the total syntheses of (+)-Isodeoxypodophyllotoxin,[108] Imperanene, (–)-enterolactone and (*R*)-(–)-baclofen.[109-112]

Scheme 1.10: Intramolecular C–H insertion.

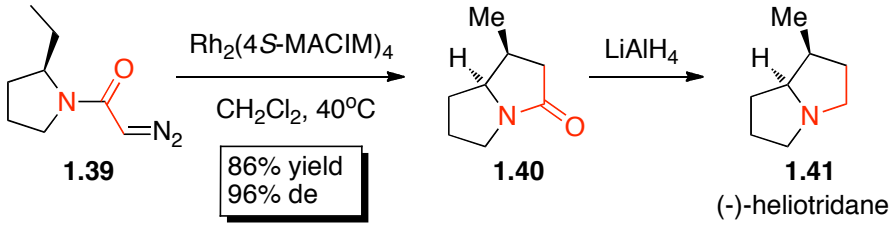

Dirhodium carboxamidates have had an important role in ylide chemistry.[1] Very high levels of asymmetric induction was obtained in an oxonium ylide/[2,3]-sigmatropic rearrangement reaction of **1.42** with ethyl diazoacetate **1.43**, catalyzed by **1.35b**. This generated the two diastereomers **1.44a-b**, both in >94% ee (Scheme 1.11).[113] A recently

discovered vista for the dirhodium(II) carboxamidates is macrocyclization through ylide intermediates, but has not yet been fully developed.[114,115]

Scheme 1.11: Oxonium ylide/[2,3]-sigmatropic rearrangement.

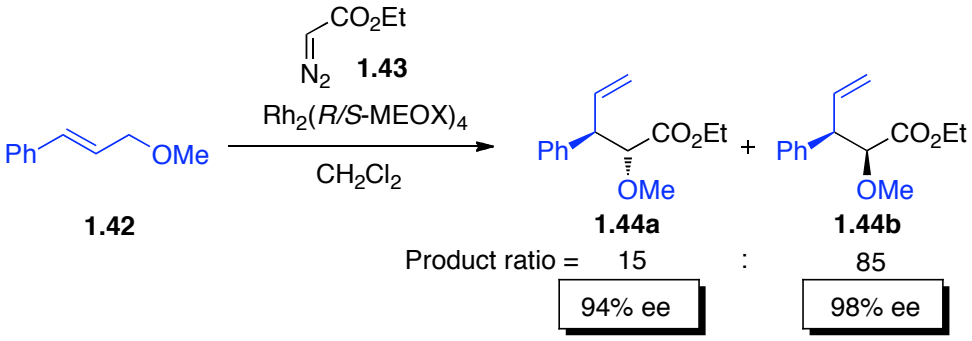

Lewis acid induced stereocontrol has been an area of extensive studies over the last two decades.[116] Although several chiral Lewis acids have been developed, a major challenge remains to achieve high levels of enantioselectivity accompanied by relatively high turnover numbers. Hetero-Diels Alder reactions traditionally have required high catalyst loadings as low turnover frequencies is a common problem.[34] Doyle et. al. described that dirhodium(II) carboxamidates could catalyze the hetero-Diels Alder reaction between **1.45** and diene **1.46** to form **1.47** in an effective manner (Scheme 1.12). 95% ee was observed when the reaction was catalyzed by $Rh_2(4S\text{-MPPIM})_4$ (**1.35f**).[25] Impressive turnover numbers up to 10,000 were achieved.

Scheme 1.12: Hetero Diels-Alder reaction.

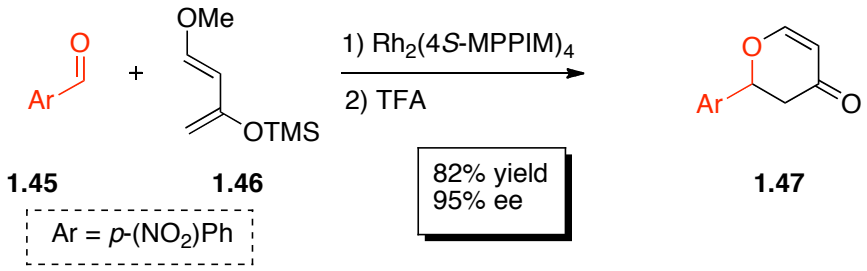

A new class of dirhodium catalyst, containing two carboxylate ligands and two orthometallated phophine ligands, was introduced by Lahuerta et. al.[117] Several variations of these complexes have been prepared. The phosphine ligands are arranged in a *cis*-manner oriented opposite to each other, giving overal C_2-symmetric complexes. These complexes have not been extensively tested as catalysts, but up to 95% ee was obtained in the intramolecular cyclopropanation chemistry of diazoketones.[118] Also intramolecular C–H insertion afforded up to 74% ee.[117]

Selective Ligand Exchange. The reaction between $Rh_2(OAc)_4$ and trifluoroacetic acid was first investigated by Bear et. al. in a kinetics study by NMR.[119] Corey and co-workers recently described the synthesis and characterization of mixed acetate/trifluoroacetate dirhodium complexes from this reaction.[44,45] The products were unambiguously identified by X-ray crystallography. The reported structures of *cis*-and *trans*-$Rh_2(OAc)_2(O_2CCF_3)_2$ are shown in Figures 1.10 and 1.11 respectively. It was reasoned that, due to the electron-withdrawing nature of the trifluoroacetate ligands, they would be more labile than acetate ligands in ligand exhange reactions carried out under kinetic conditions. From these considerations, the rational synthesis of well-defined mixed ligand acetate/carboxamidate complexes was achieved by Corey and co-workers.[44,45]

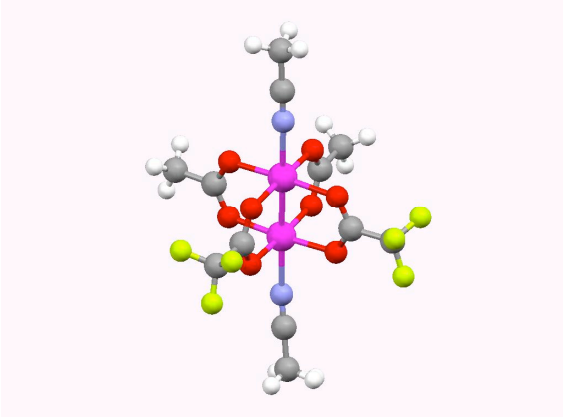

Figure 1.10: Bis-acetonitrile complex of *cis*-$Rh_2(TFA)_2(OAc)_2$.[44,45]

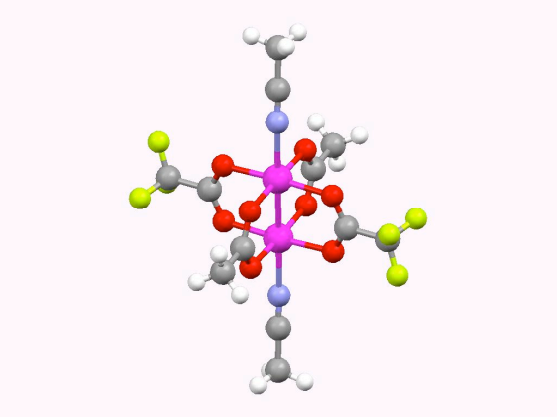

Figure 1.11: Bis-acetonitrile complex of *trans*-$Rh_2(TFA)_2(OAc)_2$.[44,45]

The synthesis and characterization of the mixed dirhodium trifluoroacetate/acetate systems opens up new opportunities for catalyst design based on selective ligand exchange. In terms of complexes with two chiral ligands, access to new complexes of C_2 and D_2-symmetry can be achieved, as shown schematically in Figure 1.12. Particularly interesting is the D_2-symmetric complex, due to its high symmetry. The remaining two achiral ligands (R) can be designed to either provide solubility, steric bulk and/or subtle electronic influences to the complex. Use of the achiral ligands to tune the properties of such complexes is of great interest and has not been explored in detail to date.

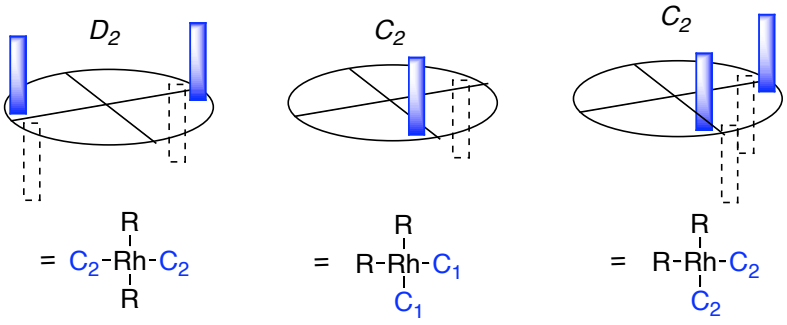

Figure 1.12: Symmetry considerations of mixed ligand complexes with two chiral ligands.

In this chapter, studies to determine the viability of achieving a selective ligand exchange in dirhodium(II) carboxylate systems are described. The synthesis of activated precursors, $Rh_2(OAc)_n(TFA)_{4-n}$ (n=1-3), and their use in controlled ligand exchange with carboxylate ligands, such as arylsulfonylprolinates, has been investigated in detail. Such a process has been described for the dirhodium carboxamidate complexes by Corey and Doyle, but has not been developed for the carboxylate family.[44,45,94] One of the major differences between the carboxylates and the carboxamidates as ligands, is the difference in basicity of these ligands. The relatively high basicity of the carboxamidates makes the ligand exchange process highly favorable if the anionic form is used and, consequently, the reactions must be carried out at very low temperatures to control the selectivity. Selectivity in the ligand exchange process arises from kinetic control. The carboxylate anions are much less basic, making the ligand exchange fairly slow, even at ambient temperature. Although this may be benefitial for the selectivity, it may hamper product yields of such reactions. Selective ligand exchange reactions of the dirhodium carboxylates are described herein in an effort to design specific mixed-ligand complexes. Furthermore, an evaluation of how such complexes perform in rhodium carbenoid

chemistry in terms of asymmetric induction, as a function of the ligand arrangement, has been adressed. The second part of the chapter describes the initial discoveries towards the design of a novel class of chiral dirhodium carboxylates for carbenoid chemistry based on optically active triarylcyclopropane acids.

1.2 Results and Discussion

1.2.1 Mixed Ligand Dirhodium Carboxylates

Synthesis of Precursors $Rh_2(O_2CCH_3)_n(O_2CCF_3)_{4-n}$. In order to control the exchange of carboxylate ligands, it was necessary to synthesize complexes in the mixed trifluoroacetate/acetate series, $Rh_2(TFA)_n(OAc)_{4-n}$ (n=1-3). These would then serve as starting materials to achieve mixed acetate/chiral carboxylate complexes by selectively exchanging trifluoroacetates. The syntheses of complexes $Rh_2(TFA)_n(OAc)_{4-n}$ with n=1, *cis*-2 and n=3 can be achieved by stirring $Rh_2(OAc)_4$ in neat trifluoroacetic acid at ambient temperature. Bear and co-workers deduced rate constants for a stepwise exchange mechanism, in which the acetate ligands are exchanged with trifluoroacetate ions in a sequential manner, based NMR and MS data.[119] The distribution of products during the course of the reaction is highly time dependent, as the reaction will proceed completely to $Rh_2(TFA)_4$ as $t \rightarrow \infty$. Using the rate constants found by Bear et.al., the five differential rate equations for the system were solved for time dependence of the concentrations of each species, using the Maple 10.05 software package. The time dependence of the concentration of each species is shown in Figure 1.13, using 17 mM as the initial concentration of $Rh_2(OAc)_4$. There is a significant *trans*-effect operating in the first two exchange reactions, leading to the rapid formation of complexes $Rh_2(TFA)(OAc)_3$ (**1.48**) and *cis*-$Rh_2(TFA)_2(OAc)_2$ (**1.49**), as seen in Figure 1.13.[41,119] Optimal yield of the former would be achieved after ~20 minutes of reaction time, whereas it would take about 1.4 hours for the latter. Exchanges of the last trifluoroacetate ligands are considerably slower processes, since the effective electrostatic attraction to

the dirhodium core has been significantly increased by introduction of the first two electron-withdrawing ligands, and because there is no *trans*-effect operating for the last two steps. The optimal yield of $Rh_2(OAc)(TFA)_3$ (**1.50**) can be achieved after circa 8.3 hours (~58% in theory). Only ~26% yield of the initial complex **1.48** can possibly be generated, based on the maximum point of its concentration curve, whereas ~78% of the *cis*-**1.49** could be obtained in theory. In practice, 40-60% isolated yield of the bis-acetonitrile adduct of *cis*-**1.49** was obtained following reaction times of ~1.5-2 hours.

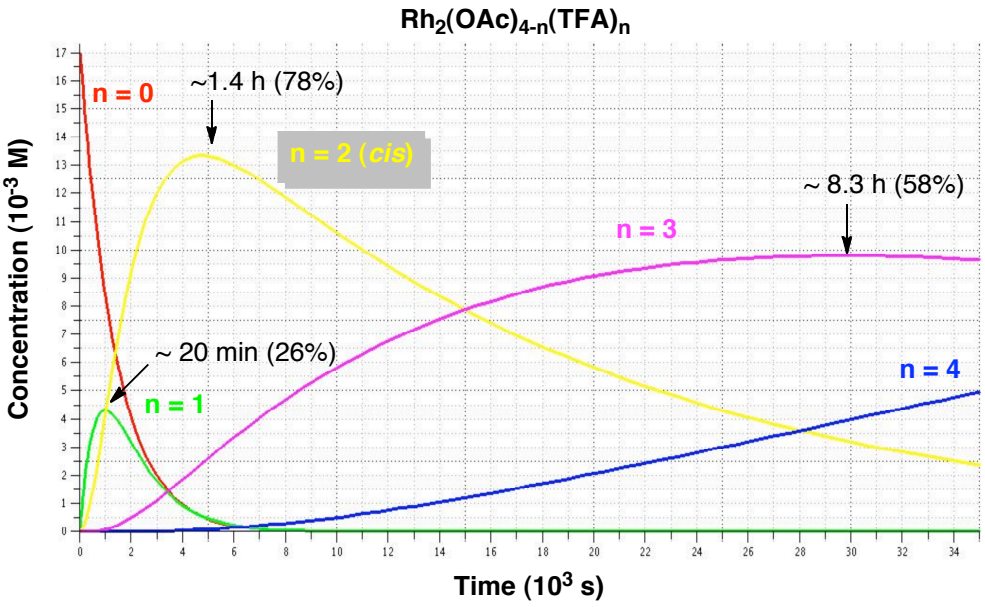

Figure 1.13: Time dependence of product distribution for formation of complexes $Rh_2(OAc)_n(TFA)_{4-n}$. n = 4 (red), n = 3 (**1.48**, green), n = 2 (*cis*-**1.49**, yellow), n = 1 (**1.50**, purple) and n = 0 (**1.51**, blue). Maxima are indicated along with the approximate theoretical yields.

A rational synthesis of *trans*-$Rh_2(OAc)_2(TFA)_2$ (*trans*-**1.49**) was described by Corey and co-workers.[44] By treating a solution of $Rh_2(TFA)_4$ (**1.51**) at 0°C with *n*-butyl ammonium acetate, and then allowed for the mixture to stir for ~15 minutes, the desired

trans-**1.49** could be isolated in 38-51% yield after column chromatography (Scheme 1.13), usually as the bis-acetonitrile complex. No *cis*-isomer can be observed in the reaction mixture. The only observed by-products were either starting materials and $Rh_2(OAc)_3(TFA)$ (**1.48**), if less than two equivalents of the acetate source was used, or $Rh_2(OAc)(TFA)_3$ (**1.50**), if more than two equivalents was added. The preference for *trans*-disubstitution can be rationalized by the *trans*-effect excerted by the first acetate group introduced. This will make the trifluoroacetate ligand in the *trans*-position kinetically more labile for substitution.

Scheme 1.13: Synthesis of *trans*-**1.49**.

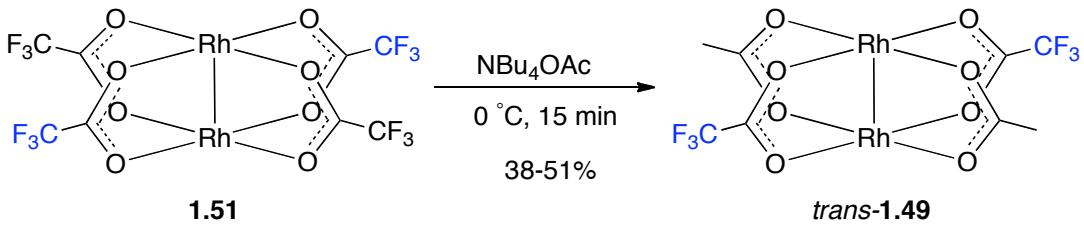

Synthesis of Mixed-Ligand Dirhodium(II) Prolinates. Given the success of the dirhodium(II) tetraprolinates as chiral catalysts for a variety of carbenoid reactions, arylsulfonylprolinate ligands were initially used to study the selective ligand exchange process. In addition to demonstrate the viabiliy of a selective ligand exchange process, the resulting complexes could be used to probe how the chiral ligand arrangement influences the asymmetric induction that is often observed in carbenoid chemistry. This could be very informative, particularly considering the importance of solvent effects in these reactions for achieving good enantiocontrol.[46,53]

The study was initiated by examining the feasibility of achieving the selective exchange of a single ligand. The mono-trifluoroacetate complex, $Rh_2(TFA)(OAc)_3$

(**1.48**), was employed, as a selective exchange with the trifluoroacetate ligand would be expected under kinetic conditions. Although the catalyst based on the chiral prolinate ligand DOSP (4-dodecylphenylsulfonylprolinate), is the most commonly effective catalyst, it was decided to use the related systems TISP (2,4,6-*tri*-isopropylphenylsulfonylprolinate) and TBSP (4-*tert*-butylphenylsulfonylprolinate) in this study, in order to simplify the characterization of the resulting complexes. It was decided to carry out the exchange reactions in a weakly coordinating solvent, THF, in order to: (1) not slow down the exchange process too much and, (2) stabilize the product complexes by solvent coordination. Furthermore, the addition of triethylamine would generate the corresponding ammonium salt with the arylsulfonylproline acids, thereby generating a more reactive ligand for the exchange process. In practice, this involved pre-mixing the arylsulfonylproline with triethylamine followed by addition of the activated dirhodium precursor complex. The reactions were initially conducted at ambient temperature, but it was found that, gentle heating of the mixture to ~40-50 °C, gave much improved reaction rates. If higher temperatures were employed, the rapid formation of more by-products was observed, presumably because of increased thermodynamic control. The selective ligand exchange reaction between complex **1.48** and the proline TISP-H at ambient temperature, conducted over 1-2 days, produced the new complex $Rh_2(OAc)_3$(TISP) (**1.52**) in 40% isolated yield (Scheme 1.14). The analogous complex $Rh_2(OAc)_3$(TBSP) (**1.53**) was formed in 70% isolated yield, when conducted at increased temperature over ~4 hours. The remainder of the material was mosty unreacted starting material. The complexes were readily purified by column chromatography on silica gel, using acetonitrile/benzene or acetonitrile/toluene solvent mixtures, which were also

effective for monitoring the exchange process by TLC. The use of these solvent systems ensured very effective separations of the purple acetonitrile adducts. Following isolation, the axial acetonitrile ligands could be removed by azeotropic distillation with dichloroethane and drying in a vacuum oven. The removal of acetonitrile was evident as the purple solids slowly turned dark green. However, the resulting complexes readily picked up atmospheric water when removed from the vacuum. The products were identified based on HRMS as well as the observation of the distinct 1 : 2 ratio of singlets in the ^{1}H NMR spectra, as the acetate ligands adjacent to the prolinate ligand are shifted slightly upfield from the *trans*-acetate signal. These studies demonstrate that the selective exchange of prolinate ligands with trifluoroacetates is viable.

Scheme 1.14: Synthesis of mono-substituted complexes.

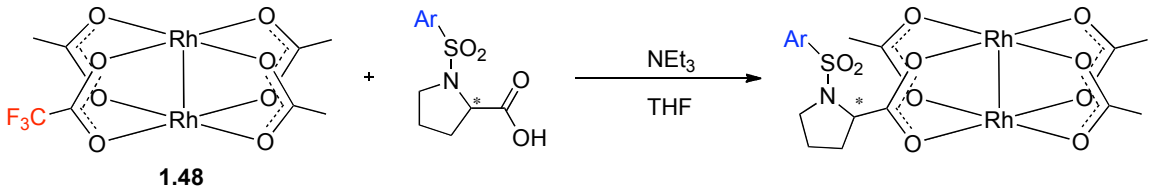

1.48

Ligand	*Product*	*Conditions*	*Yield*
Ar = (*S*)-2,4,6-Triisopropylphenyl (TISP)	**1.52**	r.t., 1-2 days	40%
Ar = (*R*)-4-*t*-Butylphenyl (TBSP)	**1.53**	40-50 °C, ~4 h	70%

The *cis*-disubstituted complexes were studied next using *cis*-**1.49** as the starting material (Scheme 1.15). The same reaction conditions as above were determined to be optimal. At ambient temperature, ligand exchange with *cis*-**1.49** produced the desired products, after 2 days, in ~20-40% yield, along with significant amounts of intermediates that had undergone a single ligand exchange in 16-50% yield. At 45-50 °C, the reactions

proceeded much faster and the products *cis*-**1.54-1.55** could be isolated in 64% and 59% yields, respectively, after only 4-5 hours of reaction time (Scheme 1.15).

Scheme 1.15: Synthesis of *cis*-prolinate/acetate complexes.

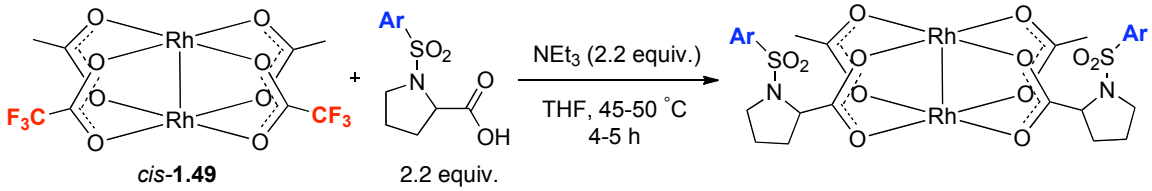

cis-**1.49** 2.2 equiv.

Ligand	*Product*	*Yield*
Ar = (*S*)-2,4,6-Triisopropylphenyl (TISP)	*cis*-**1.54**	64%
Ar = (*R*)-4-*t*-Butylphenyl (TBSP)	*cis*-**1.55**	59%

Using the established reaction conditions, the *trans*-series was also synthesized from *trans*-**1.49** (Scheme 1.16**)**. However, in this system, the double exchange proceeds at a much slower rate than the analogous process for the *cis*-series. This can again be attributed to a significant *trans*-effect operating in the *cis*-systems, rendering the ligand exchange reactions significantly faster. There is no such accelerating effect in the *trans*-system, making the ligand exchange a much slower process. At ambient temperature, at least two days of stirring was required before small amounts of the products *trans*-**1.54-1.55** were detected. At 45-55°C, the products were obtained in 48-59% yield after a reaction time of about 24 hours (Scheme 1.16). Further heating to higher temperatures produced several by-products, and was therefore avoided.

Scheme 1.16: Synthesis of *trans*-series.

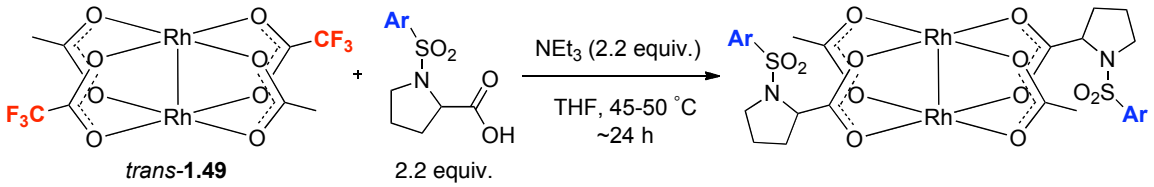

Ligand	*Product*	*Yield*
Ar = (*S*)-2,4,6-Triisopropylphenyl (TISP)	*trans*-**1.54**	48%
Ar = (*R*)-4-*t*-Butylphenyl (TBSP)	*trans*-**1.55**	59%

The observation of the singly-exchanged intermediates is important, because it strongly suggests that the reactions proceed in a stepwise manner, exchanging one ligand at a time (Scheme 1.17). The presence of each distinct species was readily monitored, by TLC, during the reaction. For the exhange reactions with (*R*)-TBSP-H, the intermediates from both the *cis* and *trans*-series were isolated (Figure 1.14). Although they display similar properties, in ^{1}H NMR, the two acetate methyl groups are inequivalent in the *cis*-complex *cis*-**1.56**, but equivalent in *trans*-**1.56**. This feature was initially used as an indirect proof of the structures of the *cis* versus *trans* prolinate complexes.

Scheme 1.17: Stepwise exchange mechanism.

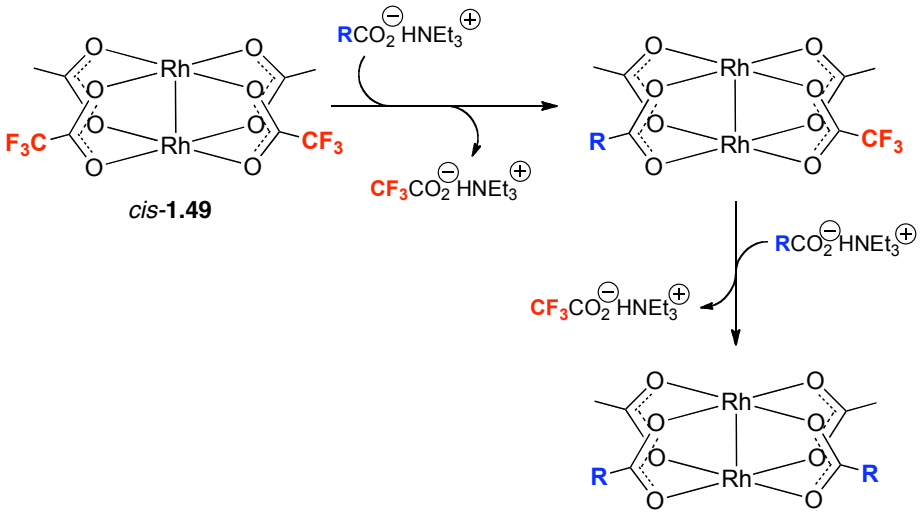

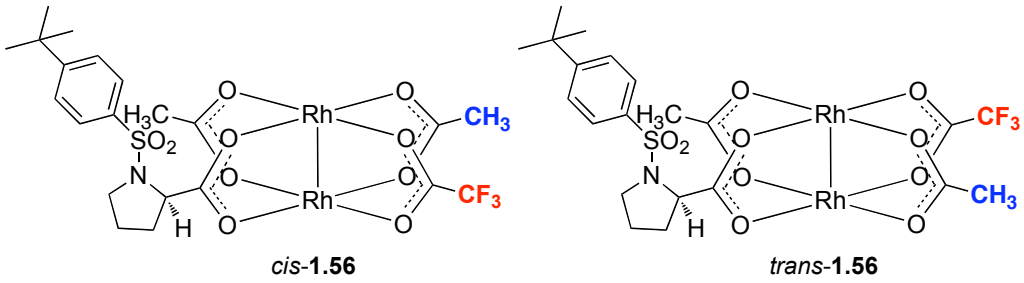

Figure 1.14: Observed intermediates from ligand exchange reactions with *R*-TBSP-H.

Although the structures of these complexes have not all been unambiguously confirmed, several observations clearly indicate that the proposed products are correct. *Cis*-versus *trans*-complexes were mainly differentiated based on two observations: (1) their different chromatographic properties and, (2) observation of the correct, singly-exchanged intermediate during the reaction. However, crystals were obtained for the bis-ethanol adduct of *trans*-**1.55**, as long, dark blue needles. The x-ray structure for this complex was determined unambiguously, and is shown in Figure 1.15.

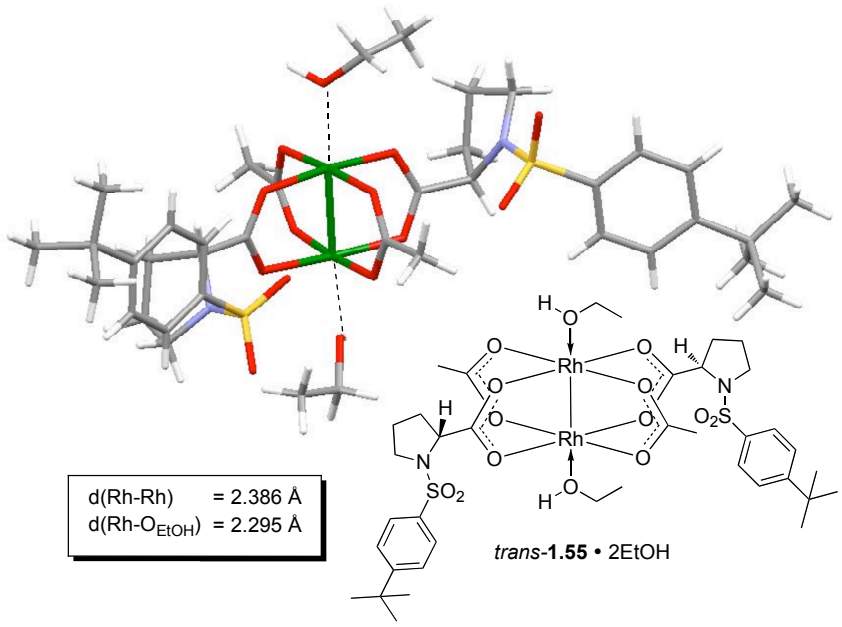

Figure 1.15: X-ray structure of bis-ethanol adduct of *trans*-**1.55**.

Catalyst evaluation. With a series of mixed ligand dirhodium prolinate complexes in hand, these were evaluated in their ability to induce asymmetry in a standard reaction. The cyclopropanation reaction between styrene and methyl phenyldiazoacetate **1.12** was used as the standard reaction (Scheme 1.18). As solvent effects have been described as important in this chemistry, considering that non-polar solvents are usually required to induce very high levels of asymmetric induction with the prolinate catalysts, both of the commonly used solvents hexanes and dichloromethane were used as reaction media. The reactions were conducted at 1 mol% catalyst loading at ambient temperature. For the complexes giving the highest enantioselectivities, the test reaction was also conducted at lower temperatures. The results of this study are summarized in Table 1.1. Up to 66% ee was obtained with *cis*-Rh_2(*R*-TBSP)$_2$(OAc)$_2$ (*cis*-**1.55**) when the reaction was carried out at low temperature. Several interesting trends emerge from the results: (1) The TBSP-complexes routinely outperform analogous TISP-complexes by at least 10% ee, (2) the enantioselectivity increases steadily with the number of ligands, (3) the *cis*-complexes always outperform the corresponding *trans*-complexes and, (4) enantioselectivity is always greater in hexanes than in dichloromethane for the TBSP-complexes, regardless of the number of chiral ligands. The latter trend seems to be opposite for TISP-complexes, but the difference is much smaller. The effects are graphically summarized in Figure 1.19. The *trans*-series data have been omitted for clarity. In general, the increase in enantioselectivity would be expected. However, the difference in enantioselectivity with single-prolinate complexes when switching solvent from dichloromethane to hexane is surprising. This can not be convincingly explained by the preference of particular

conformations in the two solvents, a previously invoked explanation model for the dirhodium tetraprolinates. The effect is not clearly understood at present.

The difference between *cis*-and *trans*-complexes is of interest. The *cis*-series routinely affords higher enantioselectivity. The preference for the up/down alignment of the ligands may be stronger in the latter case, because of the steric interactions between the adjacent ligands, thereby affording a C_2-symmetrical complex. In the *trans*-complexes, the two chiral ligands are sterically independent of each other, and may adopt a variety of conformations, one of which was shown in the x-ray structure in Figure 1.15. The tris-prolinate series was not synthesized in this work, but may be informative for future studies in this field.

Scheme 1.18: Catalyst evaluation in the cyclopropanation of styrene.

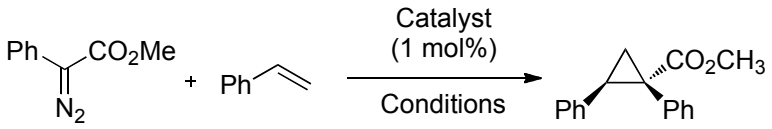

1.12 **1.57**

Table 1.1: Effect of catalyst, solvent and temperature on asymmetric induction.

Entry	*Catalyst*	*Conditions*	*Yield* (%)	*ee* (%)
1	Rh_2(*R*-TBSP)$(OAc)_3$	CH_2Cl_2, r.t.	71	24
2	*cis*-Rh_2(*R*-TBSP)$_2(OAc)_2$	CH_2Cl_2, r.t.	74	42
3	*cis*-Rh_2(*R*-TBSP)$_2(OAc)_2$	CH_2Cl_2, 0 °C	80	49
4	*trans*-Rh_2(*R*-TBSP)$_2(OAc)_2$	CH_2Cl_2, r.t.	85	30
5	Rh_2(*R*-TBSP)$_4$	CH_2Cl_2, r.t.	81	60
6	Rh_2(*S*-TISP)$(OAc)_3$	CH_2Cl_2, r.t.	76	16
7	*cis*-Rh_2(*S*-TISP)$_2(OAc)_2$	CH_2Cl_2, r.t.	76	31
8	*trans*-Rh_2(*S*-TISP)$_2(OAc)_2$	CH_2Cl_2, r.t.	63	12
9	Rh_2(*R*-TBSP)$(OAc)_3$	hexanes, r.t.	72	37
10	*cis*-Rh_2(*R*-TBSP)$_2(OAc)_2$	hexanes, r.t.	87	57
11	*cis*-Rh_2(*R*-TBSP)$_2(OAc)_2$	hexanes/CH_2Cl_2, -78°C→r.t.	69	66
12	*trans*-Rh_2(*R*-TBSP)$_2(OAc)_2$	hexanes, r.t.	80	43
13	Rh_2(*R*-TBSP)$_4$	hexanes, r.t.	86	92
14	Rh_2(*S*-TISP)$(OAc)_3$	hexanes, r.t.	78	7
15	*cis*-Rh_2(*S*-TISP)$_2(OAc)_2$	hexanes, r.t.	92	25
16	*trans*-Rh_2(*S*-TISP)$_2(OAc)_2$	hexanes, r.t.	86	8

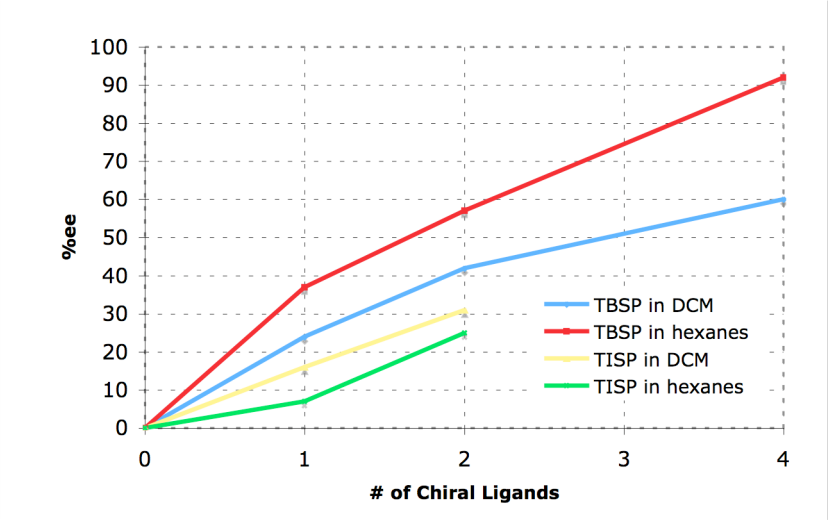

Figure 1.16: Enantioselectivity as a function of number of prolinate ligands.

Recent studies of novel catalysts have revealed that, the electronic nature of the carbenoid may have a large impact on the levels of asymmetric induction that can be obtained. Due to the relatively high level of asymmetric induction observed with *cis*-Rh_2(*R*-TBSP)$_2$(OAc)$_2$ (*cis*-**1.55**) as catalyst, it was decided to further study this complex in cyclopropanation reactions with electronically differentiated carbenoids **1.58a-d** and other alkene structures to give products **1.59a-f** (Scheme 1.19). Rotation student Jennifer Bon conducted this work under my supervision.[120] The results are summarized in Table 1.2. The results show that, variation of the carbenoid electronics did not impact the cyclopropanation chemistry of styrene much. However, when 1,1-diphenylethylene was used as the substrate, up to 74% ee was obtained with the methoxy-substituted carbenoid. This is the highest enantioselectivity that has been obtained with such complexes.

Scheme 1.19: Alkene cyclopropanation reactions.[120]

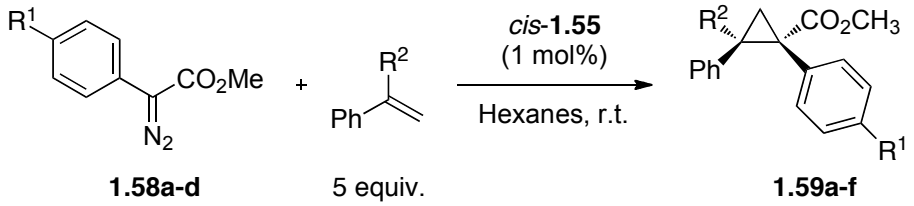

1.58a-d 5 equiv. **1.59a-f**

Table 1.2: Evaluation of *cis*-**1.55** conducted by Ms Jennifer Bon**.**[120]

Entry	*R*^{1}	*R*^{2}	**1.58**	**1.59**	*Yield* (%)	*ee* (%)
1	Br	H	**a**	**a**	53	19
2	Me	H	**b**	**b**	80	52
3	OMe	H	**c**	**c**	58	47
4	CF_3	Ph	**d**	**d**	69	47
5	Br	Ph	**a**	**e**	58	42
6	OMe	Ph	**c**	**f**	48	74

1.2.2 Design of a Novel Family of Chiral Dirhodium Tetra-carboxylates

Motivation. The design and studies of novel dirhodium catalysts for carbenoid chemistry is an area of intense current efforts in the chemical community. In order to develop new and challenging transformations for organic synthesis, new catalysts are required that display an increasing level of fine-tuned reactivity profiles. Cyclopropanation reactions, catalyzed by certain chiral rhodium(II) paddlewheel catalysts, can be remarkably chemo-, diastereo- and enantioselective. Examples of this are the cyclopropanation reactions between alkenes and aryl– or vinyldiazoacetates, to form arylcyclopropane esters with remarkable structural diversity, as discussed in Section 1.1. This methodology has been extensively applied to the syntheses of medicinally relevant compounds.

The formation of optically active esters in high enantiomeric excess is also a desirable reaction in terms of ligand design for dirhodium carboxlyates, as they can be hydrolyzed to carboxylic acids. The carboxylic acids are direct chiral ligand precursors, as chiral dirhodium complexes result from exchange reactions with dirhodium tetraacetate. The first example of using acids, formed by asymmetric cyclopropanation reactions, as ligands for the dirhodium framework was decribed by Dr. Janelle Thompson.[121] The highly enantioselective cyclopropanation reaction of styrene, using methyl phenyldiazoacetate **1.12**, afforded the diarylcyclopropane acid **1.60** upon subsequent recrystallization to >99% ee and hydrolysis. Ligand exchange with $Rh_2(OAc)_4$ gave the dirhodium tetrakis(diarylcyclopropane) carboxylate complex **1.61**. A similar method was employed to synthesize the analogous bidentate complexes **1.62-1.63**.[121]

Scheme 1.20: Synthesis of first dirhodium cyclopropane carboxylate catalyst.[121]

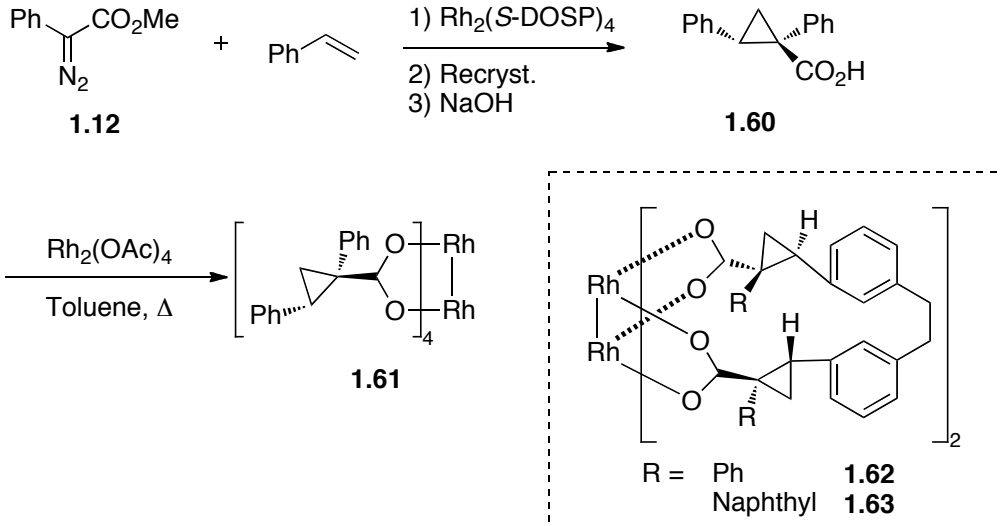

The catalyst complexes **1.61-1.63** were evaluated in the cyclopropanation reaction between styrene and various aryldiazoacetates **1.12** under several conditions (Scheme 1.21).[121] The highest enantioselectivity observed was 14% ee, using complex **1.61** in toluene as solvent. These initial results were not promising.

Scheme 1.21: Evaluation of catalysts **1.61-1.63**.[121]

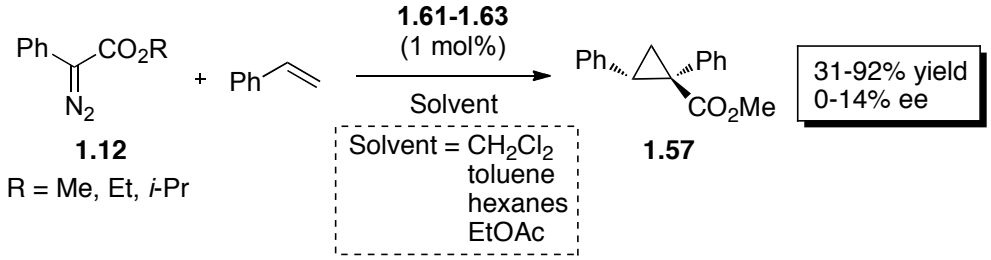

Analysis of model catalyst. Although the cyclopropyl derived dirhodium catalysts described above showed very little promise as chiral catalysts, it was decided to conduct further studies. A crucial component for further developments, would be to obtain an understanding of why complexes, such as **1.61**, failed to induce significant levels of asymmetry. If a hypothesis could be developed, these complexes would potentially

become promising catalysts by structural modifications of the system. A three-dimensional model of complex **1.61** was constructed *in silico* to shed light on the structural characteristics. It became clear that the complex may adopt many conformations in which the ligand substituents have little or no steric influence on the space around the active site of the catalyst. Figure 1.17 shows a simplified structure, in which three of the ligands have been removed for clarity. A hypothetical carbene alignment axis has been included. A crucial observation was that, the aryl groups are effectively pointing away from the space surrounding the active site, which may suggest why enantiocontrol is difficult to achieve. From this the hypothesis emerged that, if the ligand contained substituents in a *syn*-relation the carboxylate group, these would be forced to be oriented directly into the active site space. Based on the above hypothesis, the model was modified to include a phenyl substituent adjacent to the carboxylate group in a *syn*-relation. It appeared that this substituent inevitably had to influence the active site space, as shown in Figure 1.18. These observations became the impetus for the design of a modified cyclopropyl ligand, this time based on the cyclopropanation chemistry with 1,1-diarylethylenes.

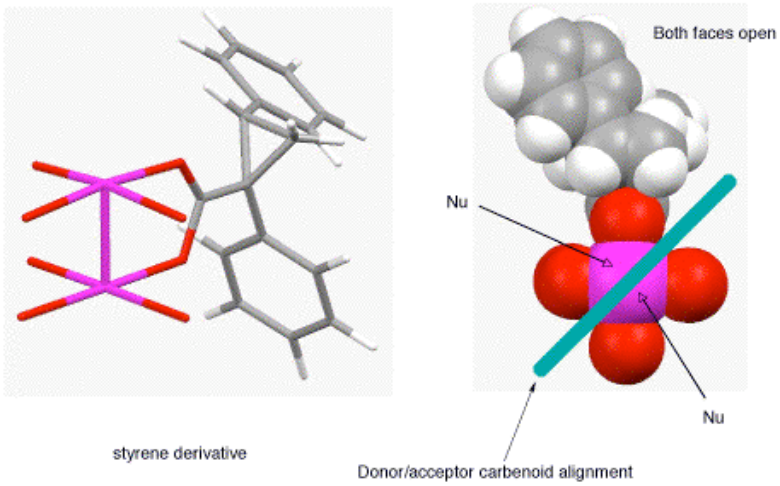

Figure 1.17: Model system for styrene-derived dirhodium complex.

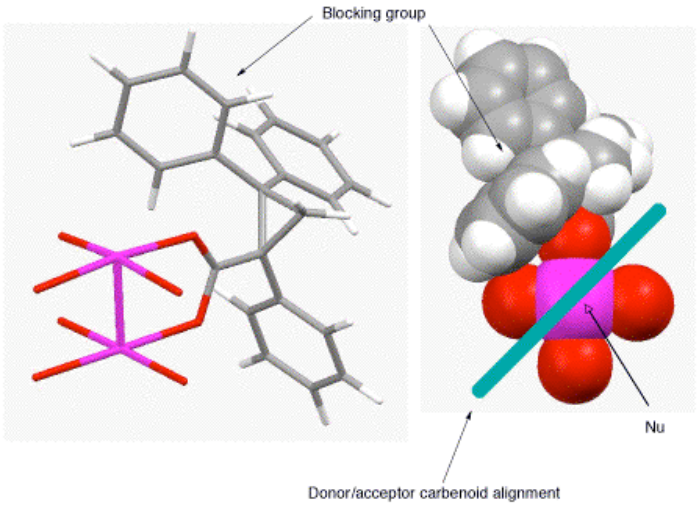

Figure 1.18: Model for triarylcyclopropane ligand system.

Modified Catalyst Synthesis. The cyclopropanation reaction between **1.12** and 1,1-diphenylethylene was conducted with Rh_2(*R*-DOSP)$_4$ in hexanes (Scheme 1.22). This reaction is precedent,[122] and affords the corresponding cyclopropane in 97% ee. The product was quantitatively hydrolyzed with KOH/MeOH to give the acid **1.64**, which was subjected to ligand exchange reaction with $Rh_2(OAc)_4$. A complex **1.65** was obtained,

which appeared to have exchanged all four acetate ligands. However, ^{1}H NMR indicated that it was formed as a mixture of isomers, which could not be separated. Partially exchanged complexes were ruled out based on the absence of any acetate peaks in the spectrum. Despite the isomeric mixture, it was decided to evaluate the obtained material **1.65.**

Scheme 1.22: Synthesis of catalyst **1.65**.

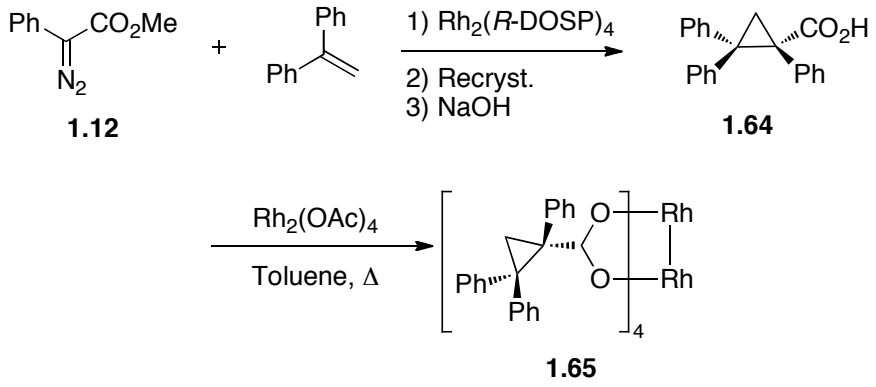

Catalyst evaluation. The initial evaluation of complex **1.65**, abbreviated Rh_2(*R*-TPCP)$_4$, gave promising results in the standard cyclopropanation reaction (Scheme 1.23, Table 1.3). In dichloromethane at ambient temperature, the reaction afforded the cyclopropane in 90% yield and 64% ee. Upon cooling the reaction to -40°C (dry ice/acetonitrile) and slowly warming to ambient temperature following addition of diazo compound, the product was isolated in 79% yield and 67% ee. In hexanes, at room temperature, only 40% ee was obtained. In all cases, the diastereoselectivity was high (>95% de). The observations that, with the modified catalyst **1.65**, more significant levels of asymmetric induction could be observed, demonstrate that the cyclopropyl acid derived dirhodium carboxylates can be a new, promising class of catalysts for carbenoid transformations.

However, challenges associated with the catalyst structure must be addressed, such as the possible formation of several rotational isomers.

Scheme 1.23: Test reaction.

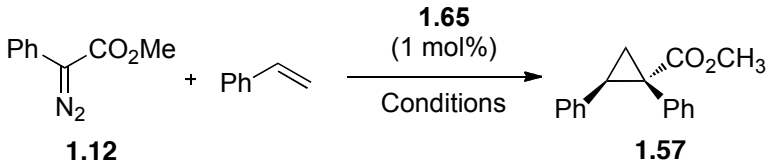

Table 1.3: Initial evaluation of catalyst **1.65**.

Entry	*Solvent*	*T* (°C)	*Yield* (%)	*ee* (%)
1	CH_2Cl_2	21	90	64
2	CH_2Cl_2	-40 to r.t.	79	67
3	Hexanes	21	88	40

In the synthesis of a complex **1.66**, analogous to **1.65**, using a *p*-bromo substituted diazo compound, it was observed that the isomers were, to some extent, chromatographically separable. A single isomeric form could be isolated, as evident from ^{1}H NMR analysis, but the exact conformation of this is unknown. When evaluated in the standard cyclopropanation reaction between **1.12** and styrene, a yield of 82% of **1.57** was obtained in 63% ee. This value is very similar to that obtained with the intial complex **1.65**. The result may indicate that steric modification of the diazo compound does not influence asymmetric induction much. This is, however, consistent with the underlying hypothesis that formed the basis of this investigation. The results also suggest that the isomer distribution of the catalyst can, to some degree, be controlled by substituents present in the diazo compound.

Scheme 1.24: Synthesis of bromo-complex **1.66**.

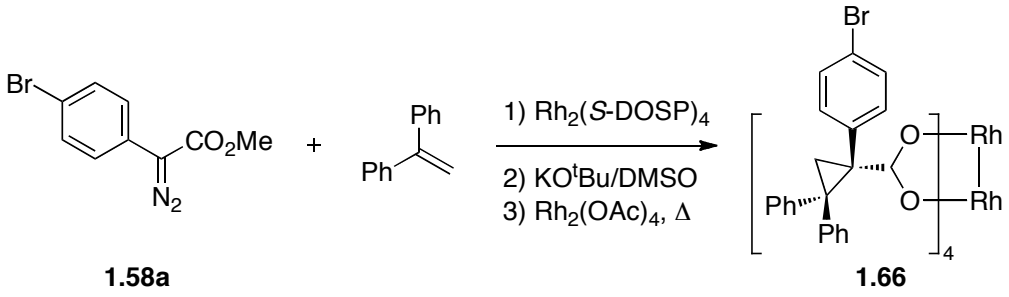

1.58a **1.66**

In order to obtain a better understanding of how catalysts such as **1.66** influence the selectivity in carbenoid reactions, the evaluation of this complex was extended to different diazo compounds and alkenes (Scheme 1.25, Table 1.4). This work was conducted by rotation student Changming Qin under my supervision. The results of these studies are shown in Table 1.4. Consistent with the initial evaluations, 62-76% ee was obtained in cyclopropanation reactions of styrene, and displayed little variation with respect to the change in substituents on the arylcarbenoids. The *ortho*-chloro substituted system **1.58e**, however, displayed a significant drop in enantioselectivity (8% ee). Enantioselectivities of 35-41% ee were obtained when 1,1-diphenylethylene was used as the trap in pentane. An improvement to 69% ee was observed when dichloromethane was used as solvent. For the methoxy-substituted diazoacetate **1.58c**, up to 76% ee was obtained in the cyclopropanation reaction with styrene in dichloromethane. Styryldiazoacetate **1.7** gave the highest enantiomeric excess (83% ee) that has been observed in the cyclopropanation reactions catalyzed by **1.66**. Further developments of this class of dirhodium catalyst should be directed towards applications that do not yet have good catalyst systems available. A crucial component of future catalyst syntheses in this family, would be to modulate the steric and electronic influences of the ligand

substituent that is in *syn*-relation to the carboxylate group, as this would be in accordance with the working hypothesis for why asymmetric induction occurs in these systems.

Scheme 1.25: Catalyst evaluation.[123]

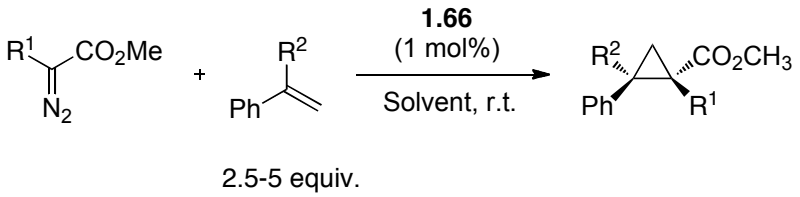

Table 1.4: Evaluation of **1.66** conducted by Mr. Changming Qin.[123]

Entry	*R^1*	*R^2*	*Solvent*	*Diazo-acetate*	*Product*	*Yield* (%)	*ee* (%)
1	(4-Br)Ph	Ph	Pentane	**1.58a**	**1.59e**	74	41
2	(4-Br)Ph	H	Pentane	**1.58a**	**1.59a**	84	69
3	Ph	Ph	Pentane	**1.12**	**1.67**	92	37
4	Ph	H	Pentane	**1.12**	**1.57**	94	62
5	(4-MeO)Ph	Ph	Pentane	**1.58c**	**1.59f**	87	35
6	(4-MeO)Ph	H	Pentane	**1.58c**	**1.59c**	63	69
7	(2-Cl)Ph	Ph	Pentane	**1.58e**	**1.68**	94	38
8	(2-Cl)Ph	H	Pentane	**1.58e**	**1.69**	89	8
9	(4-Br)Ph	Ph	CH_2Cl_2	**1.58a**	**1.59e**	69	61
10	(4-MeO)Ph	H	CH_2Cl_2	**1.58c**	**1.59c**	80	76
11	Ph	H	CH_2Cl_2	**1.12**	**1.57**	81	63
12	*E*-PhCH=CH	H	CH_2Cl_2	**1.7**	**1.70**	79	83

1.3 Conclusions

The synthesis of well-defined, mixed ligand acetate/prolinate dirhodium(II) complexes with one and two arylsulfonylprolinate ligands has been successfully achieved. This demonstrates the viability of selective ligand exchange in rhodium carboxylate complexes. The mechanism of the ligand exchange involves a stepwise exchange of ligands, which was supported by the observation and isolation of the corresponding intermediates. Up to 74% ee was observed in a test reaction using a synthesized mixed-ligand complex *cis*-$Rh_2(OAc)_2$(*R*-TBSP)$_2$ as catalyst. The corresponding *trans*-complexes displayed significantly lower control of the asymmetric induction. Overall, the enantioselectivity in the standard test reaction increased with the number of chiral ligands around the dirhodium core.

A new class of chiral dirhodium(II)-catalysts, based on triarylcyclopropyl acids, has been designed and evaluated in preliminary studies. Although significant challenges still exist in terms of catalyst synthesis, the already synthesized complexes have demonstrated great potential as they are capable of inducing significant levels of asymmetry in test cyclopropanation reactions. Up to 83% ee was observed when a styryldiazoacetate was employed as the carbenoid precursor.

1.4 Experimental Section

1.4.1 General Considerations

All reactions were conducted in flame-dried glassware under an inert atmosphere of dry argon. All reagents were used as received from commercial suppliers, unless otherwise stated. Styrene was filtered through a plug of silica before use. Dichloromethane and tetrahydrofuran solvents were obtained from drying columns (Grubbs type solvent purifier). Flash chromatography was performed on silica gel (230-400 mesh). Thin layer chromatography (TLC) was performed on aluminium backed plates, pre-coated with silica gel (0.25 mm, 60 F_{254}) which were developed using standard visualizing agents: UV fluorescence (254 nm) and phosphomolybdic acid/Δ. ^{1}H NMR spectra were recorded on Varian Nuclear Magnetic Resonance spectrometers at 600, 500, 400 or 300 MHz. Tetramethylsilane (TMS) was used as internal standard ($\delta = 0.00$) and data are reported as follows: chemical shift, multiplicity (s = singlet, d = doublet, t = triplet, q = quartet, qu = quintet, m = multiplet, and br = broad), integration and coupling constants in Hz. ^{13}C NMR spectra were recorded at 150, 125, 100 or 75 MHz. The solvent was used as internal standard ($CDCl_3$ δ =77.0) and spectra were obtained with complete proton decoupling. Infrared (IR) spectra were aquired using a Thermo Scientific Nicolet iS10 FTIR spectrometer and the wavenumbers are reported in reciprocal centimeters (cm^{-1}).

1.5.2 Procedures and Characterization Data

General procedure for preparation of $Rh_2(TFA)_n(OAc)_{4-n}$ (n=1, 2 (cis) and 3): To a flame-dry round-bottom flask purged with dry argon, was added a stir bar, $Rh_2(OAc)_4$ (1.0 equiv.) and CF_3CO_2H. The mixture was stirred vigorously for 1.5-2 h, or until the optimal reaction time for the desired product was achieved. The solvent was then removed *in vacuo,* and the resulting purple solid purified by column chromatography (10-20% CH_3CN/C_6H_6). The complexes were isolated, characterized and used for further reactions as their bis-acetonitrile adducts unless otherwise stated.

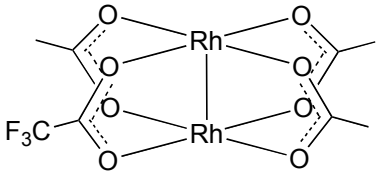

$Rh_2(OAc)_3(TFA)\bullet 2MeCN$ (1.48). TLC (10% CH_3CN/Benzene): R_f = 0.06. ^1H NMR (500 MHz, $CDCl_3$): δ 2.55 (s, 6H, coord. CH_3CN), 1.99 (s, 6H), 1.98 (s, 3H). MS (DCI, isobutene): *m/z* 496. The recorded data match previous reports.[44]

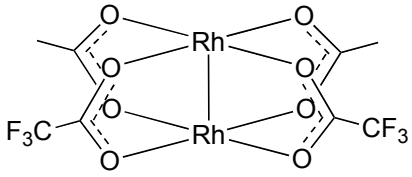

***cis*-$Rh_2(OAc)_2(TFA)_2)\bullet 2MeCN$ (*cis*-1.49)**. TLC (10% CH_3CN/Benzene): R_f = 0.24. ^1H NMR (500 MHz, $CDCl_3$): δ 2.59 (s, 6H, coord. CH_3CN), 2.00 (s, 6H). MS (DCI, isobutene): *m/z* 550. The recorded data match previous reports.[44]

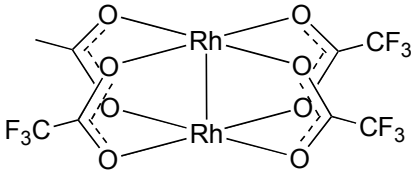

$Rh_2(OAc)(TFA)_3$•2MeCN (1.50). TLC (10% CH_3CN/Benzene): R_f = 0.50. ^1H NMR (500 MHz, $CDCl_3$): δ 2.62 (s, 6H, coord. CH_3CN), 2.00 (s, 3H). MS (DCI, isobutene): *m/z* 604. The recorded data match previous reports.[44]

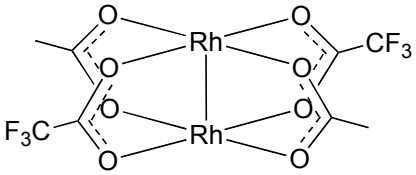

***trans*-$Rh_2(OAc)_2(TFA)_2$•2MeCN (*trans*-1.49)**. Procedure according to Corey et. al.[44] To a flame-dry round-bottom flask purged with dry argon, was added a stir bar, $Rh_2(TFA)_4$ (1.0 equiv.) and dry CH_3CN (5 mL, 17 mM solution). Vigorous stirring was initiated and the mixture was cooled to 0 °C in an ice/water bath. *N*-Butyl ammonium acetate (2.0 equiv.) was added quickly in one portion, and the reaction mixture was stirred for 15 min at 0°C. The solvent was then removed *in vacuo* to afford a purple solid. The product was purified by column chromatography (2% CH_3CN/CH_2Cl_2) to afford *trans*-**1.49** • 2MeCN as a purple solid. The complex was used for further reactions as the bis-acetonitrile adduct. Data for *trans*-**1.49** • 2MeCN: TLC (10% CH_3CN/Benzene): R_f = 0.51. ^1H NMR (500 MHz, $CDCl_3$): δ 2.51 (s, 6H, coord. CH_3CN) 1.99 (s, 6H). MS (FAB): *m/z* 550. The recorded data match previous reports.[44]

General procedure for synthesis of mixed-ligand dirhodium prolinates: To a flame-dry round-bottom flask kept under an atmosphere of dry argon, was added the appropriate arylsulfonylproline in its acidic form (2-2.2 equiv. for disubstituted complexes, 1-1.2 equiv. for monosubstituted complexes), then dry THF (2-3 mL) and distilled NEt_3 (equimolar amount to arylsulfonylproline). The mixture was allowed to stir for a few

minutes, and then added the appropriate dirhodium(II) carboxylate precursor (*cis/trans* di or mono-$Rh_2(TFA)_n(OAc)_{4-n}$) in one batch. The reaction was allowed to stir for 2-3 days at ambient temperature, or 1-2 days at 45-55˚C. The reactions were allowed to stir until the desired product was observed to be the major spot by periodic TLC-analysis. The solvent was then removed *in vacuo,* and the resulting residue purified by column chromatography using CH_3CN/benzene eluent mixtures. After isolation of the purple solids, they were dissolved in 1,2-dichloroethane in a round-bottom flask and then subjected to slow rotatory evaporation. This was repeated 3-5 times until a green color remained in the solid, which was then dried in a vacuum oven for ~12 h. The complexes readily picked up atmospheric water and are consequently characterized as their H_2O-adducts, unless otherwise noted.

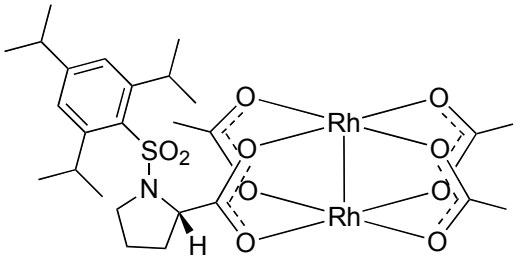

$Rh_2(OAc)_3$(*S*-TISP) (1.52). FTIR (neat): ν_{max}/cm^{-1} 2959, 1587, 1418, 1311, 1151, 730, 704, 669. ^{1}H NMR (500 MHz, CDCl3): δ 7.12 (s, 2H), 4.29 (d, 1H, *J* = 7.0 Hz), 4.07 (qu, 2H, *J* = 7.0 Hz), 3.49 (m, 1H), 3.13 (m, 1H), 2.87 (sept, 1H, *J* = 7.0 Hz), 2.10 (s, 3H), 2.07 (s, 6H), 1.98 (m, 2H), 1.85 (m, 2H), 1.23-1.19 (m, 18H). HRMS (FAB): *m/z* 764.0466 ([$C_{26}H_{39}NO_{10}Rh_2S$+H] requires 764.0478).

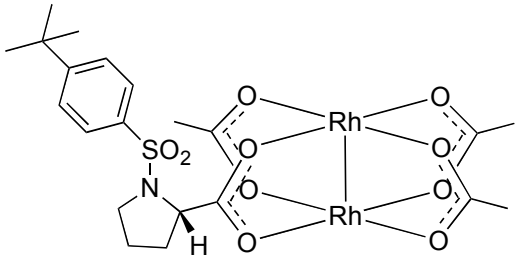

$Rh_2(OAc)_3$(*R*-TBSP) (1.53). TLC (40% CH_3CN/Benzene): R_f = 0.34. OR (c 0.88, $CHCl_3$): $[\alpha]_D^{25}$ = 115±4. FTIR (neat): ν_{max}/cm^{-1} 2965, 1586, 1418, 1347, 1199, 1162, 1114, 1089, 913. ^{1}H NMR (500 MHz, $CDCl_3$): δ 7.72 (d, 2H, *J* = 8.5 Hz), 7.48 (d, 2H, *J* = 8.5 Hz), 4.34 (bs, 1H), 3.41 (m, 1H), 3.18 (m, 1H), 2.65 (bs, coord. H_2O), 2.16 (s, 3H), 2.14 (s, 6H), 1.90 (m, 3H), 1.70 (m, 1H), 1.33 (s, 9H). ^{13}C NMR (75 MHz, $CDCl_3$): δ 192.3, 192.2, 156.2, 135.8, 127.3, 125.9, 61.6, 48.1, 35.1, 31.8, 31.1, 24.5, 23.9, 23.7. HRMS (FAB): *m/z* 693.9669 ([$C_{21}H_{29}NO_{10}Rh_2S$+H] requires 693.9664).

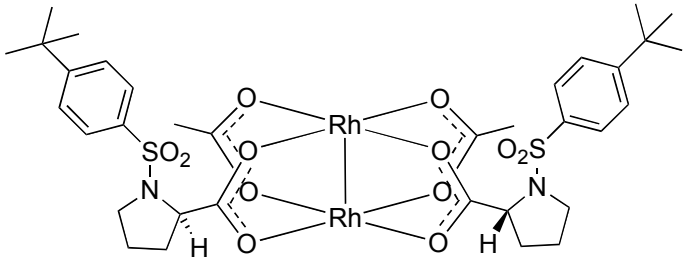

***cis*-$Rh_2(OAc)_2$(*R*-TBSP)$_2$ (*cis*-1.55).** TLC (60% EtOAc/pentane): R_f = 0.19. FTIR (neat): ν_{max}/cm^{-1} 2964, 2872, 1592, 1420, 1346, 1199, 1162, 1114, 1089, 1010, 913. ^{1}H NMR (500 MHz, $CDCl_3$): δ 7.72 (d, 4H, *J* = 8.5 Hz), 7.50 (d, 4H, *J* = 8.5 Hz), 4.39 (bs, 2H), 3.38 (s, 2H), 3.13 (m, 2H), 2.04 (s, 6H), 1.95 (m, 6H), 1.64 (m, 2H), 1.32 (s, 18H). ^{13}C NMR (75 MHz, $CDCl_3$): δ 192.6, 192.2, 156.1, 135.7, 127.4, 125.9, 61.7, 48.1, 35.1, 31.7, 24.7, 23.7. HRMS (FAB): *m/z* 945.0674 ([$C_{34}H_{46}N_2O_{12}Rh_2S_2$+H] requires 945.0675).

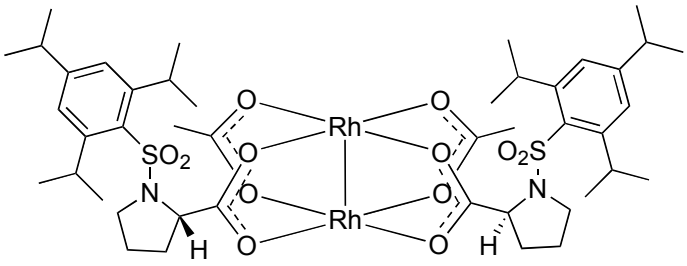

***cis*-Rh$_2$(OAc)$_2$(*S*-TISP)$_2$ (*cis*-1.54).** TLC (20% CH_3CN/Benzene): R_f = 0.21. FTIR (neat): ν_{max}/cm^{-1} 2959, 2870, 1591, 1417, 1384, 1363, 1348, 1312, 1151, 1076, 733, 668. ^{1}H NMR (500 MHz, $CDCl_3$): δ 7.11 (s, 4H), 4.28 (bs, 2H), 4.08 (qu, 4H, *J* = 7.0 Hz), 3.49 (m, 2H), 3.07 (m, 2H), 2.86 (sept, 2H, *J* = 7.0 Hz), 2.04 (s, 6H), 1.94 (m, 6H), 1.79 (m, 2H), 1.22 (m, 24H), 1.18 (d, 12H, *J* = 7.0 Hz). ^{13}C NMR (75 MHz, $CDCl_3$): δ 192.6, 192.3, 152.6, 151.2, 132.0, 123.7, 60.9, 47.1, 34.0, 31.8, 29.3, 24.9, 23.9, 23.7, 23.5. HRMS (FAB): *m/z* 1085.2241 ([$C_{44}H_{66}N_2O_{12}Rh_2S_2$+H] requires 1084.2167).

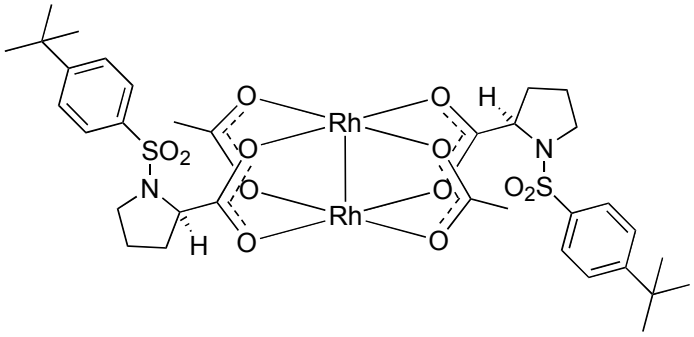

***trans*-Rh$_2$(OAc)$_2$(*R*-TBSP)$_2$ (*trans*-1.55).** OR (c 0.1, $CHCl_3$): $[\alpha]_D^{23}$ = 180±2. TLC (20% CH_3CN/Benzene): R_f = 0.29. FTIR (neat): ν_{max}/cm^{-1} 2965, 2906, 2872, 1590, 1529, 1419, 1346, 1268, 1199, 1163, 1115, 1088, 1011, 913, 732, 640, 591. ^{1}H NMR (500 MHz, $CDCl_3$): δ 7.72 (d, 4H, *J* = 8.5 Hz), 7.50 (d, 4H, *J* = 8.5 Hz), 4.39 (bs, 2H), 3.45 (m, 2H), 3.18 (m, 2H), 2.09 (s, 6H), 1.94 (m, 6H), 1.69 (m, 2H), 1.32 (s, 18H). ^{13}C NMR (75 MHz, $CDCl_3$): *δ* 192.5, 192.0, 156.1, 135.3, 127.3, 126.0, 61.7, 48.4, 35.0, 31.8, 31.0, 24.6, 23.5. HRMS (FAB): *m/z* 944.0617 ([$C_{34}H_{46}N_2O_{12}Rh_2S_2$+H] requires 944.0637).

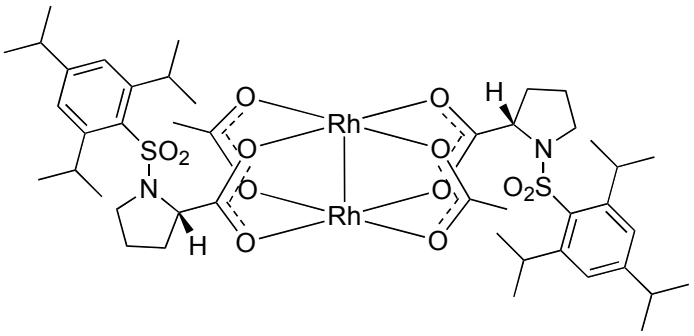

***trans*-Rh$_2$(OAc)$_2$(*S*-TISP)$_2$ (*trans*-1.54).** TLC (20% CH_3CN/Benzene): R_f = 0.29. OR (c 0.07, $CHCl_3$): $[\alpha]_D^{24}$ = -157±2. FTIR (neat): ν_{max}/cm^{-1} 2960, 2870, 1593, 1418, 1348, 1311, 1151, 1077, 911, 732, 669. ^{1}H NMR (500 MHz, $CDCl_3$): δ 7.12 (s, 4H) 4.29 (bs, 2H), 4.07 (sept, 4H, *J* = 7.0 Hz), 3.45 (bs, 2H), 3.15 (m, 2H), 2.98 (bs, 1H), 2.87 (sept, 2H, *J* = 6.5 Hz), 2.00 (s, 6H), 1.97 (m, 4H), 1.83, (m, 4H), 1.25 (d, 24H, *J* = 7.0 Hz), 1.20 (d, 12H, *J* = 6.5 Hz). ^{13}C NMR (75 MHz, $CDCl_3$): δ 192.5, 191.8, 152.7, 151.3, 131.7, 123.7, 60.6, 47.3, 34.1, 31.9, 29.3, 25.0, 24.8, 24.0, 23.5. HRMS (FAB): *m/z* 1085.2224 ([$C_{44}H_{66}N_2O_{12}Rh_2S_2$] requires 1084.2167).

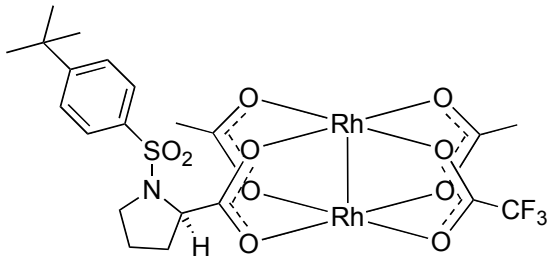

***cis*-Rh$_2$(OAc)$_2$(*R*-TBSP)(O$_2$CCF$_3$) (*cis*-1.56).** TLC (20% CH_3CN/Benzene): R_f = 0.43. FTIR (neat): ν_{max}/cm^{-1} 2963, 1636, 1566, 1418, 1341, 1200, 1158, 1009, 983. ^{1}H NMR (500 MHz, $CDCl_3$): δ 7.70 (d, 2H, *J* = 8.5 Hz), 7.47(d, 2H, *J* = 8.5 Hz), 4.34 (bs, 1H), 3.47 (m, 1H), 3.15 (m, 1H), 2.18 (s, 6H), 2.09 (bs, 2H), 2.05-1.88 (m, 2H), 1.68 (m, 1H), 1.31 (s, 9H). ^{13}C NMR (75 MHz, $CDCl_3$): δ 193.5, 192.9, 157.9, 136.6, 128.5, 127.2,

62.7, 36.0, 32.5, 31.4, 25.4, 23.1. HRMS (FAB): *m/z* 747.9429 ([$C_{21}H_{26}NO_{10}F_3Rh_2S_1$+H] requires 747.9412).

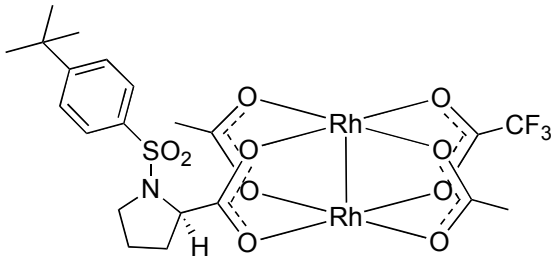

***trans*-$Rh_2(OAc)_2$(*R*-TBSP)(O_2CCF_3) (*trans*-1.56).** TLC (20% CH_3CN/Benzene): R_f = 0.43. FTIR (neat): ν_{max}/cm^{-1} 2965, 1635, 1558, 1419, 1347, 1200, 1161, 1114, 1088. ^{1}H NMR (500 MHz, $CDCl_3$): δ 7.70 (d, 2H, *J* = 8.5 Hz), 7.47(d, 2H, *J* = 8.5 Hz), 4.34 (bs, 1H), 3.47 (m, 1H), 3.15 (m, 1H), 2.18 (s, 6H), 2.09 (bs, 2H), 2.05-1.88 (m, 2H), 1.68 (m, 1H), 1.31 (s, 9H). ^{13}C NMR (75 MHz, CD_3OD): δ 194.1, 192.9, 157.9, 136.6, 128.5, 127.3, 62.5, 36.0, 32.5, 31.5, 30.7, 25.5, 23.2. HRMS (FAB): *m/z* 747.9425 ([$C_{21}H_{26}NO_{10}F_3Rh_2S_1$+H] requires 747.9412).

General procedure for initial evaluation of mixed-ligand dirhodium prolinates: To a flame-dried round-bottom flask, kept under a dry atmosphere of argon, was added styrene (5.0 equiv.), dry hexanes or CH_2Cl_2 (3.0 mL) and catalyst (0.01 equiv.). Methyl phenyldiazoacetate **1.12** (0.2 mmol , 1.0 equiv.), dissolved in dry hexanes or CH_2Cl_2 (3 mL), was then added to the former solution drop-wise over 3-20 min at ambient temperature. The mixture was allowed to stir for at least 30 min after addition, and was then concentrated *in vacuo*. The crude residue was analyzed by ^{1}H NMR and purified by flash column chromatography (10% Et_2O/pentane) to afford the cyclopropane as a white solid.

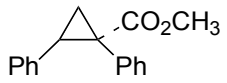

(±)-Methyl 1β, 2β-diphenylcyclopropane-1α-carboxylate (1.57): ^{1}H NMR (400 MHz, $CDCl_3$): δ 7.11-7.09 (m, 3H), 7.03-7.00 (m, 5H), 6.76-6.74 (m, 2H), 3.63 (s, 3H), 3.11 (dd, 1H, *J* = 7.0, 9.5 Hz), 2.13 (dd, 1H, *J* = 5.0, 9.5 Hz), 1.86 (dd, 1H, *J* = 5.0, 7.0 Hz). The data match previously reported results.[124]

General procedure for test reactions with ***cis*-$Rh_2(OAc)_2$(*R*-TBSP)$_2$ (*cis*-1.55).** To a flame-dried round-bottom flask kept under a dry atmosphere of argon, was added catalyst (0.002 mmol, 0.01 equiv.), alkene (1.0 mmol, 5.0 equiv.) and dry, degassed hexanes (2.0 mL). A solution of diazo compound (0.2 mmol , 1.0 equiv.) in dry, degassed hexanes (3.0 mL), was then added to the former solution drop-wise over 30 min at ambient temperature. The mixture was allowed to stir for 15 min after addition, and then concentrated *in vacuo*. The crude residue was analyzed by ^{1}H NMR and purified by flash column chromatography using Et_2O/pentane or EtOAc/hexanes mixtures to afford the pure cyclopropane.

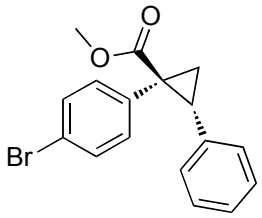

1*S*-(4-Bromophenyl)-2R-phenylcyclopropanecarboxylic acid methyl ester (1.59a). The data was collected by Ms Jennifer Bon. HPLC (S,S-Whelk, 2.0% *i*-PrOH/hexanes, 1.0 mL/min, 2mg/mL, UV 254 nm): t_R = 12.1 (major), 15.8 min (minor). ^{1}H NMR (400 MHz, $CDCl_3$) δ 7.25-7.23 (m, 2H), 7.10-7.06 (m, 3H), 6.90-6.87 (m, 2H), 6.78-6.78 (m,

2H), 3.65 (s, 3H), 3.10 (dd, 1H, *J* = 7.2, 9.6 Hz), 2.13 (dd, 1H, *J* = 4.8, 9.6 Hz), 1.83 (dd, 1H, *J* = 5.2, 7.2 Hz). Consistent with previously reported data.[121]

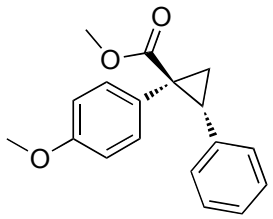

1*S*-(4-Methoxyphenyl)-2R-phenylcyclopropanecarboxylic acid methyl ester (1.59c). The data was collected by Ms Jennifer Bon. HPLC (Chiracel OD-H, 0.7% 2-PrOH in hexanes, 1.0 mL/min, 2mg/mL): t_R = 10.8 (major), 15.0 min (minor), UV. ^{1}H NMR (400 MHz, $CDCl_3$) δ 7.06-7.04 (m, 3H), 6.92-6.90 (m, 2H), 6.76-6.74 (m, 2H), 6.66-6.64 (m, 2H), 3.71 (s, 3H), 3.65 (s, 3H), 3.05 (dd, 1H, *J* = 7.2, 9.6 Hz), 2.10 (dd, 1H, *J* = 4.8, 9.2 Hz), 1.80 (dd, 1H *J* = 5.2, 7.6 Hz). Consistent with previously reported data.[121]

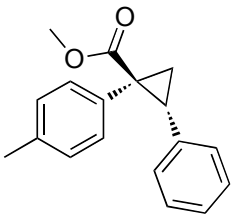

1*S*-(4-Methylphenyl)-2*R*-phenylcyclopropanecarboxylic acid methyl ester (1.59b). The data was collected by Ms Jennifer Bon. HPLC (S,S-Whelk, 1.0% 2-PrOH in hexanes, 1.0 mL/min, 2mg/mL): t_R = 10.1 (major), 13.6 (minor). ^{1}H NMR (400 MHz, $CDCl_3$) δ 7.06-7.04 (m, 3H), 6.93-6.88 (m, 4H), 6.77-6.75 (m, 2H), 3.64 (s, 3H), 3.06 (dd, 1H, *J* = 7.6, 9.2 Hz), 2.23 (s, 3H), 2.10 (dd, 1H, *J* = 5.2, 9.6 Hz), 1.83 (dd, 1H, *J* = 4.8, 7.2 Hz). Consistent with previously reported data.[121]

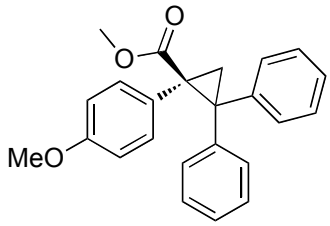

(*R*)-methyl 1-(4-methoxyphenyl)-2,2-diphenylcyclopropanecarboxylate (1.59f). The data was collected by Ms Jennifer Bon. HPLC (Chiracel OD-H, 0.7% 2-PrOH in hexanes, 1.0 mL/min, 2mg/mL): t_R = 13.3 (minor), 15.9 (major). ^{1}H NMR (300 MHz, $CDCl_3$) δ 7.50 (d, 2H, *J* = 8.7 Hz), 7.33 (t, 2H, *J* = 7.2 Hz), 7.26-7.22 (m, 3H), 7.00-6.96 (m, 5H), 6.68 (d, 2H, *J* = 6.6), 3.72 (s, 3H), 3.35 (s, 3H), 2.67 (d, 1H, *J* = 5.7 Hz), 2.37 (d, 1H, *J* = 5.4 Hz). Consistent with previously reported data.[121]

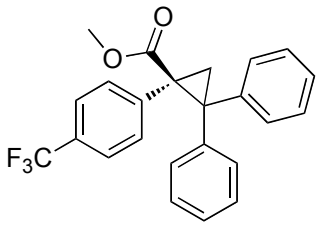

(*R*)-methyl 2,2-diphenyl-1-(4-(trifluoromethyl)phenyl)cyclopropanecarboxylate (1.59d). The data was collected by Ms Jennifer Bon. HPLC (S,S-Whelk, 2.0% 2-PrOH in hexanes, 1.0 mL/min, 2mg/mL): t_R = 7.0 (major), 7.8 (minor). ^{1}H NMR (300 MHz, $CDCl_3$) δ 7.51-7.25 (m, 9H), 7.04-6.97 (m, 5H), 3.36 (s, 3H), 2.73 (d, 1H, *J* = 5.7 Hz), 2.46 (d, 1H, *J* = 5.4 Hz). Consistent with previously reported data.[121]

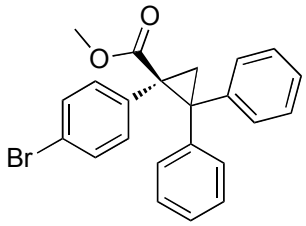

(R)-methyl 1-(4-bromophenyl)-2,2-diphenylcyclopropanecarboxylate (1.59e). The data was collected by Ms Jennifer Bon. HPLC (Chiralcel OD-H, 0.5% 2-PrOH in hexanes, 1.0 mL/min, 2mg/mL): t_R = 7.9 (major), 9.40 (minor). ^{1}H NMR (300 MHz, $CDCl_3$) δ 7.47 (d, 2H, *J* = 6.9 Hz), 7.33 (t, 2H, *J* = 6.9 Hz), 7.27-7.18 (m, 5H), 7.05-6.95 (m, 5H), 3.72 (s, 3H), 3.35 (s, 3H), 2.68 (d, 1H, *J* = 5.4 Hz), 2.39 (d, 1H, *J* = 5.7 Hz). Consistent with previously reported data.[121]

General procedure for synthesis of triarylcyclopropyl acid ligands. To a flame-dry round-bottom flask, kept under a dry atmosphere of argon, was added catalyst (0.004-0.01 equiv.), dry hexanes or pentane (150 mL) and 1,1-diphenylethylene (1.5-2.5 equiv.). The appropriate aryldiazoacetate (30 mmol, 1.0 equiv) in dry hexanes or pentane (50 mL) was added drop-wise to the former solution by syringe pump addition over 1.5-2 h. The mixture was allowed to stir for 3 h after addition and then concentrated *in vacuo*. The resulting residue was used without further purification in the next step. To a new round-bottom flask, containing the methyl ester cyclopropane residue, was added a large excess of KOH/MeOH or LiOH, THF and H_2O (2 : 1). The mixture was then heated to near reflux, until TLC analysis showed full conversion of the cyclopropane. The reaction mixture was then cooled to ambient temperature, acidified by addition of 10% HCl until pH ~ 3 and concentrated *in vacuo.* The residue was treated with water and extracted with ethyl acetate or dichloromethane (3X). The organics were then washed with brine (1X),

dried over anhydrous $MgSO_4$ and filtered. The filtrate was concentrated *in vacuo* to afford the carboxylic acid in near quantitative yield.

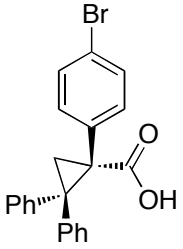

Modified hydrolysis procedure used for methyl 1-(4-bromophenyl)-2,2-diphenylcyclopropanecarboxylate: Conducted by Mr. Changming Qin. To a round-bottom flask at ambient temperature was added KO*t*-Bu (7.35g, 65.6 mmol, 15 equiv) and DMSO (30 mL). The ester (1.7g, 4.2 mmol, 1.0 equiv) dissolved in DMSO (5 mL) was added drop-wise. 10 minutes after addition, TLC-analysis showed that the ester was consumed. The system was acidified by adding 10% HCl until pH ~ 2. Then, the solution was poured into ice water (100 mL). Yellow solids precipitated and were collected by filtration. The solids were recrystallized from pentane/ether = 20/1 to give the desired product as white solid in 26 % yield (450 mg, 1.14 mmol). Data: ^{1}H NMR (400 MHz, $CDCl_3$) δ 7.47 (d, 2H, J = 7.2 Hz), 7.31-7.15 (m, 5H), 7.21 (d, 2H, J = 8.4 Hz), 7.01-6.96 (m, 5H), 2.63 (d, 1H, J = 5.6 Hz), 2.39 (d, 1H, J = 5.6 Hz). Consistent with previously reported data.[121]

Procedure for ligand exchange reactions. To a round-bottom flask fitted with a Dean-Stark apparatus, and immersed in an oil bath, was added dirhodium tetrakis(acetate) (1.0 equiv.), the carboxylic acid (5-10 equiv.) and toluene. The mixture was next heated to reflux with continuous removal and refilling of toluene, until the distillate showed no sign of acetic acid content. The mixture was then concentrated by distilling off excess toluene.

The residue was then purified by flash column chromatography (MeCN/toluene or MeCN/benzene mixtures). Upon isolation, the complexes typically have axially coordinated toluene and/or MeCN, which can be removed by repeated azeotropic distillation of the complexes from 1,2-dichloroethane (4-5X) by rotatory evaporation.

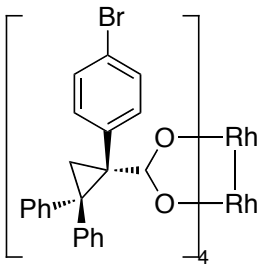

Rh_2(*S*-BrTPCP)$_4$ (1.66). The data was collected by Mr. Changming Qin. FTIR (film): ν_{max}/cm^{-1} 1577, 1490, 1447, 1397, 1379,1277, 1156, 1076, 1010, 991, 906, 823, 777, 733. ^{1}H NMR (400 MHz, $CDCl_3$): δ 7.23−7.15 (m, 7H), 6.90-6.81 (m, 7H), 2.30 (d, 1H, J = 5.2 Hz), 2.39 (d, 1H, J = 4.8 Hz). ^{13}C NMR (100 MHz, $CDCl_3$) δ 188.9, 142.4, 140.8, 135.7, 132.8, 130.6, 129.9, 129.2, 128.3, 127.9, 126.6, 126.4, 120.9, 46.9, 42.7, 23.6.

References

(1) Doyle, M. P.; McKervey, M. A.; Ye, T. *Modern Catalytic Methods for Organic Synthesis with Diazo Compounds: From Cyclopropanes to Ylides*; Wiley-interscience: New York, 1998.

(2) Doyle, M. P.; Ojima, I.; (Ed) *Catalytic Asymmetric Synthesis, Second Edition*, 2000.

(3) Lydon, K. M.; McKervey, M. A.; Jacobsen, E. N. (Ed); Pfaltz, A. (Ed); Yamamoto, H.; (Ed) *Comprehensive Asymmetric Catalysis I-III, Volume 2*, 1999.

(4) Davies, H. M. L.; Beckwith, R. E. J. *Chem. Rev.* **2003**, *103*, 2861-2903.

(5) Doyle, M. P. *Chem. Rev.* **1986**, *86*, 919-939.

(6) Doyle, M. P.; Forbes, D. C. *Chem. Rev.* **1998**, *98*, 911-935.

(7) Lebel, H.; Marcoux, J. F.; Molinaro, C.; Charette, A. B. *Chem. Rev.* **2003**, *103*, 977-1050.

(8) Ye, T.; McKervey, M. A. *Chem. Rev.* **1994**, *94*, 1091-1160.

(9) Timmons, D. J.; Doyle, M. P. *J. Organomet. Chem.* **2001**, *617*, 98-104.

(10) Davies, H. M. L.; Xiang, B.; Kong, N.; Stafford, D. G. *J. Am. Chem. Soc.* **2001**, *123*, 7461-7462.

(11) Sulikowski, G. A.; Cha, K. L.; Sulikowski, M. M. *Tetrahedron Asym.* **1998**, *9*, 3145-3169.

(12) Li, Z. J.; Davies, H. M. L. *J. Am. Chem. Soc.* **2010**, *132*, 396-401.

(13) Davies, H. M. L.; Hansen, J. In: *Catalytic Asymmetric Synthesis 3rd ed.* (Ed. Ojima, I.), John Wiley & Sons, Hoboken, New Jersey, **2010**, p.163-226.

(14) Espino, C. G.; Du Bois, J.; Evans, P. A. (Ed.) In: *Modern Rhodium-Catalyzed Organic Reactions*, 2005.

(15) Espino, C. G.; Du Bois, J. *Angew. Chem. Int. Ed.* **2001**, *40*, 598-600.

(16) Li, Z.; He, C. *Eur. J. Org. Chem.* **2006**, 4313-4322.

(17) Yu, X.-Q.; Huang, J.-S.; Zhou, X.-G.; Che, C.-M. *Org. Lett.* **2000**, *2*, 2233-2236.

(18) Halfen, J. A. *Curr. Org. Chem.* **2005**, *9*, 657-669.

(19) Anada, M.; Washio, T.; Shimada, N.; Kitagaki, S.; Nakajima, M.; Shiro, M.; Hashimoto, S. *Angew. Chem. Int. Ed.* **2004**, *43*, 2665-2668.

(20) Doyle, M. P.; Phillips, I. M.; Hu, W. H. *J. Am. Chem. Soc.* **2001**, *123*, 5366-5367.

(21) Long, J.; Hu, J.; Shen, X.; Ji, B.; Ding, K. *J. Am. Chem. Soc.* **2002**, *124*, 10-11.

(22) Doyle, M. P.; Valenzuela, M.; Huang, P. *Proc. Natl. Acad. Sci. U. S. A.* **2004**, *101*, 5391-5395.

(23) Valenzuela, M.; Doyle, M. P.; Hedberg, C.; Hu, W. H.; Holmstrom, A. *Synlett* **2004**, 2425-2428.

(24) Davies, H. M. L. *Eur. J. Org. Chem.* **1999**, 2459-2469.

(25) Doyle, M. P. *J. Org. Chem.* **2006**, *71*, 9253-9260.

(26) Fritschi, H.; Leutenegger, U.; Pfaltz, A. *Angew. Chem. Int. Ed.* **1986**, *25*, 1005-1006.

(27) Mueller, D.; Umbricht, G.; Weber, B.; Pfaltz, A. *Helv. Chim. Acta* **1991**, *74*, 232-40.

(28) Hikichi, K.; Kitagaki, S.; Anada, M.; Nakamura, S.; Nakajima, M.; Shiro, M.; Hashimoto, S. *Heterocycles* **2003**, *61*, 391-401.

(29) Evans, D. A.; Woerpel, K. A.; Hinman, M. M.; Faul, M. M. *J. Am. Chem. Soc.* **1991**, *113*, 726-8.

(30) Lowenthal, R. E.; Abiko, A.; Masamune, S. *Tetrahedron Lett.* **1990**, *31*, 6005-8.

(31) Lowenthal, R. E.; Masamune, S. *Tetrahedron Lett.* **1991**, *32*, 7373-6.

(32) Brunner, H.; Nishiyama, H.; Itoh, K.; Ojima, I. (Ed) *Catalytic Asymmetric Synthesis, Second Edition*, 2000.

(33) Nishiyama, H.; Itoh, Y.; Sugawara, Y.; Matsumoto, H.; Aoki, K.; Itoh, K. *Bull. Chem. Soc. Jpn.* **1995**, *68*, 1247-62.

(34) Davies, H. M. L.; Doyle, M. P.; Phillips, I. M.; Hu, W. *Chemtracts* **2001**, *14*, 642-645.

(35) Park, S. B.; Nishiyama, H.; Itoh, Y.; Itoh, K. *J. Chem. Soc., Chem. Commun.* **1994**, 1315-16.

(36) Chen, Y.; Zhang, X. P. *J. Org. Chem.* **2007**, *72*, 5931-4.

(37) Maxwell, J. L.; O'Malley, S.; Brown, K. C.; Kodadek, T. *Organometallics* **1992**, *11*, 645-52.

(38) Callot, H. J.; Piechocki, C. *Tetrahedron Lett.* **1980**, *21*, 3489-92.

(39) O'Malley, S.; Kodadek, T. *Tetrahedron Lett.* **1991**, *32*, 2445-8.

(40) Cotton, F. A.; Murillo, C. A.; Walton, R. A. (Eds.) *Multiple Bonds Between Metal Atoms, Third Edition*, 2005.

(41) Boyar, E. B.; Robinson, S. D. *Coord. Chem. Rev.* **1983**, *50*, 109-208.

(42) Ren, T. *Coord. Chem. Rev.* **1998**, *175*, 43-58.

(43) Felthouse, T. R. *Prog. Inorg. Chem.* **1982**, *29*, 73-166.

(44) Lou, Y.; Horikawa, M.; Kloster, R. A.; Hawryluk, N. A.; Corey, E. J. *J. Am. Chem. Soc.* **2004**, *126*, 8916-8918.

(45) Lou, Y.; Remarchuk, T. P.; Corey, E. J. *J. Am. Chem. Soc.* **2005**, *127*, 14223-14230.

(46) Davies, H. M. L.; Bruzinski, P. R.; Lake, D. H.; Kong, N.; Fall, M. J. *J. Am. Chem. Soc.* **1996**, *118*, 6897-6907.

(47) Brunner, H.; Kluschanzoff, H.; Wutz, K. *Bull. Soc. Chim. Belg.* **1989**, *98*, 63-72.

(48) Doyle, M. P. *Rec. Trav. Chim. Pays-Bas* **1991**, *110*, 305-316.

(49) Singh, V. K.; DattaGupta, A.; Sekar, G. *Synthesis* **1997**, 137-149.

(50) Kennedy, M.; McKervey, M. A.; Maguire, A. R.; Roos, G. H. P. *J. Chem. Soc. Chem. Commun.* **1990**, 361-362.

(51) McKervey, M. A.; Ye, T. *J. Chem. Soc. Chem. Commun.* **1992**, 823-824.

(52) Roos, G. H. P.; McKervey, M. A. *Synth. Commun.* **1992**, *22*, 1751-1756.

(53) Wynne, D. C.; Olmstead, M. M.; Jessop, P. G. *J. Am. Chem. Soc.* **2000**, *122*, 7638-7647.

(54) Davies, H. M. L.; Kong, N. *Tetrahedron Lett.* **1997**, *38*, 4203-4206.

(55) Davies, H. M. L.; Kong, N.; Churchill, M. R. *J. Org. Chem.* **1998**, *63*, 6586-6589.

(56) Davies, H. M. L.; Hu, B. H. *Tetrahedron Lett.* **1992**, *33*, 453-456.

(57) Davies, H. M. L.; Townsend, R. J. *J. Org. Chem.* **2001**, *66*, 6595-6603.

(58) Davies, H. M. L.; Boebel, T. A. *Tetrahedron Lett.* **2000**, *41*, 8189-8192.

(59) Davies, H. M. L.; Hansen, T.; Churchill, M. R. *J. Am. Chem. Soc.* **2000**, *122*, 3063-3070.

(60) Davies, H. M. L.; Jin, Q. H. *Tetrahedron Asym.* **2003**, *14*, 941-949.

(61) Davies, H. M. L.; Gregg, T. M. *Tetrahedron Lett.* **2002**, *43*, 4951-4953.

(62) Davies, H. M. L.; Walji, A. M.; Townsend, R. J. *Tetrahedron Lett.* **2002**, *43*, 4981-4983.

(63) Davies, H. M. L.; Dal, X.; Long, M. S. *J. Am. Chem. Soc.* **2006**, *128*, 2485-2490.

(64) Davies, H. M. L.; Beckwith, R. E. J.; Antoulinakis, E. G.; Jin, Q. H. *J. Org. Chem.* **2003**, *68*, 6126-6132.

(65) Davies, H. M. L.; Antoulinakis, E. G. *Org. Lett.* **2000**, *2*, 4153-4156.

(66) Davies, H. M. L.; Yang, J.; Nikolai, J. *J. Organomet. Chem.* **2005**, *690*, 6111-6124.

(67) Davies, H. M. L.; Hansen, T.; Hopper, D. W.; Panaro, S. A. *J. Am. Chem. Soc.* **1999**, *121*, 6509-6510.

(68) Davies, H. M. L.; Beckwith, R. E. J. *J. Org. Chem.* **2004**, *69*, 9241-9247.

(69) Davies, H. M. L.; Stafford, D. G.; Hansen, T. *Org. Lett.* **1999**, *1*, 233-236.

(70) Davies, H. M. L.; Jin, Q. H. *Proc. Natl. Acad. Sci. U. S. A.* **2004**, *101*, 5472-5475.

(71) Anada, M.; Kitagaki, S.; Hashimoto, S. *Heterocycles* **2000**, *52*, 875-883.

(72) DeAngelis, A.; Dmitrenko, O.; Yap, G. P. A.; Fox, J. M. *J. Am. Chem. Soc.* **2009**, *131*, 7230.

(73) Ghanem, A.; Gardiner, M. G.; Williamson, R. M.; Muller, P. *Chem. Eur. J.* **2000,** *16*, 3291-3295.

(74) Lindsay, V. N. G.; Lin, W.; Charette, A. B. *J. Am. Chem. Soc.* **2009**, *131*, 16383.

(75) Hashimoto, S.-i.; Watanabe, N.; Ikegami, S. *Synlett* **1994**, 353-355.

(76) Watanabe, N.; Ogawa, T.; Ohtake, Y.; Ikegami, S.; Hashimoto, S.-i. *Synlett* **1996**, 85-86.

(77) Hashimoto, S.; Watanabe, N.; Ikegami, S. *Tetrahedron Lett.* **1990**, *31*, 5173-4.

(78) Watanabe, N.; Ohtake, Y.; Hashimoto, S.; Shiro, M.; Ikdgami, S. *Tetrahedron Lett.* **1995**, *36*, 1491-4.

(79) Mueller, P.; Bernardinelli, G.; Allenbach, Y. F.; Ferri, M.; Flack, H. D. *Org. Lett.* **2004**, *6*, 1725-1728.

(80) Denton, J. R.; Sukumaran, D.; Davies, H. M. L. *Org. Lett.* **2007**, *9*, 2625-2628.

(81) Reddy, R. P.; Lee, G. H.; Davies, H. M. L. *Org. Lett.* **2006**, *8*, 3437-3440.

(82) Tsutsui, H.; Yamaguchi, Y.; Kitagaki, S.; Nakamura, S.; Anada, M.; Hashimoto, S. *Tetrahedron Asym.* **2003**, *14*, 817-821.

(83) Anada, M.; Watanabe, N. *Chem. Commun.* **1998**, 1517-1518.

(84) Chen, Z.; Chen, Z.; Jiang, Y.; Hu, W. *Synlett* **2003**, 1965-1966.

(85) Liang, C.; Robert-Peillard, F.; Fruit, C.; Mueller, P.; Dodd, R. H.; Dauban, P. *Angew. Chem. Int. Ed.* **2006**, *45*, 4641-4644.

(86) Reddy, R. P.; Davies, H. M. L. *Org. Lett.* **2006**, *8*, 5013-5016.

(87) Sawamura, M.; Sasaki, H.; Nakata, T.; Ito, Y. *Bull. Chem. Soc. Jpn.* **1993**, *66*, 2725-2729.

(88) Ishitani, H.; Achiwa, K. *Synlett* **1997**, 781-782.

(89) Pierson, N.; FernandezGarcia, C.; McKervey, M. A. *Tetrahedron Lett.* **1997**, *38*, 4705-4708.

(90) Pirrung, M. C.; Zhang, J. *Tetrahedron Lett.* **1992**, *33*, 5987-90.

(91) McCarthy, N.; McKervey, M. A.; Ye, T.; McCann, M.; Murphy, E.; Doyle, M. P. *Tetrahedron Lett.* **1992**, *33*, 5983-5986.

(92) Hodgson, D. M.; Stupple, P. A.; Pierard, F. Y. T. M.; Labande, A. H.; Johnstone, C. *Chem. Eur. J.* **2001**, *7*, 4465-4476.

(93) Mueller, P.; Baud, C.; Jacquier, Y.; Moran, M.; Naegeli, I. *J. Phys. Org. Chem.* **1996**, *9*, 341-347.

(94) Welch, C. J.; Tu, Q.; Wang, T. B.; Raab, C.; Wang, P.; Jia, X. J.; Bu, X. D.; Bykowski, D.; Hohenstaufen, B.; Doyle, M. P. *Adv. Synth. Catal.* **2006**, *348*, 821-825.

(95) Ahsan, M. Q.; Bernal, I.; Bear, J. L. *Inorg. Chem.* **1986**, *25*, 260-5.

(96) Doyle, M. P. *Aldrichimica Acta* **1996**, *29*, 3-11.

(97) Doyle, M. P. *Russ. Chem. Bull.* **1994**, *43*, 1770-1782.

(98) Doyle, M. P.; Winchester, W. R.; Simonsen, S. H.; Ghosh, R. *Inorg. Chim. Acta* **1994**, *220*, 193-199.

(99) Doyle, M. P.; Winchester, W. R.; Hoorn, J. A. A.; Lynch, V.; Simonsen, S. H.; Ghosh, R. *J. Am. Chem. Soc.* **1993**, *115*, 9968-9978.

(100) Doyle, M. P.; Winchester, W. R.; Protopopova, M. N.; Muller, P.; Bernardinelli, G.; Ene, D.; Motallebi, S. *Helv. Chim. Acta* **1993**, *76*, 2227-2235.

(101) Doyle, M. P.; Dyatkin, A. B.; Protopopova, M. N.; Yang, C. I.; Miertschin, C. S.; Winchester, W. R.; Simonsen, S. H.; Lynch, V.; Ghosh, R. *Rec. Trav. Chim. Pays-Bas* **1995**, *114*, 163-170.

(102) Doyle, M. P.; Zhou, Q. L.; Raab, C. E.; Roos, G. H. P.; Simonsen, S. H.; Lynch, V. *Inorg. Chem.* **1996**, *35*, 6064-6073.

(103) Doyle, M. P.; Austin, R. E.; Bailey, A. S.; Dwyer, M. P.; Dyatkin, A. B.; Kalinin, A. V.; Kwan, M. M. Y.; Liras, S.; Oalmann, C. J.; Pieters, R. J.; Protopopova, M.

N.; Raab, C. E.; Roos, G. H. P.; Zhou, Q. L.; Martin, S. F. *J. Am. Chem. Soc.* **1995**, *117*, 5763-5775.

(104) Doyle, M. P.; Zhou, Q. L.; Simonsen, S. H.; Lynch, V. *Synlett* **1996**, 697-&.

(105) Doyle, M. P.; Davies, S. B.; Hu, W. H. *Org. Lett.* **2000**, *2*, 1145-1147.

(106) Charette, A. B.; Wurz, R. *J. Mol. Cat. A Chem.* **2003**, *196*, 83-91.

(107) Davies, H. M. L.; Dal, X.; Crabtree, R. (Ed); Mongos, M. (Ed) In: *Comprehensive Organometallic Chemistry III,* 13 Volume Set, 2006.

(108) Doyle, M. P.; Dyatkin, A. B.; Tedrow, J. S. *Tetrahedron Lett.* **1994**, *35*, 3853-3856.

(109) Doyle, M. P.; Hu, W. H. *Chirality* **2002**, *14*, 169-172.

(110) Bode, J. W.; Doyle, M. P.; Protopopova, M. N.; Zhou, Q. L. *J. Org. Chem.* **1996**, *61*, 9146-9155.

(111) Doyle, M. P.; Hu, W. H.; Valenzuela, M. V. *J. Org. Chem.* **2002**, *67*, 2954-2959.

(112) Doyle, M. P.; Tedrow, J. S.; Dyatkin, A. B.; Spaans, C. J.; Ene, D. G. *J. Org. Chem.* **1999**, *64*, 8907-8915.

(113) Doyle, M. P.; Forbes, D. C.; Vasbinder, M. M.; Peterson, C. S. *J. Am. Chem. Soc.* **1998**, *120*, 7653-7654.

(114) Weathers, T. M.; Wang, Y. H.; Doyle, M. P. *J. Org. Chem.* **2006**, *71*, 8183-8189.

(115) Doyle, M. P.; Hu, W. H. *Synlett* **2001**, 1364-1370.

(116) Pons, J.-M.; Santelli, M.(Eds): *Lewis Acids and Selectivity in Organic Synthesis*, 1995.

(117) Estevan, F.; Herbst, K.; Lahuerta, P.; Barberis, M.; Perez-Prieto, J. *Organometallics* **2001**, *20*, 950-957.

(118) Barberis, M.; Perez-Prieto, J.; Herbst, K.; Lahuerta, P. *Organometallics* **2002**, *21*, 1667-1673.

(119) Bear, J. L.; Kitchens, J.; Willcott, M. R., III *J. Inorg. Nucl. Chem.* **1971**, *33*, 3479-86.

(120) Bon, J. *Davies Group Rotation Report* **2009**.

(121) Thompson, J. L. *Ph.D. Thesis* **2006**, *University at Buffalo, SUNY*.

(122) Davies, H. M. L.; Nagashima, T.; Klino, J. L. *Org. Lett.* **2000**, *2*, 823-826.

(123) Qin, C. *Davies Group Rotation Report* **2009**.

(124) Thompson, J. L.; Davies, H. M. L. *J. Am. Chem. Soc.* **2007**, *129*, 6090-6091.

- Chapter 2 -

Density Functional Studies on the Selectivity of Donor/Acceptor-Substituted Rhodium Carbenoids

2.1 Introduction

Transformations of transient metallocarbenoids, derived from reactions of diazo compounds with a variety of different metal complexes, have become important in mainstream organic synthesis.[1] These species have emerged as versatile intermediates.[1] The rhodium(II)-catalyzed reactions of donor/acceptor-substituted carbenoids have been explored for over two decades, and it has become clear that they display much greater selectivity when compared to the more conventional acceptor-substituted carbenoids.[2-5] A Hammett-analysis of intermolecular cyclopropanation of styrenes with different diazo compounds effectively demonstrates the effect (Scheme 1).[6] The relative reaction rates of methyl phenyldiazoacetate **2.1** with *para*-substituted styrenes *versus* styrene, are strongly influenced by the electronic nature of the styrene (ρ = -0.9 (σ^+ substituent constants)). In comparison, ethyl diazoacetate **2.2** displays no significant selectivity in this study.[6]

Scheme 2.1: Competition reactions with styrene using metallocarbenoids.[6]

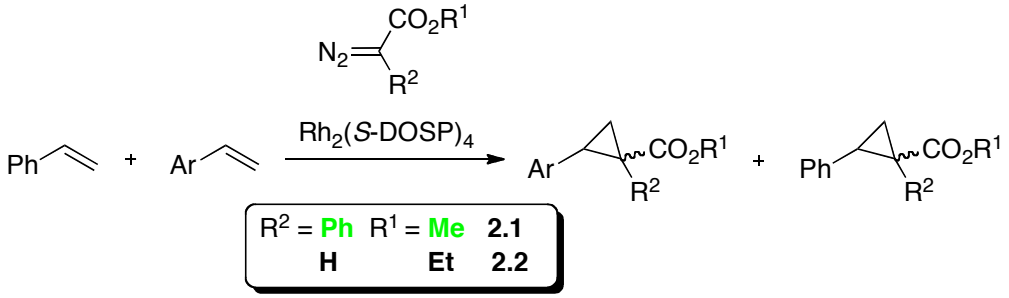

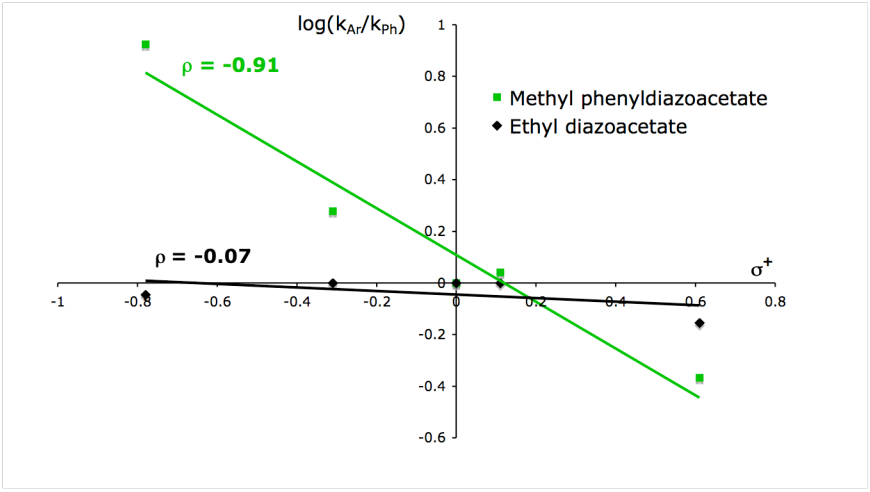

Figure 2.1: Hammett plots of intermolecular cyclopropanation with Rh_2(*S*-DOSP)$_4$.[6]

The greater selectivity of the donor/acceptor carbenoids has made available a number of transformations that were previously not viable with conventional carbenoid-systems (Figure 2.2). In particular, C–C bond forming reactions catalyzed by rhodium(II)-catalysts have found numerous applications in syntheses of biologically relevant compounds and complex natural products.[2] The effectiveness in a number of important intermolecular reaction types, such as cyclopropanation,[7-9] –propenation,[10] [4+3]– and [3+2]-cycloaddition[11-13] is significantly enhanced with donor/acceptor-substituted carbenoids (Figure 2.2). The application of donor-acceptor carbenoids in intermolecular C–H insertions, arguably the most versatile current catalytic technology for enantioselective C–H functionalization, is perhaps the most impressive demonstration of

the synthetic power of these species.[2,4,14-18] Recently, enantioselective intermolecular ylide transformations with allylic alcohols have also been developed that rely on the high selectivity displayed by these carbenoids.[19] The enhanced selectivity has also allowed for a variety of new applications to be developed that were previously not compatible with metallocarbenoid chemistry, such as solid-phase synthesis,[20,21] selective tagging of complex natural products[22] and even functionalization of proteins.[23,24] The emerging qualitative picture is that, the selectivity of these carbenoids is related to their relatively high stability compared to the conventional systems lacking the donor group.[15] However, studies on the extent of the stabilization are few.[14,25] One computational study has described a direct comparison of a donor/acceptor– and acceptor–carbenoid, but only an unsubstituted rhodium vinylcarbenoid model was investigated.[25] The synthetic potential of the donor/acceptor substituted rhodium carbenoids, as demonstrated by the remarkable range of applications, warrants a closer study of their properties and reaction pathways at the microscopic level.

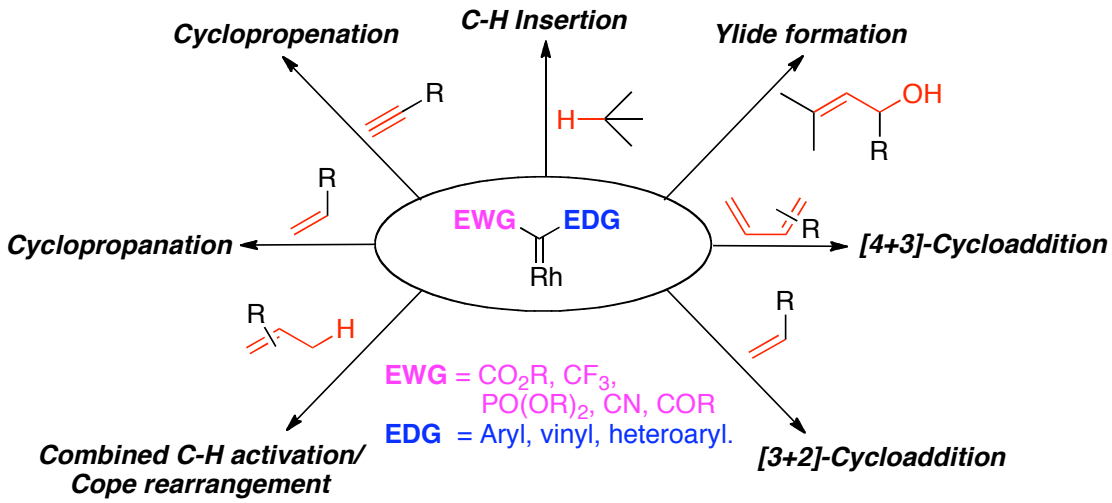

Figure 2.2: Asymmetric synthetic technologies based on donor/acceptor-substituted rhodium carbenoids.[2-5,26-29]

There are only a few reports dedicated to theoretical studies of the *intermolecular* reactions of dirhodium carbenoids,[15,25,30-32] although several studies describe the intramolecular chemistry.[33-35] In-depth information on the details of the mechanism has only emerged from theoretical methods in recent years, however, the current mechanistic picture is strongly supported by experimental observations. Singleton and Davies reported a combined theoretical and experimental study of the cyclopropanation chemistry of the unsubstituted vinyldiazo compound **2.3a** and methyl diazoacetate **2.3b** (Scheme 2.2).[25] The reaction pathway involved complexation of the diazo compounds to dirhodium tetrakisformate, which served as the catalyst model, nitrogen extrusion through **TS-Ia/b** with formation of the carbenoid complexes **2.5a-b**.[25] The nitrogen extrusion barrier through **TS-Ib** was found to be consistent with an experimental activation enthalpy reported by Teyssie et.al.[36] The potential energy surface also shows that the vinylcarbenoid complex is much more stabilized than the acceptor-carbenoid complex,[15] but this was not emphasized in the study. Furthermore, it was reported that the cyclopropanation reaction with styrene for the latter was barrierless, as a located transition structure **TS-IIb** was less stable than the carbenoid.[25] For the vinylcarbenoid model, however, a barrier of 0.5 kcal/mol was found, and it was argued that this small barrier in addition to entropic factors was responsible for the selectivity observed for donor/acceptor-substituted rhodium carbenoids.[25] Another important discovery was the explanation of how diastereoselectivity occurs in these systems. The ester group was found to be the dominant steric interaction disfavoring an approach of the alkene substituent over this moiety. The approach over the donor-group is therefore favored.[25] Hansen and Bonge have reported a closely related computational study of the

intermolecular cyclopropanation chemistry of halo-substituted diazoacetates, and concluded that also these carbenoids could be classified as donor/acceptor-carbenoids as they display relatively high diastereoselectivity.[37] However, such diazo compounds have not yet found much use in synthesis.[37-39]

Scheme 2.2: Potential energies of structures in the reaction between diazo compounds **2.3a-b** reported by Singleton and Davies calculated at the B3LYP/6-31G*[Rh-LA2] level of theory.[25]

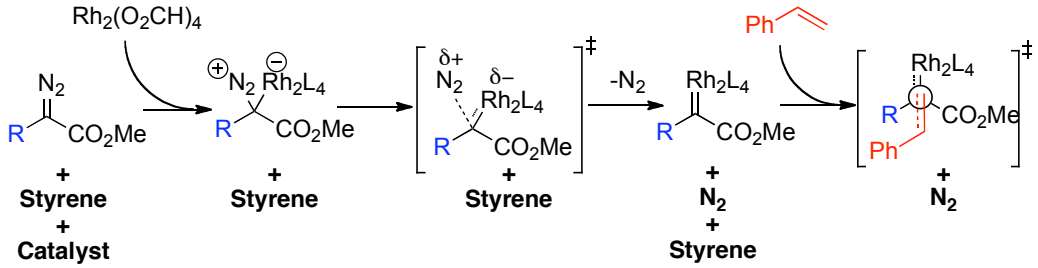

R = **vinyl**	**2.3a**	**2.4a**	**TS-Ia**	**2.5a**	**TS-IIa**
$(E+ZPE)_{rel}$	0.0	-7.9	+3.6	-12.5	-12.1 kcal/mol
R = **H**	**2.3b**	**2.4b**	**TS-Ib**	**2.5b**	**TS-IIb**
$(E+ZPE)_{rel}$	0.0	-12.8	+2.5	-2.6	-5.3 kcal/mol

An important outcome of the Singleton/Davies study was that it resulted in a revision of the transition state model used to explain absolute and relative stereochemistry in the cyclopropanation chemistry.[25] The first generation model for the cyclopropanation reaction had the alkene approaching the carbenoid in an "end-on" approach, over the ester group (Figure 2.3b).[7] Note also that, the chirality of the chiral prolinate catalyst Rh_2(*S*-DOSP)$_4$ was accounted for by placing a steric blocking group in the front right-hand quadrant and the back left-hand quadrant in this model.[7] This could be done since the catalyst was proposed to exist in a D_2-symmetric arrangement in solution, in which the arylsulfonyl groups were arranged in an up-down-up-down arrangement around the

dirhodium core, as shown in Figure 2.3a.[7,26] Since both faces of the dirhodium catalyst are equivalent in this model, the problem reduces to the scheme shown in Figure 2.3b when the carbene ligand is coordinated to the axial site.[7,26] However, it was not necessarily evident from this model what quadrants the blocking groups had to be situated in. The Singleton/Davies study adressed this problem, and it was found that an "end-on" transition state for cyclopropanation was the preferred approach.[25] Furthermore, molecular mechanics calculations on a simplified prolinate catalyst model indicated that the blocking groups would have to be situated in opposite quadrants to what was previously proposed.[25] This led to the second-generation model (Figure 2.3b, right), which accurately accounts for absolute and relative stereochemistry in the cyclopropanation products, as well as an explanation model for the steric influences of various substrates.[25]

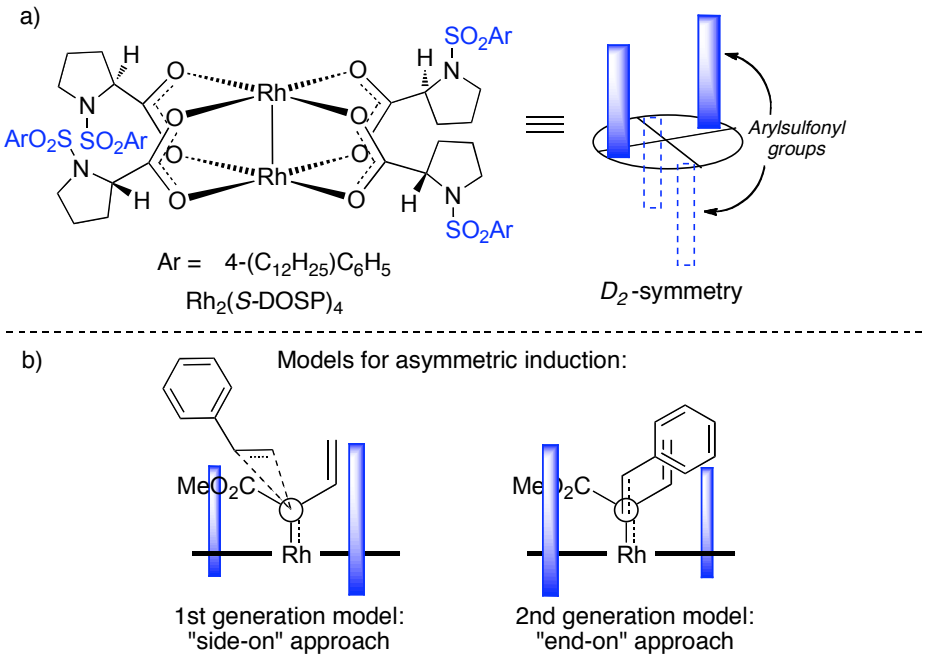

Figure 2.3: (a) D_2-symmetry of Rh_2(*S*-DOSP)$_4$.[7,26] (b) Evolution of models for prediction of asymmetric induction in cyclopropanation chemistry.[7,25]

Although factors influencing the cyclopropanation chemistry have been largely elucidated, it is of interest to extend the analysis to other systems of synthetic importance. For example, the cyclopropenation chemistry of terminal arylacetylenes with aryldiazoacetates is a favorable process that occurs with high stereoselectivity.[10] Recently, the Davies group has also disovered that highly enantioselective cyclopropenation reactions between vinyldiazoacetate **2.6** and terminal alkynes are feasible (Scheme 2.3).[40] However, the reaction does not work with any diazo compounds if the alkyne is disubstituted.[10,40] This observation has been utilized to distinguish between the two proposed approaches of the alkyne towards the carbenoid complex (Figure 2.4).[10] Analogous to the cyclopropanation chemistry, the alkyne can approach in a "side-on" transition state, in which the alkyne is parallell with the rhodium catalyst wall, or in an "end-on" transition state, parallell to the carbenoid Rh–C bond.[10] If the "side-on" approach is accurate, disubstituted alkynes could possibly be accommodated. In the "end-on" model, however, the second substituent would clash into the catalyst "wall" in the transition state. The experimental observations have been interpreted as supporting the "end-on" approach.[10] However, when considering the influence of the chiral prolinate catalyst, a problem is evident. As the alkyne is neither approaching over the donor nor the acceptor-group, but along the carbenoid axis, both prochiral faces of the carbenoid should be equally exposed to the alkyne – and hence lead to no asymmetric induction.[10,40] An explanation of how effective asymmetric induction occurs is still not available in this chemistry as the exact transition state is unknown.

Scheme 2.3: Cyclopropenation of alkynes.[40]

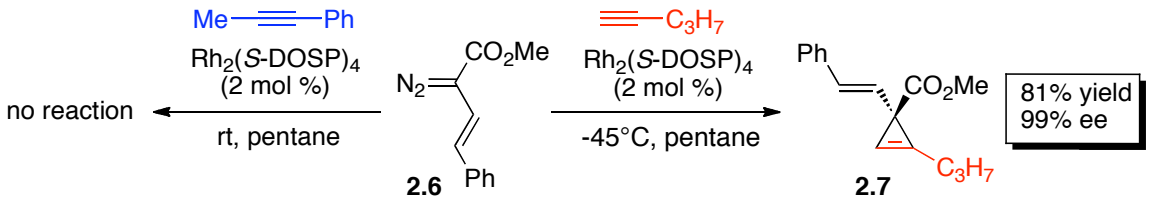

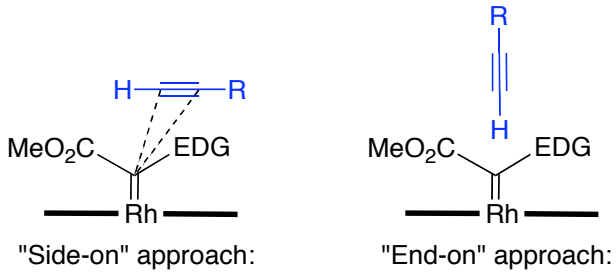

Figure 2.4: Proposed approaches of terminal alkynes towards the rhodium carbenoid.[10]

Selective C–H functionalization is one arena of widespread current interest. The versatility and novelty introduced when considering C–H bonds as functional groups, could have enormous impact on the practice of retrosynthetic analysis.[2,16,17] Directed oxidative addition of C–H bonds with metal complexes has been explored for several years, but is still only applicable to select system.[17,41] Intramolecular carbenoid C–H insertions have also been developed exhaustively and found many applications.[34,42-45] Selective *intermolecular* C–H functionalization was only realized with the introduction of the donor/acceptor-substituted rhodium carbenoids.[14,46] This approach has since been explored extensively and found many applications in complex molecule synthesis.[4,16,28,47] Computational studies of rhodium carbenoid C–H insertions published to date do not offer detailed insights into the differential nature of donor/acceptor *versus* acceptor systems or the influence of these carbenoids towards activation of C–H bonds of different electronic character.[25,32,35]

The leading computational study of intermolecular C–H functionalization to date is that of Nakamura et. al. for reactions of diazomethane and **2.3b** with methane and other simple hydrocarbons.[32] Several important mechanistic details of the C–H insertion events were extracted from the study that influence the course of the reaction. Also the role of the dirhodium paddlewheel catalyst scaffold in this chemistry was studied.[32] At the carbenoid stage of the catalytic cycle (**2.5b**), it was proposed that the dirhodium core had acted as a redox pool, affording a formal Rh(III)-carbenoid appended with a *trans*-Rh(I) "ligand" (Scheme 2.4).[32] The cationic nature of the rhodium carbenoid end would induce high electrophilic reactivity at the carbenoid carbon, a feature believed to be important in, for instance, cyclopropanation chemistry. The hydrogen of the C–H bond to be functionalized, would then initiate a hydride transfer process towards the carbenoid carbon, which involves interactions between the filled C–H bonding σ-orbital and the carbenoid p-orbital (LUMO of carbenoid complex).[32] This would result in positive charge build-up at the carbon to be functionalized in the transition state **TS-III**, and the C–C bond formation then occurs (Rh–C bond cleavage is assisted by the second rhodium).[32] These events would occur in a concerted, but asynchronous manner, consistent with previous proposals.[14,32,46]

Scheme 2.4: C–H functionalization mechanism studied by Nakamura et. al.[32]

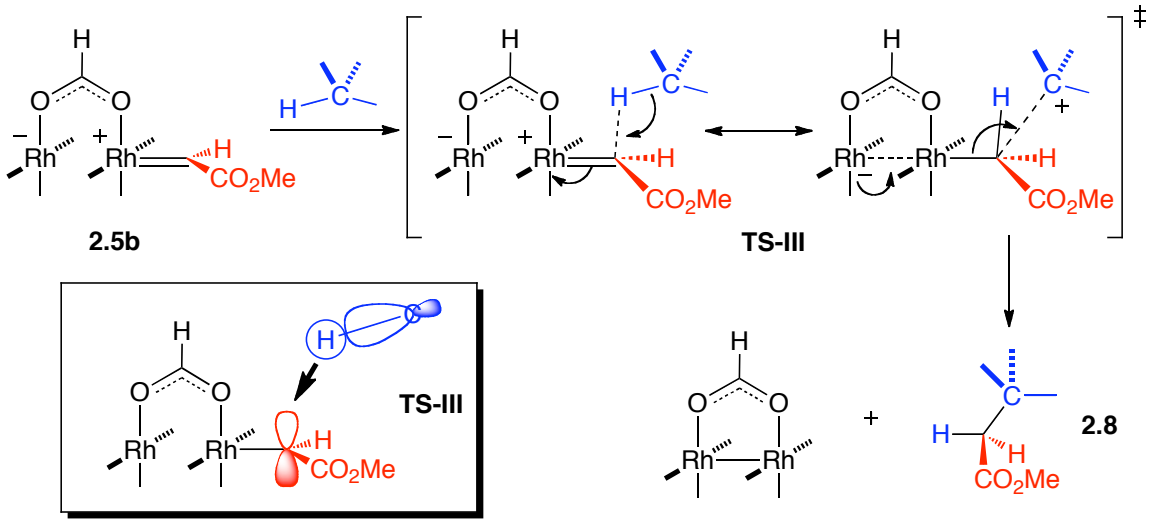

The studies of Nakamura and co-workers had large impact of how the C–H functionalization events would be considered.[32] The initial hypothesis related to asymmetric C–H insertions of donor/acceptor-substituted carbenoids, was analogous to the first generation model for the cyclopropanation chemistry.[7] The substrate was believed to approach over the ester group with the C–H bond in a "side-on" orientation (Figure 2.5).[4,14,46,48] The preferred orientation of the other three groups on the substrate (S = small size group, M = medium size group and L = large size group) was readily rationalized based on this, as the small group would prefer to be into the plane towards the bulky carbenoid, and the large group away from the catalyst "wall".[14,46] The correct absolute and relative stereochemistry could be predicted from this model. The studies of Nakamura[32] and Singleton/Davies[25] showed, however, that the C–H bond would likely approach more in an "end-on" manner and that the blocking groups (influence of the chiral prolinate catalyst), most likely were situated in opposite quadrants to what was first hypothesized.[25] Although the studies by Nakamura were only based on an acceptor-substituted rhodium carbenoid system, these results led to a second-generation model for

the C–H insertion event (Figure 2.5, right).[32,49] Although widely applied in the Davies group, this model was never published.[49] To obtain a more complete picture of the C–H functionalization event with donor/acceptor-substituted rhodium carbenoids, further studies would be required.

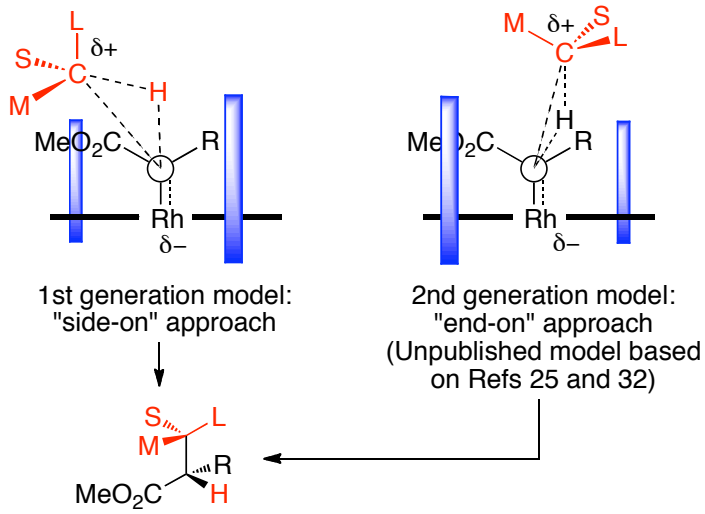

Figure 2.5: First and second generation models of intermolecular C–H insertion.[14,46,49]

A well-established C–H functionalization reaction is the so-called combined C–H activation/Cope rearrangement (CHCR, Scheme 2.5).[50-60] This occurs when a substrate containing an allylic C–H bond (**2.9**) reacts with a vinyldiazoacetate **2.10** through a reaction believed to involve a C–H insertion event interrupted by a Cope rearrangement, as depicted in **TS-IV**.[55] The product **2.11** is that of a formal C–H insertion followed by a Cope rearrangement. This reaction has been demonstrated, in a plethora of applications, ranging from medicinal syntheses to complex molecule assembly, to be a valuable tool in organic synthesis (Chart 2.1, Scheme 2.6).[50-55,57-61] The extremely high diastereoselectivity and asymmetric induction that can be achieved in selected systems (>99% ee, >50 : 1 d.r.), have added significant momentum to the chemistry. The current empirical model for the prediction of stereochemical outcome is based on the transition

state hypothesis **TS-IV**, involving a chair-like structure.[50,52] Although the synthetic utility may be unquestionable, and the model gives the correct predictions, the exact mechanism of the transformation is totally unknown. Further developments of reaction and catalyst design in this chemistry would require a detailed knowledge of the mechanism and substrate orientation that is involved.

Scheme 2.5: The combined CH activation/Cope rearrangement reaction.

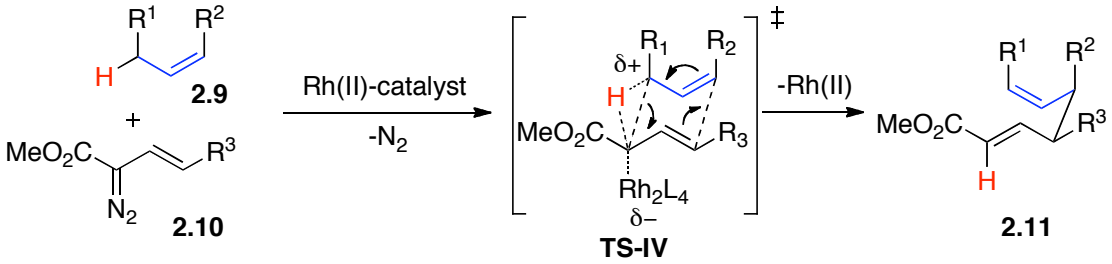

Chart 2.1: Complex marine natural products synthesized using the CHCR reaction.[51,52,61]

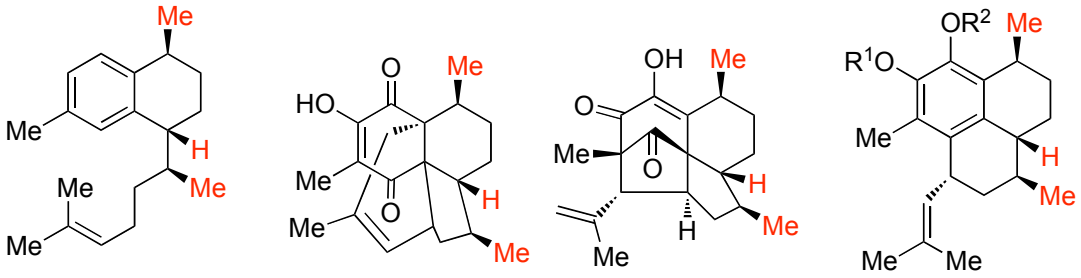

Scheme 2.6: Application of the CHCR reaction in medicinal synthesis.[58]

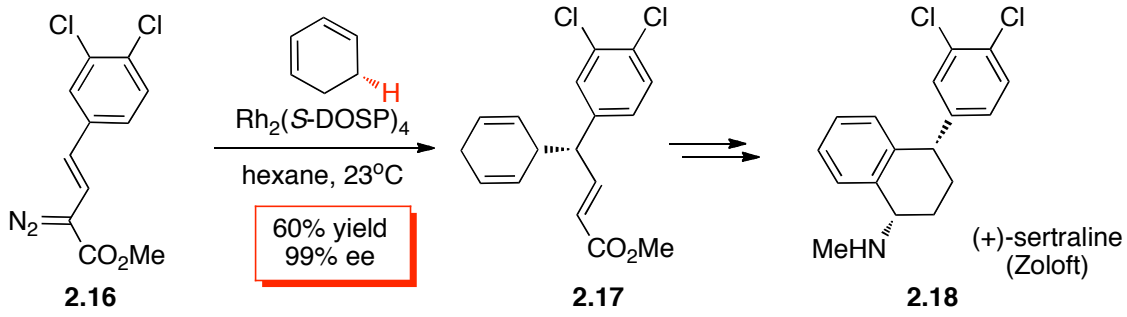

In this chapter, a DFT study of the mechanism of reactions between diazo compounds and dirhodium(II) carboxylates will be presented. Several computational studies have been conducted on rhodium-carbenoids, the more recent ones using the B3LYP hybrid functional with a composite basis set consisting of LANL2DZ on Rh and 6-31G* on smaller atoms.[25,32,33,62] This combination has been demonstrated to give reasonably accurate results.[25,32] In the studies presented herein, however, a more flexible basis set for rhodium has been applied,[15] resulting in a more accurate description of the heavy atom fragments. The results have been related to the previous calculations. The studies will attempt to shed light on several of the unanswered questions that were presented in the above introductory text: (1) what is the influence of donor/acceptor substituted rhodium carbenoids *versus* acceptor-only carbenoids on cyclopropanation reactions and C–H functionalization chemistry? (2) What is the preferred substrate orientation in intermolecular C–H insertions of donor/acceptor substituted rhodium carbenoids? (3) What is the exact structure of the transition state involved in the cyclopropenation chemistry of these carbenoids, and how does this influence the predictive model for absolute stereochemistry? (4) What is the likely mechanism of the Combined C–H activation/Cope rearrangement and what controls selectivity in this reaction? This chapter will describe efforts to address these important problems through quantum-chemical calculations.

2.2 Results And Discussion

2.2.1 On the Selectivity of Donor/Acceptor *versus* Acceptor-only Rhodium Carbenoids

Basis sets and cyclopropanation chemistry. The detailed energetics involved in reactions of diazo compounds with dirhodium complexes from previous density functional studies were shown to be fairly consistent with experimental kinetic parameters and kinetic isotope effect studies.[25,32] Singleton and Davies studied reaction models of methyl diazoacetate (**2.3b**) and methyl vinyldiazoacetate (**2.3a**) (acceptor-only and donor/acceptor systems).[25] The acceptor-only carbenoid (derived from **2.3b**) displayed a barrierless reaction with styrene, whereas the vinylcarbenoid reaction had a barrier of +0.5 kcal/mol (the zero-point energy corrected potential energy surface was reported at the B3LYP/6-31*[Rh-LA2] level of theory).[25] The small potential energy barrier and entropic factors combined, were suggested to result in the observed high selectivity in the cyclopropanation reactions of donor/acceptor-substituted rhodium carbenoids.[25] However, the small potential energy barrier, even for the simple model system, was not consistent with experimental studies demonstrating that donor/acceptor carbenoids are quite selective.[2,4,6,7] For example, the competition studies previously reported in the cyclopropanation chemistry of aryl– and vinyldiazoacetates, indicated that the flexibility of the barrier (with respect to the variation in substituent effects) must be at least ~1.8 kcal/mol, which should be reflected as electronic effects, in order to give the observed substituent effects.[6] One hypothesis was that, the barrier of the carbenoid trapping step in the catalytic cycle was not adequately described by the 6-31G*[Rh-LA2] basis set used, which could be the cause of the low predicted barrier.[15] It was decided to

employ a basis set for Rh that would offer more flexibility in the valence shell [Stuttgart RSC 1997 ECP][63-65], further augmented with a 4f polarization function,[15,66] as described in the literature for other rhodium-catalyzed reactions,[66] to obtain a more accurate description of rhodium (See Experimental Section for more details). To evaluate the performance of the new composite basis set, the geometry of $Rh_2(OAc)_4 \bullet 2H_2O$ was fully optimized and shown to reproduce the published x-ray crystallographic data for this complex[67] (Figure 2.6). For comparison, structural parameters obtained with B3LYP/6-31G*[Rh-LA2] by Nakamura are also included.[32] Overall, five out of the seven indicated structural parameters were improved using the new basis set. The bond between rhodium and the axial substituent (H_2O) was particularly interesting, as the new predicted value was much more accurate than with the former basis set (2.6% *versus* 3.8% difference between calculations and experiments). This may be of great importance in this work, since axially coordinated carbenes are the main topic.

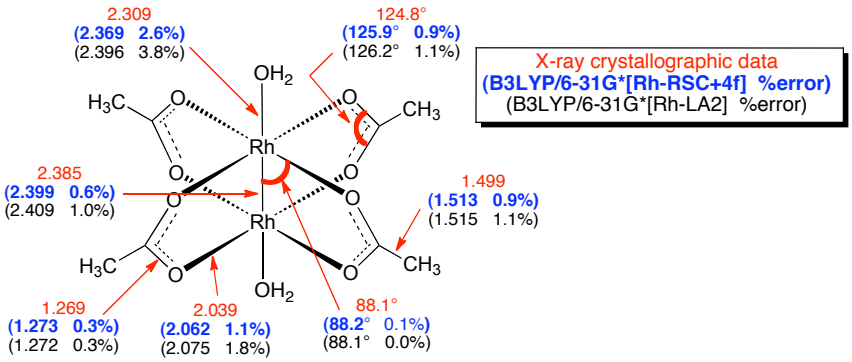

Figure 2.6: The structure of $Rh_2(OAc)_4 \bullet 2H_2O$. Bond lengths (Å) and bond angles are indicated. X-ray crystallographic data in red,[67] calculated average values with the 6-31G*[Rh-RSC+4f] basis set in **blue** and calculated average values with the 6-31G*[Rh-LA2] basis set in black.[32]

The cyclopropanation reaction pathway for the vinyldiazoacetate model **2.3a**, previously described by Singleton/Davies (Figure 2.7),[25] was re-evaluated with the composite basis set 6-31G*[Rh-RSC+4f].[15] A barrier of +2.4 kcal/mol (zero-point corrected potential energies) for the cyclopropanation step was identified (Figure 2.7, black pathway), about 1.9 kcal/mol higher than the previously reported barrier.[25] Further evaluation at the B3LYP/6-311G(2d,2p)[Rh-RSC+4f]//B3LYP/6-31G*[Rh-RSC+4f] level gave $\Delta E^{\neq}$ = 3.0 kcal/mol for this barrier. These results are more consistent with the observed selectivity in the cyclopropanation chemistry.[6] Although the composite basis set described herein gave a significantly altered barrier for the carbenoid trapping step, the remainder of the pathway was in good agreement with previously described energetics. However, overall higher stability of all the stationary points on the potential energy surface were predicted.[15]

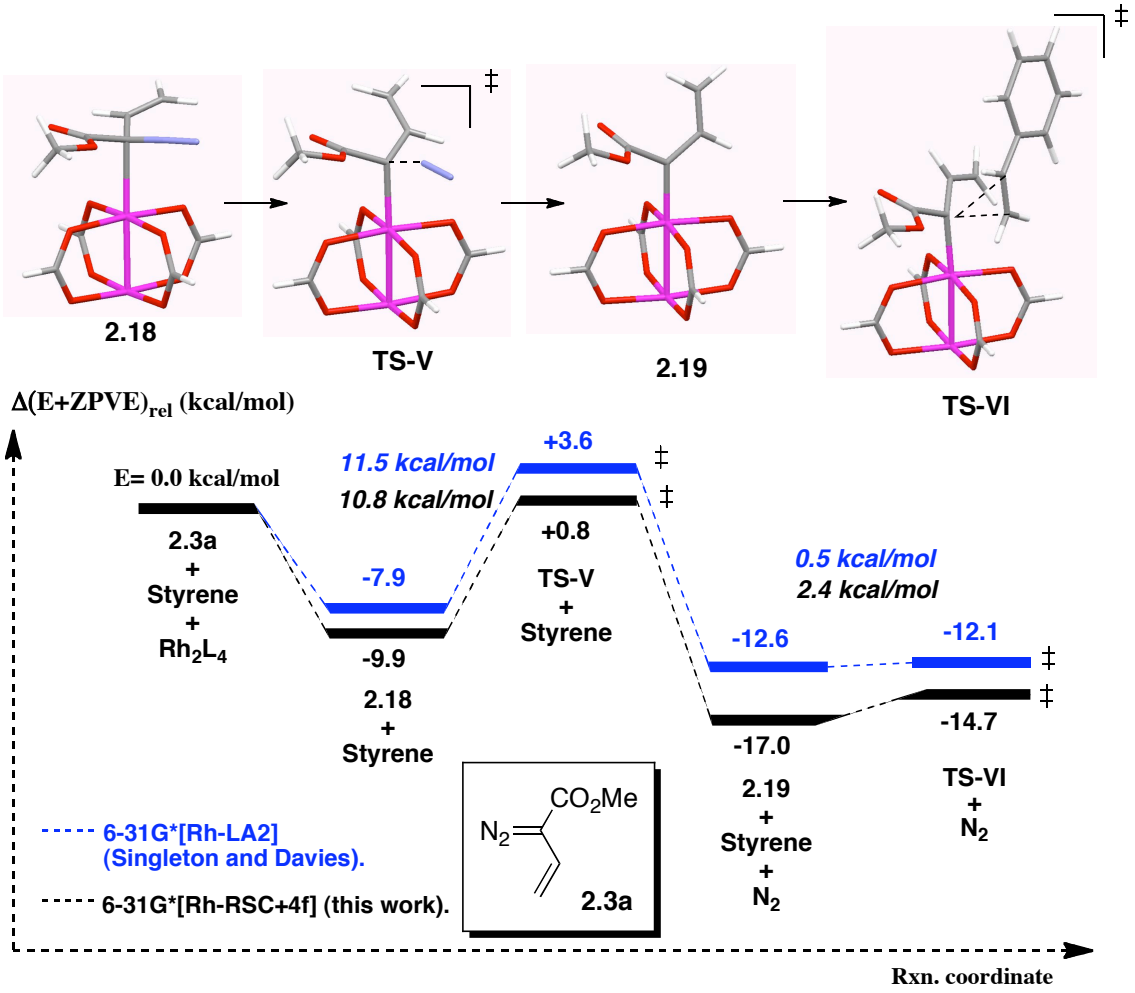

Figure 2.7: Comparison of metal basis set influence on reaction pathway. Energies (B3LYP+ZPVE) are given in kcal/mol. Structures of key intermediates **2.18** through **TS-VI** are shown above.[15,25]

The most common precursors used to generate donor/acceptor-substituted rhodium carbenoids are aryldiazoacetates. Methyl phenyldiazoacetate **2.3c** can be regarded as the parent compound for this class.[6,59] It was desired to expand the computational model studies to the reaction between **2.3c** and styrene, as it represents a more commonly employed selective carbenoid transformation.[5] Furthermore, a comparison with the cyclopropanation chemistry of methyl diazoacetate **2.3b** would be of interest, with

emphasis on how the former is able to undergo more selective reactions. As a catalyst model, dirhodium tetrakisformate, $Rh_2(O_2CH)_4$, has been employed. This is the simplest rhodium carboxylate complex, and it has been demonstrated to be a suitable carboxylate model in previous computational studies.[25,32,37] This complex does not have much synthetic utility because of its low solubility in most organic solvents.[37] The potential energy surface for the reaction pathway is reported relative to the free reactants. Solvent effects have not been taken into account, mainly because the chemistry is often carried out in non-polar hydrocarbon solvents, such as pentane or hexane, which have negligible dielectric constants. Also, the main interest of this study lies in the different intrinsic electronic effects of the model systems. The mechanism evaluated in the calculations is shown in Scheme 2.7, and is related to that of Yates for Cu-chemistry.[1,32,68,69]

Scheme 2.7: Reaction pathway for carbenoid formation and cyclopropanation of styrene.[15,25]

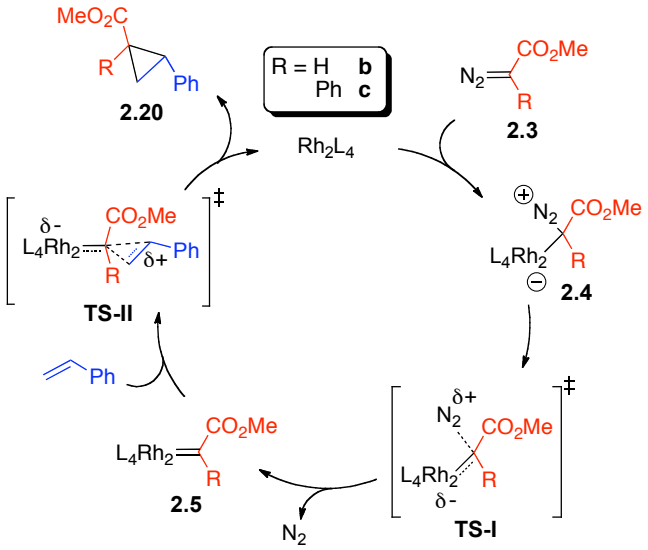

Figure 2.8 shows the calculated reaction coordinate potential energy surfaces for **2.3c** (red) and **2.3b** (black) in the cyclopropanation of styrene.[15] Coordination of **2.3c** to the dirhodium catalyst through the carbon bearing the diazonium moiety, is exoergic by -7.4 kcal/mol (Figure 2.8). The same event for **2.3b** is even more exoergic by -10.7 kcal/mol. The exoergicity of this step is consistent with previous findings.[25] A potential energy barrier of +11.3 kcal/mol for nitrogen extrusion from **2.4c** must be overcome in order to form the metallocarbenoid complex **2.5c**. The latter is stable relative to free reactants (**2.3c** + styrene + catalyst) by -16.5 kcal/mol. Adduct **2.4b** undergoes the nitrogen extrusion facing a +11.9 kcal/mol potential energy energy barrier. The gas-phase activation enthalpy for this step can be calculated from the B3LYP/6-31G*[Rh-RSC+4f] calculations, and was found to be $\Delta H^{\neq}$ = +13.4 kcal/mol. This can be compared to results obtained in a kinetic study of the reaction of ethyl diazoacetate and styrene, catalyzed by rhodium acetate, reported by Teyssié et. al.[36] $\Delta H^{\neq}$ = +15.0 kcal/mol was reported, based on an Eyring-analysis,[36] which compares reasonably well with the predicted activation enthalpy. It should be noted, however, that application of the Eyring equation is only strictly appropriate for elementary reaction steps, which would render it questionable what quantity the experimental value is actually describing in the study. The predicted energies are also consistent with observed Michaelis-Menten kinetics in these reactions, as reported by Pirrung and et. al.[70] An estimated free energy barrier for a diazoketone system was reported to be +13.3 kcal/mol, which can also be compared to the calculations herein.[70] Similar values have also been obtained in previous computational studies.[25,32] The acceptor-substituted carbenoid **2.5b** is less stable than complex **2.4b**, which renders the nitrogen extrusion process endoergic by +5.1 kcal/mol. A

cyclopropanation transition structure for reaction with styrene could not be located for reaction with **2.5b**. Similar results were reported by Singleton/Davies, and the studies concluded that this process had no potential energy barrier.[25] An approximate transition structure, estimated from the free energy surface through an iterative procedure, was reported.[25] However, this structure was more stable than the carbenoid complex **2.5b** .[25] These observations are in agreement with the aforementioned Hammett-study.[6] The phenyl-substituted carbenoid complex **2.5c** displays a potential energy barrier of +4.5 kcal/mol for the cyclopropanation reaction with styrene. The existence of this barrier is strongly associated with the high stability of the carbenoid. This stability renders the nitrogen extrusion process (**2.4c→2.5c**) exoergic by -9.1 kcal/mol.

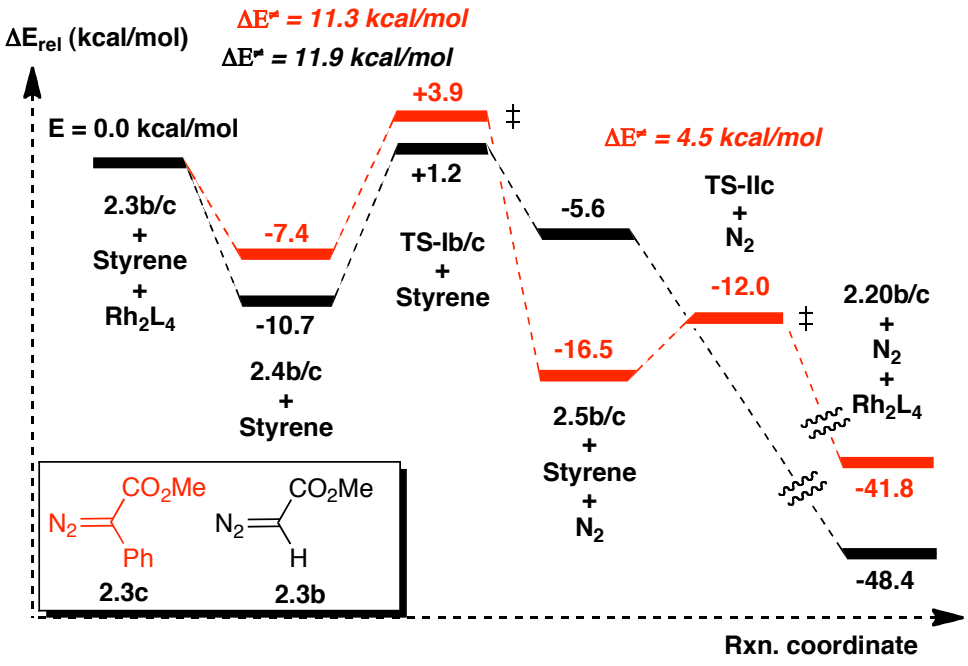

Figure 2.8: Calculated relative energies on the potential energy surface for **2.3b-c** in the cyclopropanation reaction with styrene. [15]

Figures 2.9 and 2.10 show the theoretical structures of intermediates and transition states involved in the reactions by **2.3b** and **2.3c** respectively.[15] The cyclopropanation transition state **TS-IIc** is relatively early and highly asynchronous (Figure 2.9). The C_1-C_3 bond order in the TS is 0.23, whereas C_2–C_3 have only slight bond formation (BO = 0.09).[15] These observations are consistent with a concerted, highly asynchronous transition state. The accuracy of this transition structure has also been supported by comparison of experimental and predicted kinetic isotope effects in B3LYP/6-31G*[Rh-LA2] calculations.[25] The Rh–C bond is somewhat elongated relative to free carbenoid complex **2.5c** (2.130 *vs* 2.010 Å).

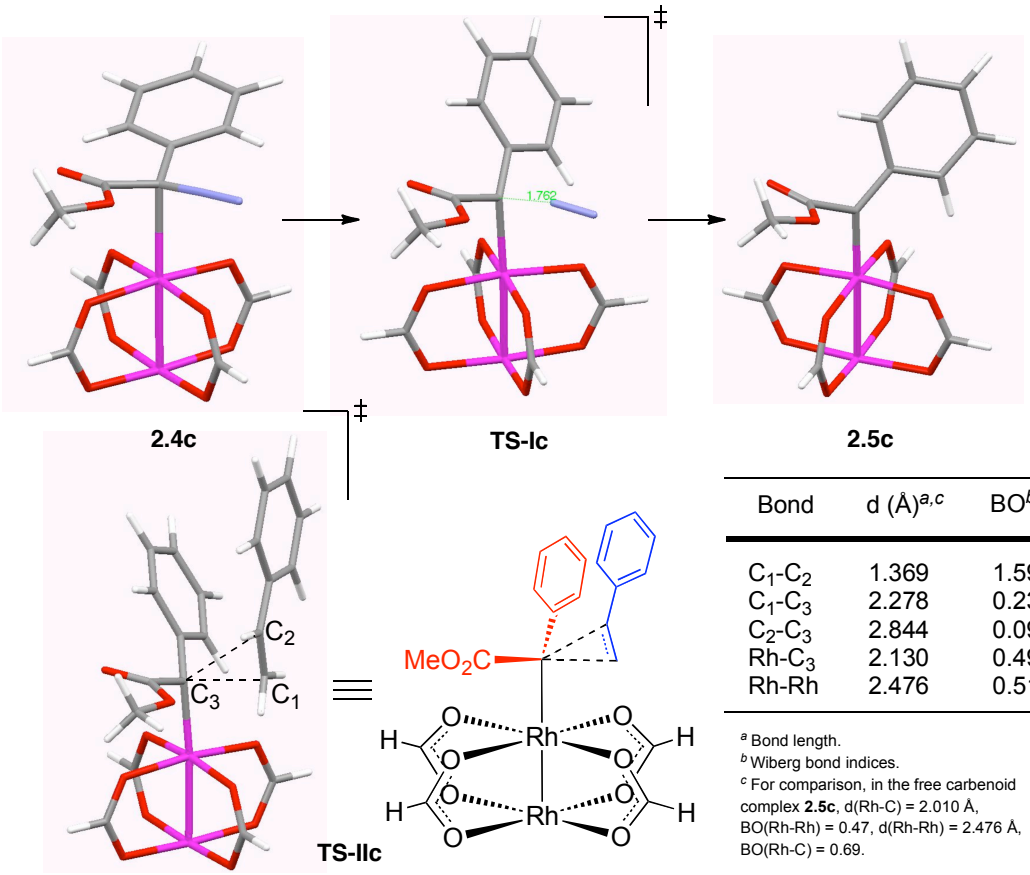

Bond	d (Å)[a,c]	BO[b,c]
C_1-C_2	1.369	1.59
C_1-C_3	2.278	0.23
C_2-C_3	2.844	0.09
Rh-C_3	2.130	0.49
Rh-Rh	2.476	0.51

[a] Bond length.
[b] Wiberg bond indices.
[c] For comparison, in the free carbenoid complex **2.5c**, d(Rh-C) = 2.010 Å, BO(Rh-Rh) = 0.47, d(Rh-Rh) = 2.476 Å, BO(Rh-C) = 0.69.

Figure 2.9: Theoretical structures for the pathway with **2.3c**.[15]

One important geometrical feature of the carbenoid **2.5b** *vs* **2.5c** is the preference of alignment on the rhodium active site (Figure 2.10).[15] Whereas **2.5b** prefers an eclipsed conformation, carbenoid **2.5c** adopts a staggered arrangement. There is an intrinsic electronic preference for the eclipsed conformation, however the phenyl group does not permit this conformation for carbenoid **2.5c**. These observations could have major implications for models that have been developed for chiral dirhodium systems,[1,4,7] since the preferred orientation of the two carbenoids will be different with respect to a given chiral ligand arrangement.

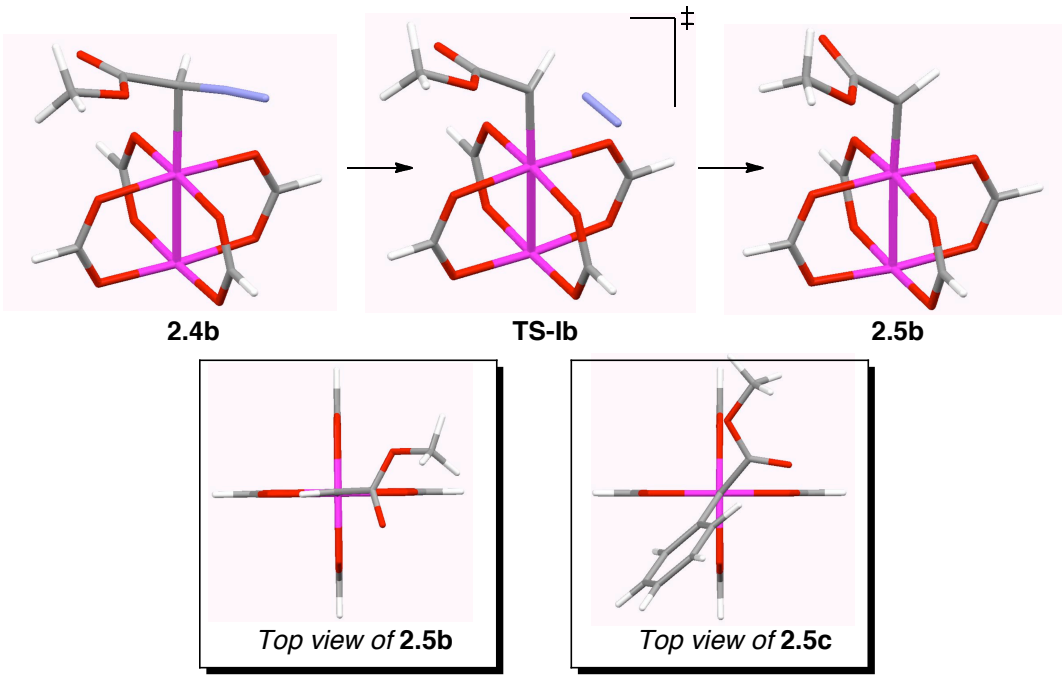

Figure 2.10: Theoretical structures for the reaction with **2.3b**. Top view of both carbenoids.[15]

C–H insertion chemistry. The aforementioned carbenoid systems were next studied in C–H insertion reactions. Two model substrates were chosen for this study; (1) cyclopentane and, (2) 1,4-cyclohexadiene. Both these substrates have been demonstrated

to give selective C–H insertions with donor/acceptor-substituted rhodium carbenoids,[14,71] and are of interest because of their difference in reactivity.[14] Competition studies have showed that the relative rate of insertion of carbenoid **2.5c** (with Rh_2(*S*-DOSP)$_4$ as catalyst) into 1,4-cyclohexadiene *versus* cyclopentane is approximately 42,400 : 1.[14] Because of this large difference in reactivity, cyclopentane requires very slow addition of the carbenoid precursor under moisture and air-free conditions,[14] whereas 1,4-cyclohexadiene undergoes facile insertion,[71] even under neat conditions.[72] These model systems will give insights into how two extremely different C–H bonds undergo the C–H insertion event. A comparison with acceptor-only carbenoid **2.5b** will shed light on how the two carbenoids behave differently in this chemistry.

Figure 2.11 shows the potential energy surface for C–H functionalization of cyclopentane with carbenoids **2.5b-c** (Scheme 2.8, Figure 2.11).[15] The phenyl-substituted carbenoid **2.5c** undergoes C–H insertion with a potential energy barrier of +17.4 kcal/mol, whereas carbenoid **2.5b** displays a barrier of only +3.5 kcal/mol. This value can be compared to that reported by Nakamura et. al. for insertion into the methylene C–H bond of propane (+0.2 kcal/mol) at the B3LYP/6-31G*[Rh-LA2] level of theory.[32] As the carbenoid derived from ethyl diazoacetate (**2.2**) displays some selectivity in C–H insertions of branched alkanes, it is expected that a small barrier would exist.[4] The large barrier for carbenoid **2.5c** is consistent with a considerably more selective reaction. Both carbenoid systems give overall very exoergic reactions (-50.1 and -56.2 kcal/mol respectively). The difference in barrier heights is primarily due to the stability of carbenoid **2.5c**, which in turn leads to a relatively much later transition state. This further implies that more steric interactions are involved between the substrate and the carbenoid

substituents. A significantly higher charge build-up in the donor/acceptor-substituted system results from this. The charge on the carbon to be functionalized (Mulliken charges) increases from -0.27q in free cyclopentane to -0.17q in the transition state (Δq = +0.10). In comparison, the same change in charge for carbenoid **2.5b** is only Δq = +0.05, consistent with a much earlier transition state.[32] These calculations interestingly predicts that, C–H insertion with carbenoid **2.5c** will have a much higher potential energy barrier (+17.4 kcal/mol) than the nitrogen extrusion step through **TS-Ic** (+11.3 kcal/mol). Gibbs free activation energies from the B3LYP/6-31G*[Rh-RSC+4f]-calculations were +32.3 kcal/mol (C–H insertion step) and +10.4 kcal/mol (nitrogen extrusion step), strongly suggesting that the functionalization process is rate-limiting. The functionalization process is highly exoergic by -50.1 kcal/mol and -56.2 kcal/mol for carbenoids **2.5c** and **2.5b**, respectively.

Scheme 2.8: C–H functionalization of cyclopentane.

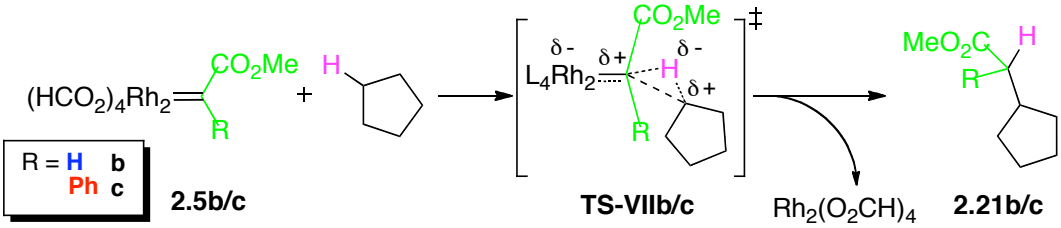

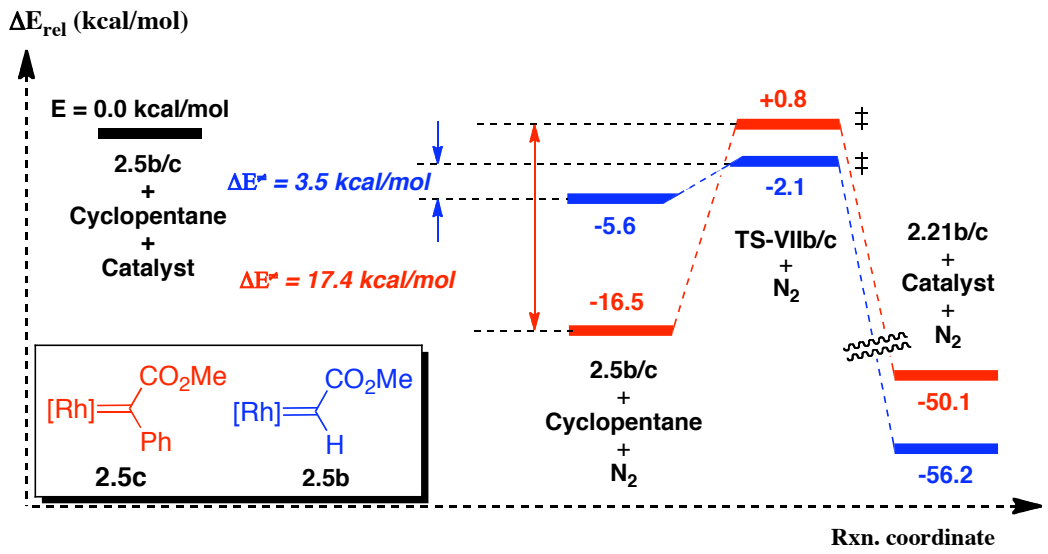

Figure 2.11: Relative energies on the potential energy surface for C–H functionalization of cyclopentane. Values are given in kcal/mol.[15]

1,4-cyclohexadiene is significantly more activated towards carbenoid C–H insertions (Scheme 2.9, Figure 2.12).[71,72] Since the C–H bonds are doubly allylic, they are expected to be much weaker than in alkanes because of hyperconjugative interactions of the type π(C=C)→σ*(C–H).[29] Transition states for insertions with both carbenoids **2.5b** and **2.5c** were located, and were found to display much smaller activation barriers than in their reactions with cyclopentane, consistent with the more reactive nature of 1.4-cyclohexadiene. A potential energy barrier of +6.2 kcal/mol for insertion of carbenoid **2.5c** was predicted. In contrast, a barrier of only +1.2 kcal/mol was found for **2.5b**. Experimentally, the cyclopropanation of the double bond is a much more favorable reaction in the latter case.[71]

The forward intrinsic reaction coordinate drive from **TS-VIIIc** did not afford insertion product directly. The system appeared to undergo a hydride transfer to the carbenoid and then reach a very flat area of the potential energy surface following this event. Geometry

optimization in this area gave a zwitterionic structure **2.23c** (Figure 2.12), with a rhodium coordinated enolate and a closly associated cyclohexadienyl cation (C–C distance = 2.574 Å). Although this structure appeared to lie in an energy minimum, a relaxed scan of the C–C bond forming coordinate showed that the pathway towards product displayed no barrier (see Experimental Section). The wavefunction stability was also confirmed here by stability analyses for **2.23c** and **TS-VIIIc**.[73,74] It is believed that the flat nature of the PES makes it problematic for the optimization algorithm and may have caused the job to converge. Nevertheless, these observations convincingly show that, systems with very good positive charge stabilizing abilities, proceed by a very asynchronous, almost step-wise, hydride transfer/C–C bond formation mechanism. Full hydride transfer pathways have been reported for certain carbenoid systems in the literature, and therefore strongly supports the mechanistic predictions by Nakamura et. al. and the work presented herein.[32,75] The reaction with carbenoid **2.5b** did not have a similar charge-separated structure, but afforded the insertion product **2.22b** directly.

In terms of the overall reaction energy, carbenoid system **2.5b** was highly exoergic by -55.5 kcal/mol. The reaction of carbenoid **2.5c** has a predicted exoergicity of -49.1 kcal/mol. The energy surface again shows that, the high reactivity of carbenoid **2.5b** is because of its instability. The stabilization present in the donor/acceptor carbenoid **2.5c** leads to a significantly higher energy barrier.[15]

Scheme 2.9: C–H insertions with 1,4-cyclohexadiene.

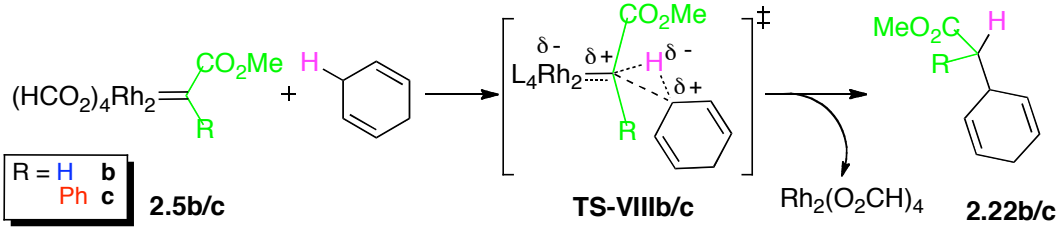

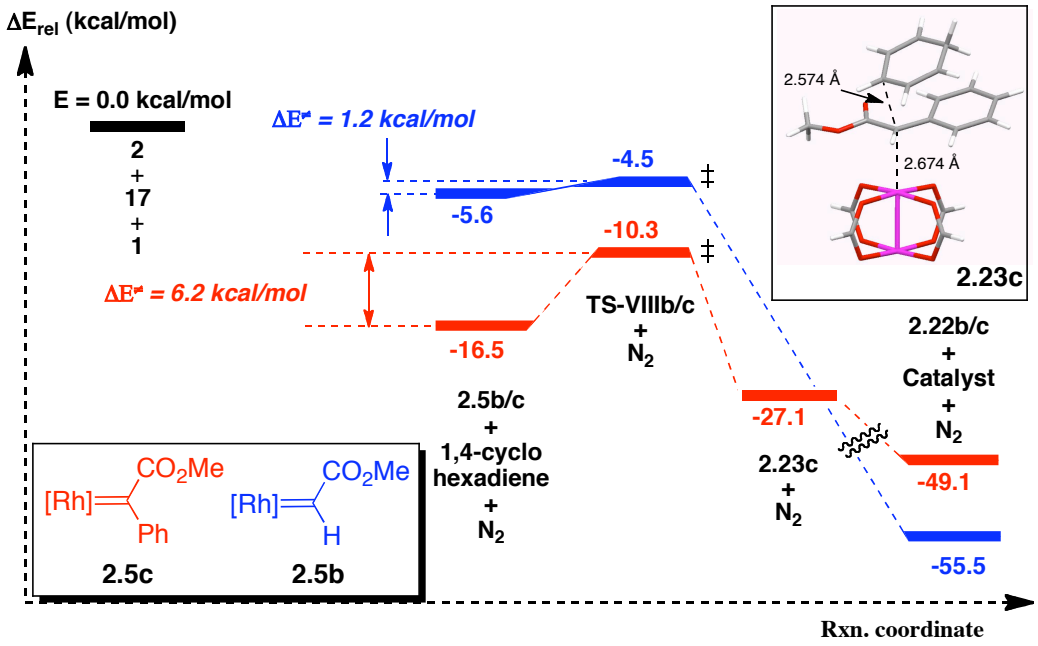

Figure 2.12: Relative energies on the potential energy surface for C–H functionalization of 1,4-cyclohexadiene.[15]

This study is qualitatively in good agreement with experimental results which indicate that 1,4-cyclohexadiene and styrene are much more reactive substrates than cyclopentane towards carbenoid **2.5c**.[14] Table 2.1 shows an overview of contributions from activation enthalpies and entropies to the Gibbs free activation energy, based on gas-phase B3LYP/6-31G*[Rh-RSC+4f]-calculations. It is clear that for both C–H insertion events, the entropic contribution to the free activation barrier are the same (14.1 kcal/mol), and that the reactivity difference between the two originates from enthalpic differences only. This is consistent with the relative bond strengths of the two substrates.[14] Furthermore, 1,4-cyclohexadiene has a higher enthalpic barrier to reaction than does styrene. The origin of the higher reactivity of the former, stems from the smaller entropic barrier involved in the C–H insertion event compared to the cyclopropanation.

Table 2.1: Contributions from gas-phase activation enthalpies and entropies to the Gibbs free activation energy for trapping of carbenoid **2.5c** at 298K.

Entry	*Trap*	$\Delta H^{\ddagger}$	$-T\Delta S^{\ddagger}$	$\Delta G^{\ddagger}$
		(kcal/mol)		
1	Styrene	4.54	15.4	19.9
2	1,4-Cyclohexadiene	4.63	14.1	18.7
3	Cyclopentane	18.3	14.1	32.3

Transition states. The theoretical transition state geometries, selected bond lengths and bond orders for the C–H insertion reactions of carbenoid **2.5c** are shown in Figure 2.13.[15] Insertion with 1,4-cyclohexadiene occurs with an early transition state which displays only hydride transfer character ($BO(C_5\text{-}H_1) = 0.36$), although not very pronounced compared to **TS-VIIc**. C–C bond formation is not evident from the structure (BO = 0.13). A C–H–C bond angle of 165° supports this observation as well. For the cyclopentane system, significant differences can be observed. A much later transition state is observed relative to **TS-VIIIc**. Furthermore, **TS-VIIc** reveals considerably advanced Rh–C bond breakage (2.320 Å, BO = 0.26). An almost complete hydride transfer is evident in this transition state ($BO(C_7\text{-}H_2) = 0.69$) along with a high degree of the C–C bond developed (BO = 0.36).[15] This analysis is in good agreement with that of Nakamura[32] for C–H insertions with **2.3b** and diazomethane, in which the hydride transfer component was also described as dominant in the transition state. However, it was claimed that, for C–H insertion processes, the Rh–C bond cleavage process was more important than having a very electrophilic carbenoid, and *vice versa* for cycloaddition chemistry. The results presented here indicate that, if the C–H bond is very activated, similar transition state

characteristics are present in both the C–H insertion and cyclopropanation chemistries. C–C bond formation is considerably more progressed in the transition state for less activated substrates. A more asynchronous event is characteristic for very reactive traps, such as styrene and 1,4-cyclohexadiene.[15]

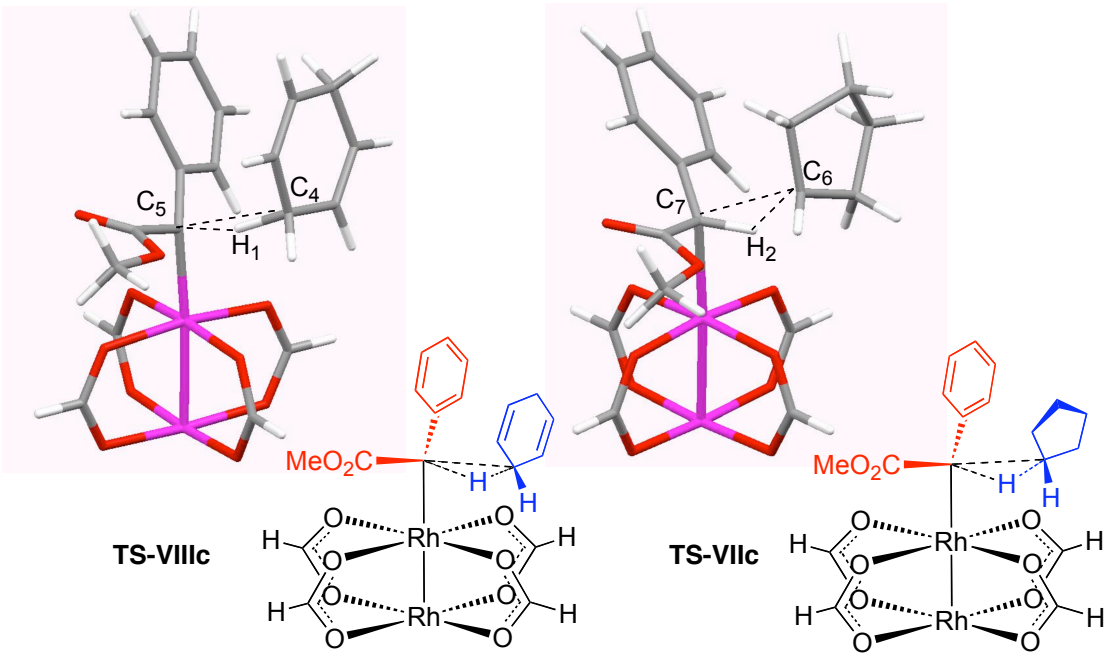

Bond	d (Å)[a]	BO[b]
C_4-C_5	2.662	0.13
C_5-H_1	1.419	0.36
C_4-H_1	1.266	0.51
Rh-C_5	2.137	0.45
Rh-Rh	2.474	0.52
∠(C_4-H_1-C_5) = 165.0°		

Bond	d (Å)[a]	BO[b]
C_6-H_2	1.543	0.19
C_7-H_2	1.148	0.69
C_6-C_7	2.409	0.36
Rh-C_7	2.320	0.26
Rh-Rh	2.451	0.60
∠(C_6-H_2-C_7) = 126.5°		

[a] Bond length. [b] Wiberg bond indices. [c] For comparison, in the free carbenoid complex **2.5c**, d(Rh-C) = 2.010 Å, BO(Rh-Rh) = 0.47, d(Rh-Rh) = 2.476 Å, BO(Rh-C) = 0.69.

Figure 2.13: Structural characteristics and selected bond orders in calculated transition state structures for carbenoid C–H insertions with **2.5c**.[15]

Axial *versus* equatorial C–H insertion and kinetic isotope effects. As demonstrated above, the use of quantum-chemical calculations to study transition states and energetics

in carbenoid transformations can be an effective tool to obtain molecular level understanding of the reaction details. Due to the selectivity displayed by the donor/acceptor-substituted rhodium carbenoids in the C–H functionalization chemistry, it was decided to study the reaction between carbenoid **2.5c** and cyclohexane (Figure 2.14).[14] This is an interesting system, because it has two types of C–H bonds, equatorial and axial. The question arises of whether selective rhodium carbenoids, such as **2.5c**, can distinguish between these two types of C–H bonds? Transition structures for equatorial and axial C–H insertion were located (**TS-IX$_{ax}$** and **TS-IX$_{eq}$**, Figure 2.14). Insertion into the equatorial bond was predicted to be more favorable by 1.5 kcal/mol over axial insertion (from gas-phase Gibbs free energies), corresponding to a relative rate of k_{eq}/k_{ax} ~ 12 : 1. This prediction will have implications for the design of C–H functionalization strategies for substrates involving cyclohexane fragments.

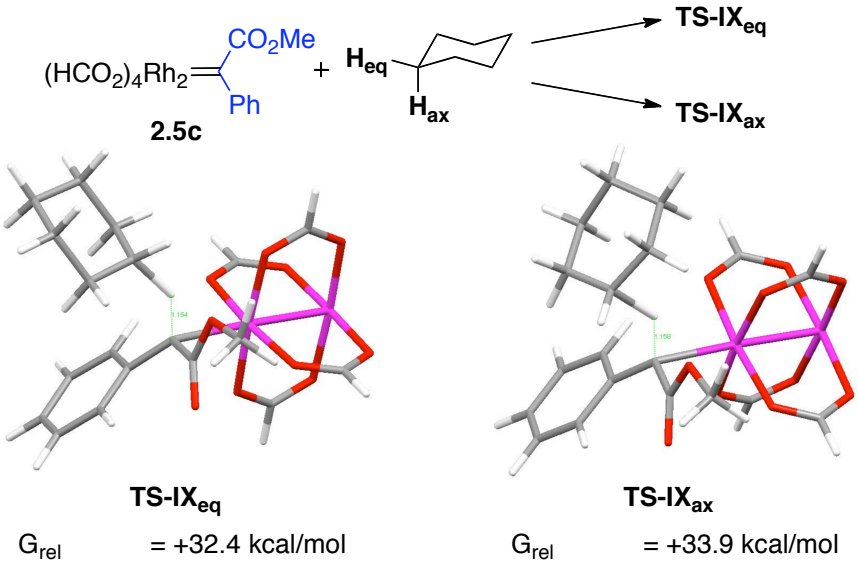

Figure 2.14: Axial *versus* equatorial C–H insertion with cyclohexane.

The reaction between methyl phenyldiazoacetate and cyclohexane catalyzed by Rh$_2$(*S*-DOSP)$_4$ has been reported.[14] A kinetic isotope effect of k_H/k_D = 2.0 was measured for this

reaction.[14] It was decided to calculate the kinetic isotope effect based on transition structures **TS-IX$_{eq}$** and **TS-IX$_{ax}$** in order to support the accuracy of these transition structures and to lend support to the above claims that equatorial C–H insertion is indeed favored over axial. The kinetic isotope effects were calculated from gas-phase Gibbs free energies obtained in B3LYP/6-31G*[Rh-RSC+4f]-calculations, and by applying Transition State Theory to the reactions with d_{12}-cyclohexane and cyclohexane (Scheme 2.10). Due to the relatively high activation barriers involved, tunneling effects were not expected to contribute significantly, and were consequently neglected. The equatorial insertion reaction gave a predicted kinetic isotope effect of k_H/k_D = 2.21, in very good agreement with the experimental value of 2.0 obtained in the Rh_2(*S*-DOSP)$_4$-catalyzed reaction,[14] particularly considering the simplifications involved in the model system. For the axial insertion, a predicted value of k_H/k_D = 2.82 was obtained. These observations strongly support the accuracy of the preferred equatorial C–H insertion transition state for cyclohexanes.

Scheme 2.10: Computed *versus* experimental[14] primary kinetic isotope effects.

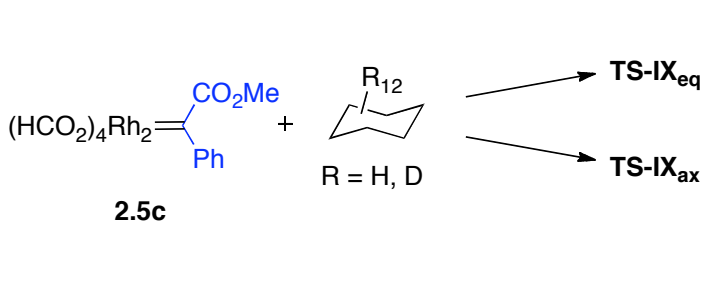

C-H bond	k_H/k_D
Axial	2.82
Equatorial	2.21
Experimental	2.0

Predictive model for C–H insertion chemistry. C–H functionalization reactions with donor/acceptor-substituted rhodium carbenoids can occur in a highly diastereo– and enantioselective manner.[2-4,18] Methylene site insertions occur with attenuated diastereoselectivity because of difficulties involved in controlling the stereogenic center

forming at the insertion site. However, if the two non-hydrogen substituents are sterically well-differentiated, very high diastereoselectivity is usually observed.[2-4] To be able to predict the stereoselectivity, an understanding of how the substrate preferentially approaches the carbenoid complex is crucial. As discussed in the introductory text on previous C–H insertion models, the orientation of the C–H bond is a particularly critical element as these reactions occur without control of the substrate orientation by pre-coordination to the metal. From computed transition state geometries presented in this work,[15] one can obtain an informative idea of how the substrate C–H bond approaches the carbenoid. In the early days of considering the C–H insertion as a concerted, three-centered, non-synchronous process, it was assumed that the C–H bond had to be almost parallel to the carbenoid plane in order to accommodate the three-centered transition structure.[14,46] This is shown schematically in Figure 2.15, in which the C–H bond is approaching: (a) parallel to the Rh–C bond ("end-on"),[49] and, (b) perpendicular to the Rh–C bond, yet parallel to the carbenoid plane ("side-on").[4,46] Ideally, the C–H–C angles would be ≤ 90° in theses cases. The calculations presented herein, however, show that the C–H functionalization event initiates with considerable hydride transfer character, also for carbenoid **2.5c**.[15] With 1,4-cyclohexadiene as substrate, the C–H–C angle is 165°, while with cyclopentane and cyclohexane, it is somewhat smaller (127° and 125° respectively). In other words, the C–H bond is almost orthogonal to the carbenoid plane, as illustrated in Figure 2.15c. C–H–C angles in the range 117-128° were also found by Nakamura et. al. for insertions with simple alkanes using diazomethane and methyl diazoacetate.[32]

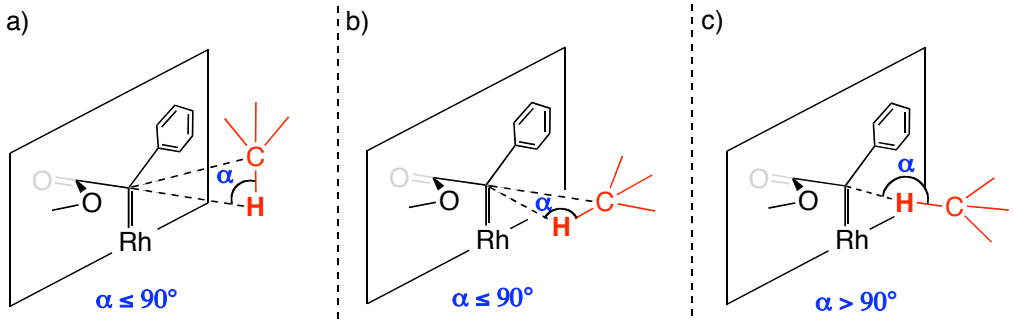

Figure 2.15: Approach modes of the C–H bond vector towards the carbenoid plane: (a) parallel with Rh–C bond, (b) perpendicular to Rh–C bond, parallel to carbenoid plane, and (c) orthogonal to carbenoid plane.

A revised perspective on how the C–H insertion transition state should be analyzed has emerged from the large observed C–H–C angles. As the C–H bond is pointing almost directly towards the carbenoid center, the remaining three substituents at the site of insertion prefer to adopt a staggered relation to the three substituents on the carbenoid.[15] The least crowded orientation is presumably preferred, and, since both the catalyst "wall" and the ester group act as sterically demanding substituents (the O–C–O plane is almost perpendicular to the carbenoid plane), the small group on the insertion site would be oriented towards the most hindered sector, which is 'gauche' to both the ester and the catalyst. A Newman projection along the C–C bond forming coordinate can be proposed as a basis for a predictive model, based on the above analysis, as shown in Figure 2.16a.[15] This model rationalizes the preferred relative orientation of the largest (R_L), medium-sized (R_M) and small (R_S) substituents on the substrate in the insertion process. When the influence of a chiral catalyst, such as Rh_2(*S*-DOSP)$_4$, is considered (by adding blocking groups as discussed in the introductory text),[4d] the Newman projection model can

successfully predict the absolute and relative stereochemistry of the major product (Figure 2.16b).[15]

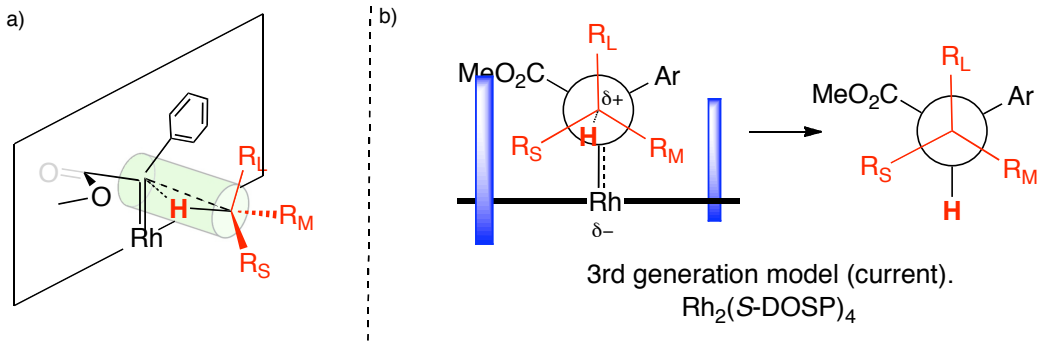

Figure 2.16: (a) Perspective of model for C–H insertion event. (b) Newman projection model for prediction of absolute and relative stereochemistry in C–H insertion. R_L = large substituent, R_M = medium size substituent, R_S = small substituent.[15]

Insertions into methylene sites will occur with diastereo– and enantiostereoselectivity that can be predicted on the basis of the Newman projection model. The result will be as indicated in Equation 1 (Scheme 2.12).[15] Only if R_L and R_M are sterically well-differentiated will the reaction proceed with high diastereoselectivity. This can be rationalized from the model, since a very large group will prefer to orient itself away from the catalyst "wall". If R_L and R_M are locally of similar steric bulk, less preference for the indicated orientation is expected, and will hence lead to attenuated diastereoselectivity (Figure 2.16b).[15] Some of the most diastereoselective C–H insertion reactions reported to date are indicated in Equations 2-6 in Scheme 2.11.[48,76-78] The large group, R_L, is indicated in blue and the medium-sized group is indicated in red. For silyl enol ethers and tetraalkoxysilane substrates, the siloxy group is the most bulky group (Equations 2[76] and 3[77]). In the case of *N*-Boc pyrrolidine, the *N*-Boc portion is considered to be the largest group (Equation 4[48,78]). Allylic C–H functionalization of cyclohexenes is

a problem area for diastereoselectivity in this chemistry. High relative stereocontrol only occurs when the very bulky *t*-butyl-diphenylsilyl group is introduced (Equation 5), as it leads to steric differentiation of the methylene site.[79] In a similar fashion, allylic C–H functionalization of acyclics with high diastereocontrol is only observed when highly functionalized vinyl substituents are employed (Equation 6).[80]

Scheme 2.11: Predictions of stereochemical outcome using the Newman projection model.[48,76-80]

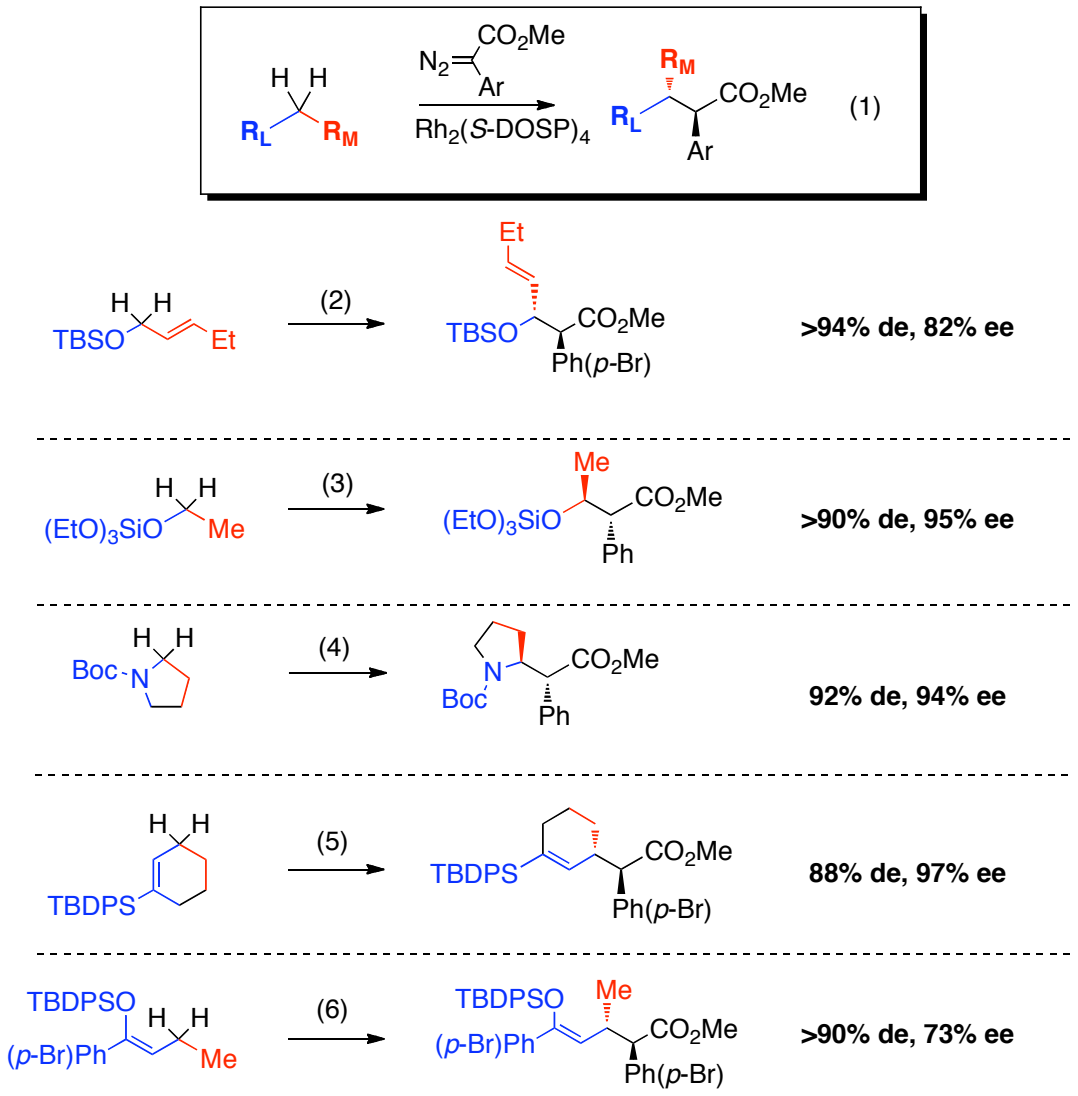

2.2.2 Cyclopropenation Chemistry

Models. Cyclopropenation reactions with termial alkynes have recently been extended to also involve styryldiazoacetates as carbenoid precursors.[40] These reactions are highly enantioselective, however, the cyclopropene products are amenable to rearrangement to achiral cyclopentadienes.[40] As mentioned in the introductory text, there are two proposed extreme orientations for approach of the alkyne towards the rhodium carbenoid in the cyclopropenation reaction, a "side-on" approach and the "end-on" approach (Figure 2.4).[10] While the "side-on" model was largely discarded, based on the experimental evidence that disubstituted alkynes did not undergo the reaction,[10] the "end-on" model fails to explain why asymmetric induction occurs in the cyclopropenation reaction as it does not have any influence from the catalyst blocking groups in the transition state (Rh_2(*S*-DOSP)$_4$ model).[10,40] Density functional calculations were performed in order to determine the exact transition structure involved. The discussion here is based on energy calculations at the B3LYP/6-311+G(2d,2p)[Rh-RSC+4f]//B3LYP/6-31G*[Rh-RSC+4f] level of theory, with zero-point corrections from B3LYP/6-31G*[Rh-RSC+4f] calculations. As the recent chemistry is carried out largely with styrylvinyldiazoacetates, the styrylsubstituted donor/acceptor carbenoid **2.24** was used in the calculations (Scheme 2.12).[40] The approach of propyne to this carbenoid was considered, as it is a representative model for this chemistry. The simple rhodium tetrakisformate catalyst model was still employed for simplicity. Only the step involving reaction between the rhodium vinylcarbenoid complex and the alkyne was considered, as the pathway leading to the carbenoid complex has been described previously.[15,25]

Potential energies and the transition state. The cyclopropenation reaction displays a relatively high potential energy activation barrier of +11.6 kcal/mol, 7.1 kcal/mol higher than that predicted for the cyclopropanation of styrene.[15] Furthermore, the reaction was exoergic by -14.6 kcal/mol. These observations suggest that a relatively late transition state occurs in the cyclopropenation chemistry compared to the related cyclopropanation reactions, which would be consistent with the superior levels of stereoselectivity.[10,40] The initial guess for transition state geometries were based on the "end-on" and "side-on" models.[10] Regardless of what the starting geometry was, the alkyne eventually optimized to approximately the same structure in all the calculations. The favored transition structure, **TS-X**, shown in Figure 2.17, displays a most striking feature that has not been considered in previous models. The close proximity and directional property of the terminal alkyne hydrogen to one of the carboxylate oxygens (d(O–H) = 1.956 Å), strongly indicates the presence of a hydrogen bonding interaction.[10] This may be an important factor leading to a tilted alkyne (18.2° clockwise tilt from the idealized "end-on" approach). The opposite, counter-clockwise tilt was imposed on the structure, but led to a transition structure of higher energy, presumably because of the increased steric interaction with the ester group. This transition state model is consistent with the experimental fact that disubstituted alkynes are usuitable substrates for this chemistry,[10,40] as this would remove the favorable interaction and place a substituent into a sterically crowded sector. Furthermore, the tilt would lead to a preferred approach over the styryl portion, making the model consistent with asymmetric induction through the D_2-symmetry model of Rh_2(*S*-DOSP)$_4$.[40]

Scheme 2.12: Reaction model between styrylcarbenoid **2.24** and propene.[40]

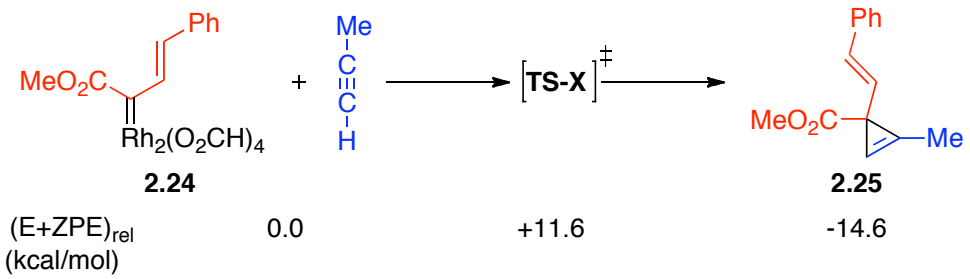

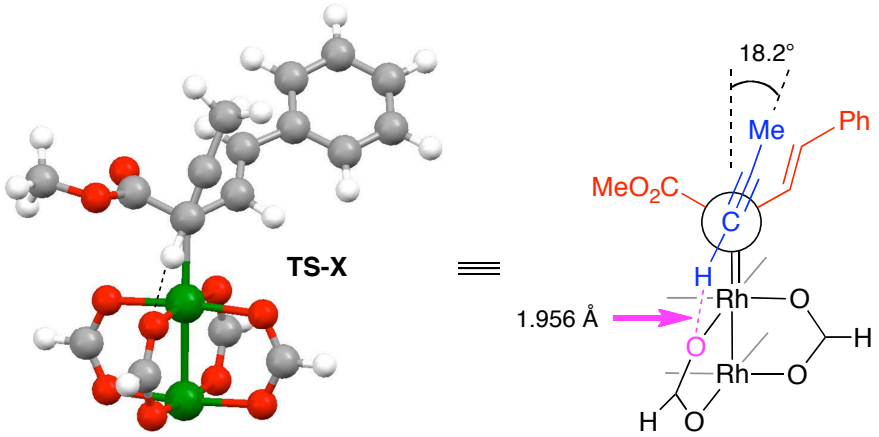

Figure 2.17: Transition structure **TS-X** for the cyclopropenation of propene.[40]

2.2.3 The Combined C–H Activation/Cope Rearrangement

Chemical models. The so-called "combined C–H Activation/Cope rearrangement" (CHCR) is, in many cases, the most stereoselective of all carbenoid C–H functionalization reactions. The most successful substrates in this chemistry have been cyclic 1,3-diene-like systems such as 1,3-cyclohexadienes,[81] cycloheptatriene,[59] and 1,2-dihydronaphthalenes.[50-52,54] The simplest model chemistry for the reaction with a 1,3-diene-like substrate, would be the reaction between the unsubstituted vinylcarbenoid model complex **2.5a** and 1,3-cyclohexadiene to produce CHCR product **2.26** (Scheme 2.13). Simple cyclic alkenes, such as cyclohexene have also been studied to some extent,

but they usually give mixtures because of competing direct C–H insertion as well as cyclopropanation in most cases.[55] Such substrates may therefore shed light on factors controlling direct C–H insertion *versus* the combined C–H activation/Cope rearrangement and cyclopropanation chemistry.[55] Another interesting potential substrate for the combined C–H activation/Cope rearrangement would be 1,4-cyclohexadiene, to produce **2.28**, because the reaction represents a desymmetrization of the substrate.[81] Herein is undertaken a study of the CHCR reaction with all three types of alkenes to obtain a more accurate picture of how the mechanism is affected by substrate structure (Scheme 2.13). Dirhodium tetraformate has been employed as a dirhodium carboxylate model in this study.[15] The main discussion is based on calculations at the B3LYP/6-311+G(2d,2p)[Rh-RSC+4f]//B3LYP/6-31G*[Rh-RSC+4f] level of theory, with zero-point corrections from B3LYP/6-31G*[Rh-RSC+4f] calculations.[15]

Scheme 2.13: Model chemistries for the CHCR reaction.

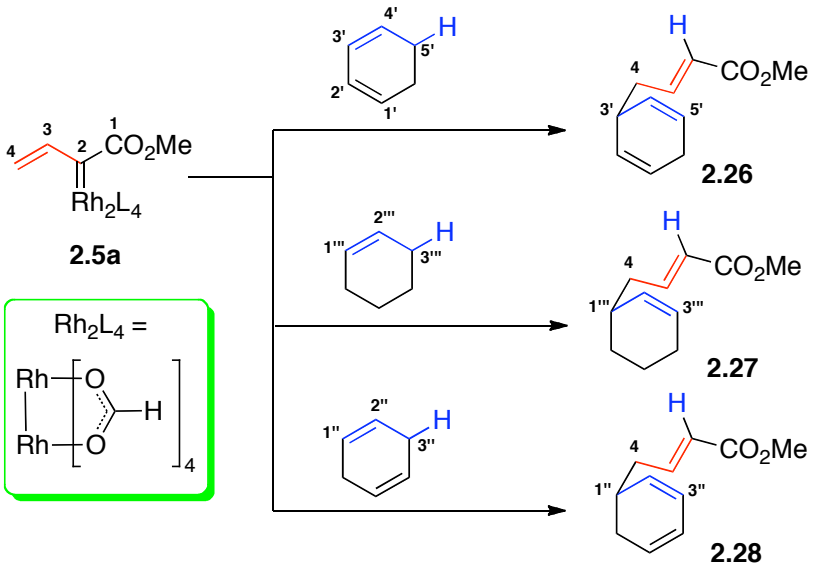

Mechanistic hypotheses. The mechanism of the CHCR reaction has been subject to several hypotheses since its discovery in the late 1990s.[58] Five plausible mechanistic

scenarios have been proposed, which will be discussed here (Scheme 2.14). Some may be ruled out on the basis of available experimental data. The five proposed pathways are: (1) a direct C–H insertion, followed by thermal Cope rearrangement,[58,82] (2) an ene-type reaction, in which the vinylcarbenoid acts as a 2π-enophile, followed by hydride shift/elimination,[58] (3) a hydride transfer, followed by vinylogous C–C bond formation, (4) a concerted, synchronous transition state involving 7 atoms or,[55,58] (5) initial attack of the vinyl group onto the vinylogous position of the carbenoid complex, followed by proton transfer.[83] The latter three lie on a mechanistic continuum, as indicated in Scheme 2.14. Mechanism (1) can be eliminated, since, in several cases, the CHCR reaction has been demonstrated to produce the thermodynamically less stable (kinetic) product.[55,81] The C–H insertion product can therefore not be an intermediate in this process. Furthermore, in the majority of cases where both products are formed, the enantiomeric excess is consistently slightly different, indicating that two reaction pathways may be involved.[55] Mechanism (2) is also an unlikely pathway, particularly since hydride shift/elimination in alkyl-substituted rhodium carbenoids is well precedent and is known to form the *Z*-product preferentially.[84] In the CHCR reaction, the *E*-product is typically observed. Mechanism (3) is consistent with the observed chemistry. Hypothesis (4) is also consistent. This pathway has served as the basis of the currently used stereochemical predictive model for this reaction.[52,55] Pathway (5) may also occur, since vinylogous reactivity leading to C–C bond formation is known.[85,86] However, in 1,3-diene-like systems, this would imply that an internal position of the sp^2-system must initiate the reaction, which is inconsistent with the HOMO electron density distribution.[87] In this work, pathways (2)-(5) were considered in the calculations.

Scheme 2.14: Mechanistic proposals for the CHCR reaction.

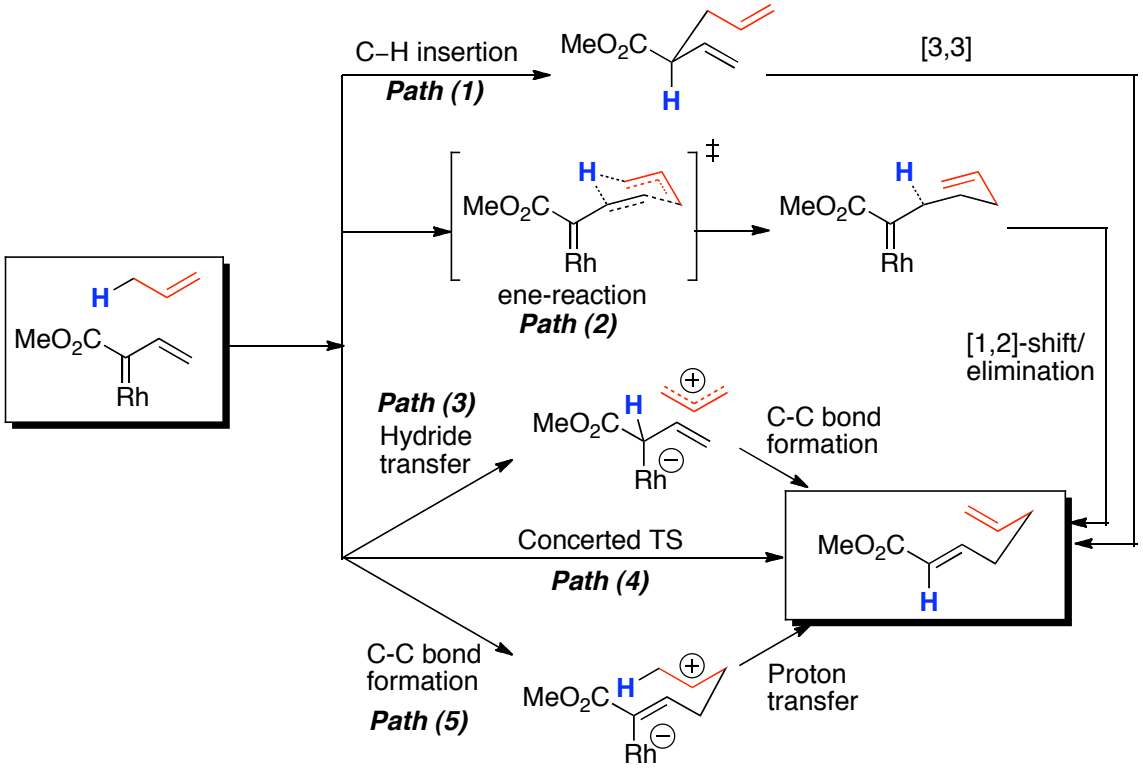

Stereochemical considerations. An important part of understanding the CHCR reaction, comes from analyzing the various stereochemical issues present in the vinylcarbenoid and substrate models. Two areas must be considered (Figure 2.18): (a) the preferred vinylcarbenoid conformation, as the vinyl group may exist in both the s-*cis* or s-*trans* orientations (Figure 2.18a)[86], and, (b) the orientation of the incoming allylic C–H bond (Figure 2.18b).

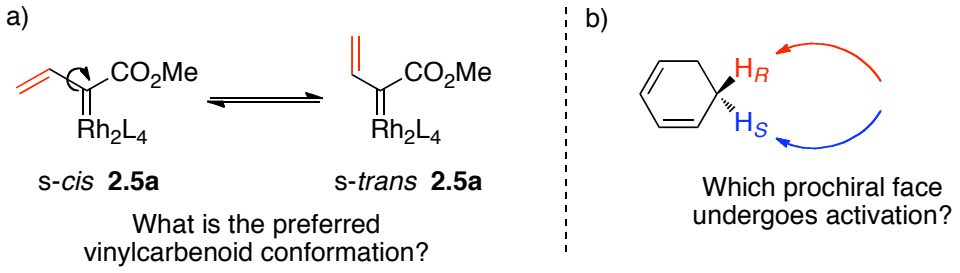

Figure 2.18: Important stereochemical considerations.

It was decided to first study the equilibrium between the s-*trans* and s-*cis* vinylcarbenoid conformations[86], with respect to substitution at the different vinyl positions, by comparing gas-phase Gibbs free energies from B3LYP/6-31G*[Rh-RSC+4f] calculations (Scheme 2.15, Table 2.2). The unsubstituted vinylcarbenoid **2.5a** has a slight preference for the s-*trans* conformer (-0.59 kcal/mol). By introducing a methyl group as R^2 (**2.29**), a commonly used vinylcarbenoid in synthesis[52], there is still a small preference for the latter conformer of -0.20 kcal/mol. When the methyl group is introduced in the 3-position (R^3), a stronger preference for the s-*cis* conformation of **2.30** is observed by +1.78 kcal/mol. This is related to the unfavorable steric interactions involved between the R^3-substituent and the catalyst "wall" in the s-*trans* conformation. This effect is reflected more strongly when introducing R^1 = Me in vinylcarbenoid **2.31**, which strongly prefers the s-*trans* conformer by -3.63 kcal/mol.[86] The R^1-group is very close to the catalyst structure in the s-*cis* conformer and leads to a somewhat distorted geometry. Another system often used in synthesis, is the styrylcarbenoid **2.24**.[81] Similar to entries 1 and 2, there is a slight preference for the s-*trans* conformer by -0.12 kcal/mol. These results are of great importance for the chemistry of vinylcarbenoids, as the orientation of the vinyl group has a crucial stereochemical role.[86] The general trends appear to be: (1) for vinylcarbenoids with only an R^2–substituent (other than hydrogen), there is no strongly preferred conformer and, hence, both potentially have to be considered in reactions involving the vinyl group. For most such systems, however, the s-*cis* conformer appears to be the more reactive.[12,25,55] (2) For vinylcarbenoids with an R^3-substituent, the s-*cis* conformation is preferred. Most likely, this is the only conformer present for the commonly used vinylcarbenoids, as the group is usually much larger than

methyl (usually siloxy-, aryl- or alkyl group).[53] (3) If R^1 > hydrogen, the s-*trans* conformer is strongly preferred. The influence of the vinyl group conformation will be discussed for the CHCR reaction below.

Scheme 2.15: Vinylcarbenoid conformations.

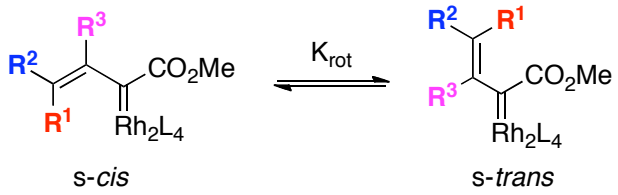

s-*cis* s-*trans*

Table 2.2: Influence of substituent pattern and nature on conformational preference.

Entry	*Carbenoid*	R^1	R^2	R^3	ΔG_{rot} (kcal/mol)	K_{rot}
1	**2.5a**	H	H	H	-0.59	2.74
2	**2.29**	H	Me	H	-0.20	1.40
3	**2.30**	H	H	Me	+1.78	0.049
4	**2.31**	Me	H	H	-3.63	462
5	**2.24**	H	Ph	H	-0.12	1.22

Reactions of vinylcarbenoids at allylic C–H sites. Transition structures were next sought for the approach of the three model substrates towards the unsubstituted vinylcarbenoid model. The analysis involved approaching both prochiral C–H bonds of 1,3-cyclohexadiene and cyclohexene, as well as the C–H bond in 1,4-cyclohexadiene, towards both vinylcarbenoid orientations. None of the located transition structures indicated a concerted, synchronous process involving all seven atoms (pathway 4, Scheme 2.14). An ene-like transition structure (pathway 2) could not be found either. A

transition structure corresponding to pathway (5) was found for the reaction with cyclohexene, but was significantly less stable than the lowest energy transition states.

The preferred transition state geometries strongly indicate a hydride transfer process from the allylic position of the substrate, with C–H–C angles of ~170°, an almost perpendicular approach of the C–H bonds to the carbenoid carbon. When animated in their imaginary vibrational modes, the transition states displayed lengthening of the substrate C–H bonds with motion towards the carbenoid carbon. These observations are consistent with what has previously been found to be characteristic for C–H insertion chemistry,[15] however, the hydride transfer component is more pronounced. The most stable transition structures **TS-XIa** through **TS-XIIIa** for the three model systems are shown in Figure 2.19, with structural characteristics indicated. In these structuctures**,** the terminal carbons are separated by 3.188-3.810 Å and display no observed rehybridization (bond lengths and angles remain approximately the same as in free substrate), indicating that no C–C bonding interactions have developed in the TS. For all three systems, there appears to be a strong cationic character developed in the allylic system of the subtrate as well as anionic character at the vinylcarbenoid portion. For **TS-XIa** and **TS-XIIIa,** the hydride transfer characteristics (C–H distances) are very similar, whereas in **TS-IIa**, the hydride transfer process is somewhat more advanced. **TS-XIa** is notably different from the other two. The distance between the bond forming carbons (3.188Å) demonstrates that a much tighter transition structure forms in comparison with **TS-XIIa** and **TS-XIIIa** (3.399 Å and 3.810 Å, respectively).

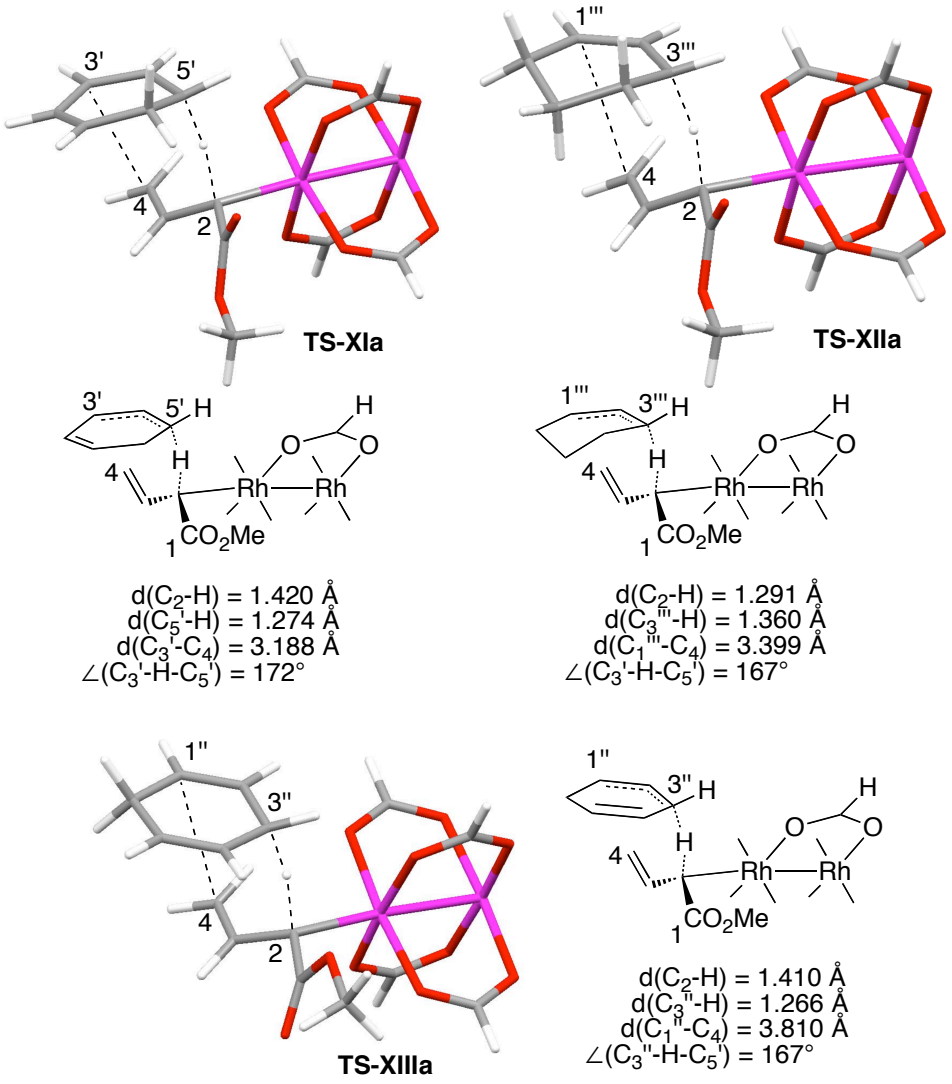

Figure 2.19: Most stable transition states found for the chemical models.

When moving forward on the potential energy surface, the hydride transfer goes to completion while reaching a very flat area of the PES, however, C–C bond formation between the terminal positions occurs before an intermediate can form. These observations indicate that the CHCR reaction proceeds through a concerted, but highly asynchronous, hydride transfer/C–C bond formation event, consistent with that of direct C–H insertion.[15] This corresponds to a mechanism shown in Figure 2.20, with the hydride transfer component occuring first.

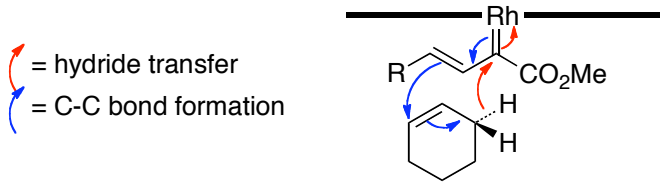

Figure 2.20: Concerted, but highly asynchronous mechanism for the CHCR reaction.

IRC analyses. Full forward intrinsic reaction coordinate analyses (IRCs) were performed for all four transition state combinations of substrate orientations (*pro-R/pro-S*) and vinylcarbenoid conformations (s-*cis*/s-*trans*) for all three model systems. The reaction with 1,3-cyclohexadiene was studied first, and the results of the forward IRC analyses are shown in Scheme 2.16. The most stable transition structure **TS-XIa** has been described above. This reaction displays a potential energy barrier of 4.2 kcal/mol and affords the product that is normally observed for the CHCR reaction through a chair-like arrangement. The absolute and relative stereochemistry is consistent with experimental observations. **TS-XIb** displayed a barrier of 6.5 kcal/mol, but the boat-like geometry was such that, for a more realistic catalyst system, severe interactions with the carboxylate ligand would likely be present, thereby strongly disfavoring this path. **TS-XIc** led to an unexpected product **2.26c**, which resulted from a hydride transfer/elimination sequence leading to aromatization of the ring and enol formation.[88] Although unusual, such elimination in the CHCR reaction has been observed.[88] The barrier for this pathway was +5.8 kcal/mol. Finally, from **TS-XId** (+4.4 kcal/mol), one could obtain product **2.26d**, which is derived from a chair-like arrangement, but, because the carbenoid vinyl group is oriented s-*trans*, has a *Z*-double bond geometry. The *Z*-CHCR product has only been observed when very electron deficient catalysts are used in reactions with styryldiazoacetates.[88,89] The similar barriers for **TS-XIa** and **TS-XId** presumably reflects

the simplicity of our model system. In practice, a significantly bulkier catalyst would be used, as well as more elaborate carbenoids. The structure of the substrate has also been shown to have a dramatic impact on the chemistry. The possibility of weak interactions, such as π-π stacking between substrate and carbenoid, may further impact the outcome of these reactions. Such interactions are not accounted for by the DFT method used herein. Nevertheless, the fact that all the barriers are relatively similar, demonstrates that they are potential pathways and suggests that test substrates can be designed that may be forced to undergo the CHCR reaction through an "unconventional" transition structure. The high propensity of the 1,3-diene model system to undergo the CHCR reaction is clearly related to the localization of charge build-up as one proceeds to the transition state. As the hydride-transfer character is strongly developed, positive charge-build-up is delocalized in the cyclohexadienyl system of the substrate, and, most of the positive charge should be localized on the central carbon of the delocalized system.[87] As a partial negative charge is present in the vinylcarbenoid portion, one would expect vinylogous bond formation with the central dienyl carbon to be highly favored.

Scheme 2.16: IRC analyses of all combinations of 1,3-cyclohexadiene and vinylcarbenoid **2.5a**. A hypothetical R-substituent has been added to demonstrate the stereochemical implications. Energy values are reported as (E+ZPE) relative to free carbenoid complex + substrate when R=H.

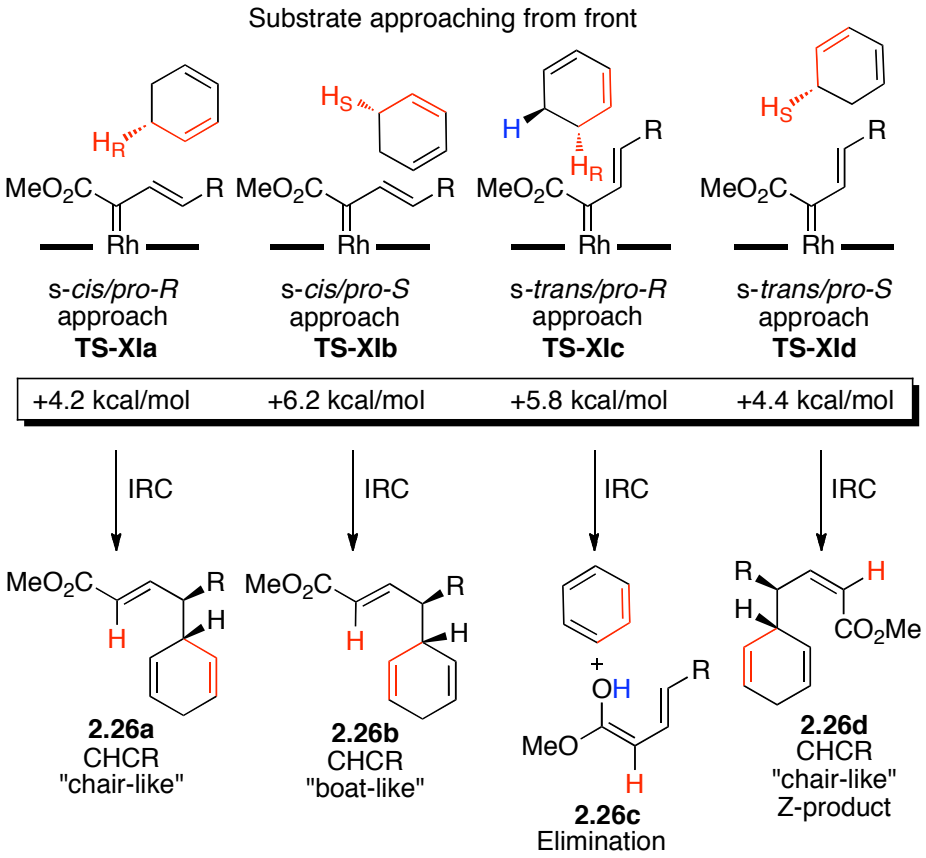

The reaction with cyclohexene was studied next. Transition state combinations analogous to those in Scheme 2.16 exist for this system and are shown in Scheme 2.17. In this system, only one of the transition structures, **TS-XIIa**, afforded the CHCR product **2.27a**, corresponding to the experimentally observed diastereomer with a potential energy barrier of +8.6 kcal/mol. Transition states **TS-XIIb** and **TS-XIId** both led to the same diastereomer of a direct C–H insertion product **2.27b**, through barriers of +9.3 kcal/mol and +8.0 kcal/mol, respectively.[55,71] **TS-XIIc** led to the other diastereomer of the insertion

product (**2.27c**) with a barrier of +9.9 kcal/mol. These results are consistent with experimental results with cyclohexene substrates in that they always produce mixtures of direct C–H insertion (as a mixture of the predicted diastereomers)[55,71] and one isomer of the CHCR product.[55] From these studies, it appears that the s-*trans* conformation of vinylcarbenoid **2.5a** somewhat enhances the direct C–H insertion pathway over the CHCR reaction. This is consistent with relatively long distances between the vinyl termini in transition states **TS-XIIb** through **TS-XIId**. In experimental work with arylvinylcarbenoids, the CHCR reaction is usually slightly favored over C–H insertion.[55,89] The discrepancy between the indicated barriers and experimental selectivities is likely to be due to the simplicity of our model system, as discussed before.

Scheme 2.17: IRC analyses of all combinations of cyclohexene and vinylcarbenoid **2.5a**. (R=H) Energy values are reported as (E+ZPE) relative to free carbenoid complex and substrate.

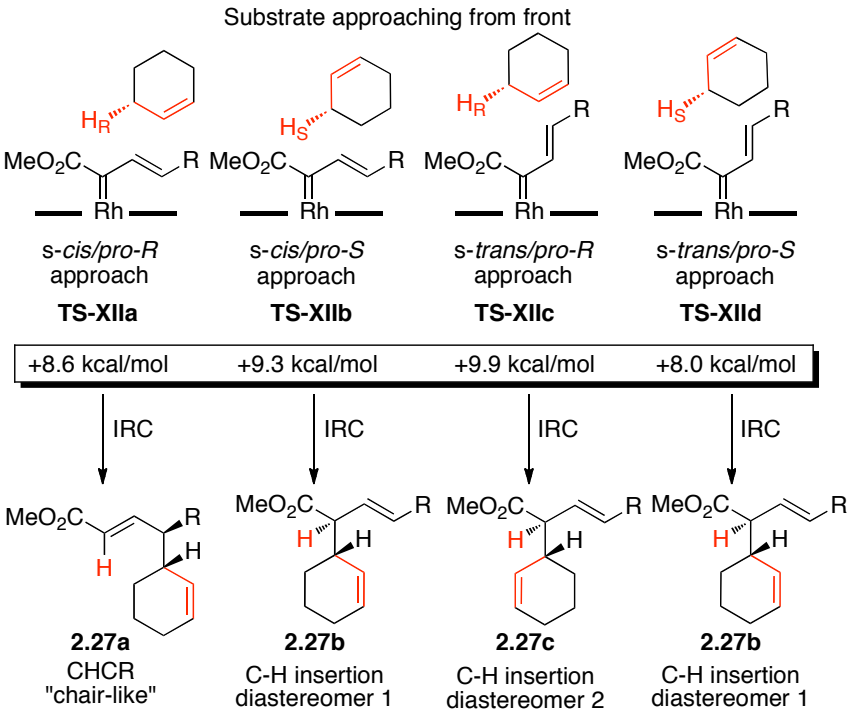

The last system to be studied was the reaction between **2.5a** and 1,4-cyclohexadiene. This system has only two transition state combinations because of the symmetry of the substrate. Reaction through **TS-XIIIa**, leads to the CHCR product **2.28a** derived from a chair-like reaction with a barrier of +5.1 kcal/mol. This is the experimentally observed major isomer in this chemistry with arylvinylcarbenoids.[81,89] The alternative transition structure **TS-XIIIb** was only 0.1 kcal/mol less stable (+5.2 kcal/mol), and led to direct C–H insertion product **2.28b**. In experimental studies with arylvinylcarbenoids, mixtures of direct C–H insertion and the CHCR are always observed, consistent with the predictions herein.[89] The observations are furthermore consistent with the cyclohexene results, which suggested a preference for direct C–H insertion for reaction trhough the s-*trans* conformation of the vinylcarbenoid. The propensity of 1,4-cyclohexadiene to give direct C–H insertion can be readily understood from the studies presented here. As in the transition states involving 1,3-cyclohexadiene, the positive-charge build-up is delocalized over the conjugated system in the substrate. In the former, however, the central carbon is situated close to the carbenoid carbon, and will hence display a higher propensity of C–C bond formation at this position, leading to direct C–H insertion.

Scheme 2.18: IRC analyses of all combinations of 1,4-cyclohexadiene and vinylcarbenoid **2.5a**. Energy values are reported as (E+ZPE) relative to free carbenoid complex+substrate (R = H).

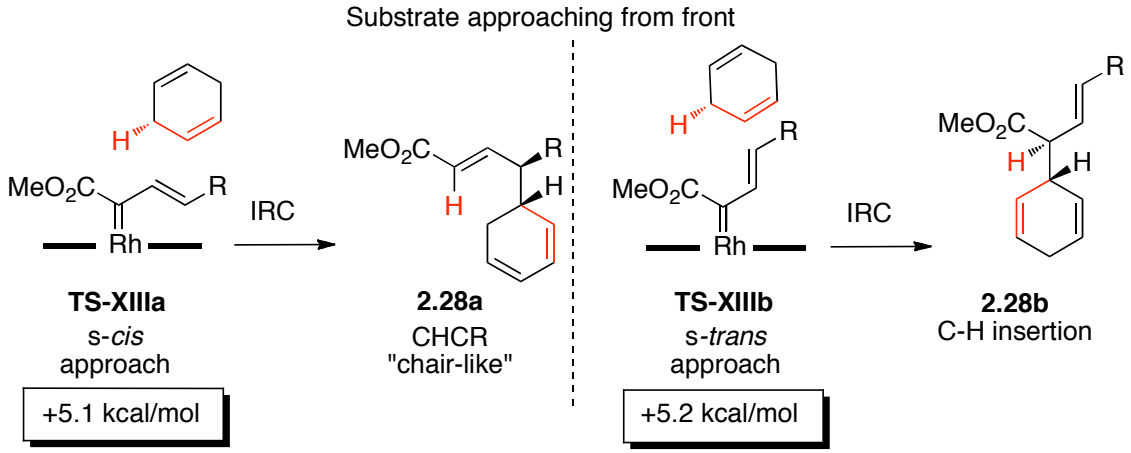

Unusual potential energy surface. A major issue in the C–H functionalization chemistry at allylic C–H sites is to understand the controlling factors that determine the reaction outcome. The major competing reaction pathways to the CHCR reaction are: (a) cyclopropanation of the double bond,[55,71] and (b) direct C–H insertion at the allylic site.[29,55] A cyclopropanation transition structure could be located for reaction with 1,3-cyclohexadiene, and it displayed a barrier of $\Delta(E+ZPE)_{rel}$ = +8.21 kcal/mol. This is consistent with the observation that minor products arising from cyclopropanation reactions can occur in some systems.[50] The issue of competing direct C–H insertion is more complex, since we have shown that the CHCR reaction proceeds initially through a transition state with considerable hydride transfer like character – the same transition state that would be expected to lead to direct C–H insertion, according to the studies presented in Section 2.2.1.[15] The idea that both reactions may occur through the same initial transition state, without an intervening intermediate, is consistent with a *potential*

energy surface bifurcation (Figure 2.21).[90-94] This phenomenon is characterized by two sequential transition states that are not connected *via* a minimum. Although the minimum energy pathway (MEP, the pathway that results from IRC calculations), from the initial transition state leads to one product (for example the CHCR product), alternative reaction trajectories over the initial transition state ridge may lead to a second product (direct C–H insertion).[91,93] In retrospect, it is sensible that the transition state valley of the hydride transfer ultimately must be connected with the Cope rearrangement transition state ridge, which again connects the two products. Bifurcations of potential energy surfaces of organic reactions are well known and have received much attention in recent years because of several examples of this phenomenon in synthetically important reaction systems.[92,93,95,96] Unfortunately, no simple, general predictors of the selectivity in such systems can be formulated, as it will be governed by the potential energy surface shape and Newtonian dynamic effects,[97] rather than traditional TST considerations.[93]

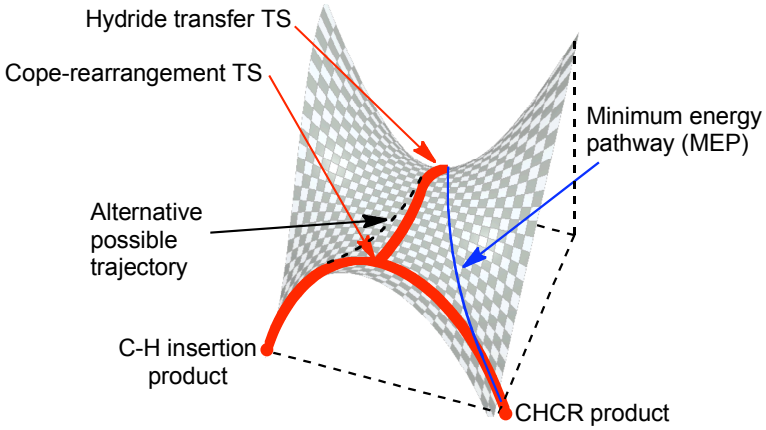

Figure 2.21: Model potential energy surface bifurcation.[93]

In order to further gather evidence of whether direct C–H insertion and the CHCR reaction are related through a bifurcated potential energy surface, it was decided to study the IRC profiles for the model reaction with 1,4-cyclohexadiene, generated from the

above analysis, more closely. The minimum energy paths are represented in Figure 2.22, starting from **TS-XIIIa** (blue data) and from **TS-XIIIb** (red data). Several characteristic features are present that support the bifurcation idea: (1) the relatively flat region of the potential energy surfaces that follows the hydride transfer TS, is a feature often observed for bifurcating systems.[92] (2) Inspection of some of the geometries from the flat regions, revealed that these structures closely resemble transition states that would be expected for Cope-rearrangements interconverting the products,[92] and, (3) by subjecting geometries from the flat regions, as indicated in Figure 2.22, to transition state geometry optimzation calculations, the corresponding Cope-rearrangement transition states **TS-XIVa** and **TS-XIVb** were obtained.[92] These transition states are indicated in Figure 2.23a. (4) Although geometry optimizations from the s-*cis* vinylcarbenoid reaction pathway (blue) always produced the same product as the IRC analysis, for the s-*trans* pathway, geometry optimization from the early part of the flat region led to an anomalous *Z*-CHCR product **2.28c** (Figure 2.23b, R = H). These results strongly suggest that, at least the pathway towards products from **TS-XIIIb** does bifurcate and, that, the pathway through **TS-XIIIa**, prefers just one product to a higher extent.

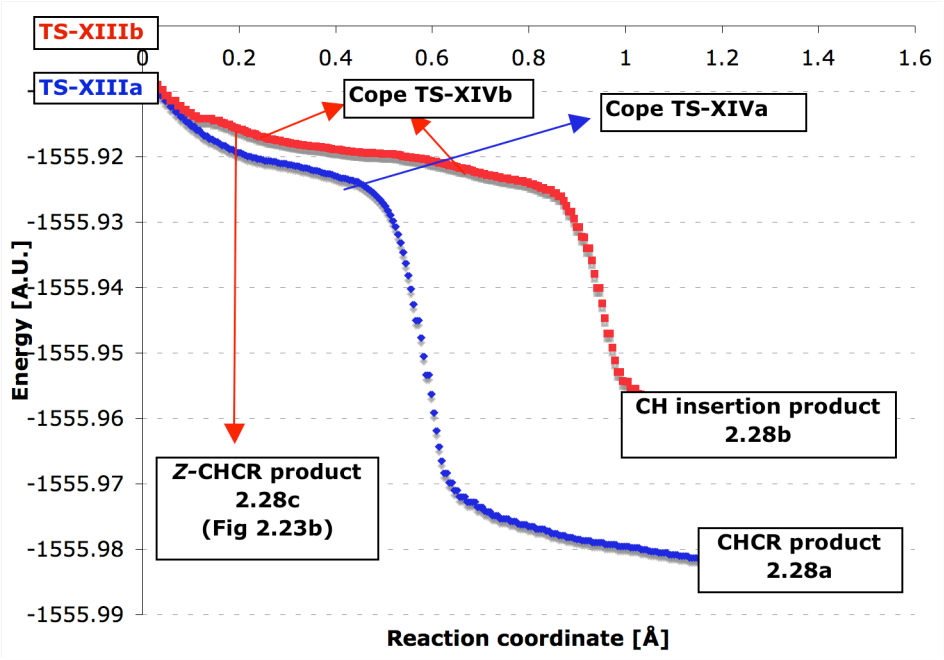

Figure 2.22: Forward IRCs for reaction of 1,4-cyclohexadiene with s-*cis* **2.5a** (blue) and s-*trans* **2.5a** (red). Upward arrows represent transition state optimizations. Downward arrows represent geometry optimizations.

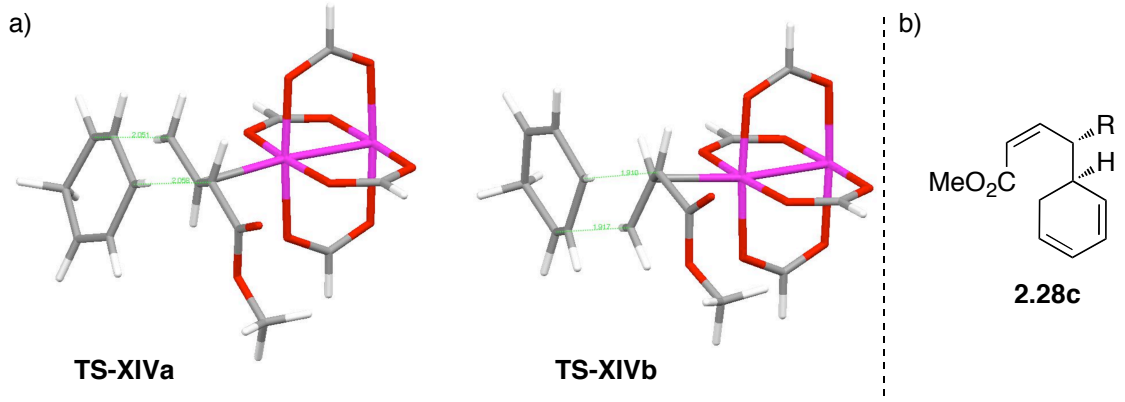

Figure 2.23: (a) Cope rearrangement transition states found from IRC geometries as indicated in Figure 2.22. (b) Anomalous CHCR product arising from **TS-XIIIb** (R = H).

Experimental evidence for the bifurcation comes from the reaction between arylvinyldiazoacetate **2.6** and 1,4-cyclohexadiene, catalyzed by Rh_2(*S*-DOSP)$_4$ (Scheme 2.19), which was conducted by Ms. Stephanie Ovalles.[89] In addition to product ratios, the stereochemical outcome of this reaction provides crucial mechanistic information. The reaction produces the "normal" CHCR product **2.32** as the major product in 72% relative yield and in 93% ee.[89] The direct C–H insertion product **2.33** was formed in 26% relative yield in 85% ee. In addition to these commonly observed products, a minor amount of 2% relative yield of a *Z*-CHCR product **2.34** was produced in 79% ee.[89] The latter product is quite unusual in this chemistry. Not only does it have the *Z*-double bond geometry, but also inverted stereogenic centers relative to product **2.32**.[83,89] The formation of products **2.32**-**2.33** can be readily rationalized, based on the IRC analyses presented in Scheme 2.18. A chair-like CHCR reaction from the s-*cis* vinylcarbenoid would produce the major product, and, considering the chiral influence of the catalyst (blocking groups, as discussed before), the predicted absolute configuration of **2.32** is consistent with the experimental results (Scheme 2.20a).[89] For direct C–H insertion to form **2.33**, the predictive model from Section 2.2.1 can be applied,[15] and the absolute configuration is again consistent with the experimental observations (Scheme 2.20b).[89] The existence of product **2.34** is believed to be related to the bifurcating nature of this reaction, and, considering the same transition state model (Scheme 2.21c), however, this time with terminal C–C bond formation occuring in a chair-like manner, the predicted absolute stereochemistry is that observed for product **2.34**. Overall, the experimental observations are in very good agreement with the computational study for 1,4-cyclohexadiene presented above, particularly since they represent evidence for a

bifurcation and since the absolute configuration of the major enantiomers could be predicted.[89] One major difference between the model system and the experimental reaction in Scheme 2.19 is that, for the former, the CHCR product **2.28a** is the thermodynamic product, whereas in the latter, both CHCR products **2.32** and **2.34** rearrange to the same direct CH insertion product **2.33** upon heating.

Scheme 2.19: Reaction between arylvinyldiazoacetate **2.6** and 1,4-cyclohexadiene conducted by Ms Stephanie Ovalles.[89]

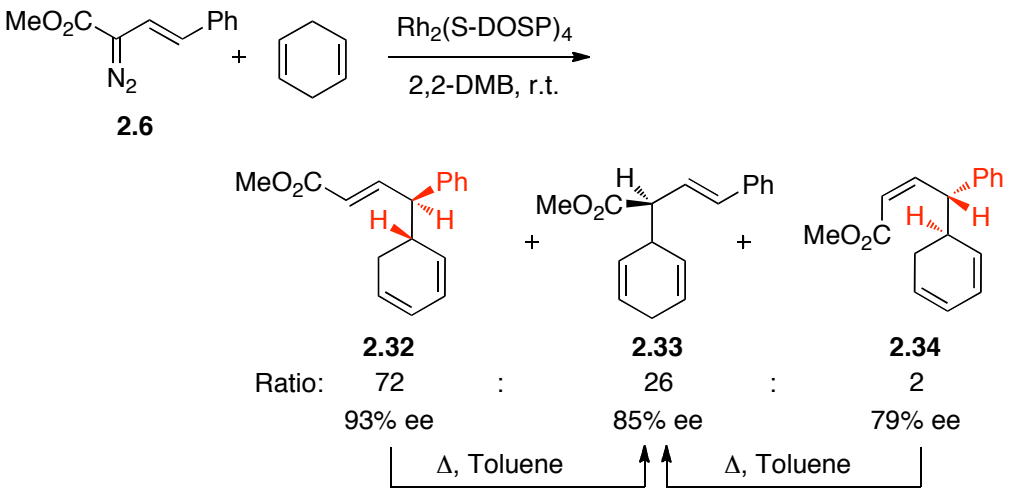

Scheme 2.20: Rationalization of stereochemical outcome.

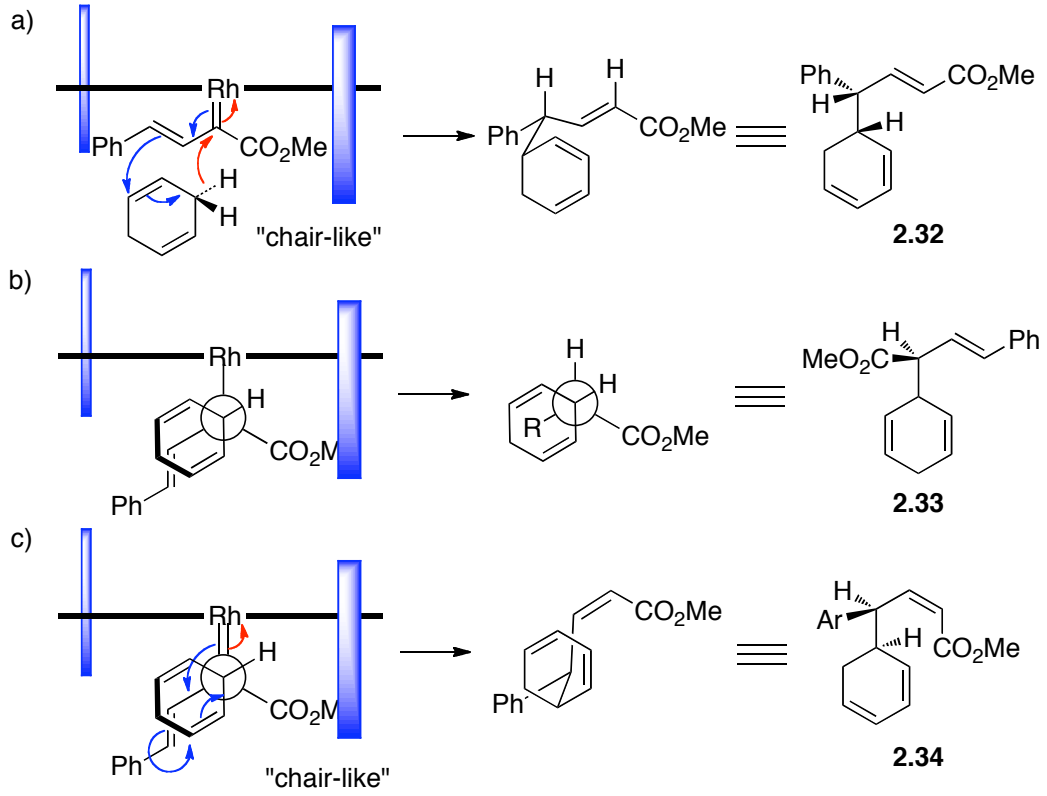

Other observations. When examining the structural details of the transition states found for reaction with 1,3-cyclohexadiene, they exhibit some notable properties different from the other transition structures. The substrate appears to prefer an unusual orientation, in which the vinyl systems of both the substrate and the vinylcarbenoid have almost perfectly aligned in an eclipsed manner. An example is shown in Figure 2.24 for **TS-XIc**. This alignment may be indicating an electrostatic attraction between the two vinyl systems, as they have strongly developed opposite charges in the transition state, in combination with the diminished steric influence (flat) of the 1,3-diene systems. The substrate has retained a hydrogen-bonding interaction with the ester carbonyl group in these unusual structures. The preferred alignment of the two vinyl systems in the TS can be characterized by the very low dihedral angles indicated in Figure 2.24. In comparison,

the ”normal” dihedral angles would be closer to ~60°. These observations can be of importance when analyzing 1,3-diene systems as the interactions between the carbenoid and the substrate are significantly different from that of cyclohexene or 1,4-cyclohexadiene systems.

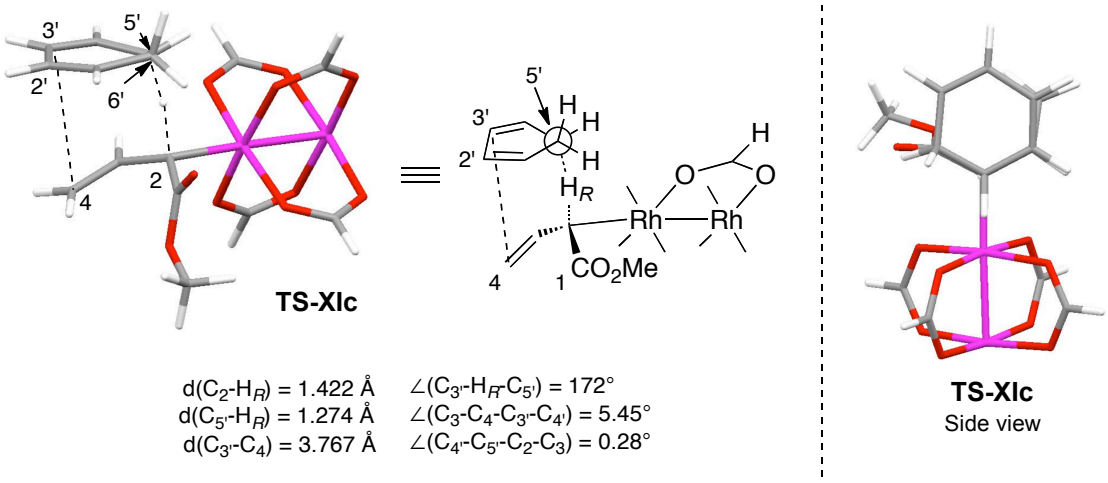

Figure 2.24: Aligned substrate with carbenoid for 1,3-cyclohexadiene reactions.

2.3 Conclusions

The Density Functional calculations presented herein demonstrate how donor/acceptor-substituted rhodium carbenoids, derived from aryl– and vinyldiazoacetates, are more stabilized than the conventionally used acceptor-only carbenoids. The stability is imparted by the donor group and implies that relatively late transition states occur. The resulting potential energy barriers reflect increased steric interactions that become important. The activation energies for carbenoid trapping are higher for donor/acceptor-substituted carbenoids, which in turn renders the system more capable of displaying selectivity between substrates with relatively subtle differences in electronic character. If the trapping agent is sterically demanding, however, electronic preference is a secondary control factor.[2d,31a,32]

The mechanism for direct C–H insertion initially displays predominantly a hydride transfer character, closely followed by C–C bond formation in an asynchronous, concerted manner. The reaction becomes more asynchronous with increasing ability of the substrate to stabilize positive charge build-up. A close inspection of the calculated transition state geometries led to a third generation predictive model for stereoselectivity in this chemistry.

A likely mechanism for the CHCR reaction has been described, which involves concerted, asynchronous hydride transfer/terminal C–C bond formation. Although Transition State Theory does not give an accurate picture of the selectivity of the reaction, this study has provided valuable insights into how the vinylcarbenoid and substrate structure influence the reaction selectivity. This is crucial for the understanding and design of new reaction systems in this chemistry. Furthermore, evidence was found

for the existence of a potential energy surface bifurcation in this reaction, which implies that both direct C–H insertion and the CHCR may proceed through the same initial transition state.

2.4 Experimental Section

2.4.1 General Considerations

All calculations were performed with the Gaussian '03 and Gaussian '09 software packages.[19] Density Functional Theory was employed with the 3-parameter hybrid functional B3LYP[20] to locate stationary points.[19] The structures involved in the CHCR reaction were initially located at the B3LYP/Lanl2DZ level of theory, but then subjected to full geometry optimization with a basis set consisting of the 1997 Stuttgart relativistic small-core ECP [Stuttgart RSC 1997 ECP][18a-c] for Rh, augmented with a 4f-function (ζ_f(Rh) = 1.350).[18d] The split valence basis set 6-31G* was used in the optimization and frequency calculations for all other atoms (C, H, N and O). This composite basis set is abbreviated 6-31G*[Rh-RSC+4f]. The main discussion of Section 2.2.1 is based on energies calculated at the B3LYP/6-311G(2d,2p)[Rh-RSC+4f]//B3LYP/6-31G*[Rh-RSC+4f] level of theory. The discussion in Sections 2.2.2 and 2.2.3 is based on B3LYP/6-311+G(2d,2p)[Rh-RSC+4f]//B3LYP/6-31G*[Rh-RSC+4f] calculations, including zero-point energy corrections calculated at the B3LYP/6-31G*[Rh-RSC+4f] level. The Gibbs free energies are calculated at the B3LYP/6-31G*[Rh-RSC+4f] level of theory. Stability of the SCF-wavefunction was confirmed by stability analyses for selected stationary points at the same level.[21a-b] Heavy atom basis set definitions and corresponding pseudopotential parameters were obtained from the EMSL basis set exchange library.[21c-d] All stationary points were characterized by normal coordinate analysis at the B3LYP/6-31G*[Rh-RSC+4f] level of theory.[22] Transition states were confirmed to have only one imaginary vibrational mode corresponding to movement along the reaction coordinate.[22] Equilibrium structures were confirmed to have zero

imaginary vibrational modes.[22] Transition states were further characterized by either full intrinsic reaction coordinate (IRC) analysis using maxpoints=50 or more, or by using default parameters, followed by geometry optimization to confirm that the stationary points were smoothly connected.[22] The calculated harmonic zero-point vibrational energies (ZPVE) are reported unscaled. Calculated structures have been visualized using Mercury.

2.4.2 Basis Sets and Pseudopotentials

Table 2.3 shows how the basis set and pseudopotential parameters were specified in the Gaussian input files used in this work. The gen-keyword was employed to generate the composite basis set input information.

Table 2.3: Basis set and pseudopotential specifications in the Gaussian input files.

```
gen=
Rh  0
 S   3  1.00
      7.91774400        -2.41557750
      6.84120700         3.09873820
      2.95984000        0.282125600
 S   1  1.00
      1.33434100         1.00000000
 S   1  1.00
     0.598810000         1.00000000
 S   1  1.00
     0.121894000         1.00000000
 S   1  1.00
     0.494520000E-01     1.00000000
 S   1  1.00
     0.160000000E-01     1.00000000
 P   2  1.00
      4.13607900        -3.34435450
      2.94628100         3.70374400
 P   2  1.00
      1.12230400        0.746225800
     0.666177000         0.269883300
 P   1  1.00
     0.365743000         1.00000000
 P   1  1.00
     0.766860000E-01     1.00000000
 P   1  1.00
```

```
     0.241700000E-01      1.00000000
 D   4  1.00
      7.03289200       -0.161604000E-01
      2.30981900        0.276398700
     0.998228000        0.485002600
     0.417057000        0.393019900
 D   1  1.00
     0.164447000         1.00000000
 D   1  1.00
     0.550000000E-01      1.00000000
 F   1  1.00
     1.350               1.00000000
****
O 0
6-31g*
****
C 0
6-31g*
****
H 0
6-31g*
****

RH  0
RH-ECP   4   28
G POTENTIAL
 1
2         1.00000000        0.00000000
S-G POTENTIAL
 2
2        11.72000000      225.34775400
2         5.82000000       32.82318900
P-G POTENTIAL
 2
2        10.42000000      158.70941200
2         5.45000000       26.44410000
D-G POTENTIAL
 2
2         8.82000000       62.75862600
2         3.87000000       10.97871900
F-G POTENTIAL
 2
2        12.31000000      -30.09345600
  2         6.16000000       -5.21848200
```

2.4.3 Calculated Properties and Geometries

Structures from Selectivity studies and Cyclopropenation

***Methyl phenyldiazoacetate* 2.1**

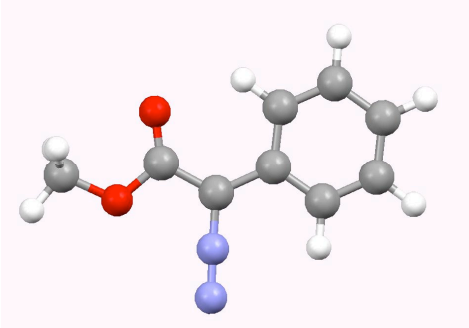

Route= #N B3LYP/6-31G* 5D OPT FREQ
Basis=6-31G(d)
B3LYP Energy=-607.67032271 Hartree
ZPE=0.158671 Hartree
Conditions=298K, 1.00000 atm
Internal Energy=-607.499905 Hartree
Enthalpy=-607.498960 Hartree
Free Energy=-607.550961 Hartree
Entropy=109.444 cal/mol-K

C	0.00000000	0.00000000	0.00000000
O	-1.15504300	0.85268100	-0.00020600
C	-2.34934400	0.20756000	-0.00006700
C	-3.47020800	1.16039500	-0.00048100
N	-3.12166200	2.43156400	-0.00087700
N	-2.84896300	3.53671400	-0.00114400
C	-4.91378200	0.83731500	-0.00041000
C	-5.35862200	-0.49753500	-0.00165500
C	-6.72425300	-0.78069700	-0.00161300
C	-7.67125400	0.24382500	-0.00039200
C	-7.23596100	1.57043200	0.00085300
C	-5.87535400	1.86591600	0.00086400
H	-5.56570800	2.90746500	0.00192800
H	-7.95663700	2.38381500	0.00185500
H	-8.73294100	0.01373800	-0.00039000
H	-7.04578100	-1.81894400	-0.00257200
H	-4.63353000	-1.30007200	-0.00254100
O	-2.45331100	-1.00447500	0.00003700
H	0.00970300	-0.63487800	0.88989300
H	0.01060200	-0.63405600	-0.89048300
H	0.85649600	0.67470700	0.00071100

***Methyl diazoacetate* 2.3b**

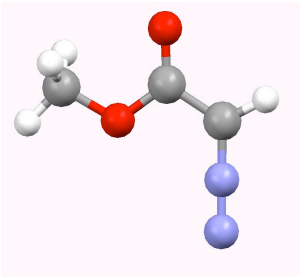

Route= #N B3LYP/6-31G* 5D OPT FREQ
Basis=6-31G(d)
B3LYP Energy=-376.616632203 Hartree
ZPE=0.077073 Hartree
Conditions=298K, 1.00000 atm
Internal Energy=-376.532333 Hartree
Enthalpy=-376.531389 Hartree

C	0.00000000	0.00000000	0.00000000
O	1.38652200	0.37203600	0.00025600
C	1.62203200	1.70849800	0.00020300
C	3.04906200	2.00997300	0.00033300
H	3.40891500	3.02854700	-0.00017800
N	3.94332800	1.05640700	-0.00019600
N	4.72187700	0.22607900	0.00018900
O	0.75543300	2.56007300	0.00003700
H	-0.50254500	0.38484900	0.89147900
H	-0.50376700	0.39023800	-0.88839100
H	-0.00773500	-1.09039700	-0.00317800

Free Energy=-376.571297 Hartree
Entropy=83.993 cal/mol-K

***Vinyldiazoacetate – s-cis* 2.3a**

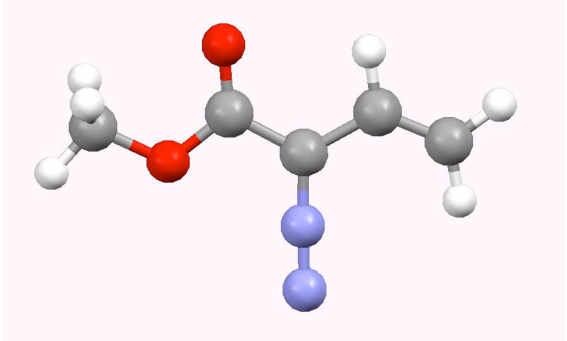

Route= #N B3LYP/6-31G* 5D OPT FREQ
Basis=6-31G(d)
B3LYP Energy=-454.01809451 Hartree
ZPE=0.110429 Hartree
Conditions=298K, 1.00000 atm
Internal Energy=-453.898128 Hartree
Enthalpy=-453.897184 Hartree
Free Energy=-453.942794 Hartree
Entropy=95.993 cal/mol-K

C	0.00000000	0.00000000	0.00000000
O	-1.38945000	0.36453700	-0.00001400
C	-2.25709600	-0.67539800	0.00005400
C	-3.65603500	-0.22777700	-0.00002300
C	-4.76634700	-1.17581800	0.00013100
C	-6.07573400	-0.89408900	0.00017400
H	-6.81022200	-1.69195000	0.00027600
H	-6.46121000	0.12282000	0.00011400
H	-4.41406000	-2.20377700	0.00020400
N	-3.89162500	1.06599300	-0.00009600
N	-4.14249700	2.17632100	-0.00039100
O	-1.92649800	-1.84503900	0.00012000
H	0.24343400	-0.58555600	0.89044400
H	0.24335400	-0.58595900	-0.89019800
H	0.54657100	0.94339200	-0.00023200

Styrene

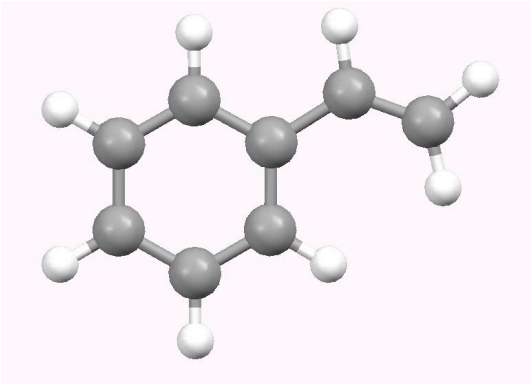

Route= #N B3LYP/6-31G* 5D OPT FREQ
Basis=6-31G(d)
B3LYP Energy=-309.641798736 Hartree
ZPE=0.133769 Hartree
Conditions=298K, 1.00000 atm
Internal Energy=-309.501262 Hartree

C	0.00000000	0.00000000	0.00000000
C	1.02274500	-0.86478400	-0.00019800
C	2.46244000	-0.55582100	-0.00016300
C	3.38439700	-1.61694500	-0.00012500
C	4.75911700	-1.38152000	-0.00007500
C	5.24350100	-0.07309200	-0.00007100
C	4.34002300	0.99484600	-0.00012200
C	2.96861700	0.75748000	-0.00017000
H	2.28334300	1.60022100	-0.00023000
H	4.70813800	2.01759000	-0.00013100
H	6.31359500	0.11571900	-0.00003700
H	5.45045400	-2.22017300	-0.00004200
H	3.01291700	-2.63939500	-0.00012700
H	0.79109400	-1.93013500	-0.00039300
H	0.13729800	1.07800000	0.00022700
H	-1.02704000	-0.35210500	-0.00005300

Enthalpy=-309.500318 Hartree
Free Energy=-309.539492 Hartree
Entropy=82.449 cal/mol-K

1,4-cyclohexadiene

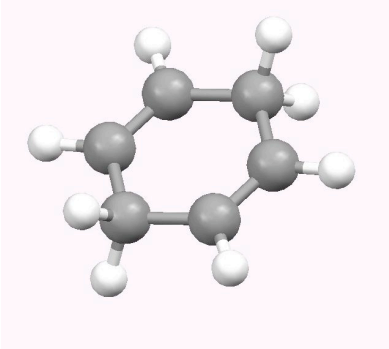

C	0.00000000	0.00000000	0.00000000
C	-0.83362500	-1.25475200	-0.00072900
C	-2.16862600	-1.25475600	-0.00071300
C	-3.00226000	-0.00000800	0.00003900
C	-2.16863500	1.25474400	-0.00071400
C	-0.83363400	1.25474800	-0.00072900
H	-0.29434400	2.20087600	-0.00130700
H	-2.70793100	2.20086800	-0.00128000
H	-3.67844800	-0.00001100	0.87150900
H	-3.68015500	-0.00001100	-0.87006500
H	-2.70791700	-2.20088300	-0.00127900
H	-0.29432900	-2.20087600	-0.00130900
H	0.67622300	0.00000300	0.87144000
H	0.67786000	0.00000300	-0.87013300

Route= #N B3LYP/6-31G* 5D OPT FREQ
Basis=6-31G(d)
B3LYP Energy=-233.413913855 Hartree
ZPE=0.122646 Hartree
Conditions=298K, 1.00000 atm
Internal Energy=-233.286022 Hartree
Enthalpy=-233.285078 Hartree
Free Energy=-233.319763 Hartree
Entropy=73.001 cal/mol-K

Cyclopentane

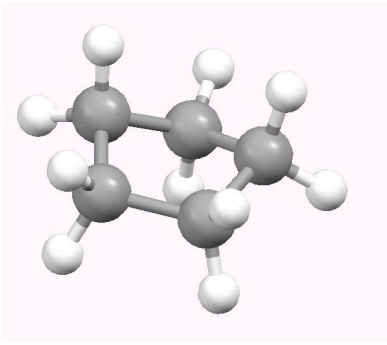

C	0.00000000	0.00000000	0.00000000
H	0.45323800	0.65056500	-0.75567900
H	0.40872200	0.31334500	0.96760800
C	0.32208200	-1.49267400	-0.26290700
C	-0.93861500	-2.24286900	0.20005800
C	-2.07834200	-1.32462200	-0.27244400
C	-1.55691800	0.10515000	0.01177400
H	-1.93069300	0.82831300	-0.72099700
H	-1.90519900	0.44609300	0.99380400
H	-3.03547300	-1.53314500	0.21846700
H	-2.23197500	-1.46266100	-1.35117600
H	-0.94906100	-2.32022200	1.29636500
H	-1.00772600	-3.26063700	-0.20067200
H	1.23451000	-1.82541000	0.24425500
H	0.47073300	-1.66243000	-1.33762500

Route= #N B3LYP/6-31G* 5D OPT FREQ
Basis=6-31G(d)
B3LYP Energy=-196.55372187 Hartree
ZPE=0.141490 Hartree
Conditions=298K, 1.00000 atm
Internal Energy=-196.407070 Hartree

Enthalpy=-196.406126 Hartree
Free Energy=-196.441192 Hartree
Entropy=73.802 cal/mol-K

Dinitrogen

Route= #N B3LYP/6-31G* 5D OPT FREQ
Basis=6-31G(d)
B3LYP Energy=-109.520718355 Hartree
ZPE=0.005600 Hartree
Conditions=298K, 1.00000 atm
Internal Energy=-109.512758 Hartree
Enthalpy=-109.511814 Hartree
Free Energy=-109.533568 Hartree
Entropy=45.785 cal/mol-K

N	0.00000000	0.00000000	0.00000000
N	0.00000000	0.00000000	-1.10530400

***Donor/acceptor carbenoid cyclopropanation product* 2.20c**

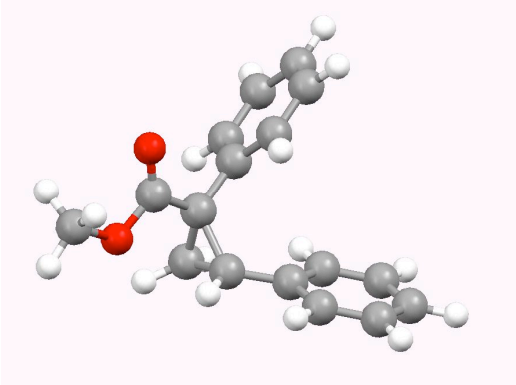

Route= #N B3LYP/6-31G(d) OPT FREQ
Basis=6-31G(d)
B3LYP Energy=-807.874908615 Hartree
ZPE=0.287567 Hartree
Conditions=298K, 1.00000 atm
Internal Energy=-807.570838 Hartree
Enthalpy=-807.569894 Hartree
Free Energy=-807.633152 Hartree
Entropy=133.138 cal/mol-K

C	0.00000000	0.00000000	0.00000000
C	1.30206300	-0.35855000	-0.66177400
O	1.80185200	-1.53899700	-0.20974800
C	3.02794800	-1.95797400	-0.82821200
H	2.89201800	-2.08748000	-1.90531900
H	3.28377400	-2.90742700	-0.35638400
H	3.81548300	-1.21915300	-0.65840000
O	1.85445000	0.30023400	-1.51675500
C	-0.47843600	1.39196600	-0.30756200
C	-0.42763500	2.39911600	0.66324300
C	-0.84805700	3.69781700	0.36886000
C	-1.32152200	4.00572100	-0.90645200
C	-1.36902500	3.00965100	-1.88475800
C	-0.94979900	1.71455400	-1.58734300
H	-0.98706600	0.94338100	-2.35075600
H	-1.73475400	3.24192000	-2.88143300
H	-1.65055900	5.01528900	-1.13833500
H	-0.80065100	4.46722100	1.13517600
H	-0.04811600	2.16775700	1.65531600
C	-1.01407200	-1.18591200	0.12236800
C	-2.47146600	-1.04751900	-0.16407000
C	-3.04987100	-1.92515500	-1.09480100
C	-4.40922500	-1.86334100	-1.39871300
C	-5.22194300	-0.91540900	-0.77585600
C	-4.66063200	-0.03514800	0.15093100
C	-3.30148900	-0.10068100	0.45550600
H	-2.88844100	0.59779400	1.17610800

H	-5.28331400	0.70761500	0.64270900
H	-6.28214400	-0.86367200	-1.00853500
H	-4.83209400	-2.55740300	-2.12043400
H	-2.42360600	-2.66904000	-1.58248500
H	-0.59693300	-2.11879600	-0.24558800
C	-0.32752700	-0.63938600	1.33485300
H	-0.91636900	-0.04002600	2.02271700
H	0.43456400	-1.25154200	1.80454300

***Donor/acceptor carbenoid C–H insertion product – 1,4 cyclohexadiene* (2.22c)**

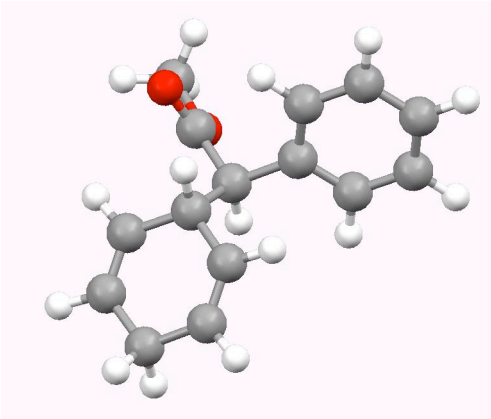

Route= #N B3LYP/6-31G* 5D OPT FREQ
Basis=6-31G(d)
B3LYP Energy=-731.639706345 Hartree
ZPE=0.275898 Hartree
Conditions=298K, 1.00000 atm
Internal Energy=-731.348304 Hartree
Enthalpy=-731.347359 Hartree
Free Energy=-731.408583 Hartree
Entropy=128.855 cal/mol-K

C	0.00000000	0.00000000	0.00000000
C	0.18654500	1.46628500	0.37458300
O	0.16612000	1.90724800	1.50644600
O	0.41062400	2.22859600	-0.71505300
C	0.65919800	3.62012400	-0.45393000
H	-0.19710500	4.07452900	0.05160100
H	0.81553300	4.07731800	-1.43134600
H	1.54632400	3.73983100	0.17371000
C	-1.12106700	-0.65148100	0.88678900
C	-1.28325400	-2.11547100	0.55635800
H	-0.41299400	-2.74768300	0.71616900
C	-2.40990600	-2.65321500	0.08177500
H	-2.44479000	-3.71978200	-0.13619200
C	-3.67138300	-1.86983100	-0.16252600
C	-3.54930900	-0.43325000	0.26805900
H	-4.44643700	0.17988200	0.19367100
C	-2.42338800	0.10223700	0.74636700
H	-2.41360500	1.14253300	1.06466300
H	-4.51504200	-2.34612000	0.36415800
H	-3.95045100	-1.92422000	-1.22874100
H	-0.77094700	-0.55097200	1.92542300
H	-0.32515700	-0.03931200	-1.04359600
C	1.34577900	-0.71305600	0.11402400
C	1.84815600	-1.44583200	-0.96891300
C	3.06545200	-2.12220500	-0.87051700
C	3.80042400	-2.07254400	0.31512100
C	3.31016100	-1.34096900	1.39925700
C	2.09306600	-0.66557400	1.30040800
H	1.72510500	-0.08429300	2.14099800
H	3.87784500	-1.29201900	2.32484900
H	4.74875900	-2.59748700	0.39319200
H	3.43874600	-2.68609000	-1.72145900
H	1.27910100	-1.48897900	-1.89431000

Donor/acceptor carbenoid C–H insertion product – cyclopentane (**2.21c**)

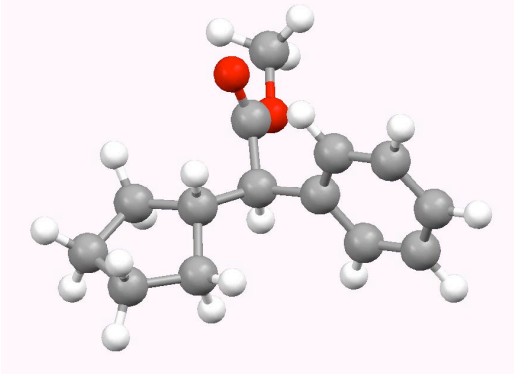

Route= #N B3LYP/6-31G* 5D OPT FREQ
Basis=6-31G(d)
B3LYP Energy=-694.780924159 Hartree
ZPE=0.294678 Hartree
Conditions=298K, 1.00000 atm
Internal Energy=-694.470908 Hartree
Enthalpy=-694.469964 Hartree
Free Energy=-694.531035 Hartree
Entropy=128.535 cal/mol-K

C	0.00000000	0.00000000	0.00000000
O	-0.01513200	-1.36562500	-0.44801400
C	-0.19827800	-2.28932800	0.51949700
C	-0.13957100	-3.70664100	-0.04169500
C	1.25807500	-4.28370600	0.17792900
C	1.97650000	-4.81637000	-0.90009200
C	3.24078700	-5.37806700	-0.71018600
C	3.80778400	-5.40978300	0.56465100
C	3.10272300	-4.87411400	1.64521700
C	1.83868000	-4.31482400	1.45476700
H	1.30179800	-3.88571200	2.29567200
H	3.53897000	-4.88873400	2.64072300
H	4.79216600	-5.84503400	0.71508100
H	3.78173700	-5.78744700	-1.55946400
H	1.54144200	-4.79217100	-1.89656500
H	-0.31299700	-3.63878600	-1.12151900
O	-0.36614800	-2.00596800	1.68843500
H	-0.94910300	0.25818300	0.47733100
H	0.15505200	0.60034600	-0.89698200
H	0.81145400	0.15969900	0.71510900
C	-1.25433400	-4.57359500	0.58539700
H	-1.08198900	-4.60223500	1.66896800
C	-2.68625800	-4.03563600	0.32817000
C	-3.62251000	-5.28008000	0.34282900
C	-2.69254800	-6.50492600	0.53762200
C	-1.31284100	-6.02089100	0.06393800
H	-0.48698600	-6.64151700	0.42527800
H	-1.26813700	-6.02338700	-1.03555200
H	-3.04263600	-7.39377200	0.00162800
H	-2.63792200	-6.77143900	1.60106200
H	-4.16615000	-5.35789200	-0.60555700
H	-4.37892700	-5.21765100	1.13218900
H	-2.72702800	-3.54285400	-0.65256700
H	-2.96955900	-3.28417200	1.07136600

Acceptor carbenoid cyclopropanation product (**2.20b**)

C	0.00000000	0.00000000	0.00000000
C	-1.35667000	-0.51423000	-0.32058400
O	-1.89654200	0.09408500	-1.40852200
C	-3.20536800	-0.36417100	-1.77770300
H	-3.18783100	-1.43157700	-2.01411600
H	-3.48311400	0.21861800	-2.65676900
H	-3.91578400	-0.19486900	-0.96402000
O	-1.92933600	-1.38204500	0.30579100

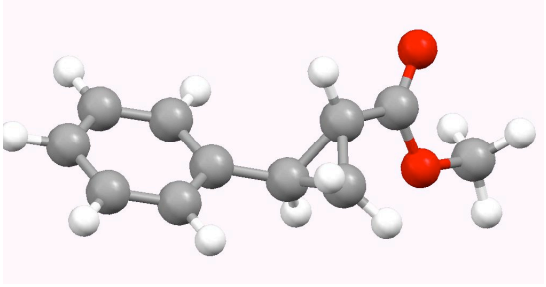

Route= #N B3LYP/6-31G* 5D OPT FREQ
Basis=6-31G(d)
B3LYP Energy=-576.816076675 Hartree
ZPE=0.206820 Hartree
Conditions=298K, 1.00000 atm
Internal Energy=-576.597324 Hartree
Enthalpy=-576.596380 Hartree
Free Energy=-576.649249 Hartree
Entropy=111.272 cal/mol-K

H	0.42134000	-0.47203600	0.88113800
C	0.97766200	0.38015100	-1.11362800
C	2.42237800	-0.00970700	-1.00516300
C	2.79662800	-1.36081800	-1.05568800
C	4.13941000	-1.73199900	-0.99126300
C	5.13229600	-0.75548000	-0.87579700
C	4.77216900	0.59189400	-0.82624600
C	3.42648000	0.96028200	-0.89112800
H	3.15007800	2.01099400	-0.85707800
H	5.53776600	1.35830100	-0.73714300
H	6.17869000	-1.04413500	-0.82310900
H	4.41116500	-2.78378400	-1.02725100
H	2.02596400	-2.12352000	-1.13836200
H	0.55256000	0.29727100	-2.11250300
C	0.37678400	1.45055100	-0.25947200
H	1.00102000	1.92233000	0.49416500
H	-0.38251500	2.09040100	-0.69666500

***Acceptor carbenoid C–H insertion product – 1,4-cyclohexadiene* (2.22b)**

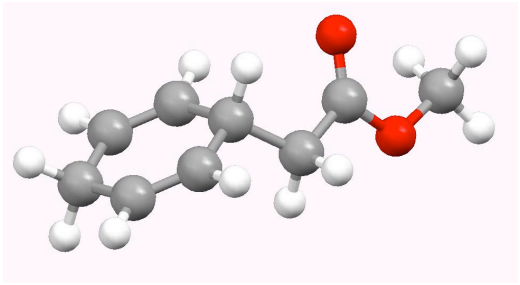

Route= #N B3LYP/6-31G* 5D OPT FREQ
Basis=6-31G(d)
B3LYP Energy=-500.59629935 Hartree
ZPE=0.194514 Hartree
Conditions=298K, 1.00000 atm
Internal Energy=-500.390863 Hartree
Enthalpy=-500.389918 Hartree
Free Energy=-500.439782 Hartree
Entropy=104.947 cal/mol-K

C	0.00000000	0.00000000	0.00000000
C	1.28504600	0.70676300	0.38955700
O	1.45620100	1.36589400	1.39367900
O	2.25316800	0.48737900	-0.52802800
C	3.52765800	1.08135200	-0.23349100
H	3.43666500	2.16820800	-0.15638000
H	4.17697300	0.80921600	-1.06624500
H	3.92638400	0.69255800	0.70757500
C	-1.23325900	0.47474200	0.80626300
C	-2.39591200	-0.46015900	0.57307800
H	-2.22985500	-1.50795000	0.82398500
C	-3.57696500	-0.07992300	0.08059300
H	-4.36444800	-0.81875400	-0.06155900
C	-3.90423400	1.34210200	-0.28936500
C	-2.76829100	2.28996100	-0.01010500
H	-2.94755700	3.34360400	-0.22005900
C	-1.58806100	1.90785500	0.48359100
H	-0.81398600	2.64624000	0.67981100
H	-4.80712200	1.67051500	0.25225000
H	-4.19011000	1.39693000	-1.35356300
H	-0.93782000	0.42385000	1.86626800
H	-0.16530700	0.12143100	-1.07594700
H	0.16437500	-1.07507600	0.16319100

***Acceptor carbenoid C–H insertion product – cyclopentane* (2.21b)**

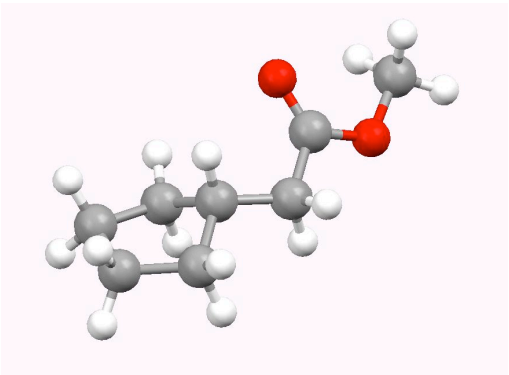

Route= #N B3LYP/6-31G* 5D OPT FREQ
Basis=6-31G(d)
B3LYP Energy=-463.737165927 Hartree
ZPE=0.213136 Hartree
Conditions=298K, 1.00000 atm
Internal Energy=-463.513148 Hartree
Enthalpy=-463.512204 Hartree
Free Energy=-463.562786 Hartree
Entropy=106.457 cal/mol-K

C	0.00000000	0.00000000	0.00000000
O	-1.21064500	-0.73511900	-0.23618400
C	-2.31280300	-0.25213600	0.38382800
C	-3.52018400	-1.12625900	0.09798700
H	-3.37130500	-2.06618800	0.64962900
H	-3.50769800	-1.40160700	-0.96440100
C	-4.85003000	-0.48001700	0.48643500
H	-4.77823400	-0.15171000	1.53227000
C	-5.26168000	0.73391900	-0.36720400
C	-6.75577800	0.93280200	-0.03723600
C	-7.29863200	-0.48420500	0.32372700
C	-6.06280200	-1.42009600	0.33618700
H	-6.11107500	-2.17963500	1.12519700
H	-5.98565100	-1.95728500	-0.61968200
H	-8.05109000	-0.82999600	-0.39293600
H	-7.78593500	-0.47047900	1.30489000
H	-7.30472000	1.39275700	-0.86575100
H	-6.86016700	1.60625400	0.82149100
H	-5.13725000	0.48535800	-1.43187700
H	-4.65319100	1.61940500	-0.16183400
O	-2.29986900	0.73733800	1.08503700
H	-0.10129800	1.03137300	-0.34892100
H	0.77428600	-0.52078800	-0.56454800
H	0.24375200	0.01081700	1.06600100

Dirhodium formate

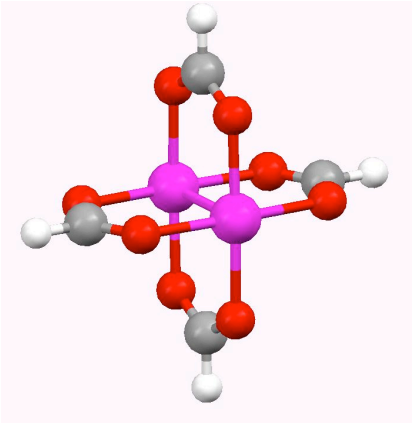

Route= #N B3LYP/gen pseudo=read gfprint OPT FREQ
B3LYP Energy=-977.981873264 Hartree
ZPE=0.101954 Hartree
Internal Energy=-977.866167 Hartree

Rh	0.00000000	0.00000000	0.00000000
Rh	-0.00000200	0.00000100	2.38968300
O	-1.44640800	-1.45404100	2.33316300
C	-1.84327100	-1.84785700	1.19484000
O	-1.45075300	-1.44970000	0.05651800
H	-2.61841200	-2.62439900	1.19483700
O	-1.45406600	1.44638800	2.33316300
C	-1.84780600	1.84332600	1.19483700
O	-1.44976300	1.45069200	0.05651700
H	-2.62466600	2.61814800	1.19483500
O	1.44635100	1.45409600	2.33316300
C	1.84338400	1.84774300	1.19484000
O	1.45069200	1.44976200	0.05651700
H	2.61800000	2.62480900	1.19483600
O	1.45405300	-1.44639000	2.33316800
C	1.84781600	-1.84330800	1.19484300
O	1.44975500	-1.45069600	0.05652200
H	2.62461500	-2.61819000	1.19484400

Enthalpy=-977.865223 Hartree
Free Energy=-977.920161 Hartree
Entropy=115.627 cal/mol-K

***Phenyl diazoacetate – dirhodium formate complex* (2.4c)**

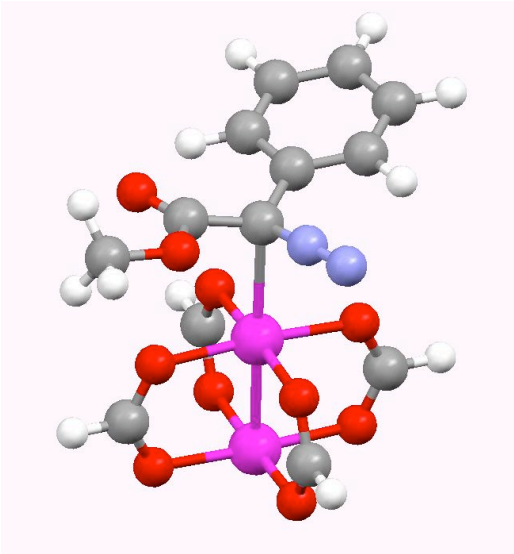

Route= # b3lyp/gen pseudo=read gfprint OPT FREQ
B3LYP Energy=-1585.66688858 Hartree
ZPE=0.261048 Hartree
Internal Energy=-1585.378329 Hartree
Enthalpy=-1585.377384 Hartree
Free Energy=-1585.464975 Hartree
Entropy=184.351 cal/mol-K

Rh	0.00000000	0.00000000	0.00000000
Rh	-2.27484600	-0.76873500	-0.33478400
O	-1.78975300	-2.46110300	0.73026100
C	-0.61476600	-2.55537500	1.18789200
O	0.34008800	-1.72717300	1.06717200
H	-0.38764900	-3.46435500	1.76073700
O	-1.65688700	-1.68485100	-2.06317600
C	-0.43760100	-1.56876000	-2.38329100
O	0.47834300	-0.95245700	-1.76047900
H	-0.13252800	-2.06356100	-3.31482400
O	-2.64578200	0.95672500	-1.38512000
C	-1.70026000	1.78695900	-1.51025400
O	-0.51644700	1.69907000	-1.06160800
H	-1.93084600	2.69985200	-2.07592000
O	-2.78350000	0.18890900	1.41570600
C	-1.87357500	0.79857000	2.04596400
O	-0.64625200	0.90653300	1.73645600
H	-2.17571200	1.29785400	2.97632900
C	2.37112900	0.64105100	0.27726300
C	2.39850700	1.87206900	-0.58471500
O	2.66733700	1.87494300	-1.76467100
O	2.07027600	2.96993800	0.12425300
C	1.92782000	4.17961400	-0.64271900
H	2.86207700	4.41843000	-1.15631100
H	1.12469900	4.05975600	-1.37260700
H	1.67850900	4.95224600	0.08434300
N	2.26228800	0.94501200	1.59252500
N	2.12856600	1.15999200	2.68979800
C	3.20836600	-0.57085900	-0.01226800
C	3.58699600	-0.87248900	-1.33102900
C	4.36113300	-2.00236000	-1.59369700
C	4.76579100	-2.84985800	-0.56216300
C	4.38711800	-2.55626800	0.74861700
C	3.61538700	-1.42935800	1.02284300
H	3.32776100	-1.23355100	2.05130300
H	4.69216000	-3.20372300	1.56613000
H	5.36842200	-3.72825300	-0.77567400
H	4.64574500	-2.21798300	-2.62010400
H	3.27469900	-0.22571700	-2.13810000

Phenyl diazoacetate – dirhodium formate complex N2 extrusion TS (TS-Ic)

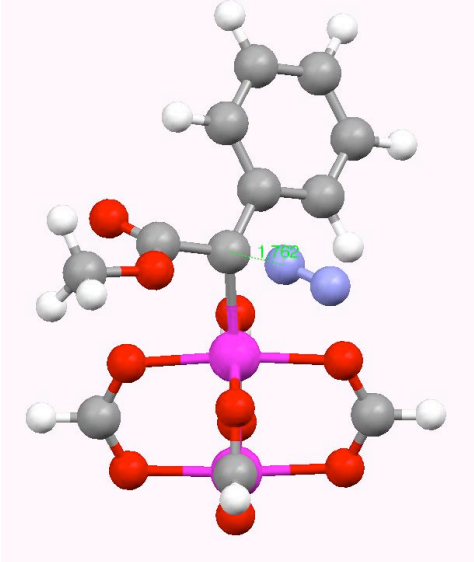

Route= # b3lyp/gen pseudo=read gfprint OPT=(TS,CalcFC,NoEigenTest) freq
B3LYP Energy=-1585.64967614 Hartree
ZPE=0.258951 Hartree
Internal Energy=-1585.363376 Hartree
Enthalpy=-1585.362432 Hartree
Free Energy=-1585.448394 Hartree
Entropy=180.923 cal/mol-K

Rh	0.00000000	0.00000000	0.00000000
C	2.12522800	0.46827100	0.13864300
C	2.36288900	1.81509700	-0.48162700
O	2.12811200	2.85317700	0.34085900
C	2.14513200	4.14814700	-0.28829200
H	3.11649400	4.33651500	-0.75215000
H	1.95561000	4.85999000	0.51477400
H	1.36201800	4.20266500	-1.04784600
O	2.65901800	1.92510500	-1.65336700
C	3.16486800	-0.57521700	-0.06188600
C	4.38342700	-0.29931600	-0.71642900
C	5.33011000	-1.30362000	-0.89906400
C	5.09521300	-2.59036800	-0.40896400
C	3.89955800	-2.87283000	0.25612300
C	2.93743900	-1.88023800	0.41879300
H	2.00613400	-2.10278700	0.92542800
H	3.71078300	-3.87207900	0.63837700
H	5.84034100	-3.36949000	-0.54599700
H	6.25672500	-1.07807100	-1.41934200
H	4.57422400	0.69090700	-1.11048900
O	-0.57812900	1.47087400	1.33192900
C	-1.82056000	1.63464300	1.54986800
O	-2.79119400	0.99969500	1.05507400
Rh	-2.38469400	-0.52397300	-0.27550400
O	-2.20237000	-1.83710600	1.30747100
C	-1.08100900	-1.94317300	1.87012200
O	0.00551500	-1.34379200	1.58013100
H	-1.02191900	-2.63805500	2.71947300
O	-2.44121700	0.81634300	-1.83072600
C	-1.37492700	1.42821100	-2.11659400
O	-0.23632100	1.32737500	-1.56282700
H	-1.43047200	2.14212900	-2.94986200
O	-1.84354900	-2.00582400	-1.59420300
C	-0.61263000	-2.16668200	-1.82684600
O	0.37175700	-1.52891900	-1.33958000
H	-0.35186700	-2.96064200	-2.54022300
H	-2.07135500	2.43274500	2.26256900
N	2.22549500	0.81636000	1.86186300
N	1.98583400	0.71676000	2.94160100

***Phenyl carbenoid complex* (2.5c)**

Rh	0.00000000	0.00000000	0.00000000
Rh	2.44038900	-0.41854200	-0.01861600
O	2.17764900	-1.45335400	-1.78495000

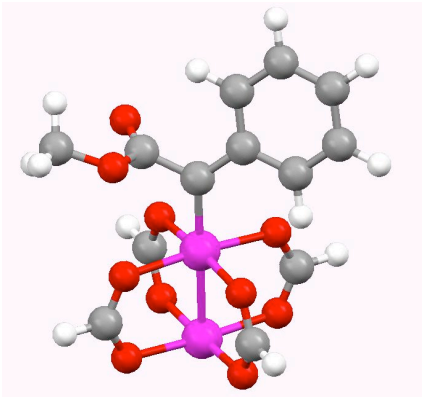

Route= # b3lyp/gen pseudo=read gfprint integral(grid=ultrafine) OPT FREQ
B3LYP Energy=-1476.15920343 Hartree
ZPE=0.251451 Hartree
Internal Energy=-1475.882383 Hartree
Enthalpy=-1475.881439 Hartree
Free Energy=-1475.963956 Hartree
Entropy=173.670 cal/mol-K

C	1.01276100	-1.54241600	-2.25218200
O	-0.07094700	-1.07424700	-1.77164200
H	0.90145000	-2.09391200	-3.19640200
O	2.07267000	-2.13923100	1.05985300
C	0.87972100	-2.41281800	1.35488000
O	-0.17739000	-1.76315700	1.06528600
H	0.71514800	-3.33088300	1.93628300
O	2.57218900	0.64204100	1.73911100
C	1.50536200	1.11458400	2.21762800
O	0.32370100	1.02418300	1.75690600
H	1.59389600	1.68028300	3.15521900
O	2.65557500	1.33159900	-1.08480900
C	1.61835700	1.99769600	-1.34556500
O	0.40932400	1.73221300	-1.04962500
H	1.76439100	2.93321100	-1.90369700
C	-1.97622400	0.36171800	0.05263100
C	-2.34758800	1.78703200	0.26714100
O	-2.48407800	2.26864100	1.37505000
O	-2.48875000	2.45214800	-0.88793400
C	-2.70974700	3.87101800	-0.76810300
H	-3.62511200	4.07196300	-0.20555500
H	-1.86236500	4.34081300	-0.26313800
H	-2.79840800	4.23527600	-1.79112000
C	-3.05263900	-0.58458400	0.01206600
C	-4.37676800	-0.21467600	0.38642300
C	-5.40978500	-1.13718400	0.34430100
C	-5.16056700	-2.44358300	-0.09803800
C	-3.87304200	-2.82822900	-0.48529100
C	-2.82464800	-1.91968800	-0.41849800
H	-1.82784700	-2.20531300	-0.72291600
H	-3.68990800	-3.84083600	-0.83227400
H	-5.97489600	-3.16209300	-0.14057500
H	-6.41088700	-0.84698800	0.64895500
H	-4.56711800	0.79201100	0.74328800

Cyclopropanation TS with styrene (**TS-IIc**)

Rh	0.00000000	0.00000000	0.00000000
C	-2.03837600	0.39647400	0.47610600
C	-2.12745700	1.73309100	1.15226900
O	-1.98648400	2.79676500	0.33412500
C	-1.80800800	4.05595800	1.00349800
H	-2.67237300	4.28903100	1.63151400
H	-1.70173100	4.79329300	0.20718100
H	-0.90978700	4.02546900	1.62413900
O	-2.19682300	1.83814200	2.36389800

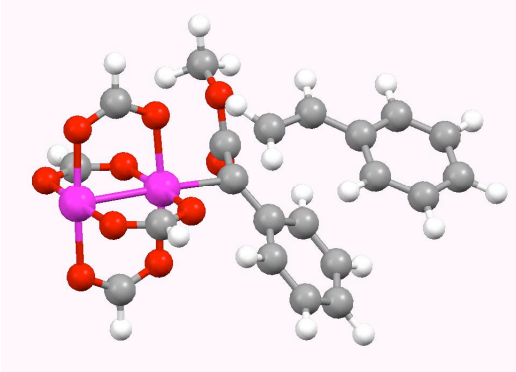

Route= # b3lyp/gen pseudo=read gfprint
OPT=(TS,CalcFC,NoEigenTest) freq
B3LYP Energy=-1785.79530531 Hartree
ZPE=0.387476 Hartree
Internal Energy=-1785.375462 Hartree
Enthalpy=-1785.374518 Hartree
Free Energy=-1785.471680 Hartree
Entropy=204.496 cal/mol-K

C	-2.95493600	-0.64393700	0.94164900
C	-2.77201700	-1.98185500	0.51516000
C	-3.61067500	-2.99956000	0.95851200
C	-4.65576100	-2.71496500	1.84106000
C	-4.86784500	-1.39949300	2.26397500
C	-4.04091800	-0.37683900	1.81439000
H	-4.20928300	0.63340400	2.16441400
H	-5.68363100	-1.17033500	2.94389000
H	-5.30422400	-3.51222600	2.19516000
H	-3.44318200	-4.01939300	0.62254100
H	-1.96111300	-2.20690000	-0.16500500
O	0.20266800	1.43469800	-1.48699000
C	1.33839600	1.60351500	-2.03378200
O	2.41670100	0.99565800	-1.79865600
Rh	2.40497800	-0.47245100	-0.35340000
O	1.84440400	-1.85977600	-1.77496500
C	0.61812100	-2.01885200	-2.00794900
O	-0.37290500	-1.42778400	-1.46721200
H	0.35819400	-2.76145700	-2.77607900
O	2.83204300	0.94113400	1.07867900
C	1.86181800	1.54163300	1.61583900
O	0.61940800	1.39371000	1.39404100
H	2.11361100	2.29360200	2.37687500
O	2.27434500	-1.90741700	1.11674200
C	1.15629200	-2.07313000	1.67743500
O	0.05942500	-1.47410800	1.44721300
H	1.11458300	-2.83528600	2.46827800
H	1.37466000	2.38103700	-2.81020500
C	-2.75925600	0.77558900	-1.65108200
C	-3.98837400	1.31334700	-1.38013900
C	-5.25652700	0.61759900	-1.27557000
C	-6.39221100	1.33743200	-0.84390300
C	-7.63084900	0.71717100	-0.71979400
C	-7.76201000	-0.64099500	-1.02413600
C	-6.64947500	-1.37010100	-1.45787900
C	-5.41175100	-0.75060500	-1.58781600
H	-4.55985500	-1.32467300	-1.93536200
H	-6.75225000	-2.42406300	-1.69997400
H	-8.72847200	-1.12854000	-0.93001700
H	-8.49292400	1.28801700	-0.38644700
H	-6.28716200	2.39316900	-0.60544900
H	-4.02311400	2.37878800	-1.16299300
H	-2.63655300	-0.25741900	-1.95694900
H	-1.91798600	1.42863500	-1.84197600

C–H insertion TS with 1,4-cyclohexadiene **(TS-VIIIc)**

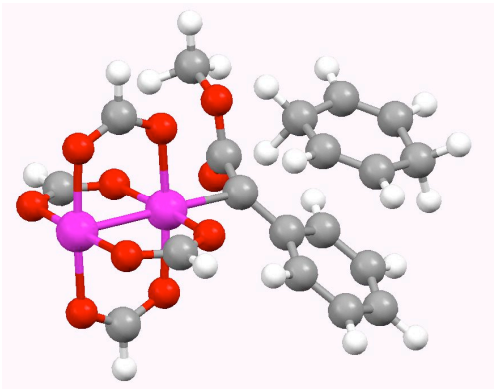

Route= #N b3lyp/gen pseudo=read gfprint integral(grid=ultrafine) OPT=(TS,CalcFC, Noeigen) freq
B3LYP Energy=-1709.5625612 Hartree
ZPE=0.371162 Hartree
Internal Energy=-1709.160090 Hartree
Enthalpy=-1709.159146 Hartree
Free Energy=-1709.253866 Hartree
Entropy=199.355 cal/mol-K

Rh	0.00000000	0.00000000	0.00000000
C	2.04095700	0.49400500	-0.39573500
C	2.13027300	1.92289600	-0.84032900
O	2.04877400	2.81484100	0.17160000
C	1.91249200	4.18629300	-0.23611300
H	2.76515000	4.49712300	-0.84604400
H	1.87129100	4.76135800	0.68943900
H	0.99265000	4.31475300	-0.81094300
O	2.18546600	2.24818200	-2.01120200
C	3.02043600	-0.42798400	-0.97342200
C	2.89348800	-1.82022600	-0.74358200
C	3.84306700	-2.71549400	-1.22759000
C	4.94622300	-2.24956400	-1.94774600
C	5.09335800	-0.87802600	-2.18832700
C	4.15279700	0.02147400	-1.70224000
H	4.26778300	1.07750000	-1.91106100
H	5.94453200	-0.51345800	-2.75691700
H	5.68259400	-2.95088500	-2.33209100
H	3.72079700	-3.78004200	-1.04699600
H	2.03867200	-2.18081900	-0.18741500
O	-0.10435900	1.06469000	1.77659700
C	-1.22818200	1.13790100	2.36854600
O	-2.32983700	0.62751900	2.02983900
Rh	-2.40339500	-0.50241200	0.30066500
O	-1.85057100	-2.17691300	1.37387900
C	-0.62335300	-2.40204600	1.53484300
O	0.36899200	-1.72149600	1.11667500
H	-0.36429600	-3.30152400	2.11265900
O	-2.83312600	1.19062100	-0.78529700
C	-1.86334100	1.88402800	-1.19655100
O	-0.62010800	1.67806400	-1.03573600
H	-2.11704100	2.78714200	-1.76955700
O	-2.31853400	-1.59009200	-1.44852500
C	-1.21237700	-1.64972900	-2.05349700
O	-0.10071800	-1.12787200	-1.72606600
H	-1.19854600	-2.22972200	-2.98714800
H	-1.22995100	1.72469300	3.29883600
C	3.15882600	0.66052800	2.01426100
C	3.24508000	-0.72752500	2.49448000
C	4.37932600	-1.44284200	2.38567000
C	5.65264300	-0.87531500	1.83400200
C	5.57606100	0.59595300	1.55280100
C	4.43761200	1.30213700	1.66617400
H	4.42577200	2.36898400	1.46482600
H	6.50045900	1.09611200	1.27135700

H	5.92379700	-1.41534300	0.90799000
H	6.48768800	-1.08345400	2.52308400
H	4.40362500	-2.47613600	2.72554100
H	2.33993600	-1.18018000	2.88601400
H	2.47568000	0.56048600	0.95328500
H	2.43713800	1.29471000	2.53265000

***C–H insertion with 1,4 cyclohexadiene – zwitterionic intermediate* (2.23c)**

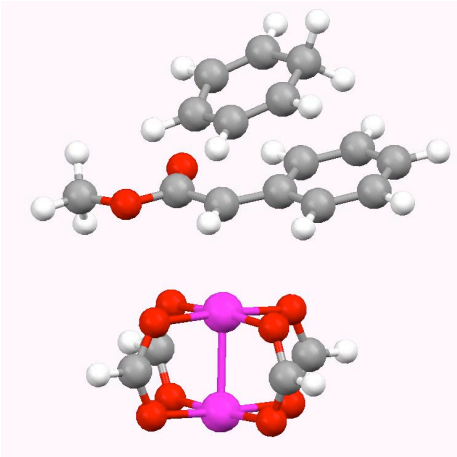

Route= #N b3lyp/gen pseudo=read gfprint OPT FREQ
B3LYP Energy=-1709.58840374 Hartree
ZPE=0.375106 Hartree
Conditions=298K, 1.00000 atm
Internal Energy=-1709.181323 Hartree
Enthalpy=-1709.180379 Hartree
Free Energy=-1709.277410 Hartree
Entropy=204.219 cal/mol-K

Rh	0.00000000	0.00000000	0.00000000
C	2.50264300	0.52625900	0.12255900
C	2.48947200	1.77181600	-0.65367900
O	2.07648900	2.82261000	0.11574800
C	1.88761200	4.05501900	-0.58687200
H	2.81553000	4.38479900	-1.06393800
H	1.57144300	4.77570300	0.16900900
H	1.11505900	3.94022900	-1.35138200
O	2.81603200	1.92101000	-1.82348100
C	3.06660900	-0.71296200	-0.33248600
C	3.17259200	-1.80066300	0.58427500
C	3.73774800	-3.01082400	0.20639400
C	4.25241700	-3.17772700	-1.08639500
C	4.14681100	-2.12833300	-2.00996900
C	3.57786300	-0.91385200	-1.64848000
H	3.48612200	-0.10789700	-2.36432800
H	4.52119400	-2.26041400	-3.02223200
H	4.69330800	-4.12621900	-1.38217200
H	3.78991000	-3.82736200	0.92238700
H	2.74802500	-1.68704400	1.57567900
O	-0.33338100	1.34214800	1.53760700
C	-1.52652400	1.52160200	1.92463200
O	-2.58149200	0.96890600	1.49505800
Rh	-2.39362600	-0.43092500	-0.00028400
O	-2.06950700	-1.89060500	1.41303300
C	-0.88056800	-2.09223500	1.79318700
O	0.17529400	-1.50006800	1.41427600
H	-0.74249500	-2.87942900	2.54761400
O	-2.60640700	1.04367500	-1.41250900
C	-1.56202600	1.65529900	-1.78335400
O	-0.36934500	1.47544800	-1.39539000
H	-1.70589900	2.44192500	-2.53682800
O	-2.08621600	-1.80789500	-1.49421000
C	-0.90099400	-1.96737600	-1.91262300
O	0.15364600	-1.38613600	-1.51992200
H	-0.76935400	-2.70282500	-2.71814600

H	-1.66120200	2.24966800	2.73677600
C	4.91417600	1.49919100	1.07390400
C	5.09929300	0.46184400	2.02396700
C	5.79720900	-0.66369400	1.69482800
C	6.46534600	-0.82255200	0.37274100
C	6.25334900	0.32200500	-0.55646600
C	5.55328600	1.43500700	-0.19199500
H	5.41573900	2.24767200	-0.89696000
H	6.71241300	0.26298100	-1.53938800
H	6.11731100	-1.76121800	-0.11082500
H	7.54804200	-1.00172800	0.51478100
H	5.92230000	-1.46295700	2.42033500
H	4.63498300	0.55164600	3.00219000
H	2.26748700	0.62385900	1.17769400
H	4.37888200	2.39781500	1.35869500

C–H insertion TS with cyclopentane
(TS-VIIc)

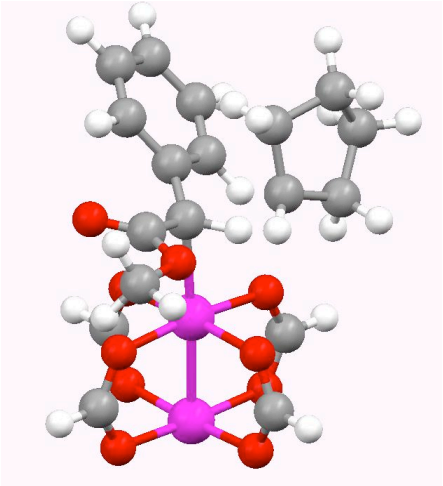

Route= #N b3lyp/gen pseudo=read gfprint integral(grid=ultrafine)
OPT=(TS,CalcFC, NoEigentest) FREQ
B3LYP Energy=-1672.68165346 Hartree
ZPE=0.391017 Hartree
Conditions=298K, 1.00000 atm
Internal Energy=-1672.259392 Hartree
Enthalpy=-1672.258447 Hartree
Free Energy=-1672.353622 Hartree
Entropy=200.312 cal/mol-K

Rh	0.00000000	0.00000000	0.00000000
O	-0.03484400	-1.59215100	-1.30986900
C	-1.13233500	-2.19948000	-1.49895400
O	-2.26005500	-1.96613200	-0.97518400
Rh	-2.39312600	-0.39691800	0.34718500
O	-1.89606800	-1.65944000	1.90069500
C	-0.67678400	-1.81590300	2.17514000
O	0.33216200	-1.28991800	1.60476500
H	-0.44894800	-2.49033900	3.01298300
O	-2.37957500	1.20636100	1.65090100
C	-1.28663500	1.80089000	1.86288200
O	-0.14430000	1.55517900	1.36242400
H	-1.32142100	2.64049200	2.57195600
O	-2.77799100	0.87480400	-1.21842700
C	-1.78872800	1.41234600	-1.79146500
O	-0.55555100	1.27338400	-1.52693700
H	-2.01978500	2.08912200	-2.62585500
H	-1.09250800	-3.03701200	-2.20912900
C	2.24352600	0.38362700	-0.44879800
C	2.24995800	1.57608000	-1.33864600
O	2.36803000	1.53401200	-2.54966000
O	2.02934800	2.74206300	-0.67627900
C	1.81651700	3.88667000	-1.51583600
H	2.68505900	4.06732700	-2.15493000
H	1.66231700	4.72257500	-0.83224800
H	0.93445300	3.73301200	-2.14120300
C	3.05927200	-0.79364200	-0.80276800

C	2.97788300	-1.95884700	-0.00525300
C	3.75914700	-3.07596200	-0.28094100
C	4.63658200	-3.07403500	-1.37061200
C	4.72660400	-1.93770200	-2.17383200
C	3.95857500	-0.80688900	-1.89263300
H	4.02512800	0.06000700	-2.53645700
H	5.40034100	-1.92453100	-3.02647400
H	5.23767600	-3.95203200	-1.59175800
H	3.67148900	-3.95955100	0.34611600
H	2.27479800	-1.98544200	0.81896300
H	2.23866800	0.64025500	0.67054900
C	3.37088000	1.33073500	1.45838100
H	2.84273200	2.27182000	1.34755300
C	3.17729800	0.52626300	2.73384100
C	4.51234000	-0.22061900	2.93878900
C	5.54928600	0.70796100	2.28084200
C	4.81086500	1.23748600	1.02529700
H	5.18923500	2.18987500	0.64042900
H	4.92057500	0.49757700	0.21711200
H	6.48464200	0.20061000	2.02544100
H	5.79423000	1.54009600	2.95305500
H	4.48662700	-1.18180000	2.41317900
H	4.72189700	-0.42182700	3.99385400
H	2.29477100	-0.12233800	2.71563000
H	3.00386200	1.25352100	3.54257600

Methyl diazoacetate – dirhodium formate complex (**2.4b**)

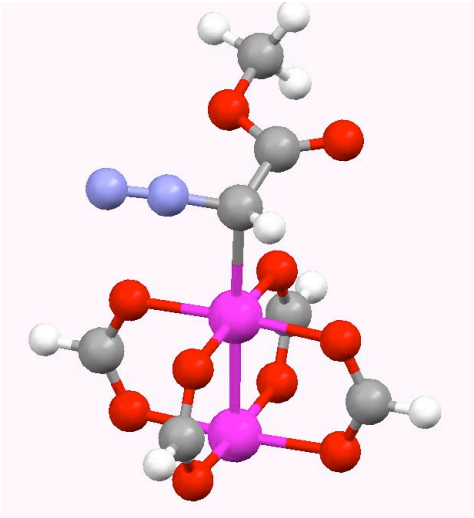

Rh	0.00000000	0.00000000	0.00000000
Rh	-2.31022700	-0.53258200	0.51001100
O	-1.62741500	-1.94717800	1.83411200
C	-0.37638200	-2.08930500	1.95548000
O	0.54725500	-1.45502900	1.35822500
H	-0.04347900	-2.85684400	2.66730600
O	-2.25871600	-1.92434700	-1.00108400
C	-1.18090600	-2.04705600	-1.65286800
O	-0.09385000	-1.41269300	-1.49443400
H	-1.18264000	-2.79419100	-2.45768900
O	-2.85663500	0.91898500	-0.84930000
C	-1.94570500	1.55761700	-1.44610300
O	-0.68662500	1.42517600	-1.32167300
H	-2.27534800	2.32255500	-2.16198400
O	-2.23479500	0.89094100	1.99738300
C	-1.15142200	1.51657700	2.16939800
O	-0.06347000	1.38851600	1.52423800
H	-1.14218800	2.26489800	2.97330800

Route= # b3lyp/gen pseudo=read gfprint OPT FREQ
B3LYP Energy=-1354.62315886 Hartree
ZPE=0.180291 Hartree
Conditions=298K, 1.00000 atm
Internal Energy=-1354.420255 Hartree
Enthalpy=-1354.419310 Hartree
Free Energy=-1354.495709 Hartree
Entropy=160.794 cal/mol-K

C	2.15137200	0.54289500	-0.68715600
C	3.09568100	-0.57197800	-0.37315900
O	3.26172800	-1.51837800	-1.10568600
O	3.70201000	-0.38695600	0.81542800
C	4.57290700	-1.45521000	1.23297700
H	4.00208400	-2.37910300	1.34920500
H	5.36783000	-1.60658200	0.49851100
H	4.98544800	-1.13300100	2.18862300
H	1.93118100	0.70744300	-1.73872600
N	2.38912300	1.70718200	-0.03724900
N	2.51293300	2.65360700	0.55576000

***Methyl diazoacetate – Nitrogen extrusion TS* (TS-Ib)**

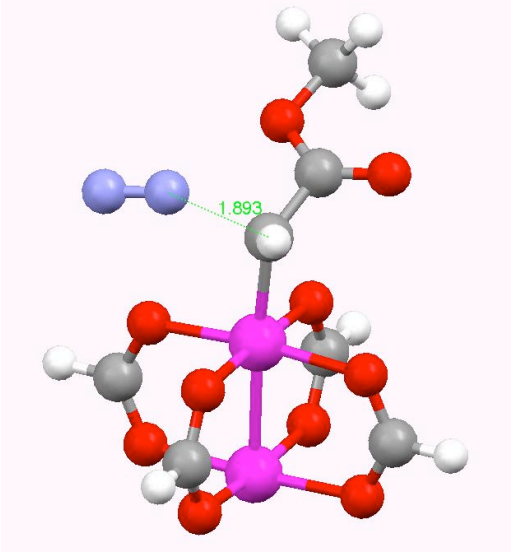

Route= # b3lyp/gen pseudo=read gfprint OPT=(TS,CalcFC,NoEigenTest) freq
B3LYP Energy=-1354.59910236 Hartree
ZPE=0.177397 Hartree
Conditions=298K, 1.00000 atm
Internal Energy=-1354.398867 Hartree
Enthalpy=-1354.397923 Hartree
Free Energy=-1354.474642 Hartree
Entropy=161.469 cal/mol-K

Rh	0.00000000	0.00000000	0.00000000
C	-1.89804200	0.22857200	-0.70052600
C	-2.99985700	-0.67322000	-0.25921800
O	-3.70757200	-0.25695500	0.79759100
C	-4.68979400	-1.19386600	1.28614100
H	-5.39059300	-1.45957000	0.49096200
H	-5.20180000	-0.67648400	2.09673000
H	-4.19427700	-2.09538500	1.65299900
O	-3.13206900	-1.73975500	-0.82392000
H	-1.96673200	0.47444100	-1.76275500
O	-0.02144500	1.51908600	1.38801600
C	1.03063700	1.74388100	2.07216200
O	2.13462100	1.14198700	2.01578700
Rh	2.33157000	-0.40476000	0.66315100
O	2.87129300	0.94709600	-0.80481400
C	1.96600000	1.48852500	-1.49434400
O	0.70496200	1.32228100	-1.41348700
H	2.29529100	2.19723500	-2.26656200
O	1.61338500	-1.72712600	2.07201100
C	0.36547100	-1.89364600	2.15428400
O	-0.55364800	-1.34284200	1.46746400
H	0.01722700	-2.60405000	2.91670800
O	2.40826100	-1.92535900	-0.71487800
C	1.36884000	-2.14981700	-1.39365000
O	0.24974200	-1.54909400	-1.34345300
H	1.42726600	-2.96663200	-2.12555600
H	0.95049600	2.56647900	2.79558800
N	-2.46646100	1.93987900	-0.12442900
N	-2.32425400	2.85051100	0.49194100

***Carbenoid complex* (2.5b)**

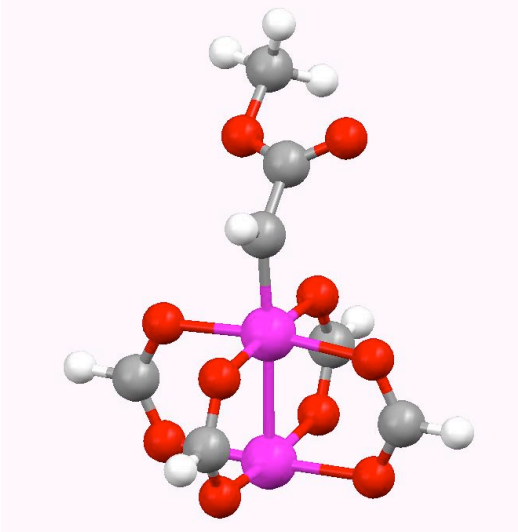

Route= # b3lyp/gen pseudo=read gfprint integral(grid=ultrafine) OPT FREQ
B3LYP Energy=-1245.08622565 Hartree
ZPE=0.169207 Hartree
Conditions=298K, 1.00000 atm
Internal Energy=-1244.896294 Hartree
Enthalpy=-1244.895350 Hartree
Free Energy=-1244.967606 Hartree
Entropy=152.075 cal/mol-K

Rh	0.00000000	0.00000000	0.00000000
C	-1.75307700	-0.59028800	-0.53591600
C	-3.03151500	-0.20380800	0.07787300
O	-3.48696300	1.01064300	-0.21170500
C	-4.71044300	1.39639800	0.45471900
H	-5.50711500	0.68322600	0.23019200
H	-4.95077100	2.38258700	0.06015800
H	-4.54860900	1.43919200	1.53407200
O	-3.54702100	-1.01455800	0.82809000
H	-1.83850700	-1.33700900	-1.33481100
O	-0.70513400	1.17066700	1.54089100
C	0.14317900	1.84678000	2.21070200
O	1.39235700	1.90745000	2.06045400
Rh	2.26998600	0.79362200	0.55601700
O	2.01203400	2.35875400	-0.75044800
C	0.91055600	2.42308200	-1.35612100
O	-0.08514100	1.63406300	-1.26998900
H	0.77494900	3.26180100	-2.05222000
O	2.45043800	-0.79808600	1.84511900
C	1.47229500	-1.58508200	1.94049700
O	0.35505300	-1.52874000	1.33181900
H	1.57937600	-2.43181300	2.63133300
O	2.94527900	-0.39325800	-0.99765200
C	2.10801500	-1.06483600	-1.65618400
O	0.84277300	-1.12367700	-1.50415800
H	2.50486700	-1.68540600	-2.47102200
H	-0.28459900	2.45136500	3.02204000

***C–H insertion TS with 1,4-cyclohexadiene* (TS-VIIIb)**

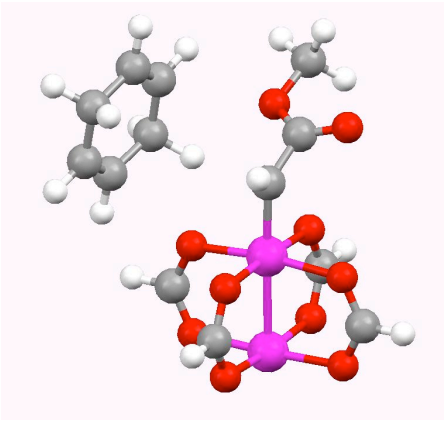

Rh	0.00000000	0.00000000	0.00000000
O	-0.86849300	0.76020600	-1.70993700
C	-2.10989500	0.57649900	-1.92095400
O	-2.94267800	-0.03531000	-1.20031200
Rh	-2.24987700	-0.85706600	0.55079200
O	-1.72326800	-2.57836200	-0.47130400
C	-0.58264600	-2.64161300	-1.00243000
O	0.34737500	-1.76995400	-0.99120900
H	-0.34497900	-3.56455100	-1.54914400
O	-1.46483500	-1.64384100	2.28424500
C	-0.23789300	-1.47074800	2.50198400
O	0.61369300	-0.86262700	1.77526100
H	0.16424300	-1.89354200	3.43301100
O	-2.58473600	0.93597500	1.51821000
C	-1.66432100	1.79645700	1.53360300

Route= #N b3lyp/gen pseudo=read gfprint
OPT=(TS,CalcFC,NoEigenTest) freq
B3LYP Energy=-1478.50250932 Hartree
ZPE=0.292042 Hartree
Conditions=298K, 1.00000 atm
Internal Energy=-1478.183568 Hartree
Enthalpy=-1478.182624 Hartree
Free Energy=-1478.270637 Hartree
Entropy=185.240 cal/mol-K

O	-0.50066800	1.72355400	1.01988600
H	-1.88203600	2.73769100	2.05705500
H	-2.48872100	1.01328500	-2.85473900
C	1.76027600	0.67289600	-0.52472100
C	2.20482000	2.06399500	-0.30387100
O	2.00344800	2.86528000	-1.19878600
O	2.72893700	2.34531800	0.89097400
C	3.03809800	3.73748200	1.11841600
H	3.73676800	4.10262500	0.36169700
H	3.48793400	3.77234400	2.10999600
H	2.12225700	4.33177900	1.08787500
H	2.30595700	0.15196600	-1.31950400
H	2.95978200	-0.28271000	0.64032900
C	3.85645600	-0.78266500	1.10868700
C	3.73007900	-2.26217600	0.91461200
C	4.63485600	-2.99211700	0.25276500
C	5.88391900	-2.41301100	-0.35500400
H	6.77015900	-2.93564700	0.04303200
C	6.02145700	-0.93251400	-0.12218600
C	5.11613100	-0.20375700	0.53998900
H	5.27730200	0.86203300	0.68917200
H	6.92020300	-0.45564500	-0.51003500
H	5.90844400	-2.62623800	-1.43714200
H	4.48873600	-4.06559800	0.14495600
H	2.84532400	-2.73338200	1.33533100
H	3.72920600	-0.50252900	2.16513300

C–H insertion TS with cyclopentane
(TS-VIIb)

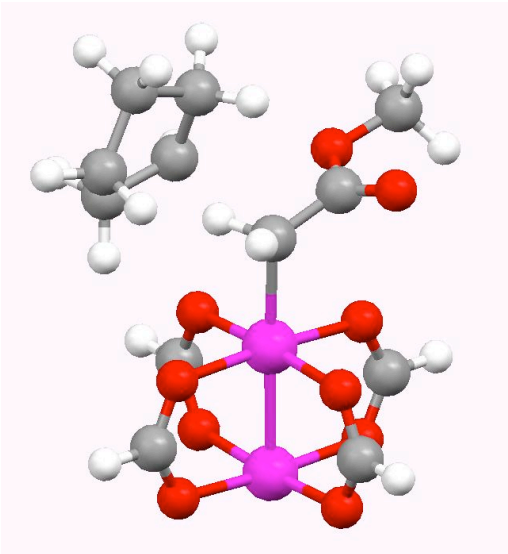

Rh	0.00000000	0.00000000	0.00000000
O	0.41411100	0.40228700	1.97858200
C	1.62447300	0.38545200	2.36279800
O	2.66139400	0.13997600	1.68374400
Rh	2.41381000	-0.29843900	-0.31240400
O	2.13524600	-2.29095500	0.16700300
C	0.97166100	-2.69090400	0.43768100
O	-0.11103200	-2.02072200	0.45270000
H	0.86945000	-3.75533100	0.69359700
O	2.00151600	-0.71535300	-2.29672700
C	0.80338600	-0.69943400	-2.68605800
O	-0.24487500	-0.45286000	-2.00590100
H	0.63193500	-0.92756700	-3.74779100
O	2.52982500	1.70854700	-0.76331900
C	1.46341200	2.38371300	-0.74201700
O	0.28436700	1.99022600	-0.47912500
H	1.56015600	3.45174400	-0.98315500

Route= #N b3lyp/gen pseudo=read gfprint OPT=(TS,CalcFC,NoEigenTest) freq
B3LYP Energy=-1441.63292535 Hartree
ZPE=0.310041 Hartree
Conditions=298K, 1.00000 atm
Internal Energy=-1441.296348 Hartree
Enthalpy=-1441.295404 Hartree
Free Energy=-1441.381573 Hartree
Entropy=181.358 cal/mol-K

H	1.78223100	0.61397900	3.42600600
C	-2.09478300	0.27419300	0.39014800
C	-2.58010200	1.67272000	0.41333100
O	-2.65056800	2.33183900	1.43209600
O	-2.87902800	2.15084900	-0.81740400
C	-3.19553700	3.55176800	-0.86802000
H	-4.04715800	3.77941400	-0.22121600
H	-3.43746800	3.75848900	-1.91088800
H	-2.33340900	4.14252200	-0.54964200
H	-2.39698500	-0.30255100	1.26136500
H	-2.36440400	-0.28184000	-0.61184300
C	-3.59391300	-0.76230100	-0.95847900
H	-3.41651500	-0.32913300	-1.94428900
C	-3.37837300	-2.26133800	-0.79924500
C	-4.29688300	-2.65664900	0.37060600
C	-5.51425500	-1.73170400	0.19421500
C	-4.91400800	-0.38158700	-0.28071400
H	-5.56190100	0.15062600	-0.98511100
H	-4.76610000	0.29097800	0.56806200
H	-6.10715800	-1.61884400	1.10667400
H	-6.17795600	-2.13682700	-0.57961500
H	-3.79545500	-2.45494100	1.32557600
H	-4.55945800	-3.71874800	0.35762100
H	-2.32760000	-2.53302900	-0.66296500
H	-3.71978000	-2.73701700	-1.73141200

***Vinyldiazoacetate – rhodium formate complex* (2.18)**

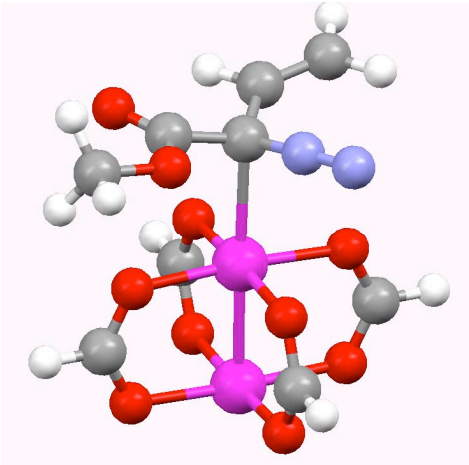

Route= # b3lyp/gen pseudo=read gfprint Integral(Grid=Ultrafine) opt freq
B3LYP Energy=-1432.01623763 Hartree

Rh	0.00000000	0.00000000	0.00000000
Rh	2.37886400	-0.46070600	0.02131100
O	2.68024100	1.48999200	0.60101900
C	1.66553100	2.22716300	0.75930300
O	0.44379300	1.92155800	0.59615900
H	1.86044700	3.26035200	1.07664200
O	2.45339000	0.11131500	-1.94863500
C	1.37120000	0.47115000	-2.49797000
O	0.21539400	0.53603400	-1.98044500
H	1.43915200	0.76503000	-3.55392300
O	1.95711900	-2.38518000	-0.56212700
C	0.74271800	-2.69978900	-0.72109200
O	-0.28262800	-1.96876900	-0.56399200
H	0.54828900	-3.73485600	-1.03308500
O	2.18350500	-1.01360900	1.99569100
C	1.03699400	-0.94312700	2.52215000
O	-0.04982900	-0.56855500	1.98118100
H	0.96605800	-1.24087700	3.57688100

ZPE=0.212829 Hartree
Conditions=298K, 1.00000 atm
Internal Energy=-1431.778145 Hartree
Enthalpy=-1431.777201 Hartree
Free Energy=-1431.858783 Hartree
Entropy=171.705 cal/mol-K

C	-2.37493000	0.57037800	-0.06443000
C	-2.48989500	1.71756500	-0.99363900
C	-2.53595700	3.01351000	-0.67501000
H	-2.60814300	3.76486000	-1.45399000
H	-2.48604700	3.37691400	0.34823500
H	-2.52568300	1.38242400	-2.02533100
C	-2.96560800	-0.74181500	-0.48670600
O	-3.18328000	-1.01713700	-1.64428800
O	-3.20438100	-1.54497700	0.56474600
C	-3.65583300	-2.87246800	0.23583000
H	-4.58625600	-2.82823700	-0.33520300
H	-2.88903500	-3.38737100	-0.34644300
H	-3.81297200	-3.36733800	1.19390700
N	-2.50873800	0.84898000	1.25018600
N	-2.55788000	1.11237500	2.34369700

Vinyldiazoacetate – rhodium formate complex Nitrogen extrusion TS **(TS-V)**

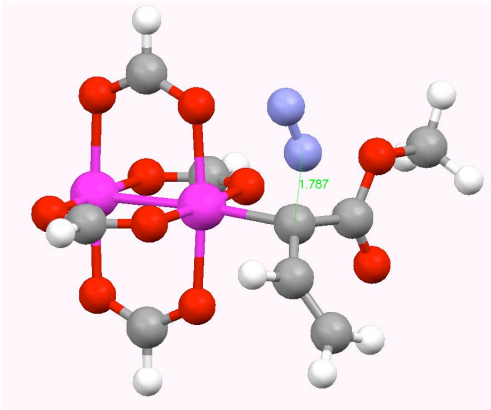

Route= #N B3LYP/gen pseudo=read OPT=(TS,CalcFC,NoEigenTest) FREQ
B3LYP Energy=-1431.99712763 Hartree
ZPE=0.210860 Hartree
Conditions=298K, 1.00000 atm
Internal Energy=-1431.761248 Hartree
Enthalpy=-1431.760304 Hartree
Free Energy=-1431.840825 Hartree
Entropy=169.470 cal/mol-K

Rh	0.00000000	0.00000000	0.00000000
C	-2.06569400	0.52809200	0.05177700
C	-2.94774000	-0.50614600	-0.58274100
O	-3.35296900	-1.46870300	0.26257700
C	-4.04661900	-2.57250000	-0.35081400
H	-4.93435500	-2.21913500	-0.88075000
H	-4.32383100	-3.23007700	0.47269100
H	-3.38191900	-3.08476400	-1.04973200
O	-3.18586800	-0.49122300	-1.77267700
C	-2.32830400	1.95508000	-0.18496000
C	-3.10514100	2.44576100	-1.16254100
H	-3.13308900	3.51609200	-1.34628900
H	-3.66678900	1.80603100	-1.83311900
H	-1.72349800	2.62915500	0.41707500
O	0.07491700	-0.96100600	1.82487500
C	1.17964900	-1.46600200	2.20703500
O	2.28701800	-1.45650400	1.60661100
Rh	2.38965300	-0.51860000	-0.22700900
O	2.77269300	1.27885000	0.71325600
C	1.79938700	1.99302900	1.07405800
O	0.55515500	1.76036700	0.93260800
H	2.04618300	2.93929800	1.57530900
O	1.84499600	-2.27772400	-1.15022400
C	0.61430000	-2.52181500	-1.28379900
O	-0.37561300	-1.81259600	-0.91837800
H	0.35673900	-3.46923400	-1.77728800
O	2.36544000	0.43990400	-2.04405000
C	1.27042700	0.93312100	-2.43376100

O	0.14709500	0.92392000	-1.84122600
H	1.28234400	1.43787900	-3.40946300
H	1.15309500	-1.96920700	3.18332900
N	-2.44434600	0.35635200	1.79001500
N	-2.21936600	0.24384400	2.87145800

***Vinylcarbenoid complex* (2.19)**

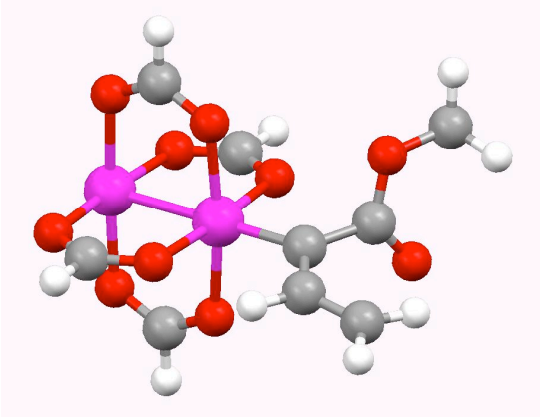

Route= #N B3LYP/gen pseudo=read gfprint OPT FREQ
B3LYP Energy=-1322.50303403 Hartree
ZPE=0.203443 Hartree
Conditions=298K, 1.00000 atm
Internal Energy=-1322.276544 Hartree
Enthalpy=-1322.275599 Hartree
Free Energy=-1322.352855 Hartree
Entropy=162.598 cal/mol-K

Rh	0.00000000	0.00000000	0.00000000
Rh	-2.39050300	-0.62521300	0.08948200
O	-2.80381700	1.21308400	-0.76003400
C	-1.84619700	1.98623200	-1.02074400
O	-0.59906100	1.79507900	-0.83262500
H	-2.10410600	2.95557400	-1.46952100
O	-2.47498000	0.22198200	1.96330000
C	-1.42016500	0.73183500	2.42582200
O	-0.27138100	0.79945900	1.88113800
H	-1.48468500	1.17956800	3.42678000
O	-1.79110700	-2.41101500	0.93453900
C	-0.55967300	-2.61175900	1.10755900
O	0.41647700	-1.84172900	0.82956900
H	-0.27717700	-3.57421400	1.55607700
O	-2.19187100	-1.44709200	-1.78727400
C	-1.06066200	-1.37262500	-2.33702900
O	0.00697200	-0.85061300	-1.88205300
H	-0.96981000	-1.81055000	-3.34058200
C	1.90881900	0.50674400	-0.05730000
C	2.34066900	1.84639200	-0.33319000
C	3.60643200	2.28661600	-0.12674600
H	3.87201600	3.32628900	-0.30005400
H	4.38635100	1.63802100	0.26148900
H	1.57630200	2.53904400	-0.67554600
C	2.92417500	-0.51551200	0.31108200
O	3.43346400	-0.54029300	1.41564100
O	3.16412300	-1.38744600	-0.67387600
C	4.05133700	-2.47431400	-0.34081800
H	5.02569100	-2.09259400	-0.02541800
H	3.61830300	-3.07549400	0.46191700
H	4.14372700	-3.05907900	-1.25530800

***Vinylcarbenoid cyclopropanation with styrene TS* (TS-VI)**

Rh	0.00000000	0.00000000	0.00000000
C	-1.95882300	0.56236800	0.44570100
C	-2.14635800	2.04898800	0.56287700
O	-2.02975600	2.73761700	-0.58647100

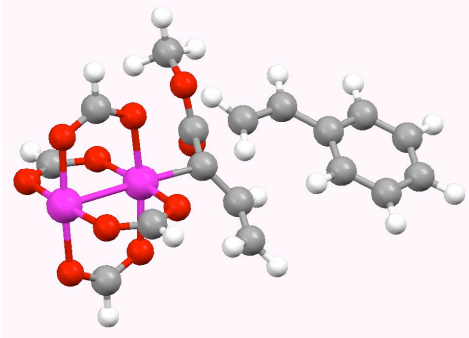

Route= #N b3lyp/gen pseudo=read
OPT=(TS,CalcFC,NoEigenTest) freq
B3LYP Energy=-1632.14299373 Hartree
ZPE=0.339148 Hartree
Conditions=298K, 1.00000 atm
Internal Energy=-1631.773688 Hartree
Enthalpy=-1631.772744 Hartree
Free Energy=-1631.865146 Hartree
Entropy=194.476 cal/mol-K

C	-2.00308400	4.16752900	-0.44090300
H	-2.91649600	4.52605700	0.04155200
H	-1.92378300	4.55982800	-1.45503400
H	-1.13899900	4.46699500	0.15684700
O	-2.30236100	2.57606300	1.64953100
C	-2.79589800	-0.17985800	1.36650600
C	-2.73439500	-1.51758600	1.53369500
H	-3.38610500	-2.01683900	2.24539200
H	-2.03876000	-2.12908100	0.97006300
H	-3.51063300	0.39196200	1.95779900
O	0.05541300	0.76199800	-1.92956400
C	1.14779100	0.71511100	-2.57929600
O	2.25540700	0.23834100	-2.21391600
Rh	2.38057700	-0.59616900	-0.33470900
O	1.73229400	-2.40267600	-1.10004900
C	0.49549400	-2.62862600	-1.14521200
O	-0.46258900	-1.87335500	-0.77414700
H	0.19057900	-3.60175700	-1.55653800
O	2.87478600	1.24381300	0.44773700
C	1.93619400	2.01389900	0.78661500
O	0.68254400	1.81123000	0.71894200
H	2.22849600	2.99172100	1.19446700
O	2.38425900	-1.39165300	1.56535800
C	1.31701200	-1.32070100	2.23281600
O	0.19754900	-0.82836900	1.88475100
H	1.34692100	-1.73835100	3.24910800
H	1.11075200	1.14734200	-3.58951600
C	-2.91509300	0.09623600	-1.62590200
C	-4.17843300	0.54581700	-1.36534800
C	-5.30139100	-0.22585500	-0.86192200
C	-6.48786300	0.45048900	-0.50553500
C	-7.58437200	-0.24035000	-0.00121000
C	-7.52228100	-1.62868200	0.15666300
C	-6.35831400	-2.31795500	-0.19518600
C	-5.25837200	-1.62842500	-0.69831200
H	-4.36967800	-2.17791200	-0.98960000
H	-6.31098900	-3.39747100	-0.08172400
H	-8.37896100	-2.17093400	0.54714900
H	-8.48737600	0.29942300	0.26961400
H	-6.53575400	1.53010700	-0.62577300
H	-4.36652300	1.61006500	-1.49860500
H	-2.65256200	-0.95459800	-1.57692300
H	-2.19139400	0.74278200	-2.10498700

TS-IX$_{eq}$

Route= #N b3lyp/gen pseudo=read gfprint
OPT=(TS,CalcFC,NoEigenTest) freq
RB3LYP Energy=-1712.00402869 Hartree
ZPE=0.421183 Hartree
Conditions=298K, 1.00000 atm
Internal Energy=-1711.550764 Hartree
Enthalpy=-1711.549820 Hartree
Free Energy=-1711.646264 Hartree
Entropy=202.982 cal/mol-K

Rh	0.00000000	0.00000000	0.00000000
O	-0.31329300	2.01811700	0.26510500
C	-1.47938700	2.48127600	0.07651300
O	-2.52484400	1.86015100	-0.27398700
Rh	-2.37474700	-0.16796000	-0.57393500
O	-1.86244400	0.15535800	-2.54500900
C	-0.64273200	0.30990600	-2.82121400
O	0.35196100	0.29530900	-2.02804300
H	-0.40102000	0.47741500	-3.88057800
O	-2.08017900	-2.19551100	-0.83167000
C	-0.91954600	-2.66167300	-0.66273800
O	0.14043400	-2.04063600	-0.33458100
H	-0.80464300	-3.74396600	-0.81890500
O	-2.78019700	-0.48122600	1.41234900
C	-1.80338800	-0.49860400	2.21382200
O	-0.57059800	-0.34805900	1.95437600
H	-2.04715600	-0.66638300	3.27216100
H	-1.58995300	3.56242300	0.23826400
C	2.23227800	0.19881300	0.62926100
C	2.27150300	-0.33195300	2.01696600
O	2.26615300	0.35991400	3.01829100
O	2.23886800	-1.68938400	2.07327400
C	2.05123100	-2.23761000	3.38677800
H	2.85965600	-1.93067100	4.05591700
H	2.05457500	-3.32005400	3.25205300
H	1.09626300	-1.90391600	3.79831500
C	2.91965200	1.46741000	0.31185400
C	2.76736400	2.04271200	-0.97010000
C	3.43379200	3.21558100	-1.31630600
C	4.25718600	3.85969500	-0.38992100
C	4.40999600	3.31371400	0.88602900
C	3.75994500	2.13093200	1.23373200
H	3.87631200	1.73027000	2.23215200
H	5.04193800	3.80930600	1.61836200
H	4.76776700	4.78116600	-0.65716500
H	3.29496600	3.63728300	-2.30855900
H	2.09826300	1.57476900	-1.68212600
H	2.31988000	-0.62223300	-0.17703700
C	3.56092900	-1.43236200	-0.46707100
C	3.53011400	-1.21550300	-1.95530300
C	4.61737000	-2.11289600	-2.60937700
C	5.99733200	-1.85545500	-1.99099600
C	5.96615600	-2.04447600	-0.46850000
C	4.87670300	-1.15528400	0.19676200

H	5.15181300	-0.10099400	0.06516200
H	4.82757900	-1.36416800	1.26896000
H	5.76733400	-3.09869200	-0.23199200
H	6.93724200	-1.79820100	-0.02280800
H	6.31678700	-0.83031400	-2.22598800
H	6.74075200	-2.52748800	-2.43734000
H	4.34346200	-3.16880700	-2.48028900
H	4.62708400	-1.91782700	-3.68840700
H	3.76242500	-0.16602800	-2.17897600
H	2.54238600	-1.43753800	-2.36856100
H	3.03083100	-2.31020000	-0.09994100

TS-IX$_{ax}$

Route= #N b3lyp/gen pseudo=read gfprint
OPT=(TS,CalcFC,NoEigenTest) freq
RB3LYP Energy=-1712.00087594 Hartree
ZPE=0.420220 Hartree
Conditions=298K, 1.00000 atm
Internal Energy=-1711.548467 Hartree
Enthalpy=-1711.547523 Hartree
Free Energy=-1711.643896 Hartree
Entropy=202.833 cal/mol-K

Rh	0.00000000	0.00000000	0.00000000
O	0.03437100	-1.95199800	-0.67153900
C	1.11285300	-2.42019700	-1.14681400
O	2.22822100	-1.83975200	-1.28322800
Rh	2.37147800	0.10196300	-0.62333100
O	1.77861900	0.78657400	-2.48045700
C	0.54609900	0.91806400	-2.70497200
O	-0.42817300	0.68689900	-1.91814900
H	0.26974000	1.28012300	-3.70570100
O	2.39254900	2.04187700	0.08040600
C	1.31929200	2.52601600	0.53465100
O	0.18050700	1.97127100	0.62974300
H	1.37173700	3.56371800	0.89491400
O	2.83455700	-0.58689100	1.25585000
C	1.87911600	-0.79126300	2.05766000
O	0.63614900	-0.63353200	1.85838600
H	2.15468600	-1.15134300	3.05866400
H	1.06598500	-3.46493200	-1.48426200
C	-2.23589100	-0.20599800	0.60349100
C	-2.18832900	-0.21607500	2.08976900
O	-2.19872700	-1.22101500	2.77624200
O	-2.05511000	1.02493400	2.63087400
C	-1.78986400	1.04595500	4.04151700
H	-2.59690200	0.56097100	4.59732300
H	-1.72098200	2.10146500	4.30842500
H	-0.84883900	0.53346300	4.25361900
C	-2.99105200	-1.27400000	-0.08936600
C	-2.87295800	-1.41322900	-1.49011300
C	-3.59511200	-2.38132800	-2.18350800
C	-4.44891000	-3.24808200	-1.49750100
C	-4.57599700	-3.13032300	-0.11151900

C	-3.86489100	-2.15538400	0.58484400
H	-3.96296000	-2.09022500	1.66057600
H	-5.23516600	-3.80086200	0.43357400
H	-5.00682500	-4.00928300	-2.03651300
H	-3.48166600	-2.46597600	-3.26123300
H	-2.19300400	-0.76200300	-2.02664500
H	-3.10486400	3.87253100	-2.95332800
C	-3.51974800	3.48852000	-2.01369200
C	-3.95623300	2.02739800	-2.19038200
C	-4.53031500	1.44546200	-0.88886900
C	-3.70580700	1.72007700	0.33008700
C	-3.00944800	3.05143300	0.43944400
C	-2.47873900	3.60395300	-0.89122400
H	-1.57766800	3.04693100	-1.17122700
H	-2.17599700	4.64806900	-0.74711700
H	-3.78849100	3.73107600	0.83575300
H	-2.22972800	3.00622900	1.20281900
H	-2.36261600	0.84812100	0.14184300
H	-4.11520100	1.34555500	1.26283600
H	-5.51050000	1.91106000	-0.67427300
H	-4.73867600	0.37317200	-0.98070900
H	-3.08820100	1.43162600	-2.49737100
H	-4.70537500	1.93434000	-2.98534100
H	-4.39517600	4.11315300	-1.77919300

Propene

Route= #N B3LYP/6-31G(d) 5d OPT FREQ
RB3LYP Energy=-116.650683194 Hartree
ZPE=0.055732 Hartree
Conditions=298K, 1.00000 atm
Internal Energy=-116.590956 Hartree
Enthalpy=-116.590012 Hartree
Free Energy=-116.619179 Hartree
Entropy=61.388 cal/mol-K
Dipole Moment=0.6857 Debye

C	0.00000000	0.00000000	0.00000000
C	1.46047400	-0.00103200	0.00083300
C	2.66775600	0.00008900	-0.00001000
H	3.73367500	0.00031400	-0.00048600
H	-0.39589200	1.01518700	-0.12351500
H	-0.39666800	-0.61396200	-0.81750700
H	-0.39754400	-0.40041400	0.94033500

Cyclopropenation TS-X
(right-tilted/s-trans conformer)

Rh	0.00000000	0.00000000	0.00000000
C	1.85412200	1.02423400	0.05862800
C	1.91944400	2.15023700	-0.93088900
O	1.27609000	3.26230200	-0.53446000
C	1.11852100	4.27054300	-1.54605500

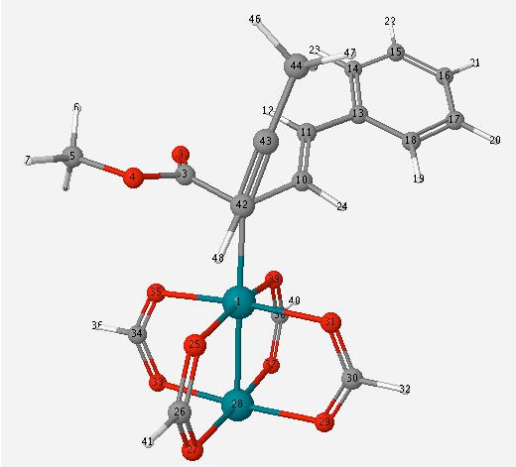

Route= #N b3lyp/gen pseudo=read gfprint OPT=(TS,CalcFC,NoEigenTest) freq
RB3LYP Energy=-1670.20993064 Hartree
ZPE=0.342298 Hartree
Conditions=298K, 1.00000 atm
Internal Energy=-1669.835776 Hartree
Enthalpy=-1669.834831 Hartree
Free Energy=-1669.932174 Hartree
Entropy=204.874 cal/mol-K
Dipole Moment=8.3677 Debye

H	2.09108700	4.59832100	-1.92279900
H	0.60001200	5.09360700	-1.05384700
H	0.52297400	3.87834500	-2.37368300
O	2.41384300	2.02511600	-2.03788900
C	2.98119000	0.14220100	0.23562200
C	4.13739100	0.15832600	-0.48627900
H	4.25562800	0.93006100	-1.24176300
C	5.22388100	-0.81505700	-0.40886900
C	6.37238600	-0.59654800	-1.19616800
C	7.45598400	-1.47004600	-1.14782600
C	7.41249700	-2.58906000	-0.31382600
C	6.27589700	-2.82823400	0.46699900
C	5.19401600	-1.95577400	0.42079300
H	4.31494100	-2.16517200	1.02240100
H	6.23360000	-3.70318600	1.10993900
H	8.25403600	-3.27523800	-0.27568500
H	8.33150900	-1.28025700	-1.76259300
H	6.40607800	0.27218400	-1.84917700
H	2.81731800	-0.63995300	0.97309400
O	-1.06996700	1.22963600	1.28177800
C	-2.30026800	0.97837700	1.50514300
O	-2.99371100	0.03789200	1.04147000
Rh	-2.08171500	-1.30836800	-0.23365500
O	-1.44532700	-2.41898600	1.39089800
C	-0.33776700	-2.13655400	1.92202300
O	0.48823700	-1.22329500	1.59664000
H	-0.03675300	-2.75476200	2.78001700
O	-2.56886300	-0.10928900	-1.83855300
C	-1.76616100	0.81176600	-2.15385800
O	-0.66185700	1.12257300	-1.60613900
H	-2.05368400	1.43373500	-3.01342200
O	-1.07050800	-2.57412300	-1.49764400
C	0.14258400	-2.32127700	-1.73719500
O	0.85488100	-1.36926900	-1.28937000
H	0.65921800	-3.01013700	-2.42004200
H	-2.80557900	1.67584100	2.18769100
C	1.61738500	2.04532900	1.92837600
C	2.78503300	2.33412500	2.17659200
C	4.21695400	2.51942200	2.25998500
H	4.69038300	1.85823200	1.51201000
H	4.51400000	3.55258500	2.04848700
H	4.60465000	2.23125100	3.24400000
H	0.54853200	2.02240500	2.04176200

Cyclopropene product 2.25

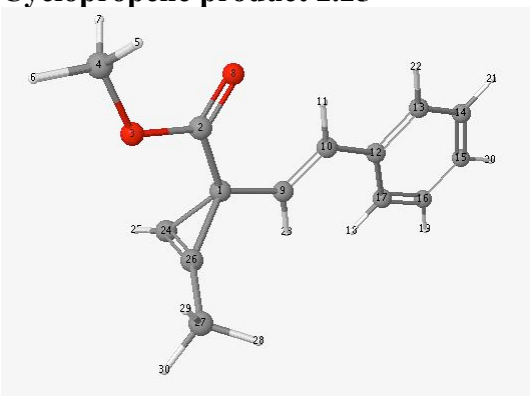

Route= #N B3LYP/6-31G(d) 5d OPT FREQ
RB3LYP Energy=-692.265420067 Hartree
ZPE=0.242562 Hartree
Conditions=298K, 1.00000 atm
Internal Energy=-692.006910 Hartree
Enthalpy=-692.005966 Hartree
Free Energy=-692.068658 Hartree
Entropy=131.946 cal/mol-K
Dipole Moment=3.2977 Debye

C	0.00000000	0.00000000	0.00000000
C	0.66785600	-1.33558700	0.20658400
O	2.02226100	-1.22708000	0.18355500
C	2.73207700	-2.45801000	0.37343600
H	2.49257900	-2.89796700	1.34574200
H	3.78984900	-2.19650700	0.32143400
H	2.47575500	-3.17748200	-0.40918200
O	0.11100400	-2.40140500	0.38373200
C	-1.49033800	0.08473800	0.04826200
C	-2.39621100	-0.88235000	0.27937000
H	-2.04063900	-1.88980900	0.46639800
C	-3.85719300	-0.70988300	0.31261300
C	-4.65177800	-1.80752600	0.69264200
C	-6.04164800	-1.71309200	0.75212000
C	-6.67650100	-0.51350100	0.42770700
C	-5.90437800	0.58679700	0.04141900
C	-4.51691500	0.49029900	-0.01717000
H	-3.94069100	1.35607900	-0.33122900
H	-6.38840300	1.52461700	-0.21999300
H	-7.75955000	-0.43524100	0.47046400
H	-6.62831600	-2.57809700	1.05103200
H	-4.16338000	-2.74550700	0.94646100
H	-1.83581100	1.10286100	-0.13170900
C	0.74222500	1.03474300	-0.84465900
H	0.97158600	1.28772700	-1.86863600
C	0.79609600	1.24765900	0.42328000
C	1.20077300	1.98412400	1.63844700
H	0.32396800	2.24560200	2.24259900
H	1.85053700	1.35550600	2.25954800
H	1.74152500	2.90181100	1.38489300

Structures from mechanism studies of the CHCR reaction

Vinylcarbenoid s-cis (2.19)

Route= # b3lyp/gen pseudo=read integral(grid=ultrafine) gfprint OPT FREQ
B3LYP Energy=-1322.50221435 Hartree
ZPE=0.203299 Hartree
Conditions=298K, 1.00000 atm
Internal Energy=-1322.275883 Hartree
Enthalpy=-1322.274939 Hartree
Free Energy=-1322.351907 Hartree
Entropy=161.994 cal/mol-K

Rh	0.00000000	0.00000000	0.00000000
Rh	-2.35602100	-0.75698300	0.02965100
O	-2.76865600	0.84877900	1.25921600
C	-1.82509400	1.62327500	1.56634500
O	-0.60203100	1.55927900	1.21302800
H	-2.07493500	2.46895800	2.22197900
O	-1.89451800	-1.89295900	1.68328800
C	-0.70723300	-1.86537300	2.10478000
O	0.27969300	-1.20642700	1.64459200

H	-0.48023000	-2.48488100	2.98302800
O	-1.79753500	-2.31553400	-1.19415200
C	-0.58493600	-2.39666400	-1.52869600
O	0.37776400	-1.62608100	-1.21542000
H	-0.31099900	-3.24016000	-2.17764300
O	-2.68163400	0.41786800	-1.63486400
C	-1.71404600	1.07791100	-2.09322400
O	-0.51589900	1.13065800	-1.65931300
H	-1.91352400	1.69362200	-2.98137700
C	1.90572500	0.60349600	0.02917700
C	2.39943500	1.94748000	0.00249900
C	1.63855300	3.00375800	-0.38026700
H	2.06508300	4.00219300	-0.43414000
H	0.60550900	2.87522400	-0.67714000
H	3.44339000	2.11874500	0.26974800
C	2.95429400	-0.41495500	0.30435800
O	3.40887700	-0.52610900	1.42740400
O	3.30533900	-1.14732900	-0.75445600
C	4.27493200	-2.18487900	-0.50169400
H	5.19347800	-1.75930700	-0.08990200
H	3.86642300	-2.91625000	0.19970900
H	4.46236800	-2.64404800	-1.47159500

s-*cis* 2.29

Route= #N b3lyp/gen pseudo=read gfprint INTEGRAL(GRID=ULTRAFINE) OPT FREQ
B3LYP Energy=-1361.82802166 Hartree
ZPE=0.231343 Hartree
Conditions=298K, 1.00000 atm
Internal Energy=-1361.571979 Hartree
Enthalpy=-1361.571035 Hartree
Free Energy=-1361.651856 Hartree
Entropy=170.102 cal/mol-K

Rh	0.00000000	0.00000000	0.00000000
O	-0.03214200	-1.56799700	-1.34268800
C	1.06951400	-2.08881700	-1.70731100
O	2.24046800	-1.77831100	-1.35799500
Rh	2.46509700	-0.23550600	-0.01324100
O	2.50803900	1.10796100	-1.58146500
C	1.41653200	1.57770800	-1.99370300
O	0.23914200	1.34139700	-1.56415100
H	1.47133600	2.28643600	-2.83221900
O	2.53722900	1.32137000	1.34181500
C	1.45355700	1.84935500	1.70317000
O	0.26831500	1.55562700	1.33704300
H	1.52502300	2.67349700	2.42693100
O	2.27109400	-1.56832700	1.54447700
C	1.10888500	-1.82831500	1.95755900
O	-0.00072200	-1.36283400	1.54377300
H	1.02911100	-2.54880100	2.78313400
H	0.97581900	-2.91801600	-2.42258200
C	-2.00240900	0.17695100	0.06436000
C	-2.79018500	-1.06175500	0.30904500

O	-3.19188800	-1.32822100	1.42566200
O	-2.98393000	-1.80822000	-0.78316700
C	-3.68711900	-3.04859200	-0.57211100
H	-3.11491400	-3.69532100	0.09740400
H	-3.77631300	-3.49957100	-1.55987800
H	-4.67399100	-2.86237900	-0.14068000
C	-2.78155900	1.36578400	0.06835600
C	-2.25213100	2.60270800	-0.16830600
C	-3.04427500	3.85999100	-0.20437100
H	-2.94477500	4.34192700	-1.18737200
H	-4.10503900	3.69797700	0.00644100
H	-2.63963900	4.57677200	0.52413200
H	-1.18767300	2.67762200	-0.36264800
H	-3.85516800	1.29088100	0.25561500

s-*trans* 2.29

Route= #N b3lyp/gen pseudo=read gfprint INTEGRAL(GRID=ULTRAFINE) OPT FREQ
B3LYP Energy=-1361.82825361 Hartree
ZPE=0.231515 Hartree
Conditions=298K, 1.00000 atm
Internal Energy=-1361.572061 Hartree
Enthalpy=-1361.571116 Hartree
Free Energy=-1361.652171 Hartree
Entropy=170.593 cal/mol-K

Rh	0.00000000	0.00000000	0.00000000
C	1.98201000	-0.11557700	-0.00277600
C	2.75479200	1.11568000	0.31261000
O	2.80798900	1.96916600	-0.71786600
C	3.42390300	3.24180800	-0.44000400
H	2.85961600	3.76759500	0.33366400
H	3.38996500	3.78858900	-1.38181200
H	4.45666800	3.10652600	-0.10839900
O	3.24079500	1.31101700	1.41102400
C	2.67592400	-1.34284500	-0.19806900
C	4.02238000	-1.48800500	-0.03206000
C	4.75778900	-2.77316000	-0.17789100
H	5.56689200	-2.66616900	-0.91401800
H	5.24489100	-3.04019500	0.77076400
H	4.10336500	-3.59412000	-0.48302700
H	4.61278300	-0.62179800	0.26361800
H	2.07371100	-2.21113100	-0.45645000
O	-0.15792200	-0.76175900	1.91168000
C	-1.31187700	-0.90389700	2.42969800
O	-2.43459100	-0.63676200	1.92449700
Rh	-2.46980000	0.13167800	0.01278200
O	-2.48619900	-1.78739600	-0.75556000
C	-1.38506400	-2.36184200	-0.95791500
O	-0.20777400	-1.91578900	-0.75524700
H	-1.43087700	-3.38277600	-1.36257300
O	-2.26226100	2.03836200	0.78092400
C	-1.10161900	2.48916600	0.97144500
O	0.01677700	1.92028300	0.75269100

H	-1.03158200	3.50702200	1.37983500
O	-2.38074800	0.89417900	-1.89828300
C	-1.24164400	1.03187500	-2.41924400
O	-0.10394100	0.76107900	-1.91837400
H	-1.21312800	1.43761500	-3.44012300
H	-1.31423700	-1.31380100	3.44910000

2.31 s-*cis*

Route= #N b3lyp/gen pseudo=read gfprint OPT FREQ
RB3LYP Energy=-1361.81819245 Hartree
ZPE=0.231721 Hartree
Conditions=298K, 1.00000 atm
Internal Energy=-1361.562120 Hartree
Enthalpy=-1361.561176 Hartree
Free Energy=-1361.640162 Hartree
Entropy=166.240 cal/mol-K

Rh	0.00000000	0.00000000	0.00000000
O	0.32190200	-1.88446700	0.78690100
C	-0.68737100	-2.61095800	1.05833800
O	-1.90993800	-2.34129200	0.91673100
Rh	-2.41879700	-0.51035200	0.11552900
O	-2.43435200	0.30173900	2.00980600
C	-1.34926300	0.73584100	2.47563100
O	-0.20334600	0.75818300	1.91868300
H	-1.38003500	1.15216500	3.49217500
O	-2.75950300	1.35327100	-0.70382700
C	-1.76699000	2.07615700	-0.98343600
O	-0.52981100	1.82747900	-0.81171300
H	-1.98618100	3.05456900	-1.43416000
O	-2.29341600	-1.30855400	-1.77468800
C	-1.16674200	-1.28032800	-2.33980300
O	-0.07078000	-0.81680900	-1.89249500
H	-1.11005300	-1.70728400	-3.35029100
H	-0.44940100	-3.60100500	1.47181200
C	1.96581600	0.34866400	-0.21291900
C	2.81347000	-0.87600300	-0.30784000
O	3.06406900	-1.40022100	-1.37477400
O	3.24562100	-1.29266100	0.88728400
C	4.00307700	-2.51910400	0.88223700
H	3.37921600	-3.34058400	0.52237500
H	4.29334600	-2.68202200	1.91967300
H	4.88473400	-2.42310100	0.24363900
C	2.66314500	1.52890500	-0.60732900
C	2.46145000	2.81747300	-0.20584900
H	3.13549900	3.55299500	-0.64763200
C	1.55429100	3.35310200	0.84381200
H	0.92921800	4.14891900	0.41719700
H	0.92089900	2.59400900	1.29824600
H	2.16163000	3.82954800	1.62797600
H	3.51672200	1.36355100	-1.26962000

2.31 s-*trans*

Route= #N b3lyp/gen pseudo=read gfprint
OPT FREQ
RB3LYP Energy=-1361.82200174 Hartree
ZPE=0.231752 Hartree
Conditions=298K, 1.00000 atm
Internal Energy=-1361.565595 Hartree
Enthalpy=-1361.564651 Hartree
Free Energy=-1361.645942 Hartree
Entropy=171.092 cal/mol-K

Rh	0.00000000	0.00000000	0.00000000
O	0.23189200	2.02821900	0.30405300
C	-0.81534200	2.74759200	0.39072500
O	-2.02072600	2.39240300	0.30495700
Rh	-2.44093100	0.39644600	-0.01186600
O	-2.32261600	0.69301200	-2.04679900
C	-1.19055800	0.58529700	-2.58916300
O	-0.07351500	0.31693300	-2.04165500
H	-1.14809600	0.74119800	-3.67609800
O	-2.68268700	-1.62964800	-0.32563200
C	-1.65384700	-2.35036000	-0.40186700
O	-0.43148900	-1.99961700	-0.31063900
H	-1.81750300	-3.42430500	-0.56858200
O	-2.43651300	0.08016800	2.02212000
C	-1.33282700	-0.18066600	2.57245100
O	-0.18580800	-0.28538200	2.03210500
H	-1.34921500	-0.34182200	3.65899500
H	-0.63069400	3.81734900	0.56190800
C	1.96977500	-0.31867100	-0.00386900
C	2.80806900	0.85860900	0.32165700
O	3.11648600	1.14070100	1.46441200
O	3.11964500	1.58178700	-0.76402600
C	3.76010000	2.84693200	-0.50558700
H	3.11407400	3.47017700	0.11657700
H	3.90719200	3.29964900	-1.48575400
H	4.71881700	2.69823200	-0.00171200
C	2.51656500	-1.60284000	-0.28048400
C	3.82630800	-2.00219800	-0.26037400
H	3.99597300	-3.04141800	-0.54752900
C	5.06792200	-1.26179600	0.10159100
H	5.66434700	-1.08705100	-0.80652600
H	4.89415100	-0.31216400	0.60392500
H	5.68731100	-1.89150600	0.75310800
H	1.78374900	-2.36203600	-0.54126200

2.29 s-*cis*

Route= #N b3lyp/gen pseudo=read gfprint
OPT FREQ
B3LYP Energy=-1361.81947287 Hartree
ZPE=0.231592 Hartree
Conditions=298K, 1.00000 atm
Internal Energy=-1361.563464 Hartree

Rh	0.00000000	0.00000000	0.00000000
Rh	-2.43147800	-0.46356100	-0.01770900
O	-2.70358200	1.38802900	0.85179200
C	-1.68763200	2.09151300	1.09151100
O	-0.46410200	1.82220400	0.85709600
H	-1.86579900	3.06841400	1.56228800

Enthalpy=-1361.562520 Hartree
Free Energy=-1361.641917 Hartree
Entropy=167.105 cal/mol-K

O	-2.22331600	-1.30194200	1.84785500
C	-1.06935400	-1.31482000	2.35661700
O	0.01533300	-0.86723600	1.86646200
H	-0.97439600	-1.76799200	3.35274900
O	-1.99838400	-2.28627400	-0.87737200
C	-0.78879000	-2.57568000	-1.07759000
O	0.24567100	-1.87463700	-0.83508700
H	-0.58775100	-3.56077000	-1.52144000
O	-2.51232000	0.39370500	-1.89202400
C	-1.44375900	0.83622500	-2.38679800
O	-0.27499500	0.83218000	-1.87701900
H	-1.51242900	1.28785700	-3.38627100
C	1.97505200	0.34925500	0.01871000
C	2.66528000	1.60955900	-0.07743700
C	2.01679500	2.65725800	-0.65483000
H	0.99376700	2.57349700	-0.99427700
H	2.53640300	3.59477600	-0.84001100
C	4.11089100	1.73123800	0.37126000
H	4.21889100	1.43452100	1.41929300
H	4.76384100	1.07961500	-0.22173700
H	4.46638000	2.75994700	0.26284200
C	2.83075600	-0.83864600	0.28023700
O	3.11282800	-1.17086100	1.41509400
O	3.22443100	-1.46299100	-0.83574000
C	3.96320700	-2.68624800	-0.64006100
H	4.87113800	-2.49772100	-0.06189300
H	3.34251000	-3.41757200	-0.11714700
H	4.20882700	-3.03642400	-1.64207300

2.29 s-*trans*

Route= #N b3lyp/gen pseudo=read gfprint integral(grid=ultrafine) OPT FREQ
B3LYP Energy=-1361.81602452 Hartree
ZPE=0.231421 Hartree
Conditions=298K, 1.00000 atm
Internal Energy=-1361.560088 Hartree
Enthalpy=-1361.559144 Hartree
Free Energy=-1361.639078 Hartree
Entropy=168.236 cal/mol-K

Rh	0.00000000	0.00000000	0.00000000
Rh	-2.42522600	-0.49133500	-0.07033500
O	-2.75095700	1.36012400	0.77605300
C	-1.75021500	2.07565400	1.04194800
O	-0.51766800	1.81795300	0.84675700
H	-1.95269500	3.05291700	1.50197700
O	-2.24639400	-1.31068300	1.80879600
C	-1.10563000	-1.30196300	2.34587200
O	-0.01538200	-0.84353800	1.87802000
H	-1.02862400	-1.74359900	3.34869200
O	-1.95480300	-2.31674100	-0.90226500
C	-0.73864500	-2.59505400	-1.07185100
O	0.28212800	-1.87875600	-0.81365800
H	-0.51565900	-3.58221100	-1.50014700

O	-2.47773400	0.34999000	-1.95172000
C	-1.39926700	0.78979600	-2.42960200
O	-0.24189900	0.79567200	-1.89812700
H	-1.44956500	1.22858800	-3.43590400
C	1.96484400	0.34940800	0.04872100
C	2.64940100	1.61955400	-0.06661000
C	3.86063700	1.75775600	0.53780900
H	4.35044800	0.93744900	1.05208700
H	4.34709900	2.72873800	0.59067900
C	1.98114900	2.79017500	-0.75180400
H	1.07557100	3.08136100	-0.21456900
H	2.66480000	3.64312600	-0.80047500
H	1.68072100	2.51873700	-1.76762100
C	2.81210600	-0.85349900	0.28381700
O	3.07656300	-1.27342100	1.39282600
O	3.21765000	-1.40044800	-0.87026400
C	3.90681800	-2.66164800	-0.75633800
H	4.82490700	-2.54545300	-0.17503300
H	3.26010400	-3.39854800	-0.27448400
H	4.13370900	-2.95815700	-1.77986400

2.24 s-*cis*

Route= #N b3lyp/gen pseudo=read gfprint OPT FREQ
RB3LYP Energy=-1553.56930325 Hartree
ZPE=0.285237 Hartree
Conditions=298K, 1.00000 atm
Internal Energy=-1553.256429 Hartree
Enthalpy=-1553.255484 Hartree
Free Energy=-1553.344386 Hartree
Entropy=187.109 cal/mol-K

Rh	0.00000000	0.00000000	0.00000000
O	-1.08683900	1.08707600	-1.38071900
C	-2.22671000	0.65401800	-1.74114800
O	-2.82589500	-0.39218800	-1.37054300
Rh	-1.88751500	-1.60513200	0.00217600
O	-0.94322300	-2.59651800	-1.54753600
C	0.15625100	-2.14570500	-1.95996600
O	0.80672300	-1.13341100	-1.53868400
H	0.62897600	-2.68820900	-2.79134800
O	-0.83182600	-2.71722400	1.38865700
C	0.29367400	-2.29319800	1.75977300
O	0.91065400	-1.24531100	1.37910900
H	0.82492600	-2.89880400	2.50784000
O	-2.71629500	-0.51205000	1.53680400
C	-2.09943200	0.51404900	1.93281400
O	-0.99250200	0.98276900	1.51659600
H	-2.56879300	1.08703000	2.74444700
H	-2.75087100	1.28284700	-2.47473400
C	1.54365700	1.30492100	0.05953400
C	1.21711500	2.74408400	0.25603600
O	1.30965600	3.26971800	1.34928200
O	0.82053900	3.36271100	-0.86360200

C	0.44007500	4.74279500	-0.70872400
H	-0.42266700	4.82351700	-0.04283300
H	0.18523900	5.08527700	-1.71130400
H	1.26831600	5.32715300	-0.29917900
C	2.92434300	1.01774600	0.11206400
C	3.42313400	-0.25196400	-0.08616600
H	2.70096700	-1.03267900	-0.29394600
C	4.80898200	-0.66182100	-0.07163100
C	5.09884400	-2.02340000	-0.31424900
C	6.40884000	-2.48954200	-0.30127300
C	7.45763900	-1.60222600	-0.04530400
C	7.19117600	-0.24835100	0.19701500
C	5.88417700	0.22014300	0.18386400
H	5.69098200	1.27082600	0.37400400
H	8.00909500	0.43781600	0.39615200
H	8.48260800	-1.96231100	-0.03381400
H	6.61430200	-3.53925400	-0.48892900
H	4.27829100	-2.70822200	-0.51140200
H	3.61505200	1.83817000	0.31036400

2.24 s-*trans*

Route= #N b3lyp/gen pseudo=read gfprint OPT FREQ
RB3LYP Energy=-1553.56991114 Hartree
ZPE=0.285402 Hartree
Conditions=298K, 1.00000 atm
Internal Energy=-1553.256906 Hartree
Enthalpy=-1553.255962 Hartree
Free Energy=-1553.344576 Hartree
Entropy=186.503 cal/mol-K

Rh	0.00000000	0.00000000	0.00000000
O	-0.83884900	1.80067600	0.55236500
C	-2.10480400	1.86360500	0.67365000
O	-2.95789300	0.95425700	0.49351200
Rh	-2.29573900	-0.92218100	-0.06864400
O	-2.39662200	-0.35780300	-2.05068000
C	-1.38422000	0.20403200	-2.54865400
O	-0.27592100	0.48135100	-1.98944200
H	-1.45525200	0.49734200	-3.60552200
O	-1.45629200	-2.72788300	-0.62263800
C	-0.20522000	-2.80062000	-0.73494600
O	0.66307400	-1.88512000	-0.55377800
H	0.20413800	-3.77825700	-1.02726500
O	-2.07357000	-1.43191100	1.91418100
C	-0.97821600	-1.16020200	2.47572900
O	0.04662700	-0.59370500	1.97827800
H	-0.88339700	-1.44485300	3.53287300
H	-2.49285300	2.84669500	0.97538600
C	1.85560100	0.73642600	0.03584200
C	2.02003400	2.19949600	0.24599800
O	2.35439200	2.67567400	1.31528800
O	1.72037000	2.91171900	-0.85001100
C	1.71850300	4.34118600	-0.68075100

H	0.97175700	4.62839200	0.06325900
H	1.46317200	4.74605900	-1.65974000
H	2.70265300	4.69490900	-0.36186100
C	2.99575200	-0.08897100	-0.06920300
C	4.28596200	0.37442700	0.06239900
H	4.42370800	1.43423200	0.26972400
C	5.50371800	-0.40118300	-0.01053000
C	6.73698200	0.26802600	0.15411900
C	7.94082900	-0.42425000	0.08144200
C	7.93608700	-1.80165200	-0.15491300
C	6.72311300	-2.48339400	-0.31786200
C	5.51934800	-1.79554400	-0.24681700
H	4.58592200	-2.33412300	-0.37210800
H	6.72285600	-3.55415300	-0.49942600
H	8.87460000	-2.34598600	-0.21117200
H	8.88046500	0.10487500	0.20941500
H	6.73550900	1.33900800	0.33982800
H	2.80899400	-1.14473500	-0.24249700

Cyclohexene

Route= #N B3LYP/6-31G(d) 5d OPT FREQ
B3LYP Energy=-234.643975482 Hartree
ZPE=0.147023 Hartree
Conditions=298K, 1.00000 atm
Internal Energy=-234.491461 Hartree
Enthalpy=-234.490517 Hartree
Free Energy=-234.525592 Hartree
Entropy=73.820 cal/mol-K

C	0.00000000	0.00000000	0.00000000
H	0.39001600	-0.13832500	-1.02131200
C	-0.80073400	-1.24031000	0.42973300
H	-0.90622600	-1.24029200	1.52371200
C	-2.19741700	-1.24037500	-0.20824000
H	-2.09191700	-1.24019200	-1.30222200
C	-2.99832400	-0.00021900	0.22158500
H	-3.38824700	-0.13856400	1.24299300
H	-3.88603400	0.11559800	-0.41594800
C	-2.16546100	1.25824700	0.16806000
C	-0.83304100	1.25828800	0.05351600
H	-0.29967800	2.20689200	-0.00223700
H	-2.69895900	2.20678700	0.22339600
H	-2.74385000	-2.15416500	0.05600600
H	-0.25419400	-2.15400100	0.16535300
H	0.88759800	0.11603400	0.63761700

1,3-cyclohexadiene

Route= #N B3LYP/6-31G(d) 5d OPT FREQ
RB3LYP Energy=-233.414357014 Hartree
ZPE=0.122862 Hartree

C	0.00000000	0.00000000	0.00000000
C	0.00346200	-1.46335700	0.47985100
H	-0.16174000	-1.49396600	1.57069200
C	1.31407100	-2.15395700	0.17531400

Conditions=298K, 1.00000 atm
Internal Energy=-233.286322 Hartree
Enthalpy=-233.285377 Hartree
Free Energy=-233.319746 Hartree
Entropy=72.335 cal/mol-K

C	2.45925100	-1.45226800	0.13586500
C	2.45580400	0.00034000	0.34418300
C	1.30727600	0.69655400	0.30431700
H	1.30699900	1.77786300	0.42382300
H	3.40526100	0.50386700	0.51198200
H	3.41114500	-1.95103100	-0.03248200
H	1.31868000	-3.23508700	0.05450500
H	-0.83744500	-2.00582900	0.03188100
H	-0.16625600	0.03049400	-1.09071700
H	-0.84324400	0.53830100	0.44868700

Vinylcarbenoid 2.5a vinyl group rotation TS

Route= # b3lyp/gen pseudo=read gfprint OPT=(TS,CalcFC,NoEigenTest) freq
B3LYP Energy=-1322.48768879 Hartree
ZPE=0.201812 Hartree
Conditions=298K, 1.00000 atm
Internal Energy=-1322.263272 Hartree
Enthalpy=-1322.262328 Hartree
Free Energy=-1322.338872 Hartree
Entropy=161.099 cal/mol-K

Rh	0.00000000	0.00000000	0.00000000
C	1.88017200	0.50779000	-0.14646500
C	2.31099300	1.83056700	-0.57580400
C	2.45773600	2.90484600	0.20887800
O	-0.61036000	1.49466000	-1.28842200
H	-2.11747400	2.44303600	-2.20428900
O	-2.49379100	0.70932700	1.82963400
C	-1.44606300	1.33124400	2.14605200
O	-0.29467500	1.26428300	1.60598700
H	-1.51929700	2.02469400	2.99466800
O	-1.78602900	-2.09709000	1.52613100
C	-0.55406700	-2.24435700	1.74253800
O	0.41879300	-1.56491000	1.27839600
H	-0.26683700	-3.06110400	2.41877000
O	-2.16963900	-1.87430700	-1.35820400
C	-1.03465200	-1.94638200	-1.89888800
O	0.03102200	-1.32338500	-1.58613100
H	-0.93540800	-2.63100100	-2.75231900
Rh	-2.38660800	-0.59623500	0.24263200
O	-2.81460400	0.95179600	-1.05421500
C	-1.85675300	1.62814500	-1.51497300
H	2.78392000	3.85167100	-0.20923200
H	2.25460200	2.86431100	1.27367500
H	2.49790200	1.89380600	-1.65249300
C	2.94405200	-0.41601000	0.32122800
O	3.35238700	-0.29325600	1.45855600
O	3.33993800	-1.31860600	-0.57397300
C	4.34591900	-2.25075300	-0.11606000
H	5.23170200	-1.71334700	0.23060500
H	3.94489500	-2.86088300	0.69625300
H	4.58013300	-2.86629700	-0.98344000

TS-XIIc-synCO

Route= #N b3lyp/gen pseudo=read gfprint
OPT=(TS,CalcFC,NoEigenTest) freq
B3LYP Energy=-1557.13062105 Hartree
ZPE=0.346813 Hartree
Conditions=298K, 1.00000 atm
Internal Energy=-1556.754302 Hartree
Enthalpy=-1556.753357 Hartree
Free Energy=-1556.845453 Hartree
Entropy=193.831 cal/mol-K

Rh	0.00000000	0.00000000	0.00000000
O	0.48883600	1.76832400	-0.95348100
C	1.69480900	1.95853700	-1.30575600
O	2.68844300	1.19598600	-1.15361000
Rh	2.37814400	-0.61671800	-0.22775500
O	2.71648000	0.26181900	1.60229400
C	1.72799400	0.77214100	2.19978700
O	0.51618900	0.82628700	1.82303400
H	1.93531700	1.23189400	3.17662100
O	1.90788300	-2.39356500	0.72097700
C	0.71602500	-2.59379400	1.07486200
O	-0.29555300	-1.83374400	0.92430900
H	0.51220600	-3.54920800	1.58030100
O	1.89345100	-1.44882400	-2.05795300
C	0.69477700	-1.40221400	-2.44183700
O	-0.30951900	-0.90200500	-1.83907500
H	0.47785800	-1.85108500	-3.42188400
H	1.89072700	2.91588200	-1.80946800
C	-2.03332500	0.60385800	0.27693700
C	-2.33295400	1.87163900	-0.45545000
O	-2.73898500	1.93693000	-1.60296800
O	-2.01681500	2.96214900	0.27578500
C	-2.03204000	4.20714500	-0.44411600
H	-1.31448600	4.16975000	-1.26672100
H	-1.74215600	4.96414800	0.28505100
H	-3.02967500	4.41359300	-0.84024500
C	-2.54403300	0.35381700	1.62368200
C	-3.12215400	1.24296300	2.45486800
H	-3.36649900	0.96124300	3.47568900
H	-3.29886600	2.27367000	2.16915900
H	-2.35112800	-0.65247500	1.99177400
C	-3.38915700	-1.14991300	-1.12975400
H	-2.58396500	-0.30202800	-0.45852400
C	-4.69977900	-0.48198000	-1.47317800
H	-5.10189900	-1.02165500	-2.34752500
C	-5.70119700	-0.54299800	-0.31220000
H	-5.32340700	0.06687100	0.51716500
C	-5.89754500	-1.98485200	0.17777000
H	-6.53377800	-2.54789500	-0.52601500
H	-6.43883100	-2.00129500	1.13288600
C	-4.59326500	-2.71647300	0.32470900
C	-3.44143100	-2.32070200	-0.26115800
H	-2.52217400	-2.87781200	-0.10785100
H	-4.59887700	-3.63763200	0.90575600

H	-6.66058100	-0.11086600	-0.61739800
H	-4.51407000	0.54266900	-1.80398200
H	-2.65991800	-1.20136400	-1.93973000

TS-XIId-synCO

Route= #N b3lyp/gen pseudo=read gfprint
OPT=(TS,CalcFC,NoEigenTest) freq
B3LYP Energy=-1557.13195326 Hartree
ZPE=0.347158 Hartree
Conditions=298K, 1.00000 atm
Internal Energy=-1556.755249 Hartree
Enthalpy=-1556.754305 Hartree
Free Energy=-1556.845901 Hartree
Entropy=192.781 cal/mol-K

Rh	0.00000000	0.00000000	0.00000000
O	0.56101800	1.76971800	-0.91109400
C	1.78150100	1.93315200	-1.22413100
O	2.74992100	1.14128700	-1.05649200
Rh	2.36346400	-0.67742200	-0.17223700
O	2.67159400	0.16202000	1.68320500
C	1.67969000	0.68766200	2.26185400
O	0.48052100	0.77928100	1.85298000
H	1.87151600	1.12535000	3.25197400
O	1.81292300	-2.45684000	0.73116600
C	0.60733900	-2.62713200	1.05278400
O	-0.37696400	-1.83411200	0.89063800
H	0.36265900	-3.58410500	1.53664100
O	1.90004900	-1.46202500	-2.03055800
C	0.71409900	-1.37209600	-2.44659800
O	-0.29292800	-0.85645800	-1.86193800
H	0.51318600	-1.79423100	-3.44196300
H	2.01823100	2.89322200	-1.70472400
C	-2.03724400	0.63485000	0.22949700
C	-2.30555300	1.91872700	-0.49243300
O	-2.71539400	2.01343200	-1.63772300
O	-1.96227100	2.98809900	0.25614300
C	-1.94115700	4.24402500	-0.44140600
H	-1.21166200	4.20668000	-1.25376000
H	-1.64726500	4.98295500	0.30456500
H	-2.92767200	4.47863600	-0.84999300
C	-2.60085700	0.41335300	1.56276600
C	-3.46603800	1.21511000	2.21207600
H	-3.78926900	0.98166300	3.22340400
H	-3.82650100	2.14600400	1.78668900
H	-2.26010400	-0.49591900	2.05496100
C	-3.53714100	-0.81425400	-1.29386200
H	-2.51562200	-0.23665900	-0.50803800
C	-4.80382100	-0.24479000	-0.88768700
H	-5.01974100	0.77176500	-1.20096200
C	-5.69847500	-0.95112400	-0.15790500
H	-6.66114700	-0.49946600	0.07681500
C	-5.47619400	-2.36932400	0.28497000
C	-3.99494600	-2.77461700	0.23851300

C	-3.31020000	-2.28766200	-1.04551300
H	-2.23938400	-2.50692200	-1.03113000
H	-3.72448200	-2.81347500	-1.92310300
H	-3.89671200	-3.86211900	0.32670600
H	-3.47535000	-2.33999100	1.09935100
H	-6.07825700	-3.02704300	-0.36479200
H	-5.88425300	-2.51055500	1.29428600
H	-3.09255700	-0.39459000	-2.19470900

TS-XIIb-synCO

Route= #N b3lyp/gen pseudo=read gfprint
OPT=(TS,CalcFC,NoEigenTest) FREQ
B3LYP Energy=-1557.129283 Hartree
ZPE=0.347095 Hartree
Conditions=298K, 1.00000 atm
Internal Energy=-1556.752756 Hartree
Enthalpy=-1556.751811 Hartree
Free Energy=-1556.842653 Hartree
Entropy=191.191 cal/mol-K

Rh	0.00000000	0.00000000	0.00000000
O	0.62018700	1.86978400	-0.63467600
C	1.83483500	2.03404800	-0.96877900
O	2.76993600	1.18676000	-0.97555700
Rh	2.32284100	-0.73571600	-0.39734200
O	2.74371400	-0.24506200	1.55648900
C	1.80885400	0.23441900	2.25760900
O	0.60262900	0.45380300	1.92688500
H	2.06626400	0.49727900	3.29367800
O	1.73804100	-2.62449600	0.21175800
C	0.54275000	-2.80056300	0.56392100
O	-0.40949400	-1.95357700	0.59031200
H	0.27564200	-3.81602700	0.89151400
O	1.75061500	-1.17457500	-2.33620700
C	0.55212000	-0.97523600	-2.67083600
O	-0.40390500	-0.52966500	-1.95904400
H	0.28912500	-1.21828900	-3.71047500
H	2.09862800	3.05078000	-1.29317600
C	-2.00082300	0.72877100	0.35338300
C	-2.21342500	2.01844800	-0.38126300
O	-2.54299400	2.14265500	-1.54827000
O	-1.93917100	3.06840000	0.42361100
C	-1.89602700	4.34765200	-0.22765600
H	-1.12671700	4.34492300	-1.00331700
H	-1.64957600	5.06411400	0.55638600
H	-2.86373200	4.58530100	-0.67761100
C	-2.57497400	0.68444500	1.70635000
C	-2.45601700	-0.36032200	2.54596100
H	-2.90216500	-0.33132400	3.53661300
H	-1.90126700	-1.25046600	2.26795200
H	-3.11420100	1.56853900	2.04511400
H	-6.33612500	-2.35650500	0.84913200
C	-5.76082800	-2.16343400	-0.06579900
H	-6.26641500	-2.74594400	-0.85458000

C	-5.85165000	-0.70801700	-0.42497600
H	-6.81696500	-0.21994900	-0.29861800
C	-4.82501400	-0.00149000	-0.94838400
H	-4.94790300	1.04406300	-1.21453700
C	-3.54065300	-0.61690900	-1.23659300
C	-3.41471300	-2.11168100	-1.03765700
C	-4.30806900	-2.63060700	0.09825500
H	-4.26288500	-3.72453400	0.14065500
H	-3.92131900	-2.25724300	1.05295900
H	-2.36857400	-2.38232500	-0.87177200
H	-3.70773400	-2.57362300	-1.99604200
H	-3.00200200	-0.19915900	-2.08563800
H	-2.60099600	-0.11871300	-0.36301400

TS-XIIa-synCO

Route= #N b3lyp/gen pseudo=read gfprint OPT=(TS,CalcFC,NoEigenTest) freq
B3LYP Energy=-1557.13222248 Hartree
ZPE=0.347180 Hartree
Conditions=298K, 1.00000 atm
Internal Energy=-1556.755856 Hartree
Enthalpy=-1556.754911 Hartree
Free Energy=-1556.844545 Hartree
Entropy=188.650 cal/mol-K

Rh	0.00000000	0.00000000	0.00000000
O	0.51530800	1.95377700	-0.43264400
C	1.72902400	2.22111100	-0.69616700
O	2.71683500	1.43650600	-0.73191400
Rh	2.38051700	-0.55269800	-0.33813000
O	2.67709500	-0.20656300	1.66920500
C	1.67948300	0.14342800	2.36032100
O	0.47680100	0.30977900	1.98788100
H	1.86987500	0.32827800	3.42725400
O	1.90607700	-2.52056100	0.07726700
C	0.70818100	-2.80401500	0.33776300
O	-0.29959600	-2.02481700	0.38192500
H	0.49440600	-3.86081100	0.55578400
O	1.93282000	-0.85539700	-2.33291500
C	0.74025800	-0.70254600	-2.71160000
O	-0.27463900	-0.37799000	-2.01607000
H	0.54237900	-0.87177400	-3.77983800
H	1.93869300	3.27649500	-0.92107800
C	-2.05552500	0.56649700	0.34352300
C	-2.34458800	1.89948900	-0.27032400
O	-2.61826000	2.10633800	-1.43960900
O	-2.21564300	2.88642600	0.64498600
C	-2.27969700	4.22269600	0.12221700
H	-1.48004400	4.37913300	-0.60566700
H	-2.14847600	4.87774200	0.98396300
H	-3.24555800	4.40398400	-0.35703200
C	-2.69311300	0.31399900	1.63097500
C	-2.59677700	-0.85159000	2.30779000
H	-1.96333800	-1.65900500	1.96081300

H	-3.12191600	-0.99071500	3.24926600
H	-3.30932400	1.11056600	2.04922000
C	-3.36540200	-1.03879300	-1.28337200
H	-2.56752400	-0.26953200	-0.49603900
C	-3.47118700	-2.23803400	-0.47639700
H	-2.58534100	-2.85574900	-0.36784300
C	-4.61648000	-2.55936000	0.17218000
H	-4.65773900	-3.48728200	0.74105100
C	-5.88378700	-1.75889400	0.06900600
H	-6.56974700	-2.30044000	-0.60440200
H	-6.39144200	-1.74030200	1.04211300
C	-5.64133600	-0.33054600	-0.44413300
H	-6.58919400	0.12836300	-0.74612200
H	-5.24370600	0.27673200	0.37742300
C	-4.64347800	-0.30194200	-1.61102900
H	-5.07884200	-0.80027100	-2.49326500
H	-4.40921100	0.72108900	-1.91663400
H	-2.60897200	-1.04945800	-2.06933100

Vinylogous TS (Path 5)

Route= #N b3lyp/gen pseudo=read gfprint
OPT=(TS,CalcFC,NoEigenTest) freq
RB3LYP Energy=-1557.12900766 Hartree
ZPE=0.351700 Hartree
Conditions=298K, 1.00000 atm
Internal Energy=-1556.748596 Hartree
Enthalpy=-1556.747652 Hartree
Free Energy=-1556.836677 Hartree
Entropy=187.368 cal/mol-K

Rh	0.00000000	0.00000000	0.00000000
O	-0.72389800	1.87981400	0.44487700
C	-1.95726100	2.01914200	0.71698200
O	-2.85807400	1.13797600	0.75914100
Rh	-2.32113600	-0.80809200	0.36889000
O	-2.65776800	-0.49212600	-1.64188300
C	-1.70720000	-0.05077900	-2.34487300
O	-0.52214900	0.23974800	-1.98851900
H	-1.92429700	0.10480000	-3.41178400
O	-1.64490300	-2.71818100	-0.05173900
C	-0.43247000	-2.87696800	-0.33429600
O	0.49562500	-2.00194100	-0.38989800
H	-0.11826600	-3.90718300	-0.56374700
O	-1.81449500	-1.05438800	2.36116000
C	-0.63919900	-0.77473600	2.72069300
O	0.33124400	-0.35394800	2.01311400
H	-0.41076500	-0.91418200	3.78777400
H	-2.27102000	3.04821400	0.94352300
C	1.89349600	0.84186100	-0.34894100
C	2.07342900	2.19645800	0.24585100
O	2.49505500	2.38407900	1.37401000
O	1.73072200	3.18830200	-0.59951500
C	1.76811300	4.51172500	-0.04251600
H	1.07552500	4.58528500	0.79987200

H	1.46077500	5.17619200	-0.85064200
H	2.77658600	4.76210900	0.29830200
C	2.94645600	0.41107400	-1.11605300
C	3.07164500	-0.91493200	-1.68832600
H	3.64207300	-0.94253800	-2.61902200
H	2.14521700	-1.47701900	-1.75446900
H	3.78764300	1.08722100	-1.29427800
C	3.45839300	-2.18752500	0.40372900
H	2.63700900	-2.89805500	0.40659400
C	4.20331400	-2.00605100	-0.78320300
H	4.17307000	-2.86492300	-1.45495000
C	5.58812900	-1.34093300	-0.65005800
C	6.01670900	-1.22497400	0.82216600
H	6.21931400	-2.23140700	1.21501400
H	6.95352900	-0.66097800	0.89145100
C	4.93256800	-0.55598800	1.67953800
H	4.84463000	0.50512200	1.42343200
H	5.20999900	-0.59745000	2.73788000
C	3.55644300	-1.24201700	1.49215300
H	2.82502300	-0.45633500	1.11022400
H	3.08682200	-1.60090600	2.41128900
H	6.31678000	-1.93697700	-1.21114000
H	5.58520700	-0.34538700	-1.10607900

TS-XIa-synCO

Route= #N b3lyp/gen pseudo=read gfprint OPT=(TS,CalcFC,NoEigenTest) freq
B3LYP Energy=-1555.91119672 Hartree
ZPE=0.323497 Hartree
Conditions=298K, 1.00000 atm
Internal Energy=-1555.559057 Hartree
Enthalpy=-1555.558113 Hartree
Free Energy=-1555.646396 Hartree
Entropy=185.808 cal/mol-K

Rh	0.00000000	0.00000000	0.00000000
C	-2.03551700	0.50145800	0.37615800
C	-2.41263300	1.81136000	-0.23635400
O	-2.35725200	2.80088000	0.68184200
C	-2.52136000	4.13246000	0.16700100
H	-3.50286400	4.24670400	-0.30104000
H	-1.74279300	4.34958200	-0.56816500
H	-2.42833200	4.79049200	1.03131000
O	-2.69623600	2.00214700	-1.40674800
C	-2.71492700	0.16915400	1.61062100
C	-2.53756200	-1.00325600	2.26471600
H	-3.10243600	-1.22791800	3.16580400
H	-1.79977000	-1.72616300	1.93781800
H	-3.45411100	0.87415500	1.99274700
O	-0.26286100	-0.28925400	-2.03142700
C	0.75714800	-0.55984300	-2.74173600
O	1.95343200	-0.70707800	-2.37238800
Rh	2.39481300	-0.47933400	-0.36714200
O	1.96806200	-2.47451700	-0.03697500

C	0.77809600	-2.79881300	0.20944900
O	-0.24885300	-2.04732000	0.28944800
H	0.58984000	-3.86939700	0.37838800
O	2.67678600	1.53450100	-0.67756300
C	1.67067500	2.29183300	-0.60245900
O	0.46489600	1.98357900	-0.34496700
H	1.85233200	3.36114700	-0.78143000
O	2.68734300	-0.21071500	1.65335800
C	1.68359300	0.07894600	2.36190000
O	0.47473800	0.22763800	2.00022700
H	1.87176300	0.22083400	3.43581500
H	0.56026700	-0.68190600	-3.81664400
C	-4.50363100	-0.50226500	-1.77032500
C	-3.26458000	-1.22545900	-1.27518400
C	-3.47816600	-2.35202000	-0.38330300
C	-4.63180500	-2.44423200	0.34067900
C	-5.71569100	-1.49683600	0.16169800
C	-5.66392300	-0.57596800	-0.82487200
H	-6.49726900	0.10330900	-0.98896500
H	-6.58004300	-1.56229900	0.81695900
H	-4.76635600	-3.26284400	1.04347500
H	-2.60126500	-0.42204600	-0.54343500
H	-2.66310000	-3.04915400	-0.22112400
H	-2.48870400	-1.35235900	-2.03046800
H	-4.24690800	0.53498200	-2.01536200
H	-4.80991700	-0.95773700	-2.73087800

TS-XId-synCO

Route= #N b3lyp/gen pseudo=read gfprint OPT=(TS,CalcFC,NoEigenTest) freq
B3LYP Energy=-1555.90984133 Hartree
ZPE=0.323185 Hartree
Conditions=298K, 1.00000 atm
Internal Energy=-1555.557682 Hartree
Enthalpy=-1555.556738 Hartree
Free Energy=-1555.646467 Hartree
Entropy=188.851 cal/mol-K

Rh	0.00000000	0.00000000	0.00000000
C	-1.98791100	0.60430000	0.24181100
C	-2.33304000	1.88070100	-0.47069400
O	-1.99827700	2.94895800	0.28188200
C	-2.04272900	4.21664700	-0.39455400
H	-1.34737100	4.21424100	-1.23725400
H	-1.73959100	4.95174800	0.35129100
H	-3.05221200	4.42761100	-0.75718800
O	-2.79217100	1.96968300	-1.59527700
C	-2.64326600	0.31367300	1.50851000
C	-3.70828900	0.98093300	2.00089100
H	-4.14808100	0.70853700	2.95706400
H	-4.13432600	1.84321000	1.49749300
H	-2.25127300	-0.54166000	2.05504600
O	-0.24917600	-0.83458800	-1.87854100
C	0.77481800	-1.32031700	-2.46005900

O	1.95774000	-1.39358100	-2.03334000
Rh	2.38555000	-0.62106500	-0.16276800
O	1.87247500	-2.42343100	0.71628000
C	0.66948100	-2.62557900	1.02659700
O	-0.33400700	-1.85617200	0.86336900
H	0.44355000	-3.59232300	1.50012900
O	2.73018600	1.21941200	-1.02202900
C	1.74472700	1.98882200	-1.18780200
O	0.52566000	1.79306200	-0.88462800
H	1.95974100	2.95986600	-1.65633800
O	2.65947500	0.20175300	1.70614000
C	1.65093100	0.69108400	2.28551200
O	0.45176700	0.75802300	1.86890900
H	1.82206200	1.11765200	3.28415100
H	0.59150800	-1.73017000	-3.46392400
C	-3.45495600	-0.92726300	-1.33429900
C	-3.15220100	-2.39881900	-1.09520800
C	-3.93924100	-3.01516000	0.02304500
C	-5.05217600	-2.42881100	0.50894800
C	-5.50946900	-1.15820400	-0.02689800
C	-4.77505000	-0.45959300	-0.93640900
H	-5.11689700	0.49758800	-1.31674600
H	-6.47631300	-0.77771900	0.29380300
H	-5.63432300	-2.90357700	1.29404400
H	-2.07803100	-2.54212700	-0.94302600
H	-3.61137300	-3.98052400	0.40071400
H	-3.38926400	-2.94409300	-2.02821100
H	-2.62657300	-0.31426400	-0.59548500
H	-3.08687900	-0.53722500	-2.28221300

TS-XIb-synCO

Route= #N b3lyp/gen pseudo=read gfprint
OPT=(TS,CalcFC,NoEigenTest) freq
RB3LYP Energy=-1555.90718239 Hartree
ZPE=0.323479 Hartree
Conditions=298K, 1.00000 atm
Internal Energy=-1555.554808 Hartree
Enthalpy=-1555.553864 Hartree
Free Energy=-1555.643734 Hartree
Entropy=189.149 cal/mol-K

Rh	0.00000000	0.00000000	0.00000000
C	-1.89562000	0.88674800	0.29330300
C	-2.05279400	2.15071900	-0.50243800
O	-1.77171400	3.22688200	0.26668700
C	-1.67910600	4.47702900	-0.43587200
H	-0.89815200	4.42100800	-1.19801400
H	-1.42381000	5.21762000	0.32246000
H	-2.63199600	4.72380100	-0.91163500
O	-2.34780000	2.22943100	-1.67998600
C	-2.54520300	0.88135800	1.59152000
C	-2.68086100	-0.23085700	2.34558100
H	-3.20284100	-0.20188500	3.29818500
H	-2.25907900	-1.17899500	2.02899100

H	-2.98738300	1.81494200	1.94023600
O	-0.23725800	-0.31323000	-2.03290700
C	0.74932700	-0.76533400	-2.69758900
O	1.88966100	-1.10181600	-2.27902800
Rh	2.28989400	-0.89581000	-0.26268100
O	1.49777200	-2.76920200	0.10017500
C	0.26455000	-2.86903000	0.33220800
O	-0.61456500	-1.94783400	0.35981600
H	-0.11323500	-3.88154800	0.53628100
O	2.93967200	1.02775600	-0.60448200
C	2.07568500	1.94632000	-0.60035600
O	0.82482600	1.85608500	-0.39555500
H	2.44487200	2.96264300	-0.79851200
O	2.56124100	-0.61973200	1.75798800
C	1.60392800	-0.13025200	2.41933000
O	0.45369200	0.21973200	2.00832200
H	1.78035200	0.01416500	3.49487100
H	0.57306400	-0.87797800	-3.77711300
C	-3.72615300	-0.46898000	-1.09525500
C	-3.22998400	-1.73800300	-1.77885900
C	-3.39104400	-2.98589900	-0.96489800
C	-4.23954100	-3.04242900	0.08255000
C	-4.99462100	-1.86736000	0.47476700
C	-4.77950400	-0.65225400	-0.10032500
H	-5.35254300	0.21224400	0.22295900
H	-5.76288700	-1.97454700	1.23705100
H	-4.38351000	-3.96593300	0.63650000
H	-2.19439200	-1.60541800	-2.10472800
H	-2.84224600	-3.86964700	-1.28098500
H	-3.81531300	-1.86363300	-2.70907300
H	-2.74171300	-0.01396500	-0.47207100
H	-3.87217500	0.36203700	-1.78564400

TS-XIc-synCO

Route= #N b3lyp/gen pseudo=read gfprint
OPT=(TS,CalcFC,NoEigenTest) freq
RB3LYP Energy=-1555.90734862 Hartree
ZPE=0.322936 Hartree
Conditions=298K, 1.00000 atm
Internal Energy=-1555.555363 Hartree
Enthalpy=-1555.554418 Hartree
Free Energy=-1555.645248 Hartree
Entropy=191.168 cal/mol-K

Rh	0.00000000	0.00000000	0.00000000
C	-2.00794200	0.45231700	0.37909500
C	-2.51207400	1.60803300	-0.42217900
O	-2.36000600	2.77093500	0.24955500
C	-2.54343500	3.96207900	-0.53517500
H	-3.56420100	4.01691600	-0.92272800
H	-1.83752300	3.97319800	-1.36877100
H	-2.34591000	4.78918600	0.14717200
O	-2.92038300	1.55344300	-1.56892500
C	-2.46570900	0.22995600	1.74427300

C	-3.45583700	0.89271900	2.37379200
H	-3.69341200	0.68187500	3.41350800
H	-4.01771600	1.68841900	1.89489100
H	-1.93777600	-0.55586300	2.28088000
O	-0.33179800	-0.92224700	-1.82248500
C	0.67231200	-1.36781100	-2.46587800
O	1.88706000	-1.34900500	-2.13309400
Rh	2.39954300	-0.48455100	-0.32745800
O	2.06079000	-2.28111200	0.64526300
C	0.89785400	-2.54449300	1.04825800
O	-0.15932400	-1.83975600	0.93982500
H	0.76550500	-3.50790900	1.56199800
O	2.55945300	1.34185600	-1.26969100
C	1.51898900	2.04610500	-1.37954800
O	0.34125200	1.79087200	-0.97411200
H	1.63750600	3.01099500	-1.89299500
O	2.76214100	0.42043400	1.48743800
C	1.77386800	0.87336000	2.12727000
O	0.54466100	0.85483900	1.80378200
H	1.99495400	1.34738400	3.09425800
H	0.43862300	-1.82987300	-3.43597500
C	-4.14935500	-1.21508100	-1.83293200
C	-3.23915100	-1.67692900	-0.70843200
C	-3.89158100	-2.25624600	0.46032000
C	-5.20392200	-2.00235400	0.71481700
C	-6.01664900	-1.20996200	-0.19058400
C	-5.52715700	-0.82857400	-1.38861900
H	-6.14135100	-0.26189600	-2.08407300
H	-7.02980700	-0.95264300	0.10605000
H	-5.67055300	-2.41123100	1.60788600
H	-2.60712700	-0.65930100	-0.27387900
H	-3.29294200	-2.83344100	1.15889800
H	-2.34635700	-2.19843100	-1.05419000
H	-3.67708100	-0.39290800	-2.37883900
H	-4.24004500	-2.04769200	-2.55599300

TS-XIIIb-antiCO

Route= #N b3lyp/gen pseudo=read gfprint
OPT=(TS,CalcFC,NoEigenTest) freq
RB3LYP Energy=-1555.90800179 Hartree
ZPE=0.323086 Hartree
Conditions=298K, 1.00000 atm
Internal Energy=-1555.555759 Hartree
Enthalpy=-1555.554815 Hartree

Rh	0.00000000	0.00000000	0.00000000
C	-1.96844600	0.54654900	0.44152100
C	-2.27515700	1.97535400	0.12076200
O	-2.61570600	2.17699800	-1.17155600
C	-2.70345500	3.55608100	-1.56969200
H	-3.45047500	4.08540700	-0.97228500
H	-2.99397700	3.53656900	-2.62044400

Free Energy=-1555.645836 Hartree
Entropy=191.570 cal/mol-K

H	-1.73228000	4.04068300	-1.44766700
O	-2.14870300	2.87681600	0.92708100
C	-2.56574900	-0.04894000	1.62884200
C	-3.40111900	0.56828000	2.48935900
H	-3.75151800	0.05651100	3.38227600
H	-3.69299100	1.60567400	2.36682300
H	-2.26530900	-1.07576600	1.82388700
O	-0.39005200	-0.79254700	-1.87552100
C	0.58693500	-1.25334400	-2.55086700
O	1.80199300	-1.31309200	-2.22797500
Rh	2.37253700	-0.57336800	-0.38153000
O	1.97443700	-2.40789100	0.48304300
C	0.80342500	-2.64167800	0.88445600
O	-0.22033300	-1.88623700	0.82981500
H	0.63269700	-3.62666600	1.34273200
O	2.60683700	1.29917300	-1.21267100
C	1.60151100	2.05866700	-1.26274700
O	0.41384700	1.82947600	-0.87017600
H	1.76384900	3.05187400	-1.70530900
O	2.79479000	0.20952800	1.47447700
C	1.83148300	0.66628500	2.15013200
O	0.60096200	0.71759700	1.83876100
H	2.07918000	1.07451700	3.13997900
H	0.32441800	-1.65001500	-3.54251900
C	-3.50937100	-0.69535300	-1.32182500
C	-3.33115300	-2.14751000	-1.12846200
C	-4.25486000	-2.90033200	-0.50856300
C	-5.55495300	-2.34825200	-0.00170200
C	-5.74375400	-0.89020400	-0.30043400
C	-4.81987200	-0.14739600	-0.93381000
H	-5.01081400	0.89782000	-1.15797600
H	-6.69721900	-0.44677600	-0.02054500
H	-5.63986500	-2.52397100	1.08399700
H	-6.39444000	-2.92297300	-0.42913400
H	-4.08666800	-3.96752400	-0.37932100
H	-2.40273900	-2.58179200	-1.48463800
H	-2.63383700	-0.17159800	-0.58384300
H	-3.09361500	-0.29695800	-2.25015600

TS-XIIIa-antiCO

Route= #N b3lyp/gen pseudo=read gfprint
OPT=(TS,CalcFC,NoEigenTest) freq
RB3LYP Energy=-1555.90872045 Hartree
ZPE=0.323341 Hartree

Rh	0.00000000	0.00000000	0.00000000
O	0.52696400	1.99585000	0.11819100
C	1.73675900	2.32682000	-0.08643000
O	2.71293700	1.58615300	-0.38391600

Conditions=298K, 1.00000 atm
Internal Energy=-1555.556513 Hartree
Enthalpy=-1555.555569 Hartree
Free Energy=-1555.644825 Hartree
Entropy=187.854 cal/mol-K

Rh	2.36369200	-0.43125500	-0.57935200
O	2.73285700	-0.68064700	1.43051900
C	1.76665700	-0.54556700	2.23184400
O	0.55215700	-0.27713000	1.97080900
H	1.99686600	-0.67799900	3.29850600
O	1.87701100	-2.43458000	-0.73593300
C	0.68920000	-2.78215700	-0.51259900
O	-0.30595700	-2.05006100	-0.19893400
H	0.47113900	-3.85693100	-0.59811300
O	1.84210100	-0.14825100	-2.55941000
C	0.63579600	0.09589200	-2.83029100
O	-0.34963100	0.20578600	-2.03216200
H	0.39347700	0.23129500	-3.89446700
H	1.95052500	3.40075500	0.00953900
C	-1.98061800	0.47966800	0.57337500
C	-2.27152800	1.94615100	0.45635200
O	-2.31871000	2.67317400	1.43034400
O	-2.40120300	2.38455800	-0.81199400
C	-2.48102600	3.81214900	-0.95865900
H	-3.33357000	4.21290100	-0.40366000
H	-2.59967500	3.98817900	-2.02815300
H	-1.56190800	4.27522000	-0.59232200
C	-2.66322500	-0.14201900	1.69479900
C	-2.54296500	-1.45200600	2.00492600
H	-3.10274800	-1.88052800	2.83243000
H	-1.86743500	-2.10151500	1.46115400
H	-3.32552500	0.48897800	2.28755000
H	-2.64029800	-0.06675600	-0.54680200
C	-3.46453700	-0.51666200	-1.39567900
C	-3.52063000	-1.94871600	-1.07817400
C	-4.61011000	-2.50995300	-0.51850600
C	-5.88105700	-1.75434000	-0.26823600
H	-6.71851500	-2.27241600	-0.76652900
C	-5.82849800	-0.32493900	-0.72274900
C	-4.73011700	0.22969600	-1.26016700
H	-4.73772000	1.26303500	-1.59252200
H	-6.74237700	0.25795700	-0.62903400
H	-6.14141800	-1.80006900	0.80229100
H	-4.60960200	-3.57140300	-0.27857700
H	-2.62461000	-2.53500900	-1.25468300
H	-2.84610200	-0.24844500	-2.25549000

2.28b

Route= #N B3LYP/6-31G(d) 5d OPT FREQ
RB3LYP Energy=-577.982507695 Hartree
ZPE=0.227565 Hartree
Conditions=298K, 1.00000 atm
Internal Energy=-577.741639 Hartree
Enthalpy=-577.740695 Hartree
Free Energy=-577.796155 Hartree
Entropy=116.726 cal/mol-K

C	0.00000000	0.00000000	0.00000000
C	1.18143200	-0.95412700	0.15994500
O	1.60157900	-1.38000400	1.21223300
O	1.72539900	-1.26999900	-1.04108500
C	2.86487600	-2.14342500	-0.99031500
H	3.67221900	-1.68681800	-0.41155200
H	3.16980800	-2.28840300	-2.02723100
H	2.59730700	-3.09888200	-0.53105700
C	0.49367600	1.31461100	-0.56064200
C	0.45600700	2.47695700	0.09220800
H	0.82747300	3.39403800	-0.35736500
H	0.05472900	2.55533100	1.10018400
H	0.90936900	1.26960500	-1.56706900
H	-0.39729300	0.15210600	1.00749600
C	-1.13162700	-0.63346400	-0.89372200
C	-2.33073500	0.28191900	-0.95103600
C	-3.55827900	-0.06915100	-0.55977800
C	-3.90786400	-1.43261400	-0.02825200
H	-4.32277500	-1.34518500	0.99012800
H	-4.73010300	-1.86694700	-0.62128000
C	-2.73103600	-2.36972600	-0.02516200
H	-2.91552900	-3.38963400	0.30885700
C	-1.50419100	-2.01721700	-0.41608500
H	-0.70589000	-2.75729000	-0.39859300
H	-4.36982700	0.65409000	-0.62687500
H	-2.15226100	1.28813400	-1.32352300
H	-0.69802700	-0.71773200	-1.90336000

2.28a

Route= #N B3LYP/6-31G(d) 5d OPT FREQ
RB3LYP Energy=-577.994949582 Hartree
ZPE=0.228493 Hartree
Conditions=298K, 1.00000 atm
Internal Energy=-577.753432 Hartree
Enthalpy=-577.752488 Hartree
Free Energy=-577.807663 Hartree
Entropy=116.125 cal/mol-K

C	0.00000000	0.00000000	0.00000000
O	-1.25739900	-0.67962500	-0.10882700
C	-2.34198800	0.12851400	-0.22030200
O	-2.26891700	1.34298900	-0.22698200
C	-3.58141000	-0.67180600	-0.32809500
C	-4.77411200	-0.07546200	-0.45998800
H	-4.78926800	1.01343500	-0.48390700
C	-6.08611900	-0.78702600	-0.57189700
H	-6.57218300	-0.50594800	-1.51701000
H	-5.92228100	-1.87229800	-0.59802900
C	-7.07978100	-0.45695600	0.58750400
C	-8.38273600	-1.27480400	0.44469800
C	-9.34247300	-0.67509900	-0.55638200

C	-9.37096900	0.65350400	-0.75538200
C	-8.44564700	1.53115400	-0.03218200
C	-7.38744900	1.02823800	0.62727800
H	-6.69385400	1.68714400	1.14440900
H	-8.62808900	2.60334800	-0.04706000
H	-10.0907920	1.10117000	-1.43656500
H	-10.0451030	-1.33168200	-1.06452400
H	-8.14272000	-2.31284000	0.18176400
H	-8.88717900	-1.31993400	1.42454000
H	-6.59044600	-0.75173800	1.52420000
H	-3.47502600	-1.75310300	-0.30101600
H	0.18207800	0.61928400	-0.88296200
H	0.75318200	-0.78501900	0.07885100
H	0.01812800	0.63981000	0.88692400

2.26a

Route= #N B3LYP/6-31G(d) 5d OPT FREQ
RB3LYP Energy=-577.993932612 Hartree
ZPE=0.228308 Hartree
Conditions=298K, 1.00000 atm
Internal Energy=-577.752500 Hartree
Enthalpy=-577.751556 Hartree
Free Energy=-577.807300 Hartree
Entropy=117.322 cal/mol-K

C	0.00000000	0.00000000	0.00000000
O	-1.24938400	-0.69139200	0.12915000
C	-2.30887500	0.08878100	0.45888300
O	-2.22324800	1.28943200	0.63518900
C	-3.54233200	-0.72224200	0.56632300
C	-4.71089800	-0.15301000	0.89093300
H	-4.70748500	0.92110100	1.07133500
C	-6.01606300	-0.87817400	1.01581100
H	-6.45731500	-0.67402300	2.00095300
H	-5.84750800	-1.96068500	0.95179000
C	-7.07316400	-0.47467900	-0.06852700
C	-8.28914600	-1.36143300	0.05424700
C	-9.52269500	-0.91333300	0.29886800
H	-10.3459110	-1.62111200	0.38514200
C	-9.86112300	0.54504200	0.45483400
H	-10.3008250	0.72522700	1.45049000
H	-10.6624360	0.82085700	-0.25076900
C	-8.66964300	1.44090800	0.24740800
H	-8.85006300	2.51406300	0.28972000
C	-7.43638700	0.98911400	0.00495000
H	-6.62945100	1.70208600	-0.15395300
H	-8.11572000	-2.43205600	-0.05217300
H	-6.59219200	-0.66872200	-1.04200500
H	-3.45086900	-1.78841500	0.37619500
H	0.27267600	0.48389900	0.94218600
H	-0.05949700	0.76239100	-0.78195000
H	0.73281800	-0.76332100	-0.26447500

C-H insertion product 2.26

Route= #N B3LYP/6-31G(d) 5d OPT FREQ
RB3LYP Energy=-577.983390571 Hartree
ZPE=0.227913 Hartree
Conditions=298K, 1.00000 atm
Internal Energy=-577.742288 Hartree
Enthalpy=-577.741344 Hartree
Free Energy=-577.796333 Hartree
Entropy=115.735 cal/mol-K

C	0.00000000	0.00000000	0.00000000
C	1.27243000	-0.81855000	0.19544600
O	1.55346700	-1.45219000	1.18929900
O	2.06435200	-0.77373800	-0.90329500
C	3.28827200	-1.51973900	-0.81232100
H	3.90141500	-1.15187700	0.01464800
H	3.79672400	-1.36681500	-1.76486700
H	3.08090900	-2.58154600	-0.65349000
C	0.34431300	1.42923700	-0.34989000
C	0.00473200	2.48739100	0.38699100
H	0.27319400	3.49773400	0.08962200
H	-0.55576300	2.38408000	1.31344400
H	0.91076700	1.56751600	-1.27021000
H	-0.52612400	-0.03052400	0.95840400
C	-0.91674800	-0.66909800	-1.09021800
C	-2.18486000	0.14527500	-1.25249500
C	-3.30077000	-0.16779100	-0.57121500
C	-3.34646400	-1.33632600	0.31196500
H	-4.18279700	-1.44043900	0.99912000
C	-2.37777200	-2.26532700	0.25507100
H	-2.40775400	-3.14725700	0.89032400
C	-1.26114000	-2.13864400	-0.75404800
H	-0.37058700	-2.67614100	-0.40947600
H	-1.57700700	-2.64084900	-1.68377600
H	-4.18794100	0.45633300	-0.65357500
H	-2.14727400	1.03575500	-1.87384000
H	-0.34950900	-0.65608700	-2.02833100

2.27b

Route= #N B3LYP/6-31G(d) 5d OPT FREQ
B3LYP Energy=-579.212012729 Hartree
ZPE=0.251971 Hartree
Conditions=298K, 1.00000 atm
Internal Energy=-578.946502 Hartree
Enthalpy=-578.945558 Hartree
Free Energy=-579.001256 Hartree
Entropy=117.227 cal/mol-K

C	0.00000000	0.00000000	0.00000000
C	1.21666400	-0.91088000	0.14114300
O	1.53368800	-1.50579400	1.14801100
O	1.91318300	-0.98961700	-1.01803200
C	3.07907400	-1.82755500	-0.98181300
H	3.78497000	-1.47070500	-0.22717800
H	3.51720800	-1.76374500	-1.97843700
H	2.80363200	-2.85976800	-0.74872300
C	0.44276800	1.38823700	-0.40398600
C	0.30151500	2.47693800	0.35283000
H	0.63980200	3.45269800	0.01430100
H	-0.15777800	2.43557400	1.33813100
H	0.91448100	1.46584300	-1.38317400

H	-0.45568700	0.04053300	0.99362300
C	-1.03076100	-0.61290000	-1.01322100
C	-2.23693500	0.28837300	-1.16277700
C	-3.46768200	-0.03104700	-0.74741800
C	-3.81262100	-1.32137800	-0.04752400
H	-4.48748000	-1.11819800	0.79552300
H	-4.38736600	-1.96406900	-0.73404200
C	-2.55774100	-2.06050600	0.43933000
H	-2.80621400	-3.09255200	0.71415900
H	-2.18066200	-1.57847100	1.35076100
C	-1.46414400	-2.04818000	-0.63833000
H	-0.60239400	-2.64013700	-0.30900600
H	-1.85125100	-2.53613800	-1.54321700
H	-4.28421600	0.66922600	-0.92180700
H	-2.06926000	1.25106900	-1.64129700
H	-0.51177200	-0.65341700	-1.98122800

2.27a

Route= #N B3LYP/6-31G(d) 5d OPT freq
B3LYP Energy=-579.223342482 Hartree
ZPE=0.252753 Hartree
Conditions=298K, 1.00000 atm
Internal Energy=-578.957255 Hartree
Enthalpy=-578.956310 Hartree
Free Energy=-579.012074 Hartree
Entropy=117.365 cal/mol-K

C	0.00000000	0.00000000	0.00000000
O	1.24718900	-0.70560100	-0.04092600
C	2.32929300	0.05296500	-0.34888100
C	3.55790500	-0.77140700	-0.36504300
C	4.74666500	-0.22625400	-0.65624600
C	6.04781600	-0.96785000	-0.69414000
H	5.86520700	-2.04382900	-0.57786100
H	6.51021200	-0.81971100	-1.68055700
H	4.76615000	0.83987100	-0.87829300
O	2.26302700	1.24646500	-0.57537600
H	0.02785700	0.79051900	0.75539100
H	-0.75266400	-0.74698400	0.25542600
H	-0.22088700	0.45078000	-0.97173500
C	8.54991300	1.47226500	-0.04206500
H	3.44653700	-1.82814400	-0.13667300
C	7.36962300	0.96473000	0.33119100
H	6.56922800	1.64318600	0.62273400
C	7.06737700	-0.51704100	0.39827500
H	6.58464400	-0.71866000	1.36602900
C	8.36912200	-1.34469000	0.32564500
H	8.87144900	-1.29256100	1.30120600
H	8.13206200	-2.40190100	0.15028400
C	9.32738300	-0.82064000	-0.75343900
H	10.2185470	-1.45717700	-0.81233500
H	8.84124200	-0.87477900	-1.73672000
C	9.72951800	0.63407800	-0.46766600

H	10.4981430	0.66546000	0.32138000
H	10.2028530	1.07955000	-1.35360200
H	8.69052200	2.55274800	-0.03429800

Cope TS from cyclohexene system

Route= #N b3lyp/gen pseudo=read gfprint
OPT=(TS,CalcFC,NoEigenTest) freq
RB3LYP Energy=-1557.15496858 Hartree
ZPE=0.353179 Hartree
Conditions=298K, 1.00000 atm
Internal Energy=-1556.773136 Hartree
Enthalpy=-1556.772192 Hartree
Free Energy=-1556.862182 Hartree
Entropy=189.399 cal/mol-K

Rh	0.00000000	0.00000000	0.00000000
O	0.16978500	2.02746200	0.36412500
C	-0.86066800	2.66662600	0.73265100
O	-2.03268200	2.22080300	0.90658800
Rh	-2.34245300	0.22339800	0.57551600
O	-2.71954100	0.61149600	-1.40732800
C	-1.74200800	0.61402900	-2.21107200
O	-0.51721300	0.40121600	-1.95489100
H	-1.98057400	0.82612400	-3.26199400
O	-2.58427400	-1.78425900	0.22904700
C	-1.56597100	-2.44246200	-0.13065300
O	-0.38499800	-2.01671600	-0.31158900
H	-1.72095900	-3.51531900	-0.30901900
O	-1.83310100	-0.17553600	2.52842100
C	-0.61502800	-0.39599900	2.79041300
O	0.36863000	-0.40393900	1.98787700
H	-0.37606700	-0.60764500	3.84121600
H	-0.71697200	3.73849600	0.92362700
C	3.11016200	0.81959700	0.51355700
C	3.36742700	2.26202600	0.68111800
O	3.64433500	2.78527000	1.74635100
O	3.31735000	2.94967200	-0.48847300
C	3.54078300	4.35977100	-0.37414200
H	2.78005700	4.82042600	0.26252700
H	3.47531900	4.75121100	-1.39014400
H	4.52673400	4.56326900	0.05351200
C	2.47300500	0.27223800	-0.60822100
C	2.37391800	-1.11740100	-0.81834700
H	1.93799400	-1.48211900	-1.74262000
H	2.28685900	-1.79239000	0.02425400
H	2.36415200	0.91944400	-1.47538100
H	3.83999400	-3.54713100	0.10139400
C	4.63120700	-2.78803700	0.13621700
H	5.57699200	-3.33731500	0.00521100
C	4.50328900	-1.82424600	-1.02819500
H	4.36842500	-2.27108300	-2.01075200
C	5.12689900	-0.57810700	-0.94737200
H	5.19328400	0.03054300	-1.84754700
C	5.35239800	0.03083700	0.27928000

C	5.48226700	-0.80251600	1.53461900
C	4.62570900	-2.08269100	1.50669600
H	4.97230400	-2.77717800	2.28065500
H	3.59401600	-1.82730500	1.77367600
H	5.23962000	-0.20119500	2.41888900
H	6.54649500	-1.06889400	1.63859600
H	5.81692700	1.01348100	0.30023700
H	3.08366500	0.28725100	1.45633500

TS-XIVb-antiCO

Route= #N b3lyp/gen pseudo=read gfprint
OPT=(TS,CalcFC,NoEigenTest) freq
RB3LYP Energy=-1555.94110689 Hartree
ZPE=0.330546 Hartree
Conditions=298K, 1.00000 atm
Internal Energy=-1555.582880 Hartree
Enthalpy=-1555.581935 Hartree
Free Energy=-1555.669138 Hartree
Entropy=183.533 cal/mol-K

Rh	0.00000000	0.00000000	0.00000000
C	3.04276800	0.75238800	0.65332200
C	3.03623000	2.05140400	-0.10795300
O	2.96744300	3.09773200	0.74010300
C	2.92922100	4.39157300	0.11778900
H	3.80887200	4.54278800	-0.51380100
H	2.91540700	5.10995600	0.93786400
H	2.02825300	4.48615300	-0.49336500
O	3.14065200	2.17343300	-1.31374600
C	2.32943100	-0.38941400	0.12175100
C	2.63494500	-0.81982100	-1.21373400
H	2.16982200	-1.75084200	-1.53734600
H	2.62470500	-0.05346800	-1.98299500
H	2.17981900	-1.18057700	0.85316400
O	-0.00753500	-0.04292600	2.07324200
C	-1.12890300	0.00982300	2.66521100
O	-2.28236700	0.08689500	2.15313200
Rh	-2.43340600	0.14203000	0.10043600
O	-2.47864600	-1.92244000	0.05368000
C	-1.37884200	-2.54096900	-0.00085900
O	-0.20506800	-2.05648100	-0.03571900
H	-1.44047300	-3.63815100	-0.02064800
O	-2.25177100	2.18858300	0.14609000
C	-1.08775600	2.68119800	0.10582300
O	0.02347500	2.07304400	0.04082800
H	-1.02932600	3.77857700	0.13028000
O	-2.44725200	0.19416400	-1.96054700
C	-1.33575400	0.14212300	-2.56124900
O	-0.17371000	0.05445400	-2.05953500
H	-1.37788000	0.17620400	-3.65888200
H	-1.08882100	-0.01537900	3.76330000
C	4.86064500	0.24872400	0.58910300
C	4.97545200	-0.89121100	1.54889000
C	4.84861500	-2.15963400	1.14386100

C	4.58683700	-2.53467000	-0.29133100
C	4.45582700	-1.31857100	-1.21728200
C	5.02012100	-0.10017100	-0.78475500
H	5.25571100	0.67149700	-1.51029700
H	4.58808100	-1.55795400	-2.27309500
H	3.68886400	-3.16374600	-0.35802100
H	5.41148900	-3.16872300	-0.65537500
H	4.95303200	-2.97534000	1.85637600
H	5.16252200	-0.65480400	2.59367000
H	2.88773500	0.92235200	1.71802800
H	5.35711800	1.16445500	0.91167300

TS-XIVb

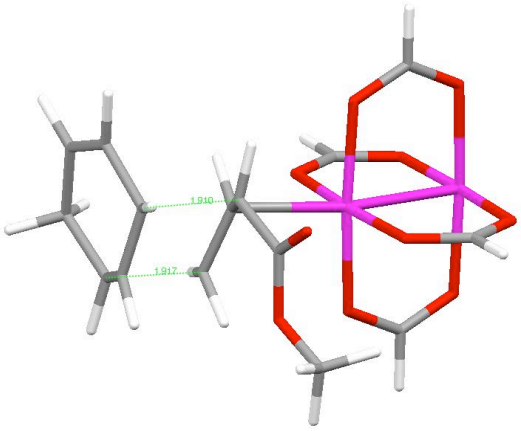

Route= #N b3lyp/gen pseudo=read gfprint OPT=(TS,CalcFC,NoEigenTest) freq
RB3LYP Energy=-1555.93782374 Hartree
ZPE=0.330323 Hartree
Conditions=298K, 1.00000 atm
Internal Energy=-1555.579701 Hartree
Enthalpy=-1555.578757 Hartree
Free Energy=-1555.665944 Hartree
Entropy=183.501 cal/mol-K

Rh	0.00000000	0.00000000	0.00000000
C	2.99477700	0.63286900	0.92571400
C	2.96398200	2.10873600	0.62646000
O	2.91029900	2.40175600	-0.69249500
C	2.80056500	3.80018800	-1.00362400
H	1.88136700	4.20556200	-0.57488300
H	2.77221600	3.85534800	-2.09226500
H	3.65759600	4.35220400	-0.60896100
O	3.03766400	2.95663900	1.49145200
C	2.34061100	-0.37488600	0.12069300
C	2.67476200	-0.50156100	-1.26632200
H	2.26333000	-1.36547100	-1.78745300
H	2.64820000	0.40090100	-1.86735500
H	2.19904600	-1.31369500	0.65222900
O	-0.02939100	-0.40656000	2.02812700
C	-1.15483200	-0.45569300	2.61252400
O	-2.30372000	-0.28952300	2.11181300
Rh	-2.43466600	0.12035500	0.09995200
O	-2.47543800	-1.90056700	-0.30587700
C	-1.37435200	-2.50094700	-0.45966300
O	-0.20088100	-2.01853700	-0.40060800
H	-1.43575500	-3.57753500	-0.67186700
O	-2.25493100	2.12648400	0.51113600
C	-1.09098300	2.61634600	0.57507000
O	0.01966300	2.02714300	0.40281000
H	-1.02979400	3.68852600	0.80772400
O	-2.43009400	0.52700900	-1.91912800
C	-1.31505100	0.58374200	-2.51189000
O	-0.15505200	0.41796900	-2.02452700
H	-1.35174400	0.80469900	-3.58802000
H	-1.12281200	-0.67069800	3.68964400
C	4.85229000	0.20833800	0.78870200

C	4.98297600	-1.11469700	1.46755300
C	4.91752300	-2.26128500	0.78171200
C	4.70867800	-2.30737600	-0.70953700
C	4.54534600	-0.91797100	-1.33641900
C	5.04278800	0.18893200	-0.62242300
H	5.25223800	1.11659000	-1.14654700
H	4.69571700	-0.90330100	-2.41641300
H	3.84380800	-2.94071700	-0.94916800
H	5.57083300	-2.80718800	-1.18064400
H	5.03496100	-3.21394200	1.29403800
H	5.13079300	-1.11594300	2.54479300
H	2.84027200	0.51578500	1.99752500
H	5.29025200	1.04693000	1.32917200

TS-XIVa

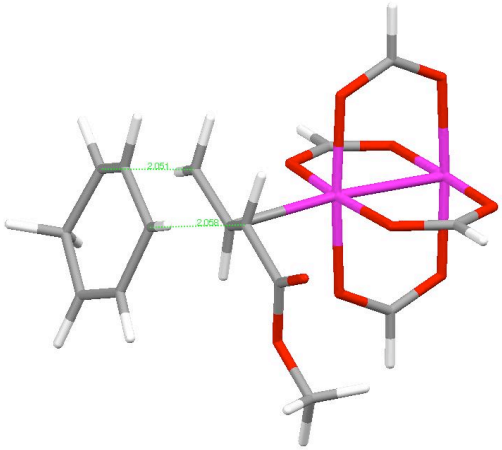

Route= #N b3lyp/gen pseudo=read gfprint OPT=(TS,CalcFC,NoEigenTest) freq
RB3LYP Energy=-1555.93970932 Hartree
ZPE=0.329726 Hartree
Conditions=298K, 1.00000 atm
Internal Energy=-1555.581840 Hartree
Enthalpy=-1555.580896 Hartree
Free Energy=-1555.670099 Hartree
Entropy=187.744 cal/mol-K

Rh	0.00000000	0.00000000	0.00000000
O	-0.20432000	1.87205800	-0.84934600
C	0.84010100	2.54442500	-1.10348900
O	2.04435100	2.22260100	-0.88883100
Rh	2.39968900	0.39291800	-0.02614200
O	2.21867100	1.23487800	1.84086900
C	1.06757600	1.26515300	2.36606400
O	-0.02703700	0.84493300	1.88251800
H	1.00596600	1.71141000	3.36817400
O	2.65833000	-1.45593200	0.83406800
C	1.62666600	-2.14278200	1.08239800
O	0.41386900	-1.84182500	0.86350300
H	1.79923900	-3.12433700	1.54530500
O	2.44678700	-0.47089500	-1.89453300
C	1.35828500	-0.87253900	-2.39611300
O	0.19581400	-0.82527200	-1.88692300
H	1.42261300	-1.31977100	-3.39759200
H	0.67403000	3.52633800	-1.56687300
C	-2.98828900	0.70543200	-0.85389600
C	-3.13782200	2.17053800	-0.61313800
O	-3.35278500	2.98051600	-1.49404000
O	-3.07154700	2.49513400	0.69663500
C	-3.18149800	3.89528400	0.98655500
H	-2.36168300	4.44588400	0.51726700
H	-3.12247300	3.97450400	2.07240700
H	-4.13159500	4.29418100	0.62031300
C	-2.45830800	-0.18736500	0.12367200
C	-2.42273100	-1.57070400	-0.18686700
H	-2.11073200	-2.26990300	0.58469400
H	-2.10589200	-1.86212700	-1.18430600

H	-2.56287300	0.10404200	1.16503200
H	-2.73870000	0.51502000	-1.89414000
C	-4.95745900	0.11815200	-0.96577000
C	-4.73362500	-1.22114400	-1.35537600
C	-4.37855900	-2.15595500	-0.37799100
C	-4.98053900	-2.03182700	1.01725800
H	-5.80340300	-2.76131900	1.11244200
C	-5.50748900	-0.65072500	1.30701500
C	-5.50100100	0.33079500	0.39519000
H	-5.88917500	1.31551600	0.64081400
H	-5.92742100	-0.47764400	2.29563100
H	-4.25127800	-2.32883200	1.78322100
H	-4.18916600	-3.17782700	-0.70445700
H	-4.53809900	-1.44186700	-2.40277200
H	-5.25971400	0.83054200	-1.72982800

2.4.4 Single Point Energy Calculations

Energies calculated for all geometries from Section 2.2.1 at the B3LYP/6-311G(2d,2p)[Rh-RSC+4f]//B3LYP/6-31G*[Rh-RSC+4f] level are given in Table 2.4.

Table 2.4: Single point energy calculations.

Structure	***B3LYP-energy [Hartree]***
Cyclopentane	-196.619472
1,4-cyclohexadiene	-233.490696
Methyl diazoacetate **2.3b**	-376.740506
Acceptor cyclopropane	-576.997396
Acceptor insertion product w/ 1,4-cyclohexadiene	-500.760267
Donor/acceptor insertion prod. w/ cyclopentane	-694.9998181
Acceptor insertion prod. w/ cyclopentane	-463.8902585
Methyl vinyldiazoacetate **2.3a**	-454.1667521
Donor/acceptor intermediate **2.23c**	-1710.058432
Donor/acceptor insertion TS w/ cyclopentane **TS-VIIc**	-1673.142644
Acceptor insertion TS w/ cyclopentane **TS-VIIb**	-1442.028017
Donor/acceptor insertion TS w/ 1,4-cyclohexadiene **TS-VIIIc**	-1478.902962
Acceptor nitrogen extrusion TS **TS-Ib**	-1354.962576
Acceptor carbenoid complex **2.5b**	-1245.414133
Acceptor diazo - catalyst complex **2.4b**	-1354.981612
Methyl vinyldiazo – catalyst complex **2.18**	-1432.402602
Methyl vinylcarbenoid cyclopropanation TS **TS-VI**	-1632.588418
Methyl vinylcarbenoid complex **2.19**	-1322.854049
Metyl vinyldiazo nitrogen extrusion TS **TS-V**	-1432.3818
Acceptor insertion TS w/ 1,4-cyclohexadiene **TS-VIIIb**	-1478.902962
Donor/acceptor insertion prod. w/ 1,4-cyclohexadiene	-731.869417

Dirhodium tetraformate	-978.2240015
Phenyldiazoacetate – rhodium complex **2.4c**	-1586.095607
Phenylcarbenoid cyclopropanation TS **TS-IIc**	-1786.28283
Phenylcarbenoid complex **2.5c**	-1476.55083
Phenyldiazo nitrogen extrusion TS **TS-IIc**	-1586.077571
Donor/acceptor insertion TS w/ 1,4-cyclohexadiene **TS-VIIIc**	-1710.031573
Donor/acceptor cyclopropane product	-808.1062574
Styrene	-309.7391593
Dinitrogen N_2	-109.5593531
Methyl phenyldiazoacetate **2.3c**	-607.8598475

References

(1) Doyle, M. P.; McKervey, M. A.; Ye, T. *Modern Catalytic Methods for Organic Synthesis with Diazo Compounds: From Cyclopropanes to Ylides*; John Wiley & Sons, Inc.: New York, 1998.

(2) Davies, H. M. L.; Manning, J. R. *Nature* **2008**, *451*, 417-424.

(3) Davies, H. M. L.; Loe, Ø. *Synthesis* **2004**, 2595-2608.

(4) Davies, H. M. L.; Beckwith, R. E. J. *Chem. Rev.* **2003**, *103*, 2861-2903.

(5) Davies, H. M. L.; Antoulinakis, E. G. *Org. Reacts.* **2001**, *57*, 1-326.

(6) Davies, H. M. L.; Panaro, S. A. *Tetrahedron* **2000**, *56*, 4871-4880.

(7) Davies, H. M. L.; Bruzinski, P. R.; Lake, D. H.; Kong, N.; Fall, M. J. *J. Am. Chem. Soc.* **1996**, *118*, 6897-6907.

(8) Davies, H. M. L.; Nagashima, T.; Klino, J. L. *Org. Lett.* **2000**, *2*, 823-826.

(9) Thompson, J. L.; Davies, H. M. L. *J. Am. Chem. Soc.* **2007**, *129*, 6090-6091.

(10) Davies, H. M. L.; Lee, G. H. *Org. Lett.* **2004**, *6*, 1233-1236.

(11) Davies, H. M. L.; Xiang, B. P.; Kong, N.; Stafford, D. G. *J. Am. Chem. Soc.* **2001**, *123*, 7461-7462.

(12) Olson, J. P.; Davies, H. M. L. *Org. Lett.* **2008**, *10*, 573-576.

(13) Reddy, R. P.; Davies, H. M. L. *J. Am. Chem. Soc.* **2007**, *129*, 10312-10313.

(14) Davies, H. M. L.; Hansen, T.; Churchill, M. R. *J. Am. Chem. Soc.* **2000**, *122*, 3063-3070.

(15) Hansen, J.; Autschbach, J.; Davies, H. M. L. *J. Org. Chem.* **2009**, *74*, 6555.

(16) Godula, K.; Sames, D. *Science* **2006**, *312*, 67-72.

(17) Bergman, R. G. *Nature* **2007**, *446*, 391-393.

(18) Davies, H. M. L.; Hansen, J. *In: Catalytic Asymmetric Synthesis 3rd ed.* (Ed. Ojima, I.), John Wiley & Sons, Hoboken, New Jersey, **2010**, p.163-226.

(19) Li, Z. J.; Davies, H. M. L. *J. Am. Chem. Soc.* **2010**, *132*, 396-401.

(20) Nagashima, T.; Davies, H. M. L. *J. Am. Chem. Soc.* **2001**, *123*, 2695-2696.

(21) Nagashima, T.; Davies, H. M. L. *Org. Lett.* **2002**, *4*, 1989-1992.

(22) Peddibhotla, S.; Dang, Y.; Liu, J. O.; Romo, D. *J. Am. Chem. Soc.* **2007**, *129*, 12222-12231.

(23) Antos, J. M.; Francis, M. B. *J. Am. Chem. Soc.* **2004**, *126*, 10256-10257.

(24) Antos, J. M.; McFarland, J. M.; Iavarone, A. T.; Francis, M. B. *J. Am. Chem. Soc.* **2009**, *131*, 6301-6308.

(25) Nowlan, D. T.; Gregg, T. M.; Davies, H. M. L.; Singleton, D. A. *J. Am. Chem. Soc.* **2003**, *125*, 15902-15911.

(26) Hansen, J.; Davies, H. M. L. *Coord. Chem. Rev.* **2008**, *252*, 545-555.

(27) Davies, H. M. L. *Eur. J. Org. Chem.* **1999**, 2459-2469.

(28) Davies, H. M. L. *J. Mol. Catal. A: Chem.* **2002**, *189*, 125-135.

(29) Davies, H. M. L.; Nikolai, J. *Org. Biomol. Chem.* **2005**, *3*, 4176-4187.

(30) Liang, Y.; Zhou, H. L.; Yu, Z. X. *J. Am. Chem. Soc.* **2009**, *131*, 17783-17785.

(31) Liu, Z. F.; Liu, J. Y. *Cent. Eur. J. Chem.*, *8*, 223-228.

(32) Nakamura, E.; Yoshikai, N.; Yamanaka, M. *J. Am. Chem. Soc.* **2002**, *124*, 7181-7192.

(33) Padwa, A.; Snyder, J. P.; Curtis, E. A.; Sheehan, S. M.; Worsencroft, K. J.; Kappe, C. O. *J. Am. Chem. Soc.* **2000**, *122*, 8155-8167.

(34) Taber, D. F.; Joshi, P. V. *J. Org. Chem.* **2004**, *69*, 4276-4278.

(35) Yoshikai, N.; Nakamura, E. *Adv. Synth. Catal.* **2003**, *345*, 1159-1171.

(36) Anciaux, A. J.; Hubert, A. J.; Noels, A. F.; Petiniot, N.; Teyssié, P. *J. Org. Chem.* **1980**, *45*, 695-702.

(37) Bonge, H. T.; Hansen, T. *J. Org. Chem.*, *75*, 2309-2320.

(38) Bonge, H. T.; Hansen, T. *Synthesis* **2009**, 91-96.

(39) Bonge, H. T.; Pintea, B.; Hansen, T. *Org. Biomol. Chem.* **2008**, *6*, 3670-3672.

(40) Briones, J. F.; Hansen, J.; Davies, H. M. L. **2010**, *Manuscript Submitted*.

(41) Dick, A. R.; Sanford, M. S. *Tetrahedron* **2006**, *62*, 2439-2463.

(42) Muller, P.; Maitrejean, E. *Collect. Czech. Chem. Commun.* **1999**, *64*, 1807-1826.

(43) Doyle, M. P.; Hu, W.; Valenzuela, M. V. *J. Org. Chem.* **2002**, *67*, 2954-2959.

(44) Muller, P.; Polleux, P. *Helv. Chim. Acta* **1994**, *77*, 645-654.

(45) Davies, H. M. L.; Grazini, M. V. A.; Aouad, E. *Org. Lett.* **2001**, *3*, 1475-1477.

(46) Davies, H. M. L.; Hansen, T. *J. Am. Chem. Soc.* **1997**, *119*, 9075-9076.

(47) Davies, H. M. L.; Jin, Q. *Tetrahedron Asym.* **2003**, *14*, 941-949.

(48) Davies, H. M. L.; Hansen, T.; Hopper, D. W.; Panaro, S. A. *J. Am. Chem. Soc.* **1999**, *121*, 6509-6510.

(49) Davies, H. M. L. *Personal Communication*.

(50) Nadeau, E.; Ventura, D. L.; Brekan, J. A.; Davies, H. M. L. *J. Org. Chem.*, *75*, 1927-1939.

(51) Dai, X.; Wan, Z.; Kerr, R. G.; Davies, H. M. L. *J. Org. Chem.* **2007**, *72*, 1895-1900.

(52) Davies, H. M. L.; Dal, X.; Long, M. S. *J. Am. Chem. Soc.* **2006**, *128*, 2485-2490.

(53) Davies, H. M. L.; Beckwith, R. E. J. *J. Org. Chem.* **2004**, *69*, 9241-9247.

(54) Davies, H. M. L.; Jin, Q. *J. Am. Chem. Soc.* **2004**, *126*, 10862-10863.

(55) Davies, H. M. L.; Jin, Q. *Proc. Natl. Acad. Sci. U. S. A.* **2004**, *101*, 5472-5475.

(56) Davies, H. M. L.; Jin, Q. *Org. Lett.* **2005**, *7*, 2293-2296.

(57) Davies, H. M. L.; Manning, J. R. *J. Am. Chem. Soc.* **2006**, *128*, 1060-1061.

(58) Churchill, M. R.; Churchill, D. G.; Ahmed, G.; Davies, H. M. L. *J. Chem. Crystallogr.* **1999**, *29*, 713-717.

(59) Davies, H. M. L.; Stafford, D. G.; Hansen, T.; Churchill, M. R.; Keil, K. M. *Tetrahedron Lett.* **2000**, *41*, 2035-2038.

(60) Davies, H. M. L.; Yang, J.; Manning, J. R. *Tetrahedron Asym.* **2006**, *17*, 665-673.

(61) Davies, H. M. L.; Walji, A. M. *Angew. Chem. Int. Ed.* **2005**, *44*, 1733-1735.

(62) Sheehan, S. M.; Padwa, A.; Snyder, P. *Tetrahedron Lett.* **1998**, *39*, 949-952.

(63) A. Bergner, M. D., W. Kuechle, H. Stoll, H. Preuss *Mol. Phys.* **1993**, *80*, 1431.

(64) M. Dolg, H. S., H. Preuss, R.M. Pitzer *J. Phys. Chem.* **1993**, *97*.

(65) M. Kaupp, P. v. R. S., H. Stoll, H. Preuss *J. Chem. Phys.* **1991**, *94*, 1360.

(66) Lam, W. H.; Lam, K. C.; Lin, Z.; Shimada, S.; Perutz, R. N.; Marder, T. B. *Dalton Trans.* **2004**, 1556 - 1562.

(67) Cotton, F. A.; Deboer, B. G.; Laprade, M. D.; Pipal, J. R.; Ucko, D. A. *Acta Cryst. B.* **1971**, *B 27*, 1664.

(68) Wong, F. M.; Wang, J. B.; Hengge, A. C.; Wu, W. M. *Org. Lett.* **2007**, *9*, 1663-1665.

(69) Yates, P. *J. Am. Chem. Soc.* **1952**, *74*, 5376-81.

(70) Pirrung, M. C.; Liu, H.; Morehead, A. T., Jr. *J. Am. Chem. Soc.* **2002**, *124*, 1014-1023.

(71) Muller, P.; Tohill, S. *Tetrahedron* **2000**, *56*, 1725-1731.

(72) Pelphrey, P.; Hansen, J.; Davies, H. M. L. *Chem. Sci.* **2010**, *Manuscript Accepted*.

(73) Bauernschmitt, R.; Ahlrichs, R. *J. Chem. Phys.* **1996**, *104*, 9047-9052.

(74) Seeger, R.; Pople, J. A. *J. Chem. Phys.* **1977**, *66*, 3045-3050.

(75) Clark, J. S.; Wong, Y.-S.; Townsend, R. J. *Tetrahedron Lett.* **2001**, *42*, 6187-6190.

(76) Davies, H. M. L.; Beckwith, R. E. J.; Antoulinakis, E. G.; Jin, Q. H. *J. Org. Chem.* **2003**, *68*, 6126-6132.

(77) Davies, H. M. L.; Antoulinakis, E. G. *Org. Lett.* **2000**, *2*, 4153-4156.

(78) Davies, H. M. L.; Venkataramani, C.; Hansen, T.; Hopper, D. W. *J. Am. Chem. Soc.* **2003**, *125*, 6462-6468.

(79) Davies, H. M. L.; Ren, P. D.; Jin, Q. H. *Org. Lett.* **2001**, *3*, 3587-3590.

(80) Davies, H. M. L.; Ren, P. D. *J. Am. Chem. Soc.* **2001**, *123*, 2070-2071.

(81) Davies, H. M. L.; Stafford, D. G.; Hansen, T. *Org. Lett.* **1999**, *1*, 233-236.

(82) Doyle, M. P.; Duffy, R.; Ratnikov, M.; Zhou, L. *Chem. Rev.*, *110*, 704-724.

(83) Hansen, J.; Gregg, T. M.; Ovalles, S.; Lian, Y.; Autschbach, J.; Davies, H. M. L. **2010**, *Manuscript in preparation*.

(84) Minami, K.; Saito, H.; Tsutsui, H.; Nambu, H.; Anada, M.; Hashimoto, S. *Adv. Synth. Catal.* **2005**, *347*, 1483-1487.

(85) Davies, H. M. L.; Hu, B. H.; Saikali, E.; Bruzinski, P. R. *J. Org. Chem.* **1994**, *59*, 4535-4541.

(86) Lian, Y.; Davies, H. M. L. *Org. Lett.*, *12*, 924-927.

(87) Fleming, I. *Frontier Orbitals and Organic Chemical Reactions*, 1976.

(88) Stafford, D. G. *Ph. D. Thesis* **2001**, University at Buffalo, The State University of New York.

(89) Ovalles, S. *M.A. Thesis* **2008**, University at Buffalo, The State University of New York.

(90) Carpenter, B. K. *in Reactive Intermediates Chemistry* **2004**, (Eds.: R.A. Moss, M. S. Platz, M. Jones Jr.), Wiley-Interscience, New York.

(91) Carpenter, B. K. *Angew. Chem. Int. Ed.* **1998**, *37*, 3341-3350.

(92) Hong, Y. J.; Tantillo, D. J. *Nature Chem.* **2009**, *1*, 384-389.

(93) Ess, D. H.; Wheeler, S. E.; Iafe, R. G.; Xu, L.; Celebi-Olcum, N.; Houk, K. N. *Angew. Chem. Int. Ed.* **2008**, *47*, 7592-7601.

(94) Carpenter, B. K. *Acc. Chem. Res.* **1992**, *25*, 520-528.

(95) Celebi-Olcum, N.; Ess, D. H.; Aviyente, V.; Houk, K. N. *J. Org. Chem.* **2008**, *73*, 7472-7480.

(96) Celebi-Olcum, N.; Ess, D. H.; Aviyente, V.; Houk, K. N. *J. Am. Chem. Soc.* **2007**, *129*, 4528.

(97) Thomas, J. B.; Waas, J. R.; Harmata, M.; Singleton, D. A. *J. Am. Chem. Soc.* **2008**, *130*, 14544-14555.

- Chapter 3 -

Influence of Ru(I)- and Ag(I)-Catalysts on The Vinylogous *versus* Carbenoid Reactivity of Transient Metallovinylcarbenoids

3.1 Introduction

A number of powerful synthetic methods have been developed based on rhodium-catalyzed reactions of vinyldiazoacetates. The transient rhodium vinylcarbenoid generated in the process can undergo highly selective transformations. Examples include cyclopropanation reactions,[1-3] [3+2] cycloadditions[4,5] and C–H functionalization processes.[3,6-10] They all involve initial nucleophilic attack at the carbenoid center, however, such conjugated electrophilic systems are also capable of exhibiting competing electrophilic reactivity at the terminal site, analogous to in allyl cation systems (Scheme 3.1).[11-14] Although commonly observed for Fischer vinylcarbenes,[15-18] this mode of reactivity has not been developed extensively for transient metallovinylcarbenoids.

Scheme 3.1: Vinylogous reactivity in metallovinylcarbenoids.

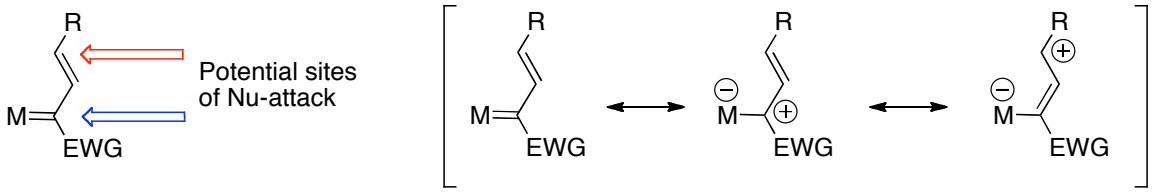

Very active catalysts are required when using vinyldiazoacetates in synthesis, particularly since competing 6π-electrocyclization to form pyrazoles is a very favorable

process.[19] Dirhodium(II) tetracarboxylates have been found to be optimal catalysts for this chemistry and have subsequently been used in all new synthetic methods based on vinyldiazoacetates.[9] Davies and co-workers discovered that vinylcarbenoids unsubstituted on the vinyl moiety were particularly prone to exhibit electrophilic reactivity at the terminal site.[12,13] Catalytic decomposition of unsubstituted vinyldiazoacetates **3.1** by various Rh(II)-carboxylates in the presence of cyclopentadiene, led to the expected product **3.2** of a tandem cyclopropanation/Cope rearrangement sequence.[13] Product **3.3** was also observed, and was thought to arise from initial nucleophilic attack at the vinyl terminus. Upon using dichloromethane as solvent, a small shift towards vinylogous reactivity was observed.[13] A major influence on the reaction pathway, however, came from the bulkiness of the ester group R and the electrophilicity of the rhodium catalyst employed. The BHT-ester gave exclusive vinylogous reactivity, whereas the methyl ester gave virtually only carbenoid reactivity in pentane when catalyzed by electron-rich Rh(II)-complexes.[13]

Scheme 3.2: Vinylogous reactivity in reaction with cyclopentadiene.[13]

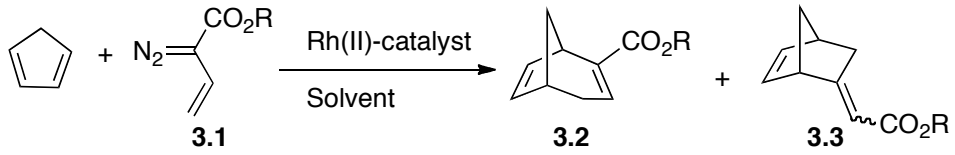

Table 3.1: Vinylogous reactivity in reaction with cyclopentadiene.[13]

Catalyst	*R =*	*Solvent*	*Ratio* (**3.2** : **3.3**)	*Yield* (%)[a]
$Rh_2(OAc)_4$	Me	CH_2Cl_2	67:33	81
$Rh_2(OAc)_4$	t-Bu	CH_2Cl_2	52:48	92
$Rh_2(OAc)_4$	BHT[b]	CH_2Cl_2	0:100	56
$Rh_2(OPiv)_4$	Me	Pentane	98:2	86
$Rh_2(OPiv)_4$	Me	CH_2Cl_2	90:10	86
$Rh_2(TFA)_4$	Me	CH_2Cl_2	32:68	60

[a] Combined yield
[b] 2,6-di(*t*-Bu)-4-MePh

The reaction is considered to proceed by initial nucleophilic attack at the vinylogous site of **3.4** to form zwitterionic intermediate **3.5** (Scheme 3.3). This intermediate then cyclizes to form a secondary metallocarbenoid intermediate **3.6**, which then undergoes a [1,2]-hydride shift and elimination to form **3.3**. The dependence of the isomer ratio of **3.3** on catalyst structure, supports the existence of the second carbenoid intermediate **3.6**.[13]

Scheme 3.3: Proposed reaction mechanism.[13]

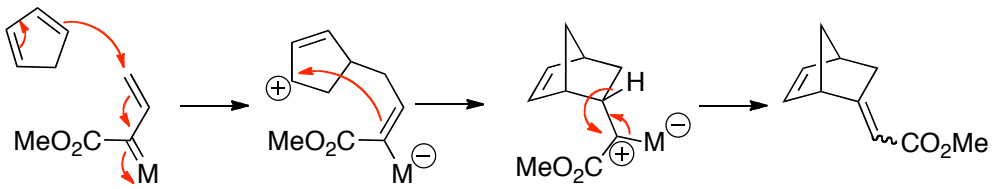

3.4 **3.5** **3.6** **3.3**

The reaction between *N*-carbomethoxypyrrole and vinyldiazoacetate **3.1** resulted in two products, **3.7** and **3.8** (Scheme 3.4), derived from a tandem cyclopropanation/Cope rearrangement and from vinylogous reactivity respectively.[12,13] The distribution of these products was dependent on the nature of the catalyst, the solvent and the size of the ester group R. A more polar solvent and electron deficient catalyst favored reaction at the

terminal site. The only solution available for the dirhodium(II) tetracarboxylates, in terms of controlling regioselectivity, was to increase the size of the ester group to make vinylogous addition the kinetically preferred pathway.[12,13,20]

Scheme 3.4: Carbenoid *versus* vinylogous reactivity.[20]

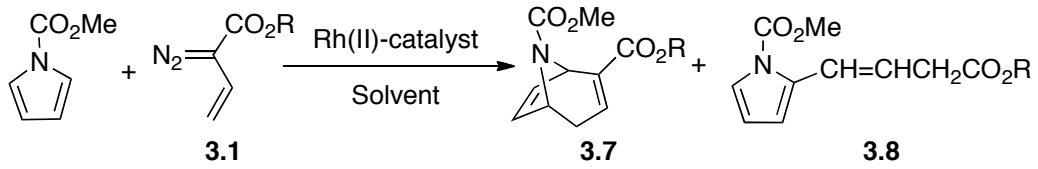

3.1 **3.7** **3.8**

Table 3.2: Influence of ester group and solvent on vinylogous reactivity with pyrroles.

R=	*Catalyst/Solvent*	*Ratio* (**3.7** : **3.8**)
Me	$Rh_2(OAc)_4/CH_2Cl_2$	55 : 45
Me	$Rh_2(OHex)_4/CH_2Cl_2$	15 : 85
Me	$Rh_2(OHex)_4$/hexane	>95 : 5
2,6-di-tBu-4-MeC_6H_2	$Rh_2(OAc)_4/CH_2Cl_2$	<5 : 95

Enhancement of reactivity at the terminal position could possibly be achieved by using other metal complexes that are inherently more electrophilic than the previously studied dirhodium tetracarboxylates. Yokota and Davies carried out preliminary studies on *in situ* generated dimolybdenum complexes (Scheme 3.5),[11] and showed that vinylogous reactivity could be achieved, even with vinylcarbenoids substituted at the terminal position. However, this system was only applicable to O–H insertion reactions. Furthermore, the actual structure of the *in situ* generated complex remains uncertain because of its instability.[11]

Scheme 3.5: Vinylogous reactivity in O–H insertion.[11]

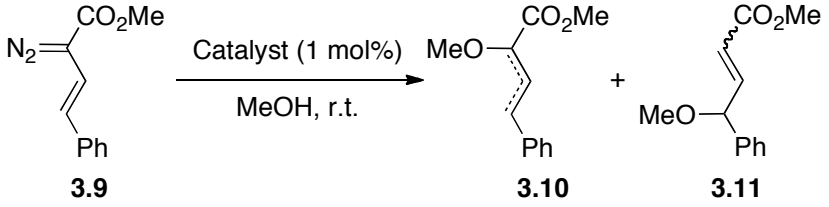

Table 3.3: Influence of catalyst on regioselectivity.[11]

Catalyst	*Ratio* (**3.10** : **3.11**)
Rh_2(S-TBSP)$_4$	>95 : 5
$Rh_2(OAc)_4$	>95 : 5
$Mo(CO)_6$/S-TBSP-H	50 : 50

Hu and co-workers described the use of mononuclear Lewis acids to control the regioselectivity of nucleophilic attack in X–H insertion chemistry (Scheme 3.6, Table 3.4).[14] Ag(I)– and Sn(II)–catalyzed reactions were reported to afford complete regiocontrol towards the 4-position in O–H insertions between benzyl alcohol and methyl phenylvinyldiazoacetate **3.9**. These reactions were, however, proposed to proceed by a Lewis acid catalyzed process of the diazoacetate, and not *via* metallocarbenoid intermediates.[14] $Cu(OTf)_2$ was also shown to give reasonable levels of 4-substitution if the substrates were benzylthiol or aniline.[14]

Scheme 3.6. Lewis acid catalyzed O–H insertions.[14]

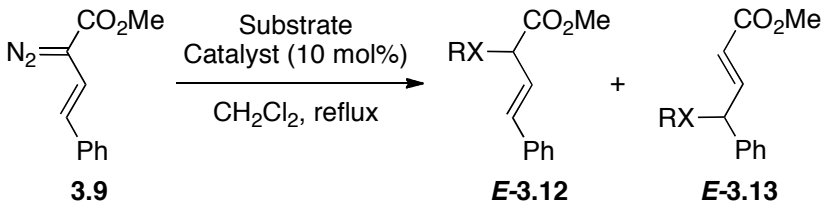

Table 3.4: Lewis-acid catalyzed X–H insertion reported by Hu et. al.[14]

Substrate	*Catalyst*	*Ratio* (***E*-3.12** : ***E*-3.13**)	*Yield* (%)[a]
$PhCH_2OH$	$AgBF_4$	2 : >98	67
	$AgClO_4$	2 : >98	71
	AgOTf	2 : >98	63
	$Sn(OTf)_2$	2 : >98	63
$PhCH_2SH$	$Cu(OTf)_2$	22 : 78	68
$PhNH_2$	AgOTf	35 : 65	66
	$Cu(OTf)_2$	15 : 85	72

[a] Overall yield.

A significant contribution to the development and understanding of vinylogous reactivity in transient metallovinylcarbenoids, was reported recently by Davies et. al. for a C–C bond forming process (Scheme 3.7).[21] It was found that the unusual *Z*-vinyldiazoacetate **3.15** could undergo selective vinylogous alkylation with sterically hindered pyrroles and indoles **3.14a-e**, catalyzed by a bidendate dirhodium(II) carboxylate complex, $Rh_2(esp)_2$.[21] A variety of substituted pyrroles and indoles **3.16a-e** were produced in good yields (Chart 3.1). The study also suggested that, for rhodium vinylcarbenoids, an s-*trans* conformation of the intermediate carbenoid could enhance vinylogous reactivity. Less hindered pyrroles and indoles gave clean carbenoid reactivity under the same reaction conditions.[21]

Scheme 3.7: Vinylogous alkylation of sterically hindered pyrroles and indoles.[21]

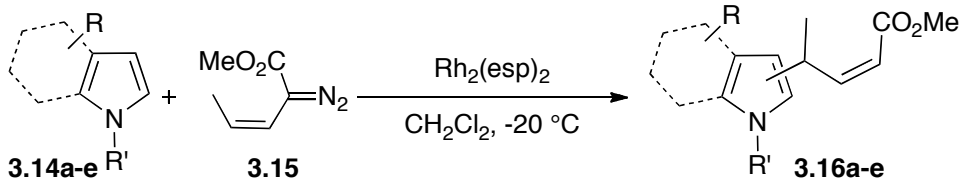

Chart 3.1: Vinylogous alkylation.[21]

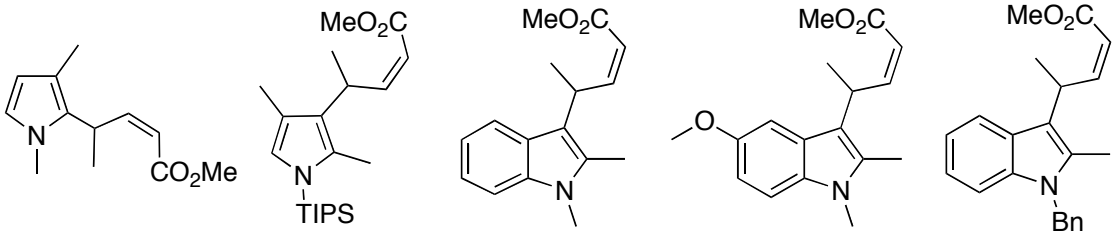

3.16a 75% yield | **3.16b** 87% yield | **3.16c** 90% yield | **3.16d** 92% yield | **3.16e** 91% yield

In this chapter, the influence of a novel family of electron-deficient diruthenium(I) carbonyl carboxylate complexes on the reactivity of the corresponding carbenoids has been studied. The catalytic activity has been evaluated in cyclopropanation reactions and O–H insertions. The ability of these catalysts to enhance vinylogous reactivity in O–H insertions and C–C bond forming reactions will be highlighted. Recent results also indicate that Ag(I)-salts can be effective in enhancing vinylogous reactivity. The scope of this chemistry has been investigated, as well as its possible application to vinylogous C–C bond forming reactions. Mechanistic studies of the O–H insertion chemistry have been conducted to evaluate viable reaction pathways involved in these transformations.

3.2 Results And Discussion

3.2.1 Electron-Deficient Ru(I) Carbonyl Carboxylates

Catalyst complexes. Diruthenium(I,I) carbonyl carboxylates of formula $[Ru_2(\mu_2\text{-}O_2CR)_2(CO)_4L_2]$ and polymeric compounds $[Ru_2(\mu_2\text{-}O_2CR)_2(CO)_4]$ have been developed for intra –and intermolecular reaction of diazoacetates and diazoacetamides by Maas and co-workers.[22-29] The complexes are often air stable, and, display roughly similar reactivity profiles to Rh(II)-dimers. A family of highly electrophilic diruthenium(I) carbonyl carboxylates of general formula $[Ru_2(\mu_2\text{-}O_2CR)_2(CO)_n]$: n = 5, R = CF_3 (**I**), $(2,4\text{-}CF_3)_2C_6H_3$ (**II**), $(3,5\text{-}CF_3)_2C_6H_3$ (**III**), $(2,3,4\text{-}F)_3C_6H_2$ (**IV**), $(2,4,6\text{-}F)_3C_6H_2$ (**V**), C_6F_5 (**VI**); n = 4, R = CF_3 (**VII**), $(3,5\text{-}CF_3)_2C_6H_3$ (**VIII**), were prepared by Petrukhina and co-workers (Figure 3.1).[30,31] These complexes were considered to be attractive catalysts for the possible enhancement of vinylogous reactivity in vinylcarbenoids due to their high electrophilicity profiles, and were consequently investigated for this purpose.

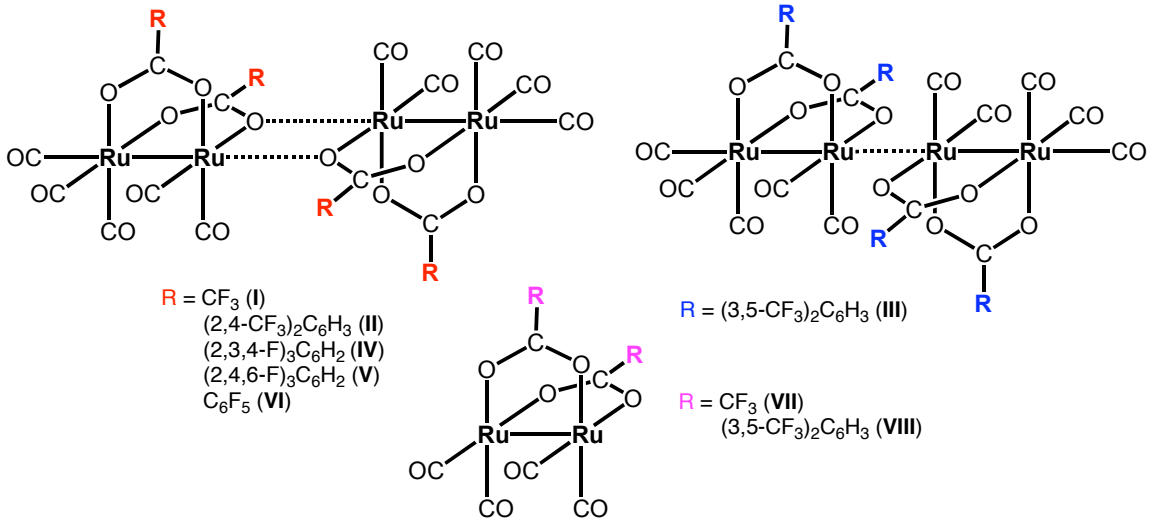

Figure 3.1: Electrophilic diruthenium(I,I) carbonyl carboxylates.[30-32]

Catalytic Activity. To determine whether the ruthenium complexes **I-VIII** were active as catalysts for carbenoid transformations, they were initially evaluated in the cyclopropanation reaction between methyl phenyldiazoacetate (**3.17**) and styrene (Scheme 3.8). This transformation is very effective with a variety of dirhodium complexes,[1-3] and was thus considered to be a good test reaction for catalytic activity of new catalysts. The reactions were conducted in dichloromethane by syringe pump addition of **3.17** to a solution of excess styrene and 1 mol% loading of the ruthenium catalyst. Reactions at room temperature gave low yields (or no reaction) for all complexes **I-VIII** (0-26%). The highest yields were obtained with complexes **I** and **IV-VI** (13-26%). Reactions in refluxing dichloromethane, however, produced the cyclopropane in moderate to good yields for all the catalysts (42-69% yield). The main side-reaction was dimerization of the diazo compound. The significantly improved reactivity with higher temperature may be attributed to thermally enhanced dissociation of the dimeric and polymeric catalyst complexes to open up the reactive axial active sites for catalysis. The lowest yields were obtained with complexes **VII** and **VIII** in reactions conducted both at room temperature and at reflux. As these two catalysts lack axial CO-ligands, they display chain polymeric structures in the solid state and are therefore expected to have lower solubility in dichloromethane compared to complexes **I-VI**. Such polymeric or oligomeric structures may also exist in solution. Complexes **I-VI**, containing axial CO ligands, form “dimer-of-dimer” type structures (see Figure 3.1) that dissociate in solution more easily than **VII** and **VIII**.

Scheme 3.8: Catalytic activity of Ru(I)-complexes.

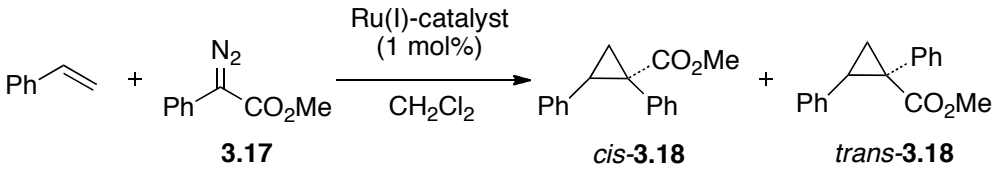

Table 3.5: Cyclopropanation reactions.

Entry	*Catalyst*	*Yield* (%)[a] (r.t.)	*Yield* (%)[b] (40 °C)	*de* (%)[c] (40 °C)
1	**I**	16[a]	55	50
2	**II**	9[a]	69	83
3	**III**	9[a]	67	69
4	**IV**	13[a]	60	51
5	**V**	26[a]	47	59
6	**VI**	16[a]	69	72
7	**VII**	0[a]	45	59
8	**VIII**	3[a]	42	64

[a] Reactions were performed by Dr. Janelle Thompson, Ref. 32
[b] Combined yield of both isomers.
[c] From ^{1}H NMR analysis of crude reaction mixture.

The diastereoselectivity of the reaction of **3.17** with styrene is generally very high when catalyzed by dirhodium complexes (routinely >94% de).[33] With the ruthenium(I) catalysts, the diastereoselectivities were somewhat attenuated (50-83% de). The relatively low diastereoselectivity observed for the ruthenium-catalyzed reactions is presumably due to the higher electrophilic character of these complexes compared to the dirhodium catalysts previously used, which lowers the abilities of the resulting carbenoid intermediates to discriminate between the diastereomeric transition states.

Vinylogous reactivity in O–H insertions. The main issue regarding the diruthenium(I,I) catalysts was whether they could enhance the vinylogous reactivity of vinylcarbenoids

derived from vinyldiazoacetates. A test reaction for this behaviour is the decomposition of the vinyldiazoacetate in neat methanol, as discussed in Section 3.1.[11] The resulting distribution of products will reflect the propensity of vinylogous *versus* carbenoid reactivity of the intermediate vinylcarbenoid as the methoxy group will be incorporated into the C4– and/or C2-positions respectively. The observed products *E/Z*-**3.11** and **3.10a-b** are derived from attack of methanol at the 4– and 2– positions, respectively. Complexes **I-III** were tested in this reaction and the results are shown in Table 3.6 along with previously reported results with dimolybdenum and dirhodium complexes. The diruthenium(I,I)-complexes shift the regioselectivity towards the terminal position quite pronounced. Products derived from vinylogous reactivity always constitute >80% of the products for these catalysts. Product yields are low, possibly due to reduced reactivity of the catalysts at room temperature. The *E/Z* ratio of **3.11** changes with catalyst as well, and the preference for the *Z*-isomer may reflect the preference of the transient vinylcarbenoid to exist in the *s*-trans conformation.

Scheme 3.9: Vinylogous reactivity in O–H insertions.

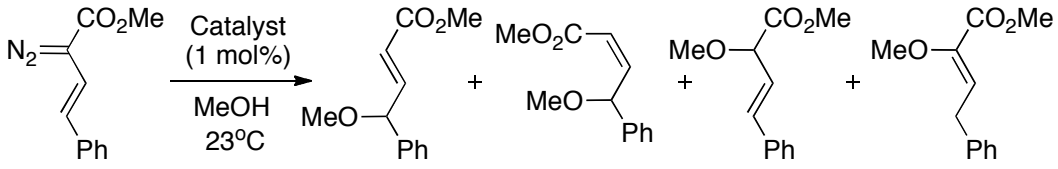

3.9 ***E*-3.11** ***Z*-3.11** ***E*-3.10a** **3.10b**

Table 3.6: O–H Insertions with Ru(I)-catalysts in comparison with other complexes.

Catalyst	*Product Ratio*								*Yield* (%)
	***E*-3.11**	:	***Z*-3.11**	:	**3.10a**	:	**3.10b**		
I[a]	11	:	75	:	14	:	0		45
II[a]	15	:	67	:	18	:	0		26
III[a]	18	:	62	:	20	:	0		28
$Mo(CO)_6$/*S*-TBSP-H[b]	17	:	34	:	40	:	9		93
Rh_2(*S*-TBSP)[b]	0	:	0	:	89	:	11		86
$Rh_2(OAc)_4$[a]	0	:	0	:	100	:	0		85

[a] Reactions performed by Dr Janelle Thompson, Ref. 32.
[b] From Ref. 11.

Vinylogous reactivity in C–C bond formation. Extension of the selective vinylogous reactivity to C–C bond forming reactions was desired, as it would greatly enhance the scope and value of the diruthenium-catalyzed process. Rhodium(II)-catalyzed reactions of vinyldiazoacetates unsubstituted at the 4-position, show enhanced vinylogous reactivity, although with poor selectivity unless the ester group is sterically demanding. The decomposition of unsubstituted vinyldiazoacetate **3.1** was therefore tested with some of the diruthenium complexes in the presence of cyclopentadiene (Scheme 3.10, Table 3.7). This reaction had previously been conducted with dirhodium(II) systems, which gave a mixture of compounds **3.3** and **3.2**, arising from vinylogous reactivity and the tandem cyclopropanation/Cope rearrangement (carbenoid reactivity) respectively, as discussed in Section 3.1.[12,13] Due to the volatility and intrinsic instability of the diazo compound, the reactions were carried out at ambient temperature and with a large excess of trapping agent (20 equivalents). The same reaction catalyzed by complexes **I**, **II** and **VI** led cleanly to the bicyclic product(s) *Z/E*-**3.3** in moderate to good yields (37-54%) with an isomer ratio of about 2 : 1 in all cases. Compared to previously reported

dirhodium-catalyzed reactions, there is remarkable control of regioselectivity and only the product(s) derived from vinylogous reactivity could be observed.

Scheme 3.10: Vinylogous reactivity in reaction with cyclopentadiene.

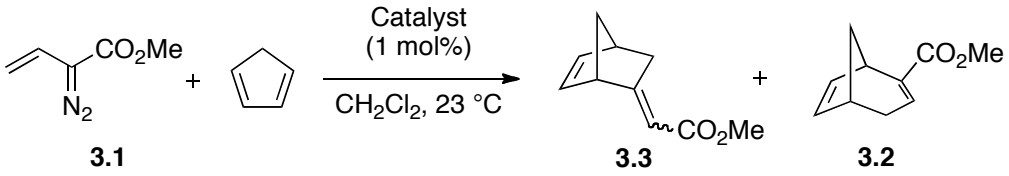

3.1 **3.3** **3.2**

Table 3.7. Reaction with cyclopentadiene.

Catalyst	*Ratio*[a] (**3.3** : **3.2**)	*Z : E ratio*[a] *of* **3.3**	*Yield* (%)[b]
I	> 98 : 2	2 : 1	54
II	> 98 : 2	2 : 1	37
VI	> 98 : 2	2.4 : 1	40
$Rh_2(OPiv)_4$[c,d]	98 : 2	0.8 : 1	86
$Rh_2(OAc)_4$[c]	67 : 33	2.5 : 1	81
$Rh_2(TFA)_4$[c]	32 : 68	1.1 : 1	60

[a] From ^{1}H NMR analysis of crude reaction mixture. [b] Combined yields of **3.2** + **3.3**.
[c] From Ref 20. [d] Carried out in pentane.

Enhancement of vinylogous reactivity in C–C bond forming reactions was furthermore demonstrated using *N*-Boc pyrrole as the trapping agent. The reaction afforded both stereoisomeric alkylation products *E/Z*-**3.8** exclusively, in moderate to good yields (45-54%). The formation of *Z*-**3.8** was strongly preferred over the *E*-isomer.

Scheme 3.11: Vinylogous reactivity in reaction with *N*-Boc pyrrole.

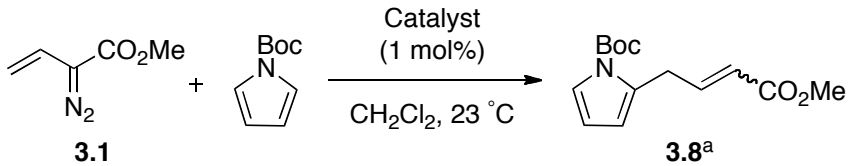

3.1 **3.8**[a]

Table 3.8: Reaction with *N*-Boc pyrrole.

Catalyst	*Z : E ratio*[b] *of* **3.8**[a]	*Yield* (%)[c]
I	11 : 1	57
II	13 : 1	45
VI	25 : 1	54

[a] For a detailed discussion of the structure of **3.8** see Section 3.2.2.
[b] From ^{1}H NMR of crude reaction mixture. [c] Isolated yield of *Z*-isomer.

3.2.2 Silver(I)-Catalyzed Reactions of Vinyldiazoacetates

Silver Catalysis. Silver(I)-complexes are well known to effect decomposition of diazo compounds.[34-39] One of the most established transformations is the Wollf rearrangement of diazoketones, a reaction that has been employed in several total syntheses of complex molecules.[38,40,41] Silver-catalyzed reactions of aryl- and vinyldiazoacetates have scarcely begun to appear in the literature.[42-45] Jørgensen and co-workers reported that silver(I) could catalyze N–H insertion reactions between anilines and aryldiazoacetates.[42] Davies and Thompson reported that a silver(I)-salt could significantly enhance the cyclopropanation chemistry or aryl– and vinyldiazoacetates as higher selectivity was observed.[44] Lovely and Dias et. al. reported recently that silver tris(pyrazolyl)borate complexes could readily catalyze intermolecular C–H insertions using ethyl diazoacetate, aryl– and vinyldiazoacetates as well as intramolecular C–H insertion.[43] The results of these studies are consistent with reactivity profiles that fit that of metallocarbenoids, and that the silver(I) carbenoid complex hence is a likely intermediate in these reactions.[42] There is, however, still an ongoing controversy on the actual mechanism, and Lewis acid-pathways have also been suggested.[14,42]

Vinylogous O–H insertion. Based on the report by Hu an co-workers,[14] we first re-investigated the reaction between methyl phenylvinyldiazoacetate **3.9** and benzyl alcohol, catalyzed by AgOTf. The reaction can afford products **3.19** and **3.20**, corresponding to carbenoid and vinylogous reactivity, respectively (Scheme 3.12, Table 3.9). Although it was reported that exclusive formation of **3.20** occurs when the reaction was carried out in refluxing dichloromethane,[14] this could not be reproduced. The best selectivity was obtained at 0°C, which gave a ~97 : 3 ratio in favor of **3.20**. It was demonstrated that, further lowering of reaction temperature, did not improve the selectivity. In addition to **3.19** and **3.20**, trace amounts of other isomers could be detected. Although these were not isolated, some of their key ^{1}H NMR chemical shifts could be assigned based on comparison with the reaction with MeOH. Furthermore, the catalyst loading could be reduced to 5 mol% without significant drop in yields. Similar results were obtained with another silver salt, $AgSbF_6$, demonstrating that the observed reactivity can be attributed to the silver component. Using dichloromethane as solvent at 0 °C with 5 mol% loading of AgOTf were chosen as standard conditions for further reactions. This represents a signficantly improved procedure compared to that reported by Hu et.al.[14]

Scheme 3.12: O–H insertions with benzyl alcohol.

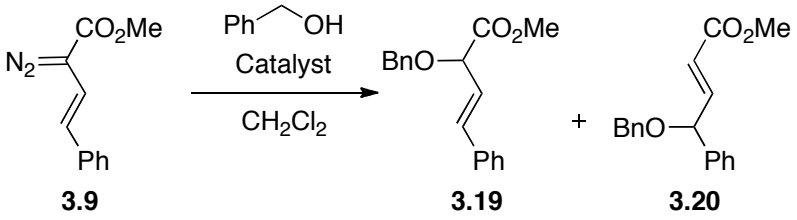

Table 3.9: Influence of loading and temperature on O–H insertion regioselectivity.

Entry	*Catalyst (Loading)*	*T* (°C)	*Product Ratio*[a] **3.19 : 3.20**	*Yield* (%)[b]
1[c]	AgOTf (10 mol%)	40	2 : >98[c]	60
2	AgOTf (10 mol%)	40	15 : 85	60
3	AgOTf (5 mol%)	40	15 : 85	60
4	AgOTf (10 mol%)	23	7 : 93	61
5	AgOTf (10 mol%)	0	~3 : 97	N/D

[a] From ^{1}H NMR of crude reaction mixture. [b] Isolated yield of **3.20**. [c] Value from Ref. 14.

A standard test reaction that has been employed to evaluate vinylogous reactivity in vinylcarbenoids, is the decomposition of **3.9** in neat methanol at ambient temperature (Scheme 3.13).[11,31] The reaction leads to four products, two of which are derived from vinylogous reactivity (*E* and *Z*-**3.11**), and two from carbenoid reactivity (**3.10a-b**). Table 3.10 shows the complementary selectivity of various catalysts in this reaction. **3.10a** and **3.10b** have been shown to be favored with common dirhodium catalysts.[11,31] However, with electron deficient diruthenium carbonyl carboxylates, *Z*-**3.11** was shown to be the favored product (75% selectivity).[31] The same reaction with AgOTf displays strong selectivity for *E*-**4** with 89% product selectivity, consistent with the reactions with benzyl alcohol. The transformation was clean and proceeded in 95% overall yield. The results from the Ru(I)-study[31] and for $Rh_2(TBSP)_4$[31] are

only included in Table 3.10 for comparison.

Scheme 3.13: O–H insertion with methanol.[11,31]

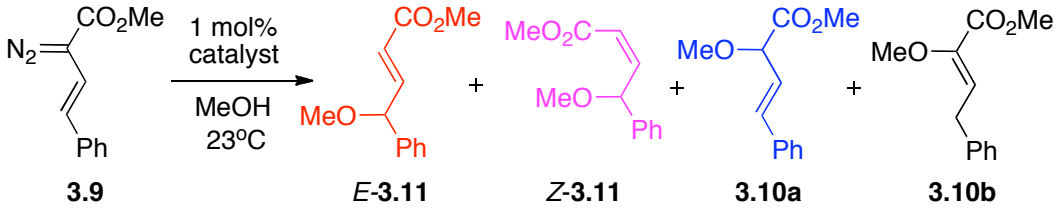

Table 3.10: Complementary selectivity of various metals.[11,31]

Catalyst (mol%)	*Product Ratio*[a]					*Yield* (%)[b]
	***E*-3.11**	:	***Z*-3.11**	:	**3.10a** : **3.10b**	
AgOTf (5%)	**89**	:	5	:	6 : 0	95
$Ru_2(TFA)_2(CO)_5$ (1%)[c]	11	:	**75**	:	14 : 0	45
Rh_2(*S*-TBSP)$_4$ (1%)[c]	0	:	0	:	**89** : 11	86

[a] From ^{1}H NMR of crude reaction mixture. [b] Combined yields. [c] From Refs 32 and 11.

To test the generality of the vinylogous insertion process with AgOTf, other substrates were studied in X–H insertion reactions with **3.9** and MeO-**3.9** (Scheme 3.14, Table 3.11). The reactions were also conducted with Rh_2OOct_4 for comparison. With benzyl alcohols, AgOTf-catalyzed reactions of **3.9** afforded 64-74% yield in a 94 : 6 product ratio in favor of the vinylogous O–H insertion products (**3.20**, **3.22a**). With *p*-nitrobenzyl alcohol, only 36% yield of the carbenoid insertion product **3.21a** could be obtained with rhodium octanoate. However, rhodium-catalyzed reactions routinely gave >95 : 5 product ratio in favor of carbenoid insertions. Attempted reactions with benzyl amine, did not give any products, presumably because of formation of silver-amine complexes. However, the reaction proceeded smoothly in the presence of aniline, but only a 56 : 44 product ratio of **3.22b** : **3.21b** was obtained with AgOTf. With rhodium octanoate, full conversion to the carbenoid insertion product **3.21b** was observed. The overall yields

were excellent 84% for both catalyst systems. The regiocontrol was maintained even when carboxylic acids were used as the source of O–H groups. AgOTf afforded >95 : 5 selectivity for the vinylogous insertion product **3.22c** in 66% yield. The same selectivity was observed with rhodium octanoate for carbenoid insertion (**3.21c**). An allylic alcohol, 3-methylbut-2-enol, gave very high selectivities in both silver– (95 : 5) and rhodium-catalyzed systems (<5 : 95), however, the rhodium-catalyzed reaction gave superior yield of **3.21d** (81% *versus* 67% of **3.22d** with AgOTf). Interestingly, a homopropargylic alcohol gave only 81 : 19 product selectivity for the vinylogous insertion product **3.22e** in 48% overall yield. No evidence for cyclopropenation chemistry was observed. With the rhodium catalyst, 74% yield of carbenoid insertion product **3.21e** was isolated. The insertion reaction could also be conducted with a diol (ethylene glycol), which gave 52% yield of **3.22f** with AgOTf and 64% yield of **3.21f** with rhodium octanoate. The reactions with benzyl alcohol were conducted using *p*-methoxyvinyldiazoacetate MeO-**3.9**, which afforded a very clean vinylogous insertion reaction with AgOTf in 77% isolated yield and with >95 : 5 product selectivity for **3.22g**. The corresponding rhodium catalyzed reaction gave 64% of the carbenoid insertion product **3.21g** exclusively. As it appeared that, the use of the more electron-rich vinyldiazo compound MeO-**3.9**, enhanced the silver-catalyzed reaction, it was also tested in the reaction with aniline. A slight increase in regioselectivity to 65 : 35 ratio was observed in favor of **3.22h**. These results demonstrate that, moderate to excellent regioselectivity can be obtained in vinylogous O–H insertions using AgOTf as catalyst, in moderate to good yields of the major isomer. Furthermore, these reactions are complementary to already established rhodium-catalyzed O–H insertions, which produce carbenoid insertion products predominantly.

Scheme 3.14: X–H insertions with arylvinyldiazoacetates.

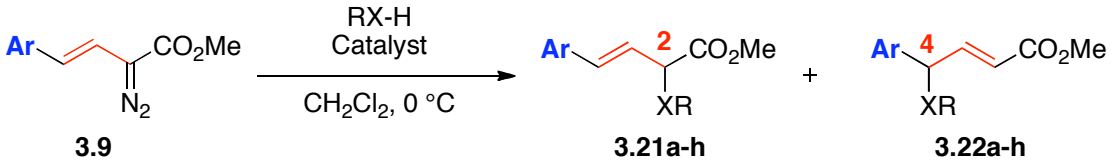

3.9 **3.21a-h** **3.22a-h**

Table 3.11: Scope of X–H insertion chemistry.

Entry	*Substrate*	*Ar =*	*Catalyst* [a]	*Product*	*Ratio*[b] *4 : 2*	*Yield (%)*[c]
1	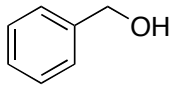	-Ph	AgOTf	**3.20**	94 : 6	74
2		-Ph	Rh_2OOct_4	**3.19**	< 5 : 95	64
3	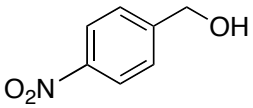	-Ph	AgOTf	**3.22a**	94 : 6	64
4		-Ph	Rh_2OOct_4	**3.21a**	< 5 : 95	36
5	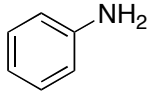	-Ph	AgOTf	**3.22b**	56 : 44	84[d]
6		-Ph	Rh_2OOct_4	**3.21b**	< 5 : 95	84
7	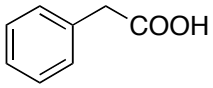	-Ph	AgOTf	**3.22c**	> 95 : 5	66
8		-Ph	Rh_2OOct_4	**3.21c**	< 5 : 95	66
9	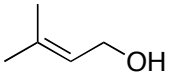	-Ph	AgOTf	**3.22d**	95 : 5	67
10		-Ph	Rh_2OOct_4	**3.21d**	< 5 : 95	81
11	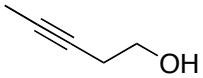	-Ph	AgOTf	**3.22e**	81 : 19	48[d]
12		-Ph	Rh_2OOct_4	**3.21e**	< 5 : 95	74
13	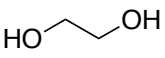	-Ph	AgOTf	**3.22f**	95 : 5	52
14		-Ph	Rh_2OOct_4	**3.21f**	< 5 : 95	64
15	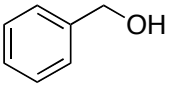	-(*p*-MeO)Ph	AgOTf	**3.22g**	> 95 : 5	77
16		-(*p*-MeO)Ph	Rh_2OOct_4	**3.21g**	< 5 : 95	64
17	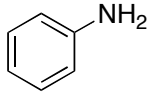	-(*p*-MeO)Ph	AgOTf	**3.22h**	65 : 35	67[d]

[a] 5 mol% of AgOTf and 1 mol% of Rh_2OOct_4 was used. [b] From ^1H NMR analysis of crude reaction mixture.
[c] Isolated yield of major product after column chromatography. [d] Overall yields.

The vinylogous addition chemistry was also observed for other diazo compounds, such as the unsubstituted vinyldiazoacetate **3.23** (Scheme 3.15). Silver triflate-catalysis gave the vinylogous addition product **3.26** in 49% isolated yield in about 5 : 1 ratio with carbenoid insertion product **3.24**. The products were assigned based on precedent with the methyl ester of this diazo compound.[11] The moderate yield may be attributed to the intrinsic instability of the diazo compound. The rhodium-catalyzed reaction was less selective in this case, producing a mixture of all three products **3.24** : **3.25** : **3.26** in a 50 : 42 : 8 ratio. This diazo compound appears to be less suitable for achieving highly regioselective reactions.

Scheme 3.15: O–H insertions with **3.23**.

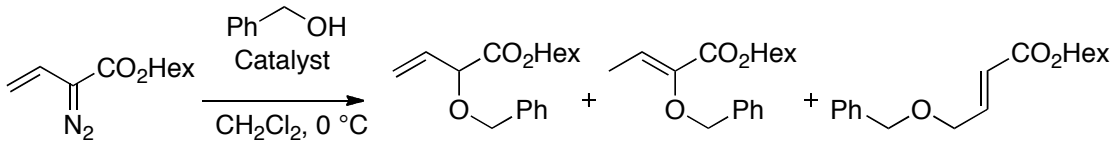

3.23 **3.24** **3.25** **3.26**

AgOTf (5 mol%)	17 : <1 : 83	49% yield of **3.24**
Rh_2OOct_4 (1 mol%)	50 : 42 : 8	

C–C Bond formation. The effective control of regioselectivity in the aforementioned O–H insertion reactions, prompted a study of C–C bond forming reactions as well, as these would be of greater synthetic impact. The reaction between unsubstituted vinyldiazo compound **3.23** and *N*-Boc pyrrole, catalyzed by AgOTf, gave an overall 49% yield of alkylation product **3.27** in a 82 : 18 *E/Z*-ratio (Scheme 3.16, Table 3.12). The *E*-product is again favored in the silver-catalyzed reactions, which is opposite to what was observed in the Ru(I)-catalyzed reactions described in Section 3.1. For comparison, both rhodium catalysts $Rh_2(TFA)_4$ and $Rh_2(OOct)_4$ were studied, and gave the *Z*-isomer preferentially

with about the same selectivity, However, the [4+3]-cycloadduct (carbenoid reactivity) was observed in both cases.

Scheme 3.16: Vinylogous reactivity in C–C bond formation with *N*-Boc pyrrole.

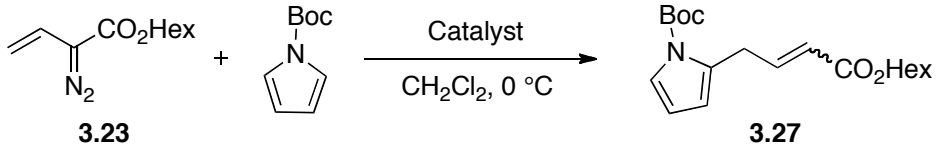

3.23 **3.27**

Table 3.12: Influence of catalyst on selectivity.

Entry	*Catalyst* (mol%)	*E/Z ratio*[a]	*Yield* (%)[b]
1	AgOTf (5 mol%)	82 : 18	49
2	$Rh_2(OOct)_4$ (1 mol%)	25 : 75	33[c]
3	$Rh_2(TFA)_4$ (1 mol%)	19 : 81	42[c]

[a] From ^{1}H NMR analysis of crude reaction mixture.
[b] Isolated yield of major isomer.
[c] Also the [4+3] cycloadduct was observed in crude mixture.

The reaction was attempted with other substrates, such as furan, benzofuran and butyl vinyl ether, but only low yields (<40%) were obtained for the desired products of vinylogous reactivity (**3.29-3.31**) despite using a massive excess of the substrates and 10 mol% loading of silver-catalyst (Chart 3.2). Methyl vinyldiazoacetate **3.28** was also tested with *N*-Boc pyrrole as the substrate, catalyzed by both AgOTf and $Rh_2(OOct)_4$. Also here, only a small amount of the desired compound **3.32** was obtained. In the analogous Rh(II)-catalyzed transformation, bis-cyclopropanation of the heterocycle occured preferentially.

Chart 3.2: Other observed products in <40% yields from vinylogous reactivity.

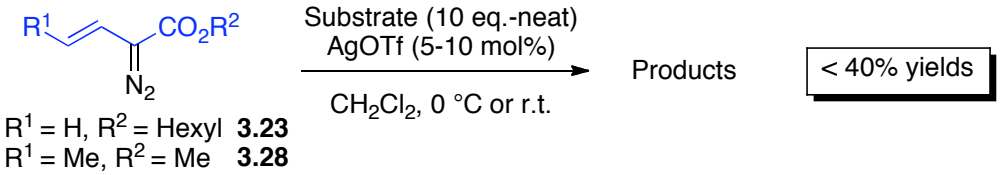

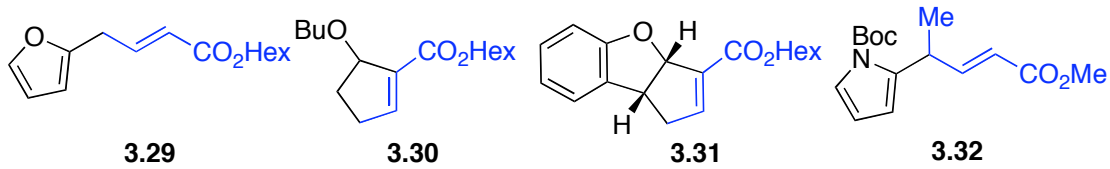

3.29 **3.30** **3.31** **3.32**

Considering the success with diazo compound **3.9** in the O–H insertion chemistry, vinylogous C–C bond formation was attempted in the reaction between **3.9** and furan, catalyzed by AgOTf (Scheme 3.17). Although a good overall yield of 80% of products **3.33-3.35** was obtained, the selectivity was rather low, producing a ratio of 21 : 79 of vinylogous- to carbenoid reactivity. It appears that, selective, high yielding vinylogous C–C bond forming reactions with silver(I)-catalysts is not a viable process with the systems that were studied herein.

Scheme 3.17: Silver-catalyzed reaction of **3.9** with furan.

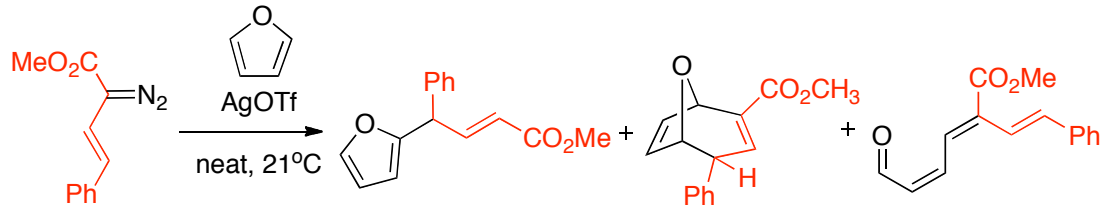

3.9 **3.33** **3.34** **3.35**

Product Ratio: 21 : 46 : 33 80% yield

Revised structure of 3.27. During studies of vinylogous C–C bond formation using silver catalysis, it was found that the spectroscopic characteristics of the major alkylation product **3.27** in the reaction between unsubstituted vinyldiazoacetate **3.23** and *N*-Boc pyrrole was different from that reported with rhodium and ruthenium catalysts. The

initially assigned structure for **3.27** from rhodium-catalyzed reactions is shown in Figure 3.2, left hand side. This had the *E*-configuration of the double bond, which was proposed to be in conjugation with the pyrrole ring. The structure was re-examined using advanced NMR analysis (HSQC, HMBC and NOESY). Key HMBC and nOe data is shown in Figure 3.2, right hand side. The key HMBC correlation, between the pyrrole carbon at 112.0 ppm and the methylene protons, suggests that the CH_2 is adjacent to the aromatic group. This is furthermore supported by nOe correlations. The double bond geometry was determined to be *Z*, consistent with nOe enhancement between the two vinylic protons and a coupling constant of circa 11 Hz.

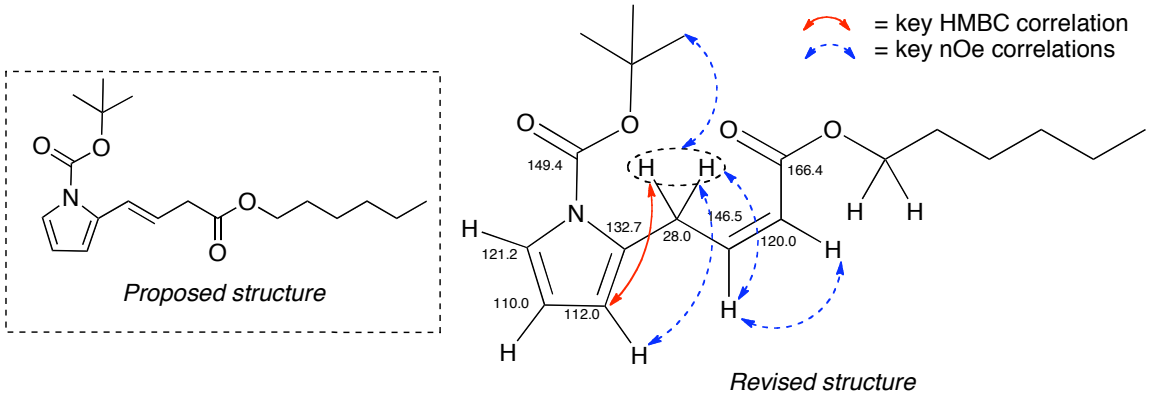

Figure 3.2: Stuctural revision of the alkylated *N*-Boc pyrrole product **3.27**.

Mechanistic studies. The likely mechanism of the vinylogous addition chemistry is of interest for future reaction design.[14,42] An increased interest in the synthetic utilization of vinylogous reactivity also necessitates a detailed understanding of the reaction pathway.[21] Scheme 3.18 describes hypothetical mechanistic scenarios for the reaction. Hu et. al. proposed that, the regioselectivity arose from an S_N2'-like attack of the alcohol onto the silver-vinyldiazoacetate complex **3.36** to form the vinylogous ylide adduct **3.37**.[14] In this process, silver acts as a Lewis acid, consistent with results obtained with other traditional

Lewis acids in this chemistry.[14] Davies et. al. have shown that silver complexes can readily catalyze cyclopropanation reactions between aryl– and vinyldiazoacetates and alkenes.[44] In this regard, the chemistry behaves as if metallocarbenoids are intermediates.[44] An alternative proposal is therefore the intermediacy of a silver vinylcarbenoid **3.38**. Jørgensen and co-workers have proposed a mixed Lewis acid/carbenoid mechanism for N–H insertion reactions of aryldiazoacetates catalyzed by silver(I)-complexes.[42] The details of the interaction of aryl- and vinyldiazoacetates with silver complexes have not been studied to great extent, despite recent developments of several important reaction systems.[42-45] The reaction pathway from ylide **3.37** has been proposed to occur through direct proton transfer, presumably via the solvent, or via a secondary silver carbenoid **3.39**, which then would undergo β-hydride elimination.[11,14]

Scheme 3.18: Mechanistic proposals for vinylogous O–H insertion.

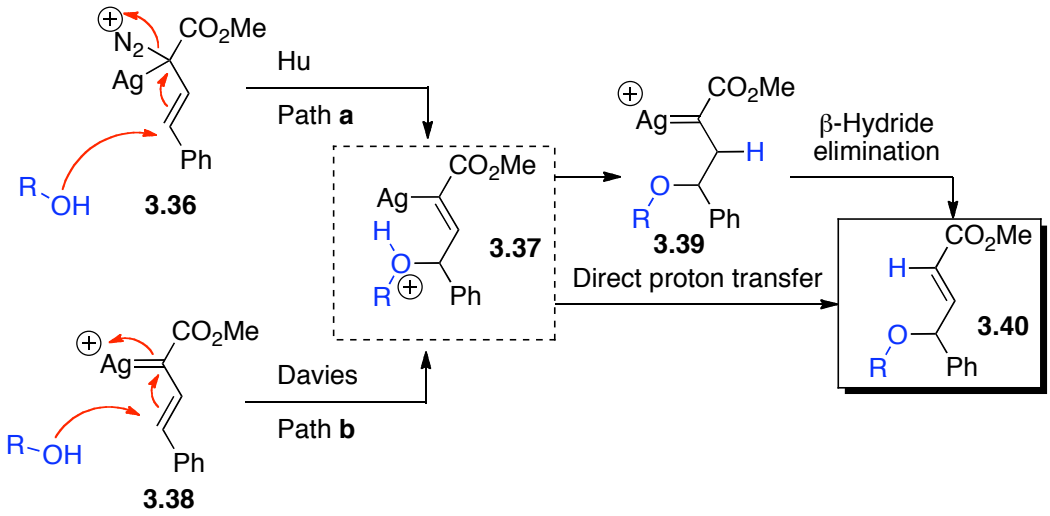

Deuterium labellig studies were conducted by using d_1-methanol in the insertion reaction with **3.9** to shed some light on the mechanism (Scheme 3.19). For comparison, the reaction was carried out using AgOTf, Rh_2OOct_4 as well as $Rh_2(TFA)_4$ as catalysts. In

all cases, the deuterium label was selectively incorporated into the 2-position of the products. This is consistent with a study of dimolybdenum-catalyzed O–H insertions by Davies and Yokota.[11] In terms of vinylogous reactivity, these observations imply that the pathway involving **3.39** is not operative, as this would lead to deuterium incorporation at the 3-position.[11] Instead, a stereospecific protonolysis of the Ag–C bond is occuring. For carbenoid insertion with rhodium catalysts, the deuterium incorporation into the 2-position is consistent with the commonly accepted mechanism for this transformation.[46,47]

Scheme 3.19: Deuterium labelling studies.

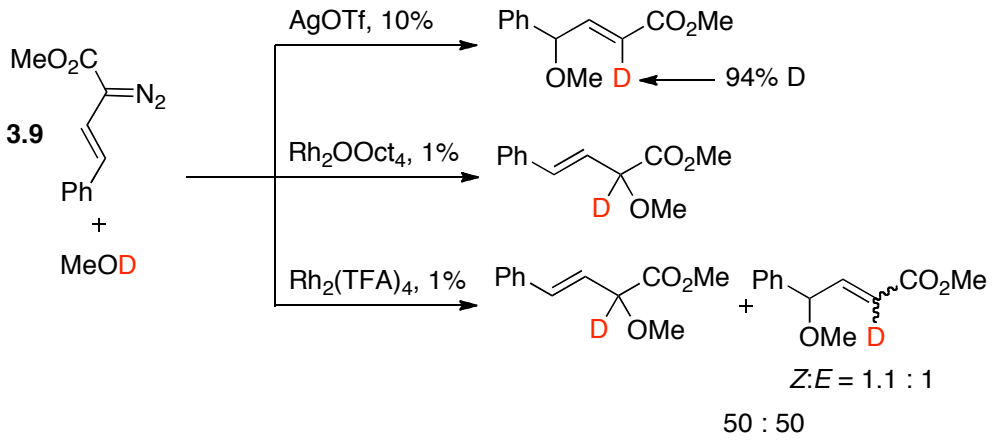

A central issue in this chemistry has been whether the reactions occur via Lewis acid-induced nitrogen loss/nucleophilic attack, or through silver-carbenoid intermediates.[42] Although recent experimental evidence suggests silver carbenoid intermediates may be involved,[39,43,44] no experiments have been conducted that can unambiguously answer this question.[42] Therefore, it was decided to conduct a density functional study to explore whether a pathway is viable through a silver-carbenoid intermediate. Furthermore, comparison of such a pathway with the proposal of Hu and co-workers on vinylogous X–H insertion, would be of interest. As model chemistry for this study was used the reaction between methanol and **3.9**, catalyzed by AgOTf (Scheme 3.20). The calculations were

performed at the B3LYP/6-311+G(2d,2p)[Ag-RSC+4f]//B3LYP/6-31G*[Ag-RSC+4f] level of theory (See section 3.4.3 for details), which employs a relativistic small-core ECP for silver. The main discussion is based on single-point energies calculated at the abovementioned level, with zero-point corrections from B3LYP/6-31G*[Ag-RSC+4f] calculations, as well as gas-phase Gibbs free energies from the latter level.

Scheme 3.20: Model reaction for computational studies.

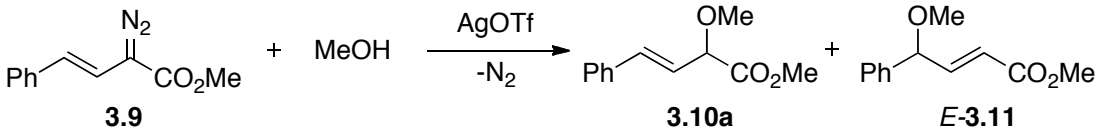

The potential energy surface for the reaction between **3.9** and methanol, catalyzed by silver triflate, is shown in Figure 3.3. A variety of adducts between silver triflate and **3.9** were explored, and it was found that the O-coordinated complex **LA-I**, in which the carbonyl group is coordinating with the silver catalyst, is the most stable adduct. This is consistent with the known Lewis acidity profile for silver salts, which are often used in Lewis acid-catalyzed processes.[39] **LA-I** lies downhill from the free reactants by -20.5 kcal/mol. In contrast, the C-coordinated complex **LA-II** was less stable (-12.7 kcal/mol) by 7.8 kcal/mol. A transition structure for loss of nitrogen from the latter (**TS-II**) was located to be at -7.1 kcal/mol, which gives a potential energy barrier of 5.65 kcal/mol from **LA-II**. The overall barrier from **LA-I** is +13.4 kcal/mol, to give the silver carbenoid complex **3.38**, which was an exoergic process by -35.6 kcal/mol. These results strongly suggest that formation of the silver vinylcarbenoid **3.38** is a facile process in this system, and that the overall process is highly exothermic. For comparison, a transition structure (**TS-I**) was also found for direct nitrogen loss from the Lewis acid adduct **LA-I**, but was strongly disfavored compared to the carbenoid pathway (+23.7 kcal/mol).

The *s*-cis vinylcarbenoid complex **3.38** was more stable than the corresponding *s*-trans isomer by about ~6.1 kcal/mol. In calculations on dirhodium carbenoids, the opposite preference is often observed (see Section 2.2). In this regard, it appears that the counter-ion is playing an important role, by forming attractive hydrogen bonds with the vinyl and aryl hydrogen, thereby stabilizing the former conformation. Transition structures were next sought for addition of methanol to both the vinylogous and carbenoid sites of **3.38**. Structures **TS-IIIa** and **TS-IIIb** were found, both which displayed strong hydrogen-bonding interactions with the triflate counterion. Vinylogous addition through **TS-IIIb** displayed a potential energy barrier of +2.33 kcal/mol, whereas carbenoid addition through **TS-IIIa** required +5.03 kcal/mol. This is consistent with experimental observations that, the former is favored. Furthermore, the stereoselectivity can now readily be rationalized since the preferred transition state has the vinylcarbenoid in an s-*cis* orientation. The proton transfer reactions of ylides **YL-IIa** and **YL-IIb** were not studied, but are likely to involve a Grotthus-type mechanism.

To obtain a more accurate picture, the two addition transition structures **TS-IIIa** and **TS-IIIb** were next fully geometry optimized at the B3LYP/6-311+G(d,p)[Ag-RSC+4f] level of theory, at 0°C with solvent effect from CH_2Cl_2 (ε=8.93) included (IEFPCM-model). From these calculations, the Gibbs free energy difference between **TS-IIIa** and **TS-IIIb** was estimated to be $\Delta\Delta G^{\neq}$ = 2.55 kcal/mol. This is in reasonable agreement with experiments (insertions with benzyl alcohol indicate $\Delta\Delta G^{\neq}$ = ∼1.9 kcal/mol, Table 3.11), considering the crude nature of our computational model and errors involved in DFT calculations.[48] Furthermore, it is not known what the actual role of the counterion is in

these reactions. In a solution containing alcohols, it may not be closely associated with the metal during the catalytic cycle.

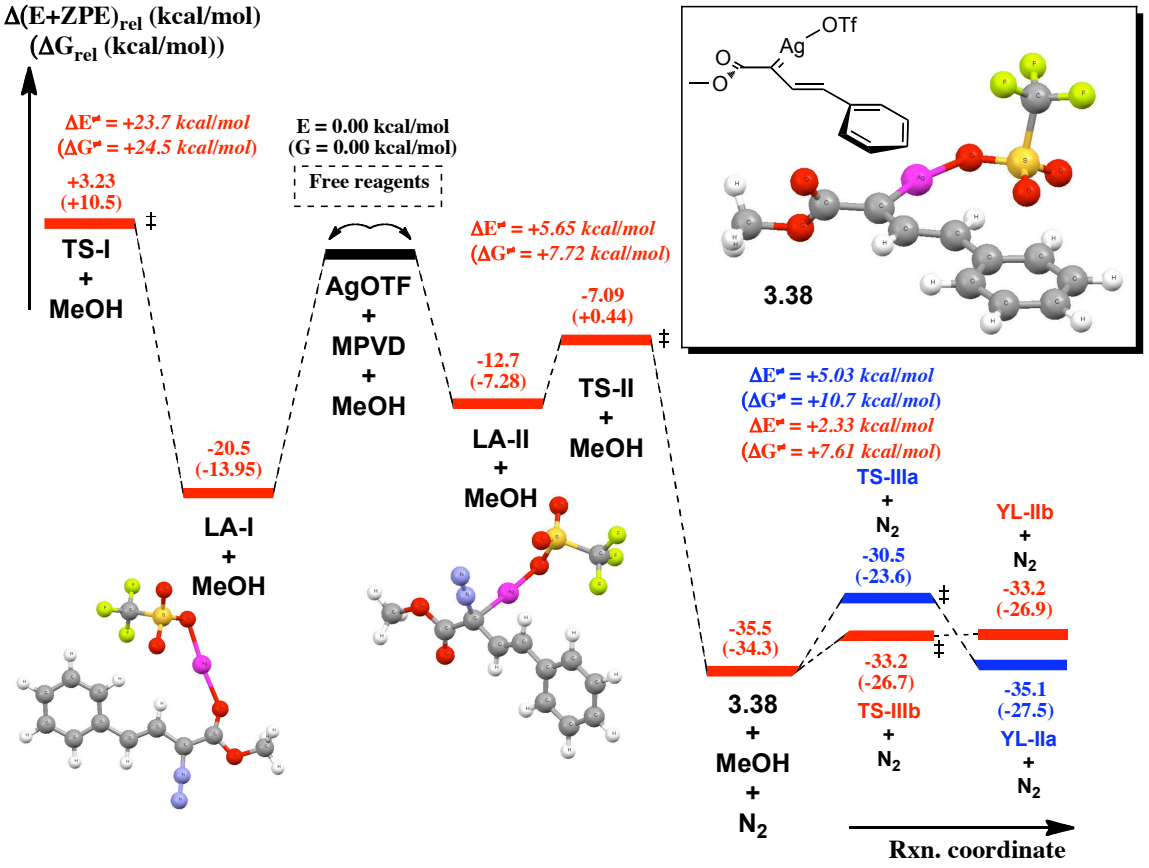

Figure 3.3: Potential energy surface for silver-catalyzed carbenoid formation and trapping by methanol. Potential energies (E+ZPE) are calculated at the B3LYP/6-311+G(2d,2p)[Ag-RSC+4f]//B3LYP/6-31G*[Ag-RSC+4f] level. Gas-phase Gibbs free energies and ZPE corrections are from B3LYP/6-31G*[Ag-RSC+4f] calculations.

Transition structures that would correspond to vinylogous addition as depicted by Hu and co-workers, could not be located despite several attempts of approaching a methanol molecule towards the vinylogous site of **LA-II**. Furthermore, the Kohn-Sham LUMO of **LA-II** is localized totally on the diazonium moiety, indicating that there is no electrophilic reactivity at the vinylogous position in this adduct. This is best illustrated by

the LUMO frontier density contour map, shown in Figure 3.4a, which shows a thermally averaged projection of the LUMO onto an isosurface of the electron density. The blue area indicates that the electrophilic site is localized on nitrogen. For comparison, the LUMO frontier density map of the silver carbenoid **3.38**, shown in Figure 3.4b, demonstrates electrophilic reactivity both at the carbenoid and vinylogous positions. This is consistent with experimental data presented herein and in previous works.[44]

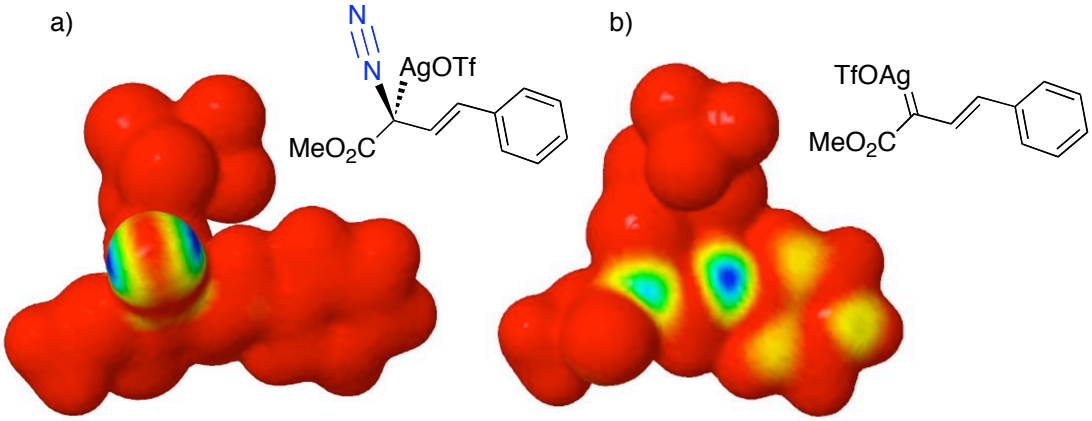

Figure 3.4: LUMO frontier density plots: (a) adduct **LA-II** and (b) silver carbenoid **3.38**.

In summary, the computational study presented above gives new insights into the reactions of diazo compounds catalyzed by silver salts. The formation of a silver vinylcarbenoid intermediates appears to be a viable process, although other pathways cannot be excluded. Furthermore, the study has presented evidence suggesting that, the mechanism proposed by Hu and co-workers on vinylogous O–H insertion with alcohols, is unlikely to operate.

Novel diazo compounds. Diazo compounds are prominent reagents in synthesis, mainly because of their role as effective precursors for the formation of metallocarbenoids in the

presence of a variety of metals.[1] The continued development of new diazo compounds is therefore of great synthetic importance. During studies of the insertion product **3.22c**, it was found that, upon treatment with DBU, deprotonation occured readily at the 4-position to form (presumably) the dienolate **3.40** (Scheme 3.21). Upon neutralization, protonation occured at the 2-position to give **3.41** (by NMR). The presumed intermediacy of dienolate **3.40**, led to the idea that this species could react, in a diazo transfer reaction with *p*-ABSA, to generate the corresponding diazo compound. This would be an entry into an interesting new class of diazo compounds.

Scheme 3.21: Double bond shift.

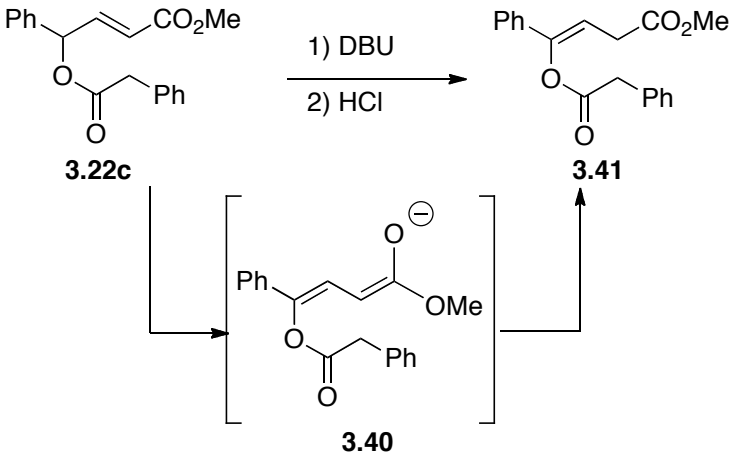

For **3.22c**, the diazo transfer reaction appeared unviable, since a very complex mixture of products was formed. For other insertion products from Table 3.11, however, the reaction proved to be very selective. Chart 3.3 shows some examples of novel diazo compounds that were prepared from O–H insertion products **3.22a**, **3.22d**, **3.22f** and **3.22g**. The dienolates were formed in a highly stereoselective manner, as only the *Z*-vinyldiazo compounds were isolated in 64-67% yield. Diazo compound **3.42b** was also formed without purification of the intermediate O–H insertion product **3.22d**. The crude

O–H insertion reaction mixture was simply washed with brine, to remove silver-catalyst, then subjected to standard diazo transfer conditions. The overall yield for the two-step process was 41%, consistent with the isolated yields of the individual steps. The double diazo compound **3.42d** arises from double vinylogous O–H insertion with ethylene glycol, followed by double diazo transfer. These studies suggest that a number of novel and unusual diazo compounds are accessible through this methodology.

Chart 3.3: Synthesis of novel diazo compounds.

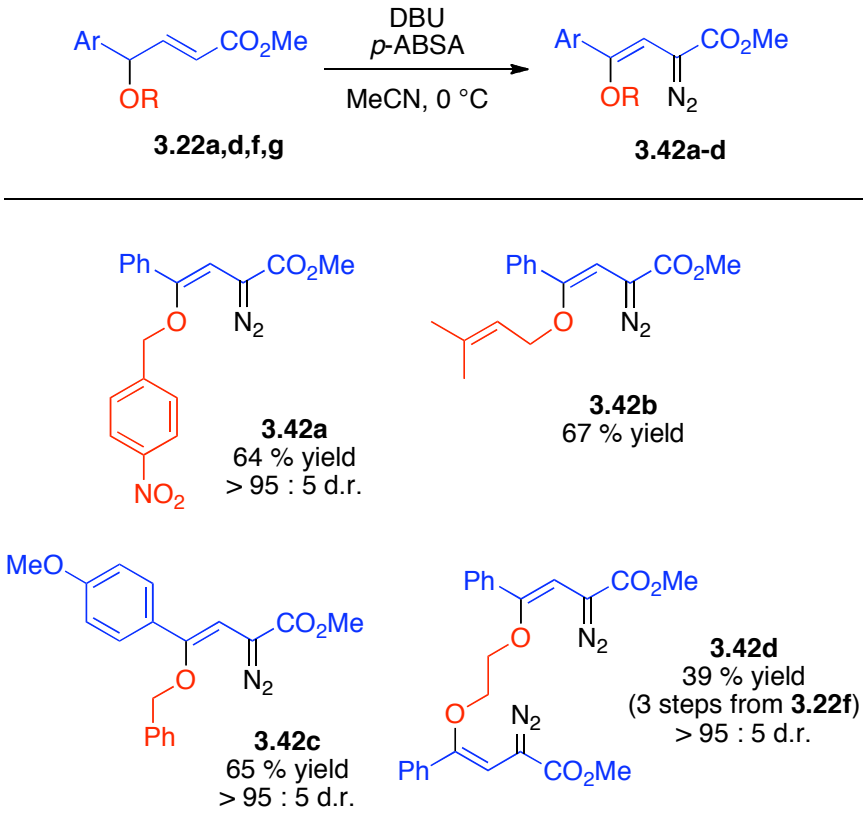

The selective dienolate formation can be explained by differential $A^{1,3}$-interactions in the deprotonation transition states that lead to both diastereomers (Scheme 3.22). The phenyl group may act as a sterically encumbering group relative to the benzyloxy group, as the latter is locally less bulky. The favored transition state for elimination then has the

oxy group proximal to the vinyl group, which would give the observed *Z*-selectivity. Furthermore, the oxygen lone pair may be involved in a favorable hydrogen bonding interaction with the α-hydrogen, thereby stabilizing this transition structure. The *Z*-stereoselectivity was proved by nOe studies of the diazo compounds, which indicated a enhancement between the vinyl hydrogen and the 4-aryl group.

Scheme 3.22: Rationalization of stereoselectivity.

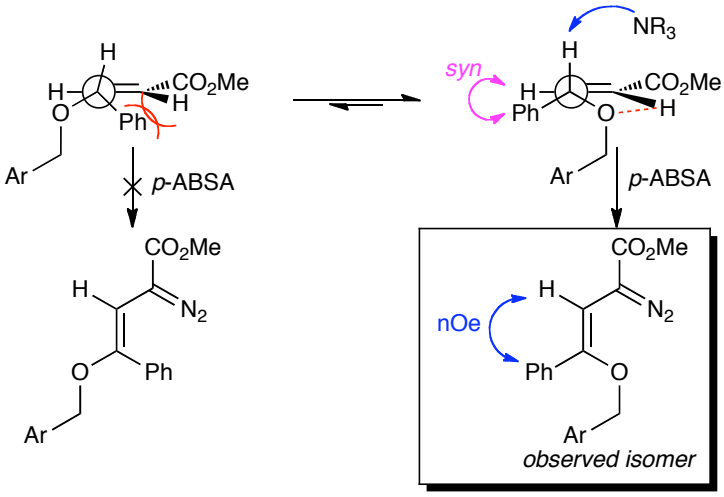

The newly formed diazo compound **3.42a** was tested for its activity as a carbenoid precursor in Rh(II)-catalyzed cyclopropanation of styrene. Using an excess of styrene and 2 mol% of the chiral catalyst Rh_2(*S*-DOSP)$_4$, cyclopropanation product **3.43** was formed in 26% ee. With Rh_2(*S*-PTAD)$_4$, 67% ee was obtained for this product, however, further optimization is needed to find good conditions for achieving highly enantioselective reactions with this new class of diazo compounds.

Scheme 3.23: Cyclopropanation of styrene with **3.42a**.

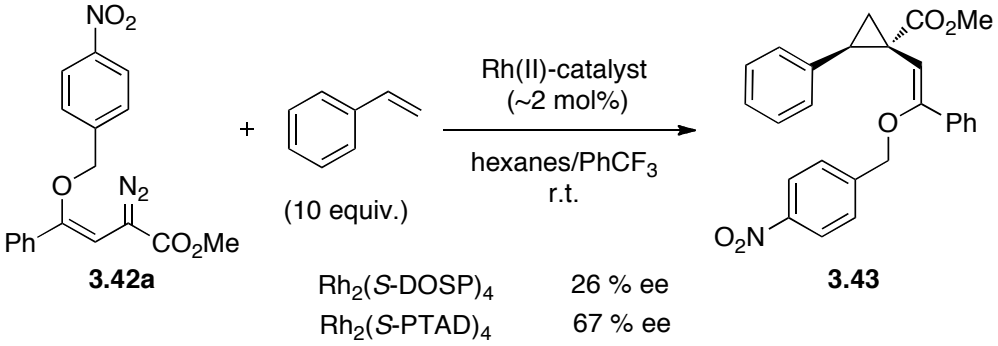

Rh_2(*S*-DOSP)$_4$ 26 % ee

Rh_2(*S*-PTAD)$_4$ 67 % ee

3.3 Conclusions

Studies herein demonstrate that a family of novel diruthenium carbonyl carboxylates can be effective catalysts for metallocarbenoid reactions at low catalyst loadings. Although these catalysts generally required more vigorous reaction conditions, when compared to dirhodium catalysts, they display significant synthetic potential as they greatly enhance vinylogous reactivity in O–H insertions and C–C bond forming reactions.

Silver(I) triflate has also been demonstrated to effectively enhance vinylogous reactivity in O–H insertion chemistry. As the rhodium(II)-catalyzed process is complementary, both regioisomeric addition products can be readily obtained. The vinylogous O–H insertion products are synthetically useful, as they have been demonstrated to be precursors to a novel family of diazo compounds. Only moderate yields and selectivities were obtained in silver-catalyzed C–C bond forming reactions. Density functional studies have demonstrated that, vinyldiazo compounds can readily generate silver vinylcarbenoids in the presence of silver(I) triflate. Furthermore, it has been shown that the vinylogous addition chemistry is likely to occur *via* this intermediate.

3.4 Experimental Section

3.4.1 General Considerations

All reactions were conducted in flame-dried glassware under an inert atmosphere of dry argon. All reagents were used as received from commercial suppliers, unless otherwise stated. Dichloromethane was obtained from drying columns (Grubbs type solvent purifier) and was degassed by bubbling argon through the solvent for >15 min prior to use. Flash chromatography was performed on silica gel (230-400 mesh). Thin layer chromatography (TLC) was performed on aluminium backed plates, pre-coated with silica gel (0.25 mm, 60 F_{254}) which were developed using standard visualizing agents: UV fluorescence (254 nm) and phosphomolybdic acid/Δ. Melting points were determined using a Mel-Temp electrothermal melting point apparatus and are uncorrected. ^{1}H NMR spectra were recorded on Varian Nuclear Magnetic Resonance spectrometers at 600, 500, 400 or 300 MHz. Tetramethylsilane (TMS) (δ = 0.00 ppm) or residual protonated solvent peak of chloroform (δ = 7.26 ppm) were used as internal standards and data are reported as follows: chemical shift, multiplicity (s = singlet, d = doublet, t = triplet, q = quartet, qu = quintet, m = multiplet, and br = broad), integration and coupling constants in Hz. ^{13}C NMR spectra were recorded at 150, 125, 100 or 75 MHz. The solvent was used as internal standard ($CDCl_3$ δ =77.0) and spectra were obtained with complete proton decoupling. Infrared (IR) spectra were aquired using a Thermo Scientific Nicolet iS10 FTIR spectrometer and the wavenumbers are reported in reciprocal centimeters (cm^{-1}). Chiral high-performance liquid chromatography was perfomed on a Varian ProStar HPLC system. Diastereomer and regioisomer ratios were determined by integration of the ^{1}H NMR spectra of crude reaction mixtures.

3.4.2 Procedures and Characterization Data

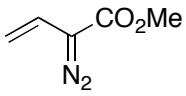

Methyl 2-diazobut-3-enoate (3.1).[49] To a solution of methyl acetodiazoacetate (9.77 g, 68.7 mmol, 1.0 eq) in MeOH/CH_2Cl_2 (1:1, 40 mL) cooled to 0°C, was added $NaBH_4$ (3.16 g, 83.5 mmol, 1.2 eq) in portions over ca 30 mins. The mixture was allowed to stir for 30 min at 0°C, then heated to r.t. and stirred for further 2 h, or until TLC-analysis shows full reduction. The reaction mixture was quenched by addition of ice water and extracted with CH_2Cl_2. The aqueous layer was extracted 6 times with CH_2Cl_2. The combined organic layers were dried over Na_2SO_4, filtered and concentrated *in vacuo* to afford the crude diazoalcohol as a yellow oil (6.38 g, 44.2 mmol, 64%) which was used further without purification. A dry 100 mL rbf was charged with diazo alcohol (3.19 g, 22.1 mmol, 1.0 eq), NEt_3 (12.5 mL, 89 mmol, 4.0 eq) and CH_2Cl_2 (10 mL). The mixture was cooled to 0°C under Ar-atmosphere and added $POCl_3$ (3.1 mL, 33.3 mmol, 1.5 eq) in CH_2Cl_2 (7 mL) by syringe pump over 30 mins. Evolution of HCl-gas was evident. The mixture was stirred at 0°C for ca 1 hr after addition, poured into a flask containing ice water and added to a separation funnel. Extracted the mixture with CH_2Cl_2 (3X), keeping the organic layers cooled in an ice bath, dried over Na_2SO_4, filtered and concentrated *in vacuo* with the flask immersed in an ice bath. The reaction afforded the highly volatile vinyldiazoacetate (564 mg, 45 mmol, 20%). Data for **3.1**: ^{1}H NMR (400 MHz, $CDCl_3$): δ 6.16 (dd, 1H, J = 17.2, 10.8 Hz), 5.12 (d, 1H, J = 10.8 Hz), 4.86 (d, 1H, J = 17.2 Hz), 3.81 (s, 3H). Consistent with published results.[49]

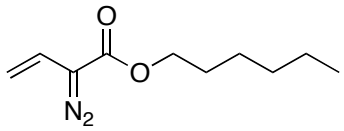

Hexyl 2-diazo-3-butenoate (3.23). According to published procedures.[7-9] A solution of 2,2,6-trimethyl-1,3-dioxolan-4-one (53.5 g, 0.38 mol) and hexanol (47 mL, 38.2 g, 0.37 mol, 1 equiv.) in xylenes (300 mL) was heated to 130-140°C for 1-1.5 h until all acetone was distilled off. The solvent was then removed *in vacuo*. The residue was diluted with MeCN (400 mL) and added *p*-ABSA (107 g, 0.45 mol, 1.2 equiv.) and NEt_3 (108 mL, 0.77 mol, 2.1 equiv.). The mixture was stirred vigorously for 10 h at ambient temperature. The thick suspension was then filtered, and the filtrate was concentrated *in vacuo*. The resulting residue was triturated with a 1:1 mixture of Et_2O/pet.ether (3 X 200 mL), dried over Na_2SO_4 and concentrated *in vacuo* to afford a yellow/orange oil. The oil was dissolved in a 1:1 mixture of CH_2Cl_2 and MeOH (500 mL) and cooled to 0°C in an ice bath. $NaBH_4$ was added in portions over 1.5 h and the mixture was stirred for several hours at ambient temperature. The mixture was then concentrated *in vacuo* and diluted with CH_2Cl_2. The organic phase was washed with water (3X), dried over Na_2SO_4 and concentrated *in vacuo* to afford a yellow oil. To a dry flask was added the oil, NEt_3 and CH_2Cl_2. The mixture was cooled to 0°C and added trifluoroacetic anhydride drop-wise over 30 min and stirred for further 2-3 h after addition at ambient temperature. The solvent was removed *in vacuo* and the residue was purified by column chromatography (5-10% Et_2O/pet.ether) to afford an orange liquid **3.23**. Data for **3.23**: TLC (10% Et_2O/pet.ether): R_f = 0.58. FTIR (neat): ν_{max}/cm^{-1} 2958, 2932, 2860, 2085, 1705, 1616, 1468, 1389, 1308, 1267, 1158, 1108. ^{1}H NMR (400 MHz, $CDCl_3$): δ 6.16 (dd, 1H, J = 17.2, 11.2 Hz), 5.11 (d, 1H, J = 11.2 Hz), 4.85 (d, 1H, J = 17.2 Hz), 4.20 (t, 2H, J = 6.4

Hz), 1.66 (m, 2H), 1.31 (m, 6H), 0.89 (t, 3H, J = 6.4 Hz). ^{13}C NMR (75 MHz, $CDCl_3$): δ 164.9, 120.5, 107.3, 65.3, 31.3, 28.7, 25.4, 22.5, 13.9. Missing carbon attributed to C=N_2. HRMS (EI): *m/z* 196.1206 ($C_{10}H_{16}N_2O_2$ requires 196.1206).

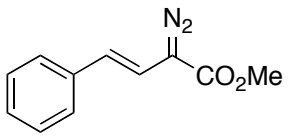

(*E*)-Methyl 2-diazo-4-phenylbut-3-enoate (3.9): See Section 5.4.2.

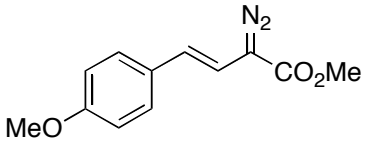

(E)-methyl 2-diazo-4-(4-methoxyphenyl)but-3-enoate (MeO-**3.9**). See Section 5.4.2.

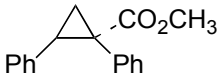

(±)-Methyl 1,2-diphenylcyclopropanecarboxylate (3.18). See Section 1.4.3.

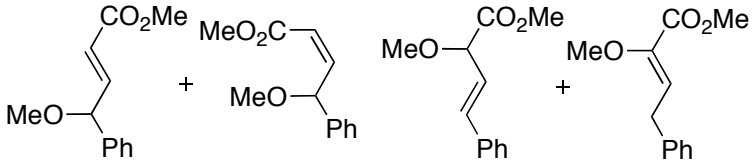

***E*-3.11** ***Z*-3.11** **3.10a** **3.10b**

Data for **(Z)-methyl 4-methoxy-4-phenylbut-2-enoate (*Z*-3.11).** ^{1}HNMR (500 MHz, $CDCl_3$): δ 7.47-7.28 (m, 5H), 6.32 (dd, 1H, J = 11.5, 9 Hz), 5.97 (d, 1H, J = 9 Hz), 5.87 (d, 1H, J = 11.5 Hz), 3.75 (s, 3H), 3.34 (s, 3H). Data for **(*E*)-methyl 4-methoxy-4-phenylbut-2-enoate (*E*-3.11)**. ^{1}H NMR (500 MHz, $CDCl_3$): δ 7.44-7.29 (m, 5H), 6.97 (dd, 1H, J = 6, 15.5 Hz), 6.10 (d, 1H, J = 15.5 Hz), 4.78 (d, 1H, J = 6 Hz), 3.72 (s, 3H), 3.33 (s, 3H). Data for **(*E*)-methyl 2-methoxy-4-phenylbut-3-enoate (3.10a) and (Z)-methyl 2-methoxy-4-phenylbut-2-enoate (3.10b)**. ^{1}H NMR (500 MHz, $CDCl_3$): δ 7.41-

7.28 (m, 5H), 6.77 (d, 1H, J = 15.5), 6.20 (dd, 1H, J = 7, 15.5), 4.43 (d, 1H, J = 7), 3.79 (s, 3H), 3.46 (s, 3H). Consistent with previously reported results.[11]

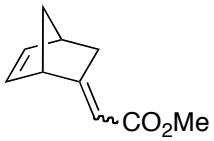

(±)-Methyl 2-(bicyclo[2.2.1]hept-5-en-2-ylidene)acetate (3.3). The diruthenium catalyst (0.002 mmol, 1 mol%) was added to a rigorously dried round-bottom flask kept under a dry argon atmosphere. Freshly distilled cyclopentadiene (0.33 g, 5.0 mmol, 20 equiv.) and CH_2Cl_2 (2 mL) was then added. Vinyldiazoacetate **3.1** (0.032 g, 0.25 mmol, 1.0 equiv.) was dissolved in CH_2Cl_2 (3 mL) and added to the reaction mixture over 2 h drop-wise by syringe pump. The mixture was then stirred for further 9-12 h at ambient temperature until complete consumption of the diazo compound was evident by TLC analysis. The solvent was removed *in vacuo* and the crude residue analyzed by ^{1}H-NMR. Purification by flash column chromatography (SiO_2, 10% Et_2O/pentane) resulted in mixture of *Z/E*-**3.3** as a colorless oil. With catalyst **I** (22 mg, 0.13 mmol, 54%): 2 : 1 isomer ratio; catalyst **II** (15.0 mg, 0.09 mmol, 37%): 2 : 1 isomer ratio; catalyst **VI** (16.4 mg, 0.10 mmol, 40%): 2.4 : 1 isomer ratio. Data for *E/Z*-**3.3**: ^{1}H NMR (400 MHz, $CDCl_3$): δ 6.28 (dd, J = 3.0, 5.5 Hz, 1H), 6.00 (dd, J = 3.0, 5.5 Hz, 1H), 5.92 (s, 1H), 3.67 (s, 3H), 3.32 (m, 1H), 3.08 (m, 1H), 2.57 (dm, 1H), 2.34 (dm, 1H), 1.70-1.67 (m, 1H), 1.47 (d, J = 8.0 Hz, 1H). Consistent with previously reported results.[44]

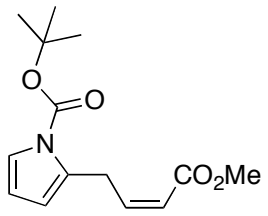

(*Z*)-*tert*-Butyl 2-(4-methoxy-4-oxobut-2-en-1-yl)-1H-pyrrole-1-carboxylate (*Z*-3.8). The diruthenium catalyst (0.002 mmol, 1 mol%) was dissolved in dry CH_2Cl_2 (2 mL) under an argon atmosphere, then added freshly distilled *N*-Boc pyrrole (20 equiv). Vinyldiazoacetate **3.1** (0.25 mmol, 1 equiv.) was dissolved in dry CH_2Cl_2 (3 mL) and added to the reaction mixture over 2 h by syringe pump addition. After addition, the reaction was stirred at ambient temperature for further 9-12 h, concentrated *in vacuo* and analyzed by ^{1}H NMR of the crude residue. Purification by flash column chromatography (10% Et_2O/pentane) resulted in *Z*-**3.8** as a colorless oil. Catalyst **I** (37.6 mg, 0.14 mmol, 57%): 11 : 1 *Z/E*-ratio; catalyst **II** (30 mg, 0.11 mmol, 45%): 13 : 1 *Z/E* -ratio; catalyst **VI** (35.6 mg, 0.13 mmol, 54%): 25 : 1 *Z/E* -ratio. Data for *Z*-**3.8**: TLC (10% Et_2O/pentane): R_f = 0.39. ^{1}H NMR (500 MHz, $CDCl_3$): δ 7.21 (m, 1H), 6.43 (dt, 1H, J = 11.5, 7.0 Hz), 6.08 (t, 1H, J = 3.0 Hz), 6.01 (m, 1H), 5.87 (m, 1H), 5.85 (m, 1H), 4.24 (d, 2H, J = 11.0 Hz), 3.73 (s, 3H), 1.59 (s, 9H). ^{13}C NMR (75 MHz, $CDCl_3$): δ 166.6, 149.4, 147.0, 132.6, 121.2, 119.5, 112.0, 110.1, 83.7, 51.1, 28.7, 28.0. FTIR (film): ν_{max}/cm^{-1} 2981, 1741, 1724, 1644, 1493, 1438, 1397, 1371, 1338, 1318, 1236, 1172, 1124, 1064. MS (ESI): *m/z* (rel.int.) 288 (31), 266 (100), 210 (17), 166 (46). HRMS (ESI): *m/z* 288.1208 ($C_{14}H_{19}O_4N$+Na requires 288.1206). Consistent with literature reports.[20]

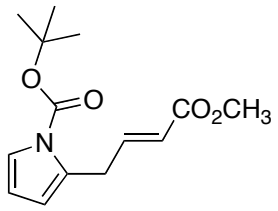

(*E*)-Methyl 4-(2-(*N*-(*tert*-butyl-1H-pyrrole-1-carboxylate)but-3-enoate. TLC (20% Et_2O/pet.ether): R_f = 0.30. FTIR (film): ν_{max}/cm^{-1} 2980, 2951, 1741, 1730, 1656, 1409, 1371, 1335, 1274, 1164, 1124, 1062. ^{1}H NMR (500 MHz, $CDCl_3$): δ 7.22 (m, 1H), 7.13 (dt, 1H, *J* = 15.5, 6.0 Hz), 6.10 (t, 1H, *J* = 3.5 Hz), 5.99 (m, 1H), 5.79 (d, 1H, *J* = 15.5 Hz), 3.77 (d, 2H, *J* = 6.0 Hz), 3.72 (s, 3H), 1.58 (s, 9H). ^{13}C NMR (125 MHz, $CDCl_3$): *δ* 166.9, 149.2, 146.4, 131.0, 121.9, 121.5, 112.6, 110.1, 83.7, 51.4, 31.5, 27.9, 79.7. HRMS (ESI): *m/z* 288.1210 ($C_{14}H_{19}O_4N$+Na requires 288.1206). Consistent with literature values.[20]

General Procedure for X–H insertions with Ag-catalyst: To a flame dry round-bottom flask, covered with Al-foil, was added Ag(I)-catalyst (0.05-0.1 equiv.), CH_2Cl_2 (5 mL) and substrate (1.5-20 equiv.) under an inert and dry argon-atmosphere. The mixture was then cooled to 0 °C in an ice/water bath. The vinyldiazoacetate (0.5 mmol, 1.0 equiv.) in CH_2Cl_2 (5 mL, 0.1 M) was added to the former solution drop-wise by syringe pump over 1-2 h. The reaction was then allowed to slowly reach ambient temperature and stirred for further 2-12 h until TLC analysis showed full conversion of the diazo compound. The solvent was then removed *in vacuo* and the residue purified by flash column chromatography (SiO_2, Et_2O/pentane mixtures) to afford the product(s).

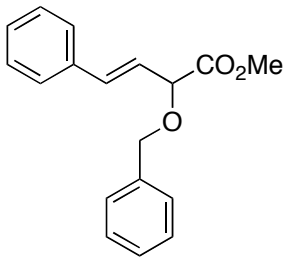

(*E*)-Methyl 2-benzyloxy-4-phenylbut-3-enoate (3.19). Colourless oil. FTIR (neat): ν_{max}/cm^{-1} 3028, 2951, 1748, 1450, 1435, 1199, 1096, 967, 734, 693. ^{1}H NMR (400 MHz, $CDCl_3$): δ 7.41-7.25 (m, 10H), 6.77 (d, 1H, J = 16 Hz), 6.25 (dd, 1H, J = 16, 7.2 Hz), 4.66 (q AB, 2H), 4.60 (d, 1H, J = 7.2 Hz), 3.77 (s, 3H). ^{13}C NMR (100 MHz, $CDCl_3$): δ 171.1, 137.1, 135.8, 134.4, 128.6, 128.5, 128.2, 128.0, 127.9, 126.7, 123.6, 78.5, 71.3, 52.3. HRMS (ESI): *m/z* 300.1592 ($C_{18}H_{18}O_3$+NH_4 requires 300.1594).

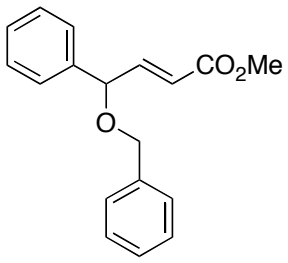

(*E*)-Methyl 4-benzyloxy-4-phenylbut-3-enoate (3.20). Colourless oil. TLC (20% Et_2O/pentane): R_f = 0.46. FTIR (neat): ν_{max}/cm^{-1} 3087, 3063, 3030, 2949, 2864, 1720, 1658, 1494, 1454, 1435, 1392, 1273, 1195, 1168, 1102, 1040, 1027. ^{1}H NMR (500 MHz, $CDCl_3$): δ 7.38-7.28 (m, 10H), 7.01 (dd, 1H, J = 16.0, 5.5 Hz), 6.15 (d, 1H, J = 16.0, 1.5 Hz), 4.98 (dd, 1H, J = 5.0, 1.5 Hz), 4.53 (d AB, 1H), 4.45 (d AB, 1H), 3.71 (s, 3H). ^{13}C NMR (75 MHz, $CDCl_3$): δ 166.7, 147.7, 138.9, 137.9, 137.8, 128.8, 128.4, 128.3, 127.7, 127.6, 127.2, 120.5, 79.7, 70.4, 51.6. HRMS (EI): *m/z* 282.1261 ($C_{18}H_{18}O_3$ requires 282.1250).

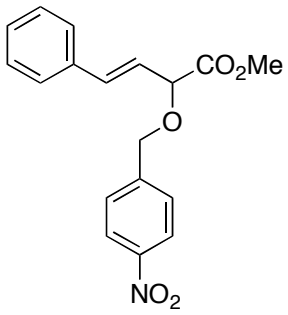

(*E*)-Methyl 2-((4-nitrobenzyl)oxy)-4-phenylbut-3-enoate (3.21a). TLC (10% Et_2O/hexane): R_f = 0.27. ^{1}H NMR (600 MHz, $CDCl_3$): δ 8.22 (d, 2H, J = 9 Hz), 7.57 (d, 2H, J = 8.4 Hz), 7.41 (d, 2H, J = 7.8 Hz), 7.34 (t, 2H, J = 8.4 Hz), 7.29 (t, 1H, J = 5.4 Hz), 6.79 (d, 1H, J = 16.2 Hz), 6.27 (dd, 1H, J = 16.2, 7.2 Hz), 4.78 (d AB, 1H, J = 13.2 Hz), 4.72 (d AB, 1H, J = 13.2 Hz), 4.64 (dd, 1H, J = 7.2, 1.2 Hz), 3.81 (s, 3H). ^{13}C NMR (150 MHz, $CDCl_3$): δ 170.6, 147.5, 144.9, 135.5, 134.9, 128.7, 128.5, 126.8, 123.7, 123.7, 123, 79.4, 70.0, 52.5. FTIR (film): ν_{max}/cm^{-1} 2924, 1747, 1518, 1344, 1107, 736, 691. MS (neg-APCI): *m/z* 326 (100%, M-H). HRMS (neg-APCI): *m/z* 326.10328 ($C_{18}H_{17}O_5N$-H requires 326.10340).

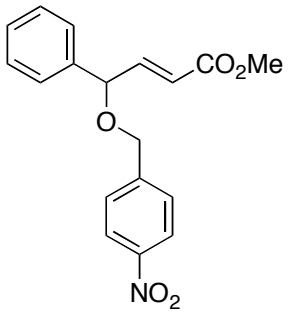

(*E*)-Methyl 4-((4-nitrobenzyl)oxy)-4-phenylbut-2-enoate (3.22a). ^{1}H NMR (400 MHz, $CDCl_3$): δ 8.21 (d, 2H, J = 8.8 Hz), 7.49 (d, 2H, J = 8.8 Hz), 7.40-7.33 (m, 5H), 7.02 (dd, 1H, J = 15.6, 5.2 Hz), 6.17 (dd, 1H, J = 15.6, 1.2 Hz), 5.02 (dd, 1H, J = 5.2, 1.2 Hz), 4.58 (t AB, 2H), 3.74 (s, 3H). ^{13}C NMR (100 MHz, $CDCl_3$): δ 166.5, 147.2, 146.9, 145.4, 138.1, 128.8, 128.6, 127.5, 127.1, 123.5, 120.5, 80.5, 69.1, 51.6. FTIR (film): ν_{max}/cm^{-1}

2950, 1720, 1519, 1344, 729, 699. HRMS (pos-APCI): *m/z* 328.11844 ($C_{18}H_{17}O_5N$+H requires 328.11795).

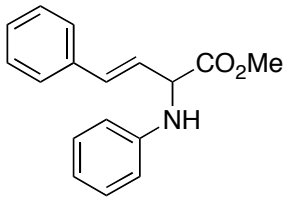

(*E*)-Methyl 4-phenyl-2-(phenylamino)but-3-enoate (3.21b). White solid. Mp = 64-66 °C. FTIR (film): ν_{max}/cm^{-1} 3396, 3024, 2952, 1735, 1601, 1504, 1432, 1202, 1158, 968, 748, 691. ^{1}H NMR (400 MHz, $CDCl_3$): δ 7.38 (dm, 2H, J = 7.2 Hz), 7.31 (tm, 2H, J = 6.8 Hz), 7.26-7.23 (m, 1H), 7.20-7.16 (tm, 2H), 6.81-6.73 (m, 2H), 6.66 (dm, 1H, J = 7.6 Hz), 6.29 (dd, 1H, J = 16, 6.0 Hz), 4.74 (br t, 1H, J = 6.0 Hz), 4.66 (br s, 1H), 3.80 (s, 3H). ^{13}C NMR (100 MHz, $CDCl_3$): δ 172.2, 146.2, 136.0, 133.0, 129.3, 128.6, 128.0, 126.7, 124.8, 118.3, 113.5, 58.8, 52.8. HRMS (ESI): *m/z* 268.13309 *(*$C_{17}H_{17}O_2N$+H requires 268.13321).

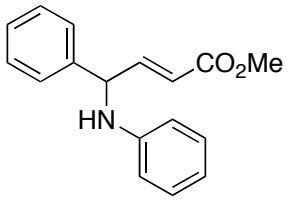

(*E*)-Methyl 4-phenyl-4-(phenylamino)but-2-enoate (3.22b). Colourless oil. FTIR (film): ν_{max}/cm^{-1} 3384, 3027, 2949, 1713, 1657, 1600, 1501, 1434, 1275, 1168. ^{1}H NMR (400 MHz, $CDCl_3$): δ 7.39-7.30 (m, 5H), 7.18-7.13 (m, 2.5H), 7.09 (d, 0.5H, J = 5.6 Hz), 6.74 (t, 1H, J = 7.6 Hz), 6.59 (d, 1H, J = 7.6 Hz), 6.10 (dd, 1H, J = 16.0, 1.6 Hz), 5.06 (d, 1H, J = 4.4 Hz), 4.05 (bs, 1H), 3.72 (s, 3H). ^{13}C NMR (100 MHz, $CDCl_3$): δ 166.8, 148.0, 146.6, 139.9, 129.2, 129.1, 128.2, 127.4, 121.4, 118.2, 113.5, 59.5, 51.6. HRMS (ESI): *m/z* 268.13315 ($C_{17}H_{17}O_2N$+H requires 268.13321).

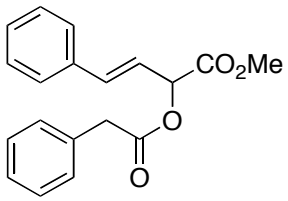

(*E*)-Methyl 4-phenyl-2-(2-phenylacetoxy)but-3-enoate (3.21c). Colourless oil. FTIR (neat): ν_{max}/cm^{-1} 3029, 2953, 1740, 1497, 1454, 1436, 1206, 1142, 1029, 967. ^{1}H NMR (400 MHz, $CDCl_3$): δ 7.38-7.25 (m, 10H), 6.73 (d, 1H, J = 16 Hz), 6.25 (dd, 1H, J = 16, 7.2 Hz), 5.65 (dd, 1H, J = 7.2, 1.2 Hz), 3.79 (bs, 2H), 3.75 (s, 3H). ^{13}C NMR (100 MHz, $CDCl_3$): δ 170.7, 168.9, 135.4, 135.2, 133.3, 129.4, 128.6, 128.6, 127.2, 126.8, 120.5, 73.3, 52.7, 40.9. HRMS (ESI): *m/z* 328.15422 (M+NH_4 requires 328.15433).

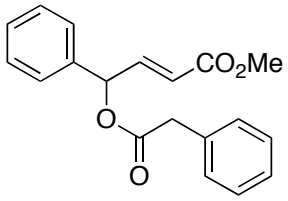

(*E*)-Methyl 4-phenyl-4-(2-phenylacetoxy)but-2-enoate (3.22c). Colourless oil. TLC (20% EtOAc/hexane): R_f = 0.42. FTIR (neat): ν_{max}/cm^{-1} 3031, 2950, 1722, 1661, 1243, 1170, 1139, 978, 696. ^{1}H NMR (400 MHz, $CDCl_3$): δ 7.36-7.25 (m, 10H), 6.98 (dd, 1H, J = 15.6, 5.2 Hz), 6.39 (dd, 1H, J = 5.2, 1.6 Hz), 5.94 (dd, 1H, J = 15.6, 1.6 Hz), 3.71 (s, 3H), 3.69 (s, 2H). ^{13}C NMR (100 MHz, $CDCl_3$): δ 170.1, 166.2, 144.6, 136.9, 133.4, 129.2, 128.7, 128.7, 128.6, 127.2, 121.2, 74.4, 51.7, 41.3 MS (ESI): *m/z* 328 (100), 278 (4). HRMS (ESI): *m/z* 328.15431 (M+NH_4 requires 328.15433).

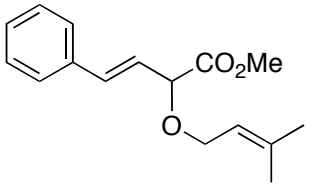

(*E*)-Methyl 2-(3-methylbut-2-enoxy)-4-phenylbut-3-enoate (3.21d). TLC (20% Et_2O/hexane): R_f= 0.24. ^{1}H NMR (400 MHz, $CDCl_3$): δ 7.41-7.39 (m, 2H), 7.35-7.31 (m, 2H), 7.28-7.24 (m, 1H), 7.76 (d, 1H, *J* = 16 Hz), 6.23 (dd, 1H, *J* = 16, 6.8 Hz), 5.40 (tt, 1H, *J* = 7.2, 1.2 Hz), 4.57 (dd, 1H, *J* = 7.2, 1.6 Hz), 4.10 (m AB, 2H), 3.78 (s, 3H), 1.77 (s, 3H), 1.68 (s, 3H). ^{13}C NMR (125 MHz, $CDCl_3$): δ 171.4, 138.4, 135.9, 134.1, 128.6, 128.2, 126.7, 124, 120.1, 78.5, 65.9, 52.3, 25.8, 18.1. FTIR (film): ν_{max}/cm^{-1} 2915, 1750, 1198, 967, 736, 691. HRMS (pos-APCI): *m/z* 261.14851 ($C_{16}H_{20}O_3$+H requires 261.14852).

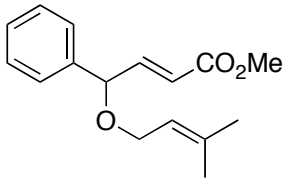

(*E*)-Methyl 4-(3-methylbut-2-enoxy)-4-phenylbut-2-enoate (3.22d). Yellow oil. FTIR (neat film): ν_{max} (cm^{-1}) 3063, 3029, 2973, 2949, 2858, 1724, 1659, 1493, 1453, 1436, 1378, 1303, 1271, 1245, 1195, 1168, 1115, 1061, 1026. ^{1}H NMR (500 MHz, $CDCl_3$): *δ* 7.37-7.30 (m, 5H), 6.99 (dd, 1H, *J* = 15.5, 5.5 Hz), 6.07 (d, 1H, *J* = 15.5 Hz), 5.36 (m, 1H), 4.94 (d, 1H, *J* = 5.5 Hz), 3.95 (d, 2H, *J* = 7.0 Hz), 3.72 (s, 3H), 1.74 (s, 3H), 1.59 (s, 3H). ^{13}C NMR (75 MHz, $CDCl_3$): *δ* 166.7, 148.0, 139.3, 137.4, 128.6, 128.1, 127.1, 120.7, 120.4, 79.6, 65.2, 51.5, 25.7, 18.0. HRMS (ESI): *m/z* 260.1406 ($C_{16}H_{20}O_3$ requires 260.1407).

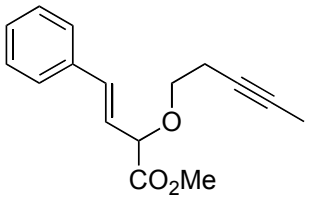

(*E*)-Methyl 2-(pent-3-ynoxy)-4-phenylbut-2-enoate (3.21e). TLC (20% Et_2O/hexane): R_f = 0.32. ^{1}H NMR (400 MHz, $CDCl_3$): δ 7.41-7.38 (m, 2H), 7.35-7.31 (m, 2H), 7.29-7.25 (m, 1H), 6.78 (d, 1H, *J* = 16 Hz), 6.22 (dd, 1H, *J* = 16, 7.2 Hz), 4.59 (dd, 1H, *J* = 7.2, 1.6 Hz), 3.78 (s, 3H), 3.70-3.59 (m, 2H), 2.54-2.48 (m, 2H), 1.77 (t, 3H, *J* = 2.4 Hz). ^{13}C NMR (125 MHz, $CDCl_3$): δ 171 (4°), 135.8 (4°), 134.2 (3°), 128.6 (3°), 128.2 (3°), 126.7 (3°), 123.6 (3°), 79.9 (3°), 77 (4°), 75.2 (4°), 68.4 (2°), 52.3 (1°), 20 (2°), 3.5 (1°). FTIR (film): ν_{max}/cm^{-1} 2919, 1749, 1198, 1107, 967, 736, 691. MS (neg-APCI): *m/z* 257 (100%, M-H), 219 (4%), 197 (3%), 190 (11%). HRMS (neg-APCI): *m/z* 257.11823 ($C_{16}H_{18}O_3$-H requires 257.11832).

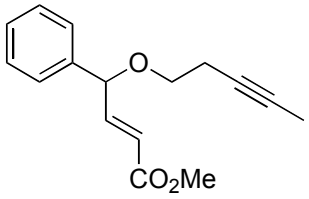

(*E*)-Methyl 4-(pent-3-ynoxy)-4-phenylbut-2-enoate (3.22e). TLC (15% Et_2O/pentane): R_f = 0.33. ^{1}H NMR (400 MHz, $CDCl_3$): δ 7.38-7.29 (m, 5H), 6.97 (dd, 1H, *J* = 15.6, 5.6 Hz), 6.12 (dd, 1H, *J* = 15.6, 1.6 Hz), 4.95 (dd, 1H, *J* = 5.2, 1.6 Hz), 3.72 (s, 3H), 3.55-3.46 (m, 2H), 2.46-2.40 (m, 2H), 1.77 (t, 3H, *J* = 2.8 Hz). ^{13}C NMR (100 MHz, $CDCl_3$): δ 166.7, 147.6, 138.9, 128.7, 128.3, 127.1, 120.4, 80.8, 76.8, 75.6, 67.6, 51.6, 20.1, 3.4. FTIR (film): ν_{max}/cm^{-1} 2918, 1722, 1271, 1167, 1103, 699. MS (neg-APCI): *m/z* 257 (100%), 219 (5%), 190 (5%). HRMS (neg-APCI): *m/z* 257.11827 ($C_{16}H_{18}O_3$-H requires 257.11832).

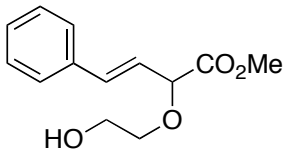

(*E*)-Methyl 2-(2-hydroxyethoxy)-4-phenylbut-3-enoate (3.21f). TLC (40% EtOAc/hexanes): R_f = 0.16. ^{1}H NMR (400 MHz, $CDCl_3$): δ 7.40 (d, 2H, *J* = 7.6 Hz), 7.35-7.26 (m, 3H), 6.78 (d, 1H, *J* = 15.6 Hz), 6.23 (dd, 1H, *J* = 16.4, 7.2 Hz), 4.60 (dd, 1H, *J* = 7.2, 1.6 Hz), 3.83-3.74 (m, 3H), 3.79 (s, 3H), 3.68-3.62 (m, 1H), 2.57 (t, 1H, *J* = 6 Hz). ^{13}C NMR (150 MHz, $CDCl_3$): δ 171.4, 135.7, 134.3, 128.6, 128.3, 126.7, 123.4, 79.9, 71.4, 61.7, 52.4. FTIR (film): ν_{max}/cm^{-1} 3456 (OH), 2952, 1736, 1065, 969, 738, 692. HRMS (ESI): *m/z* 259.09393 ($C_{13}H_{16}O_4$+Na requires 259.09408).

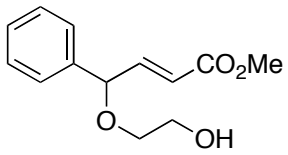

(*E*)-Methyl 4-(2-hydroxyethoxy)-4-phenylbut-2-enoate (3.22f). TLC (40% EtOAc/hexanes): R_f = 0.25. ^{1}H NMR (600 MHz, $CDCl_3$): δ 7.37 (t, 2H, *J* = 6.6 Hz), 7.33-7.30 (m, 3H), 6.99 (dd, 1H, *J* = 15.6, 5.4 Hz), 6.10 (dd, 1H, *J* = 15.6, 1.8 Hz), 4.96 (dd, 1H, *J* = 5.4, 1.2 Hz), 3.75 (bs, 2H), 3.73 (s, 3H), 3.73-3.55 (m, 1H), 3.53-3.50 (m, 1H), 2.06 (s, 1H). ^{13}C NMR (150 MHz, $CDCl_3$): δ 166.7, 147.3, 138.7, 128.8, 128.4, 127.1, 120.5, 81.2, 70.1, 61.9, 51.6. FTIR (film): ν_{max}/cm^{-1} 3428 (OH), 2950, 1719, 1274, 1169, 1042, 699. MS (ESI): *m/z* 259 (100%, M+Na). HRMS (ESI): *m/z* 259.09395 ($C_{13}H_{16}O_4$+Na requires 259.09408).

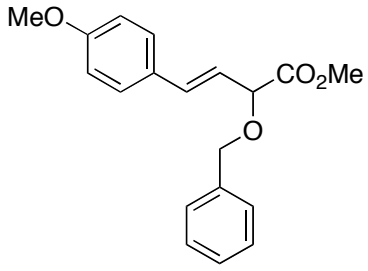

(*E*)-Methyl 2-(benzyloxy)-4-(4-methoxyphenyl)but-3-enoate (3.21g). TLC (20% EtOAc/hexanes): R_f = 0.27. ^{1}H NMR (400 MHz, $CDCl_3$): δ 7.40-7.29 (m, 7H), 6.86 (dt, 2H, *J* = 8.8, 2.8 Hz), 6.70 (d, 1H, *J* = 16 Hz), 6.11 (dd, 1H, *J* = 16, 6.8 Hz), 4.64 (q AB, 2H), 4.57 (dd, 1H, *J* = 7.6, 0.8 Hz). ^{13}C NMR (100 MHz, $CDCl_3$): δ 171.3, 159.7, 137.2, 134.2, 128.6, 128.5, 128, 128, 127.9, 121.4, 114, 78.8, 71.1, 55.3, 52.3. FTIR (film): ν_{max}/cm^{-1} 2923, 1747, 1511, 1251, 1174, 1028, 698. HRMS (ESI): *m/z* 335.12495 ($C_{19}H_{20}O_4$+Na requires 335.12538).

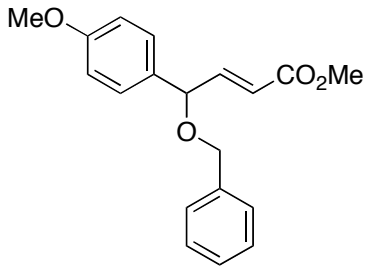

(*E*)-Methyl 4-benzyloxy-4-(4-methoxyphenyl)but-2-enoate (3.22g). TLC (20% Et_2O/pentane): R_f = 0.21. ^{1}H NMR (400 MHz, $CDCl_3$): δ 7.36-7.28 (m, 5H), 7.25 (dt, 2H, *J* = 8.8, 2.0 Hz), 7.00 (dd, 1H, *J* = 15.6, 5.2 Hz), 6.90 (dt, 2H, *J* = 8.8, 2.0 Hz), 6.13 (dd, 1H, *J* = 15.6, 2.0 Hz), 4.94 (dd, 1H, *J* = 5.2, 1.6 Hz), 4.47 (q AB, 2H), 3.81 (s, 3H), 3.72 (s, 3H). ^{13}C NMR (100 MHz, $CDCl_3$): δ 166.8, 159.6, 147.9, 137.9, 130.8, 128.6, 128.4, 127.6, 127.6, 120.1, 114.1, 79.2, 70.1, 55.3, 51.6. FTIR (film): ν_{max}/cm^{-1} 2950, 1721, 1510, 1246, 1167, 1028, 831. MS (neg-APCI): *m/z* 311 (100%, M-H), 279 (20%), 264 (9%). HRMS (neg-APCI): *m/z* 311.1287 ([$C_{19}H_{20}O_4$-H] requires 311.12888).

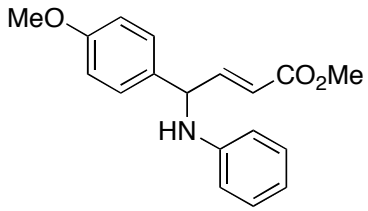

(*E*)-Methyl 4-(4-methoxyphenyl)-4-(phenylamino)but-2-enoate (3.22h). TLC (30% Et_2O/hexanes): R_f = 0.25. ^{1}H NMR (600 MHz, $CDCl_3$): δ 7.82 (d, 2H, *J* = 7.8 Hz), 7.70 (s, 1H), 7.48 (t, 1H, *J* = 7.8 Hz), 7.35 (t, 2H, *J* = 7.8 Hz), 7.21 (bs, 5H), 3.85 (s, 3H), 6.07 (dd, 1H, *J* = 15.6, 1.2 Hz), 4.99 (bt, 1H, *J* = 4.8 Hz), 4.02 (bd, 1H, *J* = 3.6 Hz), 3.78 (s, 3H), 3.70 (s, 3H). ^{13}C NMR (150 MHz, $CDCl_3$): δ 166.8, 159.4, 148.3, 146.6, 131.9, 129.1, 128.6, 121.1, 118.0, 114.3, 113.4, 58.9, 55.2, 51.5. FTIR (film): ν_{max}/cm^{-1} 3385, 2950, 1713, 1600, 1502, 1246, 1168. MS (neg-APCI): *m/z* 296 (100%, M-H), 264 (26%, M-H-OMe). HRMS (neg-APCI): *m/z* 296.12923 ($C_{18}H_{19}O_3N$-H requires 296.12922).

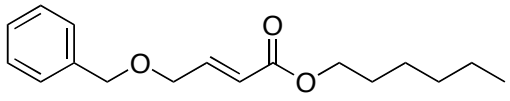

(*E*)-Hexyl 4-benzyloxybut-2-enoate (3.26). TLC (10% Et_2O/hex): R_f = 0.22. ^{1}H NMR (400 MHz, $CDCl_3$) δ 7.37-7.30 (m, 5H), 6.98 (dt, 1H, *J* = 15.6, 4.4 Hz), 6.14 (dt, 1H, *J* = 15.6, 2.0 Hz), 4.57 (s, 2H), 4.19 (dd, 2H, *J* = 4.4, 2.0 Hz), 4.14 (t, 2H, *J* = 6.4 Hz), 1.69-1.62 (m, 2H), 1.40-1.27 (m, 6H), 0.89 (t, 3H, *J* = 6.8 Hz). ^{13}C NMR (125 MHz, $CDCl_3$): δ 166.3, 144.1, 137.7, 128.4, 127.8, 127.6, 121.4, 72.7, 68.6, 64.6, 31.4, 28.6, 25.5, 22.5, 14. IR (film): ν_{max}/cm^{-1} 2930, 1718, 1271, 1169, 1119, 1022, 697. HRMS (pos-APCI): m/z 277.17979 (M+H requires 277.17982).

General procedure for preparation of 4-aryl-4-alkoxyvinyldiazoacetates from vinylogous O–H insertion products: To a flame-dry round-bottom flask purged with argon was added the appropriate 4-alkoxy-4-arylbut-2-enoate (1.0 equiv.), *p*-ABSA (1.3 equiv.) and MeCN. The mixture was cooled to 0 °C in an ice/water bath while maintaining a positive argon atmosphere, then added DBU (2.0 equiv.) in one shot, and allowed the mixture to stir for 6-12 h until full conversion of the starting material was observed by TLC. The reaction was then quenched with NH_4Cl (aq) and poured into a separation funnel. The organic layer was partitioned between Et_2O and water, then the organics were washed with water (2X), brine (1X) and dried over $MgSO_4$. The solution was filtered and concentrated *in vacuo*. The crude residue was then analyzed by ^1H NMR and purified by gradient flash column chromatography (SiO_2, Et_2O/pentane mixtures).

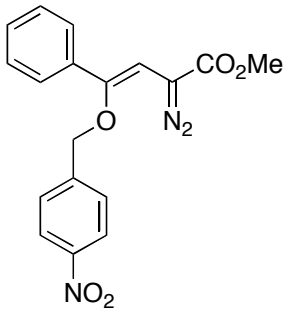

(*Z*)-Methyl-4-(4-nitrobenzyloxy)-4-phenyl-2-diazobut-3-enoate (3.42a). ^1H NMR (400 MHz, $CDCl_3$): δ 8.24 (d, 2H), 7.48 (d, 2H,), 7.45-7.31 (m, 5H), 5.55 (s, 1H), 4.79 (s, 2H), 3.81 (s, 3H). ^{13}C NMR (100 MHz, $CDCl_3$): δ 166.5, 149.6, 147.6, 143.3, 134.4, 128.8, 128.4, 128.2, 125.8, 123.7, 97, 71.2, 52.4. Missing carbon attributed to $C=N_2$. FTIR (neat film): ν_{max}/cm^{-1} 2079, 1697, 1519, 1344, 1232, 1107, 1058. HRMS (pos-APCI): *m/z* 354.10872 (M+H requires 354.10845).

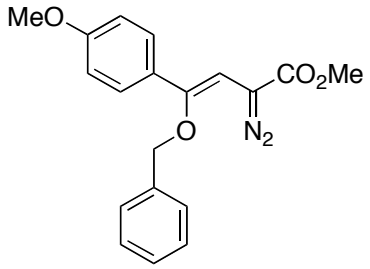

(*Z*)-Methyl 4-benzyloxy-2-diazo-4-(4-methoxyphenyl)but-3-enoate (3.42c). TLC (30% Et_2O/hexane): R_f = 0.36. ^1H NMR (600 MHz, $CDCl_3$): δ 7.40 (d, 2H, *J* = 9 Hz), 7.38-7.33 (m, 3H), 7.30 (d, 2H, *J* = 9 Hz), 6.92 (dm, 2H, *J* = 9.6 Hz), 5.34 (s, 1H), 4.68 (s, 2H), 3.84 (s, 3H), 3.79 (s, 3H). ^{13}C NMR (125 MHz, $CDCl_3$): δ 167, 159.6, 150, 136.1, 128.4, 128.2, 128.1, 127.6, 127.4, 114, 94.5, 72.6, 55.2, 52.2. Missing carbon at tributed to $C=N_2$. FTIR (film): ν_{max}/cm^{-1} 2952, 2079, 1696, 1509, 1236, 728, 697. HRMS (pos-APCI): *m/z* 311.12775 ($C_{19}H_{18}O_4$+H requires 311.12779).

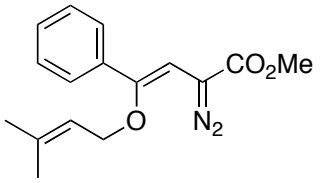

(*Z*)-Methyl 2-diazo-4-(3-methyl-but-2-enoxy)-4-phenylbut-3-enoate (3.42b). TLC (10% Et_2O/hexanes): R_f = 0.19. ^1H NMR (400 MHz, $CDCl_3$): δ 7.43 (dm, 2H, *J* = 7.2 Hz), 7.36 (tm, 2H, *J* = 7.6 Hz), 7.29 (dm, 1H, *J* = 7.6 Hz), 5.45 (s, 1H), 5.36 (tm, 1H, *J* = 7.6 Hz), 4.19 (d, 2H, *J* = 6.8 Hz), 3.83 (s, 3H), 1.76 (s, 3H), 1.54 (s, 3H). ^{13}C NMR (125 MHz, $CDCl_3$): δ 166.9, 150.1, 138.6, 135.3, 128.4, 127.8, 125.7, 118.9, 95.7, 67.3, 52.1, 25.6, 17.8. Missing carbon attributed to $C=N_2$. FTIR (film): ν_{max}/cm^{-1} 2952, 2080, 1698, 1231, 1106, 1051, 731. MS (pos-APCI): *m/z* 287 (12%, M+H), 259 (100%, M+H-N2). HRMS (pos-APCI): *m/z* 287.1389 ($C_{16}H_{18}O_3N_2$+H requires 287.13902).

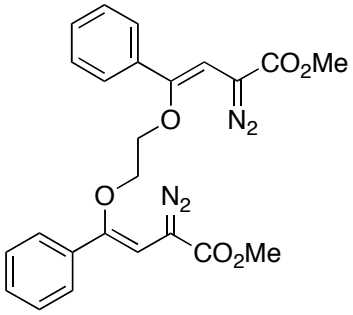

(3*Z*,3'*Z*)-dimethyl 4,4'-(ethane-1,2-diylbis(oxy))bis(2-diazo-4-phenylbut-3-enoate) (3.42d). TLC (10% Et_2O/pentane): R_f = 0.19. ^{1}H NMR (600 MHz, $CDCl_3$): δ 7.44 (d, 4H, *J* = 7.2 Hz), 7.36 (t, 4H, *J* = 7.8 Hz), 7.29 (t, 2H, *J* = 7.2 Hz), 5.50 (s, 2H), 3.86 (s, 4H), 3.82 (s, 6H). ^{13}C NMR (150 MHz, $CDCl_3$): δ 166.8, 150, 134.6, 128.6, 128.1, 125.9, 96.1, 68.7, 52.3. Missing carbon attributed to C=N_2. FTIR (film): ν_{max}/cm^{-1} 2952, 2079, 1694, 1312, 1231, 730, 697. MS (pos-APCI): *m/z* 435 (100%, M+H-N_2), HRMS (pos-APCI): *m/z* 435.15531 ($C_{24}H_{23}O_6N_2$ requires 435.15506).

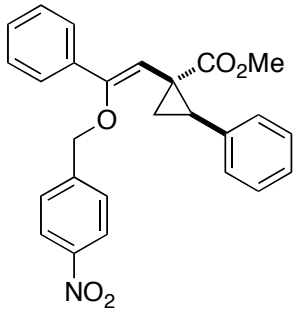

(1*S*,2*R*)-methyl 1-((*Z*)-2-((4-nitrobenzyl)oxy)-2-phenylvinyl)-2-phenylcyclopropane-carboxylate (3.43). To a flame-dry round-bottom flask, kept under a dry argon atomsphere, was added Rh(II)-catalyst (0.02 equiv.), trifluorotoluene (TFT, 10 mL) and styrene (10 equiv.), purified by passage through a plug of silica gel. (*Z*)-Methyl-4-(4-nitrobenzyloxy)-4-phenyl-2-diazobut-3-enoate (**3.42a**) (1.0 equiv.) was dissolved in TFT/CH_2Cl_2 (~9 : 1 ratio, CH_2Cl_2 added for solubility), then added drop-wise to the former solution at ambient temperature by syringe pump over 2 h. The mixture was

allowed to stir at ambient temperature for further 4-6 h. The solvent was then removed *in vacuo* and the crude residue analyzed by ^{1}H NMR. The crude product was then purified by flash column chromatography (25-35% Et_2O/pentane). Data for **3.43**: TLC (30% Et_2O/pentane): R_f = 0.28. HPLC (Chiracel OD, 3% *i*-PrOH/hexanes, 1 ml/min, ~1 mg/mL): t_R = 15.2, 18.5 min. ^{1}H NMR (400 MHz, $CDCl_3$): δ 8.24 (d, 2H, *J* = 8.8 Hz), 7.48 (d, 2H, *J* = 8.8 Hz), 7.30-7.18 (m, 8H), 7.11 (d, 1H, *J* = 7.2 Hz), 4.94 (s, 1H), 4.70 (d AB, *J* = 13 Hz), 4.54 (d AB, 1H, *J* = 13 Hz), 3.68 (s, 3H), 2.93 (dd, 1H, *J* = 9.6, 7.6 Hz), 2.07 (dd, 1H, *J* = 9.2, 4.8 Hz), 1.71 (dd, 1H, *J* = 6.8, 4.4 Hz). FTIR (film): ν_{max}/cm^{-1} 1716, 1520, 1346, 735, 697. HRMS (pos-APCI): *m/z* 430.16479 ($C_{26}H_{23}O_5N$+H requires 430.1649).

General Procedure for C–C bond forming reactions with Ag-catalyst: To a flame dry round-bottom flask covered with Al-foil was added Ag(I)-catalyst (0.05-0.1 equiv.), CH_2Cl_2 (5 mL) and substrate (1.5-20 equiv.) under an inert Ar-atmosphere. The mixture was then cooled to 0 °C in an ice/water bath. The vinyldiazoacetate (0.5 mmol, 1.0 equiv.) in CH_2Cl_2 (5 mL, 0.1 M), was added to the former solution drop-wise by syringe pump addition over 1-2 h. The reaction was then allowed to reach ambient temperature and stirred for further 2-12 h until periodic TLC analysis shows full conversion of the diazo compound. The solvent was then removed *in vacuo* and the residue purified by column chromatography (SiO_2, Et_2O/pentane mixtures) to afford the product(s).

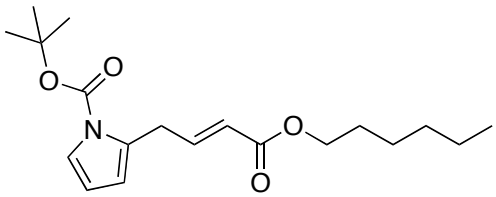

(*E*)-*tert*-butyl 2-(4-(hexyloxy)-4-oxobut-2-en-1-yl)-1*H*-pyrrole-1-carboxylate (*E*-3.27). Colourless oil. FTIR (neat): ν_{max}/cm^{-1} 2956, 2932, 2859, 1740, 1720, 1655, 1493, 1330, 1313, 1266, 1161, 1121, 1061. ^{1}H NMR (400 MHz, $CDCl_3$): δ 7.23 (dd, 1H, J = 3.2, 1.6 Hz), 7.11 (dt, 1H, J = 16.0, 6.4 Hz), 6.10 (t, 1H, J = 3.2 Hz), 5.99 (m, 1H), 5.78 (dt, 1H, J = 15.6, 1.6 Hz), 4.12 (t, 2H, J = 6.8 Hz), 3.76 (d, 2H, J = 6.4 Hz), 1.64 (m, 2H), 1.58 (s, 9H), 1.37 (m, 6H), 0.89 (t, 3H, J = 6.8 Hz). ^{13}C NMR (100 MHz, $CDCl_3$): δ 166.7, 149.2, 146.1, 131.1, 122.3, 121.5, 112.7, 110.1, 83.8, 64.4, 31.5, 31.4, 28.6, 27.9, 25.6, 22.5, 14.0. HRMS (pos-APCI): *m/z* 336.2155 ([$C_{19}H_{28}O_4N$] requires 336.2169).

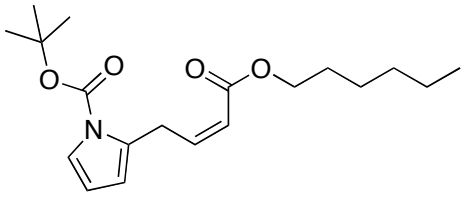

(*Z*)-*tert*-butyl 2-(4-(hexyloxy)-4-oxobut-2-en-1-yl)-1*H*-pyrrole-1-carboxylate (*Z*-3.27). Colourless oil. FTIR (neat): ν_{max}/cm^{-1} 2957, 2932, 2860, 1743, 1720, 1644, 1493, 1458, 1406, 1371, 1337, 1319, 1236, 1172, 1124, 1064. ^{1}H NMR (400 MHz, $CDCl_3$): δ 7.22 (bs, 1H), 6.40 (dt, 1H, J = 11, 7.0 Hz), 6.08 (bs, 1H), 6.01 (bs, 1H), 5.85 (d, 1H, J = 12.0 Hz), 4.23 (d, 2H, J = 6.5 Hz), 4.12 (t, 2H, J = 7.0 Hz), 1.67 (m, 2H), 1.58 (s, 9H), 1.37 (m, 2H), 1.31 (m, 4H), 0.89 (t, 3H, J = 7.0 Hz). ^{13}C NMR (75 MHz, $CDCl_3$): δ 166.4, 149.4, 146.5, 132.7, 121.2, 120.0, 112.0, 110.1, 83.7, 64.2, 31.4, 28.7, 28.6, 27.9, 25.6, 22.5, 14.0. MS (EI): *m/z* (rel. int) 336 (19), 252 (31), 236 (100). HRMS (EI): *m/z* 336.2168 ([$C_{19}H_{28}O_4N$+H] requires 336.2169).

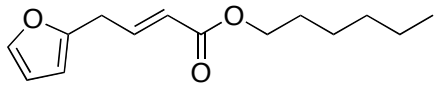

(*E*)-hexyl 4-(furan-2-yl)but-2-enoate (3.29). TLC (5% Et_2O/pentane): R_f = 0.30. FTIR (neat): ν_{max}/cm^{-1} 2956, 2931, 2859, 1721, 1658, 1597, 1506, 1467, 1384, 1333, 1305, 1275, 1185, 1061, 101, 982, 936, 731. ^{1}H NMR (500 MHz, $CDCl_3$): δ 7.34 (m, 1H), 7.02 (dt, 1H, *J* = 15.5, 7.0 Hz), 6.31 (m, 1H), 6.08 (d, 1H, *J* = 2.5 Hz), 5.88 (dt, 1H, *J* = 15.5, 1.5 Hz), 4.12 (t, 2H, *J* = 7.0 Hz), 3.54 (d, 2H, *J* = 6.5 Hz), 1.65 (m, 2H), 1.39-1.26 (m, 6H), 0.89 (t, 3H, *J* = 7.0 Hz). ^{13}C NMR (75 MHz, $CDCl_3$): δ 166.3, 151.3, 143.6, 141.8, 123.3, 110.4, 106.6, 64.6, 31.4, 30.8, 28.6, 25.6, 22.5, 14.0. LRMS (EI): *m/z* (rel.int) 236 (45), 152 (100), 135 (50), 107 (87), 79 (37). HRMS (EI): *m/z* 236.1412 ([$C_{14}H_{20}O_3$] requires 236.1407).

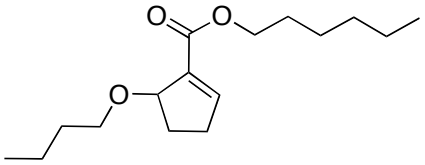

Hexyl 5-butoxycyclopent-1-enecarboxylate (3.30). Colourless oil. FTIR (neat): ν_{max}/cm^{-1} 2956, 2931, 2860, 1717, 1639, 1290, 1255, 1088. ^{1}H NMR (600 MHz, $CDCl_3$): δ 6.98 (t, 1H, *J* = 3.0 Hz), 4.68 (d, 1H, *J* = 7.2 Hz), 4.19-4.11 (m, 2H), 3.55-3.48 (m, 2H), 2.67 (dt, 1H, *J* = 18, 6.0 Hz), 2.40 (ddt, 1H, *J* = 18, 12, 3.5 Hz), 2.15-2.09 (m, 1H), 2.00-1.96 (m, 1H), 1.66 (q, 1H, *J* = 6.0 Hz), 1.54 (qu, 2H, *J* = 6.0 Hz), 1.40-1.35 (m, 4H), 1.33-1.30 (m, 6H), 0.91 (t, 3H, *J* = 6.0 Hz), 0.89 (t, 3H, *J* = 6.0 Hz). ^{13}C NMR (150 MHz, $CDCl_3$): δ 164.7, 147.8, 137.4, 82.3, 69.4, 64.3, 32.1, 31.5, 31.2, 30.5, 28.6, 25.7, 22.5, 19.3, 14.0, 13.9. HRMS (pos-APCI): *m/z* 269.2112 ([$C_{16}H_{28}O_3$+H] requires 269.2111.

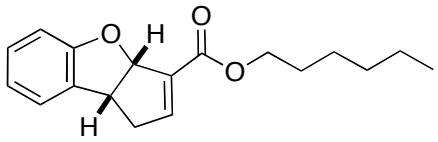

Hexyl 3a,8b-dihydro-1*H*-cyclopenta[b]benzofuran-3-carboxylate (3.31). TLC (10% EtOAc/pet.ether): R_f = 0.41. IR (neat): ν_{max}/cm^{-1} 2957, 2931, 2859, 1711, 1615, 1595, 1476, 1465, 1385, 1344, 1287, 1300, 1255, 1241, 1159, 1062, 1027, 984, 748. ^{1}H NMR (500 MHz, $CDCl_3$): δ 7.36 (d, 1H, *J* = 7.5 Hz), 7.16 (t, 1H, *J* = 7.5 Hz), 6.93 (t, 1H, *J* = 7.5 Hz), 6.82 (d, 1H, *J* = 7.5 Hz) 5.30 (dd, 1H, *J* = 17.5, 10.5 Hz), 5.19-5.16 (m, 2H), 5.09 (d, 1H, *J* = 10.5 Hz), 4.13 (t, 2H, *J* = 7.0 Hz), 3.51 (d, 1H, *J* = 4.5 Hz), 1.65 (m, 2H), 1.31 (m, 6H), 0.89 (t, 3H, *J* = 7.0 Hz). ^{13}C NMR (75 MHz, $CDCl_3$): δ 172.3, 160.6, 128.2, 125.7, 125.2, 125.2, 123.3, 121.2, 109.8, 70.9, 65.6, 37.2, 31.4, 28.5, 27.1, 25.5, 22.5, 13.9. MS (EI): *m/z* (rel.int) 202 (100), 184 (54), 157 (93), 286 (33). HRMS (EI): *m/z* 286.1558 ([$C_{18}H_{22}O_3$] requires 286.1563).

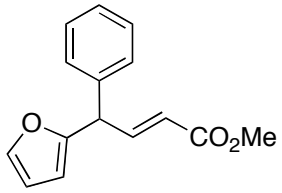

(*E*)-methyl 4-(furan-2-yl)-4-phenylbut-2-enoate (3.33). FTIR (neat): ν_{max}/cm^{-1} 3029, 2950, 1723, 1654, 1495, 1454, 1435, 1314, 1272, 1236, 1195, 1166, 1038, 1010, 982, 913, 742, 700. ^{1}H NMR (500 MHz, $CDCl_3$): δ 7.37-7.25 (m, 5H), 7.20 (d, 2H, *J* = 7.0 Hz), 6.32 (m, 1H), 6.07 (d, 1H, *J* = 3.0 Hz), 5.79 (dd, 1H, *J* = 15.5, 1.0 Hz), 4.88 (d, 1H, *J* = 7.0 Hz), 3.72 (s, 3H). ^{13}C NMR (75 MHz, $CDCl_3$): δ 166.7, 154.0, 147.3, 142.2, 139.0, 128.8, 128.3, 127.4, 122.6, 110.3, 107.3, 51.6, 47.5. MS (EI): *m/z* 242, 210, 183, 153. HRMS (EI): *m/z* 242.0944 ([$C_{15}H_{14}O_3$] requires *m/z* 242.0937).

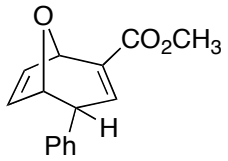

(±)-Methyl 4-phenyl-8-oxabicyclo[3.2.1]octa-2,6-diene-2-carboxylate (3.34). FTIR (neat): ν_{max}/cm^{-1} 3028, 2993, 2951, 1712, 1633, 1494, 1452, 1437, 1355, 1337, 1294, 1276, 1203, 1076, 1042. ^{1}H NMR (500 MHz, $CDCl_3$): δ 7.31-7.26 (m, 3H), 7.09 (d, 2H, J = 7.0 Hz), 6.74 (bs, 1H), 6.66 (dd, 1H, J = 6.0, 1.5 Hz), 5.53 (dd, 1H, J = 5.5, 1.5 Hz), 5.21 (bs, 1H), 5.12 (d, 1H, J = 4.5 Hz), 4.10 (dd, 1H, J = 6.5, 2.5 Hz), 3.79 (s, 3H). ^{13}C NMR (75 MHz, $CDCl_3$): δ 165.2, 139.5, 139.0, 136.3, 135.7, 128.7, 128.1, 127.7, 127.4, 82.4, 75.9, 51.8, 42.9. MS (EI): *m/z* 242, 210, 183, 153. HRMS (EI): *m/z* 242.0941 ($C_{15}H_{14}O_3$ requires *m/z* 242.0937).

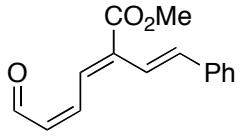

(2*E*,4*Z*)-methyl 6-oxo-2-((*E*)-styryl)hexa-2,4-dienoate (3.35). The compound could not be isolated in pure enough form for full characterization. Structure was assigned based on analogy to previous similar reactions and nOe studies. ^{1}H NMR (500 MHz, $CDCl_3$): δ 10.36 (d, 1H, J=7.5 Hz), 8.00 (d, 1H, J=12.5 Hz), 7.53-7.46 (m, 3H), 7.39-7.17 (m, 3H), 7.05 (q AB, 2H), 6.11 (dd, 1H, J=10.5, 8.0 Hz), 3.88 (s, 3H). HRMS (EI): *m/z* 242.0941 ([$C_{15}H_{14}O_3$] requires *m/z* 242.0937).

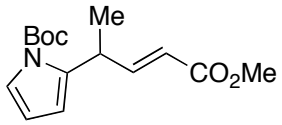

(*E*)-*tert*-butyl 2-(5-methoxy-5-oxopent-3-en-2-yl)-1H-pyrrole-1-carboxylate (3.32). Colourless oil. TLC (10% Et_2O/pentane): R_f = 0.27. FTIR (neat film): ν_{max}/cm^{-1} 2978, 1723, 1653, 1435, 1318, 1271, 1161, 1128, 1027, 1007, 979, 849, 721. ^{1}H NMR (400 MHz, $CDCl_3$): δ 7.21 (dd, 1H, J = 3.2, 1.6 Hz), 7.14 (dd, 1H, J = 15.6, 6.0 Hz), 6.10 (t, 1H, J = 3.2 Hz), 6.05 (m, 1H), 5.70 (dd, 1H, J = 15.6, 1.2 Hz), 4.38 (qu, 1H, J = 6.8 Hz), 3.71 (s, 3H), 1.57 (s, 9H), 1.39 (d, 3H, J = 7.2 Hz). ^{13}C NMR (100 MHz, $CDCl_3$): δ 167.3, 152.4, 149.1, 136.7, 121.7, 119.2, 110.8, 109.9, 83.7, 51.4, 34.3, 27.9, 19.1. MS (pos-APCI): *m/z* 280 (5), 236 (21), 180 (100). HRMS (pos-APCI): *m/z* 280.1545 ([$C_{15}H_{21}NO_4$+H] requires *m/z* 280.1543).

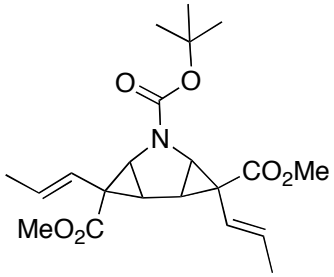

5-*tert*-butyl 3,7-dimethyl 3,7-di((*E*)-prop-1-en-1-yl)-5-azatricyclo[4.1.0.0^{2,4}]heptane-3,5,7-tricarboxylate. Major product from reaction between Methyl methylvinyldiazoacetate and *N*-Boc pyrrole catalyzed by $Rh_2(OOct)_4$. Data: White solid. Mp = 119–120 °C. TLC (15% Et_2O/pentane): R_f =0.30. FTIR (neat film): ν_{max} (cm^{-1}) 2943, 1701, 1414, 1231, 1125, 962. ^{1}H NMR (400 MHz, $CDCl_3$): δ 5.77 (dq, 2H, J = 20.4, 8.8 Hz), 5.44 (d, 2H, J = 20.8 Hz), 3.68 (s, 3H), 3.63 (s, 3H), 3.45 (d, 1H, J = 8.8 Hz), 3.33 (d, 1H, J = 8.8 Hz), 2.33 (d, 2H, J = 8.8 Hz), 1.78 (dm, 6H, J = 8.8 Hz), 1.47 (s, 9H).. ^{13}C NMR (100 MHz, $CDCl_3$): δ 172.3, 172.0, 155.1, 134.8, 119.8, 119.7, 80.7,

52.4, 52.3, 48.5, 32.8, 32.7, 32.0, 30.8, 28.3, 18.6, 18.6. MS (pos-APCI): 392 (2), 359 (2), 303 (7), 292 (100), 260 (12), 232 (17). HRMS (pos-APCI): *m/z* 392.2069 ([$C_{21}H_{29}NO_6$+H] requires *m/z* 392.2068).

3.4.3 General Computational Considerations

All calculations were performed with the Gaussian '09 software package.[50] Density Functional Theory was employed with the 3-parameter hybrid functional B3LYP[51,52] to locate stationary points on the potential energy surface (PES). The structures were subjected to full geometry optimization with a basis set consisting of the 1997 Stuttgart relativistic small-core effective core-potential [Stuttgart RSC 1997 ECP][53-55] for Ag, augmented with two 4f-functions (ζ_f(Ag) = 2.5 and 0.7).[56,57] The Ag f-exponents were obtained from Reference 56.[56] The split valence basis set 6-31G* was used in the optimization and frequency calculations for all other atoms (C, H, O, F, N and S). This composite basis set is abbreviated 6-31G*[Ag-RSC+4f].[58]. The main discussion in this chapter is based on single-point energies obtained at the B3LYP/6-311+G(2d,2p)[Ag-RSC+4f]//B3LYP/6-31G*[Ag-RSC+4f] level, corrected with zero-point energies from B3LYP/6-31G*[Ag-RSC+4f] calculations. Heavy-atom basis set definitions and corresponding pseudopotential parameters were obtained from the EMSL basis set exchange library.[59,60] All stationary points were characterized by normal coordinate analysis at the B3LYP/6-31G*[Ag-RSC+4f] level of theory. For transition states **TS-IIIa** and **TS-IIIb**, full geometry optimization was also carried out at the B3LYP/6-311+G(2d,2p)[Ag-RSC+4f] level of theory at temperature=273.15 K, also including the effects of dichloromethane as solvent (ε = 8.93) through the Integral Equation Formalism Polarizable Continuum Model (IEFPCM).[50,61] All transition states were confirmed to

have only one imaginary vibrational mode corresponding to movement along the reaction coordinate.[62] Equilibrium structures were confirmed to have zero imaginary vibrational modes.[62] Transition states were further characterized by intrinsic reaction coordinate (IRC) analysis using default parameters, followed by geometry optimization, to confirm that the stationary points were smoothly connected to each other.[7] The calculated harmonic zero-point vibrational energies (ZPVE) are reported unscaled. Calculated structures have been visualized using Mercury.[63-66]

3.4.4 Calculated Structures and Properties

The structure and properties of dinitrogen $\mathbf{N_2}$ has been reporten in Chapter 2, Section 2.4.

Structure 3.9

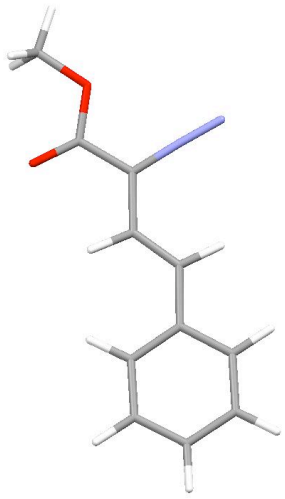

Route= #N B3LYP/6-31G(d) 5d OPT FREQ
RB3LYP Energy=-685.074915835 Hartree
ZPE=0.192102 Hartree
Conditions=298K, 1.00000 atm
Internal Energy=-684.868734 Hartree
Enthalpy=-684.867790 Hartree
Free Energy=-684.925867 Hartree
Entropy=122.234 cal/mol-K

C	0.00000000	0.00000000	0.00000000
O	-1.14345900	0.86973700	0.00015300
C	-2.34334700	0.24352200	0.00017400
C	-3.46440300	1.19519200	0.00016700
C	-4.84540200	0.74138500	0.00019700
C	-5.95071200	1.51481500	0.00000400
H	-5.83196600	2.59889600	-0.00023000
C	-7.34161200	1.05509200	0.00006400
C	-8.37151600	2.01488400	0.00004300
C	-9.71336700	1.63783900	0.00010800
C	-10.0605500	0.28624200	0.00018800
C	-9.05034600	-0.68153100	0.00019000
C	-7.71098900	-0.30515700	0.00013000
H	-6.94521800	-1.07537100	0.00011500
H	-9.30961400	-1.73708800	0.00023500
H	-11.1051270	-0.01266000	0.00022900
H	-10.4872250	2.40097800	0.00009300
H	-8.10920100	3.07057200	-0.00002500
H	-4.90493200	-0.34286000	0.00041000
N	-3.17734000	2.47980800	0.00019100
N	-2.97204100	3.60025700	0.00027500
O	-2.48871700	-0.96321200	0.00017800
H	0.00021200	-0.63394600	0.89056200
H	0.86654400	0.66160600	-0.00052400
H	-0.00044900	-0.63450300	-0.89016500

AgOTf

Route= #N b3lyp/gen pseudo=read gfprint
OPT FREQ
RB3LYP Energy=-1108.4255488 Hartree
ZPE=0.027984 Hartree
Conditions=298K, 1.00000 atm
Internal Energy=-1108.388303 Hartree
Enthalpy=-1108.387359 Hartree
Free Energy=-1108.435123 Hartree
Entropy=100.527 cal/mol-K

S	0.00000000	0.00000000	0.00000000
C	-1.26023500	-1.37231700	-0.00007400
F	-2.02450100	-1.29090400	-1.08842700
F	-0.62600500	-2.55745200	-0.00010400
F	-2.02435300	-1.29085600	1.08839700
O	0.83992200	-0.30533700	1.22535900
Ag	2.65949800	-1.01978100	-0.00004000
O	-0.74019300	1.25463200	-0.00003600
O	0.84001100	-0.30513800	-1.22543800

Ag-carbenoid 3.38, *s-cis*

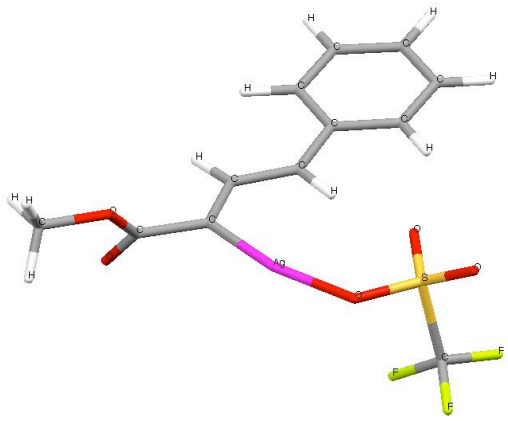

Route= #N b3lyp/gen pseudo=read gfprint
OPT FREQ
RB3LYP Energy=-1684.03545538 Hartree
ZPE=0.212141 Hartree
Conditions=298K, 1.00000 atm
Internal Energy=-1683.800273 Hartree
Enthalpy=-1683.799328 Hartree
Free Energy=-1683.882131 Hartree
Entropy=174.273 cal/mol-K

S	0.00000000	0.00000000	0.00000000
C	-0.75891600	0.16976700	1.69140200
F	-1.88543700	-0.53965000	1.77817100
F	0.10277100	-0.27665000	2.62630500
F	-1.02926700	1.45450700	1.94591300
O	-1.02154100	0.42944400	-0.94963000
O	1.25020600	0.79428700	0.09088500
Ag	2.28610900	-1.97792500	0.48186100
O	0.28245500	-1.50195000	-0.04685500
C	4.29961900	-1.99943600	0.93474800
C	5.03088200	-3.25915100	1.21420400
O	5.00391600	-4.12114500	0.18641600
C	5.66374300	-5.38316600	0.41268100
H	6.71113300	-5.22590400	0.68234700
H	5.58431600	-5.92241100	-0.53052400
H	5.16240300	-5.93077100	1.21460300
O	5.54652900	-3.47827900	2.29505700
C	5.05167700	-0.82678700	1.02590200
C	4.44152600	0.40257600	0.77770900
H	3.37080600	0.38068600	0.57274100
C	5.03329500	1.70503700	0.74533600
C	4.17081700	2.79690400	0.46904900
C	4.67102500	4.09275800	0.43231000
C	6.03083800	4.31777500	0.66846400
C	6.89834100	3.24831300	0.94145100
C	6.40965800	1.95234000	0.97889100
H	7.08224300	1.12660100	1.18736600
H	7.95207300	3.43800200	1.12159800
H	6.42255200	5.33085800	0.63939400
H	4.00799900	4.92574500	0.22059800
H	3.11720800	2.59886500	0.28785500
H	6.11238700	-0.87339100	1.27424100

Lewis Acid complex LA-I

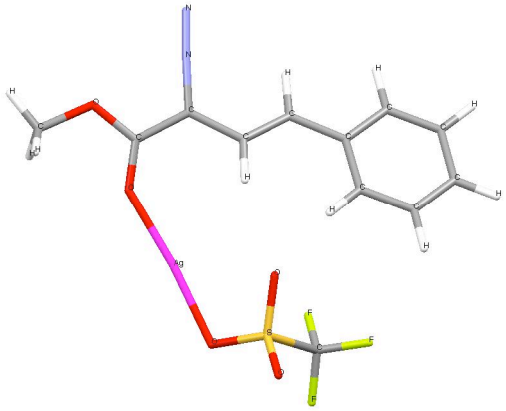

Route= #N b3lyp/gen pseudo=read gfprint OPT FREQ
RB3LYP Energy=-1793.54344838 Hartree
ZPE=0.221452 Hartree
Conditions=298K, 1.00000 atm
Internal Energy=-1793.296804 Hartree
Enthalpy=-1793.295859 Hartree
Free Energy=-1793.383213 Hartree
Entropy=183.850 cal/mol-K

C	0.00000000	0.00000000	0.00000000
Ag	2.39926400	-2.88368000	-0.41383400
F	7.04389700	-2.59168300	-1.36390600
F	5.47220100	-1.09006300	-1.50418600
F	7.03677100	-0.89473500	-0.00103700
O	6.15287100	-3.46128600	1.40049800
O	4.34544000	-1.69890500	1.17003500
C	6.26483400	-1.77157500	-0.65860400
O	4.40527200	-3.61231600	-0.39586400
C	-2.26357300	-2.86190800	-0.34747600
O	-1.75219000	-1.52778000	-0.14528300
C	-0.42596300	-1.36876700	-0.20281000
S	5.22126700	-2.72707700	0.55089800
C	1.38383900	0.48044600	0.01914800
C	1.74346800	1.76422600	-0.19235000
H	0.96113500	2.48385200	-0.43842100
C	3.09027100	2.33508100	-0.14661200
C	3.25373400	3.68601200	-0.50770200
C	4.51264300	4.28289600	-0.50498100
C	5.63564900	3.53747500	-0.14168000
C	5.48774500	2.19542100	0.22395600
C	4.23074100	1.59831000	0.22943400
H	4.14466200	0.56082700	0.53566300
H	6.35417000	1.60425300	0.50389500
H	6.61984800	3.99795100	-0.14058800
H	4.61620100	5.32705900	-0.78745800
H	2.38163300	4.26847200	-0.79730200
H	2.12572700	-0.27674800	0.25959200
N	-0.98427700	0.87376500	0.16880300
N	-1.79033000	1.66058200	0.30561400
O	0.32333400	-2.33487300	-0.41944300
H	-1.98613900	-3.22833400	-1.33839500
H	-3.34496500	-2.76346700	-0.26147900
H	-1.87474700	-3.53695200	0.41808600

Diazocomplex LA-II

C	0.00000000	0.00000000	0.00000000
Ag	1.89330400	-1.01426300	-0.73937500
F	4.15058900	-5.23900300	0.38447900
F	2.53451400	-4.54105000	-0.89783000
F	4.54022300	-4.78730400	-1.70862000
O	5.67395000	-2.60432600	0.06598400
O	3.75710400	-1.90490700	-1.40772000
C	3.84804700	-4.42252100	-0.62809700

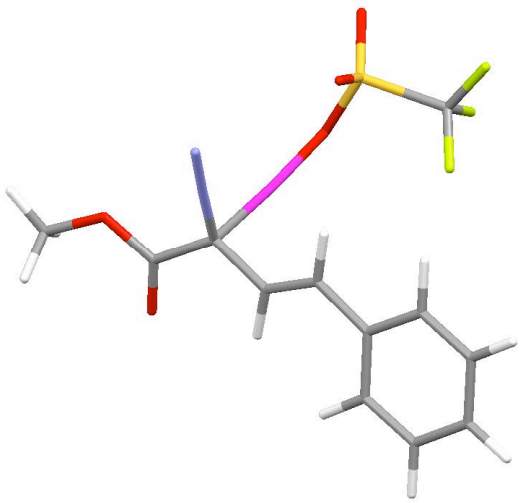

Route= #N b3lyp/gen pseudo=read gfprint OPT FREQ
RB3LYP Energy=-1793.52861111 Hartree
ZPE=0.220344 Hartree
Conditions=298K, 1.00000 atm
Internal Energy=-1793.282657 Hartree
Enthalpy=-1793.281713 Hartree
Free Energy=-1793.372585 Hartree
Entropy=191.256 cal/mol-K

O	3.31444300	-2.37206800	0.97083400
C	0.72235100	3.52900000	-0.82612800
O	0.60069800	2.27752900	-0.11407600
C	0.02163300	1.27490500	-0.79469100
S	4.23455800	-2.66059400	-0.16552600
C	-0.93255700	-1.08222700	-0.40918800
C	-1.23576600	-2.18814400	0.30032600
H	-0.74451800	-2.34834400	1.26082600
C	-2.16725100	-3.24895200	-0.09155100
C	-2.25556100	-4.39621900	0.71841700
C	-3.11692500	-5.44188600	0.39187800
C	-3.91263100	-5.36000900	-0.75153000
C	-3.84043900	-4.22354900	-1.56432500
C	-2.98158900	-3.17892900	-1.23894300
H	-2.95021700	-2.30078300	-1.87760700
H	-4.46035200	-4.15094300	-2.45364900
H	-4.58616400	-6.17253500	-1.00883700
H	-3.16510100	-6.31963000	1.03014700
H	-1.63448000	-4.46713400	1.60827600
H	-1.35791100	-0.88207700	-1.38824000
N	0.21522400	0.16685900	1.32658100
N	0.39641100	0.26320900	2.43578700
O	-0.42546500	1.34946900	-1.91796600
H	1.34405200	3.39484600	-1.71432700
H	1.19603500	4.21172000	-0.12212400
H	-0.26428500	3.89361600	-1.11955700

N_2 extrusion **TS-I**

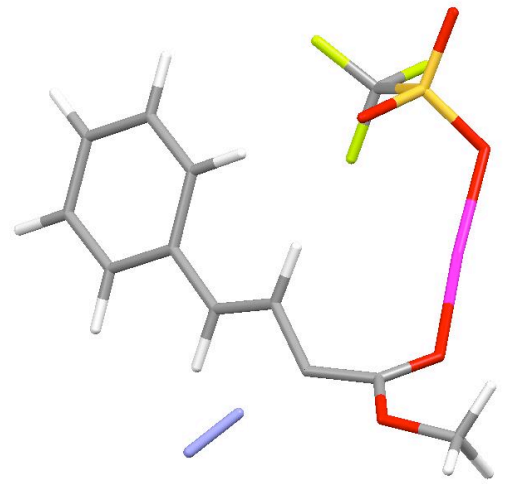

Route= #N b3lyp/gen pseudo=read gfprint OPT=(TS,CalcFC,NoEigenTest) freq
RB3LYP Energy=-1793.50054591 Hartree

C	0.00000000	0.00000000	0.00000000
F	0.72485500	-0.86033900	-0.71511200
F	-0.69856500	0.78232700	-0.84423200
F	0.82734000	0.78194900	0.70993300
S	-1.16250800	-0.89737800	1.14379000
O	-0.32667000	-1.77859900	1.95301900
O	-1.91552200	0.18637100	1.82051200
O	-2.04457100	-1.63788400	0.13763200
Ag	-3.95262900	-0.74367900	-0.07427200
O	-5.95889800	-0.03086800	-0.13579100
C	-6.41779300	1.05224700	0.32376500
C	-5.70422400	2.26812400	0.16561400
C	-4.35681000	2.52696200	0.52412600
C	-3.71708400	3.61810800	-0.01229300
H	-4.30341600	4.22278500	-0.70421500
C	-2.37460300	4.09054800	0.23981600
C	-1.96977600	5.30027900	-0.36881600

ZPE=0.218060 Hartree
Conditions=298K, 1.00000 atm
Internal Energy=-1793.256992 Hartree
Enthalpy=-1793.256047 Hartree
Free Energy=-1793.344194 Hartree
Entropy=185.520 cal/mol-K

C	-0.68776700	5.80088900	-0.17518200
C	0.21777500	5.09409200	0.62235900
C	-0.16347700	3.88872800	1.22362600
C	-1.44737100	3.38845000	1.04446600
H	-1.71922200	2.44461700	1.50543000
H	0.54591400	3.33115900	1.82668800
H	1.22274300	5.47929200	0.77185200
H	-0.39082000	6.73390900	-0.64504000
H	-2.67607800	5.84144800	-0.99376100
H	-3.83168500	1.88126900	1.23124100
O	-7.66648900	1.09712300	0.80220200
C	-8.44000500	-0.11426200	0.70502700
H	-8.57004500	-0.40354100	-0.34084100
H	-9.40100800	0.13040800	1.15718400
H	-7.95544500	-0.92644500	1.25163200
N	-6.83424100	3.53009200	1.00078900
N	-7.31572300	4.53243600	0.93771500

N_2 extrusion TS-II

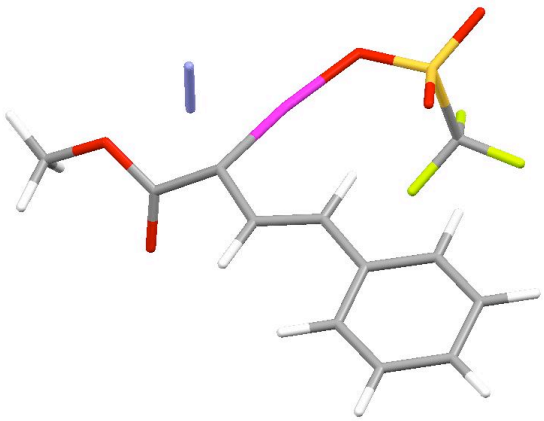

Route= #N b3lyp/gen pseudo=read gfprint OPT=(TS,CalcFC,NoEigenTest) freq
RB3LYP Energy=-1793.51738041 Hartree
ZPE=0.218744 Hartree
Conditions=298K, 1.00000 atm
Internal Energy=-1793.273272 Hartree
Enthalpy=-1793.272328 Hartree
Free Energy=-1793.360288 Hartree
Entropy=185.128 cal/mol-K

C	0.00000000	0.00000000	0.00000000
Ag	-2.05191100	-0.58050400	0.19248700
F	-5.99489000	2.05331000	-1.09238000
F	-4.33948100	0.88806200	-1.89615300
F	-6.26409900	-0.06194400	-1.52790100
O	-6.06636100	0.31443700	1.45518700
O	-4.13650300	-0.89599400	0.42143600
C	-5.40712400	0.85332400	-1.07283000
O	-3.88489300	1.51160300	0.99096600
C	1.76715600	-3.04021900	-1.18478100
O	1.15035700	-2.07269600	-0.31053900
C	0.75796300	-0.92753100	-0.90173300
S	-4.85226500	0.43881200	0.65570300
C	0.25465700	1.43155800	-0.17824700
C	-0.67681000	2.36544600	0.14673100
H	-1.63039500	2.01529600	0.54203600
C	-0.58254900	3.81095600	0.00476800
C	-1.73563500	4.56950400	0.29459200
C	-1.72181800	5.95635300	0.16793300
C	-0.55744900	6.60661300	-0.24610000
C	0.59590100	5.86607900	-0.53413300
C	0.58653800	4.48211300	-0.41017300
H	1.48876100	3.91942700	-0.63084100
H	1.50155400	6.37379900	-0.85359500
H	-0.54413000	7.68864700	-0.34394400
H	-2.61755400	6.52830900	0.39147200

H -2.63972100 4.05452600 0.61010400
H 1.21006000 1.71597800 -0.61567100
N 0.60413500 -0.38844600 1.54021200
N 0.75559400 -0.42403000 2.64147600
O 0.91908800 -0.66296500 -2.07388000
H 1.05467500 -3.36552900 -1.94671500
H 2.04840800 -3.87199400 -0.53981200
H 2.64611800 -2.60905500 -1.66931300

Vinylogous addition TS-IIIb

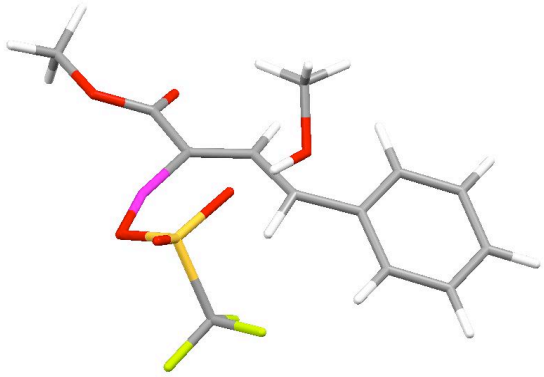

Route= #N b3lyp/gen pseudo=read gfprint OPT=(TS,CalcFC,NoEigenTest) FREQ
RB3LYP Energy=-1799.75858898 Hartree
ZPE=0.266859 Hartree
Conditions=298K, 1.00000 atm
Internal Energy=-1799.466018 Hartree
Enthalpy=-1799.465074 Hartree
Free Energy=-1799.553452 Hartree
Entropy=186.007 cal/mol-K

O 0.00000000 0.00000000 0.00000000
C 0.77396400 0.38132900 -1.60498500
F -4.51555600 -0.78953400 -3.22044200
F -2.37377700 -0.82219600 -2.82727900
F -3.69811800 -2.18392600 -1.76294600
O -5.11853900 0.04925900 -0.31517500
O -2.62737300 0.08228600 -0.04564000
O -3.73992300 1.62062900 -1.68044100
Ag -1.76070800 2.43853900 -1.93129200
C 0.28300000 2.77612500 -1.87174000
C 0.88464600 4.14883200 -1.91996900
O -0.05731600 5.10423000 -1.74241600
C 0.42501900 6.45696900 -1.75730100
H 1.16473900 6.61055500 -0.96661900
H -0.45237100 7.08183900 -1.59034300
H 0.88513700 6.68621900 -2.72226500
O 2.06081100 4.40913400 -2.09999700
C 1.17647700 1.78115000 -1.62178200
C -3.60236600 -0.95203200 -2.26601100
H -0.15693000 0.18975100 -2.13203400
C 1.75240000 -0.71611000 -1.72288000
C 1.31370500 -1.94253000 -2.25403500
C 2.19671900 -3.00896800 -2.39676200
C 3.52970300 -2.86578500 -2.00207600
C 3.97605000 -1.65434300 -1.46662600
C 3.09551200 -0.58394900 -1.32843300
H 3.45600700 0.35355500 -0.91747200
H 5.01238000 -1.54282300 -1.16140800
H 4.22100700 -3.69649400 -2.11328400
H 1.84818300 -3.94896000 -2.81417700
H 0.27406700 -2.04955300 -2.55356400
H 2.22931900 2.01856400 -1.47153700
S -3.81990000 0.31679700 -0.91735900
C 0.40934800 0.76876800 1.14767100
H -0.22714900 0.47084100 1.98362500

H	1.44840900	0.50945000	1.35623600
H	0.31219100	1.84088000	0.95616500
H	-0.99958200	0.08571800	-0.11548500

Vinylogous addition TS-IIIb in DCM at 0°C

Route= #N b3lyp/gen pseudo=read gfprint temperature=273.15
OPT=(TS,CalcFC,NoEigenTest) freq
SCRF=(PCM,Solvent=dichloromethane)
RB3LYP Energy=-1799.77810003 Hartree
ZPE=0.266453 Hartree
Conditions=273K, 1.00000 atm
Internal Energy=-1799.489191 Hartree
Enthalpy=-1799.488326 Hartree
Free Energy=-1799.566623 Hartree
Entropy=179.872 cal/mol-K

O	0.00000000	0.00000000	0.00000000
C	0.80130800	0.38750900	-1.57650500
F	-4.67078400	-0.84608600	-3.05475100
F	-2.51788500	-0.88609600	-2.73346400
F	-3.82150900	-2.14717000	-1.52870200
O	-5.19284600	0.21145600	-0.24344500
O	-2.70413300	0.20625100	0.02353300
O	-3.79040400	1.65189200	-1.71475800
Ag	-1.76466500	2.44051100	-1.98723800
C	0.28299900	2.77968000	-1.88390900
C	0.84296300	4.15644200	-1.95472100
O	0.06742300	5.04929400	-1.29855700
C	0.53655800	6.41105100	-1.30211600
H	1.53186200	6.47657900	-0.85549400
H	-0.18607700	6.96952300	-0.70791000
H	0.57235600	6.79707000	-2.32401800
O	1.86088700	4.47305100	-2.54928900
C	1.17614100	1.79872400	-1.59051200
C	-3.71827900	-0.95833700	-2.12728300
H	-0.10676500	0.17171700	-2.13439100
C	1.81645300	-0.67858700	-1.66658100
C	1.44542100	-1.90508100	-2.24812000
C	2.36893000	-2.94002200	-2.36815500
C	3.67392800	-2.76612400	-1.89742700
C	4.05220200	-1.55530800	-1.30940400
C	3.13245500	-0.51497400	-1.19572800
H	3.44200700	0.41980800	-0.73982400
H	5.06542600	-1.42058800	-0.94315200
H	4.39592900	-3.57237900	-1.98963600
H	2.07371400	-3.87901400	-2.82638100
H	0.42853400	-2.03867100	-2.60782900
H	2.22067600	2.04046700	-1.39642500
S	-3.88220600	0.40415300	-0.86777600
C	0.50113700	0.66339000	1.18484900
H	-0.10565200	0.32821400	2.02767900
H	1.53366600	0.33972100	1.31581800
H	0.44587200	1.74884900	1.07542400
H	-0.98077700	0.17076400	-0.09138100

Vinylogous Ylide YL-IIb

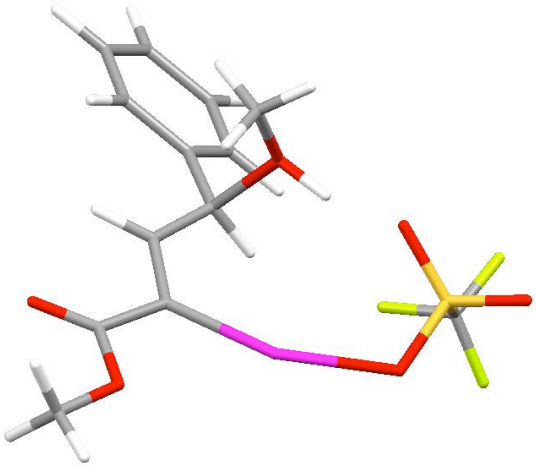

Route= #N b3lyp/gen pseudo=read gfprint OPT FREQ
RB3LYP Energy=-1799.75921383 Hartree
ZPE=0.267225 Hartree
Conditions=298K, 1.00000 atm
Internal Energy=-1799.466034 Hartree
Enthalpy=-1799.465090 Hartree
Free Energy=-1799.553743 Hartree
Entropy=186.586 cal/mol-K

O	0.00000000	0.00000000	0.00000000
C	0.76515000	0.39447400	-1.36596700
F	-4.46492200	-0.86410500	-2.98605600
F	-2.31786400	-0.86818600	-2.61771700
F	-3.61102400	-2.25046000	-1.54166500
O	-5.01709600	-0.06576900	-0.03692400
O	-2.52718200	0.03965400	0.15089100
O	-3.73310600	1.55104800	-1.44714400
Ag	-1.77857800	2.46388600	-1.69991000
C	0.26157500	2.81803200	-1.60465500
C	0.84948500	4.19761200	-1.60932900
O	-0.11890000	5.14489700	-1.64778400
C	0.34728200	6.50233200	-1.65019300
H	0.92873000	6.71104200	-0.74772600
H	-0.55036500	7.12027200	-1.68083200
H	0.97507500	6.68947300	-2.52572700
O	2.03487200	4.47830600	-1.58430000
C	1.15444000	1.83005700	-1.37134800
C	-3.53690600	-1.01812500	-2.04552000
H	-0.06906000	0.20723000	-2.04110700
C	1.82874100	-0.64889900	-1.51695800
C	1.49159500	-1.85654900	-2.14849500
C	2.43846100	-2.86691200	-2.30104000
C	3.73623600	-2.68448300	-1.81677500
C	4.08155300	-1.48931300	-1.18275800
C	3.13524700	-0.47499100	-1.03471400
H	3.42302100	0.45295800	-0.55040400
H	5.09054900	-1.34240900	-0.80827200
H	4.47709300	-3.47009100	-1.93625000
H	2.16553600	-3.79352800	-2.79760100
H	0.47904200	-1.99914400	-2.51851900
H	2.20627800	2.07210600	-1.22026500
S	-3.75595300	0.24617200	-0.69250400
C	0.47590000	0.54491200	1.25795500
H	-0.19863200	0.16414900	2.02496600
H	1.48562400	0.16379400	1.41100100
H	0.46439100	1.63567200	1.22753100
H	-1.02821300	0.10772000	-0.07562600

Carbenoid Ylide YL-IIa

O	0.00000000	0.00000000	0.00000000
C	0.56888200	0.45968900	-1.31284800
F	-0.96399100	-5.35402000	-2.34611800
F	0.64244200	-3.91396500	-2.04253000

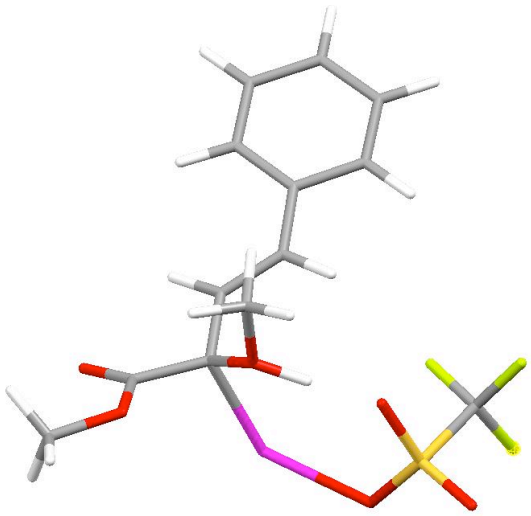

Route= #N b3lyp/gen pseudo=read gfprint OPT FREQ
RB3LYP Energy=-1799.75997515 Hartree
ZPE=0.266276 Hartree
Conditions=298K, 1.00000 atm
Internal Energy=-1799.467784 Hartree
Enthalpy=-1799.466839 Hartree
Free Energy=-1799.554658 Hartree
Entropy=184.829 cal/mol-K

F	-0.01467100	-5.17704200	-0.39493300
O	-2.79404100	-3.90302400	-0.37981900
O	-0.85789900	-2.34946600	-0.04699800
O	-1.96196100	-2.52502100	-2.30035400
Ag	-0.74284700	-0.69303200	-2.65033300
C	2.53412900	-1.10988600	-1.08154800
C	0.31417200	1.91107900	-1.51291900
O	-0.63440500	2.41462100	-0.68446700
C	-0.97605300	3.79178700	-0.91996300
H	-0.09853900	4.43320600	-0.80547300
H	-1.73160100	4.03413100	-0.17225600
H	-1.38006000	3.91800300	-1.92791400
O	0.88296400	2.57383100	-2.36160300
C	1.96733200	0.03266400	-1.52383800
C	-0.42308500	-4.50640400	-1.47294300
H	1.91489600	-1.83058000	-0.54776300
C	3.92427800	-1.53091600	-1.28799600
C	4.26920700	-2.87201300	-1.03433000
C	5.57066000	-3.33085900	-1.22949400
C	6.56230400	-2.45632600	-1.67764500
C	6.23838900	-1.11872100	-1.92553000
C	4.93912800	-0.65931800	-1.72866100
H	4.71297400	0.38871000	-1.90458000
H	7.00553800	-0.42779800	-2.26533100
H	7.57876100	-2.80991000	-1.82682300
H	5.80972000	-4.37242600	-1.03169400
H	3.49754000	-3.56036400	-0.69673100
H	2.53425800	0.73725700	-2.12868700
S	-1.66869700	-3.21002800	-0.98950700
C	0.65587900	0.34709100	1.26156400
H	1.71682200	0.10566200	1.19971500
H	0.48632500	1.41148400	1.41366800
H	0.15482500	-0.24273500	2.02908300
H	-0.36656900	-0.98006200	-0.04227100

Carbenoid addition TS-IIIa

O	0.00000000	0.00000000	0.00000000
C	0.83381400	0.33232800	-1.55664000
F	-3.33970800	-4.21338300	-2.17876200
F	-1.46921200	-3.56162000	-1.27323000
F	-3.26847300	-3.73257800	-0.05723800
O	-4.68329300	-1.52964900	-1.63545800
O	-2.49516800	-0.87179200	-0.58692500
O	-2.60110000	-1.45217600	-3.02264100
Ag	-0.61403000	-0.58804200	-2.81845400

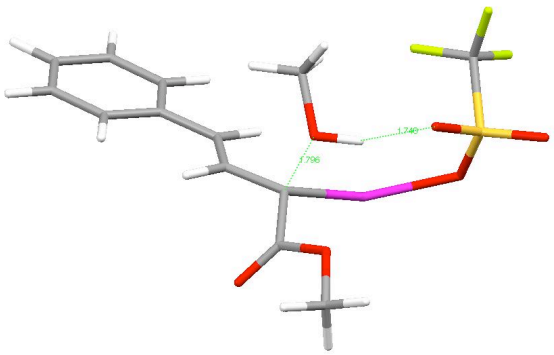

Route= #N b3lyp/gen pseudo=read gfprint OPT=(TS,CalcFC,NoEigenTest) freq
RB3LYP Energy=-1799.75390321 Hartree
ZPE=0.266259 Hartree
Conditions=298K, 1.00000 atm
Internal Energy=-1799.461766 Hartree
Enthalpy=-1799.460822 Hartree
Free Energy=-1799.548490 Hartree
Entropy=184.513 cal/mol-K

C	2.66025700	-1.30448500	-1.85738500
C	0.70028900	1.82405800	-1.59128800
O	-0.48760800	2.27761300	-1.14799500
C	-0.69505400	3.69658400	-1.26396600
H	0.07124500	4.24245300	-0.70777600
H	-1.68257100	3.87871500	-0.84091200
H	-0.66256400	4.00066700	-2.31345000
O	1.56492900	2.53502500	-2.06836000
C	2.21289000	-0.11971000	-1.38117400
C	-2.81319800	-3.39819600	-1.26657700
H	1.94113000	-1.92489600	-2.39328300
C	4.00836200	-1.86185400	-1.75632400
C	4.25565500	-3.12477300	-2.32742800
C	5.52023800	-3.70609300	-2.26555300
C	6.56557200	-3.03253600	-1.63142300
C	6.33781600	-1.77537000	-1.06038500
C	5.07518800	-1.19571600	-1.11959700
H	4.91706500	-0.21804600	-0.67476200
H	7.14976700	-1.24696000	-0.56865800
H	7.55362500	-3.48155500	-1.58216500
H	5.68969800	-4.68153000	-2.71253500
H	3.44300400	-3.64951200	-2.82433800
H	2.89891800	0.56074400	-0.87722300
S	-3.22944500	-1.62361100	-1.65079900
C	0.38687500	-1.19751800	0.71585100
H	0.22916100	-2.08867600	0.10385200
H	1.43599500	-1.09533800	0.98537700
H	-0.23558900	-1.23763400	1.61186400
H	-0.95941000	-0.12237800	-0.25859600

Carbenoid addition TS-IIIa in DCM at 0°C

Route= #N b3lyp/gen pseudo=read gfprint temperature=273.15
OPT=(TS,CalcFC,NoEigenTest) freq
SCRF=(PCM,Solvent=dichloromethane)
RB3LYP Energy=-1799.77458523 Hartree
ZPE=0.265645 Hartree
Conditions=273K, 1.00000 atm
Internal Energy=-1799.486307 Hartree
Enthalpy=-1799.485442 Hartree
Free Energy=-1799.562567 Hartree
Entropy=177.179 cal/mol-K

O	0.00000000	0.00000000	0.00000000
C	0.85372100	0.36008800	-1.64844900
F	-3.30657700	-4.24352500	-2.22810000
F	-1.47559200	-3.56796200	-1.26326000
F	-3.30871800	-3.76533900	-0.10359400
O	-4.72203600	-1.61466800	-1.70503700
O	-2.58609900	-0.87656900	-0.61855700
O	-2.63041900	-1.47189500	-3.05681500
Ag	-0.60644000	-0.56231000	-2.89413000
C	2.63455800	-1.31615100	-1.92147600
C	0.71245700	1.84557600	-1.65698100
O	-0.41253000	2.31968300	-1.09953900
C	-0.61715000	3.74300700	-1.20934300
H	0.21286900	4.28496400	-0.75044200

H	-1.54589100	3.94191200	-0.67613700
H	-0.70743300	4.03312400	-2.25906400
O	1.53157100	2.54530300	-2.23370700
C	2.21546000	-0.10742500	-1.46705500
C	-2.81373200	-3.42380300	-1.29620700
H	1.90245600	-1.92629800	-2.45062100
C	3.96492100	-1.90381800	-1.80448000
C	4.19770600	-3.15580100	-2.40855200
C	5.44937700	-3.76365500	-2.33823000
C	6.49364000	-3.12991500	-1.66057100
C	6.27870000	-1.88672400	-1.05280000
C	5.02955400	-1.27907500	-1.12092200
H	4.87892800	-0.31753100	-0.64040500
H	7.08896700	-1.39360300	-0.52365000
H	7.47094500	-3.60062100	-1.60344200
H	5.60997100	-4.72833700	-2.81056100
H	3.38545300	-3.64847100	-2.93722600
H	2.91627400	0.55711500	-0.96232700
S	-3.25688800	-1.65993200	-1.69328400
C	0.43603800	-1.18532500	0.70349400
H	0.32170700	-2.07741600	0.08259900
H	1.48037800	-1.04078700	0.97285700
H	-0.17529600	-1.26880900	1.60471600
H	-0.94323200	-0.14938400	-0.26522400

MeOH

Route= #N B3LYP/6-31G(d) 5d OPT FREQ
RB3LYP Energy=-115.712204002 Hartree
ZPE=0.051473 Hartree
Conditions=298K, 1.00000 atm
Internal Energy=-115.657440 Hartree
Enthalpy=-115.656496 Hartree
Free Energy=-115.683451 Hartree
Entropy=56.733 cal/mol-K

C	0.00000000	0.00000000	0.00000000
O	-1.41021400	0.14214000	0.00001300
H	-1.79812400	-0.74538000	-0.00002400
H	0.37469100	-0.52481100	-0.89294500
H	0.41788400	1.01051900	-0.00077500
H	0.37512500	-0.52369400	0.89342500

3.4.5 Single Point Energy Calculations

Single-point energies were calculated for the structures at the B3LYP/6-311+G(2d,2p)[Ag-RSC+2(4f)]//B3LYP/6-31G*[Ag-RSC+2(4f)] level of theory. The results are summarized in Table 3.13 below.

Table 3.13: Single point energies and calculated E+ZPE.

Structure	***Single pt Energy*** (Hartree)	***ZPE from 6-31G**** (Hartree)	***E+ZPE*** (Hartree)
TS-IIIa	-1800.244639	0.266259	-1799.97838
TS-I (Isomer 2)	-1793.972281	0.266276	-1793.706005
YL-IIa	-1800.252006	0.266276	-1799.98573
3.38 s-*trans*	-1684.470259	0.211753	-1684.258506
Silver/methanol/carbenoid complex	-1800.25491	0.265394	-1799.989516
YL-IIb	-1800.249796	0.267225	-1799.982571
TS-IIIb	-1800.249531	0.266859	-1799.982672
TS-II	-1793.998863	0.218744	-1793.780119
TS-I	-1793.981735	0.21806	-1793.763675
LA-II	-1794.009475	0.220344	-1793.789131
LA-I	-1794.02295	0.221452	-1793.801498
3.38 s-*cis*	-1684.480248	0.212141	-1684.268107
MPVD **3.9**	-685.3004567	0.192102	-685.1083547
AgOTf	-1108.688454	0.027984	-1108.66047
N_2	-109.5629655	0.0056	-109.5573655
MeOH	-115.769755	0.051473	-115.718282

References

(1) Doyle, M. P.; McKervey, M. A.; Ye, T. *Modern Catalytic Methods for Organic Synthesis with Diazo Compounds: From Cyclopropanes to Ylides*; John Wiley & Sons, Inc.: New York, 1998.

(2) Lebel, H.; Marcoux, J. F.; Molinaro, C.; Charette, A. B. *Chem. Rev.* **2003**, *103*, 977-1050.

(3) Davies, H. M. L.; Antoulinakis, E. G. *Org. Reacts.* **2001**, *57*, 1-326.

(4) Davies, H. M. L.; Hu, B. H. *Tetrahedron Lett.* **1992**, *33*, 453-456.

(5) Davies, H. M. L.; Kong, N.; Churchill, M. R. *J. Org. Chem.* **1998**, *63*, 6586-6589.

(6) Davies, H. M. L.; Nikolai, J. *Org. Biomol. Chem.* **2005**, *3*, 4176-4187.

(7) Davies, H. M. L.; Hansen, T.; Churchill, M. R. *J. Am. Chem. Soc.* **2000**, *122*, 3063-3070.

(8) Davies, H. M. L.; Yang, J.; Nikolai, J. *J. Organomet. Chem.* **2005**, *690*, 6111-6124.

(9) Davies, H. M. L. *Eur. J. Org. Chem.* **1999**, 2459-2469.

(10) Davies, H. M. L.; Beckwith, R. E. J. *Chem. Rev.* **2003**, *103*, 2861-2903.

(11) Davies, H. M. L.; Yokota, Y. *Tetrahedron Lett.* **2000**, *41*, 4851-4854.

(12) Davies, H. M. L.; Saikali, E.; Clark, T. J.; Chee, E. H. *Tetrahedron Lett.* **1990**, *31*, 6299-6302.

(13) Davies, H. M. L.; Hu, B.; Saikali, E.; Bruzinski, P. R. *J. Org. Chem.* **1994**, *59*, 4535-4541.

(14) Yue, Y.; Wang, Y.; Hu, W. *Tetrahedron Lett.* **2007**, *48*, 3975-3977.

(15) Wulff, W. D.; Yang, D. C. *J. Am. Chem. Soc.* **1983**, *105*, 6726-6727.

(16) Aoki, S.; Fujimura, T.; Nakamura, E. *J. Am. Chem. Soc.* **1992**, *114*, 2985-2990.

(17) Aumann, R.; Meyer, A. G.; Frohlich, R. *J. Am. Chem. Soc.* **1996**, *118*, 10853-10861.

(18) Nakamura, E.; Tanaka, K.; Fujimura, T.; Aoki, S.; Williard, P. G. *J. Am. Chem. Soc.* **1993**, *115*, 9015-9020.

(19) Davies, H. M. L.; Bruzinski, P. R.; Lake, D. H.; Kong, N.; Fall, M. J. *J. Am. Chem. Soc.* **1996**, *118*, 6897-6907.

(20) Davies, H. M. L.; Saikali, E.; Young, W. B. *J. Org. Chem.* **1991**, *56*, 5696-5700.

(21) Lian, Y.; Davies, H. M. L. *Org. Lett.*, *12*, 924-927.

(22) Grohmann, M.; Buck, S.; Schaeffler, L.; Maas, G. *Adv. Synth. Catal.* **2006**, *348*, 2203-2211.

(23) Werle, T.; Maas, G. *Adv. Synth. Catal.* **2001**, *343*, 37-40.

(24) Maas, G. *Chem. Soc. Rev.* **2004**, *33*, 183-190.

(25) Buck, S.; Maas, G. *J. Organomet. Chem.* **2006**, *691*, 2774-2784.

(26) Werle, T.; Schaeffler, L.; Maas, G. *J. Organomet. Chem.* **2005**, *690*, 5562-5569.

(27) Maas, G.; Werle, T.; Alt, M.; Mayer, D. *Tetrahedron* **1993**, *49*, 881-888.

(28) Maas, G.; Seitz, J. *Tetrahedron Lett.* **2001**, *42*, 6137-6140.

(29) Leger, C.-D.; Maas, G. *Z, Naturforsch. B* **2004**, *59*, 573-578.

(30) Sevryugina, Y.; Olenev, A. V.; Petrukhina, M. A. *J. Cluster Sci.* **2005**, *16*, 217-229.

(31) Petrukhina, M. A.; Sevryugina, Y.; Andreini, K. W. *J. Cluster Sci.* **2004**, *15*, 451-467.

(32) Sevryugina, Y.; Weaver, B.; Hansen, J.; Thompson, J. L.; Davies, H. M. L.; Petrukhina, M. A. *Organometallics* **2008**, *27*, 1750-1757.

(33) Davies, H. M. L.; Rusiniak, L. *Tetrahedron Lett.* **1998**, *39*, 8811-8812.

(34) Lovely, C. J.; Browning, R. G.; Badarinarayana, V.; Dias, H. V. R. *Tetrahedron Lett.* **2005**, *46*, 2453-2455.

(35) Urbano, J.; Belderrain, T. R.; Nicasio, M. C.; Trofimenko, S.; Diaz-Requejo, M. M.; Perez, P. J. *Organometallics* **2005**, *24*, 1528-1532.

(36) Dias, H. V. R.; Browning, R. G.; Richey, S. A.; Lovely, C. J. *Organometallics* **2004**, *23*, 1200-1202.

(37) Dias, H. V. R.; Browning, R. G.; Polach, S. A.; Diyabalanage, H. V. K.; Lovely, C. J. *J. Am. Chem. Soc.* **2003**, *125*, 9270-9271.

(38) Kirmse, W. *Eur. J. Org. Chem.* **2002**, 2193-2256.

(39) Naodovic, M.; Yamamoto, H. *Chem. Rev.* **2008**, *108*, 3132-3148.

(40) Honda, T.; Haze, N.; Ishige, H.; Masuda, K.; Naito, K.; Suzuki, Y. *J. Chem. Soc., Perkin Trans. 1* **1993**, 539-540.

(41) Magnus, P.; Westwood, N. *Tetrahedron Lett.* **1999**, *40*, 4659-4662.

(42) Bachmann, S.; Fielenbach, D.; Jorgensen, K. A. *Org. Biomol. Chem.* **2004**, *2*, 3044-3049.

(43) Lovely, C. J.; Flores, J. A.; Meng, X. F.; Dias, H. V. R. *Synlett* **2009**, 129-132.

(44) Thompson, J. L.; Davies, H. M. L. *J. Am. Chem. Soc.* **2007**, *129*, 6090-6091.

(45) Burgess, K.; Lim, H. J.; Porte, A. M.; Sulikowski, G. A. *Angew. Chem. Int. Ed.* **1996**, *35*, 220-222.

(46) Liu, Z. F.; Liu, J. Y. *Cent. Eur. J. Chem.*, *8*, 223-228.

(47) Liang, Y.; Zhou, H. L.; Yu, Z. X. *J. Am. Chem. Soc.* **2009**, *131*, 17783-17785.

(48) Pieniazek, S. N.; Clemente, F. R.; Houk, K. N. *Angew. Chem. Int. Ed.* **2008**, *47*, 7746-7749.

(49) Davies, H. M. L.; Hougland, P. W.; Cantrell, W. R. *Synth. Commun.* **1992**, *22*, 971-978.

(50) Gaussian 09, R. A.; M. J. Frisch, G. W. T., H. B. Schlegel, G. E. Scuseria, ; M. A. Robb, J. R. C., G. Scalmani, V. Barone, B. Mennucci, ; G. A. Petersson, H. N., M. Caricato, X. Li, H. P. Hratchian, ; A. F. Izmaylov, J. B., G. Zheng, J. L. Sonnenberg, M. Hada, ; M. Ehara, K. T., R. Fukuda, J. Hasegawa, M. Ishida, T. Nakajima, ; Y. Honda, O. K., H. Nakai, T. Vreven, J. A. Montgomery, Jr., ; J. E. Peralta, F. O., M. Bearpark, J. J. Heyd, E. Brothers, ; K. N. Kudin, V. N. S., R. Kobayashi, J. Normand, ; K. Raghavachari, A. R., J. C. Burant, S. S. Iyengar, J. Tomasi, ; M. Cossi, N. R., J. M. Millam, M. Klene, J. E. Knox, J. B. Cross, ; V. Bakken, C. A., J. Jaramillo, R. Gomperts, R. E. Stratmann, ; O. Yazyev, A. J. A., R. Cammi, C. Pomelli, J. W. Ochterski, ; R. L. Martin, K. M., V. G. Zakrzewski, G. A. Voth, ; P. Salvador, J. J. D., S. Dapprich, A. D. Daniels, ; O. Farkas, J. B. F., J. V. Ortiz, J. Cioslowski, ; and D. J. Fox, G., Inc., Wallingford CT, 2009.

(51) Lee, C.; Yang, W.; Parr, R. G. *Phys. Rev. B* **1988**, *37*, 785-789.

(52) Becke, A. D. *J. Chem. Phys.* **1993**, *98*, 5648-5652.

(53) M. Kaupp, P. v. R. S., H. Stoll, H. Preuss *J. Chem. Phys.* **1991**, *94*, 1360.

(54) A. Bergner, M. D., W. Kuechle, H. Stoll, H. Preuss *Mol. Phys.* **1993**, *80*, 1431.

(55) M. Dolg, H. S., H. Preuss, R.M. Pitzer *J. Phys. Chem.* **1993**, *97*.

(56) Martin, R. L. *J. Chem. Phys.* **1987**, *86*, 5027-5031.

(57) Balabanov, N. B.; Boggs, J. E. *J. Phys. Chem. A* **2001**, *105*, 5906-5910.

(58) Hansen, J.; Autschbach, J.; Davies, H. M. L. *J. Org. Chem.* **2009**, *74*, 6555-6563.

(59) Feller, D. *J. Comput. Chem.* **1996**, *17*, 1571-1586.

(60) Schuchardt, K. L., Didier, B.T., Elsethagen, T., Sun, L., Gurumoorthi, V., Chase, J., Li, J., and Windus, T.L. *J. Chem. Inf. Model.* **2007**, *47*, 1045-1052.

(61) Tomasi, J.; Mennucci, B.; Cammi, R. *Chem. Rev.* **2005**, *105*, 2999-3093.

(62) Foresman, J. B.; Frisch, A. *Exploring Chemistry with Electronic Structure Methods*; Gaussian, Inc.: Pittsburgh, PA, 1993.

(63) Taylor, R.; Macrae, C. F. *Acta. Cryst. B* **2001**, *57*, 815-827.

(64) Bruno, I. J.; Cole, J. C.; Edgington, P. R.; Kessler, M.; Macrae, C. F.; McCabe, P.; Pearson, J.; Taylor, R. *Acta. Cryst. B* **2002**, *58*, 389-397.

(65) Macrae, C. F.; Edgington, P. R.; McCabe, P.; Pidcock, E.; Shields, G. P.; Taylor, R.; Towler, M.; van de Streek, J. *J. Appl. Crystallogr.* **2006**, *39*, 453-457.

(66) Macrae, C. F.; Bruno, I. J.; Chisholm, J. A.; Edgington, P. R.; McCabe, P.; Pidcock, E.; Rodriguez-Monge, L.; Taylor, R.; van de Streek, J.; Wood, P. A. *J. Appl. Crystallogr.* **2008**, *41*, 466-470.

- Chapter 4 -

Bismuth–Rhodium Paddlewheel Carboxylates as Catalysts for Metallocarbenoid Transformations

4.1 Introduction

The use of dirhodium paddlewheel complexes in catalysis has been an area of continuously increasing interest for the past three decades.[1-18] These complexes are structurally characterized by a dirhodium core with a Rh–Rh single bond, bridged by four μ_2– carboxylate, carboxamidate or phosphonate ligands. A wide variety of complexes have been studied in which the bridging ligand structure has been structurally diversified. Many of these have been used in catalysis.[1-18] As catalysts, some of the complexes have been very successful in several transformations, particularly in metal nitrenoid and carbenoid chemistry.[4] This involves a variety of [2+1]-cycloadditions,[8,15,19] C–H functionalization[4,20-24] and ylide chemistry,[9,11,14,25-26] but also in Lewis acid catalyzed processes.[9,27-28] The ability of dirhodium complexes to effectively catalyze such a variety of transformations, often at low catalyst loadings, has been key to demonstrate their synthetic potential. Particularly in the context of chiral catalysis, there are numerous examples of catalytic applications in natural product synthesis and medicinal chemistry.[4,24,29-39] The dirhodium complexes are often much more attractive compared to mononuclear copper or palladium counterparts, since simple modifications of the ligands offer dramatic changes in the reactivity profile.

Electronic and steric modification of the ligands has been a dominating strategy for catalyst development in the dirhodium paddlewheel series. In the domain of chiral catalysis, the most successful classes of ligands are, the *N*-arylsulfonylprolinates,[2,13,40-41] phthaloyl-protected amino acids,[13,42-45] carboxamidates,[10,11,13,46] *ortho*-metallated arylphosphines[13,47-48] and binaphthoyl phosphonate complexes (Figure 4.1).[13-14,49] More recently, mixed valence dirhodium(II,III) species,[50,51] complexes with axially coordinated N-heterocyclic carbenes (NHCs),[52,53] and also mixed ligand (heteroleptic) systems[54,55] have been explored. Several computational and kinetic studies of dirhodium carboxylate catalyzed carbenoid reactions indicate that the carbene ligand only binds at one of the two rhodium active sites at a time.[56,57] This is supported by the observation that, immobilized dirhodium complexes (*via* coordination to one active site), still display selectivity and reactivity comparable to what is observed under homogeneous conditions.[58-60]

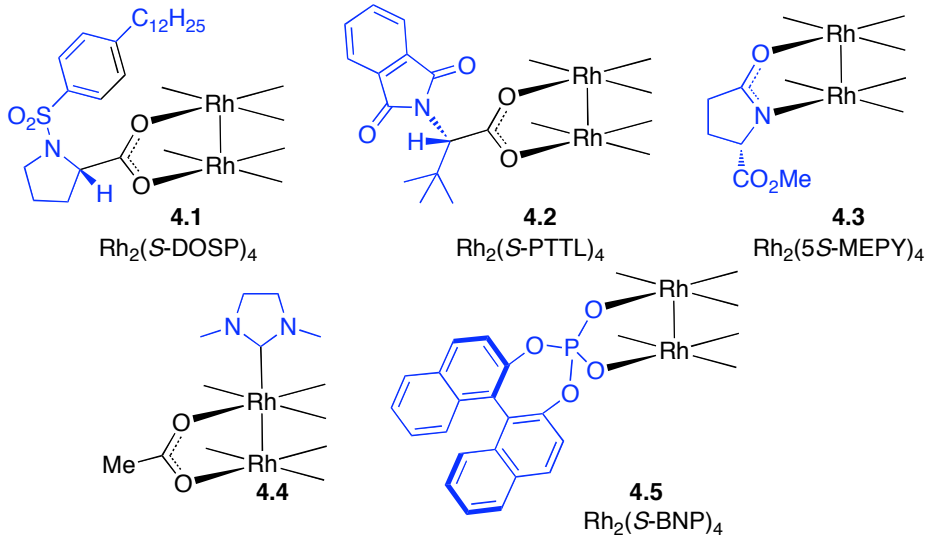

Figure 4.1: Various dirhodium catalysts.

Dikarev and co-workers have reported syntheses and structural studies of a new class of paddlewheel complexes, in which one of the rhodium atoms has been replaced by bismuth.[61-64] This group first reported the synthesis of dibismuth(II) tetrakis(trifluoroacetate) in 2004, obtained by gas-phase reduction of Bi(III) trifluoroacetate in the presence of Bi(0).[62] The dimer was reported to have a Bi–Bi single bond and only weakly coordinate aromatic groups at the axial sites.[62] It was discovered that the new Bi(II)-dimer was effectively able to act as a metalloligand towards transition metal fragments, which was utilized to prepare $BiRh(O_2CCF_3)_4$ **II** (Figure 4.2a), a heterobimetallic, homoleptic carboxylate complex.[63,64] Further developments of this technique was utilized in simple, one-pot syntheses of mixed–ligand carboxylates *cis*-$BiRh(O_2CCF_3)_2(O_2C^tBu)_2$ **I**, $BiRh(O_2CCF_3)_3(O_2CCH_3)$ **III** (Figure 4.2a)**,** as well as a chiral complex $BiRh(O_2CCF_3)_3(O_2C(S\text{-}(+)\text{-}^iBu))$.[63,64] The latter complex demonstrated that chiral ligands could be introduced in the system and hence opens up the possibility of chiral catalysis. The structures have some typical paddlewheel features, such as: (1) the bimetallic core has a bismuth–rhodium single bond, and, (2) the core acts as an anchor for four μ_2-ligands. Not unexpected, the intermetallic bond distances are intermediate of those in the pure dibismuth and dirhodium complexes (Figure 4.2b).[63,64] There is a charge asymmetry across the metal-metal bond. The bismuth end appears to reduce the positive charge on the nearby rhodium relative to dirhodium complexes, consistent with a difference in Pauling electronegativity between Rh (2.28) and Bi (2.02). The structures were shown to remain intact in solution phase and, towards basic donors, displayed Lewis acidity only at the transition metal end.[63,64]

a)

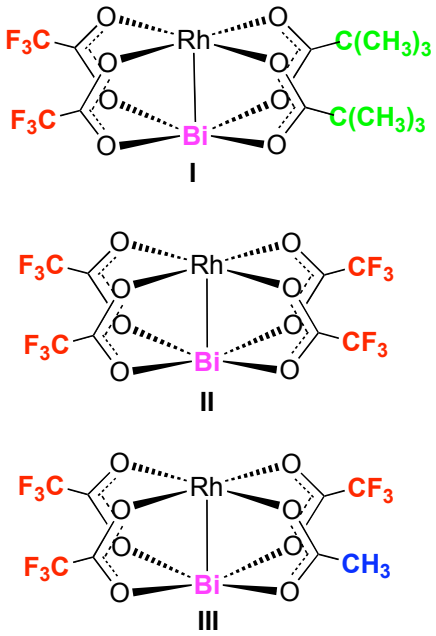

b)

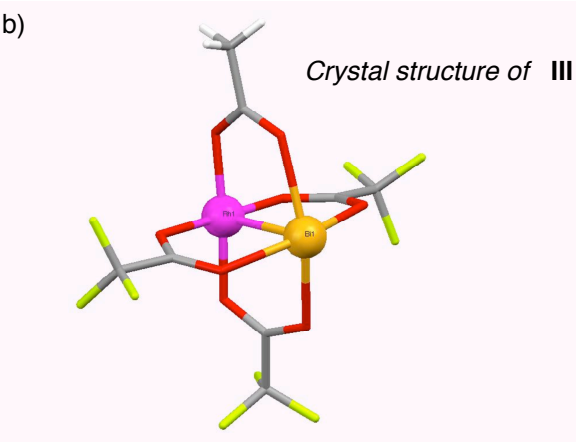

Complex	*Intermetallic bond distance* (Å)	*Mulliken Atomic Charge*	
		TM	*Bi*
$Bi_2(TFA)_4$	2.9462(3)	--	--
$BiRh(TFA)_4$	2.5493(3)	0.5201	1.3137
$Rh_2(TFA)_4$	2.3813(8)	--	--

Figure 4.2: a) RhBi carboxylate complexes. (b) Crystal structure of **III** and characteristic bond distances and charges for bimetallic complexes.[61-64]

The modification introduced in the Bi–Rh paddlewheel systems offers the opportunity to tune the reactivity of the bimetallic core itself,[64] which is a totally novel approach to reactivity control in such systems. Furthermore, such novel heterobimetallic carboxylates provide a new arena for probing the role of the dirhodium framework, a remarkably successful stuctural element in catalysis, through comparative studies of the catalytic performance. This would shed light on whether the dirhodium framework is necessary to achieve efficient, catalytic reactions and would also provide valuable insight into the influence of the bimetallic core properties on the selectivity. In this chapter, a combined experimental and computational study is presented that explores catalysis by heterobimetallic Bi–Rh carboxylates in the context of metallocarbenoid chemistry.

Furthermore, it is studied how they compare with analogous dirhodium catalysts in terms of reactivity and selectivity. The computational studies provide insights into how both the Bi–Rh core and ligands, including axial ligand effects, affect the mechanism in terms of catalytic activity and selectivity. All Bismuth-Rhodium complexes reported herein were generously provided by the Dikarev group at SUNY Albany.

4.2 Results And Discussion

4.2.1 Catalytic Activity: Cyclopropanation Chemistry

We initially studied the catalytic activity of several Bi–Rh complexes. This was evaulated in a standard cyclopropanation reaction between a diazoacetate and styrene (Scheme 4.1), a well established transformation.[19] Bi–Rh complexes **I** and **II** were evaluated in the cyclopropanation using methyl phenyldiazoacetate (**4.6a**, Table 4.1). The generally optimum conditions were determined to be 2 mol % catalyst at 40 °C, using dichloromethane as solvent (reflux), although, in some cases, full conversion could be obtained with 1 mol% catalyst at ambient temperature. The former conditions were chosen as standard in the interest of comparing all results. Full conversion was observed under these conditions and the cyclopropane was formed in excellent yield (94%) and high diastereoselectivity (>95% de) with complex **II** as catalyst (Table 4.1, Entry 2). $Rh_2(O_2CCF_3)_4$ performed similarly in this reaction, with 96% yield and >95% de (Entry 3). Complex **I** gave somewhat lower yield (74%), but still very high diastereoselectivity (Entry 1). This complex appeared to be more prone to deactivation or poisoning over time, as the performance of one catalyst batch decreased in the standard reaction when carried out a few months apart.

The effect of carbenoid structure was investigated with complex **I**. Reaction with ethyl diazoacetate **4.6b** (Entry 4) produced the corresponding cyclopropane in 47% yield as a mixture of diastereomers (21% de). The diastereoselectivity is similar to that previously reported for this reaction with dirhodium catalysts.[65] The acceptor-acceptor carbenoid, derived from methyl diazomalonate **4.6c**, was presumably not formed under the reaction conditions. Only starting materials were observed in the ^{1}H NMR spectrum of the

reaction mixture, even after prolonged reflux (>48 hours)(Entry 5). Overall, the best result was obtained with **4.6a** and, this diazo compound was therefore used for further studies. These reactions demonstrate that Bi–Rh complexes are capable of forming the carbenoid, however, it was qualitatively observed that the reactions appeared to proceed much slower than those catalyzed by dirhodium catalysts. The lack of other observable by-products indicates that the carbenoid has a similar selectivity profile to that of dirhodium carbenoids.

Scheme 4.1: Cyclopropanation of styrene.

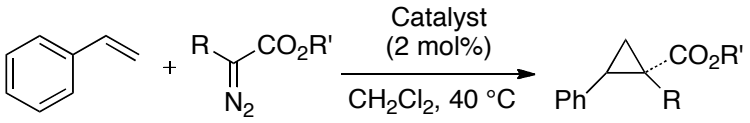

4.6a-c **4.7a-c**

Table 4.1: Influence of carbenoid structure in cyclopropanation of styrene.

Entry	*Cmpd*	*R =*	*R′ =*	*Catalyst*	*de* (%)[a]	*Yield* (%)[b]
1	**a**	Ph-	$-CH_3$	**I**	94	74
2	**a**	Ph-	$-CH_3$	**II**	>95	94
3	**a**	Ph-	$-CH_3$	$Rh_2(TFA)_4$	>95	96
4	**b**	H^-	$-CH_2CH_3$	**I**	21	47
5	**c**	MeO_2C-	$-CH_3$	**I**	N/A	N/R

[a] Measured by ^{1}H-NMR of crude reaction mixture.
[b] Isolated yields.

The reaction of methyl phenyldiazoacetate (**4.6a**) with furan, catalyzed by dirhodium catalysts, affords mono-cyclopropanation product **4.8** as well as an alkylation product (**4.9**), where the furan ring has been opened.[66,67] The latter is believed to be formed *via* a

a zwitterionic intermediate, in which the stabilization of charge build-up by the furan ring interrupts the cyclopropanation totally, and therefore undergoes a furan-unraveling reaction in competition with the cyclopropanation chemistry.[67] By increasing the electrophilicity of the catalyst, more of the ring-opened product is usually observed.[66] When the relatively electron rich bismuth–rhodium complex **I** was used as catalyst, the two products **4.8** and **4.9** were formed in a 70 : 30 ratio in 80% yield (Table 4.2, Entry 1). The more electron deficient complex **II** afforded an approximately 47 : 53 ratio of the two products in excellent 96% overall yield (Entry 2). $Rh_2(O_2CCF_3)_4$ performed almost identical to the latter (Entry 3). For these reactions, bismuth–rhodium carbenoids again appear to display similar catalytic properties as their dirhodium counterparts.

Scheme 4.2: Reaction with furan.

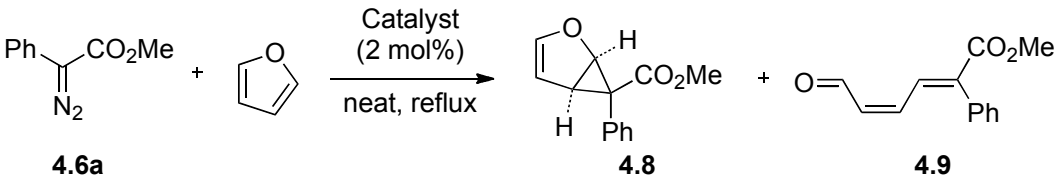

4.6a **4.8** **4.9**

Table 4.2: Reaction between **4.6a** and furan.

Entry	*Catalyst*	*Product Ratio* (**4.8** : **4.9**)[a]	*Yield (%)*[b]
1	**I**	70 : 30	80
2	**II**	47 : 53	96
3	$Rh_2(TFA)_4$	44 : 56	95

[a] Measured by ^{1}H-NMR of crude reaction mixture.
[b] Overall isolated yields.

4.2.2 Reactivity

The difference in reactivity between the two catalyst systems towards decomposition of **4.6a** was investigated next. The cyclopropanation reactions between **4.6a** and styrene, catalyzed by complexes **III** and $Rh_2(O_2CCF_3)_3(O_2CCH_3)$, were conducted with all the reagents initially present in the flask in dichoromethane solution. A solution of the catalyst was then injected by syringe and the reaction progress monitored by ReactIR. This method is well suited for monitoring such reactions as the characteristic diazo group C=N=N stretch frequency at ~2100 cm^{-1} is well separated from other bands in the IR spectrum. The measured reaction progress is shown in Figure 4.3a for $Rh_2(O_2CCF_3)_3(O_2CCH_3)$ and in Figure 4.3b for **III**. The reaction catalyzed by $Rh_2(O_2CCF_3)_3(O_2CCH_3)$ went to completion after ~16 sec with 0.2 mol % catalyst loading. This corresponds to an average TON of ~500. The reaction catalyzed by 2 mol % of **III**, went to completion after about 45 min, corresponding to an average TON of ~50. The average turnover frequencies are therefore TOF_{RhRh} ~ 31 s^{-1} and TOF_{BiRh} ~ 0.019 s^{-1} for the dirhodium complex and **III** respectively. In terms of the average turnover

frequencies, the dirhodium complex is about ~1,600 times more reactive than the Bi–Rh counterpart towards diazo decomposition. The rate of the Bi–Rh catalyzed reaction is significantly slower than that catalyzed by dirhodium, but the former can still be a high yielding process, since full conversion can be obtained. Furthermore, under the synthetically relevant conditions, the rate-limiting process is often the addition of diazo compound to the catalyst/alkene solution.

Scheme 4.3: ReactIR study of cyclopropanation reaction.

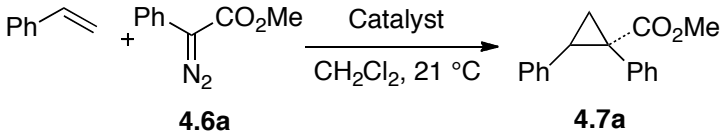

4.6a **4.7a**

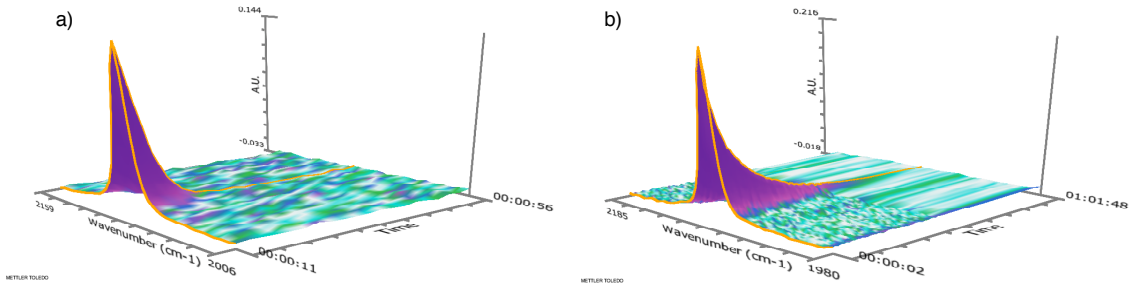

Figure 4.3: Disappearance of C=N=N stretch frequency of **4.6a** as function of time for: (a) $Rh_2(O_2CCF_3)_3(O_2CCH_3)$ (0.2 mol%, over 45 sec), and, (b) complex **III** (2 mol %, over 62 min). The catalyst was injected at t_0 = 10 s.

4.2.3 Electronic Effects

To further probe the differential properties of dirhodium and bismuth–rhodium carbenoids, competition studies were carried out. The cyclopropanation of styrene *versus* *p*-substituted styrenes gives a quantitative measure of the benzylic charge build-up in the cyclopropanation transition state *via* the Hammett reaction constant (ρ) obtained for a

series of *para*-substituents (Scheme 4.4), as well as the sign (positive or negative) of the charge build-up.[68] The Hammett equation (Equation 4.1) describes the relation between the product partition ratio rate constant k_R/k_H, ρ and the substituent constant (σ).[68,69]

$$\log\left(\frac{k_R}{k_H}\right) = \rho \cdot \sigma \qquad \text{Eq (4.1)}$$

Excellent correlations were found ($R^2 = 0.99$) when $\log(k_R/k_H)$ were plotted against σ^+ substituent constants obtained from the literature[69] for both catalyst systems (Figure 4.4). Correlation with σ^+ substituent constants indicates positive charge build-up in the transition state, consistent with the carbenoid cyclopropanation mechanism, which is expected to occur in an asynchronous manner leading to benzylic positive charge concentration. The carbenoid complex with $Rh_2(O_2CCF_3)_3(O_2CCH_3)$ appears to be slightly more sensitive to the substituent effect (ρ = -1.20 ± 0.02) than **III** (ρ = -1.00 ± 0.03). This demonstrates somewhat less positive charge build-up in the case of the carbenoid complex with catalyst **III**, indicating a *slightly* more electron rich carbenoid compared to the dirhodium system. This is consistent with a more electron-rich Rh in the heterobimetallic case *versus* homobimetallic complexes.[63,64] The Hammett analysis was also carried out for **I** (*cis*-$BiRh(OPiv)_2(O_2CCF_3)_2$) and gave ρ = -1.07 ± 0.02 (Figure 4.5), similar to the results for **III**. The dirhodium complex analogous to **I** was not available for comparison. Overall, only minor differences were detected between the systems.

Scheme 4.4: Competition studies.

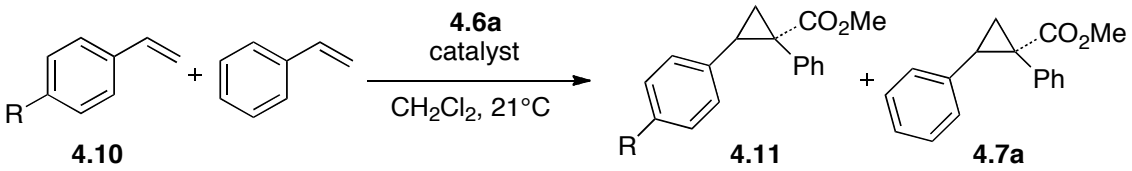

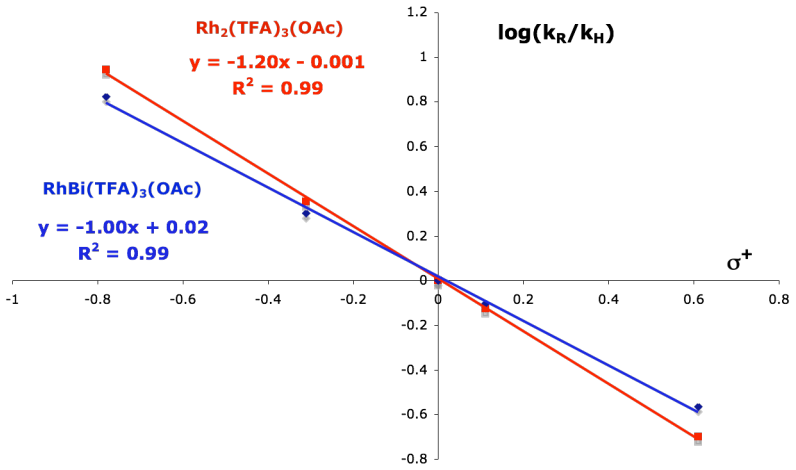

Figure 4.4: Hammet plot of cyclopropanation catalyzed by $Rh_2(O_2CCF_3)_3(O_2CCH_3)$ and **III.**

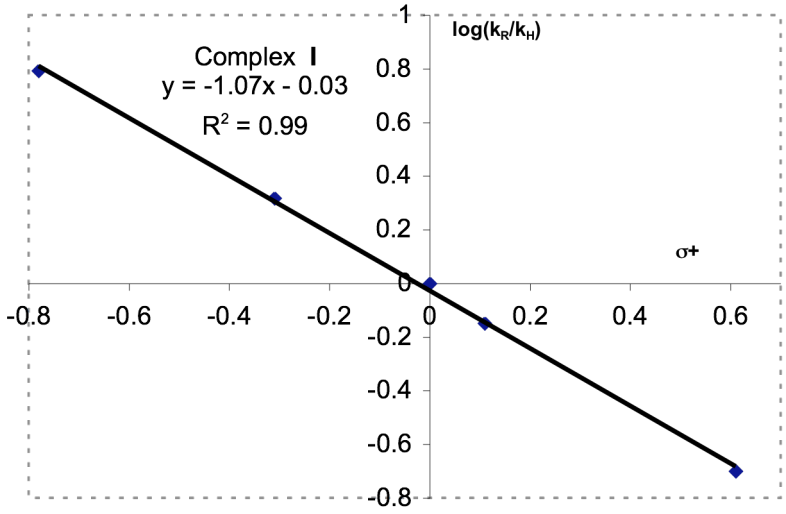

Figure 4.5: Hammet plot of cyclopropanation catalyzed by *cis*-$BiRh(OPiv)_2(TFA)_2$ (**I**).

4.2.4 C–H Insertion Chemistry

A highly activated system for C–H insertion chemistry is 1,4-cyclohexadiene. This is due to hyperconjugation between the methylene group and the two pendant double bonds, which facilitates positive charge build-up at the methylene site.[32,70] The reaction proceeds very cleanly with $Rh_2(O_2CCF_3)_4$ as well as Bi–Rh catalyst **II** under the standard reaction conditions (Scheme 4.5, Table 4.3). 84% yield of **4.12** was isolated when the reaction was catalyzed by complex **II**, comparable to the dirhodium analogue (74% yield). 47% yield was reported for complex **I**, but may have been low due to aromatization of the product. These reactions demonstrate that the heterobimetallic complexes can effectively catalyze C–H insertion processes with comparable results to that of dirhodium complexes.

Scheme 4.5: C–H insertion of 1,4-cyclohexadiene.

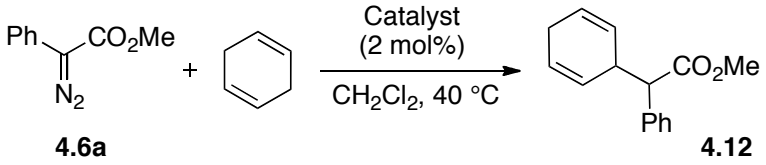

4.6a **4.12**

Table 4.3: C–H insertion.

Entry	*Catalyst*	*Yield* (%)[a]
1	**I**	47[b]
2	**II**	84
3	$Rh_2(TFA)_4$	74
4	$Rh_2(TFA)_3(OAc)$	87

[a] Isolated yields.
[b] Reaction carried out by Dr. Janelle Thompson.

The effectiveness of complex **II** in catalyzing the C–H insertion reaction led to the question of how this catalyst would perform in cases where C–H insertion occurs in competition with cyclopropanation reactions. One suitable substrate that can be used to probe this issue is cyclohexene, where both reaction pathways are observed with most dirhodium catalysts (Scheme 4.6, Table 4.4).[70] The decomposition of **4.6a** in the presence of cyclohexene, catalyzed by 2 mol % of complex **II**, afforded a 79 : 21 ratio of C–H insertion (**4.13**) to cyclopropanation (**4.14**) in an overall 52% yield. This is very similar to the results obtained with $Rh_2(O_2CCF_3)_4$, which gave 57% overall yield. For comparison, $Rh_2(O_2CCH_3)_4$ has been reported to give a 75 : 25 ratio of the two products in overall 50% yield.[70] These results show that the selectivity profile of the Bi–Rh carbenoid is very similar to that of the analogous dirhodium carbenoid in reactions where competition occurs between C–H insertion and cyclopropanation reactions.

Scheme 4.6: Reaction with cyclohexene.

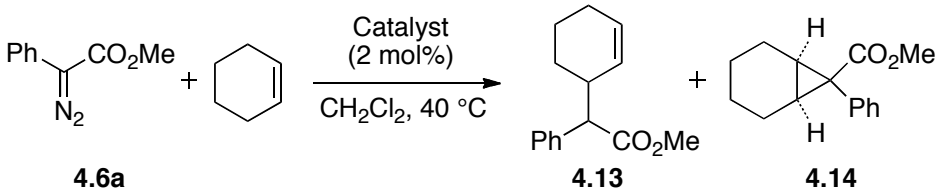

4.6a **4.13** **4.14**

Table 4.4: C–H insertion *versus* cyclopropanation.

Entry	*Catalyst*	*Product Ratio* (**4.13 : 4.14**)[a]	*Yield* (%)[b]
1	**II**	79 : 21	52
2	$Rh_2(TFA)_4$	84 : 16	57
3[c]	$Rh_2(OAc)_4$	75 : 25[c]	50[c]

[a] Measured by ^1H NMR of crude reaction mixture.
[b] Overall yield.
[c] From ref. 70

4.2.5 Vinylogous Reactivity

For metallovinylcarbenoids, electrophilic reactivity can occur at the vinylogous position in addition to the carbenoid center.[71-75] In order to test which pathway is occuring, the reaction between unsubstituted vinyldiazoacetate **4.15** and cyclopentadiene (Scheme 4.7, Table 4.5) can be carried out. The reaction can give rise to product **4.16**, derived from a tandem cyclopropanation–Cope rearrangement (carbenoid reactivity), as well as **4.17**, which comes from vinylogous reactivity of the vinylcarbenoid.[72,75] The reaction of **4.15** with cyclopentadiene, catalyzed by bismuth–rhodium complex **III**, afforded a 50 : 50 ratio of the products in overall 80% yield. The reaction with the analogous homobimetallic complex $Rh_2(O_2CCF_3)_3(O_2CCH_3)$ gave a 26 : 74 ratio of **4.16** to **4.17** in

overall 82% yield. For comparison, the more electron-rich catalyst $Rh_2(O_2CCH_3)_4$ gave 63 : 37 ratio in 79% yield. These results indicate that the bismuth–rhodium carbenoid behaves as a slightly more electron-rich system since it displays less vinylogous reactivity than the dirhodium system. Although the overall difference is not large, as demonstrated in the Hammett-studies, it is clear that the occurrence of vinylogous reactivity is very sensitive to the structure of the vinylcarbenoid complex.[72]

Scheme 4.7: Reaction with cyclopentadiene.

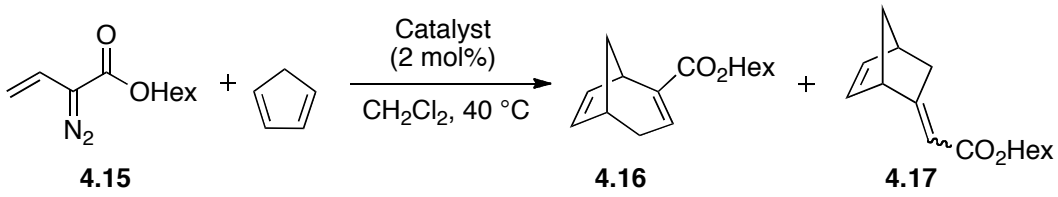

4.15 **4.16** **4.17**

Table 4.5: Vinylogous *vs* carbenoid reactivity.

Entry	*Catalyst*	*Product Ratio* (**4.16** : **4.17**)[a]	*Z/E-ratio* (**4.17**)[a]	*Yield* (%)[b]
1	$Rh_2(OAc)_4$	63 : 37	2.7 : 1	79
2	$Rh_2(TFA)_3(OAc)$	26 : 74	1.3 : 1	82
3	**III**	50 : 50	1.5 : 1	80

[a] Measured by ^1H NMR of crude reaction mixture.
[b] Overall yield.

4.2.6 Density functional studies

A density functional study of the reaction pathways for carbenoid formation as well as the [2+1]-cycloaddition steps was carried out. For model systems, the cyclopropanation reaction of styrene with methyl phenyldiazoacetate (**4.6a**) with both dirhodium and Bi–

Rh model catalysts were investigated. The calculated reaction pathway involving **4.6a** and styrene, catalyzed by $Rh_2(O_2CH)_4$, has been reported in the literature.[76] Only the currently accepted mechanism for reactions of diazo compounds with dirhodium complexes was considered (Scheme 4.8).[11,56,57,77] The catalytic cycle involves initial complexation of **4.6a** to the bimetallic catalyst, a rate-limiting nitrogen extrusion step *via* **TS-I** to form the intermediate metal carbenoid complex **4.19a** and finally, [2+1]-cycloaddition with the alkene to form the cyclopropane product **4.7a**.[11,56,57,77] Alternative mechanisms have been suggested in the literature, but were not considered since these have not yet gained general acceptance and suffer from lack of compelling experimental evidence.[54,55,78,79]

Scheme 4.8: Mechanism for catalytic cyclopropanation by dirhodium complexes.[11,56,57,77]

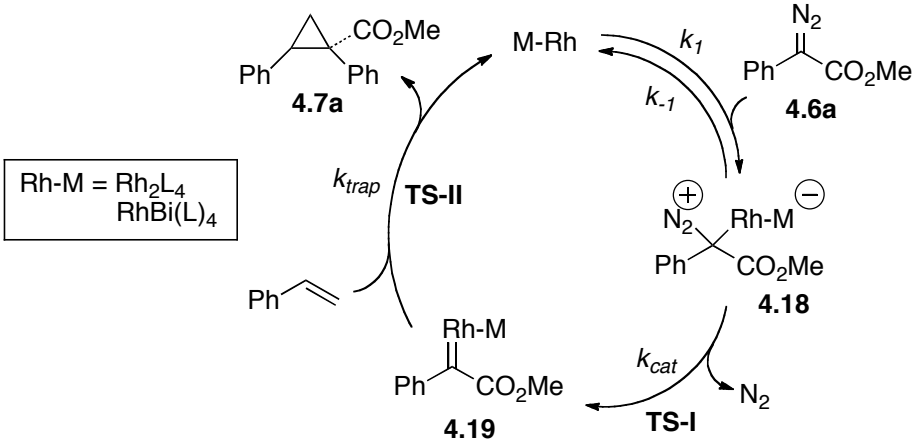

The reaction pathway potential energy diagrams calculated for the cyclopropanation reactions of **4.6a** with styrene, catalyzed by dirhodium formate[76] (red pathway) and bismuth–rhodium formate (blue pathway), are shown in Figure 4.6. The former path was reported in the literature and is only included here for comparison.[76] The calculated Bi–Rh structures are indicated and display analogous features to the dirhodium structures.

Coordination of the diazoacetate to the catalyst to form **4.18a/b** is an exoergic process in both cases, but somewhat less for the Bi–Rh system (-1.8 kcal/mol for **4.18a** *vs* -7.4 kcal/mol for **4.18b**). The nitrogen loss from **4.18a** *via* **TS-Ia** has a potential energy barrier of 19.2 kcal/mol, considerably higher than for dirhodium (11.3 kcal/mol for **4.18b** →**TS-Ib**). One striking difference between the two systems is that carbenoid formation is endoergic for Bi–Rh (+2.5 kcal/mol), but quite exoergic for dirhodium (-9.1 kcal/mol). Relative to the reactants, the Bi–Rh carbenoid complex **4.19a** is less stable by 0.7 kcal/mol, whereas the dirhodium carbenoid **4.19b** is stabilized by -16.5 kcal/mol. Despite this difference in thermodynamic stability, the kinetic stabilities of the two are not very different (3.6 kcal/mol barrier for cyclopropanation *via* **TS-IIa** for Bi–Rh system *vs* 4.5 kcal/mol for dirhodium **TS-IIb**). The difference in kinetic stabilities is presumably due to a reduced π-backbonding component in the Bi–Rh carbenoid system because of the relatively long Rh–C bond length (2.120 Å *vs* 2.010 Å in dirhodium).[80] The generally reduced σ-donor/π-acceptor bonding properties of these complexes with the axial ligand have been discussed in recent literature.[80] The presence of a significant carbenoid trapping barrier for the Bi–Rh carbenoid is a consequence of the stabilizing phenyl group on the carbenoid complex.[76] The calculations are consistent with the Hammett study, which showed only minor differences in selectivity between the two catalyst systems.

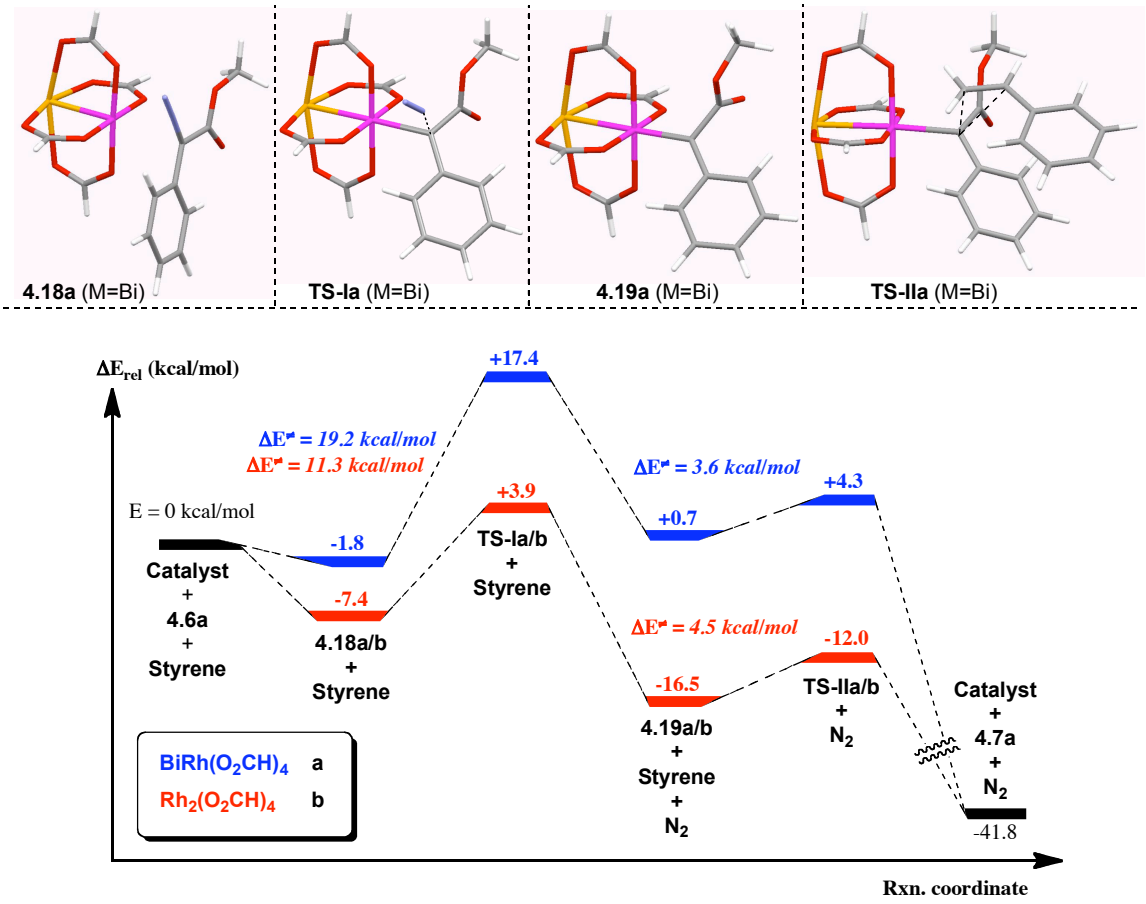

Figure 4.6: Potential energy surfaces (relative to free reactants) at B3LYP/6-311G(2d,2p)[Rh-RSC+4f][Bi-RLC]//B3LYP/6-31G*[Rh-RSC+4f][Bi-RLC] level for dirhodium[76] and Bi–Rh models.

As shown in the ReactIR studies in Section 4.2.2, the Bi–Rh catalyzed process was much slower (~1,600 times) than the corresponding dirhodium catalyzed reaction. Such a large difference in decomposition reaction rate would correspond to a much smaller difference in barrier heights of the rate-limiting step than the 7.9 kcal/mol potential energy difference obtained from the DFT computations (Entropic barriers are very similar for the two systems). In light of this difference between the two catalysts, which is in poor agreement with the experimental studies, it is likely that other effects may be

involved that are not reflected in the computational models. One possible explanation of why the barrier height difference is overestimated, could be that using formate ligands in the model catalyst systems may not give appropriate results for the Bi–Rh system. Another effect may arise from the possibility that the dirhodium catalysts have an axially coordinated ligand on the second rhodium during the catalytic cycle.[81-84] The potential influence of an axial ligand on reactions at the other metal active site has not previously been explicitly investigated computationally. Pirrung and co-workers could not demonstrate any evidence for such a pathway from kinetic data, but only a few, relatively electron-rich systems were investigated.[57] It is known that, binding of a ligand at one of the sites, weakens the binding of any ligand at the other site through the *trans*-effect.[57] It is, however, conceivable that the mechanism may proceed with an axial ligand at the other rhodium center, particularly if the catalyst is highly electrophilic. Since relatively electron-deficient catalysts were used in this study, the effect of a potential ligand at the other rhodium site has to be evaluated. The axial ligand may be adventitious water, solvent or other coordinating groups in reactants or products (π-bonds and carbonyl groups).[84] The carbonyl groups in the product, which is formed rapidly during the reaction, could be the major contribution to this effect.[85] The Bi–Rh complexes only exhibit Lewis acidity towards coordinating molecules at the Rh-end,[63] hence, the secondary axial ligand effect is absent. In order to study the axial coordination effects for the dirhodium system, the reaction pathway structures were re-optimized for the dirhodium tetraformate model, this time with an acetone molecule coordinated to the second rhodium as a model for a carbonyl donor. Figure 4.7 shows a comparison of the non-coordinated system *versus* the axial-coordination model, with the latter catalyst

structure shown. For the new catalyst system, the coordination of the diazo compound to form **4.18c** is less exoergic (-3.1 kcal/mol *vs* -7.4 kcal/mol for **4.18b**). The nitrogen extrusion potential energy barrier (**4.18c→TS-Ic**), displays a very large effect, and is now increased to 16.0 kcal/mol, 4.7 kcal/mol higher than what was previously calculated without the secondary axial ligand. The much smaller difference in potential energy barrier between the Bi–Rh and dirhodium systems ($\Delta\Delta E^{\neq}$ = 3.2 kcal/mol) is now more consistent with the experimentally observed reactivity difference. From the reactIR data reported above for $Rh_2(O_2CCF_3)_3(O_2CCH_3)$ and complex **III**, one can estimate the value of $\Delta E_a^{\neq}$ (Arrhenius activation energy difference) by applying the Arrhenius equation (Equation 4.2) to produce an expression that involves the reactivity difference k_{rel} (Eq. 4.3).

$$k = A \cdot e^{-\left(\frac{E_a}{RT}\right)} \qquad \text{Eq. (4.2)}$$

$$k_{rel} = \frac{k_1}{k_2} = e^{\frac{1}{RT}(E_{a2} - E_{a1})} \qquad \text{Eq. (4.3)}$$

A reactivity difference of ~1,600 roughly corresponds to $\Delta E_a^{\neq}$ ~ 4 kcal/mol. This would be the difference in activation barriers for the two catalyst systems. Considering the simplicity of the computational model (many approximations) and the error bars of density functional calculations, these calculations are in very good agreement with the experimental data. This agreement may suggest that secondary axial coordination effects are important when considering electron-deficient dirhodium complexes.

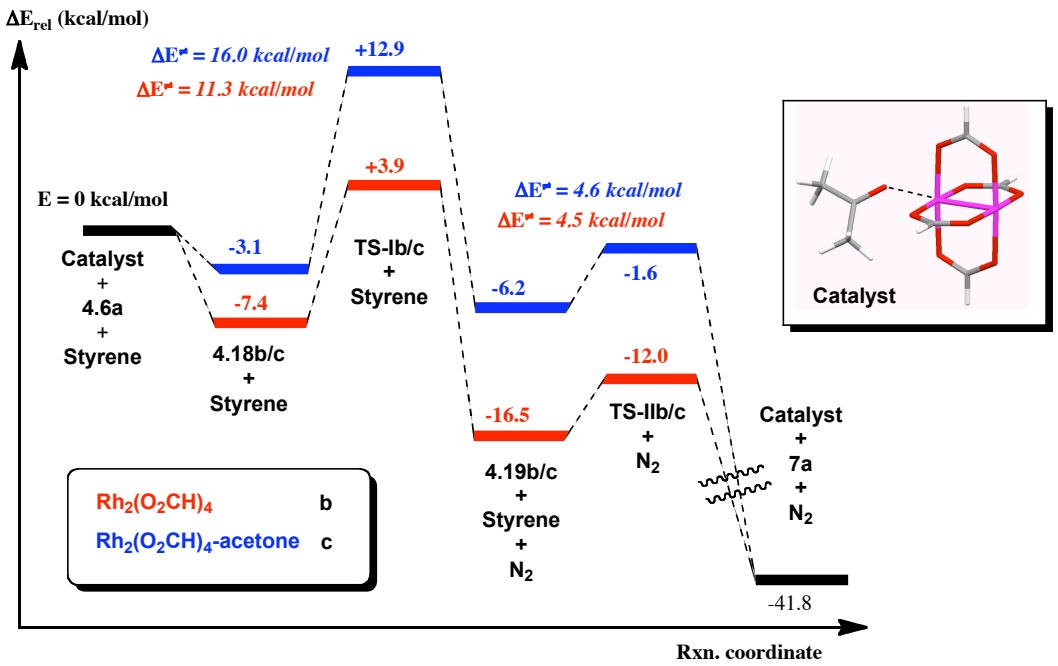

Figure 4.7: Influence of axial coordination on the reaction pathway potential energy surface compared to the coordination-free system.[76] Potential energy values (relative to free reactants) are calculated at B3LYP/6-311G(2d,2p)[Rh-RSC+4f]//B3LYP/6-31G*[Rh-RSC+4f] level of theory.

For the dirhodium system with a secondary axial ligand, the formation of the carbenoid complex **4.19c** is now less exoergic by only -3.1 kcal/mol. An interesting observation is that the potential energy barrier for the product-determining step (**4.19c→TS-IIc**) is almost unchanged by the presence of the secondary axial ligand (4.6 kcal/mol *vs* 4.5 kcal/mol for **4.19b→TS-IIb**). This suggests that the selectivity in these reactions is not much influence by the secondary axial ligand, which is generally in agreement with previously reported studies using immobilized dirhodium complexes.[58-60]

The influence of the electron-withdrawing nature of the ligands was also studied, in order to explore the differential effects on the two different bimetallic cores. Only Bi–Rh

complexes with two or more electron withdrawing ligands (trifluoroacetate) are currently available, and have therefore been used in the synthetic studies.[63,64] The reaction pathway was again re-calculated using $Rh_2(O_2CCF_3)_4$ and $BiRh(O_2CCF_3)_4$ as catalysts (Figure 4.8). As these models represent rather large computational systems for this level of density functional calculations, the role of a secondary coordinating ligand on dirhodium was not re-investigated for reasons of computational cost. Qualitatively, the reaction pathways remained the same as shown before, but significant absolute potential energy differences occur. Coordination of the diazo compound to the catalyst complexes has become much more exoergic compared to the formate model systems (-5.4 kcal/mol for Bi–Rh system **4.18d** and -13.3 kcal/mol for **4.18e**). The use of strongly electron-withdrawing trifluoroacetate ligands has made the diazo coordination process much more exoergic, which would be expected. As discussed above, it is likely that such highly electron-deficient dirhodium complexes as $Rh_2(O_2CCF_3)_4$ undergo the catalytic cycle with a secondary axial coordinating group. This is supported by the observed increase in exoergicity for the initial coordination step. For $BiRh(O_2CCF_3)_4$, the nitrogen extrusion barrier through **TS-Id** is only 1.6 kcal/mol lower than for the heterobimetallic formate model system (17.6 kcal/mol *vs* previously calculated 19.2 kcal/mol through **TS-Ia**). The same barrier decreased by 2.1 kcal/mol for the dirhodium catalyst, only by introducing the trifluoroacetate ligands. This reduction is similar reduction to that present in the Bi–Rh system. The difference between rate-limiting potential energy barriers for the two systems remains roughly the same. The thermodynamic stabilities of the carbenoid complexes **4.19d/e**, however, have changed significantly. For Bi–Rh, the carbenoid formation is now slightly exoergic (-0.4 kcal/mol), whereas it is much more exoergic for

dirhodium (-11.4 kcal/mol). In accordance with the more electron-withdrawing nature of the ligands, the [2+1]-cycloaddition barriers are somewhat lower compared to the former model barriers, but the overall trend remains the same (Bi–Rh has a slightly smaller potential energy barrier in the product-determining step).

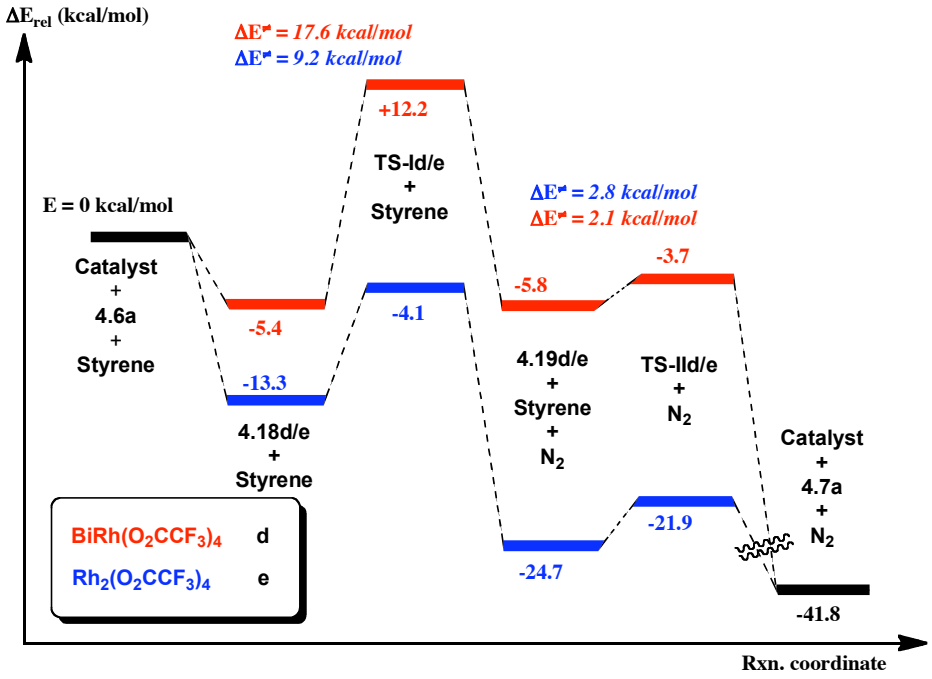

Figure 4.8: Potential energy surfaces (relative to free reactants) at B3LYP/6-311G(2d,2p)[Rh-RSC+4f][Bi-RLC]//B3LYP/6-31G*[Rh-RSC+4f][Bi-RLC] level for trifluoroacetate bridged complexes.

Charge distribution analysis. Figure 4.9 shows the calculated Mulliken charges on the bimetallic core as a function of the reaction coordinate for the catalytic cycle of the [2+1]-cycloaddition reaction with styrene. The partial charges on the two metal atoms in the dirhodium tetrakisformate (Rh^1=blue, Rh^2=red) and Bi–Rh tetrakisformate (Rh^3=violet, Bi=orange) model systems are indicated. For the dirhodium tetrakisformate pathway, coordination of the diazo compound leads to a reduction in Mulliken charge for

Rh^2 (red line) by about -0.2q. This is in accordance with calculations by Nakamura et. al. in a study of diazomethane and methyl diazoacetate in C–H insertion chemistry.[56] The charge drop signifies reduction of Rh^2 and demonstrates that it can act as an electron sink in the catalytic cycle.[56] For Bi–Rh tetrakisformate, both Bi and Rh only become partially reduced during the coordination event. Upon formation of the carbenoid complex, however, a reduction of about -0.2q occurs for Bi, a value close to that of Rh^2 in the aforementioned system. This clearly shows that Bi–Rh complexes can act as a redox pool, thereby facilitating the catalytic cycle, as shown previously in C–H insertion chemistry.[56] Further evidence comes from the elongation of the Bi–Rh intermetallic distance during the reaction (from 2.582 Å to 2.649 Å).

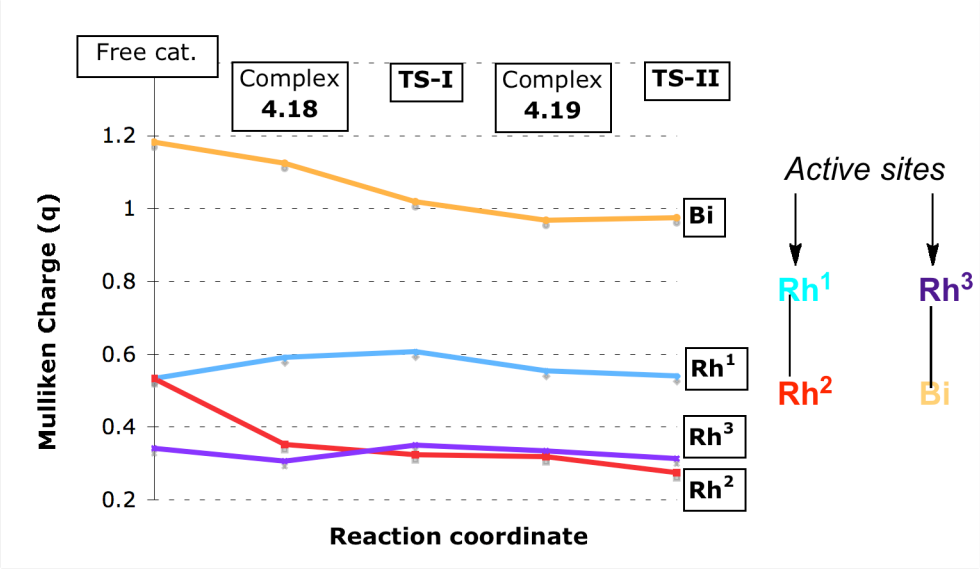

Figure 4.9: Charge distribution on bimetallic core as a function of reaction coordinate for dirhodium and Bi–Rh tetrakisformate model systems.

4.4 Conclusions

In the study described herein, heterobimetallic bismuth–rhodium paddlewheel carboxylate complexes have been demonstrated to act as effective catalysts for metallocarbenoid transformations. The studied complexes have been able to mediate [2+1]-cycloaddition reactions, C–H insertion as well as vinylogous addition chemistry with donor/acceptor carbene ligands. Similar chemo– and diastereoselectivities to the analogous dirhodium complexes were observed.

The decomposition of methyl phenyldiazoacetate in the presence of styrene, catalyzed by $BiRh(O_2CCF_3)_3(O_2CCH_3)$, was found to be about ~1,600 times slower than the corresponding dirhodium-catalyzed reaction. Density functional computed potential energy surfaces of the reaction pathway with model systems were consistent with the experimental reactivity difference if secondary axial coordination in the dirhodium catalyst model was considered. The calculations were furthermore consistent with the synthetic studies in that the selectivity profile of the Bi–Rh carbenoids was similar to that of analogous rhodium carbenoids. An analysis of the bimetallic charge distribution as a function of the reaction coordinate shows that the bismuth–rhodium core can, similar to the dirhodium framework, act as a redox pool, thereby facilitating the catalytic process.

4.5 Experimental Section

4.5.1 General Considerations for Synthetic Studies

All reactions were conducted in flame-dried glassware under an inert atmosphere of dry argon. All reagents were used as received from commercial suppliers, unless otherwise stated. Furan, styrene and 1,4-cyclohexadiene were filtered through a plug of silica before use. Cyclopentadiene was obtained from thermal cracking of commercially available cyclopentadiene dimer with subsequent distillation. Bi–Rh complexes were supplied by the Dikarev group, synthesized according to published procedures.[62-64] The dirhodium complexes were synthesized according to published procedures.[55] Dichloromethane solvent was obtained from drying columns (Grubbs type solvent purifier) and was degassed by bubbling argon through the solvent for >15 min prior to use. Flash chromatography was performed on silica gel (230-400 mesh). Thin layer chromatography (TLC) was performed on aluminium backed plates, pre-coated with silica gel (0.25 mm, 60 F_{254}) which were developed using standard visualizing agents: UV fluorescence (254 nm) and phosphomolybdic acid/Δ. Melting points were determined using a Mel-Temp electrothermal melting point apparatus and are uncorrected. ^{1}H NMR spectra were recorded on Varian Nuclear Magnetic Resonance spectrometers at 600, 500, 400 or 300 MHz. Tetramethylsilane (TMS) was used as internal standard (δ = 0.00) and data are reported as follows: chemical shift, multiplicity (s = singlet, d = doublet, t = triplet, q = quartet, qu = quintet, m = multiplet, and br = broad), integration and coupling constants in Hz. ^{13}C NMR spectra were recorded at 150, 125, 100 or 75 MHz. The solvent was

used as internal standard ($CDCl_3$ δ =77.0) and spectra were obtained with complete proton decoupling. Infrared (IR) spectra were aquired using a Thermo Scientific Nicolet iS10 FTIR spectrometer and the wavenumbers are reported in reciprocal centimeters (cm^{-1}). Diastereomeric ratios were determined by integration of the ^1H NMR spectra of crude reaction mixtures.

4.5.2 Procedures and Characterization Data

General procedure for cyclopropanation of styrene: To a flame dried round-bottom flask under an inert and dry argon-atmosphere, was added styrene (5 equiv.), dry CH_2Cl_2 (6.0 mL) and catalyst (0.02 equiv.). The flask was then placed in an oil bath and heated to 40 ˚C (reflux). The diazo compound (0.2 mmol, 1.0 equiv.) was dissolved in dry CH_2Cl_2 (3.0 mL) and added to the former solution dropwise over 2-4 h at 40 ˚C. The reaction mixture was allowed to stir for further 1 h after addition, the solvent was then removed *in vacuo*. The crude residue was analyzed by ^1H NMR and purified by flash column chromatography on silica gel with Et_2O/pentane eluent mixtures.

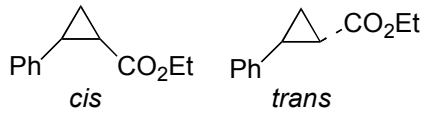

Mixture of (±)-Ethyl 2β-phenylcyclopropane-1α-carboxylate and (±)-Ethyl 2β-phenylcyclopropane-1β-carboxylate (4.7b). ^1H NMR (400 MHz, $CDCl_3$): δ 7.35-7.08 (m, 10H), 4.32-4.11 (q, 2H, *J* = 6.0 Hz), 3.92-3.81 (q, 2H, *J* = 6.0 Hz), 2.64-2.47 (m, 2H), 2.13-2.02 (m, 1H), 1.95-1.86 (m, 1H), 1.76-1.56 (m, 2H), 1.39-1.22 (m, 2H), 1.30-1.24 (t, 3H, *J* = 6.0 Hz), 1.01-0.93 (t, 3H, *J* = 6.0 Hz). The *cis*-isomer is the major diastereomer (21% de). Consistent with previously reported results.[19,65]

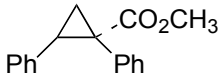

(±)-Methyl 1β, 2β-diphenylcyclopropane-1α-carboxylate (4.7a). ^{1}H NMR (400 MHz, $CDCl_3$): δ 7.11-7.09 (m, 3H), 7.03-7.00 (m, 5H), 6.76-6.74 (m, 2H), 3.63 (s, 3H), 3.11 (dd, 1H, *J*=7.0, 9.5 Hz), 2.13 (dd, 1H, *J*=5.0, 9.5 Hz), 1.86 (dd, 1H, *J*=5.0, 7.0 Hz). Consistent with previously reported results.[19]

General procedure for reactions with furan: To a flame dried round-bottom flask under an inert and dry argon-atmosphere was added furan (2.0 mL) and catalyst (0.02 equiv.). Methyl phenyldiazoacetate **4.6a** (0.5 mmol, 1.0 equiv.) was dissolved in furan (3.0 mL) and added to the former solution dropwise over 3 h at reflux. The mixture was allowed to stir for further 1 h after addition, or until periodic TLC analysis showed absence of diazo compound. The reaction mixture was then allowed to cool to ambient temperature and the remaining furan was removed *in vacuo*. The crude product was analyzed by ^{1}H NMR and purified by flash column chromatography using Et_2O/pentane eluent mixtures.

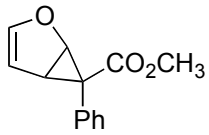

(±)-Methyl 6-phenyl-2-oxa-bicyclo[3.1.0]hex-3-ene-6-carboxylate (4.8). Structure assigned by analogy to previously reported data.[67] White solid. Mp = 79-80°C. TLC (10% Et_2O/pentane): R_f = 0.29. FTIR (neat): ν_{max}/cm^{-1} 3109, 3057, 3024, 2956, 1702, 1590, 1496, 1447, 1434, 1335, 1309, 1266, 1143, 1065, 1050, 1020, 978. ^{1}H NMR (500 MHz, $CDCl_3$): δ 7.29-7.23 (m, 3H), 7.19 (m, 2H), 5.90 (d, 1H, *J* = 2.0 Hz), 5.22 (t, 1H, *J* = 2.5 Hz), 5.13 (d, 1H, *J* = 5.5 Hz), 3.61 (s, 3H), 3.30 (dd, 1H, *J* = 5.5, 2.5 Hz). ^{13}C NMR (125 MHz, $CDCl_3$): δ 173.8, 147.3, 132.7, 130.7, 127.7, 127.2, 103.9, 70.7, 52.4, 39.2,

27.8. MS (EI, 70 eV): *m/z* (rel.int.) 216 (64), 201 (33), 184 (60), 157 (100), 128 (84). HRMS (EI, 70 eV): *m/z* 216.0780 ([$C_{13}H_{12}O_3$] requires 216.0781).

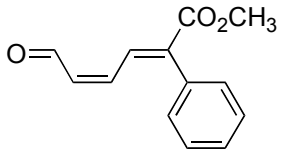

(2*E*, 4*E*)-Methyl 2-phenyl-6-oxohexa-2,4-dienoate (4.9). Structure assigned by analogy to previously reported structure as well as nOe measurements.[67] Yellow oil. TLC (30% Et_2O/pentane): R_f = 0.39. IR (neat): ν_{max}/cm^{-1} 3057, 2952, 2848, 1716, 1675, 1614, 1435, 1393, 1248, 1196, 1777, 1138, 1038, 1022. ^{1}H NMR (500 MHz, $CDCl_3$): δ 10.40 (d, 1H, *J* = 7.6 Hz), 8.31 (d, 1H, *J* = 12.0 Hz), 7.42 (m, 2H), 7.25 (m, 3H), 6.96 (dd, 1H, *J* = 12.0, 11.0 Hz), 6.04 (dd, 1H, *J* = 7.6, 11.0 Hz), 3.82 (s, 3H). ^{13}C NMR (125 MHz, $CDCl_3$): δ 190.1, 166.9, 140.9, 140.5, 133.2, 132.3, 131.3, 130.1, 128.7, 128.1, 52.6. MS (EI, 70 eV): *m/z* (rel.int.) 216 (15), 187 (65), 157 (100), 128 (72). HRMS (EI, 70 eV): *m/z* 216.0781 ([$C_{13}H_{12}O_3$] requires 216.0781).

Characteristic nOe correlations:

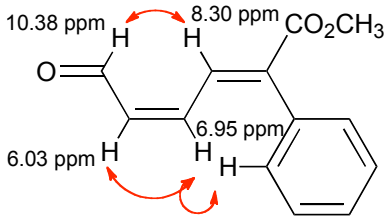

General procedure for Hammett competition experiments:[68] To a flame dried round-bottom flask under an inert and dry argon-atmosphere, was added substituted styrene (5.0 equiv.) and styrene (5.0 equiv.), dry CH_2Cl_2 (3.0 mL) and catalyst (0.01 equiv.). Methyl phenyldiazoacetate **4.6a** (0.2 mmol, 1.0 equiv.) was dissolved in dry CH_2Cl_2 (3.0 mL) and added to the former solution, drop-wise over 3 h at ambient temperature. The mixture

was allowed to stir for further 30 min – 1 h after addition. The solvent was then removed *in vacuo*. The ratio of cyclopropane products was obtained by from the crude ^{1}H NMR spectrum. The obtained product ratios are summarized in Table 4.6.

Table 4.6: Product ratios obtained in competition studies.

Entry	*R* =	σ^+	*Product ratios* (k_R/k_H)[b]		
			Complex **I**	*Complex* **III**	$Rh_2(TFA)_3OAc$
1	$-OCH_3$	-0.78[a]	6.21	6.67	8.80
2	$-CH_3$	-0.31[a]	2.08	2.00	2.26
3	-H	0.00[a]	1.00	1.00	1.00
4	-Cl	0.11[a]	0.71	0.79	0.75
5	$-CF_3$	0.61[a]	0.20	0.27	0.20

[a] Obtained from reference 69.
[b] From crude ^{1}H NMR data.

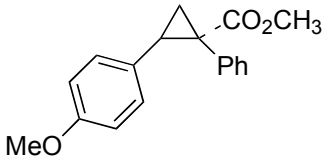

(±)-Methyl 2β-(4-methoxyphenyl)-1β-phenylcyclopropane-1α-carboxylate (MeO-4.11). ^{1}H NMR (500 MHz, $CDCl_3$): δ 7.26-6.96 (m, 9H), 3.68 (s, 3H), 3.62 (s, 3H), 3.03 (dd, 1H, *J* = 10.7, 9.3 Hz), 2.10 (dd, 1H, *J* = 9.3, 4.8 Hz), 1.79 (dd, 1H, *J* = 10.7, 4.5 Hz). Consistent with previously reported results.[68]

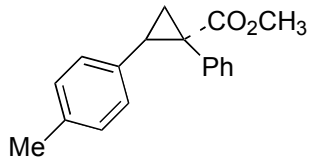

(±)-Methyl 2β-(4-methylphenyl)-1β-phenylcyclopropane-1α-carboxylate (Me-4.11). ^{1}H NMR (500 MHz, $CDCl_3$): δ 7.11 (m, 3H), 7.02 (dd, 2H, *J* = 6.8, 3.6 Hz), 6.84 (d, 2H, *J* = 8.0 Hz), 6.63 (d, 2H, *J* = 8.0 Hz), 3.62 (s, 3H), 3.06 (dd, 1H, *J* = 9.6, 6.8 Hz), 2.18 (s,

3H), 2.11 (dd, 1H, *J* = 9.6, 4.8 Hz), 1.82 (dd, 1H, *J* = 6.8, 4.8 Hz). Consistent with previously reported results.[68]

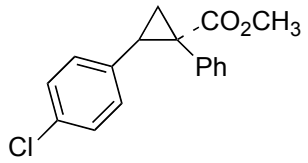

(±)-Methyl 2β-(4-chlorophenyl)-1β-phenylcyclopropane-1α-carboxylate (Cl-4.11). ^{1}H NMR (500 MHz, $CDCl_3$): δ 7.16-6.99 (m, 7H), 6.73 (m, 2H), 3.65 (s, 3H), 3.11 (dd, 1H, *J* = 9.4, 7.3 Hz), 2.15 (dd, 1H, *J* = 9.4, 4.9 Hz), 1.82 (dd, 1H, *J* = 7.3, 4.9 Hz). Consistent with previously reported results.[68]

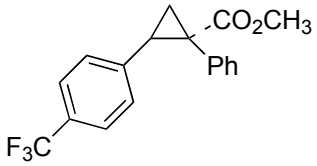

(±)-Methyl 2β-(4-trifluoromethylphenyl)-1β-phenylcyclopropane-1α-carboxylate (CF_3-4.11). ^{1}H NMR (500 MHz, $CDCl_3$): δ 7.29 (d, 2H, *J* = 8.1 Hz), 7.20-7.10 (m, 3H), 7.10-6.80 (m, 2H), 6.84 (d, 2H, *J* = 8.1 Hz), 3.66 (s, 3H), 3.15 (dd, 1H, *J* = 9.0, 6.8 Hz), 2.18 (dd, 1H, *J* = 9.0, 5.1 Hz), 1.89 (dd, 1H, *J* = 6.8, 5.1 Hz). Consistent with previously reported results.[68]

General procedure for C–H functionalization: To a flame dried round-bottom flask under an inert and dry argon-atmosphere was added the trapping agent (20 equiv.), dry CH_2Cl_2 (6.0 mL) and catalyst (0.02 equiv.). The diazo compound (0.2 mmol, 1.0 equiv.), dissolved in dry CH_2Cl_2 (3.0 mL), was added to the former solution dropwise over 2-4 h at 40 ˚C. The mixture was allowed to stir for further 1 h after addition. The solvent was

then removed *in vacuo* and the crude material analyzed by ^{1}H NMR. The residue was purified by column chromatography on silica gel with Et_2O/pentane eluent mixtures.

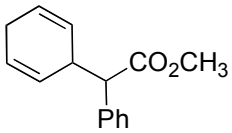

(±)-Methyl 2-(2,5-cyclohexadienyl)-2-phenylacetate (4.12). ^{1}H NMR (500 MHz, $CDCl_3$): δ 7.33-7.29 (m, 4H), 7.28-7.25 (m, 1H), 5.82-5.79 (m, 1H), 5.73-5.66 (m, 2H), 5.28-5.25 (m, 1H), 3.67 (s, 3H), 3.50-3.46 (m, 1H), 3.42 (d, 1H, J = 10.5 Hz), 2.63-2.59 (m, 2H). Consistent with previously reported results.[70]

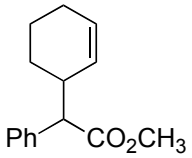

(±)-Methyl 2-(cyclohex-2-enyl)-2-phenylacetate (4.13). Obtained as mixtures of diastereomers. ^{1}H NMR (400 MHz, $CDCl_3$): δ 7.37-7.26 (m, 5H), 5.80-5.77 (m, 1H, diastereomer 1), 5.66-5.62 (m, 1H), 5.16-5.14 (m, 1H, diastereomer 2), 3.66 (s, 3H), 3.32 (d, 1H, J = 11 Hz), 2.89-2.86 (m, 1H), 2.0-0.8 (m, 6H). Consistent with previously reported results.[70]

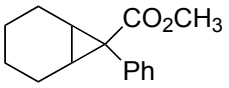

(±)-Methyl 7-phenylbicyclo[4.1.0]heptane-7-carboxylate (4.14). ^{1}H NMR (400 MHz, $CDCl_3$): δ 7.38-7.26 (m, 5H), 3.53 (s, 3H), 2.01-1.94 (m, 4H), 1.76-1.69 (m, 2H), 1.07-1.03 (m, 2H) 0.59-0.56 (m, 2H). Consistent with previously reported results.[70]

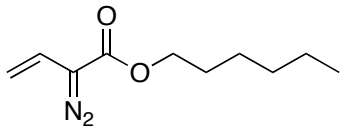

Hexyl 2-diazo-3-butenoate (4.15). See Chapter 3, Section 3.5.

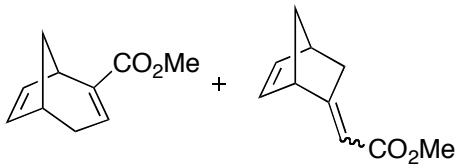

Me-4.16 **Me-4.17**

5-(2-Carbomethoxyethylidene)bicyclo[2.2.1]-hept-2-ene (Me-4.17) and Methyl Bicyclo[3.2.l]octa-2,6-diene-2-carboxylate (Me-4.16).[72,73] To a flame dried round-bottom flask under an inert and dry argon-atmosphere was added catalyst (0.02 equiv.), freshly distilled cyclopentadiene (10 equiv.) and dry CH_2Cl_2 (4.0 mL). The diazo compound **4.15** (0.2 mmol, 1.0 equiv.), dissolved in dry CH_2Cl_2 (3.0 mL), was added to the former solution dropwise over 1 h at 40 ˚C. The mixture was allowed to stir for further 1 h after addition. The solvent was then removed *in vacuo* and the crude material analyzed by ^{1}H NMR analysis. The crude residue was purified by column chromatography on silica gel with an Et_2O/pentane eluent mixture. **4.16** and **4.17** were chromatographically inseparable, and were therefore converted into their corresponding known methyl esters **Me-4.16**[72,73] and **Me-4.17**[72,73] by hydrolysis with aqueous KOH (excess) and subsequent methylation with Me_2SO_4 (excess). Data for **Me-4.16** and **Me-4.17**: ^{1}H NMR (400 MHz, $CDCl_3$): δ 6.51 (m, 1 H), 6.28 (dd, 1H, J = 3.0, 5.5 Hz), 6.23 (dd, 1 H, J = 5.6, 2.9 Hz), 6.00 (dd, 1H, J = 3.0, 5.5 Hz), 5.92 (s, 1H), 5.73 (dd, 1 H, J = 5.6, 2.7 Hz), 3.72 (s, 3 H), 3.67 (s, 3H), 3.32-3.30 (m, 2H), 3.08 (m, 1H), 2.71 (m, 1 H), 2.57 (m, 1H), 2.45 (ddd, 1 H, J = 20.0, 4.1, 4.1 Hz), 2.34 (m, 1H), 2.04 (dt, 1H, J = 9.9,

4.6 Hz), 1.91 (dd, 1H, *J* =20.0, 4.4 Hz), 1.70-1.62 (m, 2H), 1.47 (d, 1H, *J* = 8.0 Hz). The spectroscopic data are consistent with previous reports.[72,73]

General procedure for ReactIR experiments: Experiments were carried out with a Mettler Toledo ReactIR™ 45m instrument, equipped with a 9.5mm x 12" AgX 1.5m SiComp probe. A stock solution of **4.6a** in CH_2Cl_2 was prepared. Solutions of $BiRh(TFA)_3(OAc)$ (0.02 equiv.) and $Rh_2(TFA)_3(OAc)$ (0.001 equiv.) in styrene (0.1 mL each) were prepared. To a dry round-bottom flask, held under a positive nitrogen atmosphere, was added styrene (1.0 mL), CH_2Cl_2 and an aliquot of the solution of **4.6a** (1.0 equiv.). At this time, the ReactIR probe was inserted and the instrument set up for a continuous scan experiment. The scan was started and, at t_0 = 10 sec, the catalyst solution was injected by syringe in one movement with vigorous stirring. The reactions were monitored until the characteristic red colour of the diazo compound was not observable in the reaction flask. All solutions were equilibrated to ambient temperature before use (16 ˚C).

4.5.3 General Considerations for Computational Studies

All calculations were performed with the Gaussian '03 software package[86] using Density Functional Theory. The 3-parameter hybrid functional B3LYP[87,88] was employed in all calculations to locate stationary points on the potential energy surface. The structures were geometry optimized with a basis set consisting of the 1997 Stuttgart relativistic small-core ECP and corresponding basis set [Stuttgart RSC 1997 ECP][89-91] for Rh, augmented with a 4f-function (ζ_f(Rh) = 1.350),[76] the 1997 Stuttgart relativistic large-core ECP and basis set [Stuttgart RLC 1997 ECP] for Bi[92] and the split-valence basis set 6-31G* for all other atoms (C, H, N, O and F). This composite basis set is referred to as 6-

31G*[Rh-RSC+4f][Bi-RLC]. Herein, the main discussion is based on single-point potential energies, calculated at the B3LYP/6-311G(2d,2p)[Rh-RSC+4f][Bi-RLC]//B3LYP/6-31G*[Rh-RSC+4f][Bi-RLC] level of theory, for the optimized structures. Stationary points were characterized by normal coordinate analysis at the 6-31G*[Rh-RSC+4f][Bi-RLC] level of theory.[93] Transition states were confirmed to have a single imaginary vibrational mode, corresponding to movement along the reaction coordinate, whereas equilibrium structures were confirmed to have zero imaginary vibrational modes. Transition states were further characterized by intrinsic reaction coordinate (IRC) analysis, using default parameters, with subsequent geometry optimization to confirm that the stationary points were smoothly connected to each other.

The basis set and pseudopotential parameters were obtained from the EMSL basis set exchange website.[94,95] Calculated structures have been visualized using Mercury.[96-99] The GEN-keyword was utilized in Gaussian '03 to form the composite basis set.[86] An example of how the 6-31G*[Rh-RSC+4f][Bi-RLC] basis set and pseudopotential parameters[89-92,100] were specified is shown in Table 4.7 below. Note that the rhodium basis set is augmented with a 4f polarization function.[76,101]

Table 4.7: Basis set and pseudopotential definitions in the calculation input files.

```
gen=
Rh  0
 S   3  1.00
      7.91774400        -2.41557750
      6.84120700         3.09873820
      2.95984000        0.282125600
 S   1  1.00
      1.33434100         1.00000000
 S   1  1.00
     0.598810000         1.00000000
 S   1  1.00
     0.121894000         1.00000000
 S   1  1.00
     0.494520000E-01     1.00000000
```

```
 S   1  1.00
     0.160000000E-01      1.00000000
 P   2  1.00
      4.13607900         -3.34435450
      2.94628100          3.70374400
 P   2  1.00
      1.12230400         0.746225800
     0.666177000         0.269883300
 P   1  1.00
     0.365743000          1.00000000
 P   1  1.00
     0.766860000E-01      1.00000000
 P   1  1.00
     0.241700000E-01      1.00000000
 D   4  1.00
      7.03289200        -0.161604000E-01
      2.30981900         0.276398700
     0.998228000         0.485002600
     0.417057000         0.393019900
 D   1  1.00
     0.164447000          1.00000000
 D   1  1.00
     0.550000000E-01      1.00000000
 F   1  1.00
     1.350               1.00000000
****
F 0
6-31g*
****
N 0
6-31g*
****
O 0
6-31g*
****
C 0
6-31g*
****
H 0
6-31g*
****
BI  0
 S   3  1.00
      1.42538800         0.760080000E-01
     0.984914000        -0.457408000
     0.252514000         0.702184000
 S   1  1.00
     0.100619000          1.00000000
 P   3  1.00
      1.51728300         0.346682000
      1.25330700        -0.513313000
     0.207949000         0.648457000
 P   1  1.00
     0.694330000E-01      1.00000000
 D   1  1.00
     0.170000000          1.00000000
```

```
****

RH  0
RH-ECP   4   28
G POTENTIAL
 1
2         1.00000000       0.00000000
S-G POTENTIAL
 2
2        11.72000000     225.34775400
2         5.82000000      32.82318900
P-G POTENTIAL
 2
2        10.42000000     158.70941200
2         5.45000000      26.44410000
D-G POTENTIAL
 2
2         8.82000000      62.75862600
2         3.87000000      10.97871900
F-G POTENTIAL
 2
2        12.31000000     -30.09345600
2         6.16000000      -5.21848200
BI  0
BI-ECP   5   78
H POTENTIAL
 1
2         1.00000000       0.00000000
S-H POTENTIAL
 3
2         0.16115200      -0.16198800
2         1.50983500      14.03169000
2        10.00000000     122.04740100
P-H POTENTIAL
 2
2         0.76049000      -6.18852600
2         1.42641500      51.04586800
D-H POTENTIAL
 2
2         0.78022600      20.53580400
2         0.26007500      -0.13619600
F-H POTENTIAL
 1
2         0.97360800      -6.41422600
G-H POTENTIAL
 1
2         1.08819500      -6.65606400
```

4.5.4 Calculated Properties and Geometries

All structures reported in this section were geometry optimized at B3LYP/6-31G*[Rh-RSC+4f][Bi-RLC] level.[87-92,100,101] Normal coordinate analysis was carried out at the same level. Images were generated using Mercury.[96-99]

4.6a

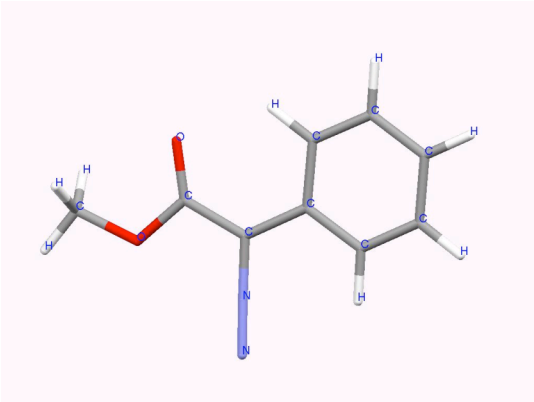

Route= #N B3LYP/6-31G* 5D OPT FREQ
B3LYP Energy=-607.67032271 Hartree
ZPE=0.158671 Hartree
Conditions=298K, 1.00000 atm
Enthalpy=-607.498960 Hartree
Free Energy=-607.550961 Hartree
Entropy=109.444 cal/mol-K
0 imaginary frequencies

C	0.00000000	0.00000000	0.00000000
O	-1.15504300	0.85268100	-0.00020600
C	-2.34934400	0.20756000	-0.00006700
C	-3.47020800	1.16039500	-0.00048100
N	-3.12166200	2.43156400	-0.00087700
N	-2.84896300	3.53671400	-0.00114400
C	-4.91378200	0.83731500	-0.00041000
C	-5.35862200	-0.49753500	-0.00165500
C	-6.72425300	-0.78069700	-0.00161300
C	-7.67125400	0.24382500	-0.00039200
C	-7.23596100	1.57043200	0.00085300
C	-5.87535400	1.86591600	0.00086400
H	-5.56570800	2.90746500	0.00192800
H	-7.95663700	2.38381500	0.00185500
H	-8.73294100	0.01373800	-0.00039000
H	-7.04578100	-1.81894400	-0.00257200
H	-4.63353000	-1.30007200	-0.00254100
O	-2.45331100	-1.00447500	0.00003700
H	0.00970300	-0.63487800	0.88989300
H	0.01060200	-0.63405600	-0.89048300
H	0.85649600	0.67470700	0.00071100

Styrene

C	0.00000000	0.00000000	0.00000000
C	1.02274500	-0.86478400	-0.00019800
C	2.46244000	-0.55582100	-0.00016300
C	3.38439700	-1.61694500	-0.00012500
C	4.75911700	-1.38152000	-0.00007500
C	5.24350100	-0.07309200	-0.00007100
C	4.34002300	0.99484600	-0.00012200
C	2.96861700	0.75748000	-0.00017000
H	2.28334300	1.60022100	-0.00023000
H	4.70813800	2.01759000	-0.00013100

H	6.31359500	0.11571900	-0.00003700
H	5.45045400	-2.22017300	-0.00004200
H	3.01291700	-2.63939500	-0.00012700
H	0.79109400	-1.93013500	-0.00039300
H	0.13729800	1.07800000	0.00022700
H	-1.02704000	-0.35210500	-0.00005300

Route= #N B3LYP/6-31G* 5D OPT FREQ
B3LYP Energy=-309.641798736 Hartree
ZPE=0.133769 Hartree
Conditions=298K, 1.00000 atm
Enthalpy=-309.500318 Hartree
Free Energy=-309.539492 Hartree
Entropy=82.449 cal/mol-K
0 imaginary frequencies

4.7a

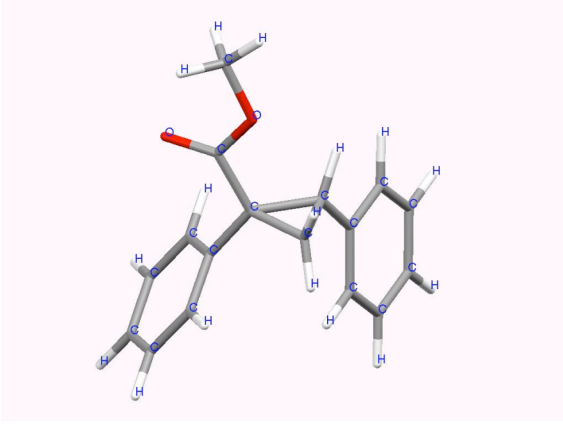

C	0.00000000	0.00000000	0.00000000
C	1.30206300	-0.35855000	-0.66177400
O	1.80185200	-1.53899700	-0.20974800
C	3.02794800	-1.95797400	-0.82821200
H	2.89201800	-2.08748000	-1.90531900
H	3.28377400	-2.90742700	-0.35638400
H	3.81548300	-1.21915300	-0.65840000
O	1.85445000	0.30023400	-1.51675500
C	-0.47843600	1.39196600	-0.30756200
C	-0.42763500	2.39911600	0.66324300
C	-0.84805700	3.69781700	0.36886000
C	-1.32152200	4.00572100	-0.90645200
C	-1.36902500	3.00965100	-1.88475800
C	-0.94979900	1.71455400	-1.58734300
H	-0.98706600	0.94338100	-2.35075600
H	-1.73475400	3.24192000	-2.88143300
H	-1.65055900	5.01528900	-1.13833500
H	-0.80065100	4.46722100	1.13517600
H	-0.04811600	2.16775700	1.65531600
C	-1.01407200	-1.18591200	0.12236800
C	-2.47146600	-1.04751900	-0.16407000
C	-3.04987100	-1.92515500	-1.09480100
C	-4.40922500	-1.86334100	-1.39871300

Route= #N B3LYP/6-31G(d) OPT FREQ
Basis=6-31G(d)
B3LYP Energy=-807.874908615 Hartree
ZPE=0.287567 Hartree
Conditions=298K, 1.00000 atm
Internal Energy=-807.570838 Hartree
Enthalpy=-807.569894 Hartree
Free Energy=-807.633152 Hartree
Entropy=133.138 cal/mol-K
0 imaginary frequencies

C	-5.22194300	-0.91540900	-0.77585600
C	-4.66063200	-0.03514800	0.15093100
C	-3.30148900	-0.10068100	0.45550600
H	-2.88844100	0.59779400	1.17610800
H	-5.28331400	0.70761500	0.64270900
H	-6.28214400	-0.86367200	-1.00853500
H	-4.83209400	-2.55740300	-2.12043400
H	-2.42360600	-2.66904000	-1.58248500
H	-0.59693300	-2.11879600	-0.24558800
C	-0.32752700	-0.63938600	1.33485300
H	-0.91636900	-0.04002600	2.02271700
H	0.43456400	-1.25154200	1.80454300

Dinitrogen N_2

Route= #N B3LYP/6-31G* 5D OPT FREQ
Basis=6-31G(d)
B3LYP Energy=-109.520718355 Hartree
ZPE=0.005600 Hartree
Conditions=298K, 1.00000 atm
Internal Energy=-109.512758 Hartree
Enthalpy=-109.511814 Hartree
Free Energy=-109.533568 Hartree
Entropy=45.785 cal/mol-K
0 imaginary frequencies

N	0.00000000	0.00000000	0.00000000
N	0.00000000	0.00000000	-1.10530400

Dirhodium tetrakisformate $Rh_2(O_2CH)_4$

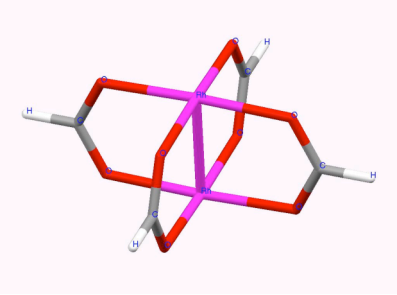

Route= #N B3LYP/gen pseudo=read gfprint OPT FREQ
B3LYP Energy=-977.981873264 Hartree
ZPE=0.101954 Hartree
Enthalpy=-977.865223 Hartree
Free Energy=-977.920161 Hartree
Entropy=115.627 cal/mol-K
0 imaginary frequencies

Rh	0.00000000	0.00000000	0.00000000
Rh	-0.00000200	0.00000100	2.38968300
O	-1.44640800	-1.45404100	2.33316300
C	-1.84327100	-1.84785700	1.19484000
O	-1.45075300	-1.44970000	0.05651800
H	-2.61841200	-2.62439900	1.19483700
O	-1.45406600	1.44638800	2.33316300
C	-1.84780600	1.84332600	1.19483700
O	-1.44976300	1.45069200	0.05651700
H	-2.62466600	2.61814800	1.19483500
O	1.44635100	1.45409600	2.33316300
C	1.84338400	1.84774300	1.19484000
O	1.45069200	1.44976200	0.05651700
H	2.61800000	2.62480900	1.19483600
O	1.45405300	-1.44639000	2.33316800
C	1.84781600	-1.84330800	1.19484300
O	1.44975500	-1.45069600	0.05652200
H	2.62461500	-2.61819000	1.19484400

Acetone – $Rh_2(O_2CH)_4$ complex

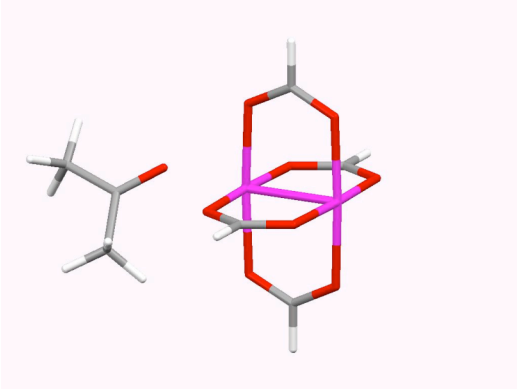

Route= # b3lyp/gen pseudo=read gfprint OPT FREQ
B3LYP Energy=-1171.16479351 Hartree
ZPE=0.187930 Hartree
Enthalpy=-1170.955386 Hartree
Free Energy=-1171.026260 Hartree
Entropy=149.168 cal/mol-K
0 imaginary frequencies

Rh	0.00000000	0.00000000	0.00000000
Rh	2.37839300	-0.41773500	-0.11568900
O	2.62411400	0.99162100	1.38003700
C	1.58206700	1.56014900	1.83239400
O	0.38217600	1.37939800	1.48151300
H	1.74845400	2.29990200	2.62762800
O	2.49776500	1.08225600	-1.53545000
C	1.42062600	1.66885600	-1.86755800
O	0.25345300	1.46003100	-1.43139900
H	1.52106900	2.45544100	-2.62812400
O	1.98627000	-1.78966400	-1.59869700
C	0.77802300	-1.97086600	-1.93735000
O	-0.25530500	-1.40093300	-1.47872900
H	0.60987900	-2.71439000	-2.72815000
O	2.11363800	-1.88158400	1.30616300
C	0.93949600	-2.08174800	1.74129300
O	-0.12684000	-1.48298700	1.41431800
H	0.83777100	-2.87401400	2.49523600
C	5.55484100	-0.29500500	-0.09870800
O	4.52956700	-0.97419000	-0.16647900
C	5.52249400	1.21194700	-0.07237900
H	4.82333200	1.58221700	-0.82733100
H	5.13179900	1.53164600	0.90115500
H	6.51480700	1.64482400	-0.22183700
C	6.89092600	-0.98826400	-0.02150600
H	6.76116500	-2.07123400	0.01230000
H	7.50042800	-0.71252000	-0.89168800
H	7.43578200	-0.64612900	0.86755600

Dirhodium tetrakis(trifluoroacetate)
$Rh_2(O_2CCF_3)_4$

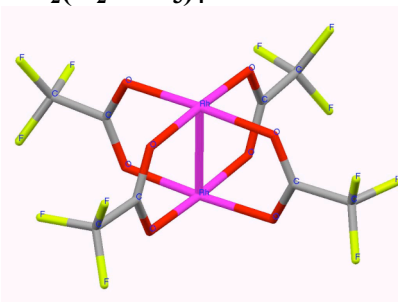

Route= # b3lyp/gen pseudo=read gfprint Integral(Grid=Ultrafine) OPT FREQ
B3LYP Energy=-2326.08424934 Hartree
ZPE=0.119592 Hartree
Enthalpy=-2325.934739 Hartree

Rh	0.00000000	0.00000000	0.00000000
Rh	-0.00015500	-0.00000200	-2.39476200
O	-1.45034300	-1.44557100	-2.33401600
C	-1.84788900	-1.82977700	-1.19723200
O	-1.45015200	-1.44562600	-0.06050800
C	-3.00228900	-2.85627900	-1.19737200
F	-4.16809900	-2.18448500	-1.20068200
F	-2.94950500	-3.63228200	-2.28373900
F	-2.95347600	-3.62845900	-0.10815500
O	1.44998000	-1.44564400	-2.33425200
C	1.84770800	-1.82980200	-1.19752700
O	1.45017100	-1.44558600	-0.06074300
C	3.00210100	-2.85631300	-1.19738600

Free Energy=-2326.032309 Hartree
Entropy=205.354 cal/mol-K
0 imaginary frequencies

F	4.16791300	-2.18452300	-1.19410500
F	2.94933000	-3.63229900	-0.11100600
F	2.95326900	-3.62851000	-2.28659100
O	1.44630500	1.44908400	-2.33415700
C	1.83217900	1.84569300	-1.19752700
O	1.44637700	1.44914600	-0.06083800
C	2.86373800	2.99562500	-1.19737400
F	2.19777000	4.16442300	-1.19393800
F	3.63948500	2.93868400	-0.11102300
F	3.63553700	2.94282500	-2.28668700
O	-1.44651700	1.44916000	-2.33392600
C	-1.83231300	1.84571500	-1.19723800
O	-1.44644400	1.44910200	-0.06060700
C	-2.86386400	2.99565400	-1.19739200
F	-2.19788800	4.16444700	-1.20080800
F	-3.63959800	2.93872900	-2.28375100
F	-3.63567500	2.94284700	-0.10808700

Bismuth–Rhodium tetrakis(formate)
$BiRh(O_2CH)_4$

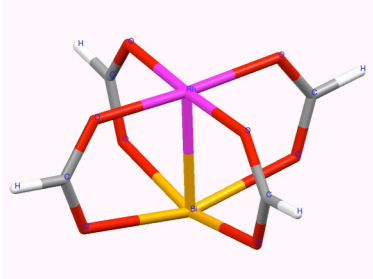

Route= # b3lyp/gen pseudo=read OPT freq
B3LYP Energy=-872.824620285 Hartree
ZPE=0.099292 Hartree
Enthalpy=-872.709168 Hartree
Free Energy=-872.768634 Hartree
Entropy=125.157 cal/mol-K
0 imaginary frequencies

Rh	0.00000000	0.00000000	0.00000000
Bi	2.58169300	-0.00042400	-0.00031800
O	2.17985900	-1.66069300	1.65849900
C	0.98238500	-1.94511300	1.94171000
O	-0.07069400	-1.44654200	1.44563400
H	0.81969200	-2.71215300	2.71186800
O	2.18043400	1.65830800	1.66014600
C	0.98305800	1.94182800	1.94466800
O	-0.07019300	1.44566000	1.44655200
H	0.82063500	2.71154100	2.71221100
O	2.18000400	1.66019300	-1.65881300
C	0.98255500	1.94475100	-1.94198900
O	-0.07056800	1.44654900	-1.44563700
H	0.81993000	2.71217200	-2.71178100
O	2.17943000	-1.65900400	-1.66074100
C	0.98188300	-1.94211800	-1.94494900
O	-0.07106900	-1.44562600	-1.44652300
H	0.81898600	-2.71181000	-2.71241300

Bismuth–Rhodium tetrakis(trifluoroacetate)
$BiRh(O_2CCF_3)_4$

Rh	0.00000000	0.00000000	0.00000000
O	-1.47006500	1.41757300	0.06957900
C	-1.96601400	1.90507000	-0.98262200

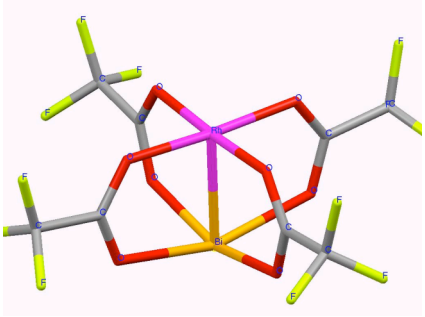

Route= #N b3lyp/gen pseudo=read gfprint integral(grid=ultrafine) opt freq
B3LYP Energy=-2220.92598707 Hartree
ZPE=0.116910 Hartree
Enthalpy=-2220.777508 Hartree
Free Energy=-2220.883365 Hartree
Entropy=222.794 cal/mol-K
0 imaginary frequencies

O	-1.67762700	1.63067300	-2.17816300
Bi	0.00079700	0.00040200	-2.59768400
O	-1.62301500	-1.68457800	-2.17804800
C	-1.90171000	-1.96925000	-0.98280900
O	-1.41809800	-1.46951300	0.06956800
C	-2.99527000	-3.04508200	-0.78743800
F	-2.70788300	-4.12570000	-1.52650500
F	-3.10830300	-3.41445400	0.48940600
F	-4.17268100	-2.54241600	-1.19844900
O	1.62909100	1.67982700	-2.17670100
C	1.90510100	1.96644100	-0.98136700
O	1.41816600	1.46942000	0.07081400
C	2.99167800	3.04942900	-0.78690600
F	2.65359700	4.15405300	-1.46817600
F	3.15257600	3.36896800	0.49825400
F	4.15847300	2.58743200	-1.26726300
O	1.68792200	-1.62076000	-2.17710000
C	1.97204300	-1.89915600	-0.98162700
O	1.47040100	-1.41704700	0.07052300
C	3.06074200	-2.97999900	-0.78724700
F	4.16690600	-2.63084200	-1.46057000
F	3.37412700	-3.14666700	0.49842700
F	2.60879900	-4.14694900	-1.27728600
C	-3.05358100	2.98718700	-0.78850400
F	-4.15793200	2.64167600	-1.46674100
F	-3.37118800	3.14949700	0.49691900
F	-2.59883600	4.15517100	-1.27262900

Methyl phenyldiazoacetate – BiRh(O$_2$CH)$_4$ complex 4.18a

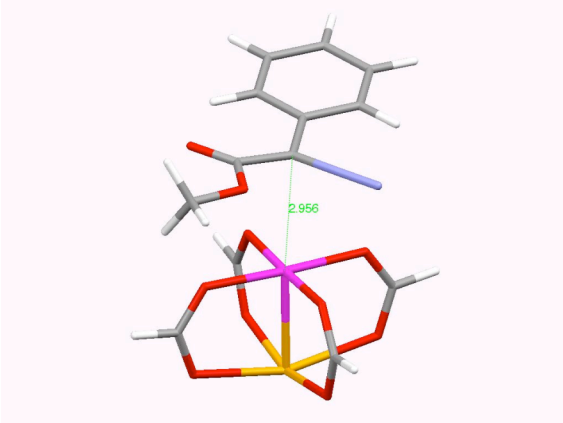

Route= #N b3lyp/gen pseudo=read gfprint integral(grid=ultrafine) OPT FREQ
B3LYP Energy=-1480.50104508 Hartree
ZPE=0.258003 Hartree

Rh	0.00000000	0.00000000	0.00000000
Bi	-2.49753700	-0.66264800	-0.19203900
O	-1.78618500	-2.27061200	1.41539600
C	-0.57706200	-2.25721400	1.77443800
O	0.34225400	-1.47858800	1.38139800
H	-0.26757900	-3.00558700	2.51791700
O	-1.60467700	-2.07165300	-1.87698100
C	-0.36293000	-2.00610500	-2.10256900
O	0.49460100	-1.27898900	-1.52248100
H	0.03479900	-2.65354100	-2.89668000
O	-2.44560700	1.12530600	-1.76628000
C	-1.35697200	1.74232800	-1.92663500
O	-0.24705500	1.52441300	-1.35593200
H	-1.35607600	2.57457100	-2.64529600
O	-2.64113500	0.94435800	1.57363000

Enthalpy=-1480.212647 Hartree
Free Energy=-1480.308021 Hartree
Entropy=200.731 cal/mol-K
0 imaginary frequencies

C	-1.57499800	1.49175100	1.96645600
O	-0.39948100	1.30976100	1.52871300
H	-1.65734700	2.21803900	2.78788600
C	2.88430200	0.53564700	0.35298900
C	2.82733800	1.71713900	-0.53781900
O	3.08427800	1.70820700	-1.72493400
O	2.45417500	2.82723000	0.14148000
C	2.27355000	4.00408300	-0.66186500
H	3.19730700	4.25573300	-1.18885600
H	1.47170800	3.84068300	-1.38542800
H	2.00441700	4.79279600	0.04100900
N	2.66824500	0.80050500	1.63742200
N	2.48357700	0.99182800	2.73910800
C	3.50843200	-0.77429800	0.03019100
C	3.89683000	-1.08315900	-1.28537500
C	4.49467300	-2.31080000	-1.56865300
C	4.71558300	-3.25188300	-0.56257400
C	4.32853200	-2.95132000	0.74465500
C	3.73204900	-1.72800400	1.03986400
H	3.43556100	-1.52370300	2.06418400
H	4.49220700	-3.66947200	1.54380100
H	5.18317800	-4.20539200	-0.79203500
H	4.79004200	-2.52796400	-2.59193500
H	3.72979100	-0.36131200	-2.07268800

BiRh(O_2CH)$_4$ complex N_2-extrusion TS (TS-Ia)

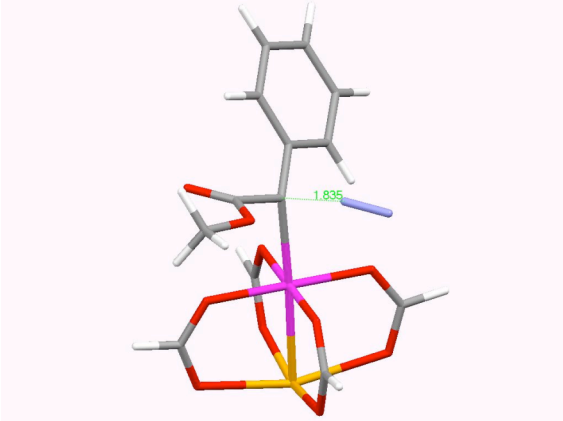

Route= #N b3lyp/gen pseudo=read gfprint integral(grid=ultrafine) OPT=(TS,CalcFC,NoEigenTest) freq
B3LYP Energy=-1480.47101923 Hartree
ZPE=0.255315 Hartree
Enthalpy=-1480.185416 Hartree
Free Energy=-1480.278112 Hartree

Rh	0.00000000	0.00000000	0.00000000
C	2.27647700	0.36677100	0.08128500
C	2.57630700	1.68954200	-0.53366200
O	2.44156200	2.75114600	0.28482800
C	2.53074700	4.03205600	-0.36217200
H	3.49295100	4.14217100	-0.86894700
H	2.43056600	4.76603000	0.43749100
H	1.72394000	4.14204800	-1.09078800
O	2.83119700	1.77536300	-1.72037800
C	3.26518100	-0.71466800	-0.10922600
C	4.51650000	-0.49251000	-0.72556800
C	5.41510100	-1.53976600	-0.90285000
C	5.09903700	-2.82170400	-0.44396000
C	3.87197600	-3.05495800	0.18205900
C	2.95824700	-2.01667400	0.33776200
H	2.00220900	-2.19437600	0.81421500
H	3.62238500	-4.05065100	0.53813200
H	5.80676700	-3.63597100	-0.57592500

Entropy=195.094 cal/mol-K
1 imaginary frequency

H	6.36726600	-1.35495700	-1.39222100
H	4.76716500	0.49475800	-1.09440200
O	-0.35097900	1.54703100	1.31956200
C	-1.51879800	1.93579900	1.63593300
O	-2.62567100	1.48133400	1.25084100
Bi	-2.58624200	-0.42513200	-0.21864700
O	-2.11319500	-1.82601000	1.69772700
C	-0.92073500	-1.90109400	2.07897100
O	0.10224200	-1.31593300	1.59519300
H	-0.70539500	-2.55225700	2.94023500
O	-2.32469300	1.07140100	-2.05024400
C	-1.17136400	1.54126700	-2.23933200
O	-0.10830000	1.30789800	-1.58854200
H	-1.04984800	2.24866000	-3.07315900
O	-1.80862500	-2.16476800	-1.66035500
C	-0.56433100	-2.25306400	-1.83259400
O	0.35658500	-1.55075400	-1.31422200
H	-0.20874100	-3.03753100	-2.51756200
H	-1.54075500	2.78054600	2.34147500
N	2.41836800	0.73542500	1.87263600
N	2.16290100	0.63036100	2.94762200

BiRh($O_2CH)_4$ carbenoid complex 4.19a

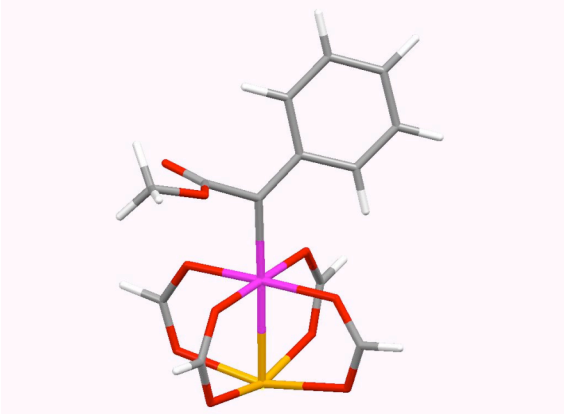

Route= #N b3lyp/gen pseudo=read gfprint integral(grid=ultrafine) OPT FREQ
B3LYP Energy=-1370.9730623 Hartree
ZPE=0.248068 Hartree
Enthalpy=-1370.696872 Hartree
Free Energy=-1370.785416 Hartree
Entropy=186.355 cal/mol-K
0 imaginary frequencies

Rh	0.00000000	0.00000000	0.00000000
Bi	2.64439700	-0.34568900	-0.04230400
O	2.06457500	-1.47545600	-2.10048100
C	0.85153600	-1.51515100	-2.41517400
O	-0.15036100	-1.03951900	-1.78871700
H	0.59038000	-2.02634900	-3.35511100
O	2.01079300	-2.30630800	1.21184600
C	0.78636800	-2.48755900	1.41839700
O	-0.19939200	-1.77049600	1.05107400
H	0.49990900	-3.38355700	1.99092400
O	2.47439000	0.90471700	1.98261500
C	1.31905400	1.24349600	2.34875500
O	0.20721700	1.02032000	1.77866800
H	1.23620100	1.81075900	3.28799700
O	2.51154400	1.72735800	-1.23773900
C	1.37064100	2.22885000	-1.39818700
O	0.24190300	1.77807000	-1.02663200
H	1.31742200	3.19025600	-1.93212200
C	-2.09626800	0.30914600	0.05725800
C	-2.51253200	1.71154000	0.26412800
O	-2.63468400	2.19386100	1.37566900
O	-2.70324200	2.37290800	-0.88871100

C	-2.93873000	3.78743600	-0.76153600
H	-3.83659200	3.97889700	-0.16808800
H	-2.08107500	4.27003600	-0.28636700
H	-3.06753600	4.15087800	-1.78081800
C	-3.14731900	-0.66151100	0.01544900
C	-4.49196700	-0.33424500	0.35889300
C	-5.49162500	-1.29156900	0.30672000
C	-5.18733900	-2.59248000	-0.11960300
C	-3.88037900	-2.93795700	-0.47698100
C	-2.86500200	-1.99340400	-0.39432400
H	-1.84976000	-2.24407300	-0.66696100
H	-3.65716400	-3.94750200	-0.80919500
H	-5.97603400	-3.33864800	-0.17198800
H	-6.50878900	-1.03500700	0.58756700
H	-4.72277400	0.67003600	0.69905000

BiRh($O_2CH)_4$ carbenoid – cycloaddition TS-IIa

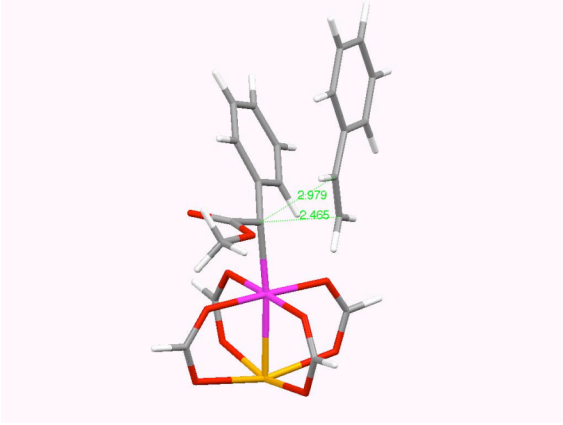

Route= #N b3lyp/gen pseudo=read gfprint integral(grid=ultrafine) OPT=(TS,CalcFC, NoEigen) freq
B3LYP Energy=-1680.6117271 Hartree
ZPE=0.383517 Hartree
Enthalpy=-1680.192798 Hartree
Free Energy=-1680.297197 Hartree
Entropy=219.728 cal/mol-K
1 imaginary frequency

Rh	0.00000000	0.00000000	0.00000000
C	-2.14473400	0.41917000	0.49020900
C	-2.27761200	1.79445100	1.04321400
O	-2.25080800	2.79851400	0.14180100
C	-2.13024100	4.11342900	0.70778300
H	-2.96403200	4.32668000	1.38250300
H	-2.14097600	4.79605900	-0.14261700
H	-1.19148200	4.20106500	1.25994700
O	-2.27554800	1.98737100	2.24871900
C	-3.07638000	-0.57720500	0.98457700
C	-2.87618100	-1.94128800	0.65224000
C	-3.72253400	-2.93123100	1.13922200
C	-4.78998600	-2.59187000	1.97519000
C	-5.01978400	-1.25238700	2.30804200
C	-4.18678600	-0.25841200	1.81207300
H	-4.36337000	0.77302200	2.09119400
H	-5.85357600	-0.98687700	2.95177200
H	-5.44434700	-3.36756600	2.36478600
H	-3.54610300	-3.97080200	0.87647200
H	-2.04480000	-2.19888500	0.00940800
O	0.08735900	1.38113800	-1.53953300
C	1.15680900	1.68797600	-2.15432300
O	2.31611000	1.23386500	-1.98746900
Bi	2.57873200	-0.50428400	-0.33821200
O	1.65325900	-2.09624600	-1.91553800
C	0.40453100	-2.15648300	-2.00823100
O	-0.47343800	-1.47860100	-1.38135900

H	-0.01289400	-2.88632600	-2.72024600
O	2.77261200	1.19569000	1.32039600
C	1.70340500	1.74631100	1.69192800
O	0.51444000	1.49187800	1.32993100
H	1.78919100	2.56058500	2.42730000
O	2.14393700	-2.03903400	1.44397900
C	0.97445800	-2.05615600	1.90745300
O	-0.03570200	-1.38288400	1.53583100
H	0.77842900	-2.74105800	2.74663700
H	1.02576400	2.45484100	-2.93395100
C	-2.90809800	0.63952800	-1.84218400
C	-4.15253400	1.12440800	-1.59329800
C	-5.38687900	0.36379900	-1.44821000
C	-6.55316700	1.03400300	-1.02380600
C	-7.75447600	0.35188400	-0.85319100
C	-7.81770100	-1.02100100	-1.10503200
C	-6.67341100	-1.70171500	-1.53420900
C	-5.47358900	-1.02007300	-1.70774100
H	-4.59764900	-1.55868800	-2.05352000
H	-6.72101600	-2.76783000	-1.73861400
H	-8.75400100	-1.55697700	-0.97527200
H	-8.64048200	0.88819100	-0.52453400
H	-6.50414300	2.10235000	-0.82637300
H	-4.24818100	2.19640700	-1.43331200
H	-2.71667500	-0.40895400	-2.04204400
H	-2.07428500	1.31080400	-1.99976100

4.18c

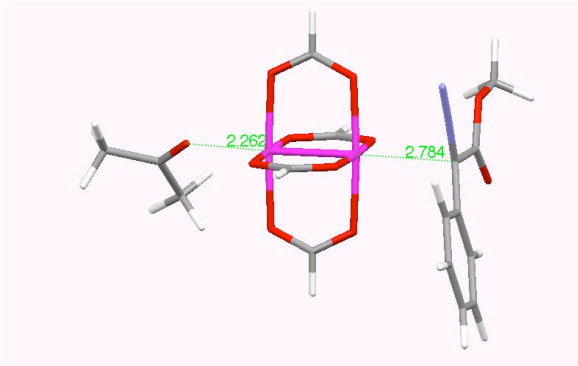

Route= #N b3lyp/gen pseudo=read gfprint integral(grid=ultrafine) OPT FREQ
B3LYP Energy=-1778.84326871 Hartree
ZPE=0.346635 Hartree
Enthalpy=-1778.460963 Hartree
Free Energy=-1778.567451 Hartree
Entropy=224.123 cal/mol-K
0 imaginary frequencies

Rh	0.00000000	0.00000000	0.00000000
C	2.76972800	0.26677000	0.06143400
C	2.77477600	1.40125500	-0.89466200
O	2.58480700	2.58001600	-0.25797300
C	2.44977000	3.72514100	-1.11506200
H	3.34428700	3.85277500	-1.72985900
H	2.32134200	4.57296500	-0.44184600
H	1.57513700	3.60563100	-1.75824800
O	2.93012200	1.29962100	-2.09464500
C	3.26526100	-1.10905800	-0.21924800
C	3.53808000	-1.52177300	-1.53511400
C	4.01251500	-2.81013900	-1.77981300
C	4.22162800	-3.70952800	-0.73397500
C	3.94759300	-3.30557100	0.57392200
C	3.47453700	-2.02119700	0.83079300
H	3.25873500	-1.73832100	1.85647800
H	4.10192100	-3.99063000	1.40337900

H	4.59256900	-4.71108100	-0.93361300
H	4.21938700	-3.10827400	-2.80441900
H	3.37688200	-0.83345500	-2.35311300
O	-0.26854100	1.39757900	1.48893800
C	-1.44674300	1.60342700	1.90664400
O	-2.51949300	1.05168100	1.52298000
Rh	-2.39722500	-0.37872100	0.04449600
O	-2.06473000	-1.82464500	1.47232700
C	-0.87229600	-2.03374400	1.84167200
O	0.18339900	-1.46201200	1.43694800
H	-0.73627200	-2.80832300	2.60903700
O	-2.58974100	1.09415300	-1.39685000
C	-1.53267300	1.67430600	-1.79033100
O	-0.34290300	1.46608100	-1.41850900
H	-1.67105900	2.45640400	-2.55036800
O	-2.13286200	-1.79311600	-1.44175200
C	-0.95028000	-1.98870100	-1.86235000
O	0.11339900	-1.42226200	-1.48689700
H	-0.84187500	-2.74550000	-2.65178200
H	-1.55081300	2.35548700	2.70103700
N	2.72164000	0.63282500	1.34297600
N	2.66959500	0.90957000	2.43937200
O	-4.62192600	-0.72984500	0.24461500
C	-5.50340300	-0.85865300	-0.60414700
C	-6.92933700	-1.07718200	-0.16484500
H	-7.29600100	-2.03197500	-0.56338900
H	-7.00111300	-1.07651100	0.92407900
H	-7.57172200	-0.29237800	-0.58447900
C	-5.20555300	-0.80048200	-2.08201000
H	-6.09156100	-0.99696000	-2.69082200
H	-4.80259400	0.18998400	-2.32135100
H	-4.41493000	-1.52001000	-2.31755400

Methyl phenyldiazoacetate – dirhodium complex N_2 extrusion TS-Ic

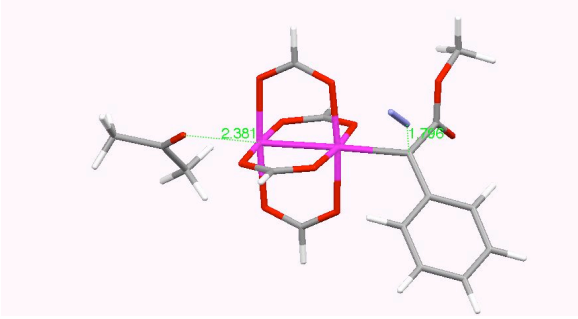

Route= #N b3lyp/gen pseudo=read gfprint integral(grid=ultrafine) OPT=(TS,CalcFC,

Rh	0.00000000	0.00000000	0.00000000
C	2.21656800	0.19247500	-0.11985900
C	2.55500900	1.43451500	-0.87596300
O	2.57105300	2.56109300	-0.13669500
C	2.68655000	3.78171500	-0.88760800
H	3.60694300	3.78555600	-1.47729000
H	2.70326900	4.57708100	-0.14240500
H	1.82851500	3.89490800	-1.55442700
O	2.70676900	1.41280300	-2.08244400
C	3.08658300	-0.99337800	-0.31023700

NoEigen) freq
B3LYP Energy=-1778.81773247 Hartree
ZPE=0.343789 Hartree
Enthalpy=-1778.438227 Hartree
Free Energy=-1778.543690 Hartree
Entropy=221.966 cal/mol-K
1 imaginary frequency

C	4.24865800	-0.95476400	-1.10914500
C	5.02972100	-2.09488600	-1.27727800
C	4.68678100	-3.28477700	-0.63026200
C	3.54716900	-3.33358100	0.17652300
C	2.74659000	-2.20476000	0.32558800
H	1.85597500	-2.24406300	0.94140100
H	3.27454800	-4.25692800	0.68025100
H	5.30432000	-4.17031400	-0.75599900
H	5.91345700	-2.05189700	-1.90788000
H	4.51850300	-0.04062800	-1.62353800
O	-0.24027500	1.67073500	1.19102500
C	-1.41925800	2.01662100	1.51257600
O	-2.50982200	1.46321000	1.20335300
Rh	-2.45037500	-0.24144100	0.03885200
O	-2.22644200	-1.38844800	1.74344800
C	-1.06480100	-1.58138700	2.18924800
O	0.03962700	-1.16309700	1.71569700
H	-0.98745300	-2.18770500	3.10338500
O	-2.53002800	0.92366900	-1.66800200
C	-1.43581700	1.36463900	-2.12460600
O	-0.26602700	1.17692000	-1.67938400
H	-1.50422800	1.99254700	-3.02488600
O	-2.23247300	-1.93175500	-1.13910400
C	-1.05946500	-2.26542700	-1.47678500
O	0.03421300	-1.70206800	-1.17902200
H	-0.97451500	-3.16113000	-2.10929600
H	-1.49252700	2.91510100	2.14246600
N	2.54767500	0.67411000	1.57840000
N	2.36534300	0.69389500	2.67438200
O	-4.81707500	-0.42505200	0.22206700
C	-5.66927300	-0.65330900	-0.63024400
C	-7.13312600	-0.65980100	-0.25534200
H	-7.56411500	-1.64830700	-0.46077600
H	-7.25897400	-0.41307100	0.80043000
H	-7.68203700	0.05940100	-0.87680900
C	-5.30047900	-0.92339600	-2.07158800
H	-6.16038500	-1.23492900	-2.67072300
H	-4.86967000	-0.00994100	-2.49790700
H	-4.51387900	-1.68308800	-2.10827800

Dirhodium carbenoid complex 4.19c

Rh	0.00000000	0.00000000	0.00000000
Rh	-2.46945700	-0.12942200	0.17918400
O	-2.40857900	1.68406100	1.16214300
C	-1.28675100	2.23245200	1.32997700

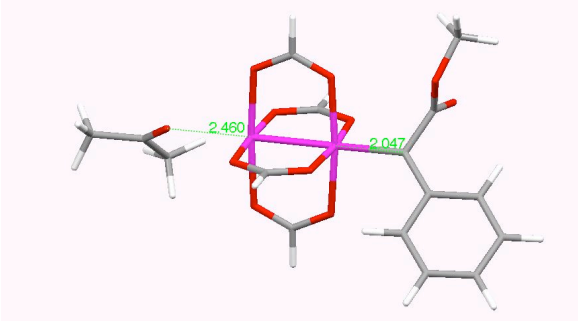

Route= #N b3lyp/gen pseudo=read gfprint integral(grid=ultrafine) OPT FREQ
B3LYP Energy=-1669.32417607 Hartree
ZPE=0.336474 Hartree
Internal Energy=-1668.954990 Hartree
Enthalpy=-1668.954046 Hartree
Free Energy=-1669.055512 Hartree
Entropy=213.553 cal/mol-K
0 imaginary frequencies

O	-0.13871700	1.81296100	0.98080100
H	-1.29046400	3.20296600	1.84726700
O	-2.21131700	-1.10866900	1.97987200
C	-1.03684600	-1.31401800	2.38151000
O	0.05894900	-0.99928800	1.81538900
H	-0.93136900	-1.83343000	3.34516500
O	-2.36566200	-1.93856600	-0.83174100
C	-1.22838500	-2.36022700	-1.17569700
O	-0.09389900	-1.82195600	-0.98285600
H	-1.20427200	-3.31994300	-1.71280800
O	-2.58113600	0.86367400	-1.63431400
C	-1.49475200	1.19015400	-2.19049500
O	-0.31143400	0.98278900	-1.78771600
H	-1.57510200	1.72287500	-3.14893600
C	2.03468200	0.12306700	-0.17844500
C	2.99943700	-0.94021900	-0.14904500
C	2.63949800	-2.21519200	0.36357200
C	3.57348100	-3.24211000	0.42475000
C	4.87224800	-3.03782900	-0.05123300
C	5.24881700	-1.79462400	-0.57739400
C	4.33287900	-0.75483600	-0.61325600
H	4.62021900	0.20389500	-1.03250500
H	6.25781800	-1.64441000	-0.95022800
H	5.59586100	-3.84801200	-0.01297700
H	3.29107200	-4.20701600	0.83573900
H	1.63416900	-2.35959000	0.73399400
C	2.55520900	1.47795500	-0.48025000
O	2.67715500	1.89896000	-1.61601200
O	2.83857300	2.17526400	0.63229500
C	3.20004800	3.55317700	0.42774000
H	4.09438900	3.62999600	-0.19636800
H	2.37767500	4.09100400	-0.05041700
H	3.39129700	3.95175600	1.42387200
C	-5.80258000	-0.57750200	-0.29918200
O	-4.90586800	-0.28264900	0.48086200
C	-5.53801600	-0.82614700	-1.76816900
H	-4.71579200	-0.19618100	-2.11420900
H	-5.22536700	-1.87197500	-1.88723500
H	-6.43300300	-0.66703900	-2.37779100
C	-7.22606300	-0.72673400	0.19275100
H	-7.26444100	-0.63571400	1.27987500
H	-7.85630600	0.04798000	-0.26324400
H	-7.63817200	-1.69470700	-0.11916200

Dirhodium carbenoid – styrene cycloaddition TS-IIc

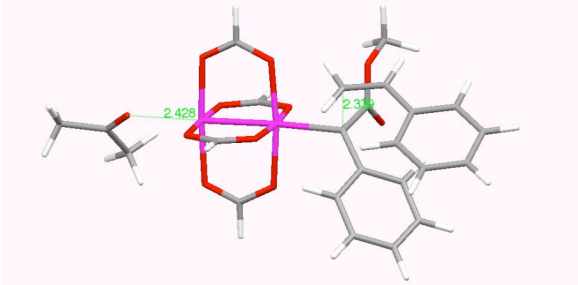

Route= #N b3lyp/gen pseudo=read gfprint integral(grid=ultrafine) OPT=(TS,CalcFC,NoEigenTest) freq
B3LYP Energy=-1978.96040295 Hartree
ZPE=0.472133 Hartree
Internal Energy=-1978.448419 Hartree
Enthalpy=-1978.447475 Hartree
Free Energy=-1978.564133 Hartree
Entropy=245.528 cal/mol-K
1 imaginary frequency

Rh	0.00000000	0.00000000	0.00000000
C	-2.09228300	0.29241100	0.49253400
C	-2.26850600	1.64147500	1.10901100
O	-2.25524600	2.67991000	0.24428300
C	-2.16616400	3.97547400	0.85707700
H	-3.01513500	4.15147800	1.52379300
H	-2.17407100	4.68695100	0.03047200
H	-1.23852400	4.05897100	1.42807600
O	-2.28698300	1.79494000	2.31922600
C	-2.94378800	-0.78114600	0.99639000
C	-2.68588600	-2.11619600	0.59980000
C	-3.45311000	-3.17154100	1.08285800
C	-4.49733000	-2.92786000	1.97850100
C	-4.78191500	-1.61730900	2.37489800
C	-4.02773600	-0.55834900	1.88384800
H	-4.24830600	0.44941200	2.21267500
H	-5.59767700	-1.42236100	3.06560100
H	-5.08975300	-3.75375500	2.36409200
H	-3.23086900	-4.18782000	0.76820000
H	-1.87238800	-2.30585300	-0.08860700
O	0.11242500	1.41282300	-1.51195100
C	1.23639800	1.63845500	-2.05952600
O	2.34884900	1.09925300	-1.81494100
Rh	2.42778600	-0.35449800	-0.35109200
O	1.92673800	-1.79028800	-1.75231200
C	0.70920100	-2.01702800	-1.97441700
O	-0.30753000	-1.47296000	-1.43561900
H	0.48638100	-2.78384100	-2.73129200
O	2.78171900	1.10579000	1.07276000
C	1.77692700	1.67383500	1.58755200
O	0.54978800	1.46129000	1.35947800
H	1.98881200	2.45592000	2.33144800
O	2.36786300	-1.78301300	1.14744900
C	1.25645900	-1.99307400	1.71119700
O	0.13771000	-1.44758000	1.47554600
H	1.25236100	-2.74844400	2.51089500
H	1.22999300	2.40461100	-2.84889400
C	-2.84315200	0.54496700	-1.70771600
C	-4.11288700	0.96837400	-1.44167700
C	-5.31079100	0.15388000	-1.31676700
C	-6.50472700	0.76361700	-0.87575300
C	-7.67662100	0.02815300	-0.72815100
C	-7.68219000	-1.33877200	-1.01916500
C	-6.51042800	-1.95984200	-1.46414700
C	-5.33960000	-1.22500600	-1.61599100

H	-4.44152400	-1.71719900	-1.97319200
H	-6.51354500	-3.02105100	-1.69719500
H	-8.59560300	-1.91645600	-0.90630800
H	-8.58452800	0.51735900	-0.38616400
H	-6.49942100	1.82678600	-0.64706300
H	-4.25116000	2.02974300	-1.24713500
H	-2.61608400	-0.48226800	-1.97049000
H	-2.05580700	1.26420600	-1.89050100
O	4.77771500	-0.73074500	-0.83445100
C	5.73198900	-0.86007000	-0.07654700
C	7.10980400	-1.15049500	-0.62799000
H	7.79966400	-0.34394200	-0.34739000
H	7.50508300	-2.07311500	-0.18371000
H	7.07419600	-1.24541500	-1.71484100
C	5.57589700	-0.74736900	1.42440200
H	6.53675800	-0.75750300	1.94640800
H	5.02118500	0.16484300	1.66382800
H	4.96151800	-1.58505600	1.77455700

Methyl phenyldiazoacetate – $Rh_2(O_2CCF_3)_4$ complex 4.18e

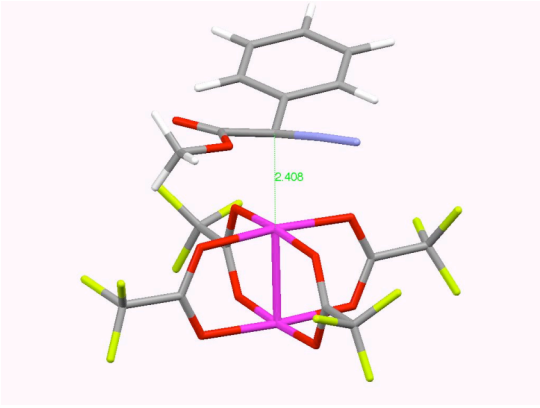

Route= #N b3lyp/gen pseudo=read gfprint integral(grid=ultrafine) OPT FREQ
B3LYP Energy=-2933.77886176 Hartree
ZPE=0.278831 Hartree
Enthalpy=-2933.456416 Hartree
Free Energy=-2933.586039 Hartree
Entropy=272.815 cal/mol-K
0 imaginary frequencies

Rh	0.00000000	0.00000000	0.00000000
Rh	0.70155300	0.66272600	-2.23934700
O	-0.67455200	2.18735800	-2.13266900
C	-1.36334000	2.28764900	-1.08288800
O	-1.32842700	1.56806800	-0.04239400
C	-2.43113600	3.40334500	-1.06788400
F	-3.61447900	2.87774400	-1.43256500
F	-2.55676100	3.92088900	0.16341400
F	-2.11860600	4.38670700	-1.91593900
O	-0.74329700	-0.57948100	-2.99562900
C	-1.44063100	-1.23013100	-2.16949800
O	-1.37666100	-1.22907700	-0.90772700
C	-2.55920100	-2.11375700	-2.76440300
F	-3.72751800	-1.45124600	-2.67604000
F	-2.32442500	-2.39645500	-4.04912100
F	-2.66733300	-3.26232200	-2.08355300
O	2.03216400	-0.90341800	-2.21843200
C	2.07978300	-1.61261600	-1.17829000
O	1.41123000	-1.49948000	-0.11115500
C	3.05228800	-2.81234900	-1.20517700
F	2.35017500	-3.94482700	-1.37595200
F	3.94147600	-2.70284300	-2.19358300
F	3.71969000	-2.89838700	-0.03868800
O	2.11604300	1.86991800	-1.35381200

C	2.16331200	1.89689900	-0.09652800
O	1.43823400	1.27596000	0.73589000
C	3.25964000	2.77547800	0.54463800
F	2.72069500	3.57538300	1.47811400
F	4.16875300	1.97990600	1.13796800
F	3.87961300	3.53119000	-0.36323300
C	-0.79566200	-0.64317000	2.18023100
C	0.11731400	-1.81188300	2.46820200
O	-0.13549000	-2.95803600	2.17893000
O	1.25345000	-1.40019800	3.05670700
C	2.26693100	-2.41286400	3.24044900
H	1.86333000	-3.25272300	3.80957700
H	2.62257600	-2.75484700	2.26730400
H	3.06495300	-1.91701700	3.79210400
N	-0.38131300	0.47837200	2.83585200
N	-0.03968200	1.43556200	3.31503900
C	-2.29248100	-0.77925600	2.10990400
C	-2.88137400	-2.01435400	1.79284100
C	-4.26968100	-2.12356400	1.71578000
C	-5.08925400	-1.01846700	1.94524400
C	-4.50660800	0.21209000	2.25259800
C	-3.12140300	0.33393600	2.33215200
H	-2.69691600	1.30816400	2.55345500
H	-5.12795200	1.08537300	2.42942300
H	-6.16953700	-1.11275800	1.88245000
H	-4.70812400	-3.08659200	1.46966200
H	-2.25673100	-2.87644400	1.60686900

Methyl phenyldiazoacetate – $Rh_2(O_2CCF_3)_4$ complex N2 extrusion TS-Ie

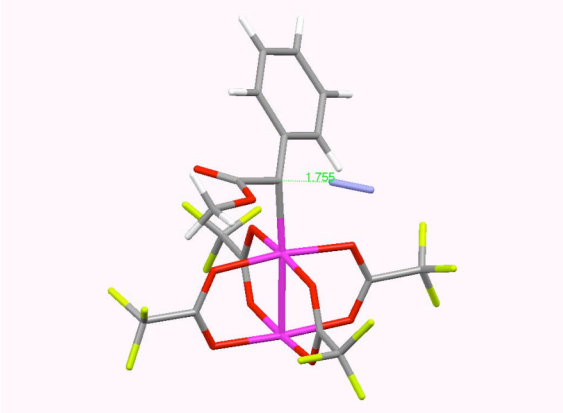

Route= #N b3lyp/gen pseudo=read gfprint OPT=(TS,CalcFC,NoEigenTest) FREQ
B3LYP Energy=-2933.76319741 Hartree

Rh	0.00000000	0.00000000	0.00000000
C	0.80237900	-1.14720800	-1.66971700
C	-0.13038500	-2.30419200	-1.90842000
O	-1.21243600	-1.99284900	-2.63694800
C	-2.24064800	-3.00710200	-2.67680800
H	-1.84268600	-3.93525700	-3.09321600
H	-3.01983300	-2.59652100	-3.31795900
H	-2.61831900	-3.18549800	-1.66822400
O	0.06718000	-3.38069600	-1.38618600
C	2.25909300	-1.38097700	-1.82767200
C	2.75945700	-2.59607000	-2.34286500
C	4.13072400	-2.79901300	-2.46440100
C	5.02646000	-1.78975200	-2.10281900
C	4.54437500	-0.57474700	-1.61010400
C	3.17532700	-0.37242200	-1.46437100

ZPE=0.276697 Hartree
Enthalpy=-2933.442928 Hartree
Free Energy=-2933.568779 Hartree
Entropy=264.877 cal/mol-K
1 imaginary frequency

H	2.81045400	0.57124100	-1.07857900
H	5.23595800	0.21359600	-1.32778000
H	6.09633600	-1.95007500	-2.20424700
H	4.50023600	-3.74593300	-2.84709400
H	2.07736400	-3.39129100	-2.61536400
O	-1.58829400	0.77335000	-1.06192200
C	-2.41494100	1.51146400	-0.44770400
O	-2.40323600	1.88329200	0.75297100
Rh	-0.88607300	1.19511300	1.97135100
O	0.29393700	2.79744700	1.42379600
C	0.96928800	2.70020400	0.37100700
O	1.05564900	1.72246900	-0.43318400
C	1.81164500	3.92568400	-0.04496800
F	3.07856100	3.54383400	-0.29084900
F	1.30335700	4.45397600	-1.17300700
F	1.82385500	4.86418200	0.90143400
O	-2.00958500	-0.47451500	2.39624600
C	-1.91478700	-1.45150200	1.61047000
O	-1.19598600	-1.57524300	0.57655700
C	-2.76891900	-2.69751500	1.93448800
F	-3.45169400	-3.08198700	0.83758100
F	-1.96782100	-3.70672400	2.31020700
F	-3.64419500	-2.45516200	2.91196800
O	0.67964600	0.41950600	3.05385700
C	1.50756200	-0.30726200	2.44514700
O	1.51650900	-0.65949100	1.22944000
C	2.71312100	-0.82186900	3.26281000
F	2.89963800	-2.13166200	3.04875400
F	3.82068000	-0.16303800	2.86848600
F	2.54209500	-0.62069800	4.57158400
C	-3.62625800	1.95970600	-1.29492100
F	-3.25672600	2.21531000	-2.55857100
F	-4.53298600	0.96274600	-1.31139500
F	-4.20226400	3.05207900	-0.78761200
N	0.41097300	-0.05292300	-2.98551600
N	0.28168200	0.90379600	-3.53239700

$Rh_2(O_2CCF_3)_4$ carbenoid complex 4.19e

Rh	0.00000000	0.00000000	0.00000000
Rh	0.81422100	1.69492400	1.62769100
O	-0.21874100	0.66313800	3.08751900
C	-0.86684500	-0.35380200	2.74204000
O	-0.98807700	-0.87289700	1.58965500
C	-1.62631700	-1.11652200	3.85041200
F	-1.59293100	-0.46175200	5.01209400

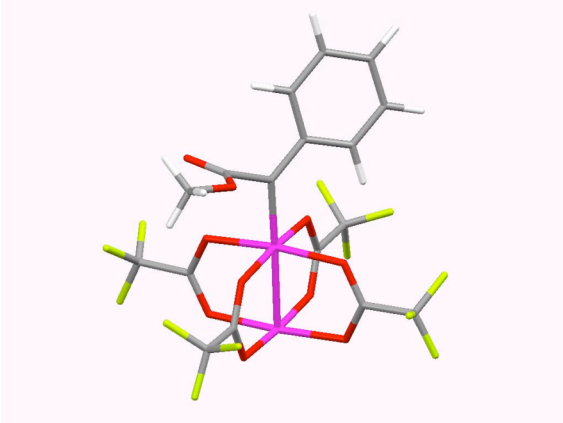

Route= #N b3lyp/gen pseudo=read gfprint integral(grid=ultrafine) OPT FREQ
B3LYP Energy=-2824.27202667 Hartree
ZPE=0.269152 Hartree
Internal Energy=-2823.962172 Hartree
Enthalpy=-2823.961228 Hartree
Free Energy=-2824.086688 Hartree
Entropy=264.054 cal/mol-K
0 imaginary frequencies

F	-2.91139700	-1.28529900	3.48904300
F	-1.07115000	-2.32880200	4.02105100
O	-0.88105000	2.78836900	1.19585800
C	-1.68583400	2.32263500	0.35324400
O	-1.61816100	1.24086800	-0.30754400
C	-2.97215800	3.13609100	0.08850800
F	-2.91032900	4.35073800	0.63573100
F	-3.18269900	3.26510800	-1.22970500
F	-4.02074300	2.47641500	0.62302500
O	1.79341200	2.61162900	0.06992600
C	1.69206600	2.08850100	-1.06887800
O	1.05673000	1.04922500	-1.41718400
C	2.41589200	2.79920700	-2.23482700
F	3.17986900	3.80342800	-1.79616700
F	3.19079700	1.92691100	-2.89651400
F	1.50233200	3.29527400	-3.08776500
O	2.45901300	0.48782000	1.93224100
C	2.53015200	-0.57986200	1.27597600
O	1.70732200	-1.06557100	0.44277400
C	3.77623700	-1.46506500	1.50098600
F	4.68432300	-0.85778900	2.26519400
F	3.41046500	-2.61484800	2.09378100
F	4.34425000	-1.76373500	0.31555000
C	-0.61504300	-1.38871800	-1.33135700
C	0.50261200	-2.02152900	-2.08644700
O	0.94676100	-1.53273400	-3.10580500
O	0.94048900	-3.13243300	-1.48541900
C	2.17522000	-3.69397400	-1.98623300
H	2.17109300	-3.72113100	-3.07721100
H	3.01125700	-3.09047900	-1.62565900
H	2.22439300	-4.69938100	-1.56944700
C	-1.94597700	-1.77256500	-1.66978300
C	-2.20719400	-2.57207300	-2.82252900
C	-3.50078100	-2.94353600	-3.14641600
C	-4.56451600	-2.55632700	-2.31843700
C	-4.33499600	-1.78630300	-1.17299700
C	-3.04606500	-1.38273900	-0.85508800
H	-2.86063400	-0.79286800	0.03103100
H	-5.16499000	-1.49759800	-0.53573600
H	-5.57759100	-2.85887500	-2.56953500
H	-3.69087500	-3.53674000	-4.03556300
H	-1.38422600	-2.85963500	-3.46839700

$Rh_2(O_2CCF_3)_4$ carbenoid styrene cycloaddition TS-IIe

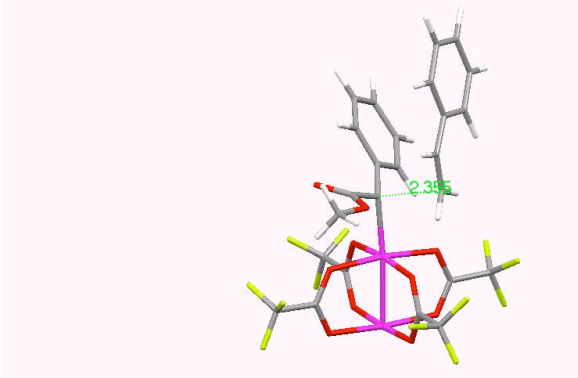

Route= #N b3lyp/gen pseudo=read gfprint OPT=(TS,CalcFC,NoEigenTest) FREQ
B3LYP Energy=-3133.91220806 Hartree
ZPE=0.405082 Hartree
Enthalpy=-3133.458442 Hartree
Free Energy=-3133.596620 Hartree
Entropy=290.820 cal/mol-K
1 imaginary frequency

Rh	0.00000000	0.00000000	0.00000000
C	-1.88353800	-0.62654500	-0.72820900
C	-1.68668500	-1.83160700	-1.60412200
O	-1.40747200	-2.96998100	-0.94537000
C	-0.93577300	-4.05525200	-1.76961500
H	-1.66929300	-4.30119100	-2.54140900
H	-0.79742600	-4.89284300	-1.08596900
H	0.01087000	-3.77899600	-2.23848300
O	-1.65677800	-1.73609200	-2.81761200
C	-2.93093300	0.31558100	-1.08698300
C	-3.02882900	1.55934000	-0.41163700
C	-3.98986900	2.49713800	-0.76981100
C	-4.88316300	2.22506500	-1.80961800
C	-4.82473300	0.99663300	-2.47518200
C	-3.87600100	0.04892400	-2.11338700
H	-3.82802600	-0.88821400	-2.65196600
H	-5.52208900	0.77836000	-3.27878200
H	-5.62423700	2.96554800	-2.09865800
H	-4.03569200	3.44701700	-0.24492600
H	-2.34198900	1.77824600	0.39510000
O	0.38857200	-1.65766200	1.17485900
C	1.50396500	-1.74009700	1.76875600
O	2.46223000	-0.92758500	1.77638600
Rh	2.26334200	0.80053000	0.66690300
O	1.36297000	1.73449800	2.27453000
C	0.12122200	1.61834400	2.40422800
O	-0.70636500	0.98789300	1.67711500
C	-0.53496000	2.33465500	3.60423400
F	0.35693000	2.99320500	4.34408100
F	-1.45346100	3.21252500	3.15386200
F	-1.16277500	1.43478800	4.38350700
O	3.01489300	-0.19038000	-0.97505100
C	2.20244700	-0.83386200	-1.68553800
O	0.94670000	-0.94223500	-1.56790800
C	2.78329200	-1.62784000	-2.87669600
F	4.10867400	-1.49797100	-2.96035600
F	2.49273900	-2.93786400	-2.72427100
F	2.23426500	-1.20494600	-4.02482200
O	1.92561200	2.47112000	-0.49035600
C	0.82943800	2.54696100	-1.10023200
O	-0.14006500	1.73221100	-1.10951700
C	0.59269200	3.80588200	-1.96362900
F	1.64223800	4.63089500	-1.93585600
F	0.35819700	3.45054000	-3.23702000

F	-0.48463800	4.46951600	-1.50222100
C	1.70445600	-3.05683900	2.55063400
F	2.69089500	-2.95649800	3.44458200
F	0.57618900	-3.40025700	3.19406000
F	2.01007900	-4.04012500	1.68120400
C	-2.69701800	-1.52664000	1.29124500
C	-3.80280300	-2.14832900	0.78480500
C	-5.13683000	-1.59494300	0.64566000
C	-6.09658000	-2.31357100	-0.10066000
C	-7.38085000	-1.81325100	-0.28705500
C	-7.73581000	-0.58240300	0.27295300
C	-6.80276800	0.13839700	1.02629500
C	-5.51918800	-0.36066100	1.21543200
H	-4.81086100	0.19961100	1.81602900
H	-7.08202700	1.08934000	1.47076300
H	-8.73890500	-0.18970600	0.13103500
H	-8.10505600	-2.37840700	-0.86674900
H	-5.81768300	-3.26988800	-0.53652000
H	-3.66678100	-3.14932000	0.38030500
H	-2.74917000	-0.55598200	1.77148100
H	-1.78326800	-2.08623900	1.44105900

Methyl phenyldiazoacetate – $BiRh(O_2CCF_3)_4$ complex 4.18d

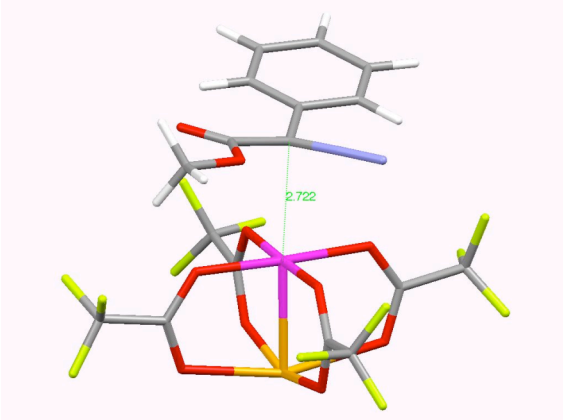

Route= #N b3lyp/gen pseudo=read gfprint integral(grid=ultrafine) OPT FREQ
B3LYP Energy=-2828.60934348 Hartree
ZPE=0.276333 Hartree
Enthalpy=-2828.287730 Hartree
Free Energy=-2828.423426 Hartree
Entropy=285.596 cal/mol-K
0 imaginary frequencies

Rh	0.00000000	0.00000000	0.00000000
Bi	0.84352500	0.88241400	-2.30335300
O	-0.66204900	2.65186100	-1.71361900
C	-1.28176000	2.55116600	-0.62507100
O	-1.21744000	1.62674600	0.23276700
C	-2.29336800	3.67528300	-0.30142400
F	-2.57562500	3.72042900	1.00771500
F	-1.81056000	4.86605800	-0.67475300
F	-3.43243900	3.44077600	-0.97605700
O	-1.03610700	-0.36697500	-3.04025800
C	-1.69492700	-0.99266300	-2.16749300
O	-1.50277100	-1.03677600	-0.92262300
C	-2.93504200	-1.76984800	-2.66886900
F	-3.97478200	-0.91771600	-2.73520400
F	-2.71632600	-2.27189100	-3.89063000
F	-3.25362700	-2.77147300	-1.84437600
O	2.05483500	-1.17719400	-2.19721500
C	1.93362700	-1.86759400	-1.15436800
O	1.22017900	-1.63994000	-0.13778700
C	2.73111900	-3.19150200	-1.07409500
F	3.41398500	-3.24855800	0.08559300

F	1.88099200	-4.22821000	-1.11939000
F	3.60051600	-3.30262300	-2.08033600
O	2.49316700	1.85614500	-0.84694600
C	2.37152200	1.66049600	0.38766200
O	1.48376300	0.99786900	0.99581500
C	3.46904300	2.24907300	1.30532300
F	2.96588700	2.61001300	2.49161400
F	4.40761400	1.30375200	1.50774000
F	4.04983200	3.31322600	0.74310100
C	-1.04318200	-0.78271100	2.38861400
C	-0.11135100	-1.92840600	2.59196700
O	-0.33493300	-3.06968000	2.24807700
O	1.02531700	-1.53066300	3.20199100
C	2.03272900	-2.54858000	3.35909600
H	1.63333700	-3.39579400	3.92131500
H	2.37881400	-2.88540800	2.38026000
H	2.84046100	-2.06617500	3.90921100
N	-0.65288300	0.33879500	3.00783100
N	-0.33982900	1.30985600	3.49411300
C	-2.50809400	-0.90078300	2.11918400
C	-3.07937000	-2.13836600	1.77766000
C	-4.44827400	-2.23054900	1.52698300
C	-5.27022700	-1.10672200	1.61075000
C	-4.70602000	0.12540100	1.94613900
C	-3.33976300	0.23123100	2.19582900
H	-2.92640400	1.20713500	2.42896200
H	-5.32792100	1.01394200	2.01235400
H	-6.33565500	-1.18753000	1.41463500
H	-4.87009900	-3.19630000	1.26229800
H	-2.45172900	-3.01557800	1.70527300

Methyl phenyldiazoacetate – $BiRh(O_2CCF_3)_4$ complex N_2-extrusion TS-Id

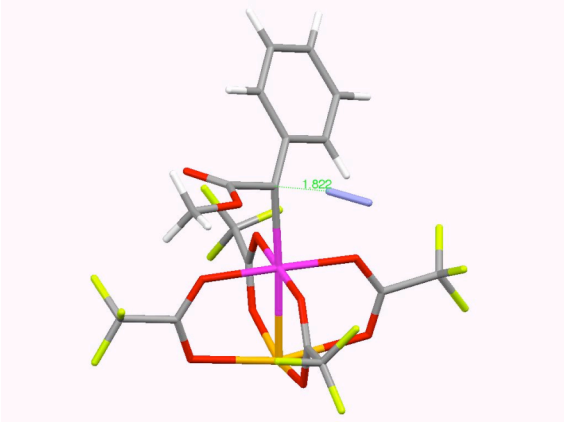

Rh	0.00000000	0.00000000	0.00000000
C	-0.99001700	1.50145200	-1.42953200
C	-0.10857800	2.70453800	-1.50783500
O	0.91759000	2.60378000	-2.36873400
C	1.89305100	3.66336000	-2.28566000
H	1.42374300	4.63012900	-2.48357500
H	2.63319800	3.42916300	-3.05030100
H	2.34784000	3.67239200	-1.29343300
O	-0.28354100	3.64253600	-0.75435300
C	-2.45092300	1.70959700	-1.48535700
C	-3.01417800	2.97875400	-1.74722100
C	-4.39442000	3.14947300	-1.77072700

Route= #N b3lyp/gen pseudo=read gfprint integral(grid=ultrafine) OPT=(TS,CalcFc, NoEigenTest) freq
B3LYP Energy=-2828.5836001 Hartree
ZPE=0.273805 Hartree
Enthalpy=-2828.264496 Hartree
Free Energy=-2828.398402 Hartree
Entropy=281.829 cal/mol-K
1 imaginary frequency

C	-5.24135100	2.05697200	-1.56468800
C	-4.70065600	0.79137700	-1.32411500
C	-3.32093600	0.61881700	-1.27384800
H	-2.90758400	-0.36402900	-1.08688400
H	-5.35494200	-0.06068600	-1.16418300
H	-6.31925600	2.19231900	-1.59100400
H	-4.81079000	4.13527400	-1.95695300
H	-2.36811700	3.83504200	-1.89632500
O	1.50532100	-0.37861400	-1.34580200
C	2.48247500	-1.14199200	-1.09156100
O	2.72038500	-1.80303400	-0.05445400
Bi	1.11179900	-1.64062700	1.74726800
O	-0.32562500	-3.20728700	0.56854500
C	-1.00684500	-2.74940600	-0.37395700
O	-1.06681700	-1.56114700	-0.81334000
C	-1.92050600	-3.72433600	-1.15451000
F	-3.18498700	-3.25982300	-1.15100200
F	-1.50595100	-3.80891400	-2.43076900
F	-1.91482000	-4.94598400	-0.62015300
O	2.20073600	0.38292700	2.40662900
C	1.92639400	1.40865300	1.73825000
O	1.11731200	1.53984000	0.77689200
C	2.65939500	2.72257700	2.10354400
F	3.33072400	3.17850500	1.02499200
F	1.77266300	3.65494900	2.47718900
F	3.53472600	2.53925800	3.09438600
O	-0.78267900	-0.93987600	3.03108900
C	-1.57639500	-0.13539200	2.48378500
O	-1.51619000	0.38428700	1.33359000
C	-2.84651700	0.24892400	3.28017400
F	-3.18723800	1.52451600	3.06338500
F	-3.86164100	-0.54000300	2.87240600
F	-2.67076700	0.06887700	4.59283500
C	3.52729900	-1.20320600	-2.23163700
F	2.92392500	-1.27134400	-3.42814800
F	4.27487200	-0.08272800	-2.19650900
F	4.33549200	-2.25816200	-2.10098300
N	-0.63231900	0.65882100	-3.00473500
N	-0.51076100	-0.19623700	-3.70087000

$BiRh(O_2CCF_3)_4$ carbenoid complex 4.19d

Rh	0.00000000	0.00000000	0.00000000
Bi	-1.06034300	-2.32652300	0.77382000
O	0.29955000	-1.81301200	2.72346900
C	0.98118400	-0.76602500	2.68272700

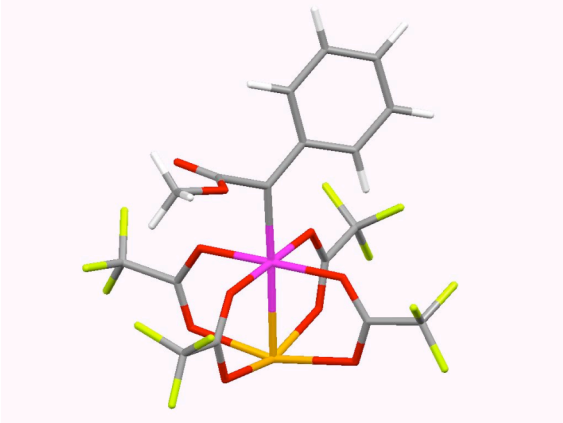

Route= #N b3lyp/gen pseudo=read gfprint integral(grid=ultrafine) OPT freq
B3LYP Energy=-2719.0853958 Hartree
ZPE=0.266354 Hartree
Enthalpy=-2718.775790 Hartree
Free Energy=-2718.906519 Hartree
Entropy=275.143 cal/mol-K
0 imaginary frequencies

O	1.05619700	0.11009300	1.76895100
C	1.90696900	-0.45785000	3.88494700
F	1.73375400	-1.33033300	4.87980700
F	3.19150800	-0.52021400	3.48003300
F	1.67111400	0.77849300	4.35117400
O	0.92282400	-3.13789400	-0.35757500
C	1.68391600	-2.27689300	-0.85064700
O	1.57114800	-1.01420400	-0.86268800
C	2.97905400	-2.76658500	-1.54336100
F	3.06299000	-4.09791900	-1.55504900
F	3.02505600	-2.32043700	-2.80864300
F	4.04765600	-2.27624900	-0.88259100
O	-2.11576000	-2.11999700	-1.36066600
C	-1.83090900	-1.10227800	-2.03808500
O	-1.04711100	-0.15029500	-1.76124100
C	-2.56072700	-0.92992800	-3.39290700
F	-3.05038200	-2.09519100	-3.83087300
F	-3.58454700	-0.07212200	-3.22528000
F	-1.73601000	-0.43609100	-4.32408400
O	-2.74732900	-0.82298000	1.61776700
C	-2.56627100	0.39828600	1.41210400
O	-1.59902200	0.98390100	0.84322800
C	-3.66103000	1.38219600	1.89233300
F	-4.63903400	0.75701100	2.54858900
F	-3.12606000	2.31318900	2.69968800
F	-4.19624500	2.01041300	0.82422900
C	0.78762000	1.88453300	-0.61208000
C	-0.25665200	2.87832900	-0.94609500
O	-0.76450800	2.92220600	-2.05079000
O	-0.57446900	3.65781100	0.09487600
C	-1.74079300	4.49406900	-0.06960300
H	-1.66206800	5.08929600	-0.98174100
H	-2.63593500	3.87000100	-0.10724600
H	-1.75982200	5.13408700	0.81185600
C	2.14218300	2.28376200	-0.79765600
C	2.47994500	3.50694000	-1.45253600
C	3.80219700	3.88032500	-1.61762500
C	4.82360600	3.06458600	-1.10745200
C	4.52316700	1.86898100	-0.44634900
C	3.20149600	1.46915700	-0.30595400
H	2.95739500	0.54656100	0.20036900
H	5.32229700	1.24835900	-0.05321600
H	5.86071100	3.36640900	-1.22814800
H	4.04947300	4.80331500	-2.13309000
H	1.68743400	4.13019400	-1.85377200

$BiRh(O_2CCF_3)_4$ carbenoid styrene cycloaddition TS-IId

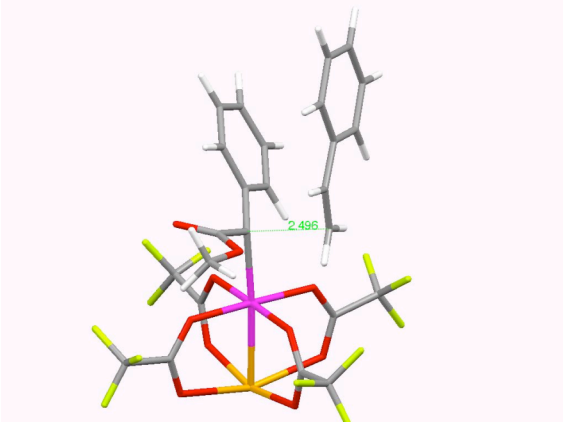

Route= #N b3lyp/gen pseudo=read gfprint OPT=(TS,CalcFC,NoEigenTest) freq
B3LYP Energy=-3028.72755939 Hartree
ZPE=0.402239 Hartree
Enthalpy=-3028.274957 Hartree
Free Energy=-3028.419284 Hartree
Entropy=303.760 cal/mol-K
1 imaginary frequency

Rh	0.00000000	0.00000000	0.00000000
C	1.99541300	0.60405700	-0.78337800
C	1.85343800	1.85109800	-1.58795100
O	1.70989200	2.98869800	-0.88447900
C	1.31579800	4.13837100	-1.65931300
H	2.05678200	4.35580900	-2.43315500
H	1.25490800	4.95755200	-0.94270000
H	0.34527200	3.95966000	-2.12567700
O	1.73972500	1.79573100	-2.80158000
C	3.03444500	-0.32493700	-1.16816300
C	3.09768300	-1.60480400	-0.55641400
C	4.05332500	-2.53744300	-0.94020100
C	4.97295000	-2.22547200	-1.94588900
C	4.94730500	-0.96495500	-2.55282200
C	4.00566100	-0.02305300	-2.16279000
H	3.98097700	0.94134400	-2.65430700
H	5.66647000	-0.71949800	-3.32884200
H	5.71096900	-2.96117200	-2.25463300
H	4.07673300	-3.51315800	-0.46341500
H	2.38956200	-1.84733200	0.22431200
O	-0.18090700	1.66521200	1.19777900
C	-1.20165500	1.92924000	1.89741200
O	-2.26333000	1.27945200	2.03335300
Bi	-2.43007600	-0.77457900	0.76129000
O	-1.10038200	-1.87928600	2.47334100
C	0.13726600	-1.72067100	2.40729900
O	0.81990800	-1.04687800	1.57776600
C	1.02164200	-2.44209800	3.45217900
F	0.29506100	-3.08972800	4.36297300
F	1.81502900	-3.33267500	2.82243000
F	1.81077600	-1.55326400	4.08281200
O	-3.03725700	0.56070100	-1.14165700
C	-2.09724800	1.12011900	-1.75452200
O	-0.85315900	1.06169600	-1.53900400
C	-2.46357100	2.03553200	-2.94866500
F	-3.78133800	2.06495500	-3.16152500
F	-2.04949700	3.29475600	-2.68997800
F	-1.85644500	1.61067800	-4.06467600
O	-1.88949300	-2.59184500	-0.71120100
C	-0.77220400	-2.54771300	-1.27967600
O	0.13575000	-1.67190800	-1.19436300
C	-0.39151400	-3.74720600	-2.18098100
F	-1.47167800	-4.43435500	-2.56393400
F	0.26792200	-3.34152400	-3.27332400

F	0.41307100	-4.57320600	-1.47989000
C	-1.08564500	3.27839000	2.64725800
F	-2.03174900	3.41011500	3.57968200
F	0.11620100	3.38580200	3.23999500
F	-1.21107700	4.28698400	1.76297000
C	2.90442900	1.41728900	1.39492000
C	4.02424100	2.00493700	0.89819700
C	5.34159700	1.40447600	0.74467000
C	6.33559200	2.11517500	0.03941400
C	7.60600400	1.57892700	-0.14871000
C	7.91239400	0.31702400	0.36764100
C	6.94262500	-0.39891600	1.07777000
C	5.67350900	0.13672300	1.26791000
H	4.93706200	-0.42233200	1.83547800
H	7.18197400	-1.37541400	1.48946800
H	8.90428500	-0.10342700	0.22606900
H	8.35707900	2.14243200	-0.69527300
H	6.09682200	3.09756300	-0.36130900
H	3.93034000	3.02290800	0.52549900
H	2.90722200	0.41929800	1.81911700
H	1.99874200	1.99242100	1.53131300

4.5.5 Single Point Energy Calculations

Table 4.8 shows single-point energies calculated at the B3LYP/6-311G(2d,2p)[Rh-RSC+4f][Bi-RLC]//B3LYP/6-31G*[Rh-RSC+4f][Bi-RLC] level for all new structures.

Table 4.8: Calculated single-point energies.

Species	***SP Energy (Hartree)***
$BiRh(O_2CH)_4$	-873.0741379
$Rh_2(O_2CH)_4$ – acetone complex	-1171.471904
$Rh_2(O_2CCF_3)_4$	-2326.777233
Complex **4.18a**	-1480.936913
TS-Ia	-1480.906279
Complex **4.19a**	-1371.373476
TS-IIa	-1681.10686
Complex **4.18e**	-2934.658315
Complex **4.19e**	-2825.117135
Complex **4.18d**	-2829.497771
TS-Id	-2829.469756
TS-IIc	-1979.514049
Complex **4.19c**	-1669.782247
TS-Ic	-1779.311123
Complex **4.18c**	-1779.336683
$BiRh(O_2CCF_3)_4$	-2221.629361
TS-IId	-3029.674871
Complex **4.19d**	-2719.939123
TS-Ie	-2934.643633
TS-IIe	-3134.851732
$Rh_2(O_2CH)_4$	-978.2240015
Product **4.7a**	-808.1062574
Styrene	-309.7391593
Dinitrogen N_2	-109.5593531
Methyl phenyldiazoacetate **4.6a**	-607.8598475

References

(1) Boyar, E. B.; Robinson, S. D. *Coord. Chem. Rev.* **1983**, *50*, 109-208.

(2) Davies, H. M. L. *Eur. J. Org. Chem.* **1999**, 2459-2469.

(3) Davies, H. M. L.; Beckwith, R. E. J. *Chem. Rev.* **2003**, *103*, 2861-2903.

(4) Davies, H. M. L.; Manning, J. R. *Nature* **2008**, *451*, 417-424.

(5) Doyle, M. P. *Chem. Rev.* **1986**, *86*, 919-939.

(6) Doyle, M. P. *Recl. Trav. Chim. Pays-Bas* **1991**, *110*, 305-316.

(7) Doyle, M. P. *Aldrichim. Acta* **1996**, *29*, 3-11.

(8) Doyle, M. P. In *Modern Rhodium-Catalyzed Organic Reactions*; Evans, P. A., Ed.; Wiley-VCH Verlag GmbH & Co. KGaA: Weinheim, 2005, p 473.

(9) Doyle, M. P. *J. Org. Chem.* **2006**, *71*, 9253-9260.

(10) Doyle, M. P.; Forbes, D. C. *Chem. Rev.* **1998**, *98*, 911-935.

(11) Doyle, M. P.; McKervey, M. A.; Ye, T. *Modern Catalytic Methods for Organic Synthesis with Diazo Compounds: From Cyclopropanes to Ylides*; Wiley-interscience: New York, 1998.

(12) Felthouse, T. R. *Prog. Inorg. Chem.* **1982**, *29*, 73-166.

(13) Hansen, J.; Davies, H. M. L. *Coord. Chem. Rev.* **2008**, *252*, 545-555.

(14) Hodgson, D. M.; Stupple, P. A.; Pierard, F. Y. T. M.; Labande, A. H.; Johnstone, C. *Chem. Eur. J.* **2001**, *7*, 4465-4476.

(15) Lebel, H.; Marcoux, J. F.; Molinaro, C.; Charette, A. B. *Chem. Rev.* **2003**, *103*, 977-1050.

(16) Ren, T. *Coord. Chem. Rev.* **1998**, *175*, 43-58.

(17) Timmons, D. J.; Doyle, M. P. *J. Organomet. Chem.* **2001**, *617*, 98-104.

(18) Ye, T.; McKervey, M. A. *Chem. Rev.* **1994**, *94*, 1091-1160.

(19) Davies, H. M. L.; Antoulinakis, E. G. *Org. Reacts.* **2001**, *57*, 1-326.

(20) Dauban, P.; Dodd, R. H. *Amino Group Chemistry* **2008**, 55-92.

(21) Davies, H. M. L.; Hansen, T.; Churchill, M. R. *J. Am. Chem. Soc.* **2000**, *122*, 3063-3070.

(22) Espino, C. G.; Fiori, K. W.; Kim, M.; Du Bois, J. *J. Am. Chem. Soc.* **2004**, *126*, 15378-15379.

(23) Flanigan, D. L.; Yoon, C. H.; Jung, K. W. *Tetrahedron Lett.* **2004**, *46*, 143-146.

(24) Godula, K.; Sames, D. *Science* **2006**, *312*, 67-72.

(25) Doyle, M. P.; Forbes, D. C.; Vasbinder, M. M.; Peterson, C. S. *J. Am. Chem. Soc.* **1998**, *120*, 7653-7654.

(26) Doyle, M. P.; Hu, W. H. *Synlett* **2001**, 1364-1370.

(27) Doyle, M. P.; Phillips, I. M.; Hu, W. H. *J. Am. Chem. Soc.* **2001**, *123*, 5366-5367.

(28) Doyle, M. P.; Valenzuela, M.; Huang, P. *Proc. Natl. Acad. Sci. U.S.A.* **2004**, *101*, 5391-5395.

(29) Davies, H. M. L. *Angew. Chem. Int. Ed.* **2006**, *45*, 6422-6425.

(30) Davies, H. M. L.; Gregg, T. M. *Tetrahedron Lett.* **2002**, *43*, 4951-4953.

(31) Davies, H. M. L.; Hansen, T.; Hopper, D. W.; Panaro, S. A. *J. Am. Chem. Soc.* **1999**, *121*, 6509-6510.

(32) Davies, H. M. L.; Stafford, D. G.; Hansen, T. *Org. Lett.* **1999**, *1*, 233-236.

(33) Doyle, M. P.; Hu, W.; Valenzuela, M. V. *J. Org. Chem.* **2002**, *67*, 2954-2959.

(34) Doyle, M. P.; Protopopova, M. N.; Zhou, Q.-L.; Bode, J. W.; Simonsen, S. H.; Lynch, V. *J. Org. Chem.* **1995**, *60*, 6654-5.

(35) Hinman, A.; Du Bois, J. *J. Am. Chem. Soc.* **2003**, *125*, 11510-11511.

(36) Kurosawa, W.; Kan, T.; Fukuyama, T. *J. Am. Chem. Soc.* **2003**, *125*, 8112-8113.

(37) Taber, D. F.; Malcolm, S. C. *J. Org. Chem.* **2001**, *66*, 944-953.

(38) Wee, A. G. H. *J. Org. Chem.* **2001**, *66*, 8513-8517.

(39) Yoon, C. H.; Nagle, A.; Chen, C.; Gandhi, D.; Jung, K. W. *Org. Lett.* **2003**, *5*, 2259-2262.

(40) Kennedy, M.; McKervey, M. A.; Maguire, A. R.; Roos, G. H. P. *J. Chem. Soc.,Chem. Commun.* **1990**, 361-362.

(41) Davies, H. M. L.; Bruzinski, P. R.; Lake, D. H.; Kong, N.; Fall, M. J. *J. Am. Chem. Soc.* **1996**, *118*, 6897-6907.

(42) Liang, C.; Collet, F.; Robert-Peillard, F.; Mueller, P.; Dodd, R. H.; Dauban, P. *J. Am. Chem. Soc.* **2008**, *130*, 343-350.

(43) Anada, M.; Kitagaki, S.; Hashimoto, S. *Heterocycles* **2000**, *52*, 875-883.

(44) Hashimoto, S.; Watanabe, N.; Ikegami, S. *Tetrahedron Lett.* **1990**, *31*, 5173-5174.

(45) Hashimoto, S.-I.; Watanabe, N.; Ikegami, S. *Synlett* **1994**, 353-355.

(46) Zalatan, D. N.; Du Bois, J. *J. Am. Chem. Soc.* **2008**, *130*, 9220-9221.

(47) Barberis, M.; Perez-Prieto, J.; Herbst, K.; Lahuerta, P. *Organometallics* **2002**, *21*, 1667-1673.

(48) Estevan, F.; Herbst, K.; Lahuerta, P.; Barberis, M.; Perez- Prieto, J. *Organometallics* **2001**, *20*, 950-957.

(49) McCarthy, N.; McKervey, M. A.; Ye, T.; McCann, M.; Murphy, E.; Doyle, M. P. *Tetrahedron Lett.* **1992**, *33*, 5983-5986.

(50) Catino, A. J.; Nichols, J. M.; Forslund, R. E.; Doyle, M. P. *Org. Lett.* **2005**, *7*, 2787-2790.

(51) Catino, A. J.; Nichols, J. M.; Choi, H.; Gottipamula, S.; Doyle, M. P. *Org. Lett.* **2005**, *7*, 5167-5170.

(52) Trindade, A. F.; Gois, P. M. P.; Veiros, L. F.; Andre, V.; Duarte, M. T.; Afonso, C. A. M.; Caddick, S.; Cloke, F. G. N. *J. Org. Chem.* **2008**, *73*, 4076-4086.

(53) Gois, P. M. P.; Trindade, A. F.; Veiros, L. F.; Andre, V.; Duarte, M. T.; Afonso, C. A. M.; Caddick, S.; Cloke, F. G. N. *Angew. Chem. Int. Ed.* **2007**, *46*, 5750-5753.

(54) Lou, Y.; Horikawa, M.; Kloster, R. A.; Hawryluk, N. A.; Corey, E. J. *J. Am. Chem. Soc.* **2004**, *126*, 8916-8918.

(55) Lou, Y.; Remarchuk, T. P.; Corey, E. J. *J. Am. Chem. Soc.* **2005**, *127*, 14223-14230.

(56) Nakamura, E.; Yoshikai, N.; Yamanaka, M. *J. Am. Chem. Soc.* **2002**, *124*, 7181-7192.

(57) Pirrung, M. C.; Liu, H.; Morehead, A. T., Jr. *J. Am. Chem. Soc.* **2002**, *124*, 1014-1023.

(58) Davies, H. M. L.; Walji, A. M. *Org. Lett.* **2003**, *5*, 479-482.

(59) Davies, H. M. L.; Walji, A. M. *Org. Lett.* **2005**, *7*, 2941-2944.

(60) Nagashima, T.; Davies, H. M. L. *Org. Lett.* **2002**, *4*, 1989-1992.

(61) Durivage, J. C.; Gruhn, N. E.; Li, B.; Dikarev, E. V.; Lichtenberger, D. L. *J. Cluster. Sci.* **2008**, *19*, 275-294.

(62) Dikarev, E. V.; Li, B. *Inorg. Chem.* **2004**, *43*, 3461-3466.

(63) Dikarev, E. V.; Gray, T. G.; Li, B. *Angew. Chem. Int. Ed.* **2005**, *44*, 1721-1724.

(64) Dikarev, E. V.; Li, B.; Zhang, H. T. *J. Am. Chem. Soc.* **2006**, *128*, 2814-2815.

(65) Doyle, M. P.; Griffin, J. H.; Bagheri, V.; Dorow, R. L. *Organometallics* **1984**, *3*, 53-61.

(66) Davies, H. M. L.; Hedley, S. J. *Chem. Soc. Rev.* **2007**, *36*, 1109-1119.

(67) Hedley, S. J.; Ventura, D. L.; Dominiak, P. M.; Nygren, C. L.; Davies, H. M. L. *J. Org. Chem.* **2006**, *71*, 5349-5356.

(68) Davies, H. M. L.; Panaro, S. A. *Tetrahedron* **2000**, *56*, 4871-4880.

(69) Hansch, C.; Leo, A.; Taft, R. W. *Chem. Rev.* **1991**, *91*, 165-195.

(70) Muller, P.; Tohill, S. *Tetrahedron* **2000**, *56*, 1725-1731.

(71) Yue, Y.; Wang, Y.; Hu, W. *Tetrahedron Lett.* **2007**, *48*, 3975-3977.

(72) Davies, H. M. L.; Hu, B.; Saikali, E.; Bruzinski, P. R. *J. Org. Chem.* **1994**, *59*, 4535-4541.

(73) Davies, H. M. L.; Saikali, E.; Clark, T. J.; Chee, E. H. *Tetrahedron Lett.* **1990**, *31*, 6299-6302.

(74) Davies, H. M. L.; Yokota, Y. *Tetrahedron Lett.* **2000**, *41*, 4851-4854.

(75) Sevryugina, Y.; Weaver, B.; Hansen, J.; Thompson, J.; Davies, H. M. L.; Petrukhina, M. A. *Organometallics* **2008**, *27*, 1750-1757.

(76) Hansen, J.; Autschbach, J.; Davies, H. M. L. *J. Org. Chem.* **2009**, *74*, 6555-6563.

(77) Yates, P. *J. Am. Chem. Soc.* **1952**, *74*, 5376-5381.

(78) Howell, J. A. S. *Dalton Trans.* **2007**, 3798-3803.

(79) Howell, J. A. S. *Dalton Trans.* **2007**, 1104-1114.

(80) Dikarev, E. V.; Li, B.; Rogachev, A. Y.; Zhang, H.; Petrukhina, M. A. *Organometallics* **2008**, *27*, 3728-3735.

(81) Pirrung, M. C.; Morehead, A. T. *J. Am. Chem. Soc.* **1996**, *118*, 8162-8163.

(82) Pirrung, M. C.; Morehead, A. T. *J. Am. Chem. Soc.* **1994**, *116*, 8991-9000.

(83) Cotton, F. A.; Hillard, E. A.; Liu, C. Y.; Murillo, C. A.; Wang, W. N.; Wang, X. P. *Inorg. Chim. Acta* **2002**, *337*, 233-246.

(84) Drago, R. S.; Long, J. R.; Cosmano, R. *Inorg. Chem.* **1982**, *21*, 2196-2202.

(85) Petrukhina, M. A.; Andreini, K. W.; Walji, A. M.; Davies, H. M. L. *Dalton Trans.* **2003**, 4221-4223.

(86) Gaussian 03 Revision C.02; M. J. Frisch, G. W. T., H. B. Schlegel, G. E. Scuseria, ; M. A. Robb, J. R. C., J. A. Montgomery, Jr., T. Vreven, ; K. N. Kudin, J. C. B., J. M. Millam, S. S. Iyengar, J. Tomasi, ; V. Barone, B. M., M. Cossi, G. Scalmani, N. Rega, ; G. A. Petersson, H. N., M. Hada, M. Ehara, K. Toyota, ; R. Fukuda, J. H., M. Ishida, T. Nakajima, Y. Honda, O. Kitao, ; H. Nakai, M. K., X. Li, J. E. Knox, H. P. Hratchian, J. B. Cross, ; C. Adamo, J. J., R. Gomperts, R. E. Stratmann, O. Yazyev, ; A. J. Austin, R. C., C. Pomelli, J. W. Ochterski, P. Y. Ayala, ; K. Morokuma, G. A. V., P. Salvador, J. J. Dannenberg, ; V. G. Zakrzewski, S. D., A. D. Daniels, M. C. Strain, ; O. Farkas, D. K. M., A. D. Rabuck, K. Raghavachari, ; J. B. Foresman, J. V. O., Q. Cui, A. G. Baboul, S. Clifford, ; J. Cioslowski, B. B. S., G. Liu, A. Liashenko, P. Piskorz, ; I. Komaromi, R. L. M., D. J. Fox, T. Keith, M. A. Al-Laham, ; C. Y. Peng, A. N.,

M. Challacombe, P. M. W. Gill, ; B. Johnson, W. C., M. W. Wong, C. Gonzalez, and J. A. Pople, ; Gaussian, I., Wallingford CT, 2004.

(87) Becke, A. D. *J. Chem. Phys.* **1993**, *98*, 5648-5652.

(88) Lee, C.; Yang, W.; Parr, R. G. *Phys. Rev. B* **1988**, *37*, 785-789.

(89) M. Kaupp, P. v. R. S., H. Stoll, H. Preuss *J. Chem. Phys.* **1991**, *94*, 1360.

(90) M. Dolg, H. S., H. Preuss, R.M. Pitzer *J. Phys. Chem.* **1993**, *97*.

(91) A. Bergner, M. D., W. Kuechle, H. Stoll, H. Preuss *Mol. Phys.* **1993**, *80*, 1431.

(92) Kuechle, W.; Dolg, M.; Stoll, H.; H., P. *Mol. Phys.* **1991**, *74*, 1245.

(93) Foresman, J. B.; Frisch, A. *Exploring Chemistry with Electronic Structure Methods*; Gaussian, Inc.: Pittsburgh, PA, 1993.

(94) Schuchardt, K. L., Didier, B.T., Elsethagen, T., Sun, L., Gurumoorthi, V., Chase, J., Li, J., and Windus, T.L. *J. Chem. Inf. Model.* **2007**, *47*, 1045-1052.

(95) Feller, D. *J. Comput. Chem.* **1996**, *17*, 1571-1586.

(96) Bruno, I. J.; Cole, J. C.; Edgington, P. R.; Kessler, M.; Macrae, C. F.; McCabe, P.; Pearson, J.; Taylor, R. *Acta. Cryst. B* **2002**, *58*, 389-397.

(97) Taylor, R.; Macrae, C. F. *Acta. Cryst. B* **2001**, *57*, 815-827.

(98) Macrae, C. F.; Bruno, I. J.; Chisholm, J. A.; Edgington, P. R.; McCabe, P.; Pidcock, E.; Rodriguez-Monge, L.; Taylor, R.; van de Streek, J.; Wood, P. A. *J. Appl. Crystallogr.* **2008**, *41*, 466-470.

(99) Macrae, C. F.; Edgington, P. R.; McCabe, P.; Pidcock, E.; Shields, G. P.; Taylor, R.; Towler, M.; van de Streek, J. *J. Appl. Crystallogr.* **2006**, *39*, 453-457.

(100) Ehlers, A. W.; Boehme, M.; Dapprich, S.; Gobbi, A.; Hoellwarth, A.; Jonas, V.; Koehler, K. F.; Stegmann, R.; Veldkamp, A.; et al. *Chem. Phys. Lett.* **1993**, *208*, 111-14.

(101) Hansen, J.; Li, B.; Autschbach, J.; Dikarev, E. V.; Davies, H. M. L. *J. Org. Chem.* **2009**, *74*, 6564-6571.

- Chapter 5 -

On the Rhodium(II)-Catalyzed Dimerization of Diazo Compounds

5.1 Introduction

The dimerization of diazo compounds in the presence of a variety of metal salts, with concominant loss of gaseous nitrogen, is a well-known transformation.[1,2] This phenomenon is often observed in reactions that involve metallocarbenoid intermediates, and is widely considered to be an undesired side-reaction even though there are some examples of useful applications in synthesis. For example, it has been demonstrated as an interesting cyclization strategy *via* intramolecular couplings.[3-6] The reaction mechanism has generally been proposed to involve: (1) reaction between a metallocarbenoid and an equivalent of diazo compound,[7] or, (2) dimerization of two carbenoids.[8] Wulfman and co-workers investigated carbene dimerization of ethyl diazoacetate and dimethyl diazomalonate in copper-catalyzed reactions, and found evidence supporting both pathways from partial rate data.[8] Trahanovsky and co-workers described the dimerization of phenyldiazomethane catalyzed by cerium(IV) ammonium nitrate (CAN).[9] The reaction gave high yields of *Z*-stilbene and was proposed to involve an oxidative chain reaction.[10] A similar proposal was put forth by Bethell et. al. for copper-catalysed dimerization of diphenyldiazomethane.[11] In the proposed process, the dimers are formed by reaction of a diazoalkane radical cation with another equivalent of diazoalkane. This mechanism is,

however, not consistent with the observed selectivity.[12] Nagai et. al reported a copper perchlorate and copper bromide-catalyzed dimerization of aryldiazoalkanes (**5.1**) to form stilbenes **5.2** (Scheme 5.1).[12] The reactions proceeded in good yields (73-92%) but with low to moderate stereoselectivity towards the *Z*-isomer (d.r. = 1.3 - 2.5 : 1). The stereoselectivity was explained by an *anti*-elimination of the thermodynamically most stable copper carbenoid – diazoalkane ylide adduct (**5.4**), as shown in Scheme 5.2.[12] It was assumed that a copper-carbenoid complex **5.3** was formed that reacts with another equivalent of **5.1**, forming the ylide adducts **5.4** and **5.5** as shown. Steric interactions were then assumed to be the controlling factor, favoring the top pathway to **5.4**, which upon internal rotation of the central C–C bond gives *trans*-elimination and, hence, *Z*-stilbene formation in preference.[12]

Scheme 5.1: Cu(II)-catalyzed homodimerization of **5.1**.[12]

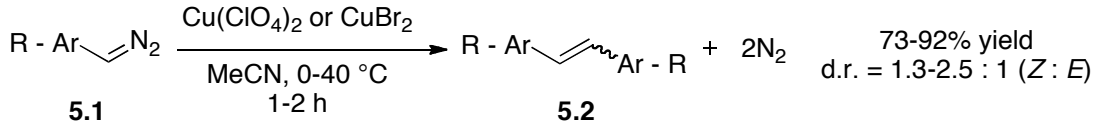

Scheme 5.2: Mechanistic explanation for preferential formation of *Z*-stilbenes.[12]

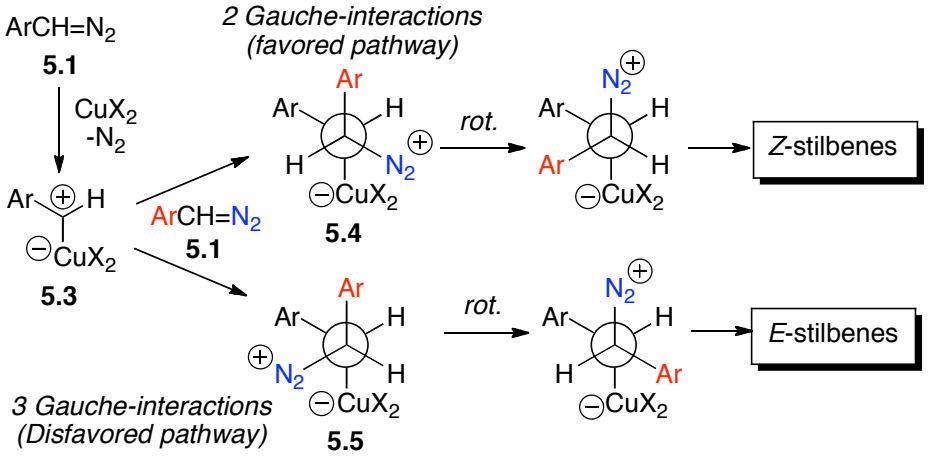

Rhodium-catalyzed dimerization of aryldiazoalkanes was reported by Shechter and Shankar.[13] Good yields (61-99%) were reported with moderate to good stereoselectivities (d.r. = 2.7-11.9 : 1) in favor of the *Z*-stilbenes **5.2** for a variety of substituted aryldiazomethanes **5.1** when the reactions were catalyzed by rhodium(II) acetate (Scheme 5.3a).[13] The stereoselectivities were generally somewhat higher than those previously observed in copper-chemistry. Analogous to the models presented previously,[12] rhodium ylides were proposed intermediates. The stereoselectivtity was proposed to be controlled by the preferred approach of the diazoalkane to the carbenoid, similar to the explanation by Nagai et. al.[12] Another interesting observation was that, for secondary aryldiazoalkanes (**5.6**) $ArC(N_2)R$ (R = Me, Ph), azine dimers **5.7** were preferentially formed (60-85% yields) with no observation of tetrasubstituted alkenes (Scheme 5.3b).[13] This was proposed to be because of the increased steric demand of the approach of the diazo compound to the carbenoid complex, which imparts nucleophilic reactivity at the nitrogen terminus of the diazo compound to become predominant.[13]

Scheme 5.3: Homodimerization of aryldiazoalkanes by Rh(II).[13]

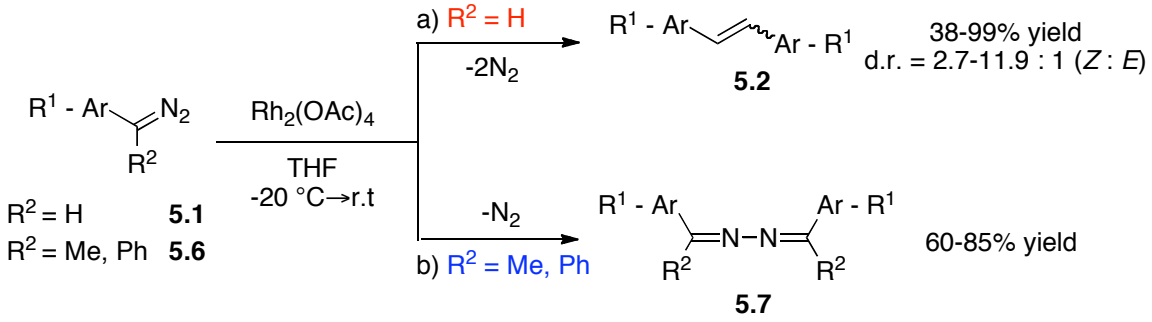

One of the most commonly used carbenoid precursors, ethyl diazoacetate (**5.8**), is notoriously prone to unselective homodimerization in the presence of most metal catalysts.[1,14-17] Good yields and *Z/E*-selectivity have been obtained in homodimerization

of ethyl diazoacetate using metal porphyrin complexes, such as [Ru(TMP)] and $[Os(TTP)]_2$ (95 and 96% yields, respectively).[14,18] Del Zotto et. al reported the first highly stereoselective formation of diethyl maleate **5.9** (>99% isomer purity) by homodimerization of **5.8** catalyzed by $[Ru(\eta^5\text{-}C_5H_5)(PPh_3)_2]Cl$ (Scheme 5.4).[19,20] This group expanded the scope of the reaction by investigating a variety of ester groups which gave quantitative homodimer formation in 95-99% *Z*-purity.[21]

Scheme 5.4: Selective homodimerization of ethyl diazoacetate. [19,20]

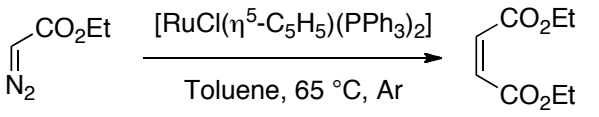

5.8 **5.9**

>99% purity

Considerable synthetic value would be added if the selective *cross*-dimerization of two different diazo compounds to form unsymmetrical alkenes could be achieved. Some examples of this have been reported. It was noted, in a study by Del Zotto and co-workers, that decomposition of equimolar amounts of two different unsubstituted diazoesters led to homo– and heterodimer mixtures.[21] A *Z*-heterodimer was formed in 60% yield from reaction between ethyl diazoacetate **5.8** and an α-diazoketone using a Ru-catalyst, affording a complementary approach for the formation of *Z*-enediones that can not be synthesized through oxidative ring-opening of 1,5-disubstituted furans.[21] An improved heterodimerization process occured when diazoketones **5.10** were reacted with TMS diazomethane **5.11** (Scheme 5.5), which gave 83-91% yields of the corresponding *Z*-heterodimers **5.12**.[21] It was noted that the selectivity probably arose from different decomposition rates of the two diazo compounds, leading to one diazo compound preferentially forming the ruthenium carbenoid complex, which could then be selectively

trapped by the second diazo compound.[21] This group later reported coupling reactions with [RuCl(cod)(Cp)], but this system displayed little selectivity.[22]

Scheme 5.5: Del Zottos cross-dimerization of diazoketones with TMS diazomethane.[21]

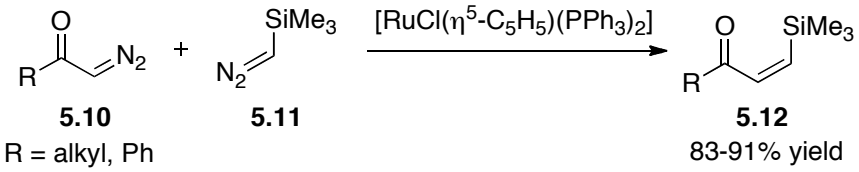

5.10 R = alkyl, Ph **5.11** **5.12** 83-91% yield

Hodgson et. al. later described dimerization of various unsubstituted diazoesters **5.13**, similar to the work described by Del Zotto, but using Grubb's metathesis catalysts (Scheme 5.6).[23-25] Grubbs' 2nd generation ruthenium catalyst effectively mediated the homocoupling of ethyl diazoacetate **5.8** affording a 95% isolated yield of diethyl maleate **5.9** (d.r. > 98 : 2). Other diazoesters gave similar high levels of selectivity.[23-25] Cross-dimerization was attempted using equimolar amounts of two different unsubstituted diazoesters **5.13a** and **5.13b**, which led to statistical mixtures of homo– and heterodimers **5.14a-c**.[24] However, all the dimers were formed with very high stereoselectivity (d.r. >96 : 4) and the heterodimers could be isolated in moderate yields (46-67%). The preferred stereoselectivity was explained in a manner identical to that of Nagai for copper-catalyzed dimerization chemistry.[12] It was noted that the amount of hetero-coupled product somewhat exceeded the expected statistical mixture if the size of the ester groups of the two coupling partners were sterically well differentiated.[24]

Scheme 5.6: Homo- and heterocoupling of unsubstituted diazoesters using Grubb's 2nd generation metathesis catalyst.[24]

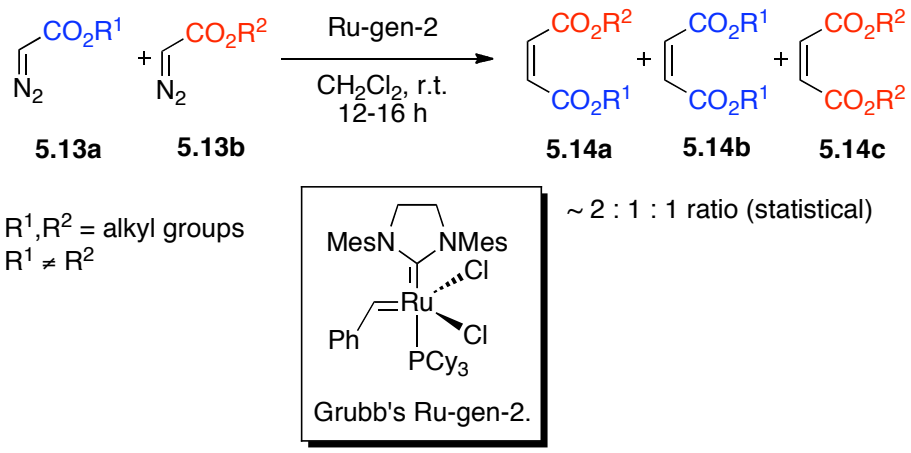

Barluenga et. al. reported that cross-coupling can occur between Fisher carbenes **5.15** and ethyl diazoacetate **5.8** when mediated by CuBr (Scheme 5.7).[26] It was shown that the coupling probably occured through the transmetallated copper carbenoid, since such a species was characterized by X-ray crystallography.[26] The Barluenga group later reported another interesting transformation that occurs when ethyl 3-methyl-2-diazobut-3-enoate **5.17** and various other diazo compounds **5.18** were decomposed in an equimolar ratio in the presence of a Cu(I)-catalyst, $[(MeCN)_4Cu]BF_4$ (Scheme 5.8).[27] The reaction resulted in formal [3+1] adducts **5.19** in good yields and occured with high regioselectivity. Several diazo compounds **5.18** could undergo the transformation to produce substituted cyclobutenes. It was reasoned that the vinyldiazoacetate would decompose slower than the other diazo component, and hence undergo cyclopropanation at the vinyl group to form **5.21** by the initially formed copper-carbenoid **5.20**.[27] Further ring expansion *via* a secondary copper cyclopropylcarbenoid **5.22** would give the observed cyclobutenes **5.19**. The methodology was highlighted by the design of a cascade sequence, composed of *in situ* copper carbenoid formation from propargylic acetates, leading to ring closure to form

furans, followed by the cyclopropanation/ring-expansion reaction with 3-substituted vinyldiazoacetates to give furyl-substituted cyclobutenes in moderate to good yields (48-73%).[27]

Scheme 5.7: Carbene cross-coupling with Fisher carbenes **5.15**. [26]

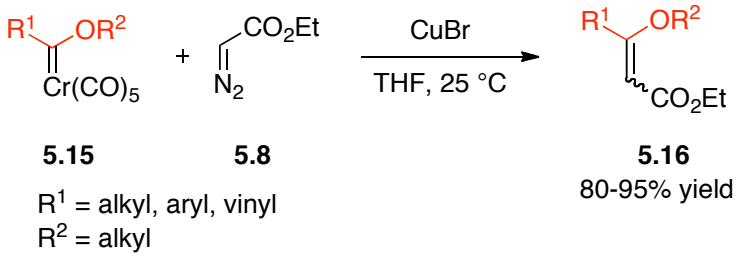

Scheme 5.8: Barluengas formal [3+1]-coupling of diazo compounds and proposed mechanism.[27]

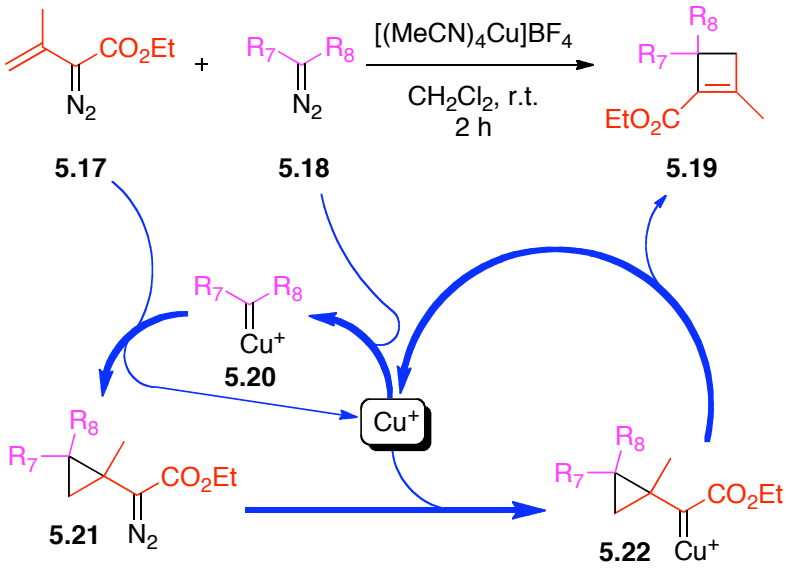

A formal carbene cross-coupling was reported by Dixneuf et. al., in which TMS diazomethane **5.11** selectively coupled with an *in situ* generated vinylcarbenoid derived from propargylic acetates **5.23** and [RuCl(cod)(Cp)].[28] The reaction could generate a variety of *Z*-coupled products **5.24** in high selectivity (68-99% yield), unless the

propargylic acetate contained a stereocenter, which led to mixtures of stereoisomeric products.[28]

Scheme 5.9: Dixneufs carbene cross-coupling with TMS diazomethane.[28]

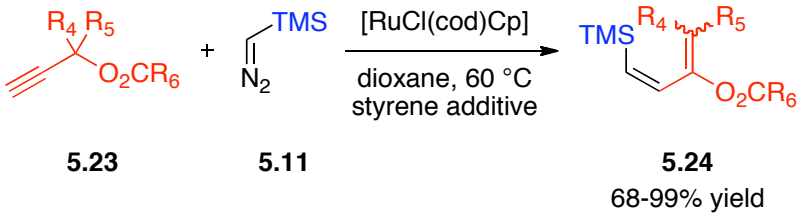

5.23 **5.11** **5.24**
68-99% yield

Donor/acceptor-substituted rhodium carbenoids, particularly those derived from aryl– and vinyldiazoacetates, have been shown to be very selective intermediates in a range of synthetically useful processes.[29-33] Highlights include intermolecular [2+1]–,[33] [3+2][34]– and [4+3]–cycloadditions,[33] ylide mediated cascade reactions[35] and also stereoselective C–H functionalization.[30,36] This chemistry has found numerous applications in syntheses of bioactive molecules and complex natural products.[36] A key factor in achieving highly chemo- and stereoselective transformations has been the utilization of these donor/acceptor-substituted rhodium carbenoids, which are much more selective than traditionally used acceptor–only carbenoids.[29,32] As a consequence of this, carbene dimerization in such reactions is not a prominent problem. Homodimerization chemistry in such systems is only observed if the carbenoid trapping agent is extremely unreactive.[37,38] Scheme 5.10 demonstrates effectively the relative propensities of dimer formation in donor/acceptor (**5.25**) *versus* acceptor systems (**5.8**),[39] particularly since a relatively unreactive trap, cyclohexane, is used as solvent. Homodimerization is predominant when ethyl diazoacetate **5.8** is used as the carbenoid precursor.[39] The three possible dimers of **5.25** (**5.28-5.29**) have been observed in minor amounts in certain reactions.[37,38]

Scheme 5.10: Dimerization propensity of donor/acceptor and acceptor-only rhodium carbenoids.[37-39]

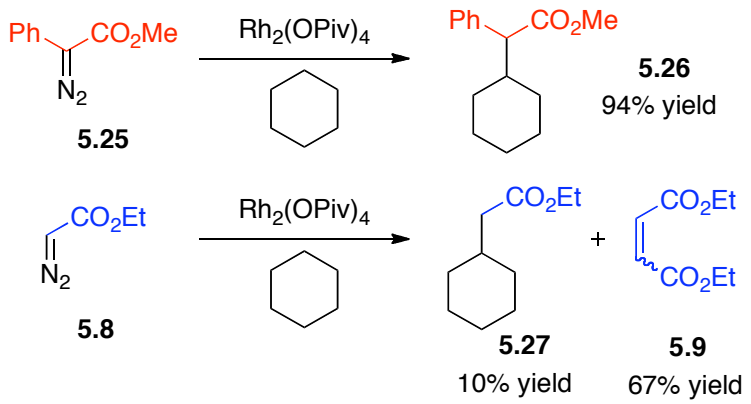

Carbene-dimers of methyl phenyldiazoacetate:

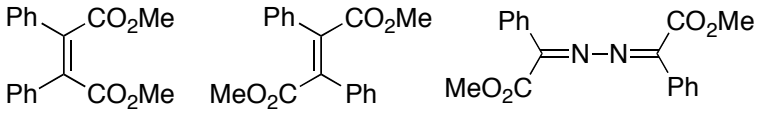

During competition studies of intermolecular C–H insertion α to nitrogen,[40] Dr. Qihui Jin discovered that the C–H insertion process was not necessarily predominant when two different diazo compounds were used in the reaction mixture.[41] The Rh_2(*S*-DOSP)$_4$-catalyzed decomposition of a 1 : 1 mixture of diazo compounds **5.8** and **5.30** in the presence of aniline **5.29**, unexpectedly resulted in a 2 : 1 mixture of cross-dimerization product **5.32** and C–H insertion product **5.31** to be isolated.[41] This suggested that the cross-dimerization of an aryldiazoacetate and ethyl diazoacetate was a very favorable process.

Scheme 5.11: Discovery of cross-dimerization.

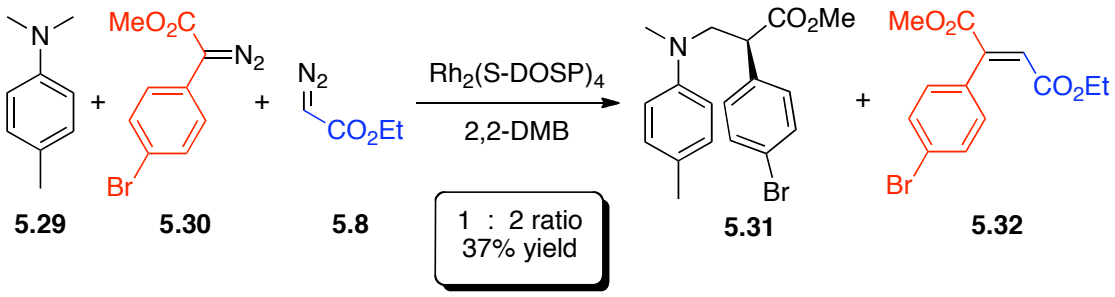

This disovery is the basis of the study presented in this chapter, which describes the development of conditions that optimize the Rh(II)-catalyzed cross-dimerization chemistry as well as an expansion of the scope of the chemistry. Mechanistic investigations of the transformation have also been conducted by competition studies, ReactIR-studies of relative decomposition rates, as well as density functional calculations. The experimental studies were carried out in collaboration with Mr. Brendan Parr under my supervision.

5.2 Results And Discussion

5.2.1 Synthetic Studies

Reaction conditions. Although the initial cross-dimerization reactions, carried out using the chiral catalyst Rh_2(*S*-DOSP)$_4$,[41] were reasonably successful, it was deemed necessary to find conditions that would: (1) optimize the cross– to homocoupling ratio, (2) maximize the stereoselectivity of **5.33**, and, (3) find an appropriate *achiral* catalyst system, as the transformation is overall achiral. Several solvents and catalysts were tested in the transformation between **5.25** and **5.8** (Scheme 5.12, Table 5.1). The reaction produces both diastereomers of the heterocoupling product as well as homodimers of **5.25** and **5.8**. Here, only the yields relative to homodimers **5.9** are recorded, as the homodimers of **5.25** do not have distinguishable signals in the ^{1}H NMR spectrum of the crude reaction mixture. However, as a 1 : 1 ratio of diazo compounds is used, the remainer of **5.25** must also form homodimers. Although the cross-dimerization could be carried out readily at ambient temperature with as low as 0.1 mol% catalyst, it was found that a much cleaner and selective reaction resulted if the diazo compounds were added drop-wise at low temperature to a solution of 1 mol% of the catalyst. The selectivity for the heterodimer increased from 63 : 37 to 91 : 9 ratio by conducting the reaction at low temperature (-63 °C). The diastereomeric ratio of **5.33** also increased to >20 : 1. A screen of different rhodium(II) catalysts furthermore demonstrated that rhodium tetrakis(pivaloate), Rh_2(OPiv)$_4$, gave the superior ratio of cross– to homocoupling in dichoromethane as solvent (91 : 9) at low temperature (Table 5.1, Entries 2-6). The stereoselectivity was also best for this system, although the very bulky Rh_2(TPA)$_4$ gave similar stereocontrol. It appears that a relatively bulky catalyst is important to achieve

high stereoselectivity. Other solvents than dichloromethane did not afford any further improvements, although trifluorotoluene gave very similar results to the reaction in dichoromethane. For convenience, the standard reaction conditions were chosen to be 1 mol % of $Rh_2(OPiv)_4$ in dichloromethane as solvent, initiated at -78 °C (dry ice/acetone bath), with slow heating to ambient temperature following the diazo compound addition. When ambient temperature was obtained, the reaction had always reached completion.

Scheme 5.12: Test reaction for optimization of reaction conditions.[a]

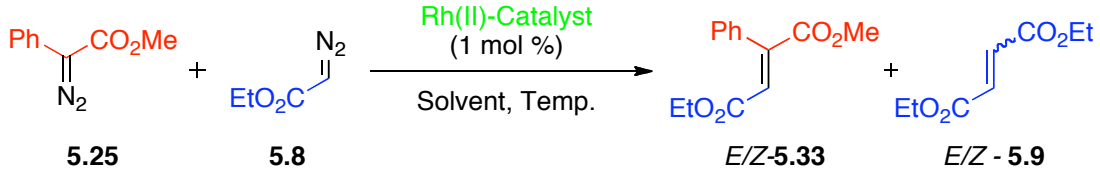

5.25 **5.8** ***E/Z*-5.33** ***E/Z* - 5.9**

Table 5.1: Influence of reaction conditions on cross-coupling selectivity.[a]

Entry	*Catalyst*	*Solvent*	*Temp.* (°C)	*Rel. Yield* (%)[b] **5.33 : 5.9**	*d.r.* **5.33** *(E : Z)*[b]
1	$Rh_2(OPiv)_4$	CH_2Cl_2	21	63 : 37	9.5 : 1
2	$Rh_2(OPiv)_4$	CH_2Cl_2	-63	91 : 9	>20 : 1
3	$Rh_2(OOct)_4$	CH_2Cl_2	-63	79 : 22	6.9 : 1
4	$Rh_2(esp)_2$	CH_2Cl_2	-63	77 : 16	12 : 1
5	$Rh_2(TPA)_4$	CH_2Cl_2	-63	64 : 36	20 : 1
6	$Rh_2(TFA)_4$	CH_2Cl_2	-63	75 : 25	7.3 : 1
7	$Rh_2(OPiv)_4$	$PhCF_3$	-63	87 : 13[d]	>20 : 1
8	$Rh_2(OPiv)_4$	Et_2O	-63	72 : 28[d]	13 : 1
9	$Rh_2(OPiv)_4$	Hexanes	-63	75 : 26	18 : 1

[a] The data was collected by Mr. Brendan Parr.
[b] From ^1H NMR of crude reaction mixture.

Aryldiazoacetates. With standard reaction conditions in hand, the scope of the reaction was the next to be investigated. The influence of the structure of the aryldiazo component

5.34 was first considered in the coupling reaction with **5.8** under the standard reaction conditions (Scheme 5.13). First, a series of *para*-substituted aryldiazoacetates **5.34a-c**, ranging from electron rich (methoxy-substituted) to electron-withdrawing (trifluoromethyl substituted), were investigated (Table 5.2). Good yields (67-73%) were obtained with excellent diastereoselectivity (> 20 : 1 d.r.) towards the fumarate products **5.35a-c**, unless the substituent was very electron-withdrawing. In the case of *para*-trifluoromethyl group (Entry 4), only 40% of the fumarate was obtained. The diastereomer ratio was reduced to 5.1 : 1 in this case. From these results, it is indicated that very electron-poor aryl groups have an adverse effect on the diastereoselectivity and reaction yield. The 2-naphthyldiazoacetate **5.34d** gave 58% yield of the desired product **5.35d** in > 20 : 1 diastereomer ratio. Consistent with the abovementioned electronic effect, benzofuranyldiazoacetate **5.34e** gave a very good (83%) yield of the desired fumarate **5.35e** with excellent diastereoselectivity. This reaction also demonstrated that heterocyclic aryl groups are tolerated in the reaction. When the aryl group was kept unsubstituted, and the electron-withdrawing group was changed to cyano or methyl ketone (Entries 7-8), the diastereomer ratio dramatically dropped to about 2-3 : 1, although good overall yields were obtained (71-85%). The phosphonate ester **5.34h** did not convert under the reaction conditions. Presumably, this diazo compound is too stable under these conditions or inhibits the reaction. Overall, a picture is emerging that the ester group is important to achieve the high levels of selectivity in addition to an electron-neutral or electron-rich donating group.

Scheme 5.13. Cross-coupling of aryldiazo compounds with **5.8**.

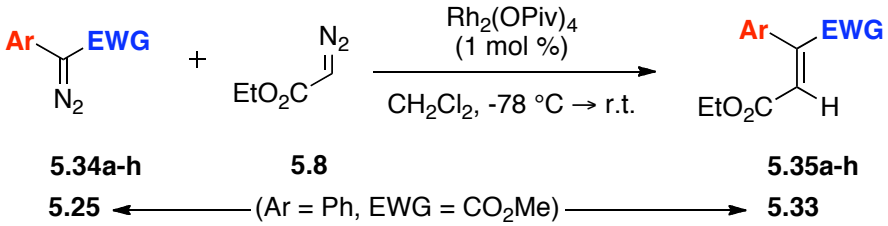

Table 5.2. Coupling of aryldiazoacetates with EDA.[a]

Entry	*Comp'd*	***Ar =***	***EWG =***	*d.r. (E : Z)*[b]	*Yield* (%)[c]
1	**5.25, 5.33**	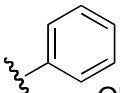	-CO_2Me	> 20 : 1	71
2	**a**	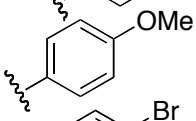	-CO_2Me	> 20 : 1	73
3	**b**	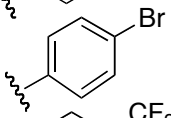	-CO_2Me	> 20 : 1	67
4	**c**	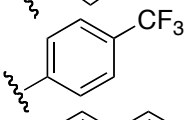	-CO_2Me	5.1 : 1	40
5	**d**	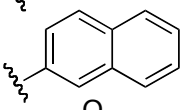	-CO_2Me	> 20 : 1	58
6	**e**	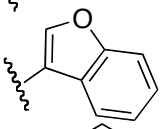	-CO_2Me	> 20 : 1	83
7	**f**	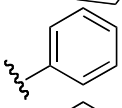	-CN	3.3 : 1	86[d]
8	**g**	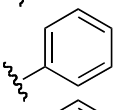	-COMe	2.0 : 1	71[d]
9	**h**	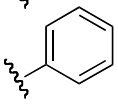	-$PO(OMe)_2$	N/A	N/R

[a] Reactions were carried out by Mr. Brendan Parr
[b] Measured from ^1H NMR of crude product.
[c] Isolated yield of major product unless otherwise stated.
[d] Overall yield.

Vinyldiazoacetates. Vinyldiazoacetates are another class of important diazo compounds used in synthesis.[42] In the cross-coupling reaction with **5.8** (Scheme 5.14), the product would be a 1,3-diene, a potentially useful synthetic intermediate. When the standard reaction conditions were applied to the reaction between arylvinyldiazoacetates **5.36a-c** and **5.8**, overall moderate to good yields were obtained (61-82%) with only moderate diastereomer ratios (~5.1-5.6 : 1), in favor of the *E*-isomeric dienes **5.37a-c**. Methyl 2-thienylvinyldiazoacetate **5.36d** afforded 61% overall yield of the corresponding diene **5.36d** in a 7.4 : 1 diastereomer ratio. Although reasonable overall reaction yields could be obtained with the vinyldiazoacetates, only moderate diastereocontrol was observed.

Scheme 5.14. Cross-coupling with vinyldiazoacetates.

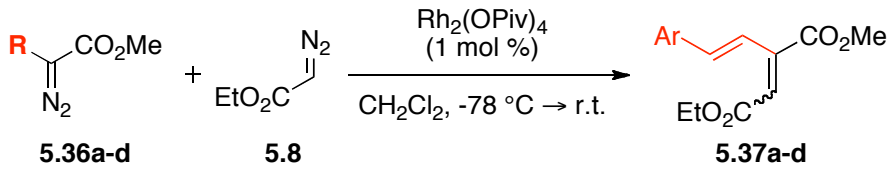

5.36a-d **5.8** **5.37a-d**

Table 5.3: Cross-coupling of various vinyldiazoacetates.[a]

Entry	*Comp'd*	***R =***	*d.r.* **5.37** (*E* : *Z*)[b]	*Yield* (%)[c]
1	**a**	Ph	5.6 : 1	82
2	**b**	(p-Br)Ph	5.1 : 1	61
3	**c**	(Mep-O)Ph	5.5 : 1	67
4	**d**	S	7.4 : 1	61

[a] Reactions were carried out by Mr. Brendan Parr
[b] Measured from ^{1}H NMR of crude product.
[c] Overall yield.

Acceptor-substituted diazo compounds. As a picture is emerging, of how the aryl– and vinyldiazoester structure influence the cross-dimerization reaction, the effects of the structure of the acceptor-substituted diazo compound remains to be understood. The reaction between methyl phenyldiazoacetate **5.25** and acceptor-substituted diazo compounds **5.38a-f** were investigated using the standard reaction conditions (Scheme 5.15, Table 5.4). The reaction with commercially available *tert*-butyl diazoacetate **5.38a** afforded the desired hetero-coupling product **5.39a** in a very clean transformation (87% yield) with excellent >20 : 1 diastereomer ratio. This strongly indicates that, by increasing the bulkiness of the acceptor-substituted diazo compound, higher selectivity can be achieved. Therefore, a series of diazoketones **5.38b-f** were synthesized[43] and studied in this reaction. Aryldiazoketones turned out to be exceptional coupling partners and gave the desired *E*- products **5.39b-f** in routinely high yields (79-87%) with a variety of aryl substituents on the diazoketone. Furthermore, excellent diastereoselectivity was observed for most of these coupling reactions (> 20 : 1 d.r.). When a less bulky vinyldiazoketone **5.38f** was used, there was virtually no diastereoselectivity, but a good overall yield of 87% was still observed. The cross-coupling of aryldiazoacetates with diazo compounds flanked by two electron-withdrawing groups were also attempted. However, this proved to be an unviable process.

Scheme 5.15: Cross-coupling of acceptor-diazo compounds with **5.25**.

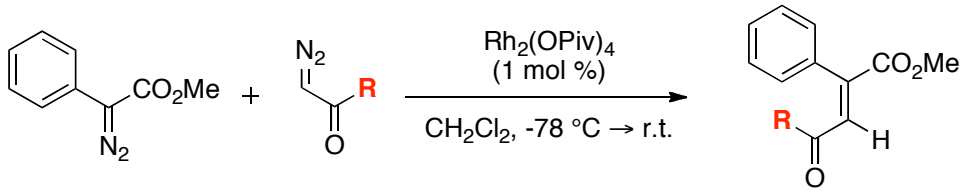

5.25 **5.38a-f** **5.39a-f**

Table 5.4: Influence of acceptor-substituted diazo compounds on cross-coupling.

Entry	*Comp'd*	***R =***	*d.r.* **5.39** (*E* : *Z*)[b]	*Yield* (%)[c]
1	**a**	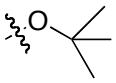	> 20 : 1	87[a]
2	**b**	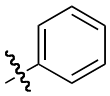	> 20 : 1	87
3	**c**	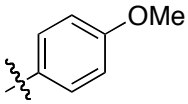	> 20 : 1	80
4	**d**	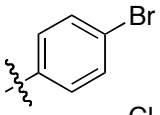	> 20 : 1	79
5	**e**	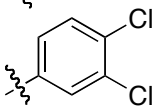	>20 : 1	87
6	**f**	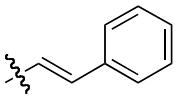	1.3 : 1	87[d]

[a] Reaction was carried out by Mr. Brendan Parr
[b] Measured from ^{1}H NMR of crude product.
[c] Isolated yield of major product.
[d] Overall yield.

The structures of the heterodimer products reported herein were determined by NMR by analogy to already established structures.[41] The diastereomers were assigned based on nOe experiments, in which the vinylic proton has a strong correlation with the methyl ester for the major diastereomer. In addition, an x-ray structure was obtained for compound **5.39d**, which shows, unambiguously, the structure and *E*-stereochemistry of this product (Figure 5.1).

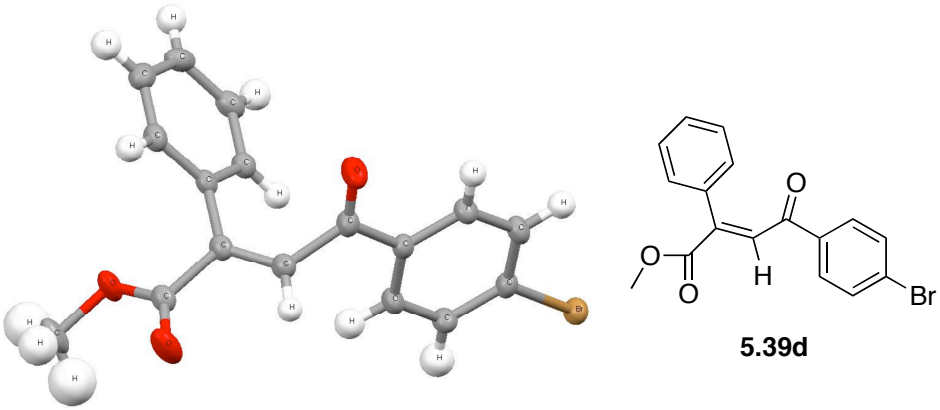

Figure 5.1 X-ray crystallographic structure determined for **5.39d**.

5.2.3 Mechanistic Studies

Competition experiments. The cross-coupling reactions are normally carried out by syringe pump addition of a 1:1 mixture of the diazo compounds to a solution of the catalyst. The slow addition is necessary under the synthetic conditions, because the catalyst appears to become inactive if the diazo compounds are added too fast. In the initial studies by Dr. Qihui Jin, it was also found that syringe pump addition of a catalyst-solution to the mixture of the diazo compounds was effective, thereby constantly adding active catalyst to the reaction mixture.[41] It was decided to study the cross-coupling reaction in experiments where both diazo compounds were present in the reaction mixture initially, and then add the catalyst from a stock solution. The disappearance of the diazo compounds could then be readily monitored by tracking the characteristic C=N=N IR stretch frequencies (~2114 cm^{-1} for ethyl diazoacetate **5.8**, ~2088 cm^{-1} for methyl phenyldiazoacetate **5.25**) using ReactIR.[44] These experiments could shed light on the origin of the catalyst poisoning effect as well as the mechanism of the cross-coupling reaction.

In a ReactIR experiment (Scheme 5.16, Table 5.5), using an equimolar mixture of **5.8** and **5.25**, the catalyst was injected in one movement and transient IR spectra were collected for several minutes (~2-3 scans/sec). The reaction was initially very fast, but came to a complete stop at about 26% conversion (Entry 1). Addition of an equivalent of styrene **5.40** (Entry 2), appeared to increase the conversion to about 45%. Addition of two equivalents led to full conversion of both diazo compounds in a very fast reaction (Entry 3, $t_{1/2}$ ~ 10 sec). An ^{1}H NMR analysis of the crude reaction mixture revealed that a mixture of heterodimer **5.33** : cyclopropane **5.41** (from **5.25**) : cyclopropanes **5.42** (from **5.8** as diastereomer mixture) in a 68 : 19 : 13 ratio was formed. By increasing the amount of **5.40** to 20 equivalents, the three products were obtained in a 44 : 30 : 26 ratio. These experiments demonstrate that the cross-coupling reaction is a remarkably favorable event, since it was the major product present even in the presence of a vast excess of styrene, a relatively reactive trap in such reactions.[38] The influence of the **5.25** : **5.8** ratio was investigated next. When **5.8** was reacted in the presence of 20 equivalents of **5.40**, only 56% conversion was obtained. The catalyst appeared to become inactive during the reaction. With **5.25**, full conversion to the cyclopropane was observed under the same conditions. When using an excess of **5.8** (1.5 : 1 ratio of **5.8** : **5.25**), this time with two equivalents of **5.40**, only about 19% conversion was observed. In the reverse case, using 1.5 equivalents of **5.25** and 1 equivalent of **5.8**, the reaction went to completion very fast. The latter reaction afforded a mixture of 53 : 41 : <6 of the three possible products.

Scheme 5.16: Competition studies of cross-dimerization reaction.

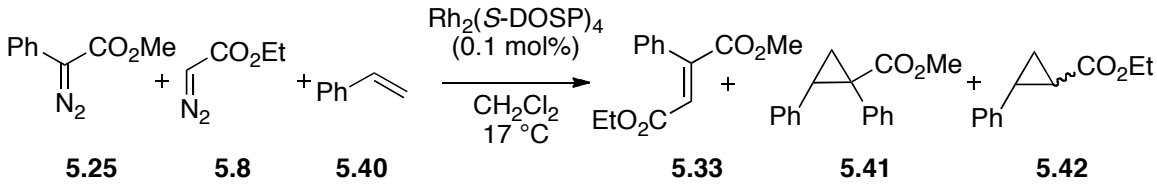

5.25 **5.8** **5.40** **5.33** **5.41** **5.42**

Table 5.5: Influence of additive and molar ratio on conversion.

Entry	*Molar ratio*			*Conversion* (%)	$t_{1/2}$ (s)
	5.25	**5.8**	**5.40**		
1	1	1	0	29	N/A
2	1	1	1	45	N/A
3	1	1	2	100[a]	10
4	1	1	20	100[b]	7
5	0	1	20	56	N/A
6	1	0	20	100	4
7	1	1.5	2	19	N/A
8	1.5	1	2	100[c]	3

[a] Afforded a 68 : 19 : 13 mixture of **5.33** : **5.41** : **5.42.**
[b] Afforded a 44 : 30 : 26 mixture of **5.33** : **5.41** : **5.42.**
[c] Afforded a 53 : 41 : <6 mixture of **5.33** : **5.41** : **5.42.**

These results demonstrate convincingly that both diazo compounds form their respective carbenoid complexes under the reaction conditions, however not at the same rate.[45] Furthermore, it appears that the acceptor carbenoid complex, derived from **5.8**, can follow a destructive pathway to render the catalyst inactive unless it is effectively trapped.[46] Formation of the acceptor-substituted rhodium carbenoid, with subsequent break-down of this complex into unreactive Rh-species, is therefore deemed to be the most likely origin of the catalyst poisoning effect. The results also suggest that the productive pathway for hetero-coupling, occurs through the donor/acceptor-substituted carbenoid intermediate derived from **5.25** reacting with **5.8**.

Relative decomposition rates. In light of the results of the abovementioned study, it was decided to conduct experiments to determine the relative reaction rates of the two diazo compounds, since this has crucial impact on the mechanistic interpretation of the cross-coupling reaction.[46] The reactions of **5.25** and **5.8** in the presence of excess styrene, added in order to prevent homodimerization reactions, catalyzed by $Rh_2(OPiv)_4$, were studied in reactIR experiments conducted in a similar fashion to those described earlier (Figure 5.2). It is clear that the rates are quite similar for the two systems, as only an initial rate difference of about 5 : 1 was obtained for the data collected at -15 °C. However, this is consistent with the observation that homodimerization of **5.8** is always occuring to some extent, even under the optimized reaction conditions. Figure 5.2 supports the idea, however, that **5.25** undergoes decomposition somewhat faster.

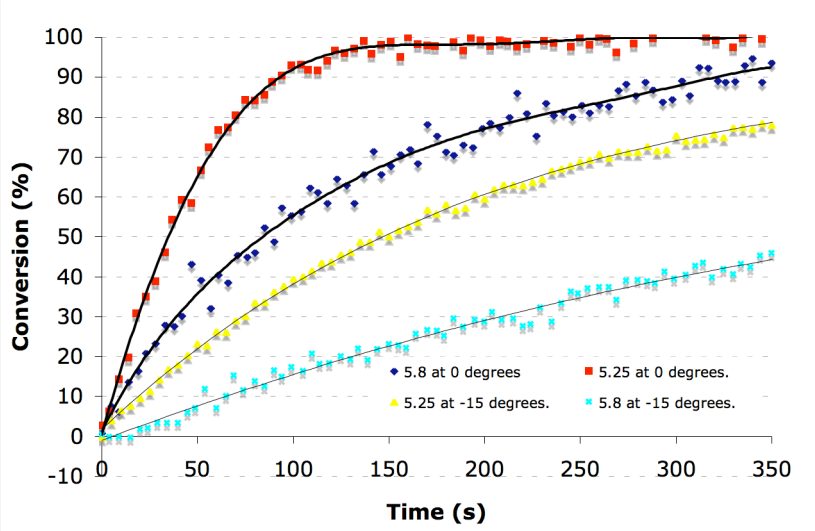

Figure 5.2: Conversion rates for decomposition of **5.25** and **5.8** at 0 °C and -15 °C. The data was collected by Mr. Brendan Parr.

DFT calculations. From the reactIR data gathered above, it appears that formation of the donor/acceptor-substituted rhodium carbenoid complex is a key initial component of the

mechanism. The most likely second event in the dimerization process, is capture of ethyl diazoacetate **5.8** by this carbenoid. To shed more light on the dimerization process, we carried out density functional calculations. As a model system, the possible dimerization reactions between methyl diazoacetate **5.43** and **5.25** were investigated using dirhodium formate (**5.44**) as catalyst (Scheme 5.17). Such rhodium carbenoid systems have been studied previously in cyclopropanation[47] and C–H insertion chemistry.[29,48] The main discussion here is based on gas-phase enthalpies and free energies calculated at the B3LYP/6-31G*[Rh-RSC+4f] level of theory.[29]

Scheme 5.17: Model chemistry for dimerization reaction.

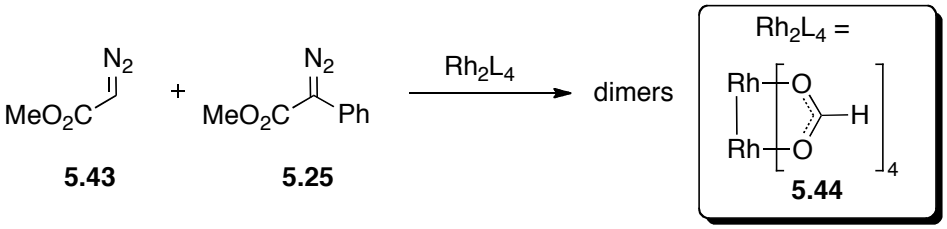

The calculations were carried out considering four possible dimerization scenarios (Scheme 5.18). The donor/acceptor carbenoid complex **5.45** can react with an equivalent of **5.25** giving rise to the homodimer **5.46**, or it can react with **5.43** to give the heterodimer **5.47**. In a similar fashion, the acceptor-carbenoid **5.48** can give either homo– (**5.47**) or heterodimerization (**5.49**). The possibility of dimerization of two carbenoids was deemed unlikely. This would be an extremely slow pathway, as the process is bimolecular and the catalyst concentration is very low (1 mol%).

Scheme 5.18: Possible dimerization scenarios.

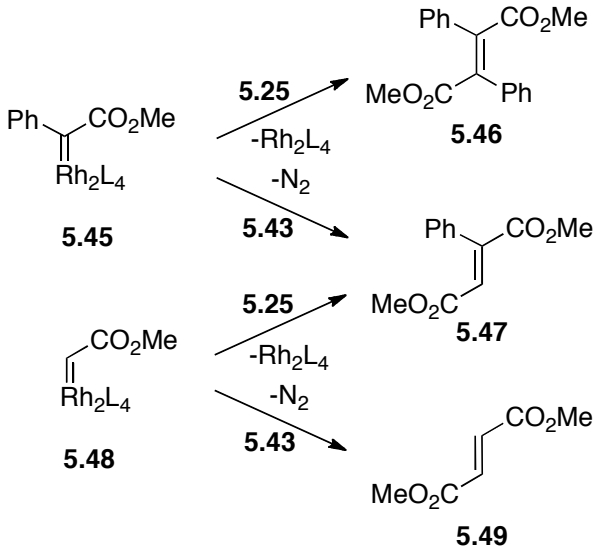

It was deemed informative to calculate and compare gas-phase activation parameters at the B3LYP/6-31G*[Rh-RSC+4f] level of theory for the pathways in Scheme 5.18, as this would indicate the relative propensities of the different dimerization events to occur. Two transition structures could be located for the homodimerization of **5.25** to give **5.46** (*E* and *Z* isomers). The transition states involve nucleophilic attack of **5.25** at carbenoid **5.45**, and the most stable structure **TS-I** is shown in Figure 5.3. The gas-phase activation enthalpy was calculated to be 15.5 kcal/mol relative to free carbenoid and diazo compound. The gas-phase activation Gibbs free energy was found to be 32.2 kcal/mol. The results demonstrate why aryldiazoacetates do not easily dimerize,[39] since most carbenoid reactions have significantly lower activation barriers (cyclopropanation of styrene has a potential energy barrier of only 4.5 kcal/mol).[29] Only C–H insertion of alkanes have barriers of this magnitude (see Section 2.2.1), which explains why the chemistry is challenging for unactivated C–H bonds and homodimerization is observed.[29]

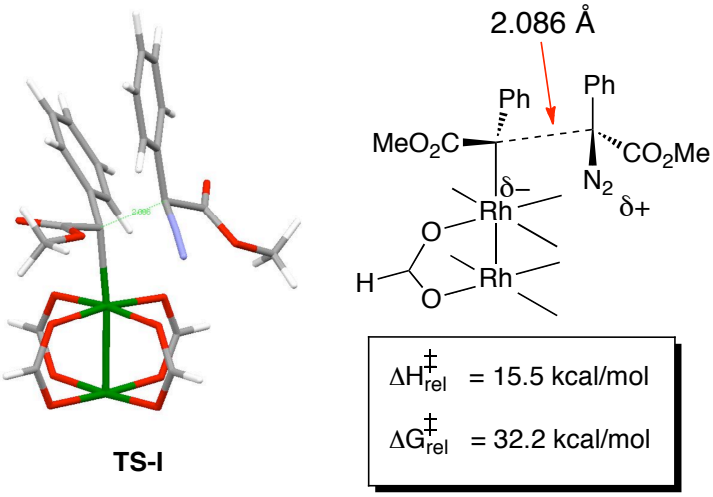

Figure 5.3: Lowest energy **TS-I** for homodimerization of **5.25**. Gas-phase activation enthalpy and Gibbs free energy are calculated relative to free carbenoid complex **5.45** + free **5.25** at the B3LYP/6-31G*[Rh-RSC+4f] level of theory.

The reaction between carbenoid complex **5.45** and methyl diazoacetate **5.43** was considered next. Six transition states for the approach of **5.43** to **5.45** were located. The three lowest energy transition structures and their respective pathways to products are shown in Scheme 5.19. The last three transition structures were not included in the discussion, as they were >4 kcal/mol less stable than the former.

When considering the Newman projections along the forming C–C bond for approach of **5.43** towards carbenoid complex **5.45**, there is a distinct steric preference for the orientation of the substitutents on the incoming substrate. This representation is analogous to models previously presented by Nagai[12], Wulfman[8] and Shechter[13] in homodimerization chemistry. In **TS-IIa**, the hydrogen substituent on **5.43** is situated towards the lower, left-hand sector of the carbenoid, which is the most sterically encumbered sector as it is flanked by the ester group, as well as the catalyst "wall". Furthermore, the diazonium moiety is oriented *anti*-periplanar to the Rh–C bond, which

allows for a concerted Rh–C and C–N bond breaking process to occur. Indeed, intrinsic reaction coordinate analysis forward from **TS-IIa** leads to the product *E*-**5.47** directly. The calculated enthalpic activation barrier for this reaction is +4.21 kcal/mol (Table 5.6). **TS-IIb** is the most stable of all the located transition structures with an enthalpic activation barrier of +2.80 kcal/mol. The structure is indicated in Table 5.6. The difference, compared to **TS-IIa**, reflects the decreased steric interactions involved when orienting the medium-sized diazonium group towards the lower, right-hand sector, and the largest group (ester) away from the bulky catalyst "wall". The forward IRC-drive from **TS-IIb** leads to ylide **YL-IIb**, which is -8.27 kcal/mol enthalpically more stable than the carbenoid. The further pathway of this ylide crucially determines the diastereomeric outcome. The most favored pathway was found by performing a potential energy surface scan of the Rh–C coordinate, which indicated that a slight, clock-wise rotation of the front fragment of **YL-IIb** occurs readily to give *syn*-elimination with a very low energy barrier (< 0.5 kcal/mol) to afford the product *E*-**5.47**. For comparison, the counterclock-wise rotation was imposed on **YL-IIb** to give **TS-IIIb**, leading to *Z*-**5.47**. This step displayed an enthalpic barrier of +5.17 kcal/mol. This considerably larger barrier reflects an increase in energy when the bonds go through the ecclipsed conformation. The most stable transition structure leading to *Z*-**5.47** was **TS-IIc**, which displayed an enthalpic activation barrier of +4.05 kcal/mol. The dimerization reaction is overall highly exothermic ΔH_{rxn} = -66.4 kcal/mol. Note that, the homodimerization of **5.25** is considerably disfavored compared to the cross-dimerization, consistent with the experimental observations.

Scheme 5.19: Heterodimerization pathways via the donor/acceptor carbenoid.

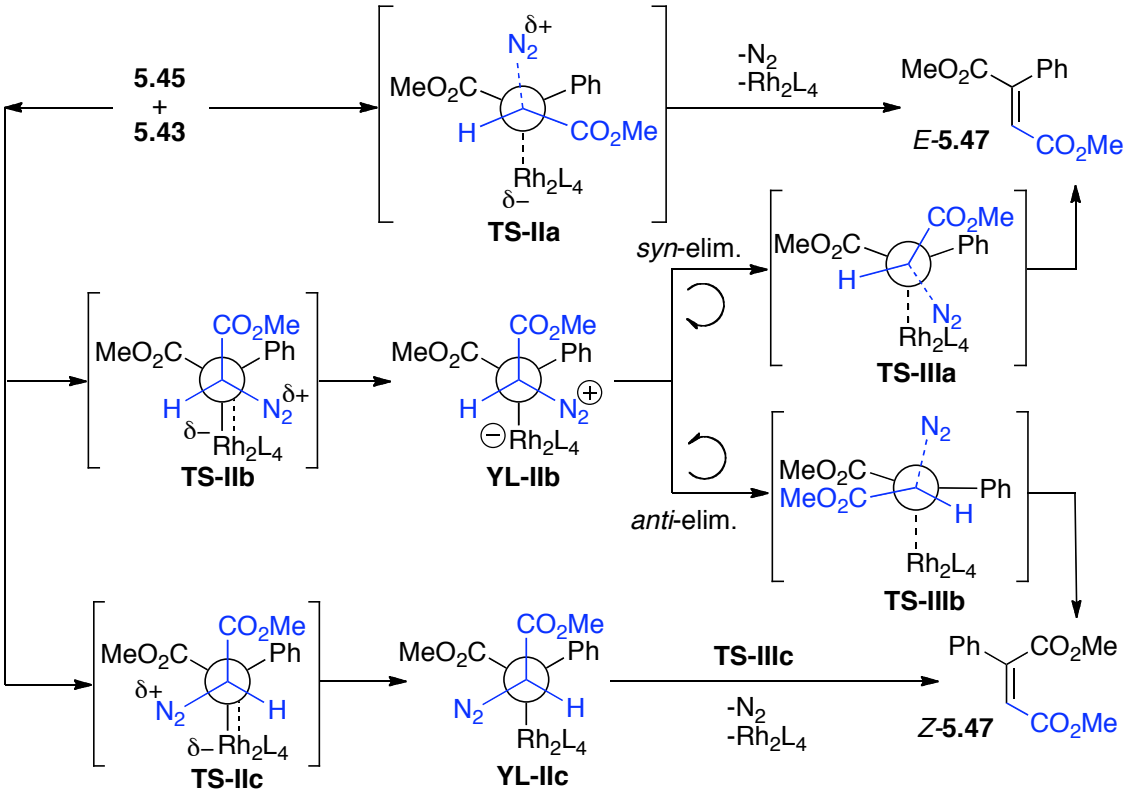

Table 5.6: Calculated gas-phase relative enthalpies and Gibbs free energies.

Entry	*Structure(s)*	H_{rel} [a] (kcal/mol)	G_{rel} [a] (kcal/mol)
1	**5.45+5.43**	0.00	0.00
2	**TS-IIa**	+4.21	+18.9
3	**TS-IIb**	+2.80	+17.2
4	**YL-IIb**	-8.27	+6.16
5	**TS-IIIa**	< -7.77[b]	N/D[b]
6	**TS-IIIb**	-3.10	+13.7
7	**TS-IIc**	+4.05	+19.0
8	**YL-IIc**	-9.85	+4.45
9	**TS-IIIc**	N/D[b]	N/D[b]
10	*E*-**5.47**+N_2+Rh_2L_4	-66.4	-76.7

[a] Gas-phase values at 298K calculated at the B3LYP/6-31G*[Rh-RSC+4f] level of theory.
[b] TS could not be located. PES scans towards product side indicate near barrierless reaction.

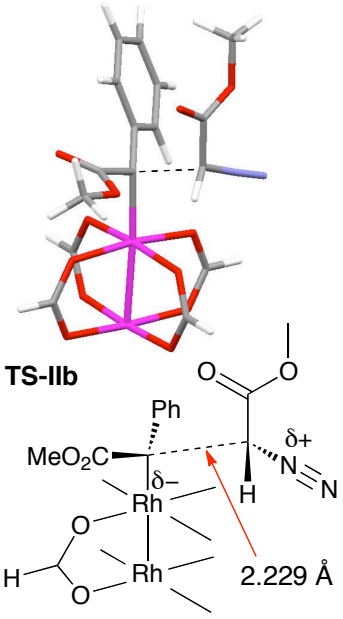

Based on the discussion above, it is clear that the stereoselectivity of the heterodimerization reaction would depend on which approach transition state is favored. The results of Table 5.6 show that, indeed, **TS-IIb** leading to the observed major product, is favored. However, under the synthetic conditions, the reaction is carried out in dichloromethane solvent at -78 °C. Therefore, all three transition states **TS-IIa-c** were re-submitted to full geometry optimization at the B3LYP/6-311+G(d,p)[Rh-RSC+4f] level of theory at -78 °C (195.15 K) for more accuracy. Furthermore, the IEF Polarizable Continuum solvent Model (IEFPCM) for dichloromethane ($\varepsilon = 8.93$) was included. The results are shown in Table 5.7. The solution-phase Gibbs free energies indicate that **TS-IIb** is still the most favored, but that the lowest-energy transition state that leads to the minor diastereomer (**TS-IIc**), is only $\Delta\Delta G^{\neq} = +1.15$ kcal/mol higher in energy, 0.65 kcal/mol lower than what the gas-phase calculations predicted. By applying the Eyring equation, an expression for the relative rates of reaction through **TS-IIb** and **TS-IIc** ($k_{TS\text{-}IIb}/k_{TS\text{-}IIc}$) can be deduced (Equation 5.1), and using only **TS-IIb** and **TS-IIc** to estimate the selectivity, the Gibbs free energy difference corresponds to a diastereomer ratio of about ~19 : 1. This can be compared to experimental diastereomer ratios from Table 5.1, which range from 6.9-22 : 1 ($\Delta\Delta G^{\neq} = 0.81$-$1.29$ kcal/mol) for various rhodium catalysts at -63 °C. Considering the simplifications involved in the model and errors in DFT-calculations,[49] the agreement between experiment and theory is very good.

Table 5.7: Relative solution-phase enthalpies and Gibbs free energies of main transition states calculated at the B3LYP/6-311+G(d,p)[Rh-RSC+4f] level of theory applying the IEFPCM solvent model for dichloromethane at 195.15 K (-78 °C).

Entry	*Structure(s)*	H_{rel} (kcal/mol)	G_{rel} (kcal/mol)
1	**TS-IIa**	+1.07	+1.39
2	**TS-IIb**	0.00	0.00
3	**TS-IIc**	+0.81	+1.15

$$\frac{k_{TS-IIb}}{k_{TS-IIc}} = e^{-\frac{\Delta\Delta G^{\ddagger}}{RT}} \qquad \text{Eq. (5.1)}$$

Although the above results strongly indicate a likely pathway for the cross-dimerization, reactions were also considered that could proceed via the acceptor-substituted carbenoid **5.48** (Scheme 5.18). In order to attempt localization of a transition structure for the homodimerization of **5.43**, the approach trajectory (C–C bond formation coordinate) of **5.43** to carbenoid **5.48** was scanned (Figure 5.4). The results indicate a barrierless bimolecular reaction, as the initial geometries (at a C–C distance of ~2.7 Å) smoothly proceeded downhill towards the *E*-homodimer **5.49**. By increasing the C–C distance from the initial point, the system was found to lower its energy as a hydrogen-bonding adduct was formed. By performing a transition state optimization of the initial structure, a transition state **TS-IV** was found that appears to connect the adduct to **5.49**. The animated imaginary frequency displayed movement along the C–C bond forming coordinate. This transition state was enthalpically less stable than the reactants (**5.43** + **5.48**) by -4.07 kcal/mol, however, the gas-phase Gibbs free energy was higher by +9.22 kcal/mol. This suggests that homodimerization of **5.43** is enthalpically barrierless, but has

an entropic barrier leading to a free energy barrier of +9.22 kcal/mol. Note that the barrier is much smaller than that found for heterodimerization before. A similar transition structure **TS-V** was found for nucleophilic attack of **5.25** at carbenoid **5.48**, which also displayed less enthalpic stability than the free reactants by -1.67 kcal/mol. The Gibbs free activation energy barrier was +13.4 kcal/mol. These results demonstrate that, in the presence of both diazo compounds, the acceptor carbenoid **5.48** would strongly prefer the homodimerization pathway.

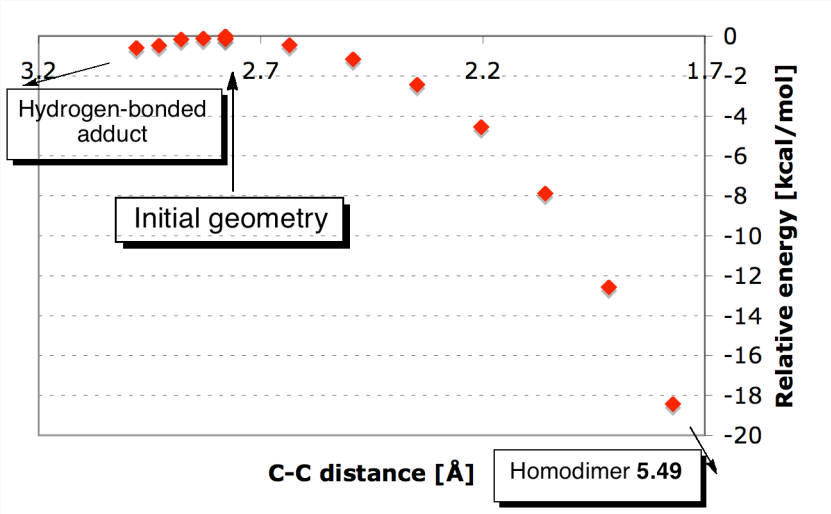

Figure 5.4: Potential energy surface scan of homodimerization of **5.43**.

The computational analysis described above, in conjuction with the reactIR studies, lends strong support to a mechanistic interpretation of the cross-coupling reaction that involves formation of the donor/acceptor-substituted rhodium carbenoid, with subsequent trapping of the unsubstituted diazoester. Furthermore, we have demonstrated that this is crucial for explaining the stereochemical outcome and selectivity of the reaction, as observed experimentally. A catalytic cycle for productive cross-coupling can therefore be formulated as shown in Scheme 5.20.

Scheme 5.20: Proposed catalytic cycle for productive cross-dimerization.

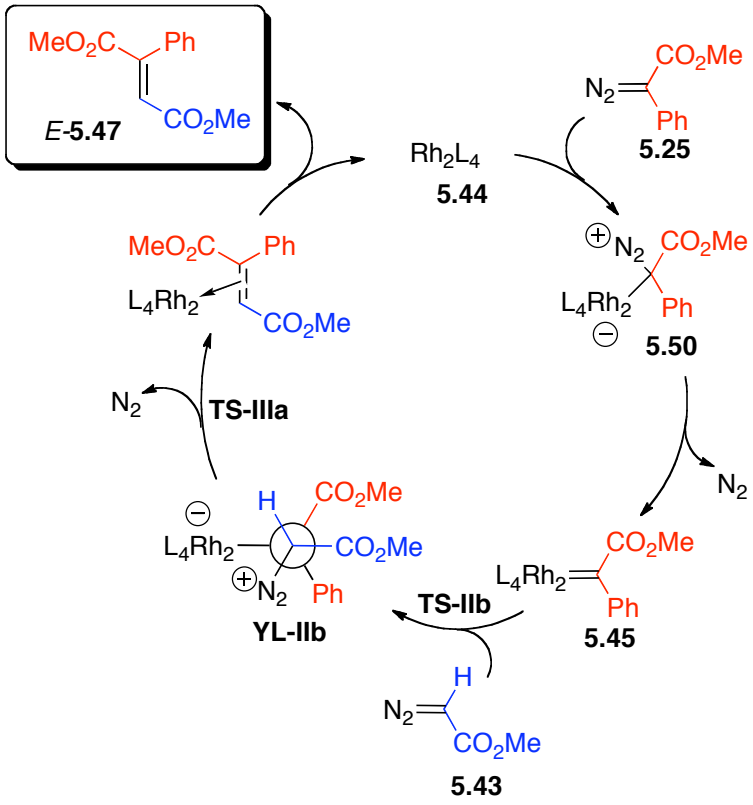

5.3 Conclusions

A convenient process for cross-coupling of a variety of diazo compounds to give electron-deficient, trisubstituted alkenes in useful yields has been developed. The study represents significant progress towards synthetic utilization of diazo coupling reactions, since valuable insight into factors controlling stereo- and chemoselectivity in the dimerization events have been identified. Firstly, it has been demonstrated that, the intermediacy of a donor/acceptor-substituted rhodium carbenoid intermediate plays a key role in achieving high stereo– and chemoselectivity. Secondly, steric differentiation of substituents on the coupling partner (acceptor-subtituted diazo compound) also increases the stereoselectivity. Furthermore, the decomposition rates of the two diazo coupling partners must be sufficiently differentiated to allow for preferential formation of one of the carbenoid complexes, which can then undergo selective reaction with the other diazo component. In this regard, the donor/acceptor-substituted carbenoids derived from aryldiazoesters are good coupling partners to a variety of acceptor-substituted diazo compounds, as they decompose relatively fast, even at lower temperatures. The control elements articulated in this chapter can be used to design viable diazo coupling reactions and provide a framework for a detailed analysis of such transformations.

5.4 Experimental Section

5.4.1 General Synthetic Considerations

All reactions were conducted in flame-dried glassware under an inert atmosphere of dry argon. All reagents were used as received from commercial suppliers, unless otherwise stated. Dichloromethane, trifluorotoluene, hexane and diethyl ether solvents were obtained from drying columns (Grubbs type solvent purifier) and were degassed by bubbling argon through the solvent for >15 min prior to use. Flash chromatography was performed on silica gel (230-400 mesh). Thin layer chromatography (TLC) was performed on aluminium backed plates, pre-coated with silica gel (0.25 mm, 60 F_{254}) which were developed using standard visualizing agents: UV fluorescence (254 nm) and phosphomolybdic acid/Δ. Melting points were determined using a Mel-Temp electrothermal melting point apparatus and are uncorrected. ^{1}H NMR spectra were recorded on Varian Nuclear Magnetic Resonance spectrometers at 600, 500, 400 or 300 MHz. Tetramethylsilane (TMS) (δ = 0.00 ppm) or residual protonated solvent peak of chloroform (δ = 7.26 ppm) were used as internal standards and data are reported as follows: chemical shift, multiplicity (s = singlet, d = doublet, t = triplet, q = quartet, qu = quintet, m = multiplet, and br = broad), integration and coupling constants in Hz. ^{13}C NMR spectra were recorded at 150, 125, 100 or 75 MHz. The solvent was used as internal standard ($CDCl_3$ δ =77.0) and spectra were obtained with complete proton decoupling. Infrared (IR) spectra were aquired using a Thermo Scientific Nicolet iS10 FTIR spectrometer and the wavenumbers are reported in reciprocal centimeters (cm^{-1}). Diastereomeric ratios were determined by integration of the ^{1}H NMR spectra of crude reaction mixtures.

5.4.2 Procedures And Characterization Data

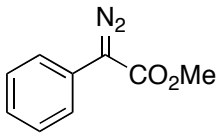

Methyl 2-diazo-2-phenylacetate (5.25). Synthesized according to published procedure.[50] Data: ^{1}H NMR (300 MHz, $CDCl_3$): δ 7.50 (m, 2H), 7.47 (m, 2H), 7.41 (m, 1H), 3.84 (s, 3H). Consistent with published data.[50]

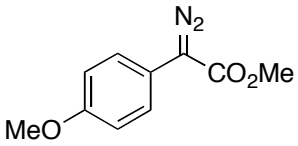

Methyl 2-diazo-2-(4-methoxy)phenylacetate (5.34a). Synthesized according to published procedure.[50] Data: ^{1}H NMR (500 MHz, $CDCl_3$): δ 7.37 (d, 2H, J = 9.2 Hz), 6.92 (d, 2H, J = 9.2 Hz), 3.84 (s, 3H), 3.81 (s, 3H). Consistent with published data.[50]

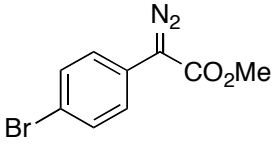

Methyl 2-diazo-2-(4-bromo)phenylacetate (5.34b). Synthesized according to published procedure.[50] Data: ^{1}H NMR (400 MHz, $CDCl_3$) δ 7.50 (d, 2H, J = 8.8 Hz), 7.37 (d, 2H, J = 8.8 Hz), 3.87 (s, 3H). Consistent with published data.[50]

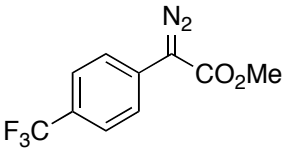

Methyl 2-diazo-2-(4-trifluoromethyl)phenylacetate (5.34c). A sample of this diazo compound was obtained from the Davies group diazo compound library.

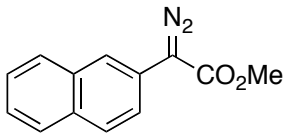

Methyl 2-diazo-2-(2-naphthyl)acetate (5.34d). A sample of this diazo compound was obtained from the Davies group diazo compound library.

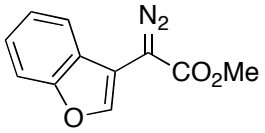

Methyl 2-diazo-2-(3-benzofuranyl)acetate (5.34e). A sample of this diazo compound was obtained from the Davies group diazo compound library.

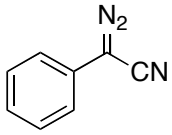

2-diazo-2-phenylacetonitrile (5.34f). Synthesized by published procedure.[51] To an Erlenmeyer flask was added 1-phenyl-1-cyanoammonium chloride (1.0 equiv.) and a 2.5 : 1 mixture of water : Et_2O (170 mL). The flask was cooled to 0 °C in an ice/water bath. Sodium nitrite (1.5 equiv.) in water was added drop-wise over ~2 min and the solution was stirred for 5 min. The organic layer was separated out. Et_2O was added to the reaction mixture, stirred for 5 min and separated out. The combined organics were washed with saturated $NaHCO_3$ (3 x 50 mL), brine (1x) and dried over $MgSO_4$. The solution was then concentrated *in vacuo*. The residue was subjected to column chromatography (SiO_2, 5% Et_2O/pentane) and afforded the product as a red solid upon isolation. Data: ^{1}H NMR (400 MHz, $CDCl_3$): δ 7.40 (t, 2H, J = 7.6 Hz), 7.20 (t, 1H, J = 7.6 Hz), 7.10 (d, 2H, J = 8.4 Hz). The spectroscopic properties were consistent with published data.[51]

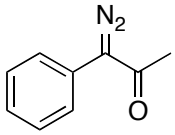

1-Diazo-1-phenylpropan-2-one (5.34g). A sample of this diazo compound was obtained from the Davies group diazo compound library.

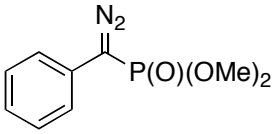

Dimethyl (diazo(phenyl)methyl)phosphonate (5.34h). A sample of this diazo compound was obtained from the Davies group diazo compound library.

General procedure for synthesis of Methyl arylvinyldiazoacetates. Prepared by following published *Organic Syntheses* procedure.[52] To a flame-dry 500 mL round-bottom flask charged with a stir bar, was added 2-carboxyethyltriphenylphosphonium chloride (28.9 g, 78 mmol, 1.3 equiv.). The flask was then fitted with a rubber septum, purged three times with dry argon and then kept under a constant positive atmosphere of dry argon. The appropriate benzaldehyde (60.0 mmol, 1.0 equiv.) and dry THF (130 mL) were then added via syringe followed by cooling of the flask to ~ -10 °C in a ice/brine bath. A solution of potassium *tert*-butoxide (150 mmol, 2.5 equiv.) in THF (80 mL) cooled to 0 °C was then added to the flask slowly *via* cannulation over a period of ~30 min - 1h. The brine/ice bath was then removed and the reaction mixture was allowed to stir for 20 min or more (until aldehyde fully converted) at ambient temperature. Dimethyl sulfate (15.1 g, 120 mmol, 2.0 equiv.) was then added *via* syringe rapidly, and the solution was stirred at ambient temperature for 2.5-5 h. *p*-acetamidobenzenesulfonyl azide (*p*-ABSA) (18.7 g, 78.0 mmol, 1.3 equiv.) was then added and the solution was again cooled down to 0 °C in

an ice/water bath. DBU (11.9, 78 mmol, 1.3 equiv.) was added rapidly *via* syringe and the solution was stirred for ~5 h at 0 °C, then 0.5 h at ambient temperature. The crude reaction mixture was then concentrated in *vacuo* and the resulting oily residue was quenched with a saturated NH_4Cl (aq, 150 mL) and added diethyl ether (200 mL). The mixture was poured into a separation funnel, mixed and the ether layer was again washed with saturated NH_4Cl (aq, 150 mL). The organic layers were combined and washed with brine (2 x 150 mL), dried over anhydrous $MgSO_4$, filtered and concentrated *in vacuo*. The remaining residue was purified by flash chromatography on silica gel (8–10% Et_2O/pentane) to give product as a red oil.

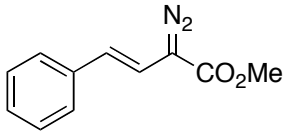

(*E*)-Methyl 2-diazo-4-phenylbut-3-enoate (5.36a). Synthesized by published procedure.[42] Data: ^{1}H NMR (500 MHz, $CDCl_3$): δ 7.38 – 7.29 (m, 4H), 7.20 (t, 1H, J = 7 Hz), 6.48 (d, 1H, J = 16 Hz), 6.20 (d, 1H, J =16 Hz), 3.85 (s, 3H). The spectroscopic properties were consistent with published data.[42]

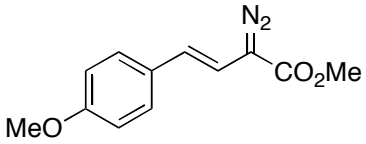

(*E*)-Methyl 2-diazo-4-(4-methoxy)phenylbut-3-enoate (5.36c). Synthesized by published procedure.[42] Data: ^{1}H NMR (500 MHz, $CDCl_3$): δ 7.29 (d, 2H, J = 8.8 Hz), 6.86 (d, 2H, J = 8.8 Hz), 6.29 (d, 1H, J = 16.0 Hz), 6.14 (d, 1H, J = 16.0 Hz), 3.84 (s, 3H), 3.80 (s, 3H). The spectroscopic properties were consistent with published data.[42]

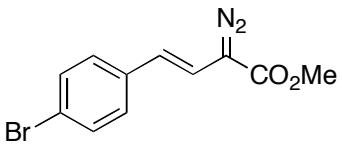

(*E*)-Methyl 2-diazo-4-(4-bromo)phenylbut-3-enoate (5.36b). Synthesized by published procedure.[42] Data: ^{1}H NMR (500 MHz, $CDCl_3$): δ 7.43 (d, 2H, J = 8.5 Hz), 7.21 (d, 2H, J = 8.5 Hz), 6.48 (d, 1H, J = 16.5 Hz), 6.13 (d, 1H, J = 16.5 Hz), 3.85 (s, 3H). The spectroscopic properties were consistent with published data.[42]

General procedure for synthesis of aryl– and vinyldiazoketones: According to a modified procedure of Danheiser et. al.[43] To a flame-dry 500 mL round bottom flask was added dry THF (70 mL) and hexamethyldisilazane HMDS (15.9 mL). The flask was cooled to 0 °C under an inert and dry argon atmosphere. BuLi (29.0 mL of 2.5 M in hexanes, 72.5 mmol, 1.08 equiv.) was added over 5-10 min by syringe. After further 10 min, the mixture was cooled to -78 °C in a CO_2/acetone bath. The appropriate ketone (67.4 mmol, 1.0 equiv) in THF (70 mL) was then added rapidly over ~1 min. The solution turned yellow, and was allowed to stir for ~ 30 min at -78 °C. Trifluoroethyl trifluoroacetate (10.1 mL) was added by syringe over ~2-3 min. The solution was stirred at -78 °C for further 3 h, then allowed to reach ambient temperature. The mixture was poured into a 1 L separatory funnel, added Et_2O (100 mL) and 5% HCL (200 mL). The aqueous layer was extracted with Et_2O (50 mL). The combined organics were washed with brine (1X), dried over $MgSO_4$ and concentrated to afford a yellow oil. The oil was placed in a dry 500 mL round bottom flask under an argon atmosphere, covered with a septum and added acetonitrile (70 mL). To this solution was added water (1.2 mL), NEt_3 (14.3 mL) and tosyl azide (or *p*-acetamidobenzenesulfonyl azide) dissolved in MeCN (10 mL). The

solution was stirred at ambient temperature for 5-8 h, then poured into a separatory funnel with Et_2O (100 mL) and 5% NaOH (200 mL). The organic layer was washed with the NaOH solution (3 x 200 mL), water (3X), brine (1X) and dried over $MgSO_4$. The product sometimes crashed out during extraction, but otherwise concentrated residue *in vacuo*. To concentrated resulting residue was added cold hexanes or pentane to precipitate solids. The solution with precipitate was then filtered and washed with cold Et_2O to afford light yellow solids.

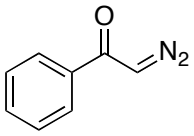

2-Diazo-1-phenylethanone (5.38b). A sample of this diazo compound was obtained from the Davies group diazo compound library.[43]

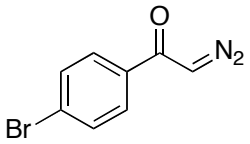

1-diazo-2-(4-bromo)phenyletan-2-one (5.38d). Synthesized by published procedure.[43] Data: ^{1}H NMR (400 MHz, $CDCl_3$): δ 7.65-7.58 (m, 4H), 5.88 (s, 1H). Consistent with published data.[43]

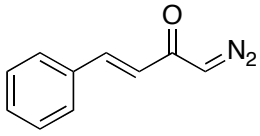

(*E*)-1-diazo-4-phenyl-3-buten-2-one (5.38f). Synthesized by published procedure.[43] Data: ^{1}H NMR (400 MHz, $CDCl_3$): δ 7.60 (d, 1H, J = 16 Hz), 7.55-7.53 (m, 2H), 7.40-7.38 (m, 3H), 6.61 (d, 1H, J = 16 Hz), 5.45 (s, 1H). Consistent with published data.[43]

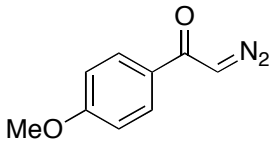

2-Diazo-1-(4-methoxyphenyl)ethanone (5.38c). This diazo compound was synthesized and kindly provided by Mr. Spandan Chennamadhavuni.[43]

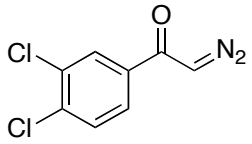

2-Diazo-1-(3,4-dichlorophenyl)ethanone (5.38e). This diazo compound was synthesized and kindly provided by Mr. Spandan Chennamadhavuni.[43]

General procedure for cross-dimerization reactions: To a flame-dried, 50 mL round-bottom flask equipped with a magnetic stir bar, a rubber septum and an argon inlet adaptor was added dirhodium(II) tetrakis(pivaloate) (0.01 equiv.). The flask was evacuated and purged with argon three times before placing it under a constant positive Ar-atmosphere. Dry and degassed CH_2Cl_2 (5.0 mL) was added by syringe and the reaction flask was cooled to -78 ^oC in an acetone/CO_2 bath. A mixed, equimolar solution of diazo compounds (1.0 mmol each, 1.0 equiv. each) was prepared by combining an acceptor- and a donor/acceptor-substituted diazo compound in CH_2Cl_2 (5.0 mL). The diazo compound solution was then added to the catalyst solution over 1 h via syringe pump. Following addition, the reaction flask was slowly allowed to obtain ambient temperature. The solvent was removed *in vacuo* and the crude material was purified by flash column chromatography.

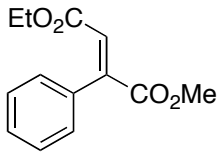

4-ethyl 1-methyl 2-phenylfumarate (5.33). The data were collected by Mr. Brendan Parr under my supervision. ^{1}H NMR (500 MHz, $CDCl_3$): δ 7.37 (m, 3H), 7.24 (m, 2H), 7.02 (s, 1H), 4.04 (q, 2H, J = 7.2 Hz), 3.80 (s, 3H), 1.06 (t, 3H, J = 7.2 Hz). ^{13}C NMR (75 MHz, $CDCl_3$): δ 167.3, 165.8, 144.2, 134.5, 129.9, 129.3, 129, 128.3, 61.4, 53.4, 14.3. FTIR (film): ν_{max}/cm^{-1} 3060, 2985, 1723, 1636, 1249, 1163, 1029. HRMS (ESI): m/z 257.0779 ($C_{13}H_{14}O_4$+Na requires 257.0784). Consistent with that reported by Dr. Qihui Jin.[41]

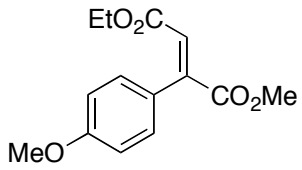

4-Ethyl 1-methyl 2-(4-methoxyphenyl)fumarate (5.35a). The data were collected by Mr. Brendan Parr under my supervision. Clear oil. ^{1}H NMR (600 MHz, $CDCl_3$): δ 7.20 (d, 2H, J = 9.6 Hz), 6.96 (s, 1H), 6.89 (d, 2H, J = 9.6 Hz), 4.08 (q, 2H, J = 7.2 Hz), 3.82 (s, 3H), 3.81 (s, 3H), 1.23 (t, 1H, J = 7.2 Hz). ^{13}C NMR (150 MHz, $CDCl_3$): δ 167.1, 165.5, 159.9, 143.3, 130.4, 128.4, 125.9, 113.2, 60.8, 55.2, 52.8, 13.9. FTIR (film): ν_{max}/cm^{-1} 2952, 1719, 1607, 1246, 1173, 1026. HRMS (pos-APCI): m/z 265.1067 ($C_{14}H_{17}O_5$ requires 265.1071). Consistent with that reported by Dr. Qihui Jin.[41]

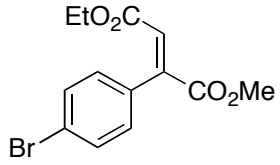

4-Ethyl 1-methyl 2-(4-bromophenyl)fumarate (5.35b). The data were collected by Mr. Brendan Parr under my supervision. ^{1}H NMR (500 MHz, $CDCl_3$): δ 7.50 (d, 2H, J = 8.5 Hz), 7.12 (d, 2H, J = 8.5 Hz), 7.04 (s, 1H), 4.07 (q, 2H, J = 7 Hz), 3.80 (s, 3H), 1.11 (t, 3H, J = 7 Hz). ^{13}C NMR (125 MHz, $CDCl_3$): δ 166.2, 164.9, 142.7, 132.7, 131, 130.5, 129.7, 122.8, 61, 53, 13.8. FTIR (film): ν_{max}/cm^{-1} 2982, 2953, 1724, 1638, 1435, 1187, 1072; HRMS (EI): m/z 311.9988 ($C_{13}H_{13}BrO_4$ requires 311.9986). Consistent with that reported by Dr. Qihui Jin.[41]

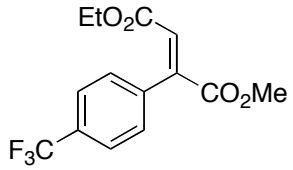

4-Ethyl 1-methyl 2-(4-(trifluoromethyl)phenyl)fumarate (5.35c). The data were collected by Mr. Brendan Parr under my supervision. ^{1}H NMR (600 MHz, $CDCl_3$): δ 7.63 (d, 2H, J = 8.4 Hz), 7.36 (d, 2H, J = 8.4 Hz), 7.10 (s, 1H), 4.05 (q, 2H, J = 7.2 Hz), 3.82 (s, 3H), 1.08 (t, 3H, J = 7.2 Hz). ^{13}C NMR (150 MHz, $CDCl_3$): δ 166, 164.7, 142.6, 137.7, 130.6, 130.4, 129.2, 124.8, 124.7, 61.1, 53.1, 13.7. FTIR (film): ν_{max}/cm^{-1} 2986, 2957, 1723, 1617, 1323, 1161, 1067. HRMS (pos-APCI): m/z 303.0839 ($C_{14}H_{14}F_3O_4$ requires 303.0839).

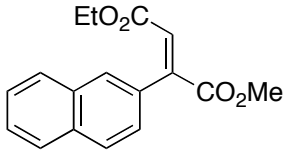

4-Ethyl 1-methyl 2-(naphthalen-2-yl)fumarate (5.35d). The data were collected by Mr. Brendan Parr under my supervision. ^{1}H NMR (600 MHz, $CDCl_3$): δ 7.83 (m, 3H), 7.73 (s, 1H), 7.49 (m, 2H), 7.35 (dd, 1H, J = 8.4, 2.4 Hz), 7.11 (s, 1H), 4.01 (q, 2H, J = 7.2 Hz), 3.82 (s, 3H), 0.98 (t, 3H, J = 7.2 Hz). ^{13}C NMR (100 MHz, $CDCl_3$): δ 166.8, 165.3, 143.6, 133.1, 132.7, 131.4, 129.7, 128.2, 127.7, 127.3, 126.6, 126.5, 126.2, 60.9, 52.9, 13.7. FTIR (film): ν_{max}/cm^{-1} 3054, 2954, 1718, 1431, 1233, 1187, 1020. HRMS (pos-APCI): m/z 285.1121 ($C_{17}H_{17}O_4$ requires 285.1121).

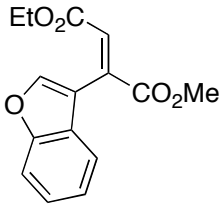

4-Ethyl 1-methyl 2-(benzofuran-3-yl)fumarate (5.35e). The data were collected by Mr. Brendan Parr under my supervision. ^{1}H NMR (600 MHz, $CDCl_3$): δ 7.86 (s, 1H), 7.51 (d, 1H, J = 7.8 Hz), 7.33 (d, 1H J = 8.4 Hz), 7.26 (m, 2H), 7.14 (s, 1H), 4.05 (q, 2H, J = 7.2 Hz), 3.83 (s, 3H), 1.02 (t, 3H, J = 7.2 Hz). ^{13}C NMR (150 MHz, $CDCl_3$): δ 166.4, 165.1, 154.6, 145.4, 133.5, 130, 126.8, 124.4, 122.9, 120.2, 113.9, 111.6, 61.1, 52.9, 13.6. FTIR (film): ν_{max}/cm^{-1} 2919, 1714, 1450, 1241, 1202, 1024, 745. HRMS (pos-APCI): m/z 275.0914 ($C_{15}H_{15}O_5$ requires 275.0914).

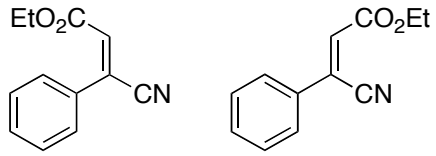

(*E*)-Ethyl 3-cyano-3-phenylacrylate (*E*-5.35f) and **(*Z*)-ethyl 3-cyano-3-phenylacrylate (*Z*-5.35f).** The data were collected by Mr. Brendan Parr under my supervision. Both *E*- and *Z*-diastereomers**.** ^{1}H NMR (600 MHz, $CDCl_3$): δ 7.45 (m, 5H), 6.64 (s, 1H), 4.17 (q, 2H, J = 7.2 Hz), 1.19 (t, 3H, J = 7.2 Hz). ^{13}C NMR (150 MHz, $CDCl_3$): δ 163.7, 132.6, 131.2, 130.8, 128.8, 128.7, 126.5, 118.1, 61.8, 14.0. FTIR (film): ν_{max}/cm^{-1} 3057, 2984, 2222, 1724, 1216, 1049, 1019. HRMS (pos-APCI): m/z 202.0861 ($C_{12}H_{12}NO_2$ requires 202.0863).

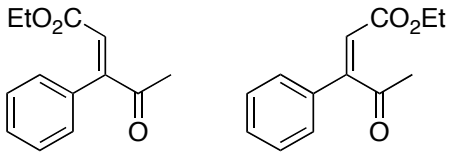

(*E*)-Ethyl 4-oxo-3-phenylpent-2-enoate (*E*-5.35g) and **(*Z*)-ethyl 4-oxo-3-phenylpent-2-enoate (*Z*-5.35g).** The data were collected by Mr. Brendan Parr under my supervision. *E*- and *Z*-diastereomers. Data for ***E*-5.35g**: ^{1}H NMR (400 MHz, $CDCl_3$): δ 7.39 (m, 3H), 7.18 (m, 2H), 6.76 (s, 1H), 4.04 (q, 2H, J = 7.2 Hz), 2.31 (s, 3H), 1.06 (t, 3H, J = 7.2 Hz). ^{13}C NMR (100 MHz, $CDCl_3$): δ 198.9, 165.5, 150.8, 134.6, 128.5, 128.4, 128.1, 126.9, 60.8, 28, 13.8. FTIR (film): ν_{max}/cm^{-1} 2918, 1716, 1697, 1367, 1215, 1187, 1027. HRMS-APCI: m/z 219.1012 ($C_{13}H_{15}O_3$ requires 219.1016). Data for ***Z*-5.35g**: ^{1}H NMR (600 MHz, $CDCl_3$): δ 7.42 (m, 5H), 6.15 (s, 1H), 4.23 (q, 2H, J = 7.2 Hz), 2.44 (s, 3H), 1.32 (t, 3H, J = 7.2 Hz). ^{13}C NMR (150 MHz, $CDCl_3$): δ 204.4, 165.4, 158.1, 132.8, 130.5, 129.1, 126.8, 115.4, 61, 30.4, 14.1. FTIR (film): ν_{max}/cm^{-1} 2982, 1710, 1615, 1369, 1218, 1182, 1156. HRMS (pos-APCI): m/z 219.1012 ($C_{13}H_{15}O_3$ requires 219.1016).

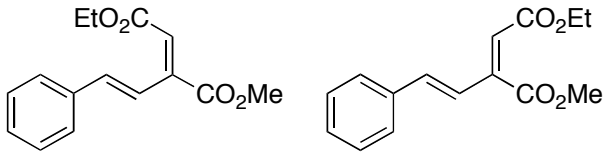

4-Ethyl 1-methyl 2-((*E*)-styryl)fumarate (*E*-5.37a) and **4-ethyl 1-methyl 2-((*E*)-styryl)maleate (*Z*-5.37a).** The data were collected by Mr. Brendan Parr under my supervision. Data for ***E*-5.37a**: ^{1}H NMR (500 MHz, $CDCl_3$): δ 8.14 (d, 1H, J = 16.5 Hz), 7.54 (d, 2H, J = 7.3 Hz), 7.33 (m, 4H), 6.34 (s, 1H), 4.25 (q, 3H, J = 7.2 Hz), 3.88 (s, 3H), 1.32 (t, 3H, J = 7.2 Hz). ^{13}C NMR (75 MHz, $CDCl_3$): δ 166.9, 165.6, 143.6, 139.2, 136.5, 129.1, 128.6, 127.5, 122.1, 120.6, 60.6, 52.4, 14.2. FTIR (film): ν_{max}/cm^{-1} 2983, 1730, 1712, 1615, 1436, 1250, 1198. HRMS (EI): m/z 260.1033 ($C_{15}H_{16}O_4$ requires 260.1043). Data for ***Z*-5.37a**: ^{1}H NMR (500 MHz, $CDCl_3$): δ 7.45 (m, 2H), 7.34 (m, 3H), 6.80 (d, 1H, J = 16.3 Hz), 6.76 (d, 1H, J = 16.3 Hz), 5.95 (s, 1H), 4.21 (q, 2H, J = 7.3 Hz), 3.97 (s, 3H), 1.30 (t, 3H, J = 7.3 Hz). ^{13}C NMR (75 MHz, $CDCl_3$): δ 167.8, 165.1, 147.6, 138.2, 135.4, 129.4, 128.8, 127.3, 124.2, 119.2, 60.8, 52.6, 14.1. FTIR (film): ν_{max}/cm^{-1} 2984, 1738, 1713, 1608, 1282, 1172, 1147. HRMS (ESI): m/z 283.0948 ($C_{15}H_{16}NaO_4$ requires 283.0941). Consistent with that reported by Dr. Qihui Jin.[41]

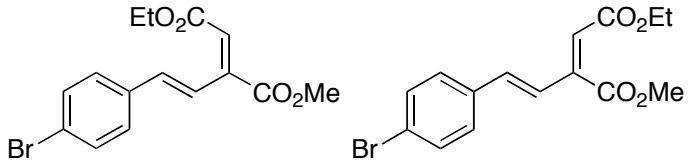

4-Ethyl 1-methyl 2-((*E*)-4-bromostyryl)fumarate (*E*-5.37b) and **4-Ethyl 1-methyl 2-((*E*)-4-bromostyryl)maleate (*Z*-5.37b).** The data were collected by Mr. Brendan Parr under my supervision. *E*- and *Z*-diastereomers. Data for ***E*-5.37b**: ^{1}H NMR (600 MHz, $CDCl_3$): δ 8.11 (d, 1H, J = 16.5 Hz), 7.45 (d, 2H, J = 7.8 Hz), 7.38 (d, 2H, J = 7.8 Hz), 7.26 (d, 1H, J = 16.5 Hz), 6.38 (s, 1H), 4.24 (q, 2H, J = 7.2 Hz), 3.86 (s, 3H), 1.32 (t, 3H,

J = 7.2 Hz). ^{13}C NMR (150 MHz, $CDCl_3$): δ 166.5, 165.4, 143, 137.7, 135.3, 131.7, 128.8, 123, 122.7, 121, 60.6, 52.4, 14.0. FTIR (film): ν_{max}/cm^{-1} 2977, 1733, 1712, 1614, 1252, 1183, 1071. HRMS (pos-APCI): *m/z* 339.0223 ($C_{15}H_{16}BrO_4$ requires 339.0227). Data for ***Z*-5.37b**: ^{1}H NMR (600 MHz, $CDCl_3$): δ 7.48 (d, 2H, J = 8.4 Hz), 7.31 (d, 2H, J = 8.4 Hz), 6.77 (d, 1H, J = 16.5 Hz), 6.69 (d, 1H, J = *1*6.5 Hz), 5.97 (s, 1H), 4.21 (q, 2H, J = 7.2 Hz), 3.96 (s, 3H), 1.30 (t, 3H, J = 7.2 Hz). ^{13}C NMR (150 MHz, $CDCl_3$) δ 167.7, 165, 147.2, 136.7, 134.3, 132, 128.7, 124.8, 123.5, 119.8, 60.9, 52.7, 14.1. FTIR (film): ν_{max}/cm^{-1} 2919, 2849, 1729, 1605, 1272, 1140, 1067. HRMS (pos-APCI): *m/z* 339.0223 ($C_{15}H_{16}BrO_4$ requires 339.0227).

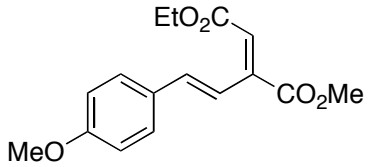

4-Ethyl 1-methyl 2-((*E*)-4-methoxystyryl)fumarate (*E*-5.37c). The data were collected by Mr. Brendan Parr under my supervision. ^{1}H NMR (600 MHz, $CDCl_3$): δ 8.05 (d, 1H, J = 16.5 Hz), 7.49 (d, 2H, J = 8.7 Hz), 7.25 (d, 1H, J = 16.5 Hz), 6.88 (d, 2H, J = 8.7 Hz), 6.25 (s, 1H), 4.25 (q, 2H, J = 7 Hz), 3.88 (s, 3H), 3.82 (s, 3H), 1.33 (t, 3H, J = 7 Hz). ^{13}C NMR (75 MHz, $CDCl_3$): δ 167.2, 165.8, 160.6, 144.2, 139, 129.3, 129.1, 120.6, 118.6, 114.2, 60.5, 55.2, 52.4, 14.2. FTIR (film): ν_{max}/cm^{-1} 3075, 2955, 1730, 1711, 1588, 1256, 1173. HRMS (ESI): *m/z* 291.1226 ($C_{16}H_{19}O_5$ requires 291.1227). Consistent with that reported by Dr. Qihui Jin.[41]

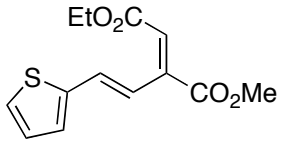

4-Ethyl 1-methyl 2-((*E*)-2-(thiophen-2-yl)vinyl)fumarate (*E*-5.37d). The data were collected by Mr. Brendan Parr under my supervision. ^{1}H NMR (500 MHz, $CDCl_3$) δ 7.95 (d, 1H, J = 16.2 Hz), 7.50 (d, 1H, J = 16.2 Hz), 7.30 (d, 1H, J = 5.2 Hz), 7.17 (d, 1H, J = 3.7 Hz), 7.02 (dd, 1H, J = 5.2, 3.7 Hz), 6.32 (s, 1H), 4.25 (q, 2H, J = 7.2 Hz), 3.87 (s, 3H), 1.34 (t, 3H, J = 7.2 Hz). ^{13}C NMR (75 MHz, $CDCl_3$): δ 166.7, 165.6, 142.9, 142.4, 132.1, 128.9, 127.9, 127.1, 121.9, 120, 60.7, 52.5, 14.2. FTIR (film): ν_{max}/cm^{-1} 2983, 1728, 1710, 1603, 1258, 1185, 1034. HRMS (ESI): m/z 289.0503 ($C_{13}H_{14}O_4SNa$ requires 289.0505). Consistent with that reported by Dr. Qihui Jin.[41]

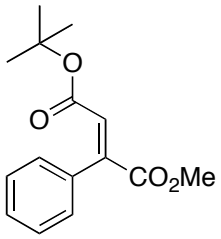

4-*tert*-Butyl 1-methyl 2-phenylfumarate (5.39a). The data were collected by Mr. Brendan Parr under my supervision. ^{1}H NMR (400 MHz, $CDCl_3$): δ 7.36 (m, 3H), 7.23 (m, 2H), 6.97 (s, 1H), 3.79 (s, 3H), 1.23 (s, 9H). ^{13}C NMR (100 MHz, $CDCl_3$): δ 167, 164.7, 141.7, 134.5, 131.5, 128.9, 128.3, 127.7, 81.8, 52.8, 27.6. FTIR (film): ν_{max}/cm^{-1} 2979, 1720, 1368, 1238, 1148, 1022, 698. HRMS (pos-APCI): m/z 263.1275 ($C_{15}H_{19}O_4$ requires 263.1278).

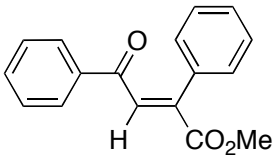

(*E*)-Methyl 4-oxo-2,4-diphenylbut-2-enoate (5.39b). Yellow oil. ^{1}H NMR (600 MHz, $CDCl_3$): δ 7.82 (d, 2H, J = 7.8 Hz), 7.70 (s, 1H), 7.48 (t, 1H, J = 7.8 Hz), 7.35 (t, 2H, J = 7.8 Hz), 7.21 (bs, 5H), 3.85 (s, 3H). ^{13}C NMR (150 MHz, $CDCl_3$): δ 193.5, 166.9, 140.3, 136.4, 136.1, 133.7, 133.6, 129.3, 128.9, 128.5, 127.8, 52.8. FTIR (film): ν_{max}/cm^{-1} 2951, 1719, 1664, 1232, 1169, 1019, 696. MS (pos-APCI): *m/z* 267 (100%, M+H), 235 (32%, M-OMe). HRMS (pos-APCI): *m/z* 267.10151 ($C_{17}H_{15}O_3$ requires 267.10157).

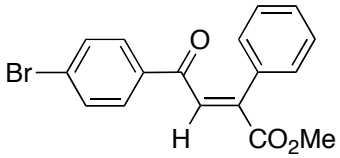

(*E*)-Methyl 4-(4-bromophenyl)-4-oxo-2-phenylbut-2-enoate (5.39d). White solid. Mp = 93.5-95.0 °C. ^{1}H NMR (600 MHz, $CDCl_3$): δ 7.66 (d, 2H, J = 8.4 Hz), 7.63 (s, 1H), 7.49 (d, 2H, J = 8.4 Hz), 7.24-7.20 (m, 3H), 7.20-7.17 (m, 2H), 3.86 (s, 3H). ^{13}C NMR (125 MHz, $CDCl_3$): δ 192.6, 166.8, 140.8, 135.7, 134.8, 133.5, 131.8, 130.3, 129.3, 128.9, 128.8, 128, 52.9. FTIR (film): ν_{max}/cm^{-1} 2950, 1719, 1665, 1583, 1171, 1069, 1008. MS (pos-APCI): *m/z* 347 (100%, M+2), 345 (99%, M), 315 (41%, $C_{16}H_{10}O_2Br$), 313 (42%, $C_{16}H_{10}O_2Br$). HRMS (pos-APCI): *m/z* 345.0122 ($C_{17}H_{13}O_3Br$+H requires 345.01208). See Appendix B for X-ray crystallographic data for this compound.

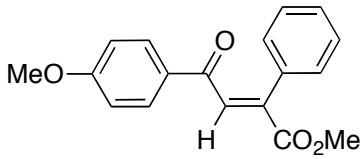

(*E*)-Methyl 4-(4-methoxyphenyl)-4-oxo-2-phenylbut-2-enoate (5.39c). ^{1}H NMR (400 MHz, $CDCl_3$): δ 7.81 (d, 2H, J = 8.8 Hz), 7.68 (s, 1H), 7.22 (m, 5H), 6.84 (d, 2H, J = 8.8 Hz), 3.85 (s, 3H), 3.82 (s, 3H). ^{13}C NMR (100 MHz, $CDCl_3$): δ 192, 167.1, 163.9, 139.5, 136.9, 133.8, 131.3, 129.3, 129.2, 128.4, 127.9, 113.8, 55.4, 52.8. FTIR (film): ν_{max}/cm^{-1} 2952, 2841, 1718, 1658, 1594, 1235, 1164. MS (pos-APCI): *m/z* 297 (100%, M), 265 (16%). HRMS (pos-APCI): *m/z* 297.11177 (M+H requires 297.11214).

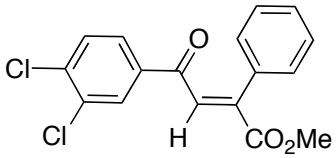

(*E*)-Methyl 4-(3,4-dichlorophenyl)-4-oxo-2-phenylbut-2-enoate (5.39e). White solid. Mp = 94.5-96.0 °C. ^{13}C NMR (125 MHz, $CDCl_3$) δ 191.4, 166.6, 141.5, 138, 135.6, 134.9, 133.4, 133.2, 130.7, 130.6, 129.3, 128.9, 128, 127.8, 53. FTIR (neat): ν_{max}/cm^{-1} 2951, 1720, 1669, 1223, 1030, 697. MS (pos-APCI): *m/z* 339 (10%, M+4), 337 (64%, M+2), 335 (100%, M), 305 (19%), 303 (30%). HRMS (pos-APCI): *m/z* 335.02372 (M+H requires 335.02363).

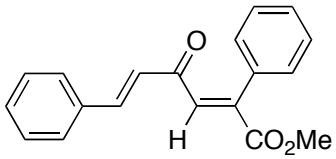

(2*E*,5*E*)-Methyl 4-oxo-2,6-diphenylhexa-2,5-dienoate (5.39f). ^{1}H NMR (400 MHz, $CDCl_3$): δ 7.45 (d, 1H, J = 12 Hz), 7.39 (s, 1H), 7.36-7.26 (m, 10H), 6.39 (d, 1H, J = 12 Hz), 3.85 (s, 3H). ^{13}C NMR (100 MHz, $CDCl_3$): δ 192.5, 167.1, 144.5, 140.4, 137.4,

134.2, 133.9, 130.7, 129.5, 129, 128.8, 128.3, 128.2, 125.6, 52.9. FTIR (neat): ν_{max}/cm^{-1} 2951, 1718, 1651, 1596, 1242, 1176, 689. MS (pos-APCI): *m/z* 293 (23%, M), 291 (16%), 262 (21%), 261 (100%, $C_{18}H_{13}O_2$). HRMS (pos-APCI): *m/z* 293.1173 (M+H requires 293.11722).

Decomposition rate studies by ReactIR. Ethyl 2-diazoacetate and methyl 2-phenyldiazoacetate stock solutions were prepared in CH_2Cl_2. A three-neck, 25 mL round bottomed flask was equipped with a magnetic stir bar and fitted with a thermometer adaptor and a rubber septum with a nitrogen inlet adaptor. A glass joint was used to fix the ReactIR probe to the flask. Aliquots of the ethyl 2-diazoacetate solution and methyl 2-phenyldiazoacetate solution were combined in the reaction flask and cooled to -42 ^{o}C in an acetonitrile/CO_2 bath while kept under an inert nitrogen atmosphere. A stock solution of rhodium(II) tetrakis(pivaloate) was prepared in a volumetric flask. After collecting background spectra for 60 s, an aliquot of the Rh(II) catalyst solution was added to the reaction flask and the reaction progress was monitored with respect to the two C=N_2 stretching frequencies observed for the diazo compounds.

5.5.3 General Considerations for Computational Studies

All calculations were performed with the Gaussian '09 software package.[53] Density Functional Theory was employed with the 3-parameter hybrid functional B3LYP[54,55] to locate stationary points on the potential energy surface (PES). The structures were subjected to full geometry optimization with a basis set consisting of the 1997 Stuttgart relativistic small-core effective core-potential [Stuttgart RSC 1997 ECP][56-58] for Rh,

augmented with a 4f-function (ζ_f(Rh) = 1.350).[29] These parameters have been demonstrated to give good accuracy for such catalyst systems described in this chapter.[29] The split valence basis set 6-31G* was used in the optimization and frequency calculations for all other atoms (C, H and O). This composite basis set is abbreviated 6-31G*[Rh-RSC+4f].[29]. Heavy atom basis set definitions and corresponding pseudopotential parameters were obtained from the EMSL basis set exchange library.[59,60] All stationary points were characterized by normal coordinate analysis at the 6-31G*[Rh-RSC+4f] level of theory, unless otherwise stated. For transition states **TS-IIa-c**, geometry optimization was also carried out at the B3LYP/6-311+G(d,p)[Rh-RSC+4f] level of theory at temperature=195.15 K, also including the effects of dichloromethane as solvent (ε = 8.93) through the default SCRF-method in Gaussian, Integral Equation Formalism Polarizable Continuum Model (IEFPCM).[53,61] All transition states were confirmed to have only one imaginary vibrational mode corresponding to movement along the reaction coordinate.[62] Equilibrium structures were confirmed to have zero imaginary vibrational modes.[62] Transition states were further characterized by intrinsic reaction coordinate (IRC) analysis using default parameters, followed by geometry optimization, to confirm that the stationary points were smoothly connected to each other.[7] The calculated harmonic zero-point vibrational energies (ZPVE) are reported unscaled. Calculated structures have been visualized using Mercury.[63-66]

5.5.4 Calculated Properties and Geometries

Structures **5.25**, **5.43, 5.45, 5.48, 5.44, N_2** are reported in Chapter 2. Images were generated using Mercury. [63-66]

***E*-5.47**

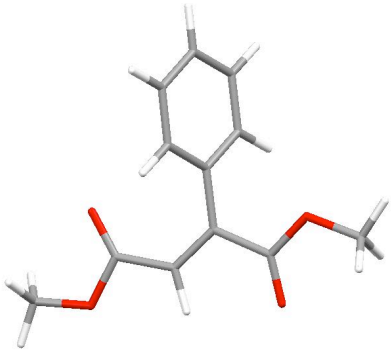

Route= #N B3LYP/6-31G(d) 5d OPT FREQ
B3LYP Energy=-765.378515285 Hartree
ZPE=0.220397 Hartree
Conditions=298K, 1.00000 atm
Internal Energy=-765.142485 Hartree
Enthalpy=-765.141541 Hartree
Free Energy=-765.203674 Hartree
Entropy=130.769 cal/mol-K
Displayed 0 imaginary frequencies.

C	0.00000000	0.00000000	0.00000000
O	0.97113500	1.05721200	0.04983900
C	2.25007600	0.65682500	0.18016200
O	2.57722500	-0.51120000	0.25066800
C	3.21490000	1.82350700	0.20363900
C	2.67600600	3.20965100	0.22437700
C	2.98645600	4.11484200	-0.80050100
C	2.45910900	5.40481300	-0.78994700
C	1.62550700	5.81430100	0.25245000
C	1.31462800	4.92245400	1.28103600
C	1.82638700	3.62628700	1.26129000
H	1.57144300	2.93354100	2.05791100
H	0.66822700	5.23353600	2.09730300
H	1.21957300	6.82234300	0.26296700
H	2.70583900	6.09260800	-1.59412600
H	3.64331700	3.80364800	-1.60600700
C	4.51495300	1.46095100	0.17867200
C	5.69509000	2.35553500	0.26360900
O	5.71412200	3.56875300	0.30571200
O	6.81917900	1.59535200	0.30561200
C	8.04695600	2.32870500	0.41055100
H	8.06343100	2.92252100	1.32881100
H	8.83686000	1.57713900	0.42525800
H	8.16904900	2.99969900	-0.44447300
H	4.73870700	0.39989600	0.14394400
H	0.19103500	-0.65337300	-0.85544300
H	-0.96492100	0.49693800	-0.10178100
H	0.03446000	-0.59640100	0.91567200

***Z*-5.47**

Route= #N B3LYP/6-31G(d) 5d FREQ
B3LYP Energy=-765.380413041 Hartree
ZPE=0.220396 Hartree
Conditions=298K, 1.00000 atm
Internal Energy=-765.144394 Hartree

C	0.00000000	0.00000000	0.00000000
O	0.48571100	-1.32761100	-0.27021300
C	0.76385900	-2.06281100	0.82150200
O	0.77380700	-1.64456200	1.95563300
C	1.16491400	-3.47558300	0.45268700
C	2.61789000	-3.74364800	0.39008400
C	3.14392800	-5.00249900	0.73254400
C	4.51180900	-5.24810200	0.64558700
C	5.38183200	-4.24160600	0.21792100
C	4.87363300	-2.98493400	-0.11613700
C	3.50568900	-2.73519400	-0.02536300
H	3.11675800	-1.75984100	-0.30147200
H	5.54292800	-2.19598000	-0.44781200
H	6.44929500	-4.43387900	0.15433400

Enthalpy=-765.143450 Hartree
Free Energy=-765.204652 Hartree
Entropy=128.812 cal/mol-K
Displayed 0 imaginary frequencies.

H	4.90138200	-6.22358000	0.92359800
H	2.47969000	-5.78003600	1.09735000
C	0.22962100	-4.42675400	0.25570800
C	-1.21868000	-4.15935500	0.34622100
O	-1.73889600	-3.09131000	0.61404400
O	-1.92498600	-5.28516000	0.08541300
C	-3.35090700	-5.14001900	0.14750900
H	-3.69503100	-4.40440600	-0.58490900
H	-3.75601600	-6.12645700	-0.08048300
H	-3.66186600	-4.81720100	1.14496900
H	0.51650600	-5.44255200	0.00515800
H	-0.95423100	-0.06070200	0.52905600
H	-0.13012600	0.46659400	-0.97675900
H	0.71737500	0.55983000	0.60537500

TS-I

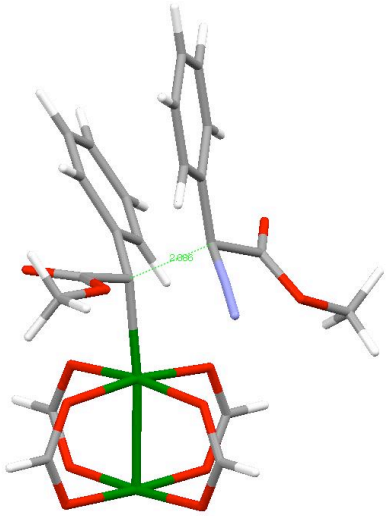

Route= #N b3lyp/gen pseudo=read gfprint FREQ
B3LYP Energy=-2083.80501512 Hartree
ZPE=0.410753 Hartree
Conditions=298K, 1.00000 atm
Internal Energy=-2083.356584 Hartree
Enthalpy=-2083.355640 Hartree
Free Energy=-2083.463534 Hartree
Entropy=227.082 cal/mol-K
Displayed 1 imaginary frequency.

Rh	0.00000000	0.00000000	0.00000000
C	-2.17216700	0.10942100	-0.40711100
C	-2.40762800	-0.81885500	-1.56551900
O	-2.53690500	-2.12988000	-1.24366100
C	-2.53385500	-3.03231000	-2.36200600
H	-3.37418100	-2.82261600	-3.02900600
H	-2.62509800	-4.03045300	-1.93051500
H	-1.59754900	-2.93534300	-2.91404400
O	-2.36964600	-0.44186800	-2.71992400
C	-2.81439400	1.43439400	-0.57250300
C	-2.32328300	2.56532500	0.11571400
C	-2.89301700	3.82283400	-0.06292400
C	-3.97228700	3.99038300	-0.93229200
C	-4.48610000	2.88557500	-1.61649100
C	-3.92386100	1.62703900	-1.43300000
H	-4.33075600	0.78789200	-1.98218400
H	-5.32707500	3.00430200	-2.29428100
H	-4.41079500	4.97458000	-1.07715200
H	-2.48825900	4.67578700	0.47509500
H	-1.48522200	2.44927900	0.78701800
O	-0.00187200	-1.69644900	1.20745700
C	1.10801400	-2.14452900	1.63641300
O	2.26715700	-1.69281400	1.43855700
Rh	2.46765900	-0.02165200	0.24272100
O	2.25024800	1.19236500	1.89722100
C	1.08602500	1.51166400	2.25039700
O	-0.02405000	1.18033800	1.72171300
H	1.00904700	2.16157400	3.13516800
O	2.56794200	-1.22686700	-1.41996500

C	1.48180200	-1.54023500	-1.97965100
O	0.29938600	-1.21577800	-1.65002400
H	1.56099400	-2.18034400	-2.87008800
O	2.53646100	1.63791100	-0.97201500
C	1.44090400	2.09076400	-1.40833300
O	0.26519100	1.66713700	-1.18547000
H	1.50438000	2.96936100	-2.06563600
H	1.03951700	-3.04570900	2.26396400
C	-3.30378000	-0.70314700	1.14507300
C	-2.93891000	0.12830400	2.37188800
O	-3.32759300	1.25753500	2.55058400
O	-2.17591600	-0.56055900	3.23074800
C	-1.74916500	0.16433600	4.40175300
H	-2.61597000	0.45124100	5.00211300
H	-1.11083200	-0.52857600	4.94883500
H	-1.19449300	1.05278600	4.09963400
N	-2.82444000	-1.98650300	1.33566000
N	-2.41671600	-3.01880600	1.44849400
C	-4.76987100	-0.74876800	0.75457700
C	-5.33110000	-1.90169500	0.17649800
C	-6.67696000	-1.93377500	-0.18111000
C	-7.48994900	-0.81813800	0.02605300
C	-6.93798300	0.32983800	0.59128000
C	-5.59055300	0.37413800	0.95303700
H	-5.18003600	1.27220800	1.39187500
H	-7.55449100	1.20904500	0.75578000
H	-8.53986800	-0.84544800	-0.25122500
H	-7.08799000	-2.83791400	-0.62138100
H	-4.72404400	-2.78093500	-0.00503700

TS-IIa

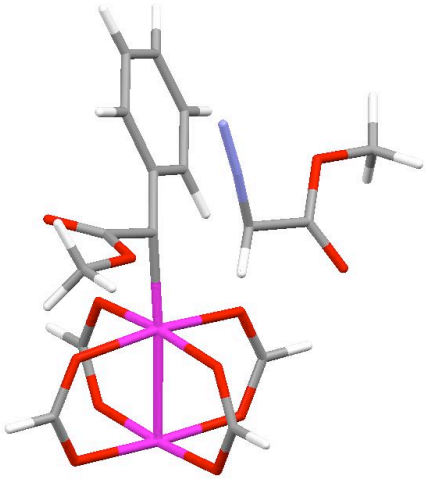

Rh	0.00000000	0.00000000	0.00000000
C	-2.02306900	0.61222200	0.13991800
C	-2.07271200	2.10978600	0.03679700
O	-1.98965100	2.61089500	-1.21677200
C	-1.81051200	4.03748300	-1.29052300
H	-2.64644200	4.55612300	-0.81406300
H	-1.76954700	4.26865400	-2.35524400
H	-0.87866600	4.31897400	-0.79642000
O	-2.09005300	2.81077400	1.02967000
C	-3.02838600	0.00766600	1.01808200
C	-2.89218900	-1.33811200	1.43417200
C	-3.83831400	-1.92902100	2.26377500
C	-4.94845500	-1.19934500	2.69975800
C	-5.10767000	0.12982200	2.30050000

Route= #N b3lyp/gen pseudo=read gfprint
OPT=(TS,CalcFC,NoEigenTest) freq
B3LYP Energy=-1852.77002955 Hartree
ZPE=0.329790 Hartree
Conditions=298K, 1.00000 atm
Internal Energy=-1852.407081 Hartree
Enthalpy=-1852.406137 Hartree
Free Energy=-1852.505234 Hartree
Entropy=208.567 cal/mol-K
Displayed 1 imaginary frequency.

C	-4.16480400	0.72745800	1.47055900
H	-4.28336000	1.77050800	1.20515200
H	-5.96350400	0.70436100	2.64351700
H	-5.68276100	-1.66241700	3.35384100
H	-3.70760300	-2.96049600	2.57983600
H	-2.03516900	-1.90447300	1.09558200
O	0.13720600	0.28616400	-2.04676400
C	1.25223400	0.06850900	-2.62239300
O	2.33875700	-0.29731600	-2.10234300
Rh	2.39235800	-0.62661800	-0.06359000
O	1.80295300	-2.57731800	-0.38526600
C	0.56858900	-2.82224600	-0.42484200
O	-0.40234200	-2.01164600	-0.28360100
H	0.28208700	-3.86848000	-0.60148800
O	2.85867100	1.34967600	0.25576300
C	1.90737600	2.17283900	0.34132700
O	0.65880400	1.94907600	0.26439300
H	2.18512800	3.22404100	0.50352100
O	2.29176400	-0.91385300	1.97365000
C	1.18899200	-0.70001500	2.54820300
O	0.08605300	-0.33181100	2.03422400
H	1.16843500	-0.85101200	3.63667600
H	1.25636000	0.22519800	-3.71012700
C	-2.79001600	0.06353200	-1.89181600
C	-2.92176300	-1.40999900	-2.11962300
O	-2.10964700	-2.06712100	-2.72498600
O	-4.05894500	-1.88562500	-1.57517800
C	-4.27524000	-3.29974800	-1.73811800
H	-3.47582000	-3.86078600	-1.24877500
H	-5.23469600	-3.50127900	-1.26269300
H	-4.30450400	-3.56057200	-2.79900400
N	-3.95231200	0.72268600	-1.85682600
N	-4.93435700	1.25638000	-1.68804400
H	-1.98378700	0.57428900	-2.40642500

TS-IIa solvent model at 195K

Route=#N b3lyp/gen pseudo=read gfprint
temperature=195.15
OPT=(TS,CalcFC,NoEigenTest) freq
SCRF=(PCM,Solvent=dichloromethane)
RB3LYP Energy=-1853.28192236 Hartree
ZPE=0.326171 Hartree
Conditions=195K, 1.00000 atm
Internal Energy=-1852.939691 Hartree
Enthalpy=-1852.939073 Hartree

Rh	0.00000000	0.00000000	0.00000000
C	-2.04151800	0.60995700	0.15316200
C	-2.10924900	2.10083600	0.01083100
O	-2.10859900	2.56978100	-1.24500800
C	-2.01923600	4.00666100	-1.39325700
H	-2.87618300	4.48934400	-0.92343700
H	-2.02101900	4.18328900	-2.46571300
H	-1.09614200	4.37048300	-0.94407500
O	-2.07552200	2.81468000	0.99263100

Free Energy=-1852.989931 Hartree
Entropy=163.535 cal/mol-K
Displayed 1 imaginary frequency.

C	-3.03774900	0.01657100	1.03768500
C	-2.86909200	-1.29988900	1.52355200
C	-3.80560200	-1.87262000	2.37180400
C	-4.94121600	-1.15519300	2.75415900
C	-5.13636900	0.14358500	2.28237700
C	-4.20054800	0.72397700	1.43711700
H	-4.35558900	1.74216000	1.10737000
H	-6.01395300	0.70536400	2.58020000
H	-5.66911300	-1.60470500	3.42020500
H	-3.65221400	-2.88030800	2.74037400
H	-1.99697100	-1.86011100	1.22386700
O	0.10690300	0.26018100	-2.05753800
C	1.20075100	0.03655500	-2.65675900
O	2.29115600	-0.33487600	-2.15141300
Rh	2.39076700	-0.64263600	-0.09859300
O	1.76681200	-2.60416000	-0.37437100
C	0.53139200	-2.84247600	-0.38707300
O	-0.41849700	-2.01611700	-0.25276100
H	0.23261500	-3.88856200	-0.53027900
O	2.86137100	1.35345500	0.17847700
C	1.92009300	2.18468500	0.27310900
O	0.67643400	1.95533600	0.23508400
H	2.20459500	3.23630500	0.40573700
O	2.31215000	-0.90063800	1.95980600
C	1.22624700	-0.67125700	2.55487100
O	0.12670300	-0.29896000	2.04966900
H	1.22394200	-0.80883200	3.64367900
H	1.18611100	0.18805000	-3.74337700
C	-2.86120000	-0.01689500	-1.90879300
C	-2.97192900	-1.49100900	-2.11230300
O	-2.16882600	-2.13301400	-2.74301600
O	-4.06899700	-1.98429800	-1.52372300
C	-4.31094600	-3.40148300	-1.69049400
H	-3.49001400	-3.97450500	-1.26108800
H	-5.23672500	-3.59776300	-1.15686200
H	-4.41809600	-3.63985200	-2.74855000
N	-4.03624700	0.61950800	-1.86682900
N	-5.01968300	1.13258000	-1.71672300
H	-2.08398700	0.50697100	-2.44826200

TS-IIb

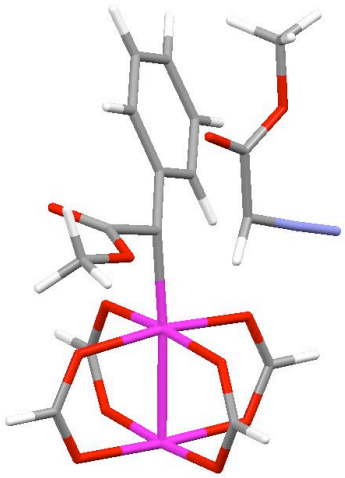

Route= #N b3lyp/gen pseudo=read gfprint OPT=(TS,CalcFC,NoEigenTest) freq
B3LYP Energy=-1852.77237968 Hartree
ZPE=0.329882 Hartree
Conditions=298K, 1.00000 atm
Internal Energy=-1852.409333 Hartree
Enthalpy=-1852.408389 Hartree
Free Energy=-1852.507905 Hartree
Entropy=209.449 cal/mol-K
Displayed 1 imaginary frequency.

Rh	0.00000000	0.00000000	0.00000000
C	2.07041400	0.21473800	-0.40506600
C	2.28812800	1.50176900	-1.15589700
O	2.13025900	2.61618300	-0.42270900
C	2.24022900	3.85075600	-1.14809700
H	3.22934200	3.93411400	-1.60511000
H	2.09608400	4.63529000	-0.40512000
H	1.47105000	3.90178500	-1.92154300
O	2.47767000	1.51104600	-2.35810900
C	2.96612200	-0.89810700	-0.75096800
C	2.64584600	-2.21368700	-0.34328100
C	3.48238300	-3.28429200	-0.65148300
C	4.65566300	-3.07364000	-1.37674700
C	4.99500200	-1.77966100	-1.78877800
C	4.16975700	-0.70594800	-1.47747400
H	4.43825700	0.28681500	-1.81606500
H	5.90294100	-1.61158900	-2.36180600
H	5.30199600	-3.91138900	-1.62544000
H	3.21052800	-4.28683100	-0.33268500
H	1.73261100	-2.38496100	0.21005700
O	-0.02544700	1.36941500	1.56338400
C	-1.14738200	1.66444000	2.09338800
O	-2.28710100	1.21152000	1.81319900
Rh	-2.44948100	-0.20844000	0.31752400
O	-2.08346000	-1.69921500	1.69687700
C	-0.88776700	-2.01295200	1.92403700
O	0.16964500	-1.52108400	1.40967200
H	-0.72079000	-2.81227900	2.66036100
O	-2.69855500	1.28021800	-1.07502900
C	-1.66285400	1.78681000	-1.58558800
O	-0.44718700	1.50194100	-1.35191800
H	-1.82223600	2.58026500	-2.32929700
O	-2.44660100	-1.60118700	-1.19972200
C	-1.34756000	-1.86560400	-1.75995200
O	-0.19381600	-1.39591500	-1.50356300
H	-1.37987700	-2.59955300	-2.57726300
H	-1.10153100	2.41068500	2.89976200
C	2.95271200	0.87084200	1.53401500
C	4.39954200	1.11597600	1.28891500
O	4.83107200	2.08764500	0.70909600
O	5.15136900	0.09424900	1.74755300
C	6.56233200	0.18855800	1.47755300
H	6.96381000	1.12658700	1.86737900
H	7.00969500	-0.66606800	1.98452900
H	6.74036100	0.13221200	0.40119900

N	2.68985700	-0.13394600	2.38339300
N	2.48655600	-1.03848400	3.01972700
H	2.25387100	1.69566500	1.59887800

TS-IIb solvent model

Route=#N b3lyp/gen pseudo=read gfprint
temperature=195.15
OPT=(TS,CalcFC,NoEigenTest) freq
SCRF=(PCM,Solvent=dichloromethane)
RB3LYP Energy=-1853.28357473 Hartree
ZPE=0.326021 Hartree
Conditions=195K, 1.00000 atm
Internal Energy=-1852.941392 Hartree
Enthalpy=-1852.940774 Hartree
Free Energy=-1852.992153 Hartree
Entropy=165.209 cal/mol-K

Rh	0.00000000	0.00000000	0.00000000
C	-2.09984700	-0.03019900	-0.46692500
C	-2.36187500	-1.16092200	-1.41381100
O	-2.37777100	-2.37060600	-0.85491700
C	-2.48141400	-3.49657000	-1.75211600
H	-3.39104500	-3.42575200	-2.34872100
H	-2.51597100	-4.37231900	-1.10938700
H	-1.61073300	-3.53233400	-2.40650200
O	-2.44046600	-0.96523300	-2.61211100
C	-2.93004400	1.15783200	-0.63730700
C	-2.50542500	2.40235000	-0.11986400
C	-3.28079700	3.54718400	-0.27938600
C	-4.49832600	3.47903100	-0.95109700
C	-4.94583500	2.25614900	-1.46415300
C	-4.17936400	1.11377200	-1.30787500
H	-4.53809000	0.17851100	-1.71674700
H	-5.89375600	2.20211900	-1.98682100
H	-5.10002100	4.37186300	-1.07878900
H	-2.93031300	4.49246700	0.11830600
H	-1.55596600	2.46350000	0.38825100
O	-0.06461600	-1.60043700	1.32967700
C	1.01074900	-2.01679200	1.85988500
O	2.17246100	-1.56960100	1.68704900
Rh	2.44489100	0.04182900	0.40144300
O	2.08762400	1.35058200	1.97289900
C	0.89962900	1.66710400	2.23289600
O	-0.15194200	1.29229000	1.63100900
H	0.74396500	2.34816000	3.07921900
O	2.64929400	-1.26965100	-1.18876600
C	1.61086700	-1.64243000	-1.79525500
O	0.41314800	-1.31237400	-1.55564900
H	1.75229600	-2.33727100	-2.63272700
O	2.54227700	1.64456600	-0.91108400
C	1.47771800	2.04788400	-1.44939900
O	0.30543700	1.59790800	-1.28522700
H	1.56715700	2.89166400	-2.14520000
H	0.90326300	-2.86568100	2.54660000
C	-2.98315700	-0.90722900	1.45284100
C	-4.35478400	-1.47067800	1.31303600

O	-4.58099800	-2.63662600	1.09301500
O	-5.28938800	-0.51699300	1.44363900
C	-6.66857800	-0.94193400	1.33724100
H	-6.89488200	-1.67544300	2.11075300
H	-7.25648200	-0.03949300	1.47984100
H	-6.85364700	-1.36998200	0.35251000
N	-2.92550600	0.19871600	2.21099500
N	-2.89117700	1.18415600	2.73214500
H	-2.14685000	-1.58052900	1.60060100

YL-IIb

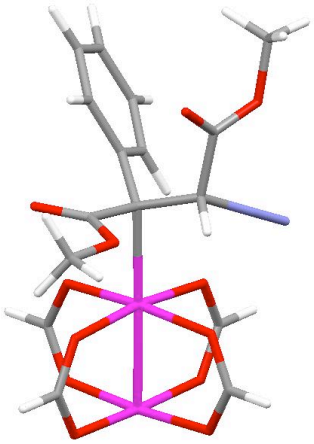

Route= #N b3lyp/gen pseudo=read gfprint OPT freq
B3LYP Energy=-1852.79164164 Hartree
ZPE=0.330917 Hartree
Conditions=298K, 1.00000 atm
Internal Energy=-1852.427233 Hartree
Enthalpy=-1852.426289 Hartree
Free Energy=-1852.525676 Hartree
Entropy=209.178 cal/mol-K
Displayed 0 imaginary frequencies.

Rh	0.00000000	0.00000000	0.00000000
C	2.29297800	0.38183300	-0.24600700
C	2.24280300	1.60556000	-1.11041900
O	2.09447300	2.75654500	-0.39306400
C	1.95054700	3.94794700	-1.17630600
H	2.82907000	4.09800500	-1.80931700
H	1.85501000	4.76155400	-0.45573600
H	1.05885900	3.88029200	-1.80273100
O	2.30994800	1.59976100	-2.32199600
C	3.10599500	-0.76398400	-0.83099200
C	2.81822100	-2.10041600	-0.50963100
C	3.62597100	-3.14529800	-0.96547500
C	4.73915300	-2.88126300	-1.76176700
C	5.03564600	-1.55888400	-2.09864600
C	4.23373600	-0.51470800	-1.63854200
H	4.47723400	0.50189700	-1.92258700
H	5.89383900	-1.33501500	-2.72746400
H	5.36326600	-3.69426500	-2.12373300
H	3.37071900	-4.16974900	-0.70528400
H	1.94103000	-2.33052300	0.08160700
O	-0.09022900	1.13577700	1.74619300
C	-1.23293100	1.29785100	2.29028000
O	-2.34353000	0.83248600	1.92699900
Rh	-2.43619300	-0.33620700	0.21345300
O	-2.06708800	-2.03368000	1.32596200
C	-0.86984300	-2.34039100	1.54929600
O	0.18199200	-1.72537900	1.17230200
H	-0.69720700	-3.24838000	2.14467700
O	-2.72262200	1.35238700	-0.91163000
C	-1.69445400	1.96078300	-1.32092900
O	-0.47659700	1.67562500	-1.11318600
H	-1.87158800	2.85557200	-1.93405200
O	-2.35064700	-1.45844700	-1.50560100
C	-1.22443800	-1.60297500	-2.06454200

O	-0.09702100	-1.15023300	-1.69964200
H	-1.21472800	-2.20072100	-2.98633600
H	-1.23858700	1.92397500	3.19448800
C	2.81626600	0.79044000	1.13657900
C	4.34853700	0.91947700	1.27632200
O	4.95016300	1.78973300	0.70163000
O	4.88063100	-0.03717200	2.04474000
C	6.32615300	-0.05232400	2.11239000
H	6.69335300	0.89616300	2.50974700
H	6.57295400	-0.87780500	2.77850100
H	6.73444400	-0.22059000	1.11388000
N	2.36839500	-0.20472800	2.15940100
N	2.03445700	-1.01343000	2.83807900
H	2.32761500	1.71322700	1.46079900

TS-IIIb

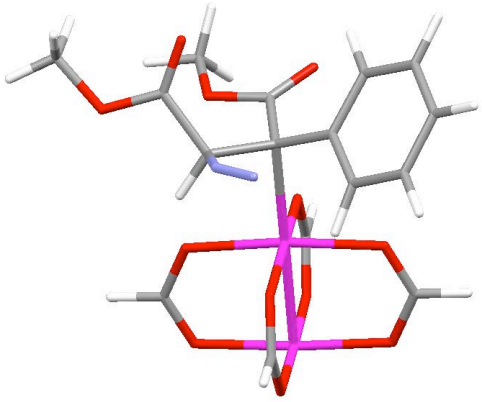

Route= #N b3lyp/gen pseudo=read gfprint OPT=(TS,CalcFC,NoEigenTest) freq
B3LYP Energy=-1852.78223693 Hartree
ZPE=0.331260 Hartree
Conditions=298K, 1.00000 atm
Internal Energy=-1852.418709 Hartree
Enthalpy=-1852.417764 Hartree
Free Energy=-1852.513386 Hartree
Entropy=201.254 cal/mol-K
Displayed 1 imaginary frequency

Rh	0.00000000	0.00000000	0.00000000
C	2.33220300	0.18279700	0.20570500
C	2.79084400	-0.63720400	-1.06003300
H	1.99808400	-1.21741600	-1.53704700
O	2.56765600	-1.94750700	1.19892300
C	2.55902400	-0.60693100	1.45537700
C	2.63244900	-2.79488700	2.35428900
H	3.54570100	-2.60201100	2.92379500
H	2.62638800	-3.81490700	1.96755000
H	1.76351500	-2.62030500	2.99178600
O	2.63018300	-0.17100500	2.58687300
C	2.75788700	1.60630400	0.26178500
C	2.27865100	2.54434600	-0.69644400
C	2.73837600	3.87575200	-0.71710500
C	3.67277000	4.30221300	0.20841500
C	4.14940300	3.39201900	1.17048800
C	3.70581000	2.07875700	1.20195100
H	4.09413700	1.40361800	1.95087300
H	4.89197100	3.71627900	1.89489900
H	4.03042000	5.32806000	0.20281700
H	2.33664500	4.56211100	-1.45738700
H	1.44161800	2.27151100	-1.32637500
O	0.11657600	-1.90255100	-0.82140700
C	-0.96386800	-2.49352700	-1.14215800
O	-2.14578200	-2.06941600	-1.03464000
Rh	-2.43777800	-0.17510000	-0.26365900
O	-2.20820300	0.61694400	-2.16116900
C	-1.04763800	0.87920300	-2.56896600
O	0.05717200	0.73961100	-1.94712400

H	-0.96717300	1.27879700	-3.59014300
O	-2.52893400	-0.95268800	1.63448600
C	-1.44186900	-1.08713900	2.26535800
O	-0.26624100	-0.80558700	1.88059900
H	-1.51930000	-1.50236100	3.27996000
O	-2.59091600	1.71639400	0.52745800
C	-1.52445600	2.30136700	0.87283200
O	-0.32968300	1.88350700	0.77921000
H	-1.64137900	3.30340600	1.30866000
H	-0.84337400	-3.50044900	-1.56647800
C	4.02940800	-1.56705700	-0.83684400
O	5.04231100	-1.20368100	-0.29153900
O	3.82746900	-2.75357600	-1.41400400
C	4.91568000	-3.69140000	-1.28744500
H	5.11104800	-3.89618700	-0.23218700
H	4.58188200	-4.59181200	-1.80182200
H	5.81918300	-3.28933000	-1.75225500
N	3.27901800	0.25830500	-2.11762200
N	3.40001500	1.34999800	-2.41111000

TS-IIc

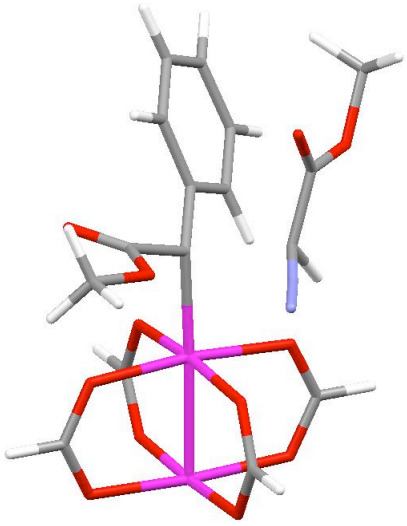

Route= #N b3lyp/gen pseudo=read gfprint OPT=(TS,CalcFC,NoEigenTest) freq
B3LYP Energy=-1852.77049096 Hartree
ZPE=0.330102 Hartree
Conditions=298K, 1.00000 atm
Internal Energy=-1852.407342 Hartree
Enthalpy=-1852.406398 Hartree
Free Energy=-1852.504966 Hartree
Entropy=207.454 cal/mol-K
Displayed 1 imaginary frequency

Rh	0.00000000	0.00000000	0.00000000
C	-2.04840400	0.26056600	0.48069400
C	-2.19607200	1.36152000	1.48760800
O	-2.11579800	2.61223300	1.00203200
C	-2.04750500	3.65297300	1.99313000
H	-2.93294800	3.63333700	2.63343900
H	-2.00173400	4.58462900	1.42876500
H	-1.15226500	3.52550900	2.60557700
O	-2.26577600	1.11064600	2.67617000
C	-2.98288300	-0.86541100	0.64345100
C	-2.72747300	-2.10358100	0.01264600
C	-3.59357900	-3.18189700	0.16999000
C	-4.74086300	-3.05403600	0.95585100
C	-5.02462000	-1.83276900	1.57703400
C	-4.16445800	-0.75199200	1.41831100
H	-4.39186100	0.18102900	1.91890900
H	-5.91421500	-1.72630500	2.19175200
H	-5.41117300	-3.89982200	1.08589200
H	-3.36930800	-4.12666100	-0.31761100
H	-1.84524500	-2.20717800	-0.60325500
O	0.15382300	1.73243900	-1.13547200
C	1.29130500	2.05188600	-1.61262800
O	2.38248400	1.43435300	-1.51117900
Rh	2.40851300	-0.34541100	-0.46422700

O	1.84440800	-1.34853900	-2.18558400
C	0.62119700	-1.44591800	-2.45447700
O	-0.37373900	-1.01334100	-1.78021700
H	0.36167800	-1.96778000	-3.38681200
O	2.81654600	0.67969900	1.27091800
C	1.84310600	1.13052400	1.93406700
O	0.60098300	1.03370100	1.68202000
H	2.09100200	1.68124700	2.85225800
O	2.29574900	-2.09182100	0.61928700
C	1.18644000	-2.39184700	1.13930400
O	0.08303900	-1.76478100	1.06604700
H	1.15877700	-3.31665200	1.73244700
H	1.31175300	2.98933000	-2.18750800
C	-2.79674300	1.05252400	-1.44699200
C	-4.27651200	0.84268100	-1.50775100
O	-5.10259800	1.65056300	-1.13808200
O	-4.54247600	-0.36926000	-2.01458100
C	-5.93655800	-0.73442400	-2.04011800
H	-6.50549300	-0.01510100	-2.63389800
H	-5.96427900	-1.72354800	-2.49576500
H	-6.33264100	-0.76771900	-1.02304400
N	-2.50314800	2.35809300	-1.61843300
N	-2.30561600	3.45893100	-1.69987100
H	-2.13817700	0.40075300	-2.01350000

TS-IIc solvent model

Route= #N b3lyp/gen pseudo=read gfprint
temperature=195.15
OPT=(TS,CalcFC,NoE
RB3LYP Energy=-1853.28244049 Hartree
ZPE=0.326331 Hartree
Conditions=195K, 1.00000 atm
Internal Energy=-1852.940094 Hartree
Enthalpy=-1852.939476 Hartree
Free Energy=-1852.990325 Hartree
Entropy=163.507 cal/mol-K
Displayed 1 imaginary frequency

Rh	0.00000000	0.00000000	0.00000000
C	-2.07494300	0.21050300	0.49289200
C	-2.25857400	1.27576400	1.52730100
O	-2.35091000	2.52977100	1.07727900
C	-2.38194200	3.57247100	2.07960900
H	-3.25435400	3.45390800	2.72206800
H	-2.44361200	4.50282400	1.52078600
H	-1.47295200	3.54254400	2.67932500
O	-2.22567800	0.98664400	2.70713200
C	-2.98693700	-0.93000800	0.61132300
C	-2.69553600	-2.15141500	-0.03226200
C	-3.53627200	-3.24903100	0.10033200
C	-4.69430000	-3.15735900	0.87245900
C	-5.01586600	-1.95310400	1.50366400
C	-4.18005800	-0.85407900	1.37086800
H	-4.44453300	0.06789300	1.87161500
H	-5.91737900	-1.87481200	2.10014000
H	-5.34585900	-4.01720200	0.98079500

H	-3.28724500	-4.17968100	-0.39635900
H	-1.80617400	-2.22773900	-0.63742100
O	0.12219000	1.76685200	-1.08688900
C	1.23444900	2.11638400	-1.58505200
O	2.33263900	1.50817500	-1.51504600
Rh	2.40772600	-0.29839900	-0.49695400
O	1.83633700	-1.27927000	-2.23905700
C	0.61254200	-1.38785200	-2.50033400
O	-0.36738600	-0.98077200	-1.80203400
H	0.34843000	-1.89115400	-3.43889300
O	2.81096800	0.71237000	1.26448100
C	1.84288500	1.13230000	1.95180700
O	0.60701700	1.00524700	1.71066700
H	2.09219400	1.67405800	2.87293000
O	2.31999600	-2.07983100	0.55854900
C	1.22456000	-2.41408600	1.08215700
O	0.12124000	-1.79562100	1.03401100
H	1.21658200	-3.35390700	1.64861100
H	1.22868200	3.06213500	-2.14188100
C	-2.85452700	1.06552300	-1.45867400
C	-4.32925200	0.86853500	-1.53130800
O	-5.15173900	1.69141400	-1.19078300
O	-4.60541700	-0.34597800	-2.00859900
C	-6.00712800	-0.70310700	-2.08649500
H	-6.53053900	-0.01492700	-2.74962900
H	-6.02079400	-1.71159400	-2.48999600
H	-6.45402200	-0.68004700	-1.09340100
N	-2.54220000	2.37103600	-1.59365100
N	-2.32345100	3.45927300	-1.65223100
H	-2.19891200	0.42295800	-2.03471200

YL-IIc

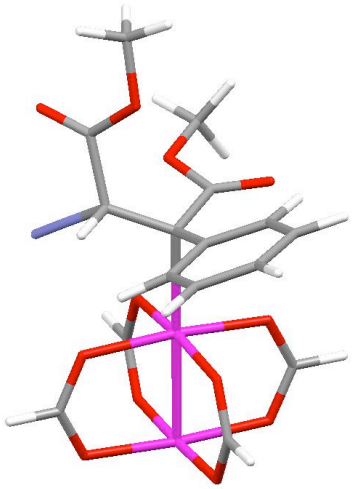

Rh	0.00000000	0.00000000	0.00000000
C	2.37261600	0.07566200	0.11559600
C	2.65744900	-0.68234600	1.35964400
O	2.88034500	-2.01415100	1.06757800
C	3.03353600	-2.87464600	2.20434200
H	3.23177000	-3.86748700	1.79771100
H	2.11702100	-2.88079000	2.79954600
H	3.86482000	-2.54236100	2.83142300
O	2.68697300	-0.28410100	2.50547600
C	2.73087100	1.54439900	0.05629600
C	2.64274800	2.26078100	-1.15487500
C	3.00361000	3.60339100	-1.24050300
C	3.44953000	4.28756700	-0.10942100

Route= #N b3lyp/gen pseudo=read gfprint
OPT FREQ
B3LYP Energy=-1852.79399624 Hartree
ZPE=0.331019 Hartree
Conditions=298K, 1.00000 atm
Internal Energy=-1852.429475 Hartree
Enthalpy=-1852.428531 Hartree
Free Energy=-1852.528166 Hartree
Entropy=209.699 cal/mol-K
Displayed 0 imaginary frequencies.

C	3.51536300	3.60297600	1.10398300
C	3.16509600	2.25538500	1.19117600
H	3.21749300	1.74809600	2.14424000
H	3.84761500	4.11823900	2.00205800
H	3.72947900	5.33571300	-0.17159100
H	2.91847600	4.11755300	-2.19474400
H	2.23104500	1.79208900	-2.04573700
O	-0.12928100	-2.07630500	0.14217100
C	-1.28248200	-2.61666700	0.11827500
O	-2.40080400	-2.05304400	-0.00375900
Rh	-2.43562100	0.00420600	-0.15874600
O	-2.13082500	-0.12650700	-2.22227800
C	-0.96571000	-0.15056500	-2.69721000
O	0.15079500	-0.12885900	-2.07107500
H	-0.88889400	-0.19992000	-3.79333200
O	-2.43330700	0.14194100	1.90733200
C	-1.32275300	0.17613400	2.51527300
O	-0.14777400	0.12844500	2.03037800
H	-1.37443700	0.25551600	3.60980900
O	-2.39763800	2.04793700	-0.28942100
C	-1.26351600	2.60508500	-0.23151800
O	-0.12671800	2.05671000	-0.12291100
H	-1.25765700	3.70248200	-0.28437200
H	-1.29378200	-3.71195800	0.21304800
C	2.95880500	-0.62725400	-1.09058700
C	4.41744000	-1.17188500	-1.07804800
O	4.75387200	-2.16716300	-1.67658600
O	5.19791700	-0.35329700	-0.39006500
C	6.59733700	-0.71140800	-0.33810500
H	7.01012700	-0.76068100	-1.34806200
H	7.07012100	0.08052400	0.24031700
H	6.71393100	-1.67915700	0.15463400
N	2.19107500	-1.86561900	-1.47630700
N	1.62114400	-2.79330000	-1.66206400
H	2.83775200	-0.01719300	-1.98976600

TS-IV

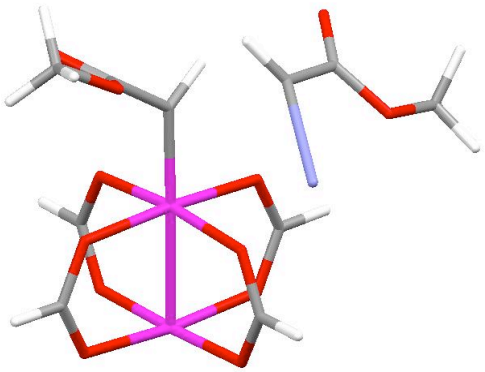

Route= #N b3lyp/gen pseudo=read gfprint OPT=(TS,CalcFC,NoEigenTest) freq
B3LYP Energy=-1621.71061877 Hartree
ZPE=0.247672 Hartree
Conditions=298K, 1.00000 atm
Internal Energy=-1621.434165 Hartree
Enthalpy=-1621.433221 Hartree
Free Energy=-1621.524207 Hartree
Entropy=191.497 cal/mol-K
Displayed 1 imaginary frequency

Rh	0.00000000	0.00000000	0.00000000
C	1.71623500	0.67765100	-0.63918600
C	2.13155600	2.08600200	-0.49994000
O	2.82126900	2.41157300	0.60096100
C	3.11121300	3.82021200	0.74908600
H	3.68831900	4.18290000	-0.10485200
H	3.68970100	3.89832900	1.66899500
H	2.18023100	4.38536400	0.82845500
O	1.78364700	2.86219800	-1.37021200
H	2.25156500	0.12183900	-1.41654500
O	0.69871300	-0.81084300	1.76269000
C	-0.11131500	-1.40744000	2.54410800
O	-1.34650700	-1.59320400	2.39052300
Rh	-2.22013200	-0.84208900	0.68289700
O	-1.75198100	-2.58435000	-0.32938200
C	-0.63627700	-2.66673700	-0.90696700
O	0.30114100	-1.80406200	-0.95402000
H	-0.43132900	-3.60327100	-1.44441800
O	-2.50416700	0.97144900	1.62840800
C	-1.58466800	1.83099400	1.57616600
O	-0.44985500	1.74602100	1.00232500
H	-1.77347400	2.78360300	2.09011700
O	-3.00420900	-0.05864600	-1.04664300
C	-2.20785500	0.53217500	-1.82410300
O	-0.95674800	0.71493100	-1.68255200
H	-2.63347800	0.94831600	-2.74702800
H	0.34063700	-1.80432700	3.46348200
C	3.85834700	-0.56891600	0.62108700
C	3.77008200	-1.73680200	-0.25544000
O	3.94768800	-1.66643200	-1.45707200
O	3.46344600	-2.86632300	0.41533500
C	3.27079500	-4.03031700	-0.40844400
H	4.18160500	-4.25917200	-0.96724100
H	3.03166900	-4.83705000	0.28452500
H	2.44813100	-3.86067100	-1.10681100
N	3.69263900	-0.68511600	1.92175600
N	3.54877600	-0.78772100	3.04019900
H	4.28608500	0.36197000	0.28147300

TS-V

Rh	0.00000000	0.00000000	0.00000000
C	-1.91031700	-0.25488400	-0.43183800
C	-2.57113100	-1.55486600	-0.17889000
O	-2.97768900	-1.77538600	1.07626000

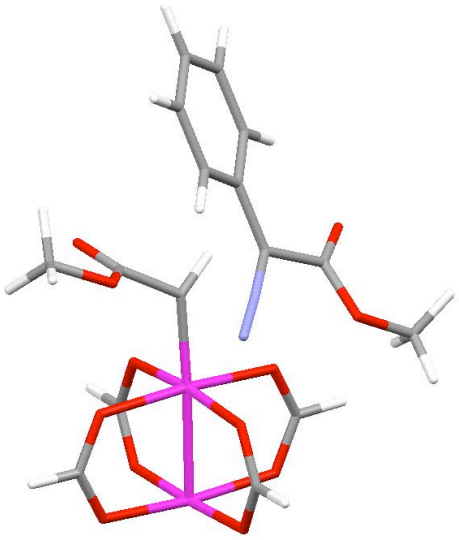

Route= #N b3lyp/gen pseudo=read gfprint OPT=(TS,CalcFC,NoEigenTest) freq
B3LYP Energy=-1852.76049028 Hartree
ZPE=0.329399 Hartree
Conditions=298K, 1.00000 atm
Internal Energy=-1852.397913 Hartree
Enthalpy=-1852.396969 Hartree
Free Energy=-1852.497172 Hartree
Entropy=210.895 cal/mol-K
Displayed 1 imaginary frequency

C	-3.50063100	-3.09433100	1.33147800
H	-4.38658600	-3.27662100	0.71831700
H	-3.75746100	-3.10159700	2.39056600
H	-2.73964900	-3.84650700	1.11368500
O	-2.61766500	-2.36710300	-1.08424600
H	-2.32632900	0.28803700	-1.28398800
O	-0.21752300	0.99963200	1.79436900
C	0.82275600	1.36985800	2.42825500
O	2.02948200	1.21632900	2.10581800
Rh	2.44006000	0.21696300	0.34824900
O	2.32787200	1.98672000	-0.71625600
C	1.20859500	2.35538100	-1.15929200
O	0.07278600	1.79411800	-1.01797300
H	1.19584700	3.28626700	-1.74407700
O	2.36035300	-1.57452000	1.36803500
C	1.24831500	-2.15779200	1.47117200
O	0.11313200	-1.78671900	1.02923300
H	1.24515900	-3.11369200	2.01334300
O	2.74093200	-0.79394700	-1.41519200
C	1.71672100	-1.14951500	-2.05761300
O	0.49404500	-0.97050000	-1.75679200
H	1.88636400	-1.68315500	-3.00262100
H	0.62763700	1.88980900	3.37670200
C	-3.67731600	1.27138900	0.69787600
C	-3.11367700	2.51687900	0.10904500
O	-3.27557200	2.84742300	-1.04777500
O	-2.42082400	3.22924000	1.01515900
C	-1.77355000	4.41103200	0.50619700
H	-2.51711600	5.11616300	0.12664600
H	-1.24095300	4.83450000	1.35749400
H	-1.08153200	4.13865100	-0.29192100
N	-3.31902400	1.03829800	1.96350800
N	-3.01872300	0.79203400	3.02317900
C	-4.94434500	0.63982400	0.23812500
C	-5.73310700	-0.12081900	1.12107000
C	-6.91605900	-0.71376700	0.68677300
C	-7.33867000	-0.56195400	-0.63535100
C	-6.56300600	0.19246000	-1.51549400
C	-5.37548500	0.78990200	-1.09255200
H	-4.78892200	1.38231500	-1.78204300
H	-6.87792200	0.32089600	-2.54729600
H	-8.26134600	-1.02489900	-0.97306100
H	-7.51155000	-1.29011100	1.38958700
H	-5.43196900	-0.24826300	2.15648800

References

(1) Doyle, M. P.; McKervey, M. A.; Ye, T. *Modern Catalytic Methods for Organic Synthesis with Diazo Compounds: From Cyclopropanes to Ylides*; John Wiley & Sons, Inc.: New York, 1998.

(2) Grundmann, C. *Liebigs Ann. Chem.* **1938**, *536*, 29-36.

(3) Nandakumar, M. V.; Ghosh, S.; Schneider, C. *Eur. J. Org. Chem.* **2009**, 6393-6398.

(4) Font, J.; Serratos.F; Valls, J. *J. Chem. Soc., Chem. Commun.* **1970**, 721.

(5) Doyle, M. P.; Hu, W.; Phillips, I. M.; Wee, A. G. H. *Org. Lett.* **2000**, *2*, 1777-1779.

(6) Li, G. Y.; Che, C. M. *Org. Lett.* **2004**, *6*, 1621-1623.

(7) Diaz-Requejo, M. M.; Belderrain, T. R.; Nicasio, M. C.; Prieto, F.; Perez, P. J. *Organometallics* **1999**, *18*, 2601-2609.

(8) Wulfman, D. S.; Peace, B. W.; McDaniel, R. S., Jr. *Tetrahedron* **1976**, *32*, 1251-1255.

(9) Trahanov.Ws; Robbins, M. D.; Smick, D. *J. Am. Chem. Soc.* **1971**, *93*, 2086.

(10) Jugelt, W.; Pragst, F. *Angew. Chem. Int. Ed.* **1968**, *7*, 290.

(11) Bethell, D.; Handoo, K. L.; Fairhurst, S. A.; Sutcliffe, L. H. *J. Chem. Soc., Perkin Trans. 2* **1979**, 707-713.

(12) Oshima, T.; Nagai, T. *Tetrahedron Lett.* **1980**, *21*, 1251-1254.

(13) Shankar, B. K. R.; Shechter, H. *Tetrahedron Lett.* **1982**, *23*, 2277-2280.

(14) Collman, J. P.; Rose, E.; Venburg, G. D. *J. Chem. Soc., Chem. Commun.* **1993**, 934-935.

(15) Park, S. B.; Nishiyama, H.; Itoh, Y.; Itoh, K. *J. Chem. Soc., Chem. Commun.* **1994**, 1315-1316.

(16) Galardon, E.; Maux, P. L.; Toupet, L.; Simonneaux, G. *Organometallics* **1998**, *17*, 565-569.

(17) Lee, H. M.; Bianchini, C.; Jia, G.; Barbaro, P. *Organometallics* **1999**, *18*, 1961-1966.

(18) Woo, L. K.; Smith, D. A. *Organometallics* **1992**, *11*, 2344-2346.

(19) Baratta, W.; Del Zotto, A.; Rigo, P. *Organometallics* **1999**, *18*, 5091-5096.

(20) Baratta, W.; DelZotto, A.; Rigo, P. *Chem. Commun.* **1997**, 2163-2164.

(21) Del Zotto, A.; Baratta, W.; Verardo, G.; Rigo, P. *Eur. J. Org. Chem.* **2000**, 2795-2801.

(22) Basato, M.; Tubaro, C.; Biffis, A.; Bonato, M.; Buscemi, G.; Lighezzolo, F.; Lunardi, P.; Vianini, C.; Benetollo, F.; Del Zotto, A. *Chem. Eur. J.* **2009**, *15*, 1516-1526.

(23) Hodgson, D. M.; Angrish, D. *Chem. Commun.* **2005**, 4902-4904.

(24) Hodgson, D. M.; Angrish, D. *Chem. Eur. J.* **2007**, *13*, 3470-3479.

(25) Hodgson, D. M.; Angrish, D. *J. Mol. Catal. A: Chem.* **2006**, *254*, 93-95.

(26) Barluenga, J.; Lopez, L. A.; Lober, O.; Tomas, M.; Garcia-Granda, S.; Alvarez-Rua, C.; Borge, J. *Angew. Chem. Int. Ed.* **2001**, *40*, 3392-3394.

(27) Barluenga, J.; Riesgo, L.; Lopez, L. A.; Rubio, E.; Tomas, M. *Angew. Chem. Int. Ed.* **2009**, *48*, 7569-7572.

(28) Vovard-Le Bray, C.; Derien, S.; Dixneuf, P. H. *Angew. Chem. Int. Ed.* **2009**, *48*, 1439-1442.

(29) Hansen, J.; Autschbach, J.; Davies, H. M. L. *J. Org. Chem.* **2009**, *74*, 6555-6563.

(30) Davies, H. M. L.; Beckwith, R. E. J. *Chem. Rev.* **2003**, *103*, 2861-2903.

(31) Davies, H. M. L. *Eur. J. Org. Chem.* **1999**, 2459-2469.

(32) Davies, H. M. L.; Panaro, S. A. *Tetrahedron* **2000**, *56*, 4871-4880.

(33) Davies, H. M. L.; Antoulinakis, E. G. *Org. Reacts.* **2001**, *57*, 1-326.

(34) Davies, H. M. L.; Xiang, B. P.; Kong, N.; Stafford, D. G. *J. Am. Chem. Soc.* **2001**, *123*, 7461-7462.

(35) Li, Z. J.; Davies, H. M. L. *J. Am. Chem. Soc.* **2010**, *132*, 396-401.

(36) Hansen, J.; Davies, H. M. L. In: *Catalytic Asymmetric Synthesis 3rd ed.* (Ed. Ojima, I.), John Wiley & Sons, Hoboken, New Jersey, **2010**, p.163-226.

(37) Davies, H. M. L.; Hansen, T. *J. Am. Chem. Soc.* **1997**, *119*, 9075-9076.

(38) Davies, H. M. L.; Hansen, T.; Churchill, M. R. *J. Am. Chem. Soc.* **2000**, *122*, 3063-3070.

(39) Davies, H. M. L.; Hedges, L. M.; Matasi, J. J.; Hansen, T.; Stafford, D. G. *Tetrahedron Lett.* **1998**, *39*, 4417-4420.

(40) Davies, H. M. L.; Venkataramani, C.; Hansen, T.; Hopper, D. W. *J. Am. Chem. Soc.* **2003**, *125*, 6462-6468.

(41) Jin, Q. *Ph.D.-Thesis* **2004**.

(42) Manning, J. R.; Davies, H. M. L. *Org. Synth.* **2007**, *84*, 334-346.

(43) Danheiser, R. L.; Miller, R. F.; Brisbois, R. G. *Org. Synth.* **1996**, *73*,134-143.

(44) Hansen, J.; Li, B.; Dikarev, E.; Autschbach, J.; Davies, H. M. L. *J. Org. Chem.* **2009**, *74*, 6564-6571.

(45) Qu, Z. H.; Shi, W. F.; Wang, J. B. *J. Org. Chem.* **2001**, *66*, 8139-8144.

(46) Pelphrey, P.; Hansen, J.; Davies, H. M. L. *Chem. Sci.* **2010**, *online article.*

(47) Nowlan, D. T.; Gregg, T. M.; Davies, H. M. L.; Singleton, D. A. *J. Am. Chem. Soc.* **2003**, *125*, 15902-15911.

(48) Nakamura, E.; Yoshikai, N.; Yamanaka, M. *J. Am. Chem. Soc.* **2002**, *124*, 7181-7192.

(49) Pieniazek, S. N.; Clemente, F. R.; Houk, K. N. *Angew. Chem. Int. Ed.* **2008**, *47*, 7746-7749.

(50) Baum, J. S.; Shook, D. A.; Davies, H. M. L.; Smith, H. D. *Synth. Commun.* **1987**, *17*, 1709-1716.

(51) Denton, J. R.; Cheng, K.; Davies, H. M. L. *Chem. Commun.* **2008**, 1238-1240.

(52) Manning, J. R.; Davies, H. M. L. *Org. Synth.* **2007**, *84*, 334-346.

(53) Gaussian 09, R. A.; M. J. Frisch, G. W. T., H. B. Schlegel, G. E. Scuseria, ; M. A. Robb, J. R. C., G. Scalmani, V. Barone, B. Mennucci, ; G. A. Petersson, H. N., M. Caricato, X. Li, H. P. Hratchian, ; A. F. Izmaylov, J. B., G. Zheng, J. L. Sonnenberg, M. Hada, ; M. Ehara, K. T., R. Fukuda, J. Hasegawa, M. Ishida, T. Nakajima, ; Y. Honda, O. K., H. Nakai, T. Vreven, J. A. Montgomery, Jr., ; J. E. Peralta, F. O., M. Bearpark, J. J. Heyd, E. Brothers, ; K. N. Kudin, V. N. S., R. Kobayashi, J. Normand, ; K. Raghavachari, A. R., J. C. Burant, S. S. Iyengar, J. Tomasi, ; M. Cossi, N. R., J. M. Millam, M. Klene, J. E. Knox, J. B. Cross, ; V. Bakken, C. A., J. Jaramillo, R. Gomperts, R. E. Stratmann, ; O. Yazyev, A. J. A., R. Cammi, C. Pomelli, J. W. Ochterski, ; R. L. Martin, K. M., V. G. Zakrzewski, G. A. Voth, ; P. Salvador, J. J. D., S. Dapprich, A. D. Daniels, ; O. Farkas, J. B. F ., J. V. Ortiz, J. Cioslowski, ; and D. J. Fox, G., Inc., Wallingford CT, 2009.

(54) Lee, C.; Yang, W.; Parr, R. G. *Phys. Rev. B* **1988**, *37*, 785-789.

(55) Becke, A. D. *J. Chem. Phys.* **1993**, *98*, 5648-5652.

(56) M. Kaupp, P. v. R. S., H. Stoll, H. Preuss *J. Chem. Phys.* **1991**, *94*, 1360.

(57) A. Bergner, M. D., W. Kuechle, H. Stoll, H. Preuss *Mol. Phys.* **1993**, *80*, 1431.

(58) M. Dolg, H. S., H. Preuss, R.M. Pitzer *J. Phys. Chem.* **1993**, *97*.

(59) Feller, D. *J. Comput. Chem.* **1996**, *17*, 1571-1586.

(60) Schuchardt, K. L., Didier, B.T., Elsethagen, T., Sun, L., Gurumoorthi, V., Chase, J., Li, J., and Windus, T.L. *J. Chem. Inf. Model.* **2007**, *47*, 1045-1052.

(61) Tomasi, J.; Mennucci, B.; Cammi, R. *Chem. Rev.* **2005**, *105*, 2999-3093.

(62) Foresman, J. B.; Frisch, A. *Exploring Chemistry with Electronic Structure Methods*; Gaussian, Inc.: Pittsburgh, PA, 1993.

(63) Taylor, R.; Macrae, C. F. *Acta. Cryst. B* **2001**, *57*, 815-827.

(64) Bruno, I. J.; Cole, J. C.; Edgington, P. R.; Kessler, M.; Macrae, C. F.; McCabe, P.; Pearson, J.; Taylor, R. *Acta. Cryst. B* **2002**, *58*, 389-397.

(65) Macrae, C. F.; Edgington, P. R.; McCabe, P.; Pidcock, E.; Shields, G. P.; Taylor, R.; Towler, M.; van de Streek, J. *J. Appl. Crystallogr.* **2006**, *39*, 453-457.

(66) Macrae, C. F.; Bruno, I. J.; Chisholm, J. A.; Edgington, P. R.; McCabe, P.; Pidcock, E.; Rodriguez-Monge, L.; Taylor, R.; van de Streek, J.; Wood, P. A. *J. Appl. Crystallogr.* **2008**, *41*, 466-470.

- Appendix A -

NMR Spectral Data for Representative Compounds

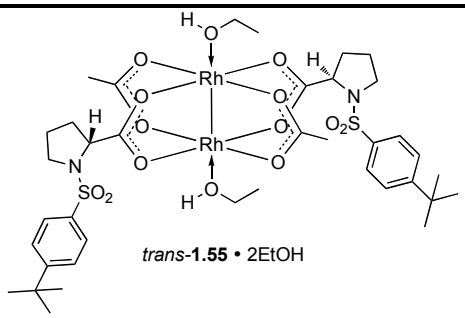

trans-**1.55** • 2EtOH

^{1}H NMR, 600 MHz, $CDCl_3$

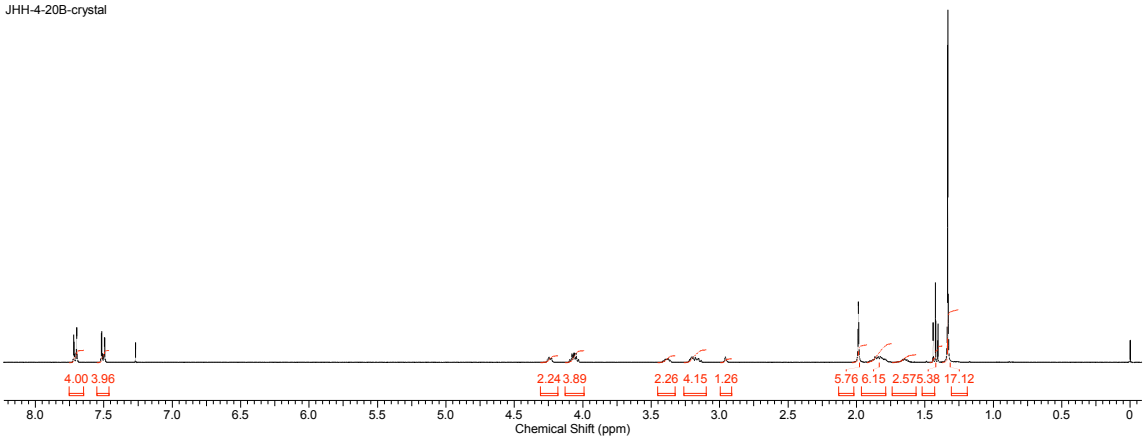

^{13}C NMR, 150 MHz, $CDCl_3$

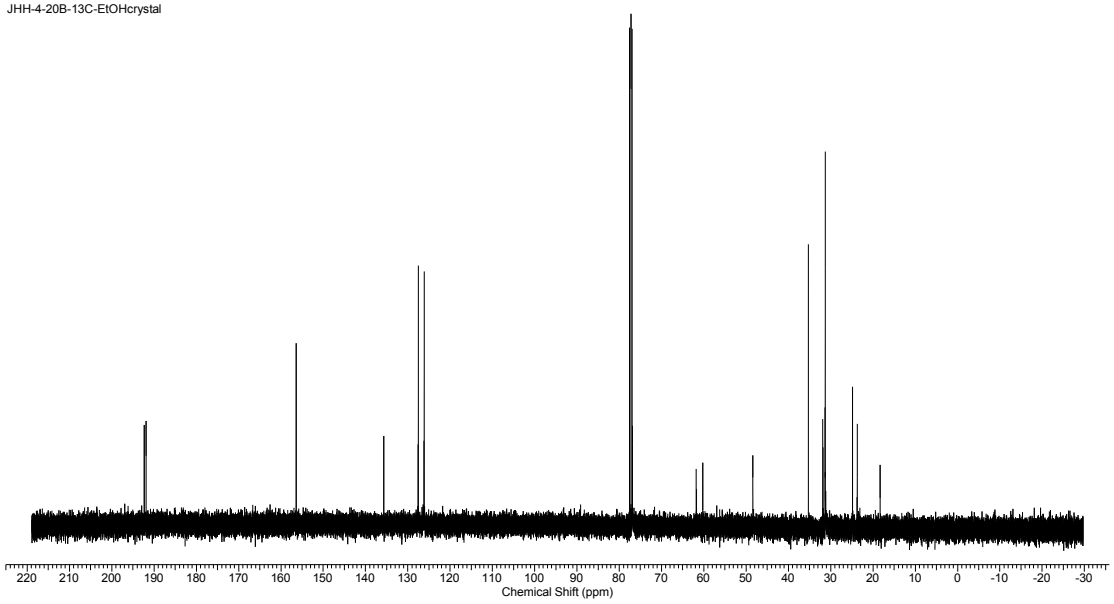

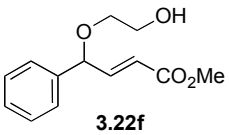

3.22f

^{1}H NMR, 600 MHz, $CDCl_3$

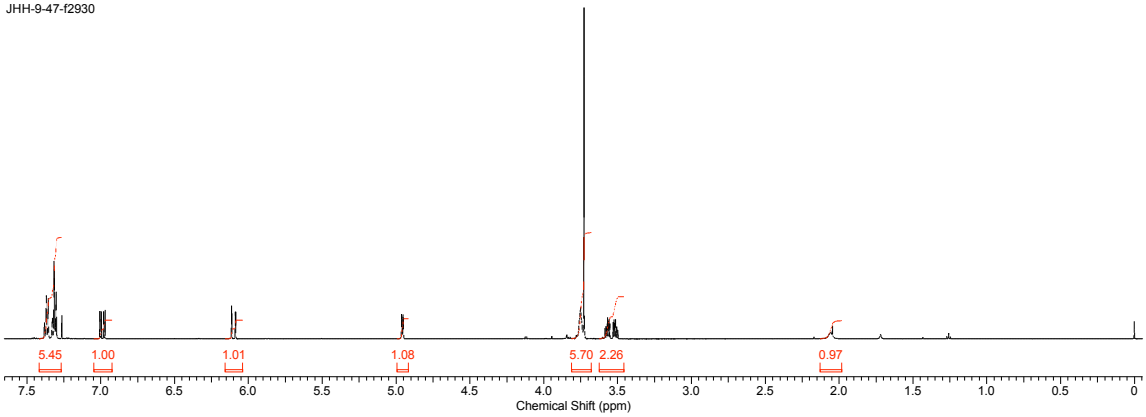

^{13}C NMR, 150 MHz, $CDCl_3$

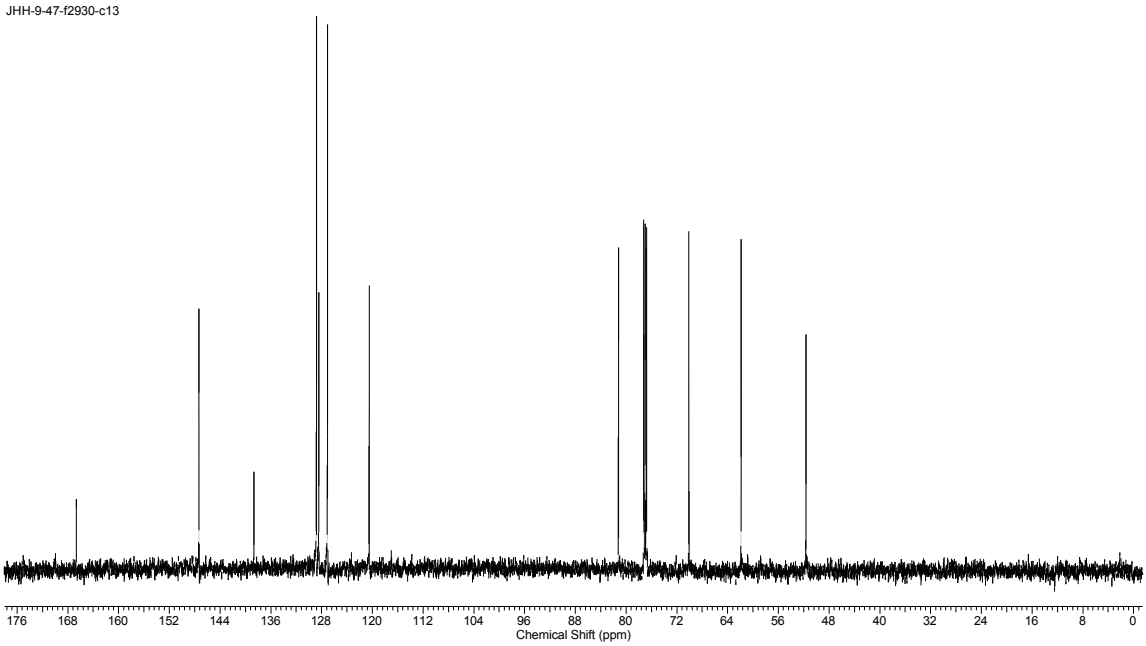

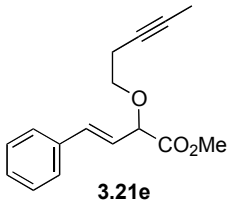

3.21e

^{1}H NMR, 400 MHz, $CDCl_3$

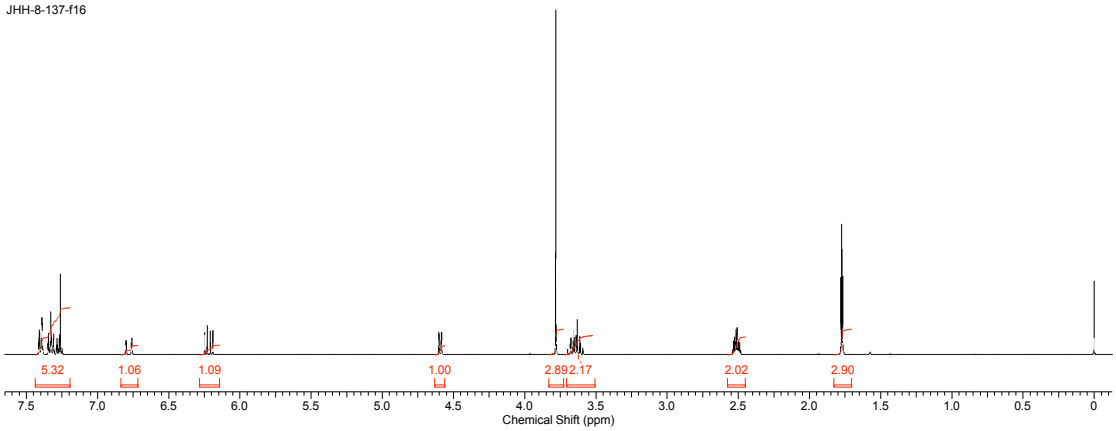

^{13}C NMR, 150 MHz, $CDCl_3$

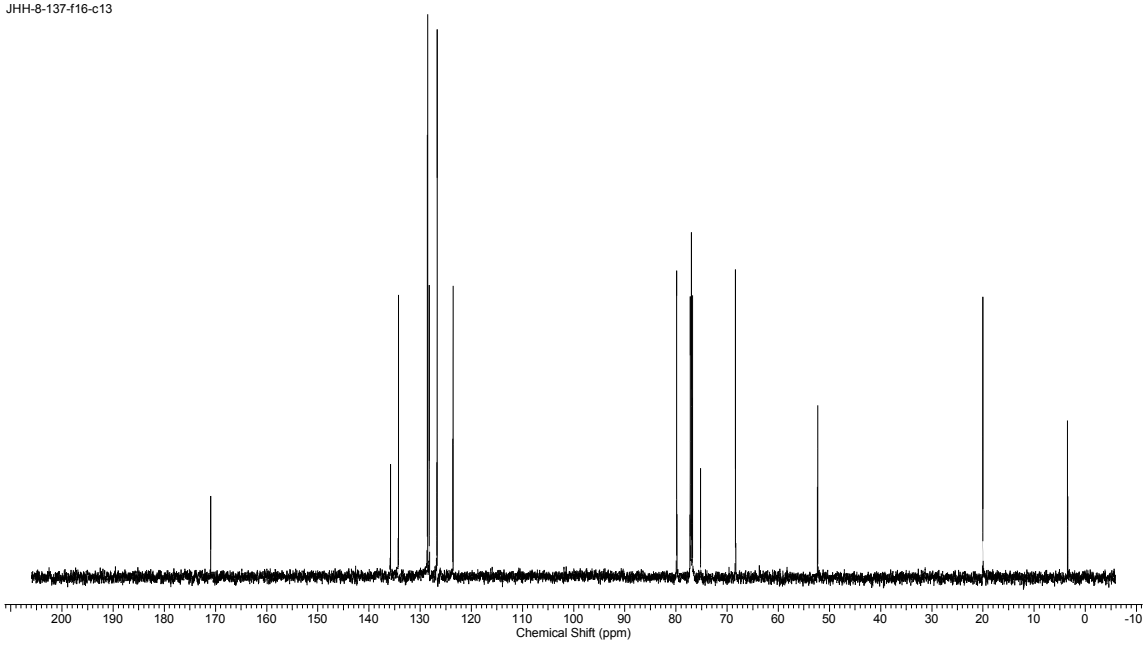

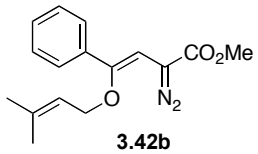

3.42b

^{1}H NMR, 400 MHz, $CDCl_3$

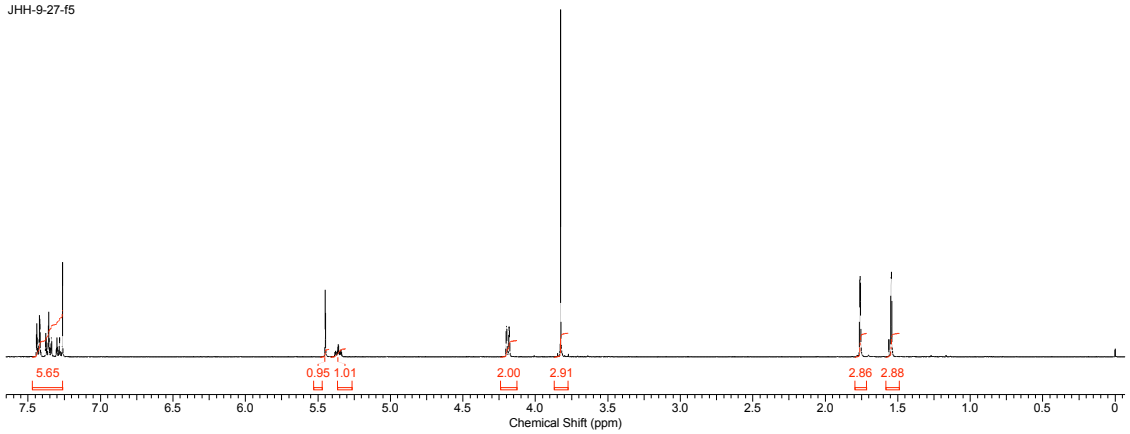

^{13}C NMR, 150 MHz, $CDCl_3$

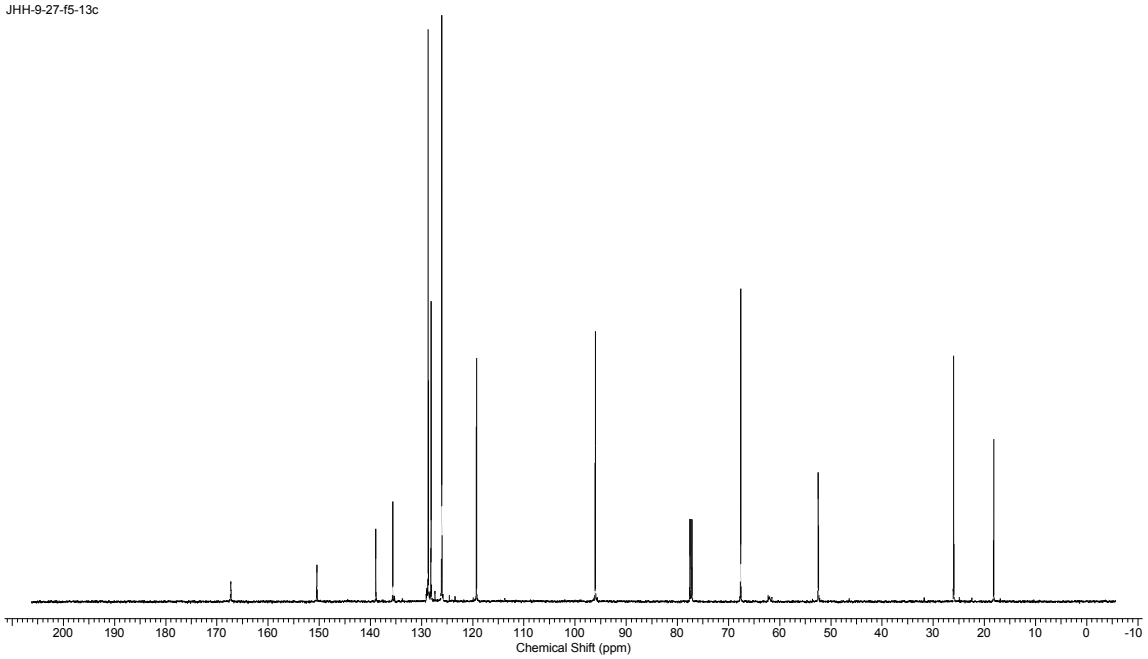

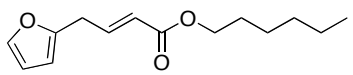

3.29

^{1}H NMR, 500 MHz, $CDCl_3$

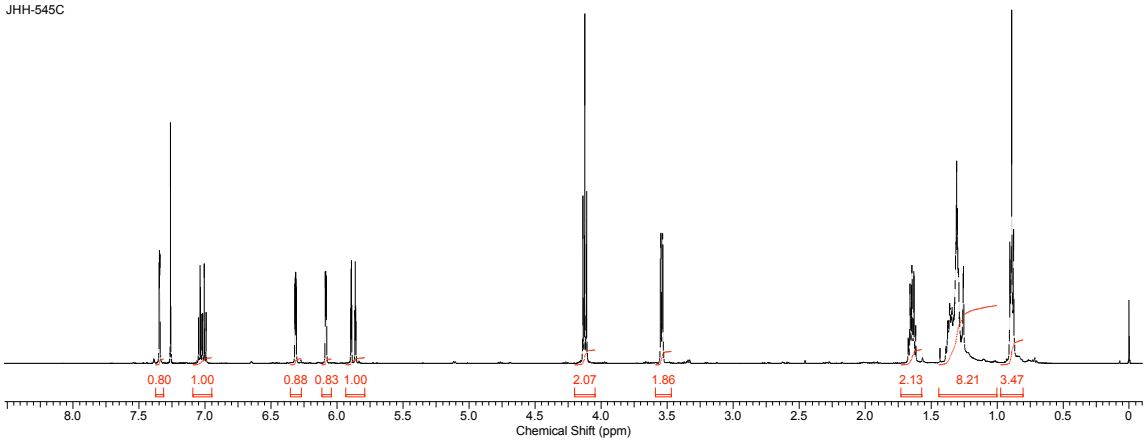

^{13}C NMR, 75 MHz, $CDCl_3$

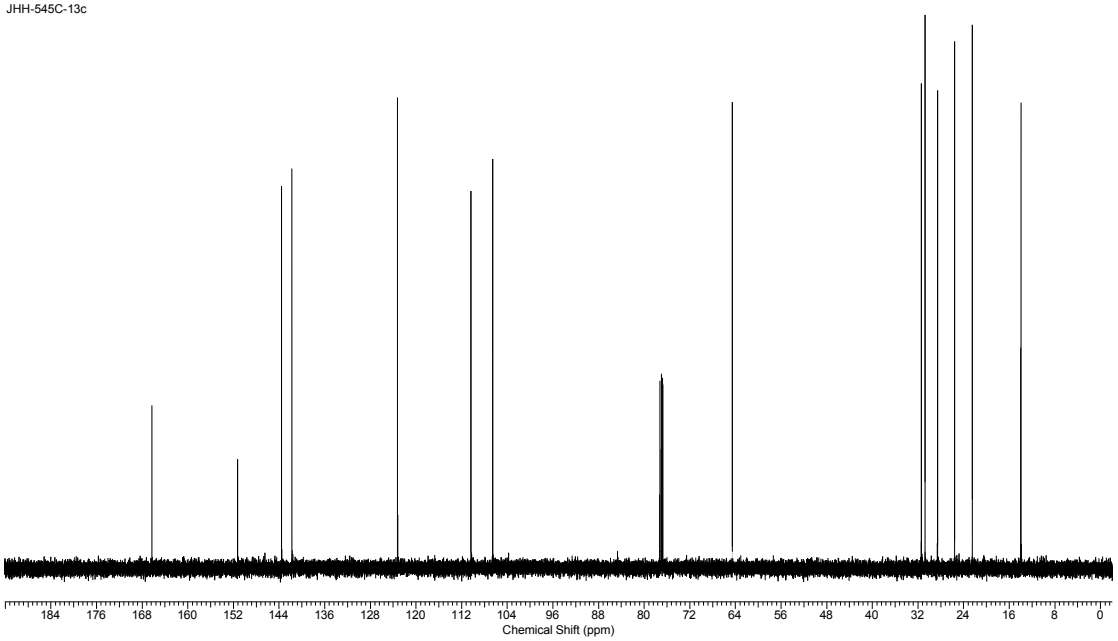

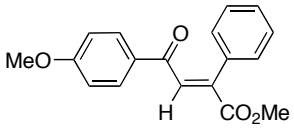

5.39c

^{1}H NMR, 400 MHz, $CDCl_3$

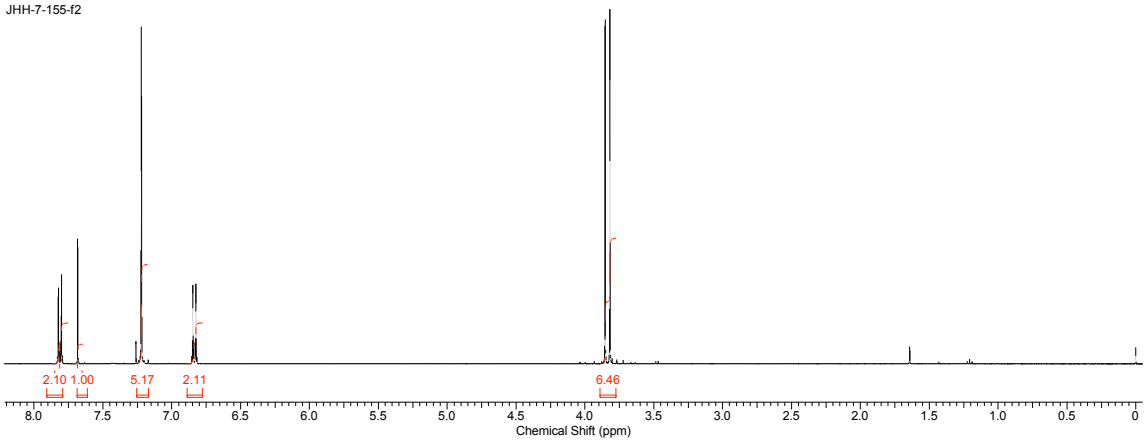

^{13}C NMR, 100 MHz, $CDCl_3$

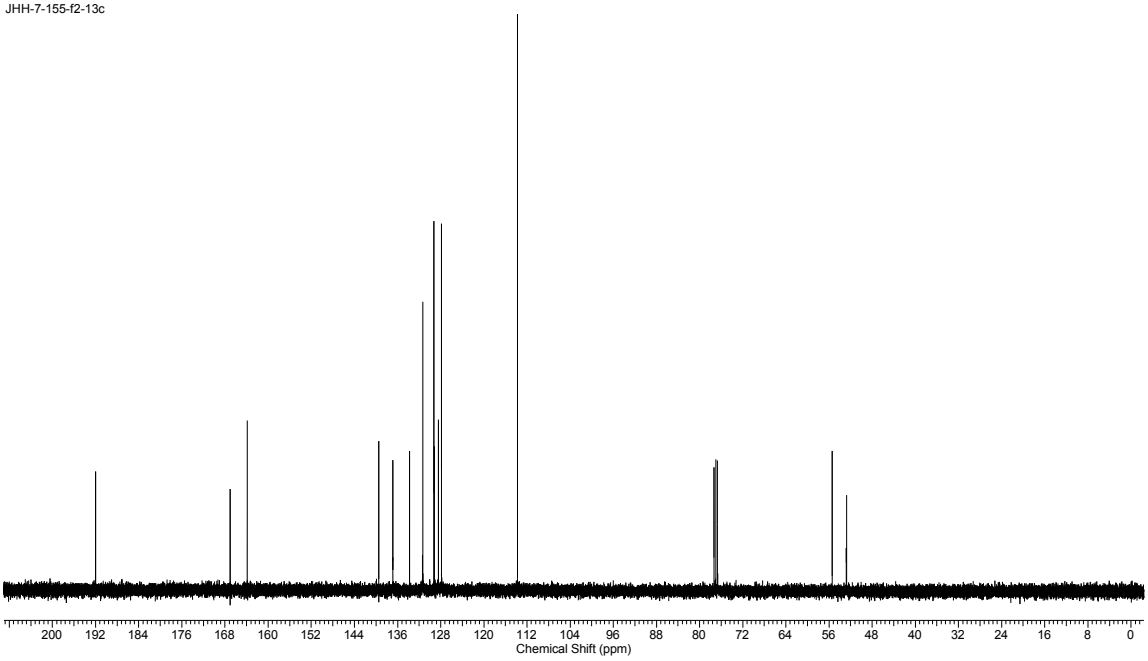

- Appendix B -

X–Ray Crystallographic Data

Appendix B1: trans-1.55• 2EtOH

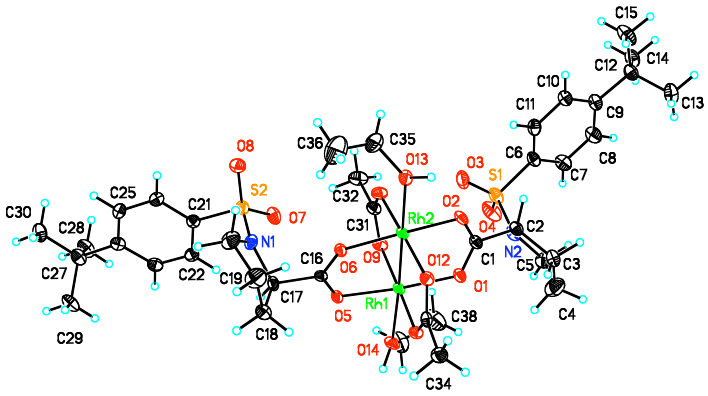

Table B1-1: Crystal data and structure refinement for *trans*-**1.55** ● 2EtOH.

Identification code	jhh_420bs	
Empirical formula	C38 H57.50 N2 O14.25 Rh2 S2	
Formula weight	1040.30	
Temperature	173(2) K	
Wavelength	0.71073 Å	
Crystal system	Orthorhombic	
Space group	P2(1)2(1)2(1)	
Unit cell dimensions	a = 16.7571(15) Å	α= 90°.
	b = 19.8743(18) Å	β= 90°.
	c = 27.847(3) Å	γ = 90°.
Volume	9273.9(14) Å^3	
Z	8	
Density (calculated)	1.490 Mg/m^3	
Absorption coefficient	0.864 mm^{-1}	
F(000)	4284	
Crystal size	0.35 x 0.17 x 0.12 mm^3	
Theta range for data collection	1.42 to 32.58°.	
Index ranges	-25<=h<=25, -29<=k<=29, -41<=l<=41	
Reflections collected	200521	
Independent reflections	32291 [R(int) = 0.0997]	
Completeness to theta = 32.58°	97.0 %	
Absorption correction	Semi-empirical from equivalents	
Max. and min. transmission	0.9034 and 0.7541	
Refinement method	Full-matrix least-squares on F^2	
Data / restraints / parameters	32291 / 7 / 1110	
Goodness-of-fit on F^2	1.019	
Final R indices [I>2sigma(I)]	R1 = 0.0482, wR2 = 0.0938	
R indices (all data)	R1 = 0.0891, wR2 = 0.1098	
Absolute structure parameter	-0.030(17)	
Largest diff. peak and hole	1.189 and -0.760 e.Å^{-3}	

Table B1-2: Atomic coordinates (x 10^4) and equivalent isotropic displacement parameters ($Å^2$x 10^3) for *trans*-**1.55** ● 2EtOH. U(eq) is defined as one third of the trace of the orthogonalized U^{ij} tensor.

	x	y	z	U(eq)
C(1)	3576(2)	10670(2)	7695(1)	28(1)
C(2)	4188(3)	10940(2)	7347(2)	30(1)
C(3)	4062(3)	11694(2)	7245(2)	44(1)
C(4)	4639(4)	12048(3)	7579(3)	68(2)
C(5)	5346(3)	11603(3)	7582(2)	51(1)
C(6)	5870(2)	10235(2)	6911(2)	34(1)
C(7)	6555(3)	10593(3)	6784(2)	43(1)
C(8)	6794(3)	10599(3)	6307(2)	45(1)
C(9)	6385(2)	10246(2)	5956(2)	35(1)
C(10)	5707(2)	9886(2)	6094(2)	35(1)
C(11)	5444(3)	9889(2)	6567(2)	37(1)
C(12)	6669(3)	10290(3)	5429(2)	41(1)
C(13)	6571(3)	11021(3)	5248(2)	54(2)
C(14)	7558(3)	10082(3)	5401(2)	49(1)
C(15)	6188(4)	9826(4)	5104(2)	68(2)
C(16)	1758(2)	9455(2)	8929(1)	24(1)
C(17)	1281(3)	9054(2)	9290(2)	29(1)
C(18)	447(3)	9346(3)	9370(2)	44(1)
C(19)	-73(3)	8962(3)	9018(2)	60(2)
C(20)	265(3)	8248(3)	9035(2)	49(1)
C(21)	1763(2)	7379(2)	9648(2)	27(1)
C(22)	2118(3)	7678(2)	10052(2)	33(1)
C(23)	2084(3)	7353(2)	10484(2)	35(1)
C(24)	1698(3)	6732(2)	10541(2)	31(1)
C(25)	1345(3)	6454(2)	10134(2)	33(1)
C(26)	1373(3)	6768(2)	9691(2)	30(1)
C(27)	1675(3)	6399(3)	11037(2)	39(1)
C(28)	2547(3)	6218(3)	11181(2)	50(1)
C(29)	1335(3)	6888(3)	11407(2)	50(1)
C(30)	1184(3)	5749(3)	11041(2)	49(1)
C(31)	3614(3)	9111(2)	8340(2)	34(1)
C(32)	4183(3)	8517(3)	8361(2)	47(1)
C(33)	1577(2)	11088(2)	8301(2)	28(1)
C(34)	944(3)	11625(2)	8314(2)	41(1)
C(35)	1430(5)	8640(3)	7333(3)	80(2)
C(36)	864(8)	8375(5)	7585(4)	183(6)
C(37)	4325(3)	10950(4)	9426(2)	62(2)
C(38)	4859(4)	11065(4)	9029(2)	83(2)
C(1A)	1736(3)	985(2)	218(1)	28(1)
C(2A)	1388(3)	1510(2)	-128(2)	31(1)
C(4A)	76(4)	1877(4)	137(3)	53(2)
C(3A)	488(3)	1402(3)	-220(2)	46(1)
C(5A)	608(3)	2478(3)	140(2)	54(1)
C(4B)	126(17)	2024(13)	-253(11)	50(6)
C(3B)	488(3)	1402(3)	-220(2)	46(1)
C(5B)	608(3)	2478(3)	140(2)	54(1)
C(6A)	2176(3)	2896(2)	-599(2)	37(1)
C(7A)	1696(3)	3429(2)	-747(2)	42(1)
C(8A)	1695(4)	3613(2)	-1224(2)	46(1)
C(9A)	2151(3)	3294(2)	-1563(2)	41(1)
C(10A)	2638(3)	2760(2)	-1408(2)	47(1)
C(11A)	2640(3)	2558(2)	-928(2)	42(1)
C(12A)	2183(4)	3527(2)	-2088(2)	66(2)

C(13A)	2484(9)	3045(7)	-2435(5)	60(4)
C(14A)	1203(6)	3519(5)	-2262(4)	50(3)
C(15A)	2339(9)	4261(7)	-2110(6)	68(4)
C(16A)	3278(2)	-518(2)	1413(1)	23(1)
C(17A)	3809(3)	-890(2)	1764(2)	28(1)
C(19A)	3914(4)	-2049(3)	1519(3)	38(2)
C(18A)	3491(3)	-1603(2)	1864(2)	36(1)
C(20A)	4747(3)	-1747(2)	1476(2)	40(1)
C(19A)	4261(11)	-2050(9)	1844(7)	45(5)
C(18B)	3491(3)	-1603(2)	1864(2)	36(1)
C(20B)	4747(3)	-1747(2)	1476(2)	40(1)
C(21A)	5778(2)	-686(2)	2158(2)	29(1)
C(22A)	6369(3)	-1163(2)	2172(2)	32(1)
C(23A)	6709(3)	-1335(2)	2608(2)	35(1)
C(24A)	6457(3)	-1049(2)	3037(2)	32(1)
C(25A)	5850(3)	-564(2)	3009(2)	36(1)
C(26A)	5507(3)	-382(2)	2579(2)	35(1)
C(27A)	6836(3)	-1249(2)	3519(2)	37(1)
C(28A)	7276(4)	-632(3)	3728(2)	48(2)
C(29A)	7451(5)	-1824(4)	3474(2)	57(2)
C(30A)	6193(4)	-1464(4)	3876(2)	48(2)
C(31A)	3585(3)	1065(2)	849(2)	28(1)
C(32A)	4261(3)	1555(3)	872(2)	49(1)
C(33A)	1308(3)	-720(2)	802(2)	29(1)
C(34A)	674(3)	-1265(2)	804(2)	43(1)
C(35A)	4082(3)	-932(3)	-177(2)	50(1)
C(36A)	4131(4)	-1638(3)	-48(3)	96(3)
C(37A)	1272(4)	1525(3)	1951(2)	58(2)
C(38A)	895(4)	1876(3)	1556(2)	72(2)
C(13B)	2014(9)	2961(7)	-2407(5)	61(4)
C(14B)	1911(9)	4199(6)	-2177(5)	52(3)
C(15B)	3175(6)	3651(6)	-2189(4)	54(3)
C(28B)	6410(17)	-818(14)	3944(10)	74(8)
C(29B)	7642(15)	-1140(13)	3488(8)	68(7)
C(30B)	6548(15)	-1943(11)	3619(8)	67(7)
N(1)	1115(2)	8375(2)	9107(1)	32(1)
N(2)	4996(2)	10929(2)	7564(1)	36(1)
N(1A)	1411(2)	2181(2)	97(1)	37(1)
N(2A)	4594(2)	-1017(2)	1540(1)	29(1)
O(1)	3617(2)	10873(2)	8124(1)	30(1)
O(2)	3068(2)	10263(2)	7522(1)	31(1)
O(3)	5004(2)	9701(2)	7578(1)	52(1)
O(4)	6215(2)	10354(2)	7816(1)	62(1)
O(5)	2309(2)	9818(1)	9099(1)	26(1)
O(6)	1557(2)	9410(1)	8494(1)	26(1)
O(7)	2538(2)	8150(2)	9064(1)	40(1)
O(8)	1576(2)	7322(2)	8729(1)	41(1)
O(9)	3750(2)	9594(2)	8623(1)	32(1)
O(10)	3049(2)	9063(1)	8039(1)	34(1)
O(11)	2099(2)	11102(1)	8627(1)	29(1)
O(12)	1527(2)	10651(1)	7964(1)	29(1)
O(13)	1600(2)	9334(2)	7375(1)	36(1)
O(14)	3509(2)	10904(2)	9294(1)	36(1)
O(1A)	1482(2)	993(1)	641(1)	30(1)
O(2A)	2233(2)	584(1)	35(1)	31(1)
O(3A)	2870(2)	2234(2)	83(1)	60(1)
O(4A)	2070(3)	3250(2)	291(1)	67(1)
O(5A)	2840(2)	-66(1)	1592(1)	24(1)

O(6A)	3299(2)	-701(2)	980(1)	30(1)
O(7A)	5884(2)	-631(2)	1233(1)	38(1)
O(8A)	4952(2)	166(2)	1636(1)	40(1)
O(9A)	3665(2)	576(2)	556(1)	33(1)
O(10A)	2990(2)	1163(1)	1121(1)	30(1)
O(11A)	1802(2)	-738(2)	456(1)	31(1)
O(12A)	1291(2)	-304(1)	1141(1)	28(1)
O(13A)	3300(2)	-662(2)	-143(1)	39(1)
O(14A)	1490(2)	866(2)	1825(1)	35(1)
O(1S)	5402(4)	207(4)	388(2)	62(2)
Rh(1)	2961(1)	10375(1)	8633(1)	23(1)
Rh(2)	2273(1)	9838(1)	7987(1)	23(1)
Rh(1A)	2115(1)	457(1)	1142(1)	22(1)
Rh(2A)	2755(1)	-92(1)	486(1)	23(1)
S(1)	5533(1)	10255(1)	7511(1)	41(1)
S(2)	1796(1)	7801(1)	9090(1)	31(1)
S(1A)	2188(1)	2653(1)	11(1)	45(1)
S(2A)	5316(1)	-487(1)	1603(1)	30(1)

Table B1-3: Bond lengths [Å] and angles [°] for *trans*-**1.55** ● 2EtOH.

C(1)-O(1)	1.263(5)	C(21)-S(2)	1.767(4)
C(1)-O(2)	1.269(5)	C(22)-C(23)	1.366(6)
C(1)-C(2)	1.509(6)	C(22)-H(22A)	0.9500
C(2)-N(2)	1.483(5)	C(23)-C(24)	1.402(6)
C(2)-C(3)	1.539(6)	C(23)-H(23A)	0.9500
C(2)-H(2A)	1.0000	C(24)-C(25)	1.392(6)
C(3)-C(4)	1.514(8)	C(24)-C(27)	1.531(6)
C(3)-H(3A)	0.9900	C(25)-C(26)	1.384(6)
C(3)-H(3B)	0.9900	C(25)-H(25A)	0.9500
C(4)-C(5)	1.479(8)	C(26)-H(26A)	0.9500
C(4)-H(4A)	0.9900	C(27)-C(29)	1.527(7)
C(4)-H(4B)	0.9900	C(27)-C(30)	1.532(7)
C(5)-N(2)	1.464(6)	C(27)-C(28)	1.556(6)
C(5)-H(5A)	0.9900	C(28)-H(28A)	0.9800
C(5)-H(5B)	0.9900	C(28)-H(28B)	0.9800
C(6)-C(11)	1.378(6)	C(28)-H(28C)	0.9800
C(6)-C(7)	1.396(6)	C(29)-H(29A)	0.9800
C(6)-S(1)	1.764(4)	C(29)-H(29B)	0.9800
C(7)-C(8)	1.388(7)	C(29)-H(29C)	0.9800
C(7)-H(7A)	0.9500	C(30)-H(30A)	0.9800
C(8)-C(9)	1.386(6)	C(30)-H(30B)	0.9800
C(8)-H(8A)	0.9500	C(30)-H(30C)	0.9800
C(9)-C(10)	1.396(6)	C(31)-O(9)	1.264(5)
C(9)-C(12)	1.545(6)	C(31)-O(10)	1.269(5)
C(10)-C(11)	1.390(6)	C(31)-C(32)	1.518(6)
C(10)-H(10A)	0.9500	C(32)-H(32A)	0.9800
C(11)-H(11A)	0.9500	C(32)-H(32B)	0.9800
C(12)-C(15)	1.522(7)	C(32)-H(32C)	0.9800
C(12)-C(13)	1.546(7)	C(33)-O(11)	1.260(5)
C(12)-C(14)	1.548(7)	C(33)-O(12)	1.282(5)
C(13)-H(13A)	0.9800	C(33)-C(34)	1.506(6)
C(13)-H(13B)	0.9800	C(34)-H(34A)	0.9800
C(13)-H(13C)	0.9800	C(34)-H(34B)	0.9800
C(14)-H(14A)	0.9800	C(34)-H(34C)	0.9800
C(14)-H(14B)	0.9800	C(35)-C(36)	1.293(11)
C(14)-H(14C)	0.9800	C(35)-O(13)	1.413(6)
C(15)-H(15A)	0.9800	C(35)-H(35A)	0.9500
C(15)-H(15B)	0.9800	C(36)-H(36A)	0.9800
C(15)-H(15C)	0.9800	C(36)-H(36B)	0.9800
C(16)-O(6)	1.261(4)	C(36)-H(36C)	0.9800
C(16)-O(5)	1.264(4)	C(37)-O(14)	1.419(6)
C(16)-C(17)	1.512(6)	C(37)-C(38)	1.440(8)
C(17)-N(1)	1.471(5)	C(37)-H(37A)	0.9900
C(17)-C(18)	1.529(6)	C(37)-H(37B)	0.9900
C(17)-H(17A)	1.0000	C(38)-H(38A)	0.9800
C(18)-C(19)	1.517(7)	C(38)-H(38B)	0.9800
C(18)-H(18A)	0.9900	C(38)-H(38C)	0.9800
C(18)-H(18B)	0.9900	C(1A)-O(1A)	1.253(5)
C(19)-C(20)	1.527(7)	C(1A)-O(2A)	1.260(5)
C(19)-H(19A)	0.9900	C(1A)-C(2A)	1.535(6)
C(19)-H(19B)	0.9900	C(2A)-N(1A)	1.475(5)
C(20)-N(1)	1.461(6)	C(2A)-C(3A)	1.545(6)
C(20)-H(20A)	0.9900	C(2A)-H(2A1)	1.0000
C(20)-H(20B)	0.9900	C(4A)-C(5A)	1.492(9)
C(21)-C(26)	1.384(6)	C(4A)-C(3A)	1.535(8)
C(21)-C(22)	1.405(6)	C(4A)-H(4A1)	0.9900

C(4A)-H(4A2)	0.9900	C(23A)-H(23B)	0.9500
C(3A)-H(3AA)	0.9900	C(24A)-C(25A)	1.404(6)
C(3A)-H(3AB)	0.9900	C(24A)-C(27A)	1.538(6)
C(5A)-N(1A)	1.474(6)	C(25A)-C(26A)	1.375(6)
C(5A)-H(5AA)	0.9900	C(25A)-H(25B)	0.9500
C(5A)-H(5AB)	0.9900	C(26A)-H(26B)	0.9500
C(4B)-H(4B1)	0.9900	C(27A)-C(29B)	1.37(3)
C(4B)-H(4B2)	0.9900	C(27A)-C(30B)	1.49(2)
C(6A)-C(11A)	1.377(7)	C(27A)-C(30A)	1.526(8)
C(6A)-C(7A)	1.392(6)	C(27A)-C(28A)	1.545(8)
C(6A)-S(1A)	1.765(4)	C(27A)-C(29A)	1.545(8)
C(7A)-C(8A)	1.376(7)	C(27A)-C(28B)	1.63(3)
C(7A)-H(7AA)	0.9500	C(28A)-H(28D)	0.9800
C(8A)-C(9A)	1.371(7)	C(28A)-H(28E)	0.9800
C(8A)-H(8AA)	0.9500	C(28A)-H(28F)	0.9800
C(9A)-C(10A)	1.406(7)	C(29A)-H(29D)	0.9800
C(9A)-C(12A)	1.533(7)	C(29A)-H(29E)	0.9800
C(10A)-C(11A)	1.396(7)	C(29A)-H(29F)	0.9800
C(10A)-H(10B)	0.9500	C(30A)-H(30D)	0.9800
C(11A)-H(11B)	0.9500	C(30A)-H(30E)	0.9800
C(12A)-C(14B)	1.434(11)	C(30A)-H(30F)	0.9800
C(12A)-C(13A)	1.451(11)	C(31A)-O(10A)	1.266(5)
C(12A)-C(13B)	1.461(12)	C(31A)-O(9A)	1.276(5)
C(12A)-C(15A)	1.484(12)	C(31A)-C(32A)	1.495(6)
C(12A)-C(15B)	1.705(11)	C(32A)-H(32D)	0.9800
C(12A)-C(14A)	1.711(11)	C(32A)-H(32E)	0.9800
C(13A)-H(13D)	0.9800	C(32A)-H(32F)	0.9800
C(13A)-H(13E)	0.9800	C(33A)-O(12A)	1.255(5)
C(13A)-H(13F)	0.9800	C(33A)-O(11A)	1.270(5)
C(14A)-H(14D)	0.9800	C(33A)-C(34A)	1.517(6)
C(14A)-H(14E)	0.9800	C(34A)-H(34D)	0.9800
C(14A)-H(14F)	0.9800	C(34A)-H(34E)	0.9800
C(15A)-H(15D)	0.9800	C(34A)-H(34F)	0.9800
C(15A)-H(15E)	0.9800	C(35A)-O(13A)	1.419(6)
C(15A)-H(15F)	0.9800	C(35A)-C(36A)	1.452(8)
C(16A)-O(6A)	1.259(4)	C(35A)-H(35B)	0.9900
C(16A)-O(5A)	1.262(4)	C(35A)-H(35C)	0.9900
C(16A)-C(17A)	1.513(5)	C(36A)-H(36D)	0.9800
C(17A)-N(2A)	1.477(5)	C(36A)-H(36E)	0.9800
C(17A)-C(18A)	1.541(6)	C(36A)-H(36F)	0.9800
C(17A)-H(17B)	1.0000	C(37A)-O(14A)	1.403(5)
C(19A)-C(18A)	1.485(8)	C(37A)-C(38A)	1.447(8)
C(19A)-C(20A)	1.525(7)	C(37A)-H(37C)	0.9900
C(19A)-H(19C)	0.9900	C(37A)-H(37D)	0.9900
C(19A)-H(19D)	0.9900	C(38A)-H(38D)	0.9800
C(18A)-H(18C)	0.9900	C(38A)-H(38E)	0.9800
C(18A)-H(18D)	0.9900	C(38A)-H(38F)	0.9800
C(20A)-N(2A)	1.484(5)	C(13B)-H(13G)	0.9800
C(20A)-H(20C)	0.9900	C(13B)-H(13H)	0.9800
C(20A)-H(20D)	0.9900	C(13B)-H(13I)	0.9800
C(19A)-H(19E)	0.9900	C(14B)-H(14G)	0.9800
C(19A)-H(19F)	0.9900	C(14B)-H(14H)	0.9800
C(21A)-C(22A)	1.372(6)	C(14B)-H(14I)	0.9800
C(21A)-C(26A)	1.396(6)	C(15B)-H(15G)	0.9800
C(21A)-S(2A)	1.773(4)	C(15B)-H(15H)	0.9800
C(22A)-C(23A)	1.382(6)	C(15B)-H(15I)	0.9800
C(22A)-H(22B)	0.9500	C(28B)-H(28G)	0.9800
C(23A)-C(24A)	1.388(6)	C(28B)-H(28H)	0.9800

C(28B)-H(28I)	0.9800
C(29B)-H(29G)	0.9800
C(29B)-H(29H)	0.9800
C(29B)-H(29I)	0.9800
C(30B)-H(30G)	0.9800
C(30B)-H(30H)	0.9800
C(30B)-H(30I)	0.9800
N(1)-S(2)	1.613(4)
N(2)-S(1)	1.621(4)
N(1A)-S(1A)	1.621(4)
N(2A)-S(2A)	1.615(4)
O(1)-Rh(1)	2.047(3)
O(2)-Rh(2)	2.040(3)
O(3)-S(1)	1.425(4)
O(4)-S(1)	1.436(4)
O(5)-Rh(1)	2.025(3)
O(6)-Rh(2)	2.039(3)
O(7)-S(2)	1.426(3)
O(8)-S(2)	1.433(3)
O(9)-Rh(1)	2.038(3)
O(10)-Rh(2)	2.021(3)
O(11)-Rh(1)	2.044(3)
O(12)-Rh(2)	2.043(3)
O(13)-Rh(2)	2.277(3)
O(13)-H(13)	0.9500
O(14)-Rh(1)	2.312(3)
O(14)-H(14)	0.9500
O(1A)-Rh(1A)	2.051(3)
O(2A)-Rh(2A)	2.036(3)
O(3A)-S(1A)	1.429(4)
O(4A)-S(1A)	1.434(4)
O(5A)-Rh(1A)	2.031(2)
O(6A)-Rh(2A)	2.047(3)
O(7A)-S(2A)	1.431(3)
O(8A)-S(2A)	1.435(3)
O(9A)-Rh(2A)	2.032(3)
O(10A)-Rh(1A)	2.030(3)
O(11A)-Rh(2A)	2.050(3)
O(12A)-Rh(1A)	2.048(3)
O(13A)-Rh(2A)	2.275(3)
O(13A)-H(13J)	0.9500
O(14A)-Rh(1A)	2.318(3)
O(14A)-H(14J)	0.9500
Rh(1)-Rh(2)	2.3872(4)
Rh(1A)-Rh(2A)	2.3839(4)

O(1)-C(1)-O(2)	126.8(4)
O(1)-C(1)-C(2)	117.2(4)
O(2)-C(1)-C(2)	116.0(3)
N(2)-C(2)-C(1)	110.7(3)
N(2)-C(2)-C(3)	102.4(4)
C(1)-C(2)-C(3)	111.9(4)
N(2)-C(2)-H(2A)	110.5
C(1)-C(2)-H(2A)	110.5
C(3)-C(2)-H(2A)	110.5
C(4)-C(3)-C(2)	104.5(4)
C(4)-C(3)-H(3A)	110.8
C(2)-C(3)-H(3A)	110.8
C(4)-C(3)-H(3B)	110.8
C(2)-C(3)-H(3B)	110.8
H(3A)-C(3)-H(3B)	108.9
C(5)-C(4)-C(3)	103.8(5)
C(5)-C(4)-H(4A)	111.0
C(3)-C(4)-H(4A)	111.0
C(5)-C(4)-H(4B)	111.0
C(3)-C(4)-H(4B)	111.0
H(4A)-C(4)-H(4B)	109.0
N(2)-C(5)-C(4)	103.0(4)
N(2)-C(5)-H(5A)	111.2
C(4)-C(5)-H(5A)	111.2
N(2)-C(5)-H(5B)	111.2
C(4)-C(5)-H(5B)	111.2
H(5A)-C(5)-H(5B)	109.1
C(11)-C(6)-C(7)	120.2(4)
C(11)-C(6)-S(1)	120.3(3)
C(7)-C(6)-S(1)	119.4(4)
C(8)-C(7)-C(6)	119.0(4)
C(8)-C(7)-H(7A)	120.5
C(6)-C(7)-H(7A)	120.5
C(9)-C(8)-C(7)	121.9(4)
C(9)-C(8)-H(8A)	119.0
C(7)-C(8)-H(8A)	119.0
C(8)-C(9)-C(10)	117.9(4)
C(8)-C(9)-C(12)	119.3(4)
C(10)-C(9)-C(12)	122.7(4)
C(11)-C(10)-C(9)	121.1(4)
C(11)-C(10)-H(10A)	119.4
C(9)-C(10)-H(10A)	119.4
C(6)-C(11)-C(10)	119.8(4)
C(6)-C(11)-H(11A)	120.1
C(10)-C(11)-H(11A)	120.1
C(15)-C(12)-C(9)	111.6(4)
C(15)-C(12)-C(13)	108.6(5)
C(9)-C(12)-C(13)	109.2(4)
C(15)-C(12)-C(14)	108.6(4)
C(9)-C(12)-C(14)	109.2(4)
C(13)-C(12)-C(14)	109.7(4)
C(12)-C(13)-H(13A)	109.5
C(12)-C(13)-H(13B)	109.5
H(13A)-C(13)-H(13B)	109.5
C(12)-C(13)-H(13C)	109.5
H(13A)-C(13)-H(13C)	109.5
H(13B)-C(13)-H(13C)	109.5
C(12)-C(14)-H(14A)	109.5
C(12)-C(14)-H(14B)	109.5
H(14A)-C(14)-H(14B)	109.5
C(12)-C(14)-H(14C)	109.5
H(14A)-C(14)-H(14C)	109.5
H(14B)-C(14)-H(14C)	109.5
C(12)-C(15)-H(15A)	109.5
C(12)-C(15)-H(15B)	109.5
H(15A)-C(15)-H(15B)	109.5
C(12)-C(15)-H(15C)	109.5
H(15A)-C(15)-H(15C)	109.5
H(15B)-C(15)-H(15C)	109.5
O(6)-C(16)-O(5)	126.6(4)

O(6)-C(16)-C(17)	117.4(3)	H(29A)-C(29)-H(29B)	109.5
O(5)-C(16)-C(17)	116.0(3)	C(27)-C(29)-H(29C)	109.5
N(1)-C(17)-C(16)	110.7(3)	H(29A)-C(29)-H(29C)	109.5
N(1)-C(17)-C(18)	103.0(3)	H(29B)-C(29)-H(29C)	109.5
C(16)-C(17)-C(18)	112.4(4)	C(27)-C(30)-H(30A)	109.5
N(1)-C(17)-H(17A)	110.2	C(27)-C(30)-H(30B)	109.5
C(16)-C(17)-H(17A)	110.2	H(30A)-C(30)-H(30B)	109.5
C(18)-C(17)-H(17A)	110.2	C(27)-C(30)-H(30C)	109.5
C(19)-C(18)-C(17)	103.9(4)	H(30A)-C(30)-H(30C)	109.5
C(19)-C(18)-H(18A)	111.0	H(30B)-C(30)-H(30C)	109.5
C(17)-C(18)-H(18A)	111.0	O(9)-C(31)-O(10)	127.1(4)
C(19)-C(18)-H(18B)	111.0	O(9)-C(31)-C(32)	117.0(4)
C(17)-C(18)-H(18B)	111.0	O(10)-C(31)-C(32)	115.9(4)
H(18A)-C(18)-H(18B)	109.0	C(31)-C(32)-H(32A)	109.5
C(18)-C(19)-C(20)	103.6(5)	C(31)-C(32)-H(32B)	109.5
C(18)-C(19)-H(19A)	111.1	H(32A)-C(32)-H(32B)	109.5
C(20)-C(19)-H(19A)	111.1	C(31)-C(32)-H(32C)	109.5
C(18)-C(19)-H(19B)	111.1	H(32A)-C(32)-H(32C)	109.5
C(20)-C(19)-H(19B)	111.1	H(32B)-C(32)-H(32C)	109.5
H(19A)-C(19)-H(19B)	109.0	O(11)-C(33)-O(12)	126.0(4)
N(1)-C(20)-C(19)	101.9(4)	O(11)-C(33)-C(34)	117.0(4)
N(1)-C(20)-H(20A)	111.4	O(12)-C(33)-C(34)	117.0(4)
C(19)-C(20)-H(20A)	111.4	C(33)-C(34)-H(34A)	109.5
N(1)-C(20)-H(20B)	111.4	C(33)-C(34)-H(34B)	109.5
C(19)-C(20)-H(20B)	111.4	H(34A)-C(34)-H(34B)	109.5
H(20A)-C(20)-H(20B)	109.3	C(33)-C(34)-H(34C)	109.5
C(26)-C(21)-C(22)	120.2(4)	H(34A)-C(34)-H(34C)	109.5
C(26)-C(21)-S(2)	120.5(3)	H(34B)-C(34)-H(34C)	109.5
C(22)-C(21)-S(2)	119.3(3)	C(36)-C(35)-O(13)	120.1(7)
C(23)-C(22)-C(21)	119.1(4)	C(36)-C(35)-H(35A)	120.0
C(23)-C(22)-H(22A)	120.5	O(13)-C(35)-H(35A)	120.0
C(21)-C(22)-H(22A)	120.5	C(35)-C(36)-H(36A)	109.5
C(22)-C(23)-C(24)	122.4(4)	C(35)-C(36)-H(36B)	109.5
C(22)-C(23)-H(23A)	118.8	H(36A)-C(36)-H(36B)	109.5
C(24)-C(23)-H(23A)	118.8	C(35)-C(36)-H(36C)	109.5
C(25)-C(24)-C(23)	116.9(4)	H(36A)-C(36)-H(36C)	109.5
C(25)-C(24)-C(27)	123.5(4)	H(36B)-C(36)-H(36C)	109.5
C(23)-C(24)-C(27)	119.6(4)	O(14)-C(37)-C(38)	114.2(5)
C(26)-C(25)-C(24)	122.2(4)	O(14)-C(37)-H(37A)	108.7
C(26)-C(25)-H(25A)	118.9	C(38)-C(37)-H(37A)	108.7
C(24)-C(25)-H(25A)	118.9	O(14)-C(37)-H(37B)	108.7
C(25)-C(26)-C(21)	119.2(4)	C(38)-C(37)-H(37B)	108.7
C(25)-C(26)-H(26A)	120.4	H(37A)-C(37)-H(37B)	107.6
C(21)-C(26)-H(26A)	120.4	C(37)-C(38)-H(38A)	109.5
C(29)-C(27)-C(24)	110.0(4)	C(37)-C(38)-H(38B)	109.5
C(29)-C(27)-C(30)	109.3(4)	H(38A)-C(38)-H(38B)	109.5
C(24)-C(27)-C(30)	112.6(4)	C(37)-C(38)-H(38C)	109.5
C(29)-C(27)-C(28)	108.9(4)	H(38A)-C(38)-H(38C)	109.5
C(24)-C(27)-C(28)	108.0(4)	H(38B)-C(38)-H(38C)	109.5
C(30)-C(27)-C(28)	107.9(4)	O(1A)-C(1A)-O(2A)	127.7(4)
C(27)-C(28)-H(28A)	109.5	O(1A)-C(1A)-C(2A)	116.9(4)
C(27)-C(28)-H(28B)	109.5	O(2A)-C(1A)-C(2A)	115.3(3)
H(28A)-C(28)-H(28B)	109.5	N(1A)-C(2A)-C(1A)	109.8(3)
C(27)-C(28)-H(28C)	109.5	N(1A)-C(2A)-C(3A)	102.9(4)
H(28A)-C(28)-H(28C)	109.5	C(1A)-C(2A)-C(3A)	112.4(4)
H(28B)-C(28)-H(28C)	109.5	N(1A)-C(2A)-H(2A1)	110.5
C(27)-C(29)-H(29A)	109.5	C(1A)-C(2A)-H(2A1)	110.5
C(27)-C(29)-H(29B)	109.5	C(3A)-C(2A)-H(2A1)	110.5

C(5A)-C(4A)-C(3A)	103.2(5)	C(12A)-C(13A)-H(13D)	109.5
C(5A)-C(4A)-H(4A1)	111.1	C(12A)-C(13A)-H(13E)	109.5
C(3A)-C(4A)-H(4A1)	111.1	H(13D)-C(13A)-H(13E)	109.5
C(5A)-C(4A)-H(4A2)	111.1	C(12A)-C(13A)-H(13F)	109.5
C(3A)-C(4A)-H(4A2)	111.1	H(13D)-C(13A)-H(13F)	109.5
H(4A1)-C(4A)-H(4A2)	109.1	H(13E)-C(13A)-H(13F)	109.5
C(4A)-C(3A)-C(2A)	104.2(4)	C(12A)-C(14A)-H(14D)	109.5
C(4A)-C(3A)-H(3AA)	110.9	C(12A)-C(14A)-H(14E)	109.5
C(2A)-C(3A)-H(3AA)	110.9	H(14D)-C(14A)-H(14E)	109.5
C(4A)-C(3A)-H(3AB)	110.9	C(12A)-C(14A)-H(14F)	109.5
C(2A)-C(3A)-H(3AB)	110.9	H(14D)-C(14A)-H(14F)	109.5
H(3AA)-C(3A)-H(3AB)	108.9	H(14E)-C(14A)-H(14F)	109.5
N(1A)-C(5A)-C(4A)	103.0(4)	C(12A)-C(15A)-H(15D)	109.5
N(1A)-C(5A)-H(5AA)	111.2	C(12A)-C(15A)-H(15E)	109.5
C(4A)-C(5A)-H(5AA)	111.2	H(15D)-C(15A)-H(15E)	109.5
N(1A)-C(5A)-H(5AB)	111.2	C(12A)-C(15A)-H(15F)	109.5
C(4A)-C(5A)-H(5AB)	111.2	H(15D)-C(15A)-H(15F)	109.5
H(5AA)-C(5A)-H(5AB)	109.1	H(15E)-C(15A)-H(15F)	109.5
H(4B1)-C(4B)-H(4B2)	109.0	O(6A)-C(16A)-O(5A)	126.9(4)
C(11A)-C(6A)-C(7A)	120.0(4)	O(6A)-C(16A)-C(17A)	117.4(3)
C(11A)-C(6A)-S(1A)	120.0(4)	O(5A)-C(16A)-C(17A)	115.7(3)
C(7A)-C(6A)-S(1A)	120.0(4)	N(2A)-C(17A)-C(16A)	109.6(3)
C(8A)-C(7A)-C(6A)	119.3(5)	N(2A)-C(17A)-C(18A)	103.1(3)
C(8A)-C(7A)-H(7AA)	120.3	C(16A)-C(17A)-C(18A)	111.3(4)
C(6A)-C(7A)-H(7AA)	120.3	N(2A)-C(17A)-H(17B)	110.9
C(9A)-C(8A)-C(7A)	122.7(5)	C(16A)-C(17A)-H(17B)	110.9
C(9A)-C(8A)-H(8AA)	118.6	C(18A)-C(17A)-H(17B)	110.9
C(7A)-C(8A)-H(8AA)	118.6	C(18A)-C(19A)-C(20A)	104.6(5)
C(8A)-C(9A)-C(10A)	117.4(4)	C(18A)-C(19A)-H(19C)	110.8
C(8A)-C(9A)-C(12A)	122.4(4)	C(20A)-C(19A)-H(19C)	110.8
C(10A)-C(9A)-C(12A)	120.1(5)	C(18A)-C(19A)-H(19D)	110.8
C(11A)-C(10A)-C(9A)	120.9(5)	C(20A)-C(19A)-H(19D)	110.8
C(11A)-C(10A)-H(10B)	119.5	H(19C)-C(19A)-H(19D)	108.9
C(9A)-C(10A)-H(10B)	119.5	C(19A)-C(18A)-C(17A)	105.5(4)
C(6A)-C(11A)-C(10A)	119.6(5)	C(19A)-C(18A)-H(18C)	110.6
C(6A)-C(11A)-H(11B)	120.2	C(17A)-C(18A)-H(18C)	110.6
C(10A)-C(11A)-H(11B)	120.2	C(19A)-C(18A)-H(18D)	110.6
C(14B)-C(12A)-C(13A)	127.5(9)	C(17A)-C(18A)-H(18D)	110.6
C(14B)-C(12A)-C(13B)	123.4(9)	H(18C)-C(18A)-H(18D)	108.8
C(13A)-C(12A)-C(13B)	32.3(7)	N(2A)-C(20A)-C(19A)	102.6(4)
C(14B)-C(12A)-C(15A)	29.8(6)	N(2A)-C(20A)-H(20C)	111.3
C(13A)-C(12A)-C(15A)	124.0(10)	C(19A)-C(20A)-H(20C)	111.3
C(13B)-C(12A)-C(15A)	139.9(9)	N(2A)-C(20A)-H(20D)	111.3
C(14B)-C(12A)-C(9A)	115.9(7)	C(19A)-C(20A)-H(20D)	111.3
C(13A)-C(12A)-C(9A)	116.6(7)	H(20C)-C(20A)-H(20D)	109.2
C(13B)-C(12A)-C(9A)	109.9(6)	H(19E)-C(19A)-H(19F)	108.9
C(15A)-C(12A)-C(9A)	110.1(7)	C(22A)-C(21A)-C(26A)	120.6(4)
C(14B)-C(12A)-C(15B)	98.4(8)	C(22A)-C(21A)-S(2A)	119.7(3)
C(13A)-C(12A)-C(15B)	69.2(8)	C(26A)-C(21A)-S(2A)	119.6(3)
C(13B)-C(12A)-C(15B)	101.5(8)	C(21A)-C(22A)-C(23A)	119.6(4)
C(15A)-C(12A)-C(15B)	71.2(8)	C(21A)-C(22A)-H(22B)	120.2
C(9A)-C(12A)-C(15B)	103.6(6)	C(23A)-C(22A)-H(22B)	120.2
C(14B)-C(12A)-C(14A)	69.8(8)	C(22A)-C(23A)-C(24A)	121.9(4)
C(13A)-C(12A)-C(14A)	98.0(8)	C(22A)-C(23A)-H(23B)	119.0
C(13B)-C(12A)-C(14A)	68.6(8)	C(24A)-C(23A)-H(23B)	119.0
C(15A)-C(12A)-C(14A)	99.6(8)	C(23A)-C(24A)-C(25A)	117.0(4)
C(9A)-C(12A)-C(14A)	103.5(5)	C(23A)-C(24A)-C(27A)	121.4(4)
C(15B)-C(12A)-C(14A)	152.9(6)	C(25A)-C(24A)-C(27A)	121.6(4)

C(26A)-C(25A)-C(24A)	122.1(4)	C(33A)-C(34A)-H(34E)	109.5
C(26A)-C(25A)-H(25B)	119.0	H(34D)-C(34A)-H(34E)	109.5
C(24A)-C(25A)-H(25B)	119.0	C(33A)-C(34A)-H(34F)	109.5
C(25A)-C(26A)-C(21A)	118.8(4)	H(34D)-C(34A)-H(34F)	109.5
C(25A)-C(26A)-H(26B)	120.6	H(34E)-C(34A)-H(34F)	109.5
C(21A)-C(26A)-H(26B)	120.6	O(13A)-C(35A)-C(36A)	113.6(5)
C(29B)-C(27A)-C(30B)	118.5(16)	O(13A)-C(35A)-H(35B)	108.8
C(29B)-C(27A)-C(30A)	141.2(11)	C(36A)-C(35A)-H(35B)	108.8
C(30B)-C(27A)-C(30A)	52.4(9)	O(13A)-C(35A)-H(35C)	108.8
C(29B)-C(27A)-C(24A)	108.1(11)	C(36A)-C(35A)-H(35C)	108.8
C(30B)-C(27A)-C(24A)	105.7(10)	H(35B)-C(35A)-H(35C)	107.7
C(30A)-C(27A)-C(24A)	110.5(4)	C(35A)-C(36A)-H(36D)	109.5
C(29B)-C(27A)-C(28A)	55.0(10)	C(35A)-C(36A)-H(36E)	109.5
C(30B)-C(27A)-C(28A)	145.0(10)	H(36D)-C(36A)-H(36E)	109.5
C(30A)-C(27A)-C(28A)	108.2(5)	C(35A)-C(36A)-H(36F)	109.5
C(24A)-C(27A)-C(28A)	108.7(4)	H(36D)-C(36A)-H(36F)	109.5
C(29B)-C(27A)-C(29A)	56.9(11)	H(36E)-C(36A)-H(36F)	109.5
C(30B)-C(27A)-C(29A)	62.9(10)	O(14A)-C(37A)-C(38A)	112.0(4)
C(30A)-C(27A)-C(29A)	108.5(5)	O(14A)-C(37A)-H(37C)	109.2
C(24A)-C(27A)-C(29A)	113.3(4)	C(38A)-C(37A)-H(37C)	109.2
C(28A)-C(27A)-C(29A)	107.4(5)	O(14A)-C(37A)-H(37D)	109.2
C(29B)-C(27A)-C(28B)	113.2(14)	C(38A)-C(37A)-H(37D)	109.2
C(30B)-C(27A)-C(28B)	102.1(13)	H(37C)-C(37A)-H(37D)	107.9
C(30A)-C(27A)-C(28B)	50.4(10)	C(37A)-C(38A)-H(38D)	109.5
C(24A)-C(27A)-C(28B)	108.6(10)	C(37A)-C(38A)-H(38E)	109.5
C(28A)-C(27A)-C(28B)	61.1(10)	H(38D)-C(38A)-H(38E)	109.5
C(29A)-C(27A)-C(28B)	137.9(10)	C(37A)-C(38A)-H(38F)	109.5
C(27A)-C(28A)-H(28D)	109.5	H(38D)-C(38A)-H(38F)	109.5
C(27A)-C(28A)-H(28E)	109.5	H(38E)-C(38A)-H(38F)	109.5
H(28D)-C(28A)-H(28E)	109.5	C(12A)-C(13B)-H(13G)	109.5
C(27A)-C(28A)-H(28F)	109.5	C(12A)-C(13B)-H(13H)	109.5
H(28D)-C(28A)-H(28F)	109.5	H(13G)-C(13B)-H(13H)	109.5
H(28E)-C(28A)-H(28F)	109.5	C(12A)-C(13B)-H(13I)	109.5
C(27A)-C(29A)-H(29D)	109.5	H(13G)-C(13B)-H(13I)	109.5
C(27A)-C(29A)-H(29E)	109.5	H(13H)-C(13B)-H(13I)	109.5
H(29D)-C(29A)-H(29E)	109.5	C(12A)-C(14B)-H(14G)	109.5
C(27A)-C(29A)-H(29F)	109.5	C(12A)-C(14B)-H(14H)	109.5
H(29D)-C(29A)-H(29F)	109.5	H(14G)-C(14B)-H(14H)	109.5
H(29E)-C(29A)-H(29F)	109.5	C(12A)-C(14B)-H(14I)	109.5
C(27A)-C(30A)-H(30D)	109.5	H(14G)-C(14B)-H(14I)	109.5
C(27A)-C(30A)-H(30E)	109.5	H(14H)-C(14B)-H(14I)	109.5
H(30D)-C(30A)-H(30E)	109.5	C(12A)-C(15B)-H(15G)	109.5
C(27A)-C(30A)-H(30F)	109.5	C(12A)-C(15B)-H(15H)	109.5
H(30D)-C(30A)-H(30F)	109.5	H(15G)-C(15B)-H(15H)	109.5
H(30E)-C(30A)-H(30F)	109.5	C(12A)-C(15B)-H(15I)	109.5
O(10A)-C(31A)-O(9A)	125.6(4)	H(15G)-C(15B)-H(15I)	109.5
O(10A)-C(31A)-C(32A)	118.0(4)	H(15H)-C(15B)-H(15I)	109.5
O(9A)-C(31A)-C(32A)	116.4(4)	C(27A)-C(28B)-H(28G)	109.5
C(31A)-C(32A)-H(32D)	109.5	C(27A)-C(28B)-H(28H)	109.5
C(31A)-C(32A)-H(32E)	109.5	H(28G)-C(28B)-H(28H)	109.5
H(32D)-C(32A)-H(32E)	109.5	C(27A)-C(28B)-H(28I)	109.5
C(31A)-C(32A)-H(32F)	109.5	H(28G)-C(28B)-H(28I)	109.5
H(32D)-C(32A)-H(32F)	109.5	H(28H)-C(28B)-H(28I)	109.5
H(32E)-C(32A)-H(32F)	109.5	C(27A)-C(29B)-H(29G)	109.5
O(12A)-C(33A)-O(11A)	127.1(4)	C(27A)-C(29B)-H(29H)	109.5
O(12A)-C(33A)-C(34A)	116.9(4)	H(29G)-C(29B)-H(29H)	109.5
O(11A)-C(33A)-C(34A)	116.0(4)	C(27A)-C(29B)-H(29I)	109.5
C(33A)-C(34A)-H(34D)	109.5	H(29G)-C(29B)-H(29I)	109.5

H(29H)-C(29B)-H(29I)	109.5	O(9)-Rh(1)-Rh(2)	87.90(8)
C(27A)-C(30B)-H(30G)	109.5	O(11)-Rh(1)-Rh(2)	88.18(8)
C(27A)-C(30B)-H(30H)	109.5	O(1)-Rh(1)-Rh(2)	87.40(8)
H(30G)-C(30B)-H(30H)	109.5	O(14)-Rh(1)-Rh(2)	174.48(8)
C(27A)-C(30B)-H(30I)	109.5	O(10)-Rh(2)-O(6)	90.64(12)
H(30G)-C(30B)-H(30I)	109.5	O(10)-Rh(2)-O(2)	86.62(12)
H(30H)-C(30B)-H(30I)	109.5	O(6)-Rh(2)-O(2)	175.05(11)
C(20)-N(1)-C(17)	112.9(4)	O(10)-Rh(2)-O(12)	176.70(11)
C(20)-N(1)-S(2)	124.4(3)	O(6)-Rh(2)-O(12)	89.55(12)
C(17)-N(1)-S(2)	121.7(3)	O(2)-Rh(2)-O(12)	92.95(12)
C(5)-N(2)-C(2)	111.5(4)	O(10)-Rh(2)-O(13)	92.08(12)
C(5)-N(2)-S(1)	122.5(3)	O(6)-Rh(2)-O(13)	92.48(10)
C(2)-N(2)-S(1)	118.9(3)	O(2)-Rh(2)-O(13)	91.74(11)
C(5A)-N(1A)-C(2A)	111.9(4)	O(12)-Rh(2)-O(13)	91.20(12)
C(5A)-N(1A)-S(1A)	120.9(3)	O(10)-Rh(2)-Rh(1)	88.65(8)
C(2A)-N(1A)-S(1A)	118.8(3)	O(6)-Rh(2)-Rh(1)	87.12(7)
C(17A)-N(2A)-C(20A)	111.8(3)	O(2)-Rh(2)-Rh(1)	88.69(8)
C(17A)-N(2A)-S(2A)	120.7(3)	O(12)-Rh(2)-Rh(1)	88.06(8)
C(20A)-N(2A)-S(2A)	121.4(3)	O(13)-Rh(2)-Rh(1)	179.17(9)
C(1)-O(1)-Rh(1)	118.1(3)	O(10A)-Rh(1A)-O(5A)	86.51(11)
C(1)-O(2)-Rh(2)	117.5(2)	O(10A)-Rh(1A)-O(12A)	175.70(11)
C(16)-O(5)-Rh(1)	117.7(2)	O(5A)-Rh(1A)-O(12A)	91.52(11)
C(16)-O(6)-Rh(2)	118.5(3)	O(10A)-Rh(1A)-O(1A)	89.74(12)
C(31)-O(9)-Rh(1)	118.1(3)	O(5A)-Rh(1A)-O(1A)	174.06(11)
C(31)-O(10)-Rh(2)	118.0(3)	O(12A)-Rh(1A)-O(1A)	91.91(12)
C(33)-O(11)-Rh(1)	118.7(3)	O(10A)-Rh(1A)-O(14A)	96.20(11)
C(33)-O(12)-Rh(2)	118.2(3)	O(5A)-Rh(1A)-O(14A)	86.78(10)
C(35)-O(13)-Rh(2)	126.2(4)	O(12A)-Rh(1A)-O(14A)	87.50(11)
C(35)-O(13)-H(13)	116.8	O(1A)-Rh(1A)-O(14A)	98.22(11)
Rh(2)-O(13)-H(13)	117.0	O(10A)-Rh(1A)-Rh(2A)	88.22(8)
C(37)-O(14)-Rh(1)	128.2(3)	O(5A)-Rh(1A)-Rh(2A)	88.25(7)
C(37)-O(14)-H(14)	115.8	O(12A)-Rh(1A)-Rh(2A)	87.90(8)
Rh(1)-O(14)-H(14)	115.9	O(1A)-Rh(1A)-Rh(2A)	87.03(8)
C(1A)-O(1A)-Rh(1A)	117.3(3)	O(14A)-Rh(1A)-Rh(2A)	173.13(8)
C(1A)-O(2A)-Rh(2A)	116.9(2)	O(9A)-Rh(2A)-O(2A)	87.14(12)
C(16A)-O(5A)-Rh(1A)	117.9(2)	O(9A)-Rh(2A)-O(6A)	89.28(12)
C(16A)-O(6A)-Rh(2A)	117.4(2)	O(2A)-Rh(2A)-O(6A)	174.83(11)
C(31A)-O(9A)-Rh(2A)	118.7(3)	O(9A)-Rh(2A)-O(11A)	176.08(11)
C(31A)-O(10A)-Rh(1A)	118.7(3)	O(2A)-Rh(2A)-O(11A)	93.09(12)
C(33A)-O(11A)-Rh(2A)	117.4(3)	O(6A)-Rh(2A)-O(11A)	90.22(12)
C(33A)-O(12A)-Rh(1A)	118.2(3)	O(9A)-Rh(2A)-O(13A)	95.61(12)
C(35A)-O(13A)-Rh(2A)	127.6(3)	O(2A)-Rh(2A)-O(13A)	91.49(10)
C(35A)-O(13A)-H(13J)	116.2	O(6A)-Rh(2A)-O(13A)	92.57(11)
Rh(2A)-O(13A)-H(13J)	116.2	O(11A)-Rh(2A)-O(13A)	88.30(12)
C(37A)-O(14A)-Rh(1A)	130.5(3)	O(9A)-Rh(2A)-Rh(1A)	87.97(8)
C(37A)-O(14A)-H(14J)	114.9	O(2A)-Rh(2A)-Rh(1A)	88.72(7)
Rh(1A)-O(14A)-H(14J)	114.6	O(6A)-Rh(2A)-Rh(1A)	87.42(8)
O(5)-Rh(1)-O(9)	86.74(12)	O(11A)-Rh(2A)-Rh(1A)	88.12(8)
O(5)-Rh(1)-O(11)	90.57(11)	O(13A)-Rh(2A)-Rh(1A)	176.42(9)
O(9)-Rh(1)-O(11)	175.29(12)	O(3)-S(1)-O(4)	121.6(2)
O(5)-Rh(1)-O(1)	175.42(11)	O(3)-S(1)-N(2)	106.3(2)
O(9)-Rh(1)-O(1)	90.60(12)	O(4)-S(1)-N(2)	106.0(2)
O(11)-Rh(1)-O(1)	91.82(12)	O(3)-S(1)-C(6)	107.7(2)
O(5)-Rh(1)-O(14)	87.26(10)	O(4)-S(1)-C(6)	107.9(2)
O(9)-Rh(1)-O(14)	95.70(12)	N(2)-S(1)-C(6)	106.4(2)
O(11)-Rh(1)-O(14)	88.03(11)	O(7)-S(2)-O(8)	120.8(2)
O(1)-Rh(1)-O(14)	96.73(11)	O(7)-S(2)-N(1)	105.93(19)
O(5)-Rh(1)-Rh(2)	88.77(7)	O(8)-S(2)-N(1)	107.9(2)

O(7)-S(2)-C(21)	107.6(2)
O(8)-S(2)-C(21)	107.1(2)
N(1)-S(2)-C(21)	106.74(19)
O(3A)-S(1A)-O(4A)	121.0(3)
O(3A)-S(1A)-N(1A)	106.5(2)
O(4A)-S(1A)-N(1A)	106.7(2)
O(3A)-S(1A)-C(6A)	107.7(2)
O(4A)-S(1A)-C(6A)	107.2(2)
N(1A)-S(1A)-C(6A)	107.0(2)
O(7A)-S(2A)-O(8A)	120.61(19)
O(7A)-S(2A)-N(2A)	106.82(19)
O(8A)-S(2A)-N(2A)	106.11(19)
O(7A)-S(2A)-C(21A)	106.99(19)
O(8A)-S(2A)-C(21A)	109.4(2)
N(2A)-S(2A)-C(21A)	106.03(19)

Symmetry transformations used to generate equivalent atoms:

Table B1-4: Anisotropic displacement parameters ($Å^2 x\ 10^3$) for *trans*-**1.55**●2EtOH. The anisotropic displacement factor exponent takes the form: $-2\pi^2[\ h^2\ a^{*2}U^{11} + \ldots + 2\ h\ k\ a^*\ b^*\ U^{12}\ ]$

	U^{11}	U^{22}	U^{33}	U^{23}	U^{13}	U^{12}
C(1)	26(2)	37(2)	22(2)	0(2)	0(2)	-3(2)
C(2)	28(2)	39(2)	24(2)	0(2)	-2(2)	-3(2)
C(3)	51(3)	48(3)	33(3)	7(2)	6(2)	-2(2)
C(4)	64(4)	48(3)	93(5)	-7(3)	7(4)	-9(3)
C(5)	40(3)	52(3)	62(4)	-14(3)	1(3)	-12(2)
C(6)	28(2)	45(3)	27(2)	5(2)	2(2)	6(2)
C(7)	30(2)	61(3)	40(3)	-6(2)	-2(2)	-7(2)
C(8)	29(2)	64(3)	43(3)	-5(2)	4(2)	-15(2)
C(9)	24(2)	47(3)	34(2)	5(2)	0(2)	-2(2)
C(10)	27(2)	44(2)	33(2)	2(2)	0(2)	-2(2)
C(11)	29(2)	42(2)	40(2)	8(2)	1(2)	-1(2)
C(12)	35(2)	52(3)	36(2)	3(2)	9(2)	-1(2)
C(13)	42(3)	70(4)	51(3)	25(3)	6(3)	6(3)
C(14)	41(3)	64(3)	44(3)	9(3)	11(2)	7(2)
C(15)	62(4)	107(5)	35(3)	-2(3)	2(3)	-21(4)
C(16)	27(2)	25(2)	19(2)	-4(2)	-2(2)	1(2)
C(17)	35(2)	33(2)	19(2)	4(2)	0(2)	-10(2)
C(18)	47(3)	42(3)	43(3)	-4(2)	15(2)	-2(2)
C(19)	37(3)	56(3)	86(5)	-6(3)	7(3)	6(3)
C(20)	37(3)	44(3)	66(4)	-7(3)	-3(3)	-11(2)
C(21)	24(2)	28(2)	29(2)	0(2)	0(2)	4(2)
C(22)	33(2)	32(2)	33(2)	-3(2)	-2(2)	-3(2)
C(23)	35(2)	41(2)	28(2)	-5(2)	-5(2)	2(2)
C(24)	30(2)	35(2)	30(2)	-2(2)	-4(2)	7(2)
C(25)	31(2)	28(2)	39(3)	4(2)	-1(2)	-2(2)
C(26)	29(2)	30(2)	32(2)	-1(2)	-7(2)	2(2)
C(27)	35(3)	51(3)	31(2)	5(2)	-2(2)	7(2)
C(28)	43(3)	72(4)	35(3)	11(3)	-4(2)	14(3)
C(29)	48(3)	72(4)	29(3)	-1(2)	8(2)	7(3)
C(30)	54(3)	54(3)	39(3)	13(2)	3(2)	-2(3)
C(31)	36(3)	39(2)	26(2)	-1(2)	0(2)	3(2)
C(32)	46(3)	52(3)	43(3)	-11(2)	-13(2)	19(3)
C(33)	26(2)	31(2)	27(2)	6(2)	4(2)	-5(2)
C(34)	44(3)	39(3)	39(3)	0(2)	2(2)	7(2)
C(35)	110(6)	49(3)	81(5)	-11(3)	30(4)	-36(4)
C(36)	262(16)	107(7)	179(11)	-29(8)	97(11)	-117(10)
C(37)	50(3)	92(5)	45(3)	1(3)	-12(3)	-22(3)
C(38)	55(4)	134(7)	60(4)	-30(4)	0(3)	-36(4)
C(1A)	31(2)	34(2)	19(2)	1(2)	-3(2)	7(2)
C(2A)	39(2)	32(2)	21(2)	2(2)	-1(2)	6(2)
C(4A)	43(4)	70(5)	45(4)	17(3)	1(3)	24(3)
C(3A)	37(3)	62(3)	39(3)	7(2)	-13(2)	-3(2)
C(5A)	62(4)	50(3)	51(3)	6(3)	6(3)	24(3)
C(3B)	37(3)	62(3)	39(3)	7(2)	-13(2)	-3(2)
C(5B)	62(4)	50(3)	51(3)	6(3)	6(3)	24(3)
C(6A)	44(3)	32(2)	33(2)	7(2)	-8(2)	-11(2)
C(7A)	63(3)	31(2)	33(3)	-1(2)	2(2)	-1(2)
C(8A)	78(4)	29(2)	31(3)	1(2)	-2(3)	6(2)
C(9A)	63(3)	25(2)	34(2)	2(2)	5(2)	0(2)
C(10A)	63(3)	35(2)	42(3)	-5(2)	5(3)	2(2)

C(11A)	43(3)	35(2)	49(3)	0(2)	-10(2)	-2(2)
C(12A)	125(6)	39(3)	32(3)	4(2)	7(4)	-1(3)
C(13A)	82(11)	56(7)	42(7)	-2(6)	16(8)	1(8)
C(14A)	72(8)	49(6)	29(5)	8(4)	-16(5)	-9(5)
C(15A)	68(10)	76(9)	61(9)	32(7)	-15(8)	-16(8)
C(16A)	23(2)	30(2)	17(2)	2(2)	-2(2)	5(2)
C(17A)	29(2)	34(2)	23(2)	-2(2)	-3(2)	3(2)
C(19A)	37(4)	24(3)	55(4)	2(3)	-8(3)	-3(3)
C(18A)	38(3)	40(2)	31(2)	10(2)	5(2)	8(2)
C(20A)	28(2)	31(2)	60(3)	-8(2)	0(2)	5(2)
C(19A)	48(11)	42(10)	47(11)	28(8)	19(9)	21(8)
C(18B)	38(3)	40(2)	31(2)	10(2)	5(2)	8(2)
C(20B)	28(2)	31(2)	60(3)	-8(2)	0(2)	5(2)
C(21A)	28(2)	30(2)	28(2)	0(2)	-3(2)	-9(2)
C(22A)	30(2)	43(2)	24(2)	-6(2)	3(2)	3(2)
C(23A)	29(2)	44(3)	33(2)	-6(2)	-5(2)	8(2)
C(24A)	33(2)	37(2)	27(2)	-4(2)	2(2)	-12(2)
C(25A)	47(3)	33(2)	26(2)	-5(2)	7(2)	2(2)
C(26A)	36(2)	31(2)	38(3)	-4(2)	-1(2)	4(2)
C(27A)	47(3)	40(2)	25(2)	5(2)	-2(2)	-5(2)
C(28A)	50(4)	63(4)	31(3)	0(3)	-5(3)	-12(4)
C(29A)	63(5)	81(5)	26(3)	-7(3)	-16(3)	31(4)
C(30A)	44(4)	62(4)	37(4)	22(3)	1(3)	-5(3)
C(31A)	35(2)	32(2)	18(2)	4(2)	-1(2)	-2(2)
C(32A)	50(3)	48(3)	48(3)	-3(2)	6(3)	-11(3)
C(33A)	28(2)	34(2)	25(2)	1(2)	-7(2)	1(2)
C(34A)	37(3)	43(3)	49(3)	-6(2)	-2(2)	-4(2)
C(35A)	38(3)	66(4)	47(3)	3(3)	11(2)	14(3)
C(36A)	42(4)	74(5)	173(9)	33(5)	5(5)	21(3)
C(37A)	81(4)	43(3)	50(3)	-19(3)	-8(3)	18(3)
C(38A)	114(6)	46(3)	57(4)	-8(3)	-2(4)	35(4)
C(13B)	74(10)	78(9)	32(6)	7(6)	8(7)	-26(9)
C(14B)	82(11)	44(6)	29(6)	10(5)	-8(7)	6(7)
C(15B)	62(7)	58(7)	43(6)	6(5)	12(6)	1(6)
N(1)	37(2)	29(2)	29(2)	3(2)	-7(2)	-10(2)
N(2)	24(2)	52(2)	31(2)	1(2)	0(2)	-4(2)
N(1A)	53(2)	32(2)	25(2)	2(2)	-6(2)	7(2)
N(2A)	26(2)	30(2)	32(2)	-3(2)	-1(2)	4(1)
O(1)	32(2)	37(2)	22(2)	-1(1)	1(1)	-11(1)
O(2)	29(2)	47(2)	16(1)	-4(1)	2(1)	-11(1)
O(3)	60(2)	52(2)	45(2)	19(2)	17(2)	9(2)
O(4)	43(2)	106(3)	38(2)	6(2)	-8(2)	22(2)
O(5)	33(2)	32(1)	16(1)	-2(1)	-2(1)	-9(1)
O(6)	32(2)	30(2)	17(1)	-2(1)	-1(1)	-12(1)
O(7)	32(2)	54(2)	35(2)	5(2)	3(1)	-8(1)
O(8)	53(2)	39(2)	31(2)	-5(1)	-2(2)	-3(2)
O(9)	30(2)	40(2)	26(2)	-6(1)	-6(1)	3(1)
O(10)	39(2)	34(2)	28(2)	-9(1)	-8(1)	3(1)
O(11)	34(2)	31(1)	22(1)	-5(1)	-2(1)	-2(1)
O(12)	30(2)	33(2)	23(1)	1(1)	-5(1)	1(1)
O(13)	51(2)	37(2)	20(2)	1(1)	-11(1)	-15(2)
O(14)	40(2)	46(2)	22(2)	-11(1)	1(1)	-7(2)
O(1A)	36(2)	34(2)	20(1)	3(1)	4(1)	14(1)
O(2A)	44(2)	33(2)	16(1)	2(1)	2(1)	14(1)
O(3A)	58(2)	75(3)	48(2)	23(2)	-23(2)	-8(2)
O(4A)	116(4)	50(2)	37(2)	-6(2)	-20(2)	-11(2)
O(5A)	28(1)	29(1)	16(1)	-3(1)	1(1)	9(1)
O(6A)	36(2)	38(2)	17(1)	0(1)	-2(1)	16(1)

O(7A)	33(2)	50(2)	30(2)	5(1)	6(1)	-3(1)
O(8A)	50(2)	29(2)	40(2)	5(1)	-6(2)	4(2)
O(9A)	33(2)	40(2)	27(2)	-3(1)	9(1)	-2(1)
O(10A)	34(2)	30(1)	24(1)	-3(1)	3(1)	-2(1)
O(11A)	37(2)	33(2)	24(2)	-4(1)	-1(1)	-3(1)
O(12A)	28(1)	34(2)	21(1)	-2(1)	3(1)	0(1)
O(13A)	45(2)	59(2)	14(1)	-7(1)	-7(1)	21(2)
O(14A)	46(2)	37(2)	23(2)	0(1)	12(1)	10(2)
O(1S)	52(5)	89(6)	44(4)	18(4)	2(3)	11(4)
Rh(1)	26(1)	28(1)	15(1)	-2(1)	-2(1)	-4(1)
Rh(2)	25(1)	29(1)	14(1)	-2(1)	-2(1)	-3(1)
Rh(1A)	26(1)	26(1)	14(1)	0(1)	2(1)	6(1)
Rh(2A)	28(1)	28(1)	14(1)	-1(1)	2(1)	6(1)
S(1)	36(1)	57(1)	30(1)	8(1)	1(1)	8(1)
S(2)	34(1)	34(1)	26(1)	0(1)	-1(1)	-5(1)
S(1A)	60(1)	45(1)	30(1)	3(1)	-18(1)	-7(1)
S(2A)	31(1)	30(1)	27(1)	3(1)	-2(1)	-1(1)

Table B1-5: Hydrogen coordinates (x 10^4) and isotropic displacement parameters ($Å^2$x 10^3) for *trans*-**1.55** ● 2EtOH.

	x	y	z	U(eq)
H(2A)	4179	10676	7042	36
H(3A)	4184	11800	6906	53
H(3B)	3505	11829	7314	53
H(4A)	4777	12501	7456	82
H(4B)	4410	12093	7905	82
H(5A)	5690	11688	7300	62
H(5B)	5664	11666	7879	62
H(7A)	6853	10828	7021	52
H(8A)	7252	10853	6219	54
H(10A)	5421	9635	5860	42
H(11A)	4972	9654	6653	44
H(13A)	6007	11149	5263	81
H(13B)	6759	11052	4915	81
H(13C)	6885	11324	5451	81
H(14A)	7617	9617	5512	74
H(14B)	7876	10381	5606	74
H(14C)	7744	10118	5068	74
H(15A)	5624	9953	5117	102
H(15B)	6249	9360	5212	102
H(15C)	6382	9867	4773	102
H(17A)	1575	9028	9602	35
H(18A)	267	9271	9704	52
H(18B)	437	9834	9300	52
H(19A)	-30	9153	8690	72
H(19B)	-639	8969	9119	72
H(20A)	35	7988	9304	59
H(20B)	166	8005	8730	59
H(22A)	2379	8101	10025	39
H(23A)	2331	7555	10755	42
H(25A)	1075	6036	10162	39
H(26A)	1128	6566	9419	36
H(28A)	2547	6004	11498	75
H(28B)	2870	6629	11192	75
H(28C)	2772	5907	10943	75
H(29A)	783	7000	11321	75
H(29B)	1657	7299	11411	75
H(29C)	1345	6678	11725	75
H(30A)	630	5850	10955	74
H(30B)	1201	5549	11362	74
H(30C)	1408	5431	10807	74
H(32A)	4016	8175	8128	70
H(32B)	4176	8323	8685	70
H(32C)	4725	8669	8284	70
H(34A)	576	11562	8045	61
H(34B)	1196	12069	8290	61
H(34C)	648	11595	8617	61
H(35A)	1733	8368	7120	96
H(36A)	836	7891	7520	274
H(36B)	355	8586	7499	274
H(36C)	971	8448	7927	274
H(37A)	4482	10528	9589	75
H(37B)	4388	11322	9660	75

H(38A)	5410	11085	9148	125
H(38B)	4723	11492	8873	125
H(38C)	4809	10697	8797	125
H(2A1)	1690	1511	-438	37
H(4A1)	-468	1996	27	63
H(4A2)	41	1671	460	63
H(3AA)	346	1520	-555	55
H(3AB)	335	928	-160	55
H(5AA)	491	2780	-133	65
H(5AB)	553	2734	444	65
H(4B1)	-448	1994	-172	60
H(4B2)	183	2213	-580	60
H(3BA)	409	1148	-522	55
H(3BB)	249	1140	46	55
H(5BA)	607	2961	54	65
H(5BB)	388	2422	468	65
H(7AA)	1373	3663	-522	51
H(8AA)	1364	3976	-1321	55
H(10B)	2969	2534	-1633	56
H(11B)	2961	2189	-829	51
H(13D)	3059	2983	-2386	90
H(13E)	2387	3213	-2760	90
H(13F)	2211	2613	-2392	90
H(14D)	871	3358	-1996	75
H(14E)	1139	3219	-2538	75
H(14F)	1039	3975	-2351	75
H(15D)	2895	4349	-2020	102
H(15E)	1982	4496	-1888	102
H(15F)	2245	4423	-2438	102
H(17B)	3869	-630	2069	34
H(19C)	3641	-2053	1204	46
H(19D)	3940	-2516	1643	46
H(18C)	3607	-1739	2199	44
H(18D)	2907	-1624	1811	44
H(20C)	5106	-1921	1730	48
H(20D)	4984	-1842	1158	48
H(19E)	4541	-2046	2158	54
H(19F)	4127	-2521	1760	54
H(18E)	3102	-1743	1615	44
H(18F)	3234	-1629	2183	44
H(20E)	4582	-1900	1153	48
H(20F)	5319	-1853	1525	48
H(22B)	6543	-1375	1885	39
H(23B)	7127	-1657	2614	42
H(25B)	5670	-355	3296	43
H(26B)	5093	-56	2570	42
H(28D)	7790	-578	3565	72
H(28E)	7366	-700	4072	72
H(28F)	6951	-228	3679	72
H(29D)	7537	-1929	3134	85
H(29E)	7250	-2225	3640	85
H(29F)	7957	-1684	3620	85
H(30D)	6051	-1935	3819	71
H(30E)	5720	-1180	3834	71
H(30F)	6397	-1413	4204	71
H(32D)	4137	1906	1108	73
H(32E)	4339	1760	556	73
H(32F)	4749	1319	969	73

H(34D)	325	-1205	1083	65
H(34E)	930	-1707	820	65
H(34F)	356	-1234	509	65
H(35B)	4440	-671	36	60
H(35C)	4276	-875	-510	60
H(36D)	4685	-1791	-76	145
H(36E)	3792	-1902	-264	145
H(36F)	3949	-1698	284	145
H(37C)	1754	1777	2051	69
H(37D)	901	1510	2227	69
H(38D)	749	2331	1658	108
H(38E)	414	1632	1458	108
H(38F)	1266	1901	1284	108
H(13G)	2502	2699	-2456	92
H(13H)	1821	3130	-2716	92
H(13I)	1605	2673	-2261	92
H(14G)	2349	4516	-2120	78
H(14H)	1466	4304	-1962	78
H(14I)	1733	4237	-2512	78
H(15G)	3478	3533	-1900	81
H(15H)	3270	4124	-2269	81
H(15I)	3350	3366	-2457	81
H(28G)	5892	-1020	4021	111
H(28H)	6331	-354	3836	111
H(28I)	6750	-822	4230	111
H(29G)	7865	-1415	3229	102
H(29H)	7895	-1263	3793	102
H(29I)	7742	-663	3421	102
H(30G)	6775	-2254	3383	100
H(30H)	5965	-1954	3599	100
H(30I)	6716	-2077	3942	100
H(13)	1417	9616	7122	43
H(14)	3142	11120	9503	43
H(13J)	2965	-726	-414	47
H(14J)	1359	533	2057	42

Table B1-6: Torsion angles [°] for *trans*-**1.55** ● 2EtOH.

O(1)-C(1)-C(2)-N(2)	44.8(5)
O(2)-C(1)-C(2)-N(2)	-135.8(4)
O(1)-C(1)-C(2)-C(3)	-68.7(5)
O(2)-C(1)-C(2)-C(3)	110.6(4)
N(2)-C(2)-C(3)-C(4)	-21.5(5)
C(1)-C(2)-C(3)-C(4)	97.1(5)
C(2)-C(3)-C(4)-C(5)	36.9(6)
C(3)-C(4)-C(5)-N(2)	-37.0(6)
C(11)-C(6)-C(7)-C(8)	0.5(7)
S(1)-C(6)-C(7)-C(8)	-177.0(4)
C(6)-C(7)-C(8)-C(9)	-1.7(8)
C(7)-C(8)-C(9)-C(10)	1.0(8)
C(7)-C(8)-C(9)-C(12)	178.4(5)
C(8)-C(9)-C(10)-C(11)	0.9(7)
C(12)-C(9)-C(10)-C(11)	-176.4(4)
C(7)-C(6)-C(11)-C(10)	1.3(7)
S(1)-C(6)-C(11)-C(10)	178.9(3)
C(9)-C(10)-C(11)-C(6)	-2.1(7)
C(8)-C(9)-C(12)-C(15)	175.4(5)
C(10)-C(9)-C(12)-C(15)	-7.3(7)
C(8)-C(9)-C(12)-C(13)	-64.5(6)
C(10)-C(9)-C(12)-C(13)	112.7(5)
C(8)-C(9)-C(12)-C(14)	55.4(6)
C(10)-C(9)-C(12)-C(14)	-127.4(5)
O(6)-C(16)-C(17)-N(1)	42.6(5)
O(5)-C(16)-C(17)-N(1)	-139.4(4)
O(6)-C(16)-C(17)-C(18)	-72.0(5)
O(5)-C(16)-C(17)-C(18)	106.1(4)
N(1)-C(17)-C(18)-C(19)	-26.1(5)
C(16)-C(17)-C(18)-C(19)	93.0(4)
C(17)-C(18)-C(19)-C(20)	38.2(5)
C(18)-C(19)-C(20)-N(1)	-34.5(6)
C(26)-C(21)-C(22)-C(23)	1.1(6)
S(2)-C(21)-C(22)-C(23)	179.3(3)
C(21)-C(22)-C(23)-C(24)	-0.8(7)
C(22)-C(23)-C(24)-C(25)	0.0(7)
C(22)-C(23)-C(24)-C(27)	-179.3(4)
C(23)-C(24)-C(25)-C(26)	0.5(6)
C(27)-C(24)-C(25)-C(26)	179.8(4)
C(24)-C(25)-C(26)-C(21)	-0.2(7)
C(22)-C(21)-C(26)-C(25)	-0.6(6)
S(2)-C(21)-C(26)-C(25)	-178.8(3)
C(25)-C(24)-C(27)-C(29)	-125.3(5)
C(23)-C(24)-C(27)-C(29)	54.0(6)
C(25)-C(24)-C(27)-C(30)	-3.0(6)
C(23)-C(24)-C(27)-C(30)	176.2(4)
C(25)-C(24)-C(27)-C(28)	115.9(5)
C(23)-C(24)-C(27)-C(28)	-64.8(5)
O(1A)-C(1A)-C(2A)-N(1A)	48.6(5)
O(2A)-C(1A)-C(2A)-N(1A)	-133.2(4)
O(1A)-C(1A)-C(2A)-C(3A)	-65.2(5)
O(2A)-C(1A)-C(2A)-C(3A)	113.0(4)
C(5A)-C(4A)-C(3A)-C(2A)	37.1(5)
N(1A)-C(2A)-C(3A)-C(4A)	-22.3(5)
C(1A)-C(2A)-C(3A)-C(4A)	95.7(5)
C(3A)-C(4A)-C(5A)-N(1A)	-36.7(5)

C(11A)-C(6A)-C(7A)-C(8A)	-0.2(7)
S(1A)-C(6A)-C(7A)-C(8A)	179.9(4)
C(6A)-C(7A)-C(8A)-C(9A)	-0.2(8)
C(7A)-C(8A)-C(9A)-C(10A)	-0.3(8)
C(7A)-C(8A)-C(9A)-C(12A)	-176.4(5)
C(8A)-C(9A)-C(10A)-C(11A)	1.3(8)
C(12A)-C(9A)-C(10A)-C(11A)	177.5(5)
C(7A)-C(6A)-C(11A)-C(10A)	1.2(7)
S(1A)-C(6A)-C(11A)-C(10A)	-179.0(4)
C(9A)-C(10A)-C(11A)-C(6A)	-1.7(8)
C(8A)-C(9A)-C(12A)-C(14B)	18.0(11)
C(10A)-C(9A)-C(12A)-C(14B)	-158.0(8)
C(8A)-C(9A)-C(12A)-C(13A)	-162.2(9)
C(10A)-C(9A)-C(12A)-C(13A)	21.8(11)
C(8A)-C(9A)-C(12A)-C(13B)	-127.7(9)
C(10A)-C(9A)-C(12A)-C(13B)	56.3(10)
C(8A)-C(9A)-C(12A)-C(15A)	49.8(10)
C(10A)-C(9A)-C(12A)-C(15A)	-126.2(8)
C(8A)-C(9A)-C(12A)-C(15B)	124.5(7)
C(10A)-C(9A)-C(12A)-C(15B)	-51.5(7)
C(8A)-C(9A)-C(12A)-C(14A)	-55.9(7)
C(10A)-C(9A)-C(12A)-C(14A)	128.1(6)
O(6A)-C(16A)-C(17A)-N(2A)	41.0(5)
O(5A)-C(16A)-C(17A)-N(2A)	-141.1(3)
O(6A)-C(16A)-C(17A)-C(18A)	-72.4(5)
O(5A)-C(16A)-C(17A)-C(18A)	105.6(4)
C(20A)-C(19A)-C(18A)-C(17A)	35.3(6)
N(2A)-C(17A)-C(18A)-C(19A)	-23.7(5)
C(16A)-C(17A)-C(18A)-C(19A)	93.7(5)
C(18A)-C(19A)-C(20A)-N(2A)	-32.4(6)
C(26A)-C(21A)-C(22A)-C(23A)	-1.3(7)
S(2A)-C(21A)-C(22A)-C(23A)	-177.8(3)
C(21A)-C(22A)-C(23A)-C(24A)	1.6(7)
C(22A)-C(23A)-C(24A)-C(25A)	-1.4(7)
C(22A)-C(23A)-C(24A)-C(27A)	179.5(4)
C(23A)-C(24A)-C(25A)-C(26A)	0.9(6)
C(27A)-C(24A)-C(25A)-C(26A)	-180.0(4)
C(24A)-C(25A)-C(26A)-C(21A)	-0.6(7)
C(22A)-C(21A)-C(26A)-C(25A)	0.8(6)
S(2A)-C(21A)-C(26A)-C(25A)	177.3(3)
C(23A)-C(24A)-C(27A)-C(29B)	56.3(12)
C(25A)-C(24A)-C(27A)-C(29B)	-122.8(11)
C(23A)-C(24A)-C(27A)-C(30B)	-71.6(11)
C(25A)-C(24A)-C(27A)-C(30B)	109.3(10)
C(23A)-C(24A)-C(27A)-C(30A)	-126.8(5)
C(25A)-C(24A)-C(27A)-C(30A)	54.1(6)
C(23A)-C(24A)-C(27A)-C(28A)	114.6(5)
C(25A)-C(24A)-C(27A)-C(28A)	-64.5(6)
C(23A)-C(24A)-C(27A)-C(29A)	-4.8(7)
C(25A)-C(24A)-C(27A)-C(29A)	176.1(5)
C(23A)-C(24A)-C(27A)-C(28B)	179.5(11)
C(25A)-C(24A)-C(27A)-C(28B)	0.4(12)
C(19)-C(20)-N(1)-C(17)	18.9(6)
C(19)-C(20)-N(1)-S(2)	-172.3(4)
C(16)-C(17)-N(1)-C(20)	-116.0(4)
C(18)-C(17)-N(1)-C(20)	4.4(5)
C(16)-C(17)-N(1)-S(2)	74.9(4)
C(18)-C(17)-N(1)-S(2)	-164.8(3)

C(4)-C(5)-N(2)-C(2)	24.2(6)
C(4)-C(5)-N(2)-S(1)	174.3(4)
C(1)-C(2)-N(2)-C(5)	-120.8(4)
C(3)-C(2)-N(2)-C(5)	-1.4(5)
C(1)-C(2)-N(2)-S(1)	87.9(4)
C(3)-C(2)-N(2)-S(1)	-152.7(3)
C(4A)-C(5A)-N(1A)-C(2A)	23.8(5)
C(4A)-C(5A)-N(1A)-S(1A)	171.3(4)
C(1A)-C(2A)-N(1A)-C(5A)	-120.4(4)
C(3A)-C(2A)-N(1A)-C(5A)	-0.6(5)
C(1A)-C(2A)-N(1A)-S(1A)	91.3(4)
C(3A)-C(2A)-N(1A)-S(1A)	-148.9(3)
C(16A)-C(17A)-N(2A)-C(20A)	-115.6(4)
C(18A)-C(17A)-N(2A)-C(20A)	3.0(5)
C(16A)-C(17A)-N(2A)-S(2A)	91.5(4)
C(18A)-C(17A)-N(2A)-S(2A)	-149.9(3)
C(19A)-C(20A)-N(2A)-C(17A)	18.0(6)
C(19A)-C(20A)-N(2A)-S(2A)	170.7(4)
O(2)-C(1)-O(1)-Rh(1)	13.4(6)
C(2)-C(1)-O(1)-Rh(1)	-167.3(3)
O(1)-C(1)-O(2)-Rh(2)	-4.5(6)
C(2)-C(1)-O(2)-Rh(2)	176.2(3)
O(6)-C(16)-O(5)-Rh(1)	-1.5(5)
C(17)-C(16)-O(5)-Rh(1)	-179.3(3)
O(5)-C(16)-O(6)-Rh(2)	10.3(5)
C(17)-C(16)-O(6)-Rh(2)	-171.9(3)
O(10)-C(31)-O(9)-Rh(1)	3.3(6)
C(32)-C(31)-O(9)-Rh(1)	-176.4(3)
O(9)-C(31)-O(10)-Rh(2)	0.8(6)
C(32)-C(31)-O(10)-Rh(2)	-179.5(3)
O(12)-C(33)-O(11)-Rh(1)	0.3(5)
C(34)-C(33)-O(11)-Rh(1)	178.9(3)
O(11)-C(33)-O(12)-Rh(2)	7.3(5)
C(34)-C(33)-O(12)-Rh(2)	-171.3(3)
C(36)-C(35)-O(13)-Rh(2)	76.8(11)
C(38)-C(37)-O(14)-Rh(1)	40.3(8)
O(2A)-C(1A)-O(1A)-Rh(1A)	16.1(6)
C(2A)-C(1A)-O(1A)-Rh(1A)	-165.9(3)
O(1A)-C(1A)-O(2A)-Rh(2A)	-5.1(6)
C(2A)-C(1A)-O(2A)-Rh(2A)	177.0(3)
O(6A)-C(16A)-O(5A)-Rh(1A)	-2.6(5)
C(17A)-C(16A)-O(5A)-Rh(1A)	179.8(3)
O(5A)-C(16A)-O(6A)-Rh(2A)	13.8(5)
C(17A)-C(16A)-O(6A)-Rh(2A)	-168.5(3)
O(10A)-C(31A)-O(9A)-Rh(2A)	2.8(6)
C(32A)-C(31A)-O(9A)-Rh(2A)	-177.8(3)
O(9A)-C(31A)-O(10A)-Rh(1A)	5.1(6)
C(32A)-C(31A)-O(10A)-Rh(1A)	-174.2(3)
O(12A)-C(33A)-O(11A)-Rh(2A)	7.6(6)
C(34A)-C(33A)-O(11A)-Rh(2A)	-172.1(3)
O(11A)-C(33A)-O(12A)-Rh(1A)	2.1(6)
C(34A)-C(33A)-O(12A)-Rh(1A)	-178.1(3)
C(36A)-C(35A)-O(13A)-Rh(2A)	95.4(6)
C(38A)-C(37A)-O(14A)-Rh(1A)	44.9(7)
C(16)-O(5)-Rh(1)-O(9)	-93.9(3)
C(16)-O(5)-Rh(1)-O(11)	82.2(3)
C(16)-O(5)-Rh(1)-O(1)	-39.3(16)
C(16)-O(5)-Rh(1)-O(14)	170.2(3)

C(16)-O(5)-Rh(1)-Rh(2)	-5.9(3)
C(31)-O(9)-Rh(1)-O(5)	84.4(3)
C(31)-O(9)-Rh(1)-O(11)	29.0(16)
C(31)-O(9)-Rh(1)-O(1)	-91.9(3)
C(31)-O(9)-Rh(1)-O(14)	171.3(3)
C(31)-O(9)-Rh(1)-Rh(2)	-4.5(3)
C(33)-O(11)-Rh(1)-O(5)	-94.6(3)
C(33)-O(11)-Rh(1)-O(9)	-39.4(15)
C(33)-O(11)-Rh(1)-O(1)	81.5(3)
C(33)-O(11)-Rh(1)-O(14)	178.2(3)
C(33)-O(11)-Rh(1)-Rh(2)	-5.9(3)
C(1)-O(1)-Rh(1)-O(5)	20.7(16)
C(1)-O(1)-Rh(1)-O(9)	75.2(3)
C(1)-O(1)-Rh(1)-O(11)	-100.8(3)
C(1)-O(1)-Rh(1)-O(14)	171.0(3)
C(1)-O(1)-Rh(1)-Rh(2)	-12.7(3)
C(37)-O(14)-Rh(1)-O(5)	122.2(4)
C(37)-O(14)-Rh(1)-O(9)	35.8(4)
C(37)-O(14)-Rh(1)-O(11)	-147.1(4)
C(37)-O(14)-Rh(1)-O(1)	-55.5(4)
C(37)-O(14)-Rh(1)-Rh(2)	166.2(7)
C(31)-O(10)-Rh(2)-O(6)	-90.5(3)
C(31)-O(10)-Rh(2)-O(2)	85.4(3)
C(31)-O(10)-Rh(2)-O(12)	3(2)
C(31)-O(10)-Rh(2)-O(13)	177.0(3)
C(31)-O(10)-Rh(2)-Rh(1)	-3.4(3)
C(16)-O(6)-Rh(2)-O(10)	77.4(3)
C(16)-O(6)-Rh(2)-O(2)	21.1(15)
C(16)-O(6)-Rh(2)-O(12)	-99.3(3)
C(16)-O(6)-Rh(2)-O(13)	169.5(3)
C(16)-O(6)-Rh(2)-Rh(1)	-11.2(3)
C(1)-O(2)-Rh(2)-O(10)	-93.5(3)
C(1)-O(2)-Rh(2)-O(6)	-37.0(15)
C(1)-O(2)-Rh(2)-O(12)	83.3(3)
C(1)-O(2)-Rh(2)-O(13)	174.6(3)
C(1)-O(2)-Rh(2)-Rh(1)	-4.7(3)
C(33)-O(12)-Rh(2)-O(10)	-15(2)
C(33)-O(12)-Rh(2)-O(6)	78.1(3)
C(33)-O(12)-Rh(2)-O(2)	-97.6(3)
C(33)-O(12)-Rh(2)-O(13)	170.6(3)
C(33)-O(12)-Rh(2)-Rh(1)	-9.0(3)
C(35)-O(13)-Rh(2)-O(10)	38.6(5)
C(35)-O(13)-Rh(2)-O(6)	-52.1(5)
C(35)-O(13)-Rh(2)-O(2)	125.3(5)
C(35)-O(13)-Rh(2)-O(12)	-141.7(5)
C(35)-O(13)-Rh(2)-Rh(1)	-114(5)
O(5)-Rh(1)-Rh(2)-O(10)	-83.38(12)
O(9)-Rh(1)-Rh(2)-O(10)	3.40(12)
O(11)-Rh(1)-Rh(2)-O(10)	-174.00(12)
O(1)-Rh(1)-Rh(2)-O(10)	94.09(12)
O(14)-Rh(1)-Rh(2)-O(10)	-127.3(9)
O(5)-Rh(1)-Rh(2)-O(6)	7.32(11)
O(9)-Rh(1)-Rh(2)-O(6)	94.11(12)
O(11)-Rh(1)-Rh(2)-O(6)	-83.29(11)
O(1)-Rh(1)-Rh(2)-O(6)	-175.20(12)
O(14)-Rh(1)-Rh(2)-O(6)	-36.6(9)
O(5)-Rh(1)-Rh(2)-O(2)	-170.03(12)
O(9)-Rh(1)-Rh(2)-O(2)	-83.25(12)

O(11)-Rh(1)-Rh(2)-O(2)	99.36(12)
O(1)-Rh(1)-Rh(2)-O(2)	7.45(12)
O(14)-Rh(1)-Rh(2)-O(2)	146.0(9)
O(5)-Rh(1)-Rh(2)-O(12)	96.97(11)
O(9)-Rh(1)-Rh(2)-O(12)	-176.25(12)
O(11)-Rh(1)-Rh(2)-O(12)	6.36(11)
O(1)-Rh(1)-Rh(2)-O(12)	-85.55(12)
O(14)-Rh(1)-Rh(2)-O(12)	53.0(9)
O(5)-Rh(1)-Rh(2)-O(13)	69(6)
O(9)-Rh(1)-Rh(2)-O(13)	156(6)
O(11)-Rh(1)-Rh(2)-O(13)	-22(6)
O(1)-Rh(1)-Rh(2)-O(13)	-114(6)
O(14)-Rh(1)-Rh(2)-O(13)	25(6)
C(31A)-O(10A)-Rh(1A)-O(5A)	80.0(3)
C(31A)-O(10A)-Rh(1A)-O(12A)	17.3(17)
C(31A)-O(10A)-Rh(1A)-O(1A)	-95.4(3)
C(31A)-O(10A)-Rh(1A)-O(14A)	166.4(3)
C(31A)-O(10A)-Rh(1A)-Rh(2A)	-8.3(3)
C(16A)-O(5A)-Rh(1A)-O(10A)	-95.7(3)
C(16A)-O(5A)-Rh(1A)-O(12A)	80.4(3)
C(16A)-O(5A)-Rh(1A)-O(1A)	-44.8(12)
C(16A)-O(5A)-Rh(1A)-O(14A)	167.8(3)
C(16A)-O(5A)-Rh(1A)-Rh(2A)	-7.4(3)
C(33A)-O(12A)-Rh(1A)-O(10A)	-33.9(17)
C(33A)-O(12A)-Rh(1A)-O(5A)	-96.5(3)
C(33A)-O(12A)-Rh(1A)-O(1A)	78.6(3)
C(33A)-O(12A)-Rh(1A)-O(14A)	176.7(3)
C(33A)-O(12A)-Rh(1A)-Rh(2A)	-8.4(3)
C(1A)-O(1A)-Rh(1A)-O(10A)	72.8(3)
C(1A)-O(1A)-Rh(1A)-O(5A)	22.0(13)
C(1A)-O(1A)-Rh(1A)-O(12A)	-103.2(3)
C(1A)-O(1A)-Rh(1A)-O(14A)	169.0(3)
C(1A)-O(1A)-Rh(1A)-Rh(2A)	-15.4(3)
C(37A)-O(14A)-Rh(1A)-O(10A)	46.7(4)
C(37A)-O(14A)-Rh(1A)-O(5A)	132.8(4)
C(37A)-O(14A)-Rh(1A)-O(12A)	-135.5(4)
C(37A)-O(14A)-Rh(1A)-O(1A)	-44.0(4)
C(37A)-O(14A)-Rh(1A)-Rh(2A)	176.5(6)
C(31A)-O(9A)-Rh(2A)-O(2A)	81.6(3)
C(31A)-O(9A)-Rh(2A)-O(6A)	-94.7(3)
C(31A)-O(9A)-Rh(2A)-O(11A)	-11.9(19)
C(31A)-O(9A)-Rh(2A)-O(13A)	172.8(3)
C(31A)-O(9A)-Rh(2A)-Rh(1A)	-7.2(3)
C(1A)-O(2A)-Rh(2A)-O(9A)	-94.2(3)
C(1A)-O(2A)-Rh(2A)-O(6A)	-47.9(15)
C(1A)-O(2A)-Rh(2A)-O(11A)	81.9(3)
C(1A)-O(2A)-Rh(2A)-O(13A)	170.2(3)
C(1A)-O(2A)-Rh(2A)-Rh(1A)	-6.2(3)
C(16A)-O(6A)-Rh(2A)-O(9A)	73.3(3)
C(16A)-O(6A)-Rh(2A)-O(2A)	27.1(15)
C(16A)-O(6A)-Rh(2A)-O(11A)	-102.8(3)
C(16A)-O(6A)-Rh(2A)-O(13A)	168.9(3)
C(16A)-O(6A)-Rh(2A)-Rh(1A)	-14.6(3)
C(33A)-O(11A)-Rh(2A)-O(9A)	-6.1(19)
C(33A)-O(11A)-Rh(2A)-O(2A)	-99.4(3)
C(33A)-O(11A)-Rh(2A)-O(6A)	76.7(3)
C(33A)-O(11A)-Rh(2A)-O(13A)	169.2(3)
C(33A)-O(11A)-Rh(2A)-Rh(1A)	-10.8(3)

C(35A)-O(13A)-Rh(2A)-O(9A)	50.7(4)
C(35A)-O(13A)-Rh(2A)-O(2A)	138.0(4)
C(35A)-O(13A)-Rh(2A)-O(6A)	-38.8(4)
C(35A)-O(13A)-Rh(2A)-O(11A)	-129.0(4)
C(35A)-O(13A)-Rh(2A)-Rh(1A)	-128.6(11)
O(10A)-Rh(1A)-Rh(2A)-O(9A)	6.63(12)
O(5A)-Rh(1A)-Rh(2A)-O(9A)	-79.93(11)
O(12A)-Rh(1A)-Rh(2A)-O(9A)	-171.51(11)
O(1A)-Rh(1A)-Rh(2A)-O(9A)	96.47(12)
O(14A)-Rh(1A)-Rh(2A)-O(9A)	-123.6(7)
O(10A)-Rh(1A)-Rh(2A)-O(2A)	-80.55(12)
O(5A)-Rh(1A)-Rh(2A)-O(2A)	-167.11(11)
O(12A)-Rh(1A)-Rh(2A)-O(2A)	101.30(12)
O(1A)-Rh(1A)-Rh(2A)-O(2A)	9.28(12)
O(14A)-Rh(1A)-Rh(2A)-O(2A)	149.2(7)
O(10A)-Rh(1A)-Rh(2A)-O(6A)	96.01(12)
O(5A)-Rh(1A)-Rh(2A)-O(6A)	9.45(12)
O(12A)-Rh(1A)-Rh(2A)-O(6A)	-82.14(12)
O(1A)-Rh(1A)-Rh(2A)-O(6A)	-174.16(13)
O(14A)-Rh(1A)-Rh(2A)-O(6A)	-34.2(7)
O(10A)-Rh(1A)-Rh(2A)-O(11A)	-173.68(12)
O(5A)-Rh(1A)-Rh(2A)-O(11A)	99.76(11)
O(12A)-Rh(1A)-Rh(2A)-O(11A)	8.17(11)
O(1A)-Rh(1A)-Rh(2A)-O(11A)	-83.85(12)
O(14A)-Rh(1A)-Rh(2A)-O(11A)	56.1(7)
O(10A)-Rh(1A)-Rh(2A)-O(13A)	-174.0(12)
O(5A)-Rh(1A)-Rh(2A)-O(13A)	99.4(12)
O(12A)-Rh(1A)-Rh(2A)-O(13A)	7.8(12)
O(1A)-Rh(1A)-Rh(2A)-O(13A)	-84.2(12)
O(14A)-Rh(1A)-Rh(2A)-O(13A)	55.8(14)
C(5)-N(2)-S(1)-O(3)	171.6(4)
C(2)-N(2)-S(1)-O(3)	-40.4(4)
C(5)-N(2)-S(1)-O(4)	40.9(4)
C(2)-N(2)-S(1)-O(4)	-171.1(3)
C(5)-N(2)-S(1)-C(6)	-73.8(4)
C(2)-N(2)-S(1)-C(6)	74.2(4)
C(11)-C(6)-S(1)-O(3)	20.6(4)
C(7)-C(6)-S(1)-O(3)	-161.9(4)
C(11)-C(6)-S(1)-O(4)	153.5(4)
C(7)-C(6)-S(1)-O(4)	-28.9(4)
C(11)-C(6)-S(1)-N(2)	-93.1(4)
C(7)-C(6)-S(1)-N(2)	84.5(4)
C(20)-N(1)-S(2)-O(7)	166.6(4)
C(17)-N(1)-S(2)-O(7)	-25.5(4)
C(20)-N(1)-S(2)-O(8)	36.0(5)
C(17)-N(1)-S(2)-O(8)	-156.1(3)
C(20)-N(1)-S(2)-C(21)	-78.9(4)
C(17)-N(1)-S(2)-C(21)	89.0(3)
C(26)-C(21)-S(2)-O(7)	-147.1(3)
C(22)-C(21)-S(2)-O(7)	34.7(4)
C(26)-C(21)-S(2)-O(8)	-15.8(4)
C(22)-C(21)-S(2)-O(8)	166.0(3)
C(26)-C(21)-S(2)-N(1)	99.6(3)
C(22)-C(21)-S(2)-N(1)	-78.7(4)
C(5A)-N(1A)-S(1A)-O(3A)	168.5(4)
C(2A)-N(1A)-S(1A)-O(3A)	-46.1(3)
C(5A)-N(1A)-S(1A)-O(4A)	38.0(4)
C(2A)-N(1A)-S(1A)-O(4A)	-176.6(3)

C(5A)-N(1A)-S(1A)-C(6A)	-76.5(4)
C(2A)-N(1A)-S(1A)-C(6A)	68.8(4)
C(11A)-C(6A)-S(1A)-O(3A)	15.5(4)
C(7A)-C(6A)-S(1A)-O(3A)	-164.6(4)
C(11A)-C(6A)-S(1A)-O(4A)	147.3(4)
C(7A)-C(6A)-S(1A)-O(4A)	-32.9(5)
C(11A)-C(6A)-S(1A)-N(1A)	-98.6(4)
C(7A)-C(6A)-S(1A)-N(1A)	81.3(4)
C(17A)-N(2A)-S(2A)-O(7A)	-161.8(3)
C(20A)-N(2A)-S(2A)-O(7A)	47.9(4)
C(17A)-N(2A)-S(2A)-O(8A)	-31.9(4)
C(20A)-N(2A)-S(2A)-O(8A)	177.8(4)
C(17A)-N(2A)-S(2A)-C(21A)	84.4(3)
C(20A)-N(2A)-S(2A)-C(21A)	-65.9(4)
C(22A)-C(21A)-S(2A)-O(7A)	-26.8(4)
C(26A)-C(21A)-S(2A)-O(7A)	156.7(3)
C(22A)-C(21A)-S(2A)-O(8A)	-159.0(3)
C(26A)-C(21A)-S(2A)-O(8A)	24.5(4)
C(22A)-C(21A)-S(2A)-N(2A)	87.0(4)
C(26A)-C(21A)-S(2A)-N(2A)	-89.5(4)

Symmetry transformations used to generate equivalent atoms:

Table B1-7: Hydrogen bonds for *trans*-**1.55** ● 2EtOH [Å and °].

D-H...A	d(D-H)	d(H...A)	d(D...A)	<(DHA)
O(13)-H(13)...O(5A)#1	0.95	2.13	2.782(4)	124.8
O(14)-H(14)...O(2A)#2	0.95	2.38	3.039(4)	126.5
O(13A)-H(13J)...O(5)#3	0.95	2.05	2.850(4)	140.3
O(14A)-H(14J)...O(2)#4	0.95	2.26	3.059(4)	141.2

Symmetry transformations used to generate equivalent atoms:
#1 -x+1/2,-y+1,z+1/2 #2 x,y+1,z+1 #3 x,y-1,z-1
#4 -x+1/2,-y+1,z-1/2

Appendix B2: 5.39d

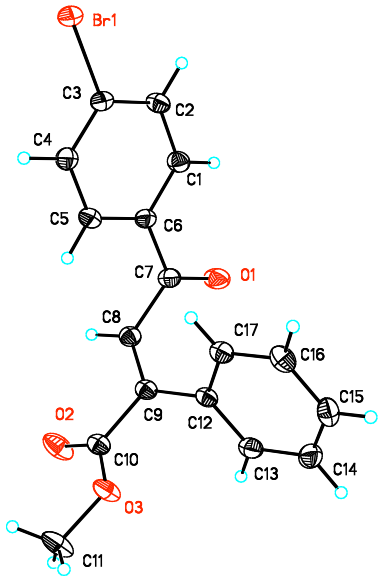

Table B2-1. Crystal data and structure refinement for **5.39d**

Identification code	jhh_8_51_0m	
Empirical formula	C17 H13 Br O3	
Formula weight	345.18	
Temperature	173(2) K	
Wavelength	1.54178 Å	
Crystal system	Monoclinic	
Space group	C2/c	
Unit cell dimensions	a = 13.9442(5) Å	α= 90°.
	b = 13.8353(4) Å	β= 98.0910(10)°.
	c = 15.3372(5) Å	γ = 90°.
Volume	2929.43(17) Å^3	
Z	8	
Density (calculated)	1.565 Mg/m^3	
Absorption coefficient	3.891 mm^{-1}	
F(000)	1392	
Crystal size	0.28 x 0.19 x 0.16 mm^3	
Theta range for data collection	4.52 to 69.36°.	
Index ranges	-16<=h<=13, -16<=k<=15, -17<=l<=18	
Reflections collected	15893	
Independent reflections	2641 [R(int) = 0.0160]	
Completeness to theta = 69.36°	96.4 %	
Absorption correction	Semi-empirical from equivalents	
Max. and min. transmission	0.5748 and 0.4088	
Refinement method	Full-matrix least-squares on F^2	
Data / restraints / parameters	2641 / 0 / 242	
Goodness-of-fit on F^2	1.111	
Final R indices [I>2sigma(I)]	R1 = 0.0234, wR2 = 0.0634	
R indices (all data)	R1 = 0.0236, wR2 = 0.0635	
Largest diff. peak and hole	0.337 and -0.356 e.Å^{-3}	

Table B2-2. Atomic coordinates (x 10^4) and equivalent isotropic displacement parameters ($Å^2$x 10^3) for **5.39d**. U(eq) is defined as one third of the trace of the orthogonalized U^{ij} tensor.

	x	y	z	U(eq)
Br(1)	12400(1)	6769(1)	1109(1)	29(1)
C(1)	10643(1)	9186(1)	1047(1)	28(1)
C(2)	11439(1)	8593(1)	1022(1)	28(1)
C(3)	11340(1)	7610(1)	1171(1)	25(1)
C(4)	10474(1)	7218(1)	1344(1)	29(1)
C(5)	9684(1)	7818(1)	1369(1)	29(1)
C(6)	9762(1)	8805(1)	1224(1)	24(1)
C(7)	8918(1)	9463(1)	1233(1)	27(1)
C(8)	8013(1)	9047(1)	1505(1)	25(1)
C(9)	7180(1)	8919(1)	974(1)	23(1)
C(10)	6357(1)	8498(1)	1390(1)	25(1)
C(11)	4906(2)	7592(2)	1121(2)	43(1)
C(12)	7047(1)	9109(1)	9(1)	23(1)
C(13)	6303(1)	9710(1)	-383(1)	28(1)
C(14)	6184(1)	9884(1)	-1281(1)	33(1)
C(15)	6802(2)	9454(1)	-1803(1)	33(1)
C(16)	7536(1)	8854(1)	-1423(1)	32(1)
C(17)	7662(1)	8684(1)	-521(1)	26(1)
O(1)	8958(1)	10312(1)	1043(1)	40(1)
O(2)	6329(1)	8473(1)	2167(1)	45(1)
O(3)	5684(1)	8110(1)	788(1)	33(1)

Table B2-3. Bond lengths [Å] and angles [°] for **5.39d**

Br(1)-C(3)	1.8938(17)	C(9)-C(8)-C(7)	125.18(17)
C(1)-C(2)	1.386(3)	C(9)-C(8)-H(8)	119.2(13)
C(1)-C(6)	1.398(2)	C(7)-C(8)-H(8)	115.5(13)
C(1)-H(1)	0.92(2)	C(8)-C(9)-C(12)	124.08(16)
C(2)-C(3)	1.388(3)	C(8)-C(9)-C(10)	116.27(16)
C(2)-H(2)	0.97(2)	C(12)-C(9)-C(10)	119.54(15)
C(3)-C(4)	1.384(3)	O(2)-C(10)-O(3)	123.94(16)
C(4)-C(5)	1.384(3)	O(2)-C(10)-C(9)	124.45(16)
C(4)-H(4)	0.98(3)	O(3)-C(10)-C(9)	111.52(15)
C(5)-C(6)	1.390(3)	O(3)-C(11)-H(11A)	112.8(19)
C(5)-H(5)	0.95(2)	O(3)-C(11)-H(11B)	111(2)
C(6)-C(7)	1.489(2)	H(11A)-C(11)-H(11B)	97(3)
C(7)-O(1)	1.214(2)	O(3)-C(11)-H(11C)	106(2)
C(7)-C(8)	1.499(2)	H(11A)-C(11)-H(11C)	123(3)
C(8)-C(9)	1.333(2)	H(11B)-C(11)-H(11C)	106(3)
C(8)-H(8)	0.93(2)	C(17)-C(12)-C(13)	118.73(17)
C(9)-C(12)	1.488(2)	C(17)-C(12)-C(9)	120.31(16)
C(9)-C(10)	1.507(2)	C(13)-C(12)-C(9)	120.96(16)
C(10)-O(2)	1.198(2)	C(14)-C(13)-C(12)	120.62(17)
C(10)-O(3)	1.332(2)	C(14)-C(13)-H(13)	119.6(13)
C(11)-O(3)	1.451(2)	C(12)-C(13)-H(13)	119.8(13)
C(11)-H(11A)	0.94(3)	C(13)-C(14)-C(15)	120.04(18)
C(11)-H(11B)	0.97(4)	C(13)-C(14)-H(14)	118.8(14)
C(11)-H(11C)	0.88(4)	C(15)-C(14)-H(14)	121.1(14)
C(12)-C(17)	1.392(2)	C(16)-C(15)-C(14)	119.81(18)
C(12)-C(13)	1.398(2)	C(16)-C(15)-H(15)	120.8(14)
C(13)-C(14)	1.385(3)	C(14)-C(15)-H(15)	119.4(14)
C(13)-H(13)	0.95(2)	C(15)-C(16)-C(17)	120.28(18)
C(14)-C(15)	1.390(3)	C(15)-C(16)-H(16)	120.9(14)
C(14)-H(14)	0.99(2)	C(17)-C(16)-H(16)	118.7(14)
C(15)-C(16)	1.381(3)	C(16)-C(17)-C(12)	120.52(18)
C(15)-H(15)	0.91(2)	C(16)-C(17)-H(17)	120.3(14)
C(16)-C(17)	1.390(3)	C(12)-C(17)-H(17)	119.2(14)
C(16)-H(16)	0.95(3)	C(10)-O(3)-C(11)	116.37(16)
C(17)-H(17)	0.93(2)		
C(2)-C(1)-C(6)	120.76(17)		
C(2)-C(1)-H(1)	119.2(14)		
C(6)-C(1)-H(1)	120.0(14)		
C(1)-C(2)-C(3)	118.46(16)		
C(1)-C(2)-H(2)	122.7(13)		
C(3)-C(2)-H(2)	118.7(13)		
C(4)-C(3)-C(2)	121.71(16)		
C(4)-C(3)-Br(1)	118.49(13)		
C(2)-C(3)-Br(1)	119.78(13)		
C(3)-C(4)-C(5)	119.30(17)		
C(3)-C(4)-H(4)	121.5(15)		
C(5)-C(4)-H(4)	119.2(15)		
C(4)-C(5)-C(6)	120.28(17)		
C(4)-C(5)-H(5)	119.4(14)		
C(6)-C(5)-H(5)	120.2(14)		
C(5)-C(6)-C(1)	119.49(16)		
C(5)-C(6)-C(7)	121.27(15)		
C(1)-C(6)-C(7)	119.22(16)		
O(1)-C(7)-C(6)	121.78(16)		
O(1)-C(7)-C(8)	120.51(16)		
C(6)-C(7)-C(8)	117.70(15)		

Symmetry transformations used to generate equivalent atoms:

Table B2-4. Anisotropic displacement parameters ($Å^2 x\ 10^3$) for **5.39d**. The anisotropic displacement factor exponent takes the form: $-2\pi^2[\ h^2\ a^{*2}U^{11} + \ldots + 2\ h\ k\ a^*\ b^*\ U^{12}\ ]$

	U^{11}	U^{22}	U^{33}	U^{23}	U^{13}	U^{12}
Br(1)	24(1)	30(1)	36(1)	1(1)	8(1)	6(1)
C(1)	25(1)	23(1)	35(1)	0(1)	5(1)	-3(1)
C(2)	22(1)	28(1)	34(1)	-2(1)	7(1)	-3(1)
C(3)	21(1)	28(1)	25(1)	-2(1)	2(1)	3(1)
C(4)	26(1)	24(1)	37(1)	4(1)	5(1)	1(1)
C(5)	21(1)	30(1)	35(1)	3(1)	5(1)	-3(1)
C(6)	19(1)	25(1)	26(1)	0(1)	2(1)	-1(1)
C(7)	21(1)	28(1)	31(1)	-1(1)	3(1)	1(1)
C(8)	24(1)	25(1)	28(1)	-1(1)	7(1)	3(1)
C(9)	22(1)	20(1)	29(1)	-3(1)	8(1)	3(1)
C(10)	25(1)	23(1)	30(1)	-5(1)	9(1)	0(1)
C(11)	35(1)	52(1)	44(1)	-9(1)	17(1)	-22(1)
C(12)	20(1)	22(1)	28(1)	-1(1)	5(1)	-4(1)
C(13)	23(1)	27(1)	36(1)	-1(1)	7(1)	0(1)
C(14)	31(1)	28(1)	39(1)	6(1)	0(1)	-1(1)
C(15)	41(1)	30(1)	27(1)	4(1)	5(1)	-8(1)
C(16)	35(1)	30(1)	32(1)	-4(1)	12(1)	-5(1)
C(17)	24(1)	25(1)	31(1)	-2(1)	6(1)	-1(1)
O(1)	27(1)	26(1)	68(1)	6(1)	11(1)	3(1)
O(2)	43(1)	63(1)	31(1)	-10(1)	16(1)	-21(1)
O(3)	26(1)	45(1)	31(1)	-5(1)	10(1)	-13(1)

Table B2-5. Hydrogen coordinates (x 10^4) and isotropic displacement parameters ($Å^2$x 10^3) for **5.39d**.

	x	y	z	U(eq)
H(1)	10695(15)	9835(17)	931(14)	29(5)
H(2)	12047(17)	8828(16)	866(14)	32(5)
H(4)	10411(18)	6530(20)	1467(16)	49(7)
H(5)	9080(18)	7546(17)	1461(15)	38(6)
H(8)	8064(14)	8844(14)	2084(14)	25(5)
H(13)	5879(16)	10005(16)	-32(14)	32(5)
H(14)	5657(17)	10321(17)	-1540(15)	38(6)
H(15)	6724(16)	9579(16)	-2390(16)	36(6)
H(16)	7948(18)	8531(18)	-1774(16)	40(6)
H(17)	8145(17)	8271(15)	-268(15)	28(5)
H(11A)	4600(20)	7960(20)	1520(20)	64(8)
H(11B)	5160(30)	7090(30)	1530(30)	95(12)
H(11C)	4580(30)	7290(30)	660(20)	90(11)

Table B2-6. Torsion angles [°] for **5.39d**.

C(6)-C(1)-C(2)-C(3)	0.4(3)
C(1)-C(2)-C(3)-C(4)	-0.2(3)
C(1)-C(2)-C(3)-Br(1)	178.21(14)
C(2)-C(3)-C(4)-C(5)	0.0(3)
Br(1)-C(3)-C(4)-C(5)	-178.37(15)
C(3)-C(4)-C(5)-C(6)	-0.1(3)
C(4)-C(5)-C(6)-C(1)	0.4(3)
C(4)-C(5)-C(6)-C(7)	178.94(18)
C(2)-C(1)-C(6)-C(5)	-0.5(3)
C(2)-C(1)-C(6)-C(7)	-179.11(17)
C(5)-C(6)-C(7)-O(1)	-174.46(18)
C(1)-C(6)-C(7)-O(1)	4.1(3)
C(5)-C(6)-C(7)-C(8)	6.8(2)
C(1)-C(6)-C(7)-C(8)	-174.59(16)
O(1)-C(7)-C(8)-C(9)	69.6(3)
C(6)-C(7)-C(8)-C(9)	-111.7(2)
C(7)-C(8)-C(9)-C(12)	4.5(3)
C(7)-C(8)-C(9)-C(10)	-179.31(15)
C(8)-C(9)-C(10)-O(2)	17.1(3)
C(12)-C(9)-C(10)-O(2)	-166.52(18)
C(8)-C(9)-C(10)-O(3)	-159.66(16)
C(12)-C(9)-C(10)-O(3)	16.7(2)
C(8)-C(9)-C(12)-C(17)	53.5(2)
C(10)-C(9)-C(12)-C(17)	-122.57(18)
C(8)-C(9)-C(12)-C(13)	-126.76(19)
C(10)-C(9)-C(12)-C(13)	57.2(2)
C(17)-C(12)-C(13)-C(14)	-0.3(3)
C(9)-C(12)-C(13)-C(14)	179.95(16)
C(12)-C(13)-C(14)-C(15)	0.5(3)
C(13)-C(14)-C(15)-C(16)	-0.1(3)
C(14)-C(15)-C(16)-C(17)	-0.3(3)
C(15)-C(16)-C(17)-C(12)	0.5(3)
C(13)-C(12)-C(17)-C(16)	-0.2(3)
C(9)-C(12)-C(17)-C(16)	179.57(16)
O(2)-C(10)-O(3)-C(11)	-3.1(3)
C(9)-C(10)-O(3)-C(11)	173.70(17)

Symmetry transformations used to generate equivalent atoms: